NAM

Assurance Meeting on Exposure, Fragility and Fatality Models for the Groningen Building Stock

Presentations	**Participants Workshop**
Letter and Report	**Assurance Panel**

Date March 2018

Editors Jan van Elk & Dirk Doornhof

General Introduction

On 21st and 22nd February 2018, NAM organised, under the auspices of the Ministry of Economic Affairs and Climate, an Assurance Meeting on Exposure, Fragility and Fatality Models for the Groningen Building Stock at Schiphol Airport, Amsterdam.

Objective of the Meeting

To assure the following elements of the Groningen Risk Assessment:

1. The building typologies classification and the process used to combine inspection data and inference rules in the development of the Exposure Model
2. The experimental and numerical modelling programmes used in the development of the Fragility Model, and the underlying methodology behind the latter
3. The use of numerical and empirical data for the development of the Fatality Model
4. The implementation of the above models, and associated uncertainty, in the risk engine

The assurance scope will focus on fatality risk estimation, rather than non-life threatening structural and non-structural damage.

Meeting Format

In the meeting, the attendees will have the following roles:

1. **Development Team**. The study programme and the models developed by this team were subjected to the assurance. The team prepared pre-read documents and make these available to the Assurance Team at least one month prior to the meeting and present their work.
2. **Assurance Team**. Experts asked to assure the study programme and the models developed. The assurance team prepared a report with opinion of the work and suggestions for further work. Table 1 lists the members of the assurance team.
3. **Domain Experts**. Experts potentially presenting their views on one or more of the Assurance Meeting topics and taking part in the discussions. These experts have not been involved in the study programme and the development of the models subject to the assurance.
4. **Observers**. Experts in other fields (e.g. hazard modelling) with an interest in the assurance process. Representatives of the regulator, SodM, will be invited to attend as observers.

Some of the Assurance Team also performed assurance on the studies for the development of the exposure, fragility and fatality models in October 2015.

The Assurance Team

The assurance team was chosen from internationally recognised experts in the field.

External Expert	Affiliation	Main Expertise Area
Jack Baker (Chair)	Stanford University, USA	PSHA, Fragility Development and Risk Analysis
Matjaz Dolsek	University of Ljubljana, Slovenia	Structural Modelling, Fragility Development and Risk Analysis
Paolo Franchin	University of Rome “La Sapienza”, Italy	Structural Modelling, Fragility Development and Risk Analysis
Ron Hamburger	Simpson Gumpertz and Heger, USA	Structural Modelling and Performance Assessment of Structures
Ihsan Engin Bal	Hanze Hoogeschool, Groningen	Structural Modelling and Performance Assessment of Structures
Marco Schotanus	RUTHERFORD + CHEKENE, USA	Structural Modelling and Performance Assessment of Structures
Nico Luco	United States Geological Survey, USA	PSHA, Fragility Development and Risk Analysis
Dimitrios Vamvatsikos	NTUA, Greece	Structural Modelling, Fragility Development and Risk Analysis

Table 1: The Assurance Team

The Domain Experts were selected from local experts involved with seismic assessment of buildings in Groningen. Representatives from the Ministry of Economic Affairs and Climate, the regulator (SodM), National Coordinator Groningen (NCG), TNO, Exxonmobil and EBN were present as Domain Experts.

Timing and Place

The meeting was held:

> Wednesday 21st February and Thursday 22nd February 2018, plenary sessions with Development Team, Assurance Team, Domain Experts and Observers. During these session, the Development Team and selected Domain Experts made presentations to the Assurance Team. These formed the basis for discussions.
>
> Friday 23rd February 2018 morning, a session exclusive to the Assurance Team was held. The Development Team was available to the Assurance Team to provide clarifications upon request for Assurance Team (if required).

Preparation and Agenda

Technical reports were made available to the Assurance Team and the Domain Experts one month prior to the event. Domain Experts were asked to indicate, up to two weeks prior to the event, if they would be interested in delivering a presentation at the meeting. A proposal for the meeting agenda was submitted by the Development Team to the Assurance Team, two weeks ahead of the event. The Assurance Team prepared the final agenda for the plenary sessions.

Wednesday 21st February

Start	End	Topic	Speaker
09:00	09:30	Welcome and Introduction Request by Minister and Life Safety Norm in The Netherlands	Ruud Cino
09:30	10:30	Risk metrics Overview of NAM's Hazard and Risk Assessment programme Objectives and Meeting format	Thijs Jurgens Jan van Elk
10:30	11:00	*Coffee break*	
11:00	11:20	Seismological model	Stephen Bourne
11:20	11:40	Ground Motion model	Julian Bommer
11:40	12:00	Hazard modelling and results + Risk Engine	Stephen Bourne
12:00	13:00	Groningen Building Stock and Exposure Database	Rinke Kluwer
13:00	14:00	*Lunch*	
14:00	14:30	Experimental testing programme for URM materials characterisation at TU Delft	Jan Rots
14:30	15:30	Experimental testing programme for URM components and structures at Eucentre and LNEC	Guido Magenes
15:30	16:00	*Coffee break*	
16:00	16:30	Experimental testing programme for RC structures at Eucentre	Rui Pinho
16:30	17:00	Verification and calibration of numerical models using test data	Rui Pinho
17:00	18:00	Discussion	All

Thursday 22nd February

Start	End	Topic	Speaker
09:00	09:30	Summary of first impressions/feedback from Review Panel	Jack Baker
09:30	10:15	Numerical modelling of Groningen buildings using Finite Element Analysis (with LS-Dyna software)	Richard Sturt
10:15	11:00	Numerical modelling of Groningen buildings using the Applied Element Method (with ELS software)	Andrea Penna
11:00	11:30	*Coffee break*	
11:30	13:00	Exposure, Fragility and Consequence models	Helen Crowley
13:00	14:00	*Lunch*	
14:00	14:30	Overview of risk results	Stephen Bourne
14:30	15:00	Discussion	All
15:00	15:30	*Coffee break*	
15:30	16:30	Final discussions	All
16:30	17:00	Closure	Jan van Elk

The current document

The current document contains:

- A general instruction providing information on the objectives, agenda and other specifics of the meeting. This section also introduces the Assurance Panel
- An Assurance Letter sent to the Ministry of Economic Affairs and climate by the Assurance Panel
- An Assurance Report prepared by the Assurance Panel
- All presentations used in the discussions during the meeting.

NAM

Title	**Assurance Meeting on Exposure, Fragility and Fatality Models for the Groningen Building Stock**	**Date**	March 2018
		Initiator	NAM
Autor(s)	Jack Baker (Chair), Matjaz Dolsek Paolo Franchin, Ron Hamburger Ihsan Engin Bal, Marco Schotanus Nico Luco, Dimitrios Vamvatsikos	**Editors**	Jan van Elk and Dirk Doornhof
Organisation	Assurance Panel	**Organisation**	NAM
Place in the Study and Data Acquisition Plan	Study Theme: Exposure, Fragility and Fatality Models Comment: On 21st and 22nd February 2018, NAM organised under the auspices of the Ministry of Economic Affairs and Climate an Assurance Meeting on Exposure, Fragility and Fatality Models for the Groningen Building Stock at Schiphol Airport, Amsterdam. The current document contains: ▪ A general instruction providing information on the objectives, agenda and other specifics of the meeting. This section also introduces the Assurance Panel ▪ An Assurance Letter sent to the Ministry of Economic Affairs and climate by the Assurance Panel ▪ An Assurance Report prepared by the Assurance Panel ▪ All presentations used in the discussions during the meeting.		
Directliy linked research	(1) Modelling Seismic Building Response (2) Experiments on buildings (3) Risk Assessment		
Used data			
Associated organisation	NAM		
Assurance	Assurance Panel		

27 April 2018

Mr. Jan van Herk
Ministry of Economic Affairs and Climate Policy
Bezuidenhoutseweg 73
2594 AC The Hague
The Netherlands

Dear Mr. van Herk:

Under the auspices of the Ministry of Economic Affairs and Climate, the NAM convened a panel consisting of the undersigned experts in structural engineering, earthquake engineering and risk analysis to review the NAM Research Team's Version 5 exposure, fragility, and fatality models for the Groningen building stock. Our review included the project reports associated with these models, and presentations from the research team on 21 and 22 February 2018 at the World Trade Center conference facility at Schiphol Airport. Some members of our panel also reviewed previous versions of these models in 2015. Our review focused on the selection of building archetypes, and the development of the fragility models and consequence functions for these archetypes. Attached with this letter is a report of our assessment from this Version 5 model review.

In general, we found this work to meet, and in many cases advance, international state-of-the art in structural testing and modeling, and prediction of consequences. They are suitable for the purpose of assessing Local Personal Risk from induced seismicity in the Groningen field. The attached report includes some recommendations for refinements and opportunities for future development, but these issues do not impact the fundamental appropriateness of these models for their intended purpose.

Sincerely,

Jack Baker (Chair)
Ihsan Engin Bal
Matjaz Dolsek
Paolo Franchin
Ronald Hamburger
Nicolas Luco
Marko Schotanus
Dimitrios Vamvatsikos

Review report: Exposure, fragility, and fatality models for the Groningen building stock

27 April, 2018

Jack Baker (Chair), Ihsan Engin Bal, Matjaz Dolsek, Paolo Franchin, Ronald Hamburger, Nicolas Luco, Marko Schotanus, Dimitrios Vamvatsikos

Introduction and Scope

This report summarizes the findings from the Assurance Panel, tasked with reviewing the Version 5 exposure, fragility, and fatality models for the Groningen Risk Assessment effort.

We reviewed these models to judge their suitability to evaluate Local Personal Risk. We understand that these models may have additional utility for other purposes, but have not performed a comprehensive review of their suitability for those other purposes.

We understand our scope of work to consist of review of:

1. The building typologies classification and the process used to combine inspection data and inference rules in the development of the Exposure Model;
2. The experimental and numerical modeling programs used in the development of the Fragility Model, and the underlying methodology behind the latter;
3. The use of numerical and empirical data for the development of the Fatality Model;
4. The implementation of the above models, and associated uncertainty, in the risk engine.

The assurance scope focuses on fatality risk estimation, rather than non-life threatening structural and non-structural damage.

Our review relied upon analysis reports provided by the NAM Research Team, as well as presentations made during an Assurance Workshop that took place on February 21 and 22, 2018 at the World Trade Center conference facility at Schiphol Airport. The subset of materials we reviewed that most directly relate to this report are:

- “Induced Seismicity in Groningen: Assessment of Hazard, Building Damage and Risk” Dated November 2017;
- “Report on the v5 Fragility and Consequence Models for the Groningen Field” Dated October 2017;
- “A Probabilistic Model to Evaluate Options for Mitigating Induced Seismic Risk” Draft manuscript received 9 February 2017.

While we carefully reviewed this information, we have not independently verified surveys or analysis results. We also note that results from the study expressed in terms of Local Personal

Risk for individual structures were not compared to acceptability of the same structure based on an assessment in accordance with NPR 9998, the Dutch Standard for “Assessment of buildings in case of erection, reconstruction and disapproval – basic rules for seismic actions: induced earthquakes” and that review of the Standard was beyond our scope.

Findings

The basic approach to risk evaluation properly follows the commonly accepted international framework for such studies. In general, we found this work to meet, and in many cases advance, the international state-of-the art in defining structural fragility and consequences informed by structural testing and modeling. The project team is world-class, and includes well-qualified experts in all aspects of the project scope. In some ways this project will be a model for future seismic risk assessments worldwide.

Assessing life safety risk in Groningen is extremely difficult, given the complete lack of empirical data on earthquake-induced structural collapses or fatalities for the region. This makes the modeling more challenging than in other regions where past deadly earthquakes provide observational constraints. The project team is well aware of this challenge, and has carefully thought about the many necessary extrapolations.

The goal of linking from gas extraction, to earthquake occurrence, to ground motion, to building exposure, to structural collapse and ultimately life safety, is an ambitious one. The interfaces between these models have been handled with more care than is standard, and care has been taken to identify and track uncertainties associated with the component models.

In the following subsections, we comment on specific model components this Panel reviewed.

Exposure model

The exposure model developed for the region is extremely detailed given the size of the region. The use of national databases, combined with inspections, local engineering expertise and other data sources, is appropriate and ensures utilization of all plausibly relevant data. It is appropriate that efforts have emphasized developing index buildings for the building stock contributing most to risk.

In general, the developed data and building archetypes are well suited for the purposes of identifying potentially vulnerable buildings and evaluating Local Personal Risk. It appears that the exposure models have utility for other purposes as well (e.g., later identification of buildings that may be identified for retrofit), though we have not considered those purposes in detail.

Fragility model

The overall testing and modeling effort underlying the fragility model is frankly incredible. The testing program is very substantial, with care taken to replicate typical construction details and as-built conditions in experimental specimens, and to identify and quantify potential failure modes of the buildings. The combination of material, component and full-scale tests is extremely extensive.

The iterative development of numerical models, with software chosen based on suitability for the given objectives, builds substantial confidence that potential failure mechanisms are well characterized. The LS Dyna modeling is very sophisticated and not often employed even in regions of high natural seismicity. The application of Applied Element Method to masonry, coupled with supporting experimental tests, is pioneering. The use of parallel model development quality assurance is beyond best practices in almost any application; the only analog to this that the Panel knows of is in assessment of nuclear power plant risk.

The conversion of detailed numerical models into simplified single-degree-of-freedom (SDOF) models is understandable, given the wide range of building types to be studied, and the high computational cost of the detailed models. The consideration of soil-structure-interaction, and ground motion duration effects, could be important, given the somewhat unique circumstances present in Groningen.

Fatality model

The choice to use empirical models to predict fatalities, with only supplementary consideration of theoretical or numerical simulations, is appropriate. Prediction of fatalities is an extremely difficult problem to address numerically, so utilizing past observations from elsewhere in the world is the best available path to solving this problem. The empirical data utilized to establish potential fatality rates appears appropriate for the considered building typologies, given the fact that there are only a handful of empirical relationships available for this purpose.

Recommendations

While our review of the models is positive, there are several issues that we recommend the project team further address moving forward.

The mapping of detailed multi-degree-of-freedom (MDOF) structural models into simplified SDOF models is a challenging aspect of the process that needs care. The project documentation should include dynamic analysis validation results, such as those presented at the in-person meeting with the Panel; a comparison of SDOF and MDOF model pushover curves should also be provided. The specific approach to fit SDOF backbones, and choice of hysteresis models could be refined, but these choices did not appear to have impacted drift predictions for the cases we saw, and so ultimately these refinements may not impact Local Personal Risk estimates significantly.

For validation of the SDOF-based fragility functions, we suggest that the project team develops a fragility function directly for one MDOF model, for comparison with a corresponding SDOF-based function. A good candidate building would be the URM4L archetype that governs the risk in the area, or a ductile building where the impact of the SDOF conversion is likely to be the largest.

The project would benefit from an evaluation of end-to-end interfaces and epistemic uncertainties. While the individual model components appear to have been well-studied and reviewed, a systematic study of the model interfaces, and the epistemic uncertainties associated with each model, would be beneficial. At present, the risk analysis includes consideration of some epistemic uncertainties (e.g., maximum possible earthquake magnitude, building fragility), but not others such as earthquake source model parameters and building inventory. As we deem the confidence intervals on Local Personal Risk estimates to be important, a systematic uncertainty study, and resulting expanded logic tree, is recommended. Additionally, the metrics used to quantify epistemic uncertainties could be improved relative to the current tornado diagram representation.

Finally, while the model sub-components are well documented, there is an opportunity to produce some aggregated model predictions for review, and for comparison of models against external data sources. An internal comparison of fragility functions for all architypes would be useful to evaluate whether the relative fragilities of the various buildings are ordered consistently with engineering judgement. Some suggested external comparisons are:

- Compare fragility models to empirical fragility functions for similar construction types from elsewhere in the world.
- Compute fatality rates as a function of ground shaking intensity (by combining the fragility and fatality models), and compare the results to empirical models (from, e.g., PAGER) for similar construction types.
- Compute regional predictions of the numbers of fatalities from the M>3 earthquakes that have happened in the past in Groningen (with the anticipation that the predictions would be of essentially zero fatalities).

These comparisons would not be done with the implication that the external models are “correct” for application in Groningen, or that the comparisons should result in close matches. After all, the anticipation is that the extensive testing and modeling program has produced fragility functions that are better suited for Groningen than any alternatives. Rather, the goal of these comparisons would be to provide general confirmation of the reasonableness of the results, and a benchmark to evaluate any differences; for example, if the Groningen fragilities for unreinforced masonry buildings suggest lower collapse probabilities than masonry fragilities from elsewhere in the world, would that relative difference make sense given what is known about Groningen construction methods?

Opportunities for future refinement

The insights established by the Version 5 models provide a foundation for even further exploration of risks and potential mitigation actions in Groningen. In this section we offer thoughts on potential opportunities for extension of the work scope, which may be useful if the project undertakes further stages of study.

Reduce conservatism

It appears that the project effort has appropriately aimed to characterize expected performance of the buildings, rather than taking a conservative view as is the case with building code analysis. There are, however, potentially a few subtle sources of conservatism remaining (i.e., sources that might result in overestimation of Local Personal Risk), which might be refined in future efforts:

- The large numbers of cycles of loading during testing and analysis may be producing conservatism in damage predictions relative to behavior under the very short duration shaking anticipated in Groningen. To some extent this may indirectly account for impacts of cumulative damage or pre-existing damage to buildings, but nonetheless some further evaluation of this issue may yield further insights.
- It has been assumed that the experimental buildings are near collapse at termination of the tests, but they may possibly have substantial remaining capacity.
- The ground motions used for analysis may be stronger in the demands they produce than actual ground motions that could be observed in Groningen. This is addressed to some extent by the use of vector ground motion intensity measures. But now that more is known about the ground motions contributing to risk, some follow-up study using hazard-consistent ground motions would offer the opportunity to better understand this issue.
- Take advantage of any further shake table tests as an opportunity for assessing the fidelity of the models and the currently employed fragility functions. Perform blind predictions (e.g., before and after knowing the material properties), perhaps sending the results to an independent third party before the test, and assess the fidelity of the models with an eye for improving the uncertainty bounds employed in the relevant fragilities.

Further refine structural modeling

As noted above, the structural modeling effort is in general extremely strong given the scope of study. Nonetheless, there are opportunities to further explore the impact of modeling assumptions on calculated risks. A few opportunities identified by the Panel include:

- Split building typologies and corresponding fragilities for critical cases (e.g., separate one- and two-story unreinforced masonry buildings, or separate older and newer variants of broadly defined typologies).
- Consider the impacts of including foundation flexibility in MDOF models, with an eye to differential settlement.
- Introduce a refined representation of soil-structure interaction in the SDOF model. Frequency dependence of stiffness and damping can be described for the purpose of time-domain analysis through a lumped-parameter model (LPM). Even with a relatively simple LPM the frequency-dependent coupled rocking-sway dynamic impedance can be described in the frequency range of interest. Care should then be taken to the way foundation input motion is applied, while incorporating the effective SDOF model height could be considered to better understand any issues of overturning moment coupled with foundation rotation.

- Consider the role of non-structural elements on structural response and life safety - in particular, internal masonry partitions.
- Consider developing simplified MDOF models as an alternative to SDOF models. Simplified structural models are capable of predicting various failure modes that can cause fatalities, but they are not as computationally demanding as refined Finite Element Models.

Study sensitivities in fatality models

There is an opportunity to better understand the implications of the fatality model, with respect to assumptions associated with that model. Parameters that could be explored include:

- Percent of time that occupants spend inside versus outside of the building;
- Percent volume loss associated with building collapse modes;
- Considered radius around the exterior of buildings;
- Combined impacts of exterior debris from adjacent buildings.

Extend project scope

Finally, there are topics that are not the current focus of the NAM modeling effort, but that could be well addressed by the models that NAM has developed. We recommend that these topics would benefit from study by the project team.

- Develop fragility functions and fatality models for retrofitted buildings, to evaluate benefits and necessary levels of retrofits for risk reduction. There seem to be some planned experiments with strengthening works, thus their outcomes could be useful for this purpose.
- Assess index buildings according to NPR. Parallel analyses using NPR and the NAM fragility functions, especially of the experimentally tested buildings, will help reconcile any differences in assessment results and support informed decision-making in cases where the two approaches result in different outcomes.
- The developed models could be utilized to quantify aggregate risk measures (i.e., group risk) rather than individual Local Personal Risk. This scope extension would require further refinements to address issues such as correlation of damage states of buildings, and spatial correlation of ground motions.
- Explore the potential impacts of cumulative damage or pre-existing damage to buildings mentioned above.

NAM

Introduction
Assurance Workshop on Building Response, Fragility and Consequence Model

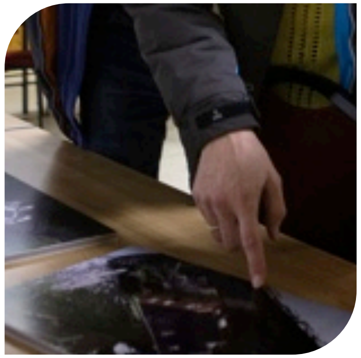

BRON VAN ONZE ENERGIE

Groningen Gasfield

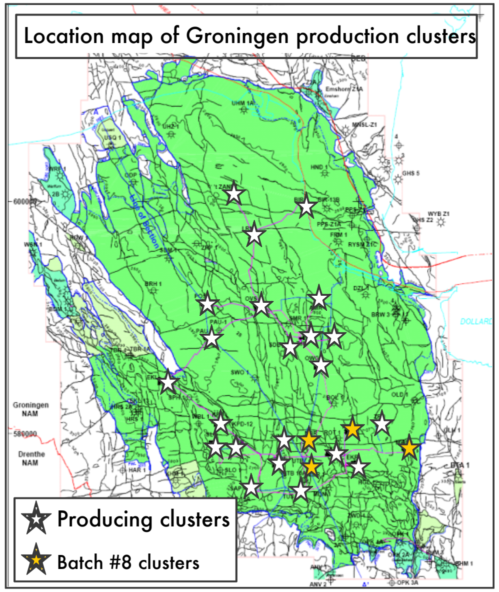

- The Groningen gas field is the 7th largest gasfield in the world, based on initial reserves. Some 70% of the gas has already been produced, but based on current reserves, it is still 13th in the world ranking,
- The field was discovered in 1959 and taken into production in 1963,
- The field is located in rural the north-eastern part of the country (Groningen province), close to the city of Groningen,
- The gas contains 14% nitrogen and has a lower calorific content than gas from other fields,
- The field is operated by NAM (a joint venture of Shell and Exxonmobil),
- Some 93% of the gross revenue is paid in taxes to the Dutch state. If the tax income had been put into a bank account, it would now contain some 1 trillion Euro.

Huizinge Earthquake on 16th Augustus 2012

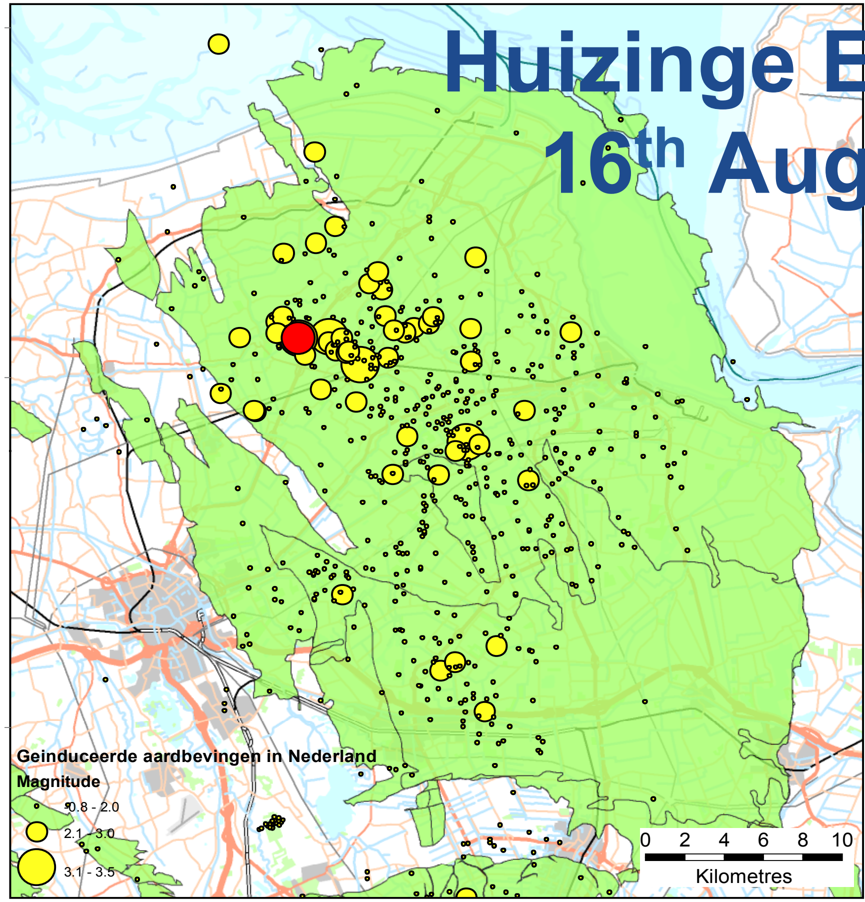

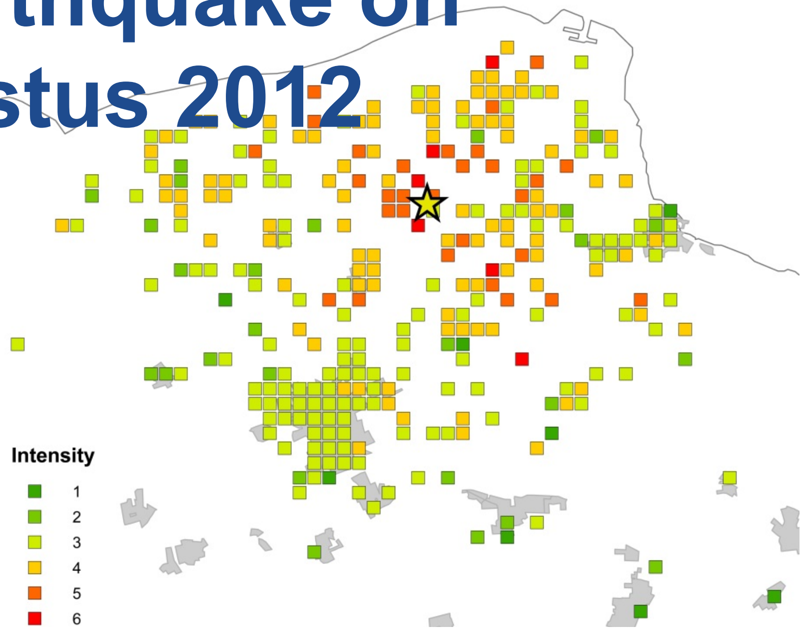

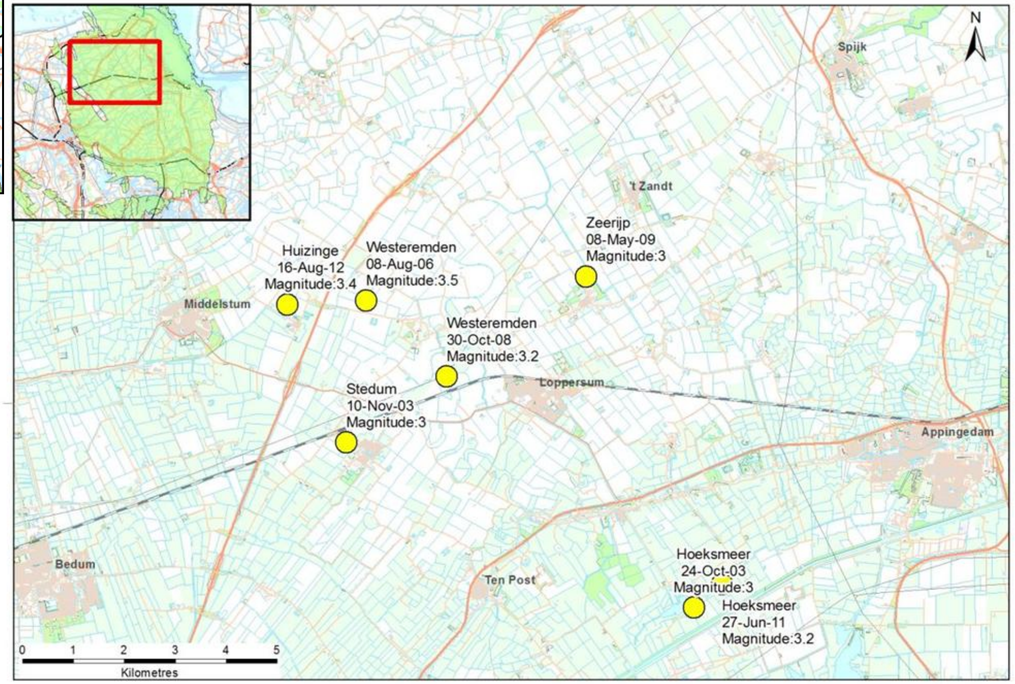

Societal Events

Political debates in House of Commons

Many Court Cases; Reimbursement Declining House Prices, Immaterial Damage, etc.

Protests

Criminal Case against NAM

National Coordinator Groningen (NCG)

Raad van State review of Ministerial Decision

NAM

NAM

Assurance Meeting on Exposure, Fragility and Fatality Models for the Groningen Building Stock

21 - 22 February 2018, Schiphol Airport, Amsterdam

BRON VAN ONZE ENERGIE

Earthquake studies cover 7 themes

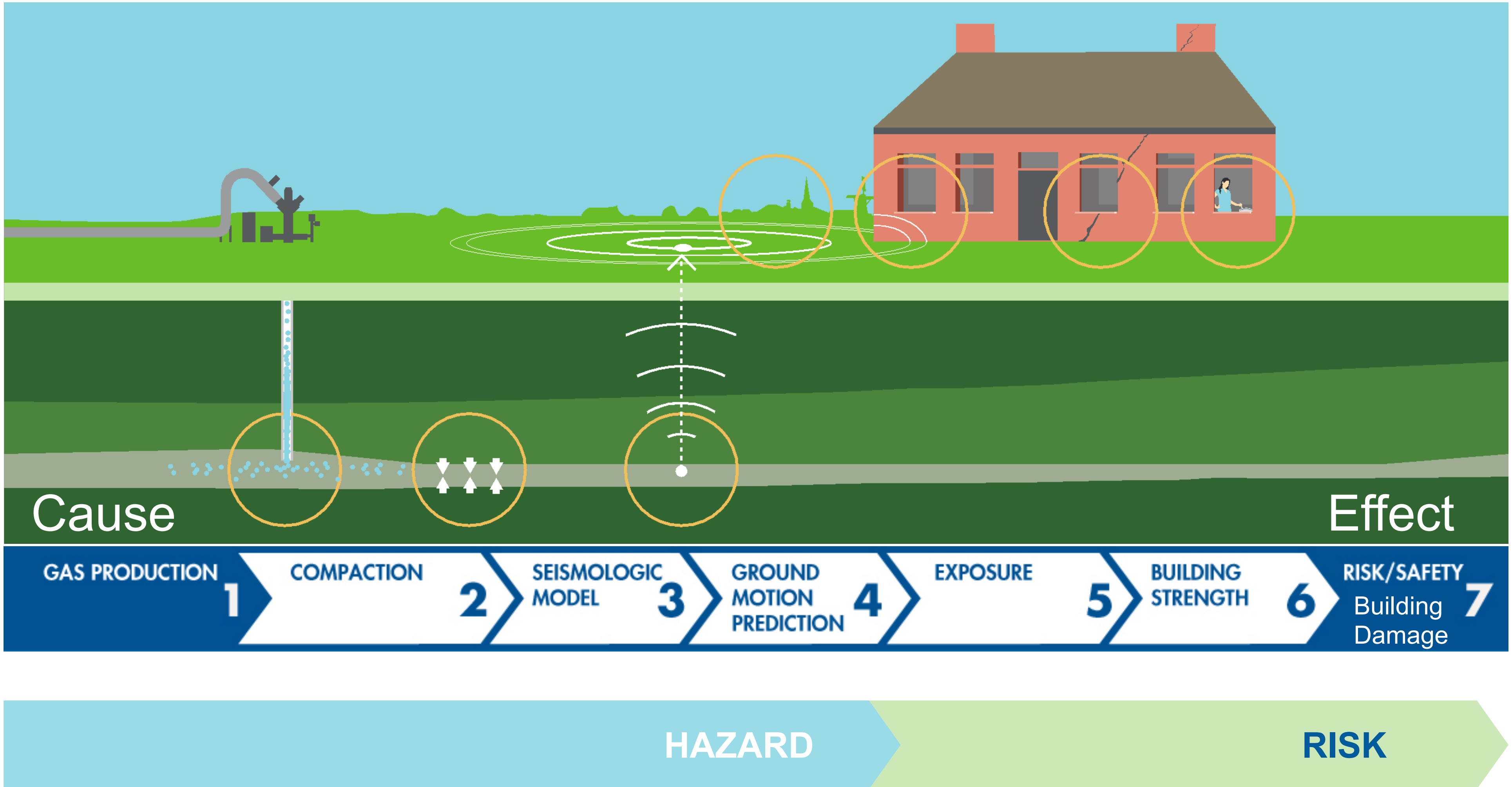

Introduction
Hazard and Risk Assessment

- The hazard- and risk assessment spans from cause (gas production) to effect (accidents, harm and building damage).
- The uncertainties in each step of the assessment are identified, estimated and consistently incorporated in the assessment.
- A traditional Probabilistic Seismic Hazard and Risk Framework is used (based on Cornell, 1968).
- Implementation is based on Monte Carlo Method (C- and Python Code)
- NAM has sought the assistance and advice of external experts from academia and knowledge institutes for each expertise area. Rigorous assurance processes are in place.
- Key is the collection of data in Groningen to prepare a hazard and risk assessment specific to the Groningen situation.

Study and Data Acquisition Plan

COOPERATION AND ASSURANCE

Staatstoezicht op de Mijnen
Ministerie van Economische Zaken

MOSAYK
Modelling and Structural Analysis Konsulting

ROSSINGH DRILLING
Drilling, Supply & Handling

Schlumberger

Magnitude
A Baker Hughes Company

TNO

Deltares

ARUP

Deltares
Enabling Delta Life

ASL
Avalon Sciences Ltd

TU Delft

BAKER HUGHES

Universiteit Utrecht

EUCENTRE
European Centre for Training and Research in Earthquake Engineering

Koninklijk Nederlands Meteorologisch Instituut
Ministerie van Infrastructuur en Milieu

rijksuniversiteit groningen

中国地震局
China Earthquake Administration

anteagroup

Assurance and Supervision of Studies:

1. Voluntary: by independent international experts and publication in scientific journals
2. Government: Scientific Advisory Committee, SodM, KNMI en Tcbb
3. Public Review: Sharing reports on www.NAM.nl

Field Measurements and Monitoring

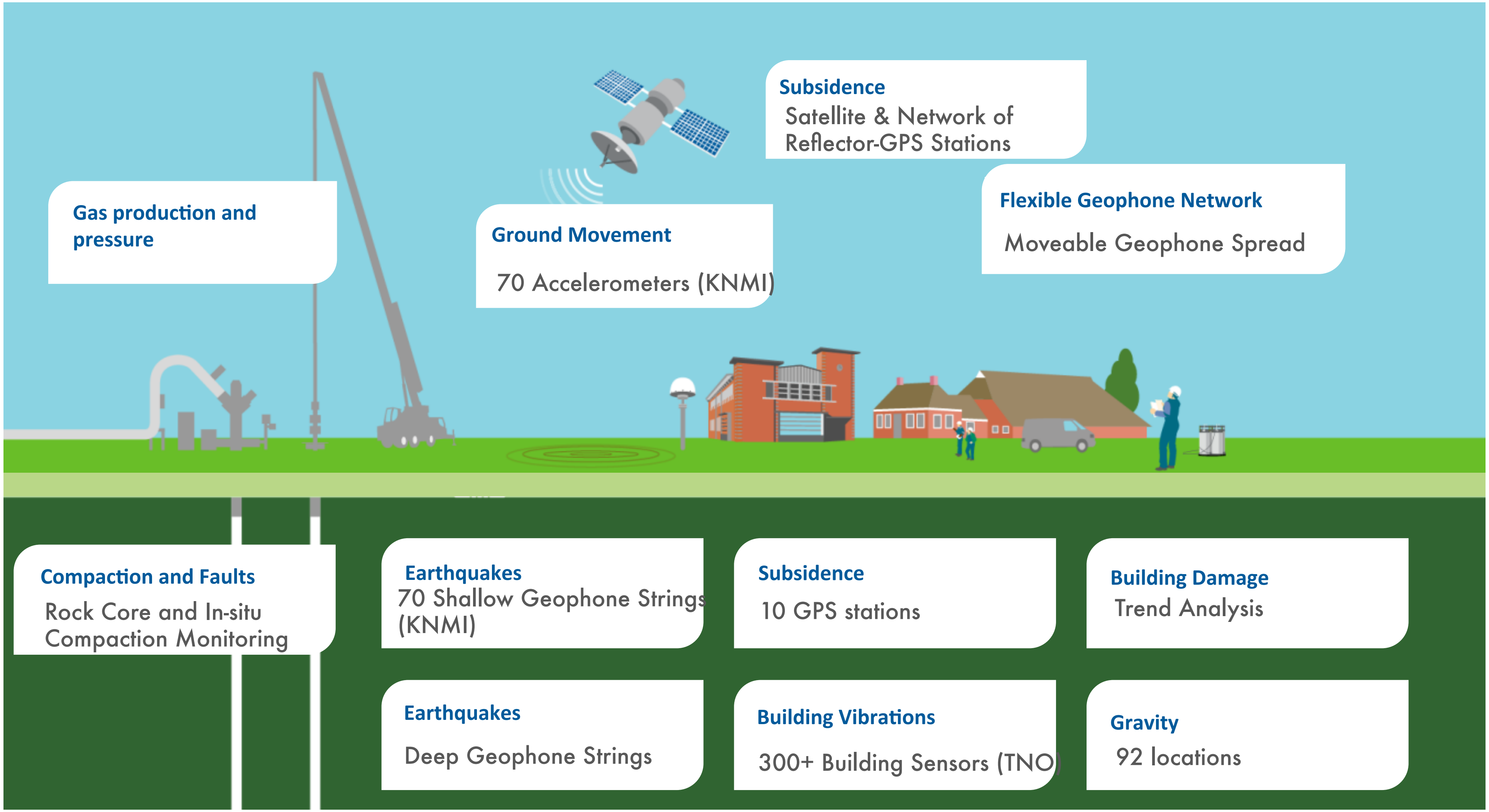

Principles of the "buildings component" of the NAM research programme

- Construction practice in Groningen region is distinct from what is found in areas of the world with a long history of damaging earthquakes.
- Therefore, building classification and fragility/fatality models developed for other regions could not be employed in the seismic risk analyses for Groningen.
- NAM decided to deploy an extensive programme of building data collection, structural testing and numerical modelling validation/ calibration, that could then feed the development of the exposure, fragility and fatality models.
- In this Assurance Workshop, we are aiming at a review of this entire effort, from building data gathering to the development of the models

Risk Norm for Earthquakes in The Netherlands

Eindadvies

Handelingsperspectief voor Groningen

Adviescommissie 'Omgaan met risico's van geïnduceerde aardbevingen'
(Commissie-Meijdam)

14 december 2015

- Living and working in Groningen must be as safe as elsewhere in the Netherlands and in Groningen the same safety standards must apply as elsewhere in the Netherlands.
- The committee adheres to the generally accepted safety standards for all kinds of risks in The Netherlands:
  - for existing construction to temporarily accept a mean individual local personal risk (chance of death) that residents run of 1 in 10,000 years (10^{-4}) and
  - for new construction to accept a mean individual local personal risk (chance of death) that residents run of 1 in 100,000 years (10^{-5}).

Introduction Assurance Panel

External Expert	Affiliation
Jack Baker (Chair)	Stanford University, USA
Matjaz Dolsek	University of Ljubljana, Slovenia
Paolo Franchin	University of Rome “La Sapienza”, Italy
Ron Hamburger	Simpson Gumpertz and Heger, USA
Ihsan Engin Bal	Hanze Hoogeschool, Groningen
Marco Schotanus	RUTHERFORD + CHEKENE, USA
Nico Luco	United States Geological Survey, USA
Dimitrios Vamvatsikos	NTUA, Greece

Agenda – Morning Day 1

Start	End	Topic	Speaker
09:00	09:30	Welcome and Introduction	Ruud Cino & Thijs Jurgens
09:30	10:30	Overview of NAM's Hazard and Risk Assessment programme Objectives and Meeting format	Jan van Elk
10:30	11:00	Coffee break	
11:00	11:20	Seismological model	Steve Oates
11:20	11:40	Ground Motion model	Julian Bommer
11:40	12:00	Hazard modelling and results + Risk Engine	Steve Oates
12:00	13:00	Groningen Building Stock and Exposure Database	Rinke Kluwer
13:00	14:00	Lunch	

Agenda – Afternoon Day 1

Start	End	Topic	Speaker
13:00	14:00	Lunch	
14:00	14:30	Experimental testing programme for URM materials characterisation at TU Delft	Jan Rots
14:30	15:30	Experimental testing programme for URM components and structures at Eucentre and LNEC	Guido Magenes & Francesco Graziotti
15:30	16:00	Coffee break	
16:00	16:30	Experimental testing programme for RC structures at Eucentre	Rui Pinho
16:30	17:00	Verification and calibration of numerical models using test data	Rui Pinho
17:00	18:00	Discussion	All

Agenda – Day 2

Start	End	Topic	Speaker
09:00	09:30	Summary of first impressions/feedback from Review Panel	Jack Baker
09:30	10:15	Numerical modelling of Groningen buildings using Finite Element Analysis (with LS-Dyna software)	Richard Sturt
10:15	11:00	Numerical modelling of Groningen buildings using the Applied Element Method (with ELS software)	Andrea Penna
11:00	11:30	Coffee break	
11:30	13:00	Exposure, Fragility and Consequence models	Helen Crowley
13:00	14:00	Lunch	
14:00	14:30	Overview of risk results	Steve Oates
14:30	15:00	Discussion	All
15:00	15:30	Coffee break	
15:30	16:30	Final discussions	All
16:30	17:00	Closure	Rui Pinho & Jan van Elk

Objectives

To assure the following elements of the Groningen Risk Assessment:

1. The building typologies classification and the process used to combine inspection data and inference rules in the development of the Exposure Model
2. The experimental and numerical modelling programmes used in the development of the Fragility Model, and the underlying methodology behind the latter
3. The use of numerical and empirical data for the development of the Fatality Model
4. The implementation of the above models, and associated uncertainty, in the risk engine

The assurance scope will focus on fatality risk estimation, rather than non-life threatening structural and non-structural damage.

Confidentiality

- No Confidentiality Arrangement in Place for the Assurance Workshop.

- Request for Chatham House Rule:

  When a meeting, or part thereof, is held under the Chatham House Rule, participants are free to use the information received, but neither the identity nor the affiliation of the speaker(s), nor that of any other participant, may be revealed.

https://www.chathamhouse.org/about/chatham-house-rule

Transparency

- All reports (130) are published at the "onderzoeksrapporten" page of www.nam.nl. Together more than 90,000 downloads.
- More than 40 papers have been published in respected peer-reviewed journals (SCImago Journal Ranking).
- All raw data is freely available for research.
- Rigorous Assurance processes are in place.
- Latest update:
  - Hazard, Building Damage and Risk Assessment – November 2017 (currently 650 downloads).

NAM

Summary of the Groningen seismological model Probabilistic seismicity forecasts based on a model of extreme threshold failures within a heterogeneous poro-elastic thin-sheet

Stephen Bourne, Steve Oates
Projects & Technology, Shell Global Solutions International

Assurance meeting for Exposure, Fragility and Fatality Models for the Groningen building stock
World Trade Center, Schiphol, 21st February, 2018

Outline

- Model design
  - Coulomb stresses induced by poro-elastic thin sheet deformations
  - Activity rates as Extreme Threshold Failures
  - Magnitude distributions as Extreme Threshold Failures
  - Aftershocks as Epidemic Type Aftershock Sequences
- Model inference
- Model performance
- Summary

Model of seismicity induced by poro-elastic reservoir deformations

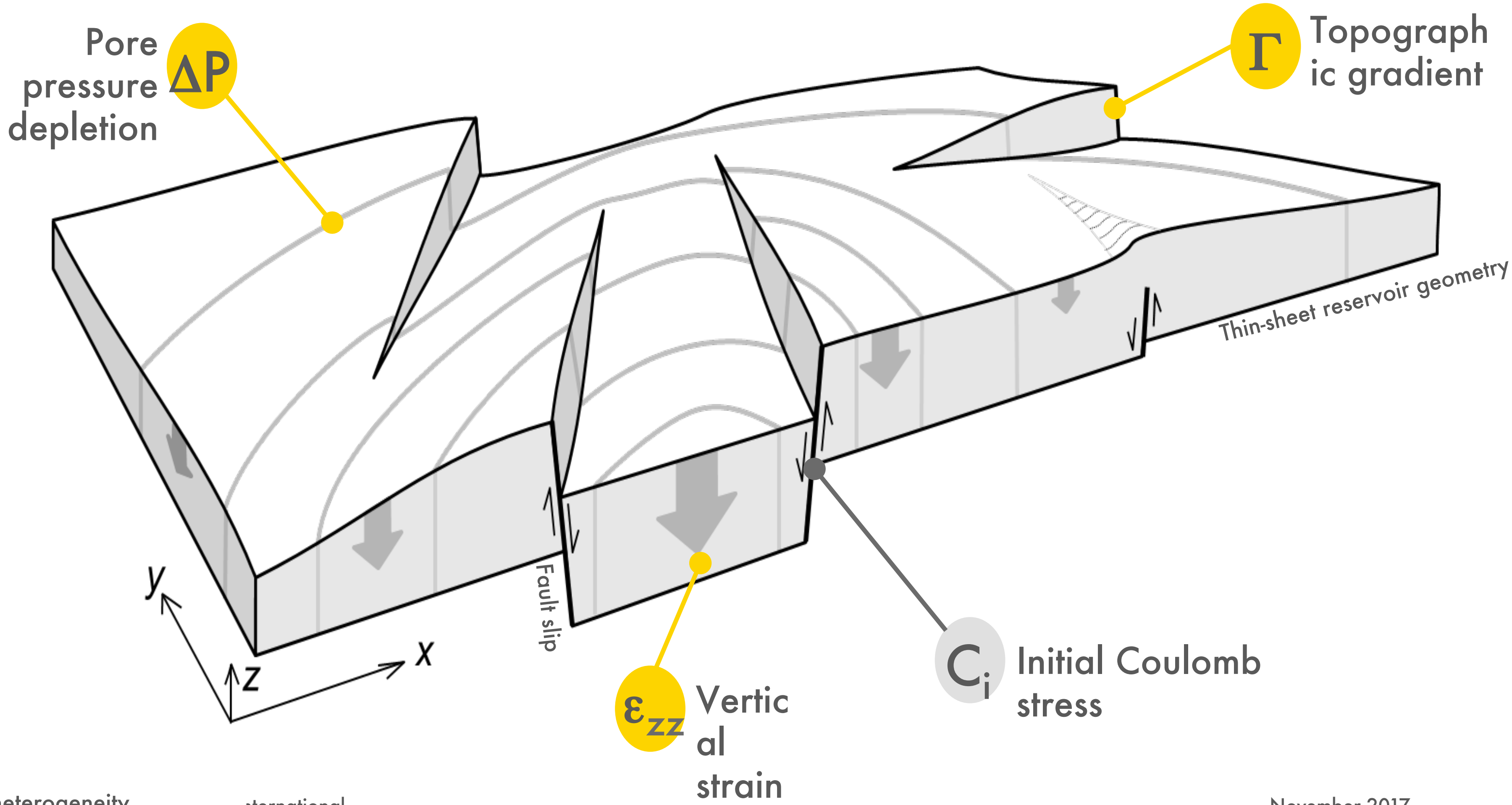

Resolved heterogeneity
Unresolved heterogeneity

Seismological model as a network of physical processes

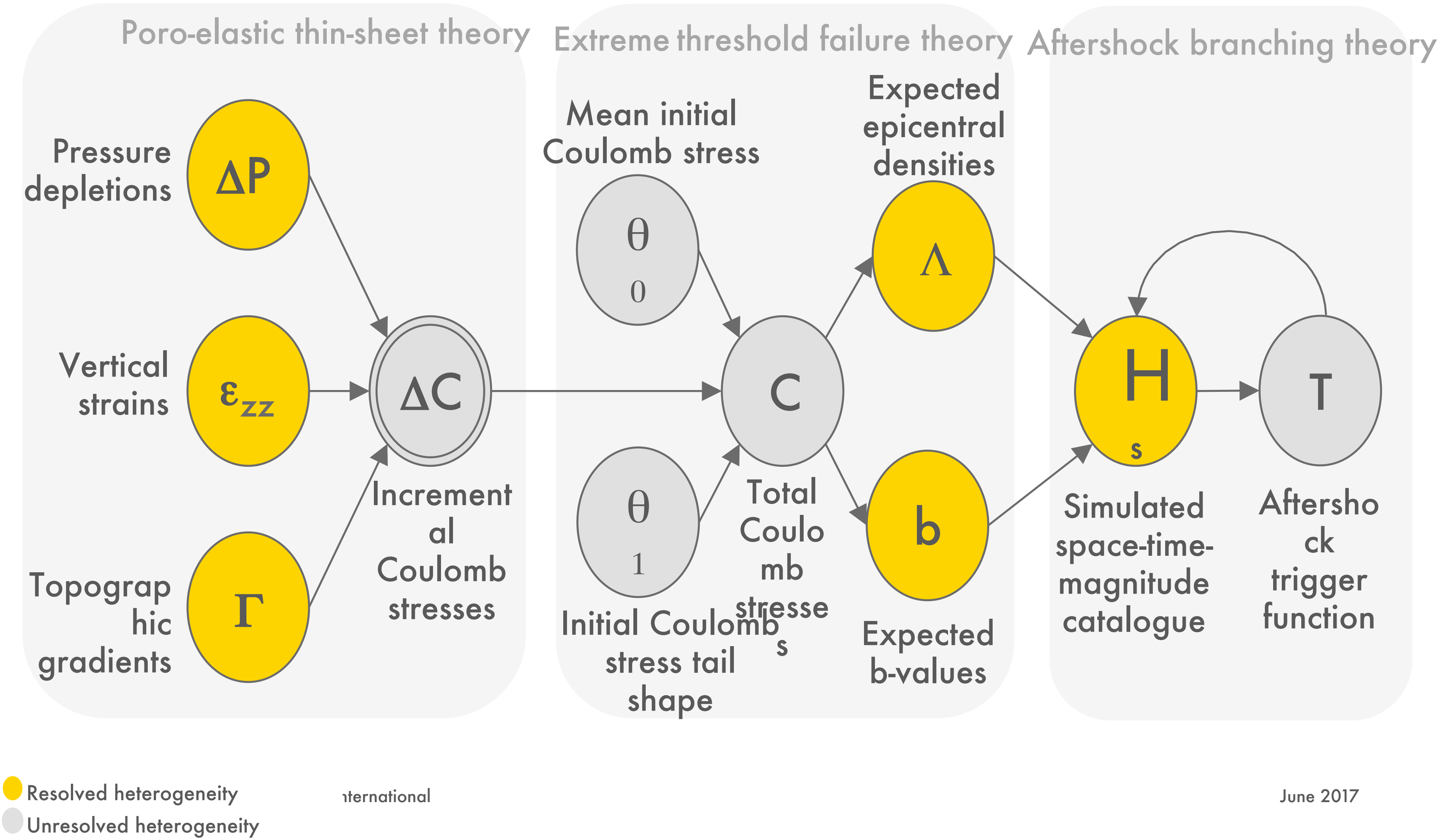

Incremental Coulomb stress model
Event rates and mean magnitude appear to increase with incremental Coulomb stress

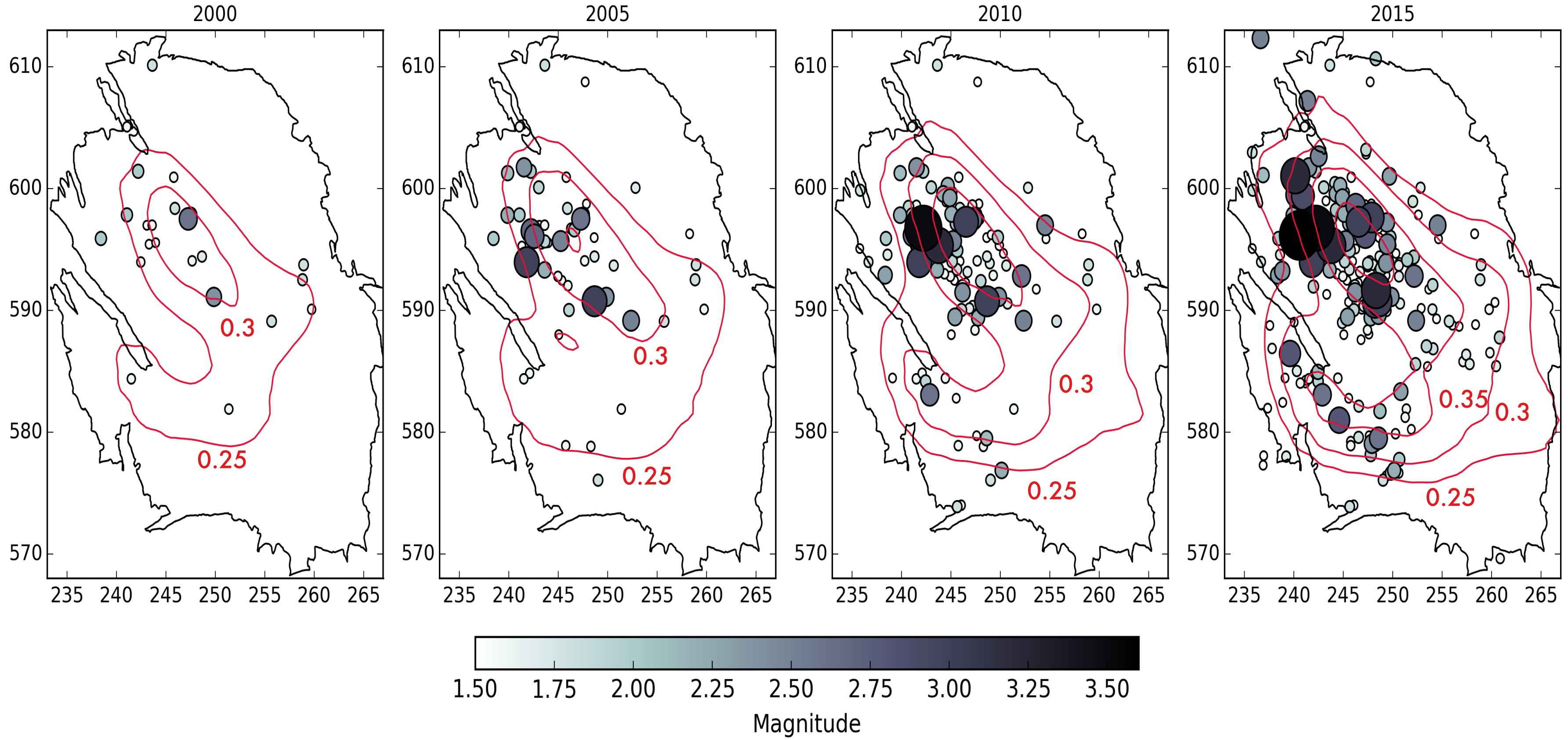

- Incremental Coulomb stress contours: 0.25, 0.30, 0.35, 0.40 MPa

Incremental Coulomb stress model
Event rates and mean magnitude appear to increase with incremental Coulomb stress

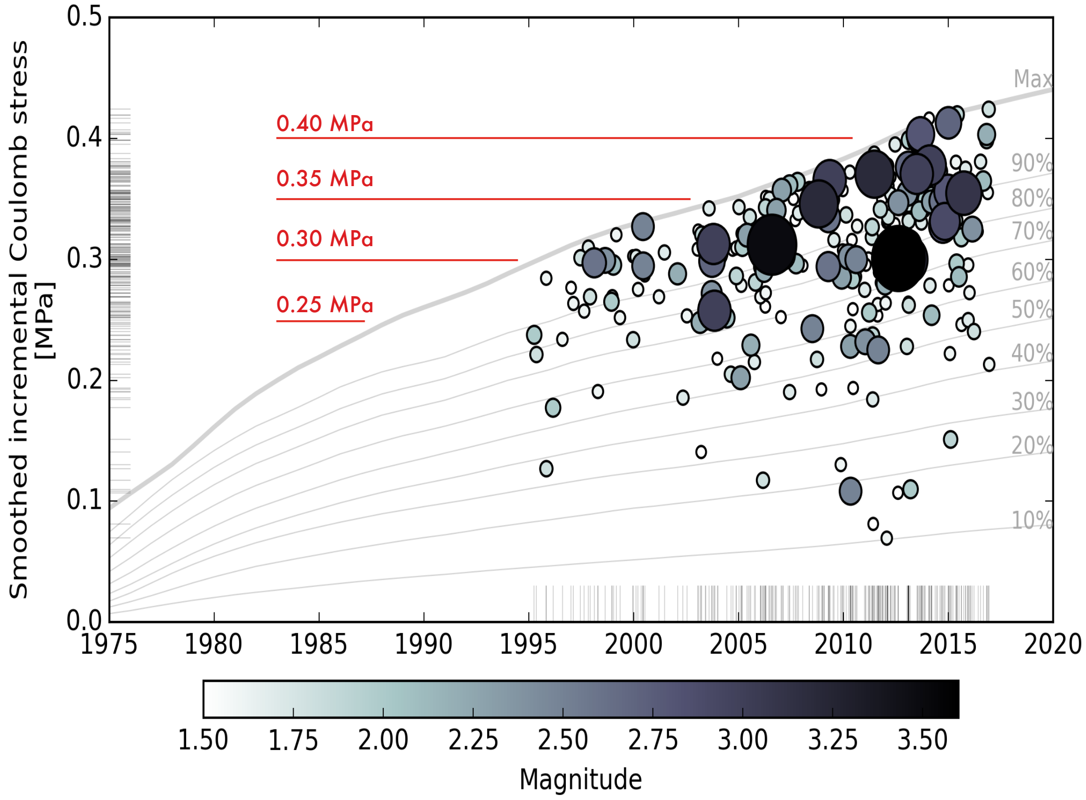

Extreme threshold theory for the probability of fault failure under a given incremental Coulomb stress load

- Initial Coulomb stresses
  - Independently and identically distributed
  - Due to unresolved frictional heterogeneities

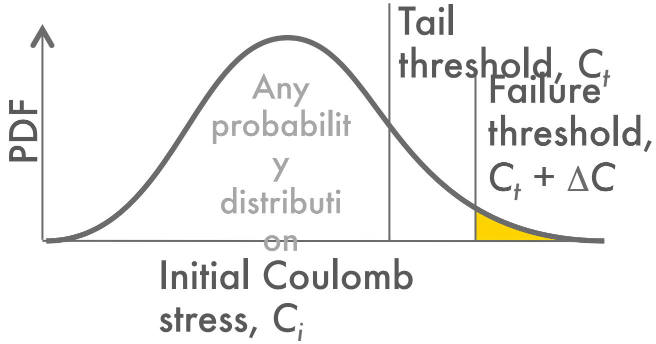

- Extreme Threshold Theory

$$Pr(C_i > -\Delta C | C_i > C_t) = \begin{cases} \left(1 - \frac{C_t + \Delta C}{\tilde{\sigma}}\right)^{-1/\zeta} & \text{if } \zeta \neq 0, \\ \exp\left(\frac{C_t + \Delta C}{\tilde{\sigma}}\right) & \text{if } \zeta = 0, \end{cases}$$

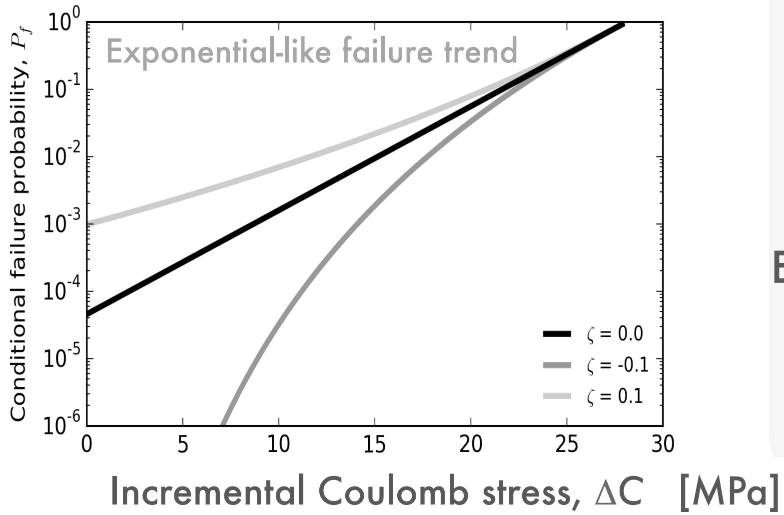

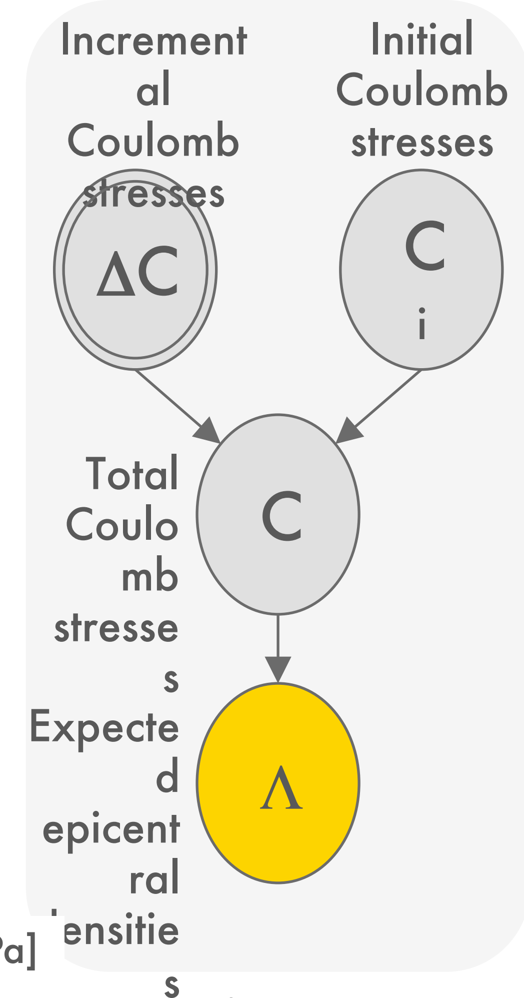

Resolved heterogeneity
Unresolved heterogeneity

Magnitude model

Inverse power-law evolution of *b*-values with smoothed incremental Coulomb stress

- Inverse power-law

$$b_i = b_{min} + \left(\Delta C_i - S_0 / S_1\right)^{-S_2}$$

- Bayesian inference with uniform priors

$$0.5 \le b_{min} \le 3.0 \quad 10^{-3} \le S_1 \le 10$$
$$-0.2 \le S_0 \le 0.2 \quad 0.1 \le S_2 \le 5$$

- Likelihood function

$$\beta_i = b_i \ln(10)$$
$$\ln p = \sum_i \left(\ln \beta_i - \beta_i \left(M_i - M_{min} + 1/2\, \Delta M\right)\right)$$

- Spline interpolation used to estimate ΔC_i

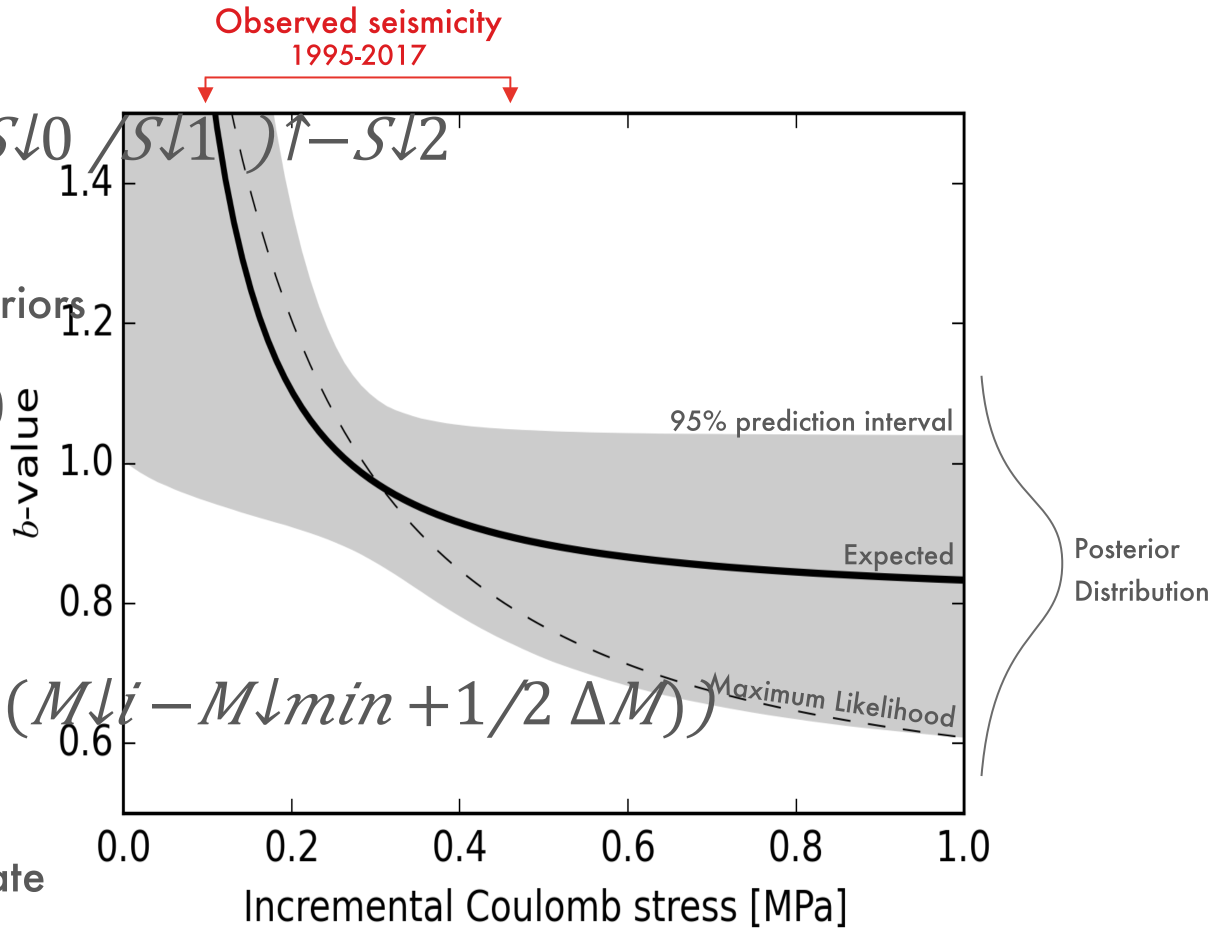

Model assumptions

- Reservoir deformations are elastic; plastic deformations are negligible.
- Fault reactivations are simple Coulomb frictional failures.
- Frictional fault failures remain limited to the tail of the initial stress distribution.
- The statistical character of the initial stress tail is invariant.
- Aftershocks are sufficiently described by the empirical ETAS model.
- Variations in *b*-value are an inverse power function of incremental Coulomb stress.

Magnitude model
Evolution of the expected *b*-value map with time

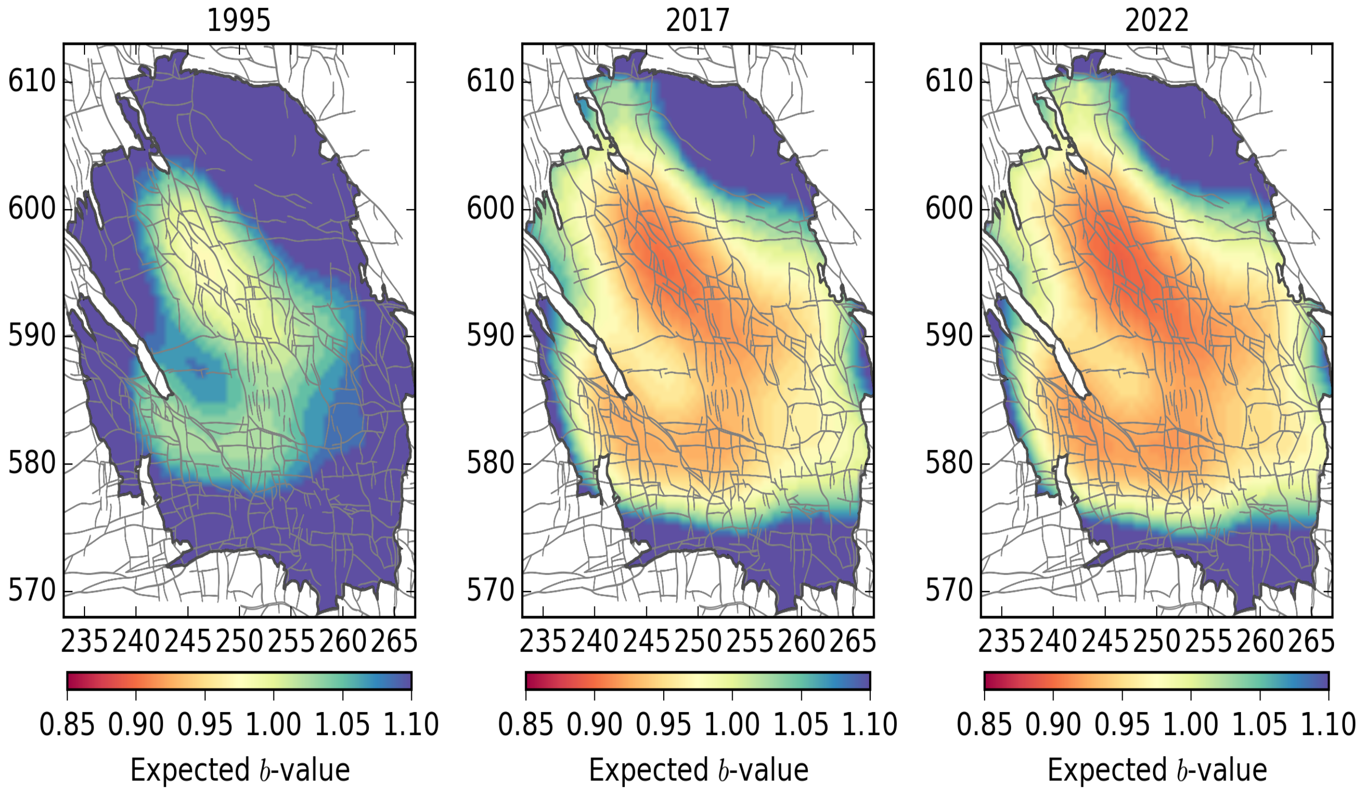

Magnitude model

Maximum magnitude distribution

- Panel of independent experts
- Proposed probability distribution
- Three-point equivalent re-samp

Source: Report by panel on Mmax for Groningen 25th April

Moment Magnitude	Weight
4	0.08625
4.5	0.4
5	0.24375
5.5	0.1125
6	0.07875
6.5	0.0525
7	0.02625

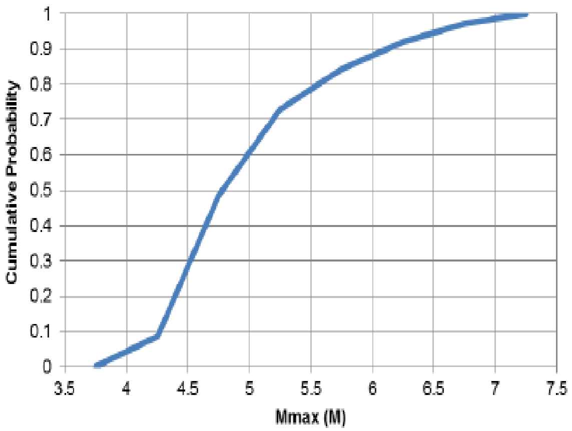

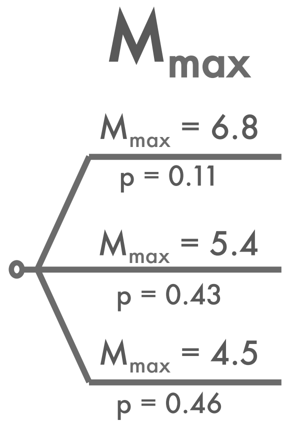

Model performance
Temporal density residuals

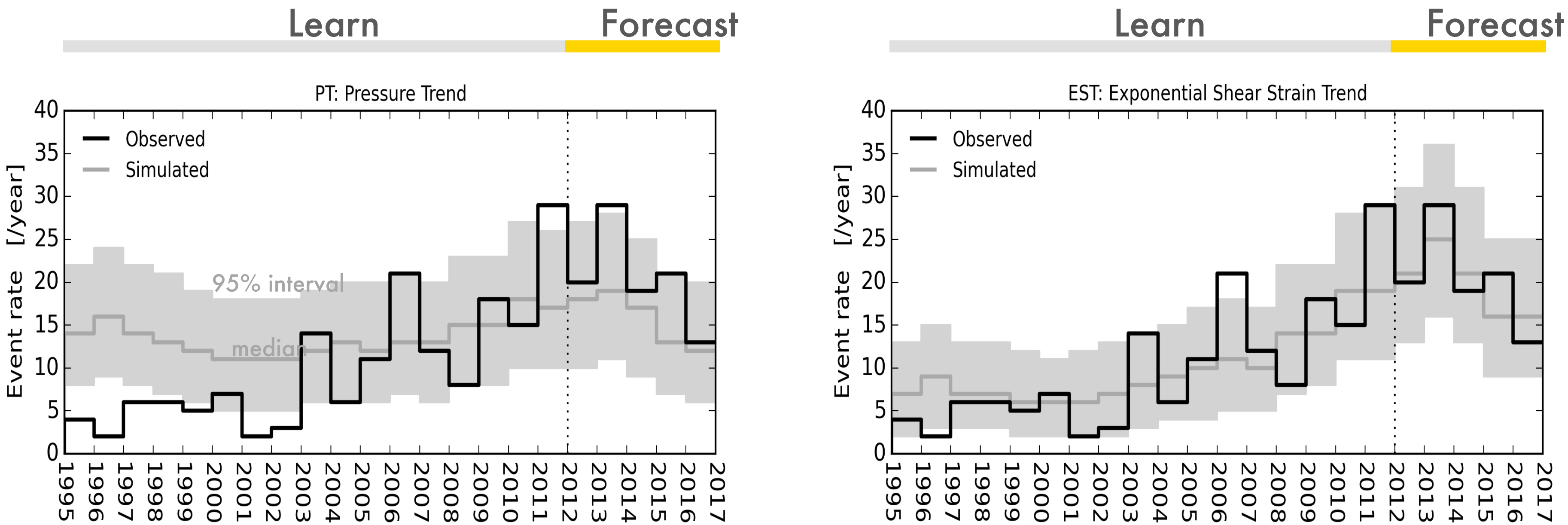

- Both models are based on Coulomb stress failure – but each represents a different type of reservoir heterogeneity
- PT: Pressure trend model includes depletion heterogeneity only
- EST: Exponential shear strain trend model includes depletion, geometric, elastic and frictional heterogeneities

Model performance
Spatial density residuals

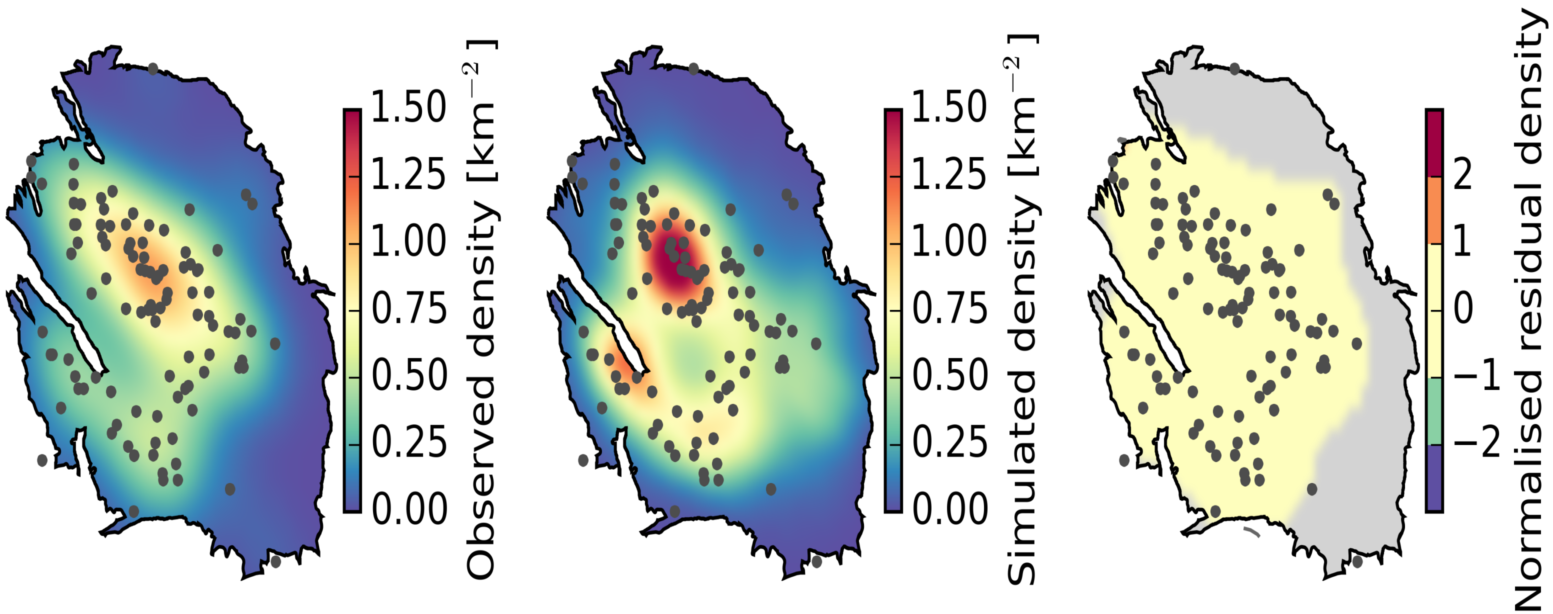

- Learning period: 1995 to 2012
- Forecast period: 2012 to 2017
- EST model forecasts spatial density consistent with observed spatial density within stochastic variability

Model performance
Magnitude distribution and aftershock clustering residuals

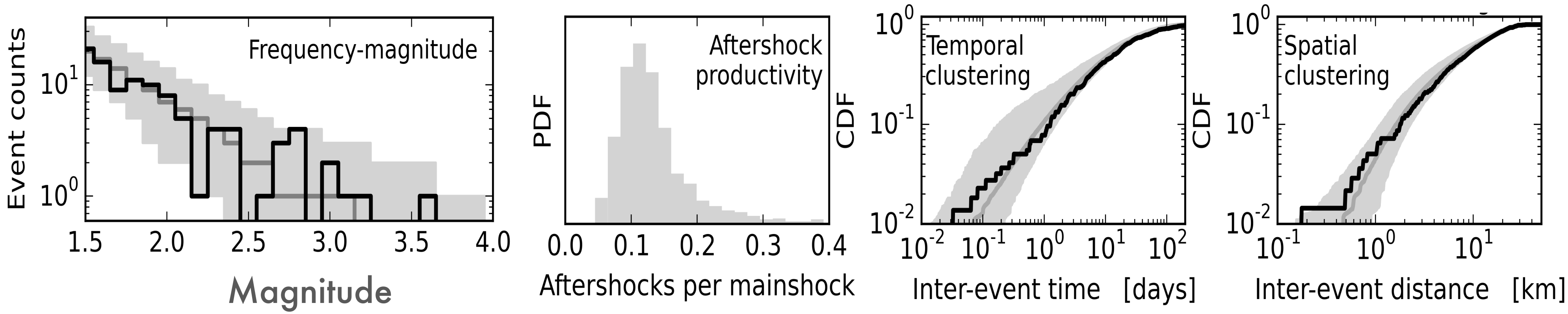

- Learning period: 1995 to 2012
- Forecast period: 2012 to 2017
- EST model forecasts magnitudes and aftershocks consistent with observed trends and variabilities

Model criticism
Prospective Testing

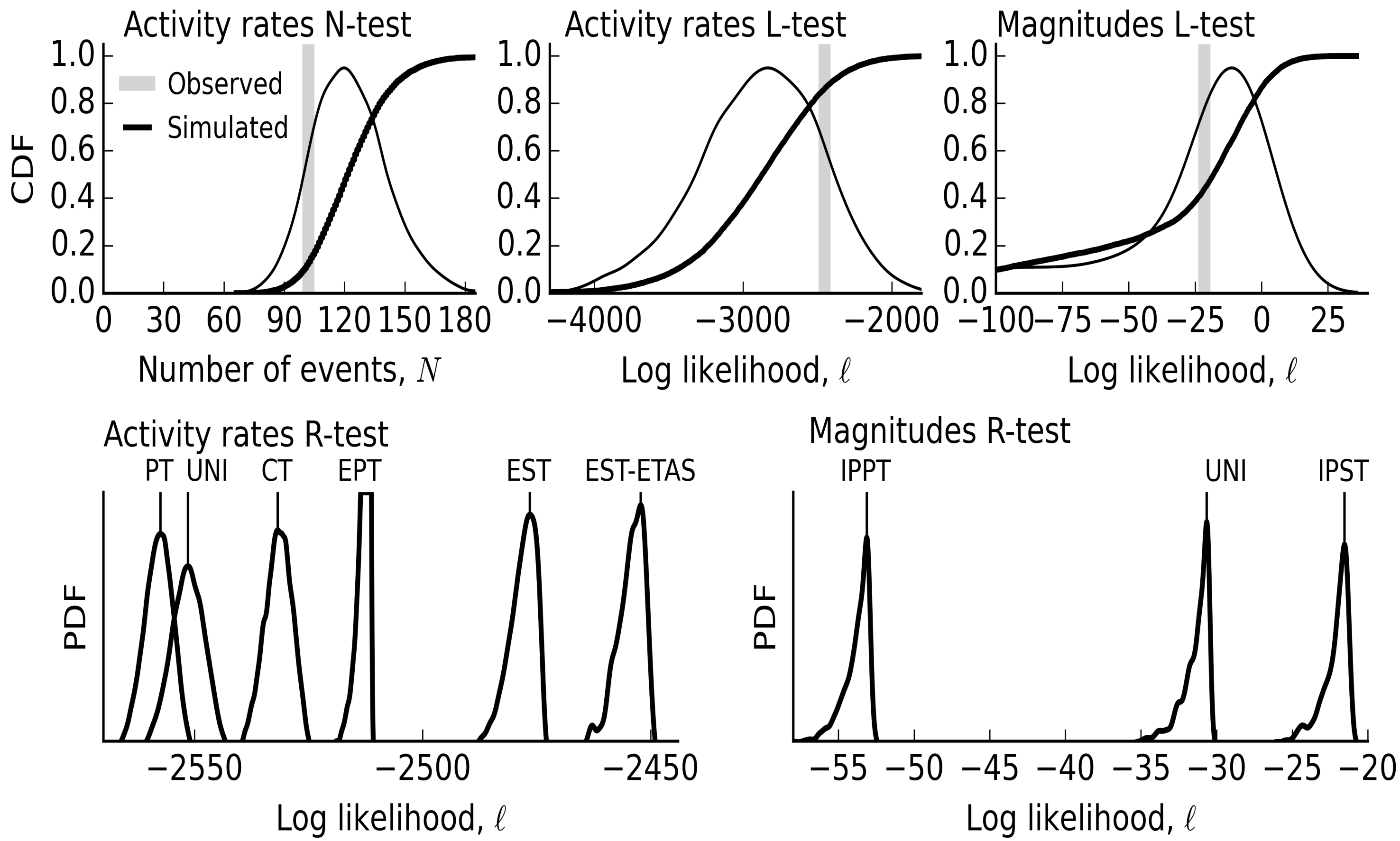

Summary

- Established a physics-based theory for the exponential shear strain activity rate model
- Pore-elastic thin-sheet theory
  - Computes smoothed incremental Coulomb stress according to resolvable geometric and elastic heterogeneities
- Extreme thresholds failure theory
  - Computes induced seismicity rates according to incremental Coulomb stress and the extremes of initial Coulomb stress
  - Computes the frequency-magnitude distribution and its dependence on incremental Coulomb stress
- Bayesian inference for hidden variables
  - Ensemble of realizations for each seismological model
  - Family of alternative seismological models represent different types of reservoir heterogeneity
- Model performance

Open access publication

JOURNAL OF GEOPHYSICAL RESEARCH
Solid Earth
AN AGU JOURNAL
JGR
Explore this journal >

Open Access

Research Article

Extreme threshold failures within a heterogeneous elastic thin-sheet and the spatial-temporal development of induced seismicity within the Groningen gas field†

S. J. Bourne, S. J. Oates

Accepted manuscript online: 7 November 2017 Full publication history

DOI: 10.1002/2017JB014356 View/save citation

Cited by (CrossRef): 0 articles Check for updates Citation tools ▾

†This article has been accepted for publication and undergone full peer review but has not been through the copyediting, typesetting, pagination and proofreading process, which may lead to differences between this version and the Version of Record. Please cite this article as doi: 10.1002/2017jb014356

Abstract

Measurements of the strains and earthquakes induced by fluid extraction from a subsurface reservoir reveal a transient, exponential-like increase in seismicity relative to the volume of fluids extracted. If the frictional strength of these re-activating faults is heterogeneously and randomly distributed, then progressive failures of the weakest fault patches account in a general manner for this initial exponential-like trend.

Allowing for the observable elastic and geometric heterogeneity of the reservoir, the spatio-temporal evolution of induced seismicity over 5 years is predictable without significant bias using a statistical-physics model of poro-elastic reservoir deformations inducing extreme threshold frictional failures of previously inactive faults. This model is used to forecast the temporal and spatial probability density of earthquakes within the Groningen natural gas reservoir, conditional on future gas production plans. Probabilistic seismic hazard and risk assessments based on these forecasts inform the current gas production policy and building strengthening plans.

The Groningen Ground-Motion Model for the Prediction of Spectral Accelerations, PGA, PGV and Duration

Julian J Bommer, Bernard Dost, Ben Edwards, Pauline P Kruiver, Michail Ntinalexis,
Adrian Rodriguez-Marek, Elmer Ruigrok, Jesper Spetzler & Peter J Stafford

Ground-Motion Recording Networks

G-stations
(borehole geophones & surface accelerographs)

B-stations
(surface accelerographs)

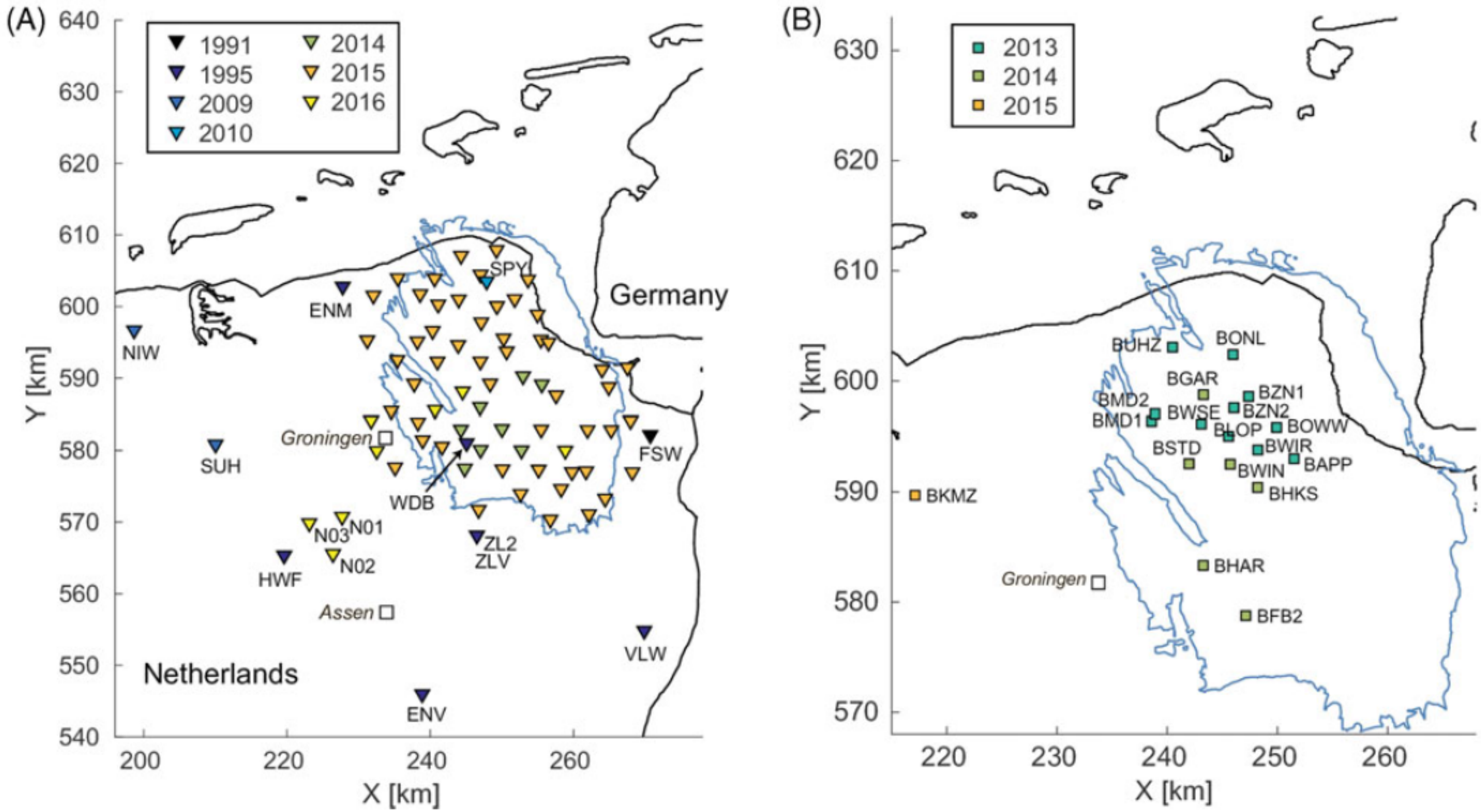

Dost *et al*. (2017

Ground-Motion Database ($M_L \geq 2.5$)

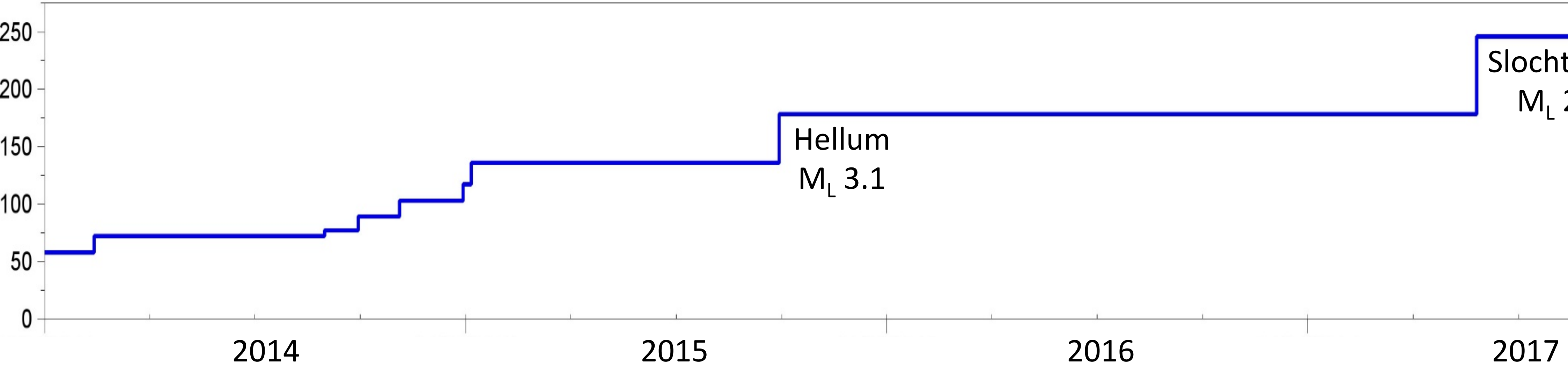

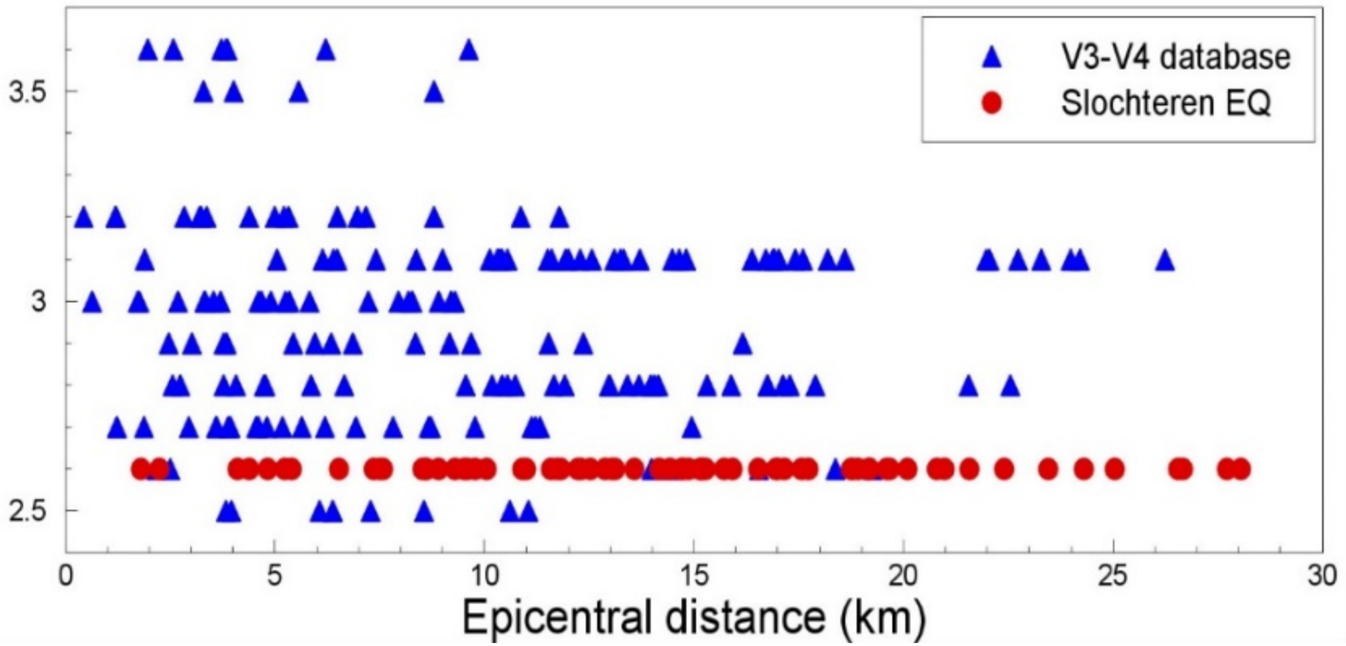

Database contains 246 records from
earthquakes with M_L from 2.5 to 3.
M_L equivalent, on average, to **M** in t
range (Dost *et al.*, 2018)

General Framework of Ground-Motion Model

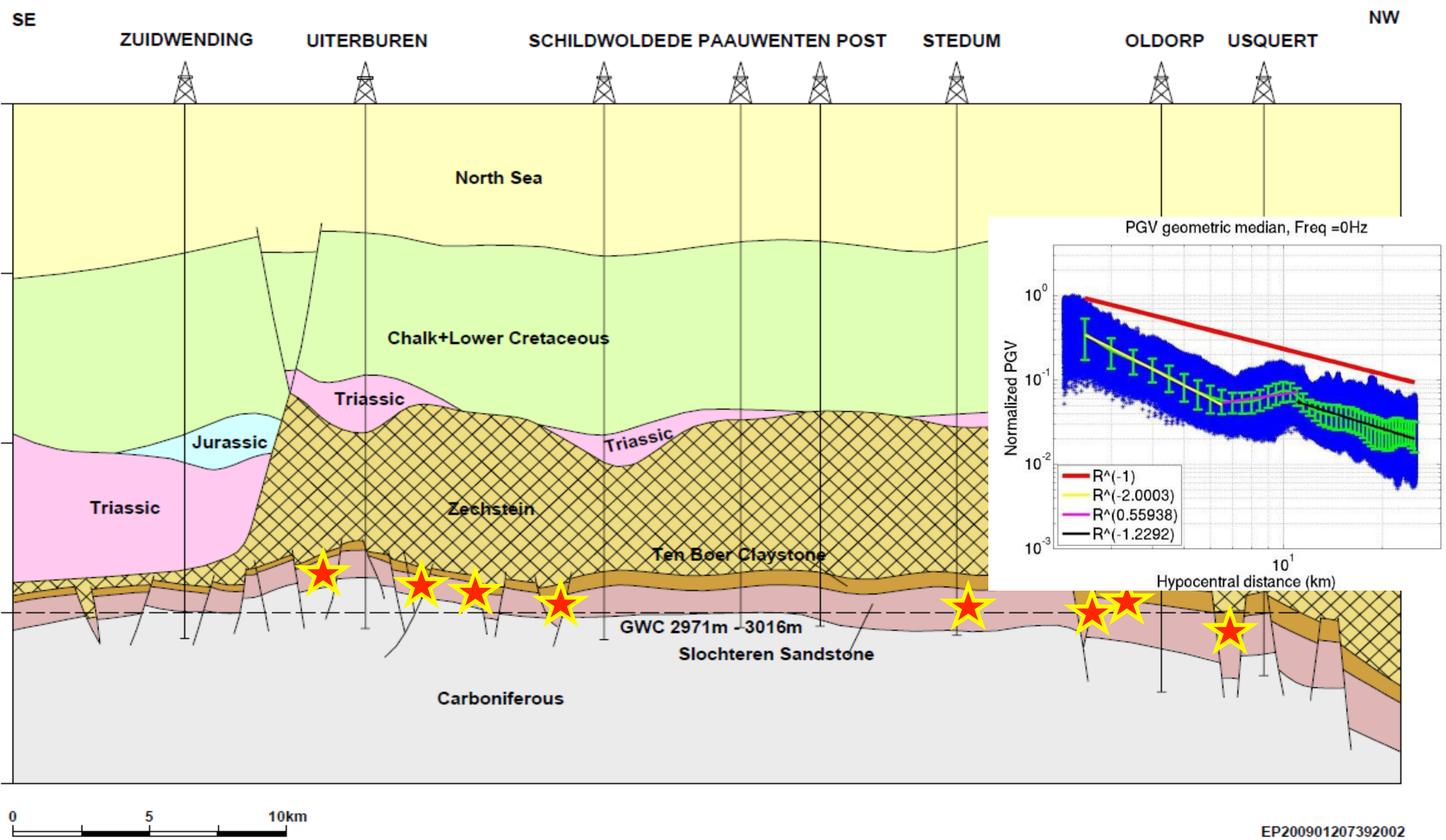

NS_B rock motions transferred t
surface via non-linear frequency
dependent amplification factors

Geometric spreading patterns—
including effects of high-velocit
Zechstein salt layer—informed b
full waveform simulations

Simulation-based GMPEs for
prediction of amplitudes at base
of the North Sea formation (NS_B)

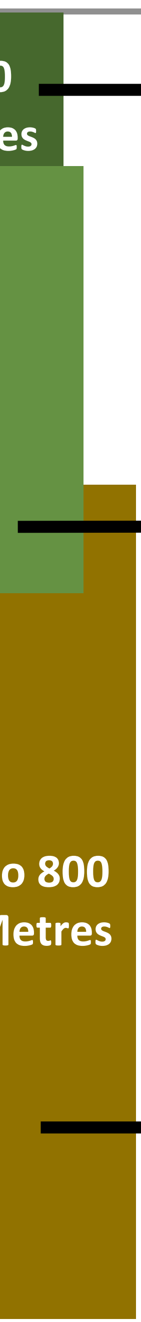

TNO GeoTop model and V_S values from CPT-based relations

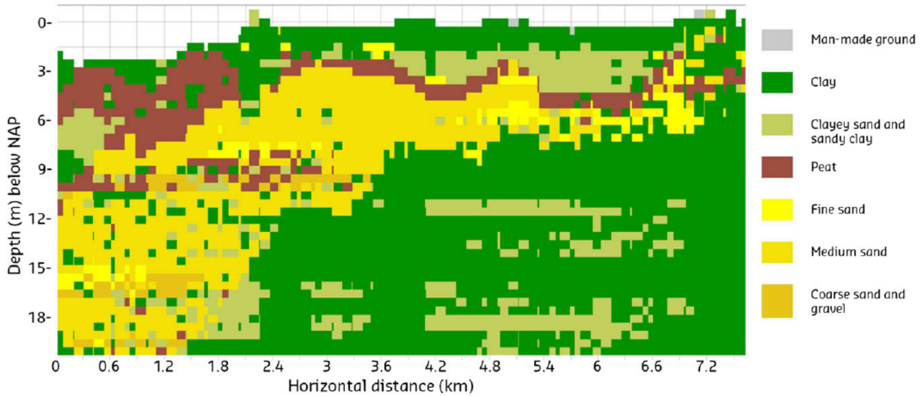

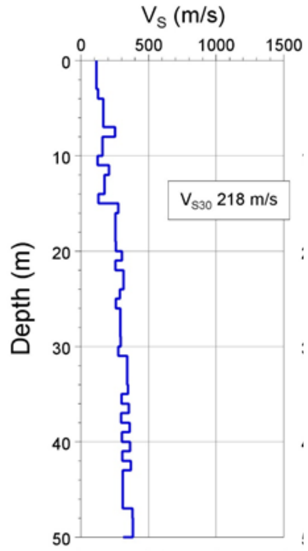

Inversion of surface-waves (ground roll) from legacy reservoir imaging

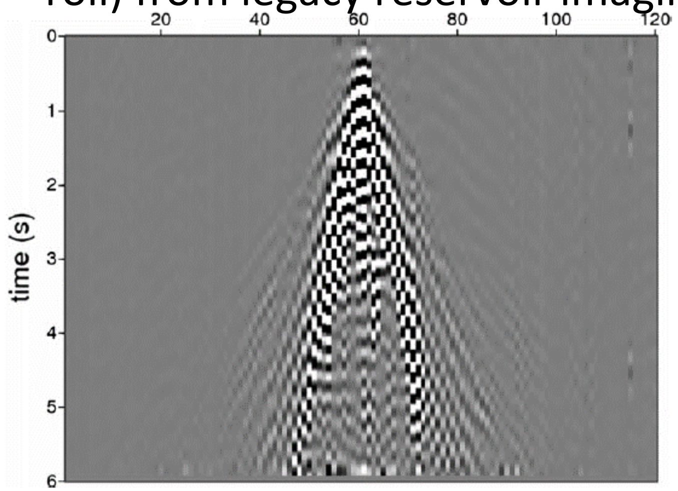

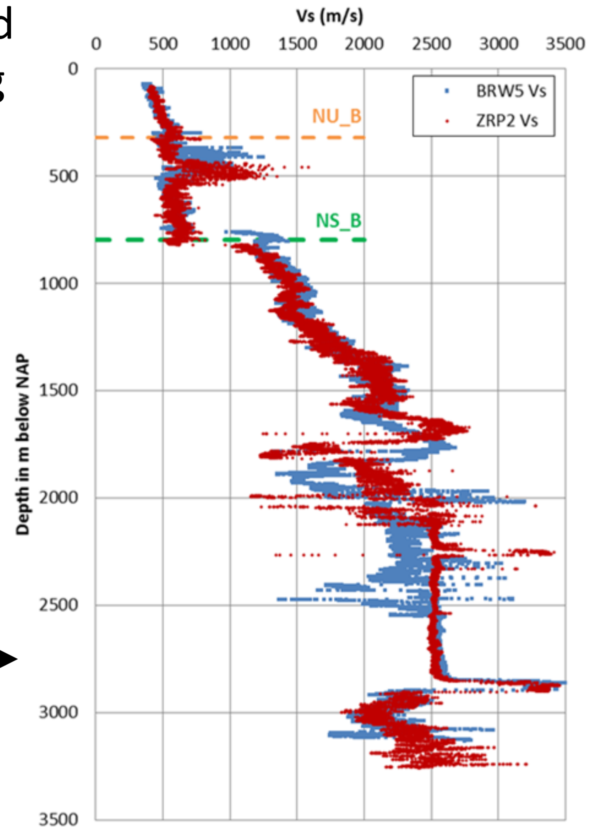

Deeper V_S profile from NAM sonic logs and V_P-V_S conversions

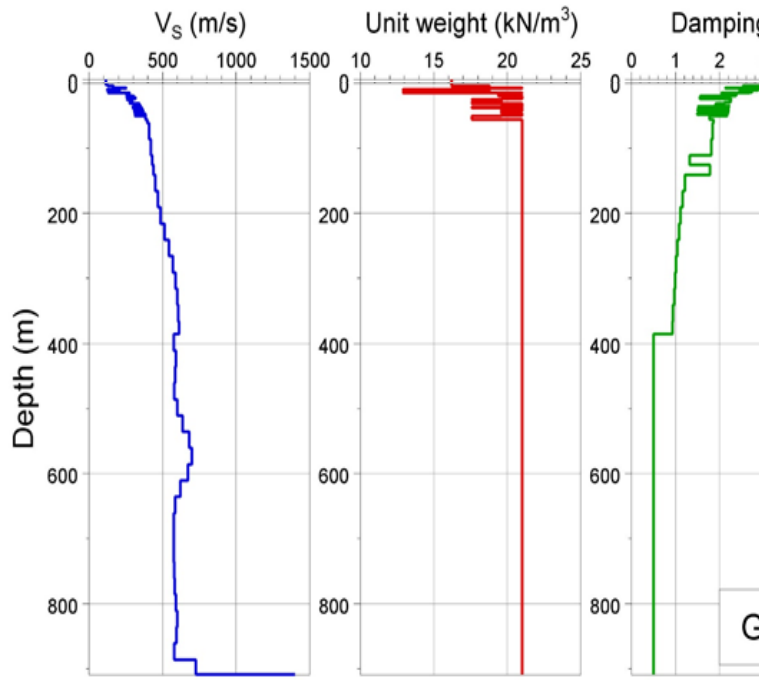

Kruiver *et al*. (2017

Shallow V_S profiles confirmed by in situ measurements (B-stations) and analysis of borehole recordings (G-stations)

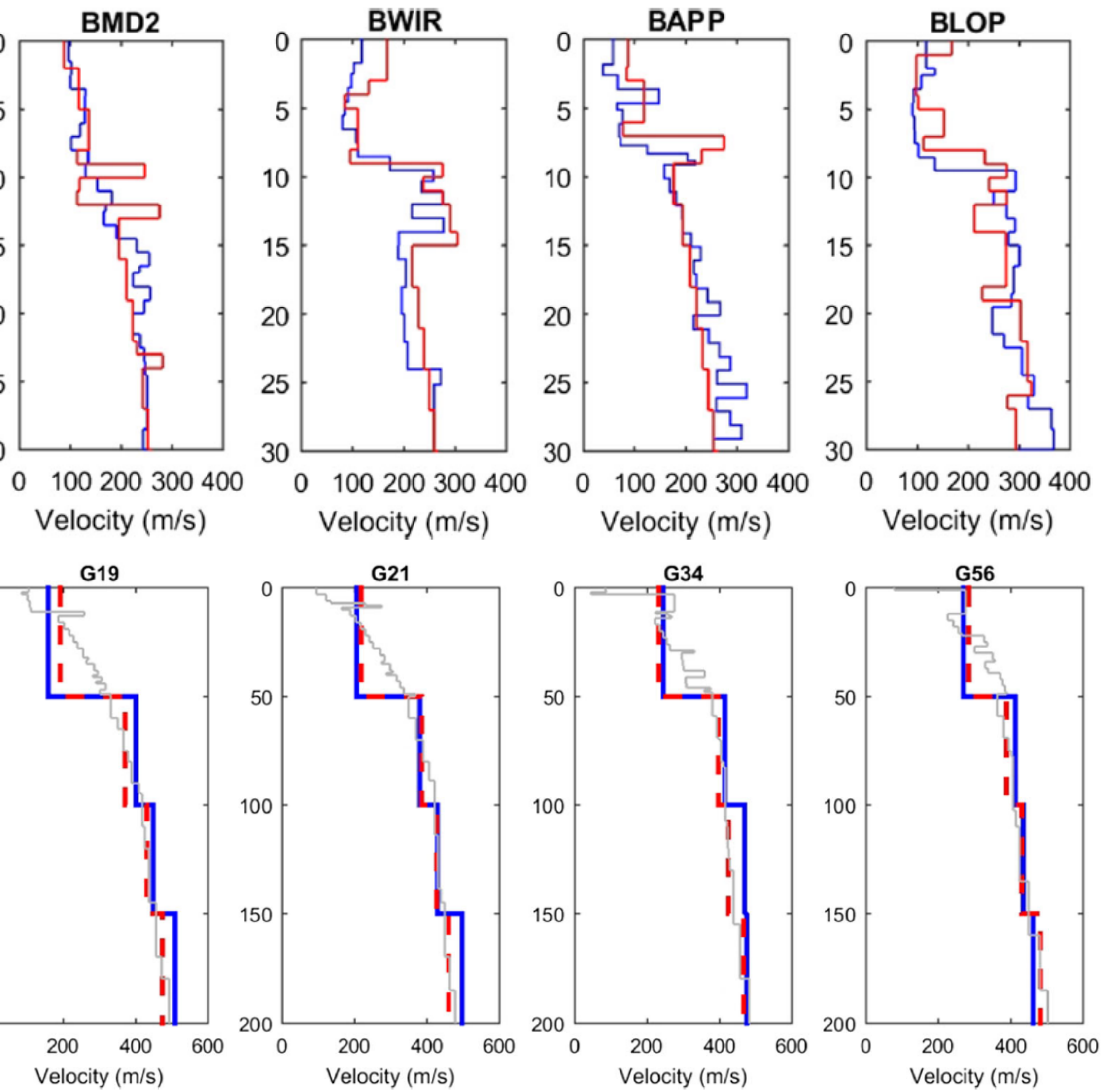

Comparison of transfer functions obtained fr inversions of surface FAS and from site respo analyses vindicate assumption of 1D propaga

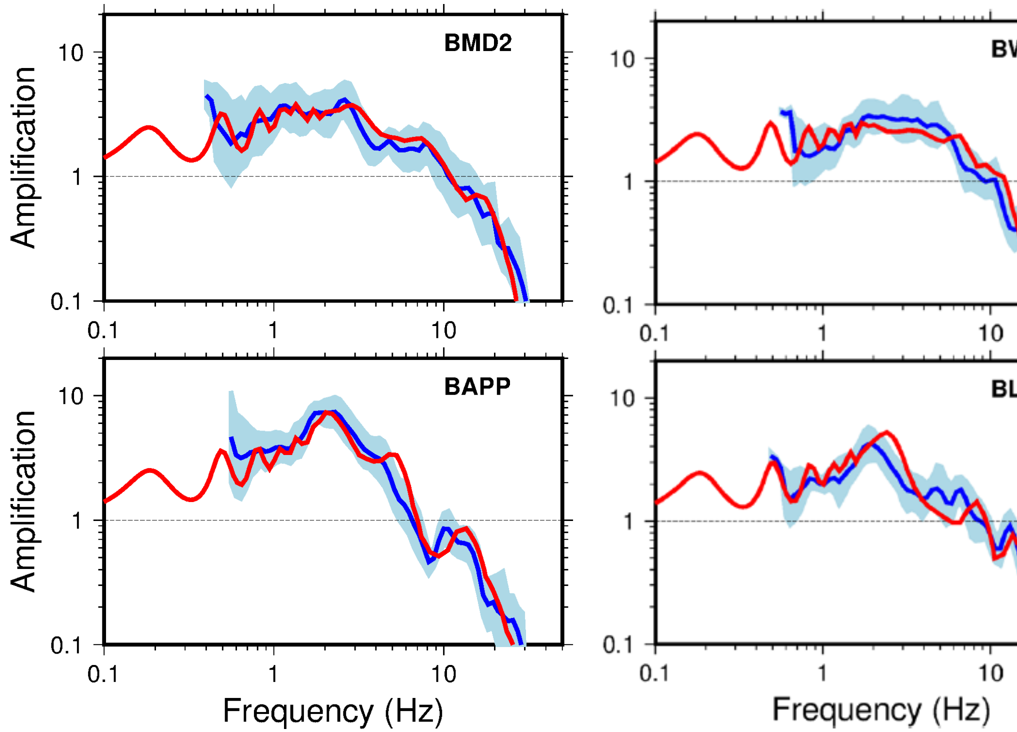

Noorlandt *et al*. (2

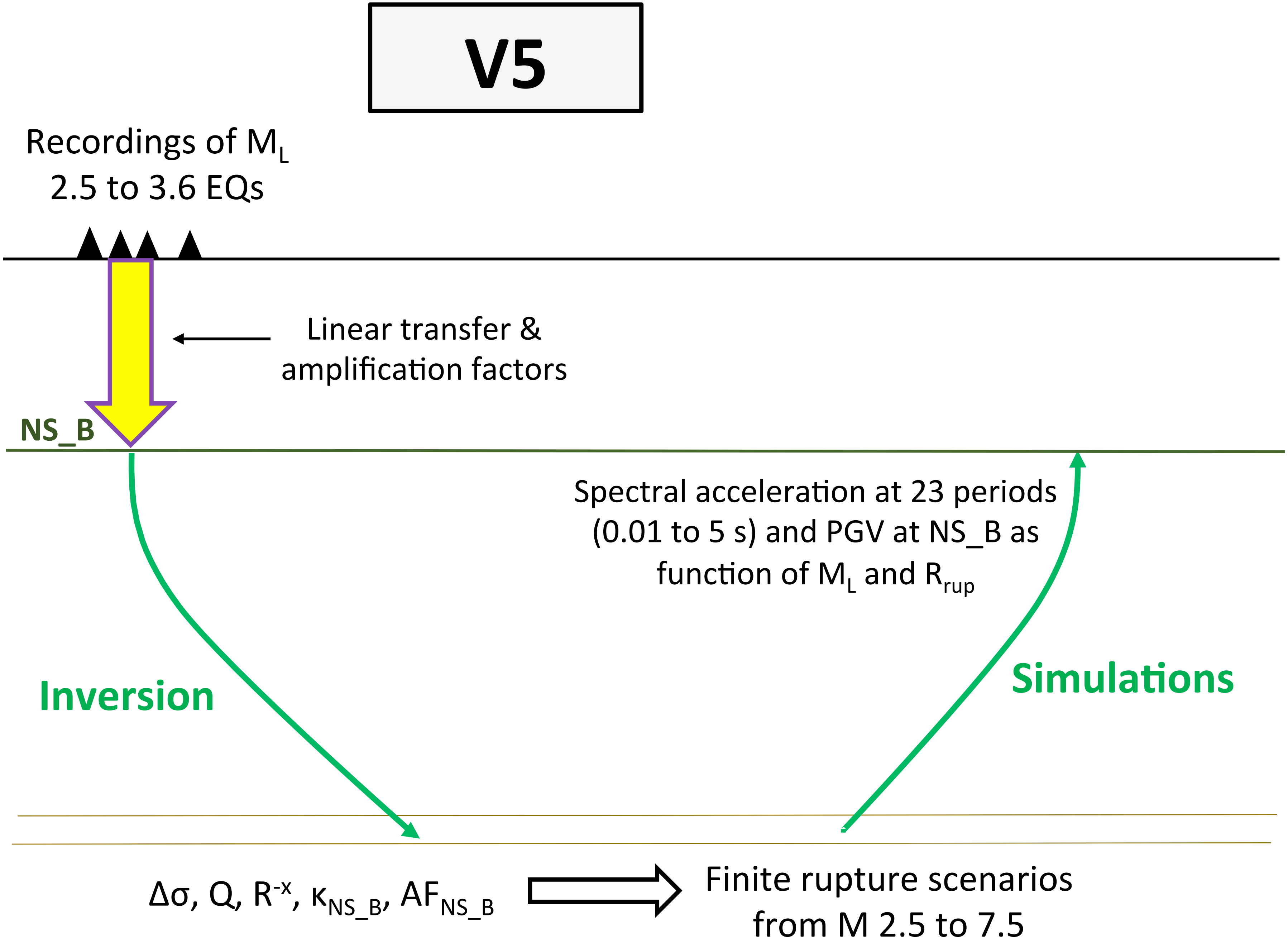

V5
Recordings of M_L 2.5 to 3.6 EQs
Linear transfer & amplification factors
NS_B
Spectral acceleration at 23 periods (0.01 to 5 s) and PGV at NS_B as function of M_L and R_{rup}
Inversion
Simulations
$\Delta\sigma$, Q, R^{-x}, κ_{NS_B}, AF_{NS_B}
Finite rupture scenarios from M 2.5 to 7.5

Upper branch of
gic-tree calibrated
match predictions
om European and
GA-West2 GMPEs

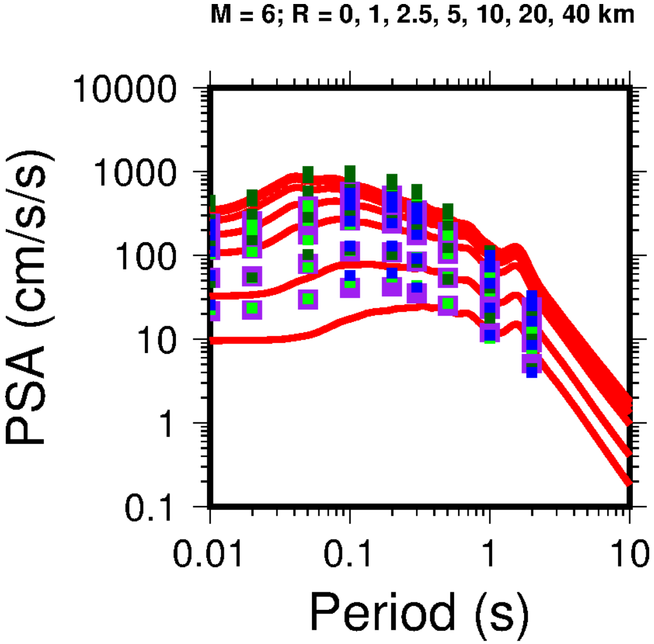

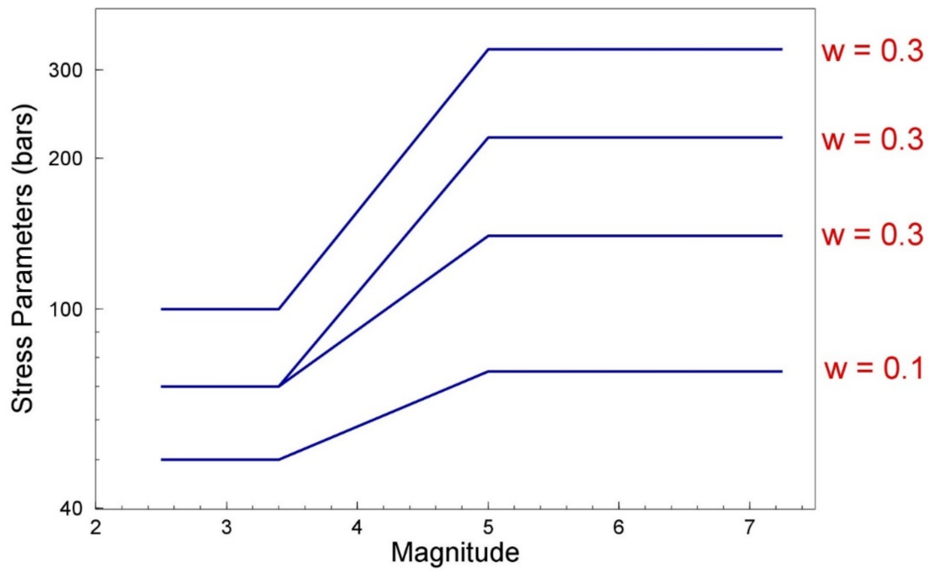

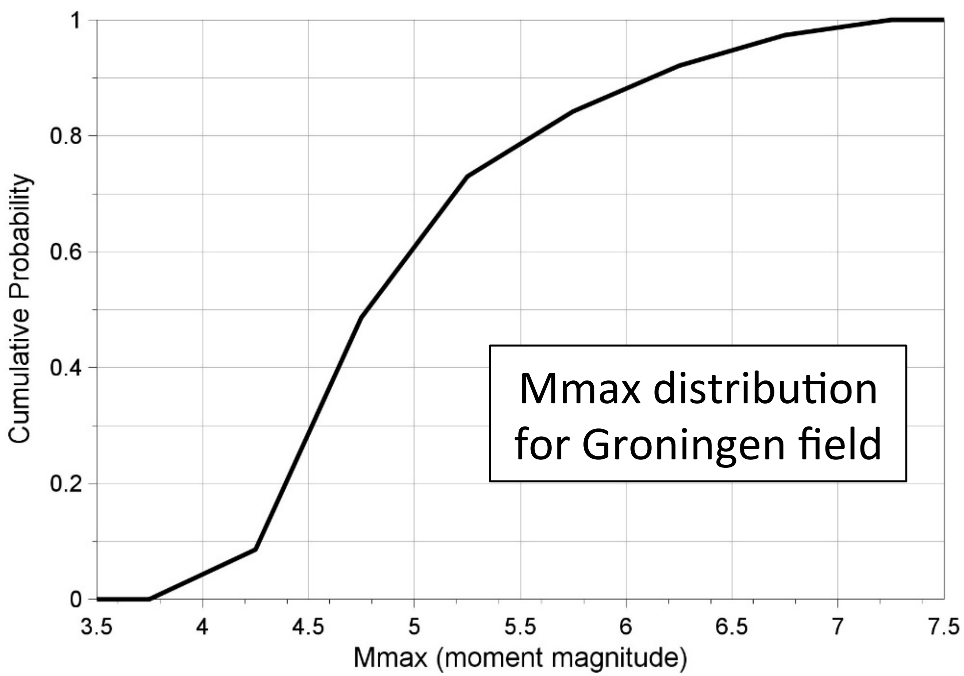

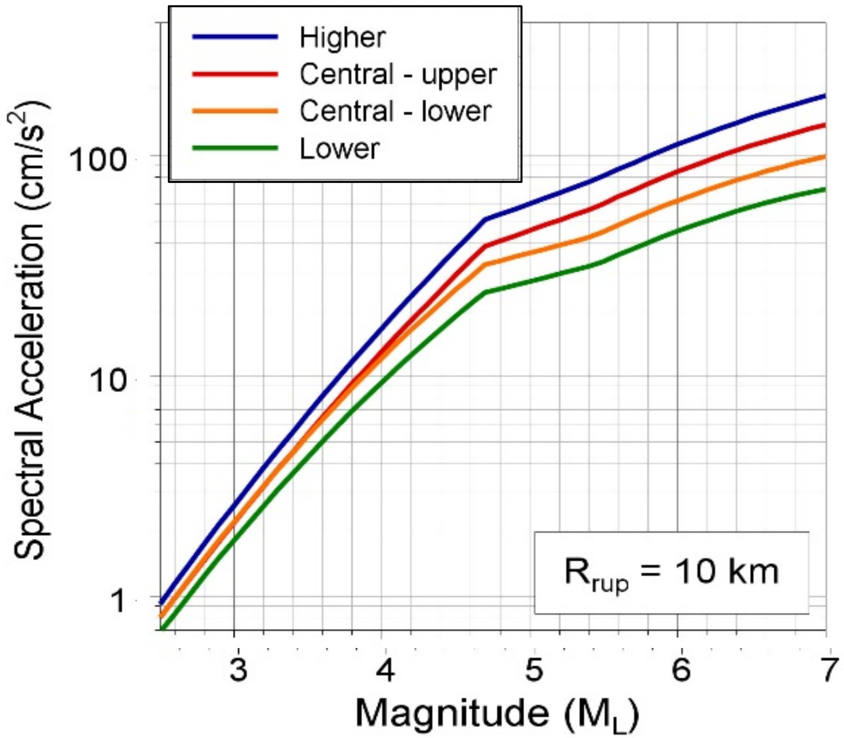

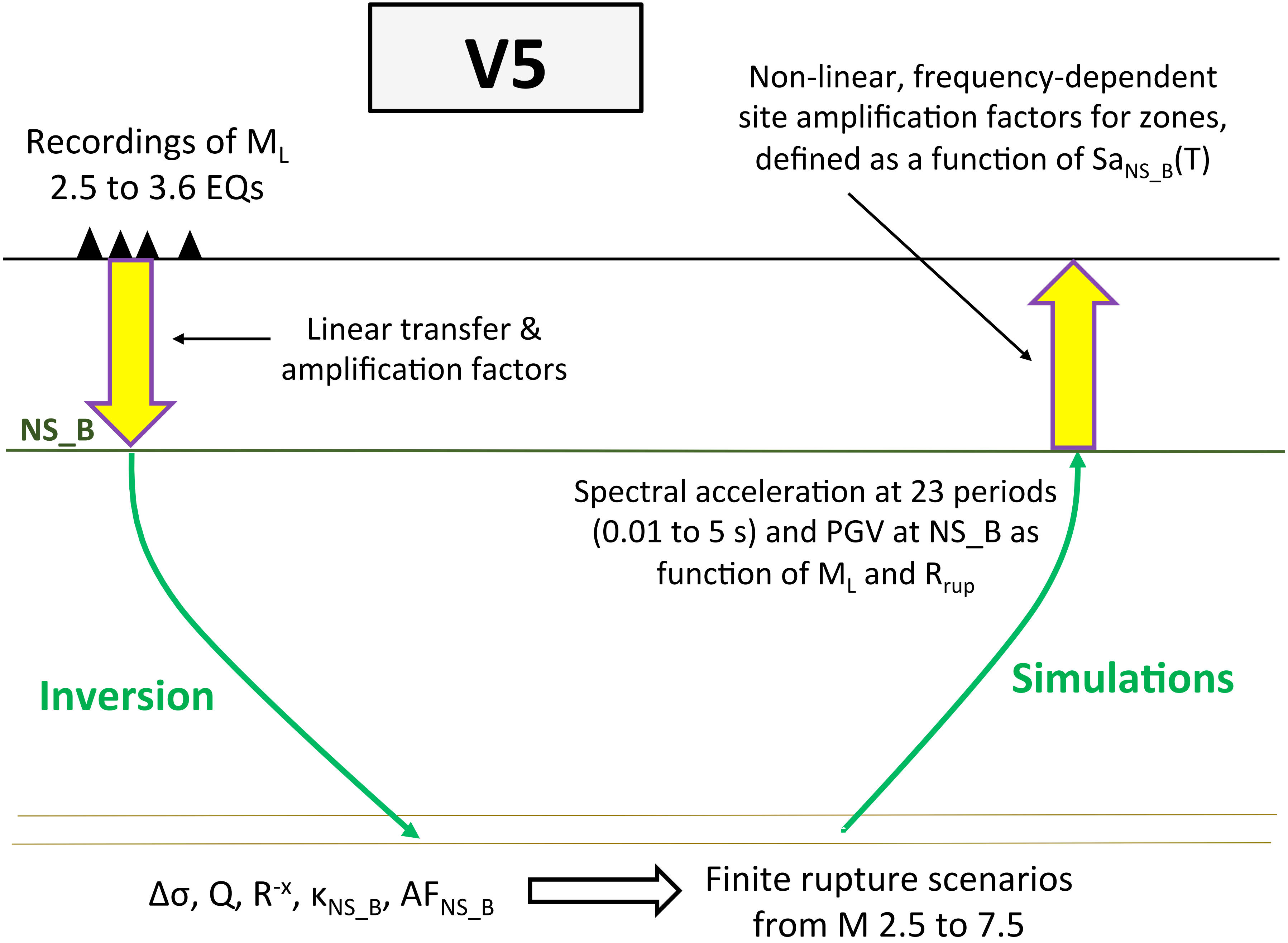

V5
Recordings of M_L 2.5 to 3.6 EQs
Non-linear, frequency-dependent site amplification factors for zones, defined as a function of $Sa_{NS\_B}(T)$
Linear transfer & amplification factors
NS_B
Spectral acceleration at 23 periods (0.01 to 5 s) and PGV at NS_B as function of M_L and R_{rup}
Inversion
Simulations
$\Delta\sigma$, Q, R^{-x}, κ_{NS_B}, AF_{NS_B}
Finite rupture scenarios from M 2.5 to 7.5

160 zones with unique AFs

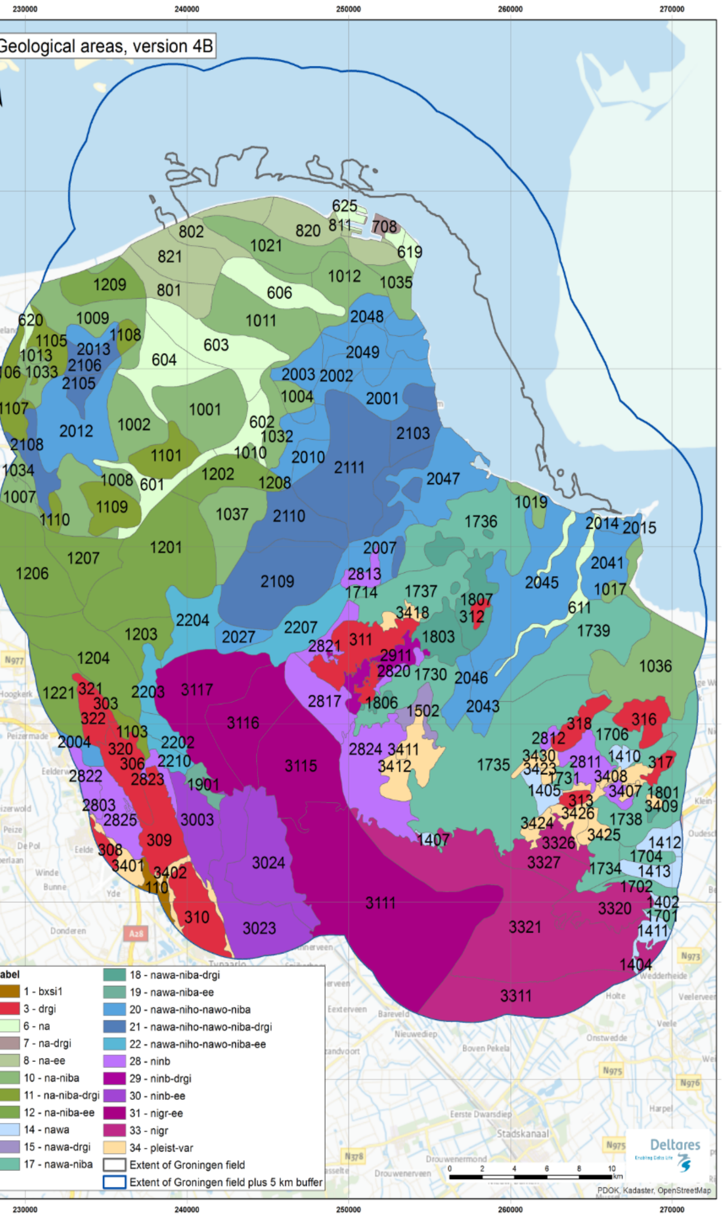

Linear part of AFs at short periods found to depend on magnitude and distance (Stafford *et al.*, 2017)

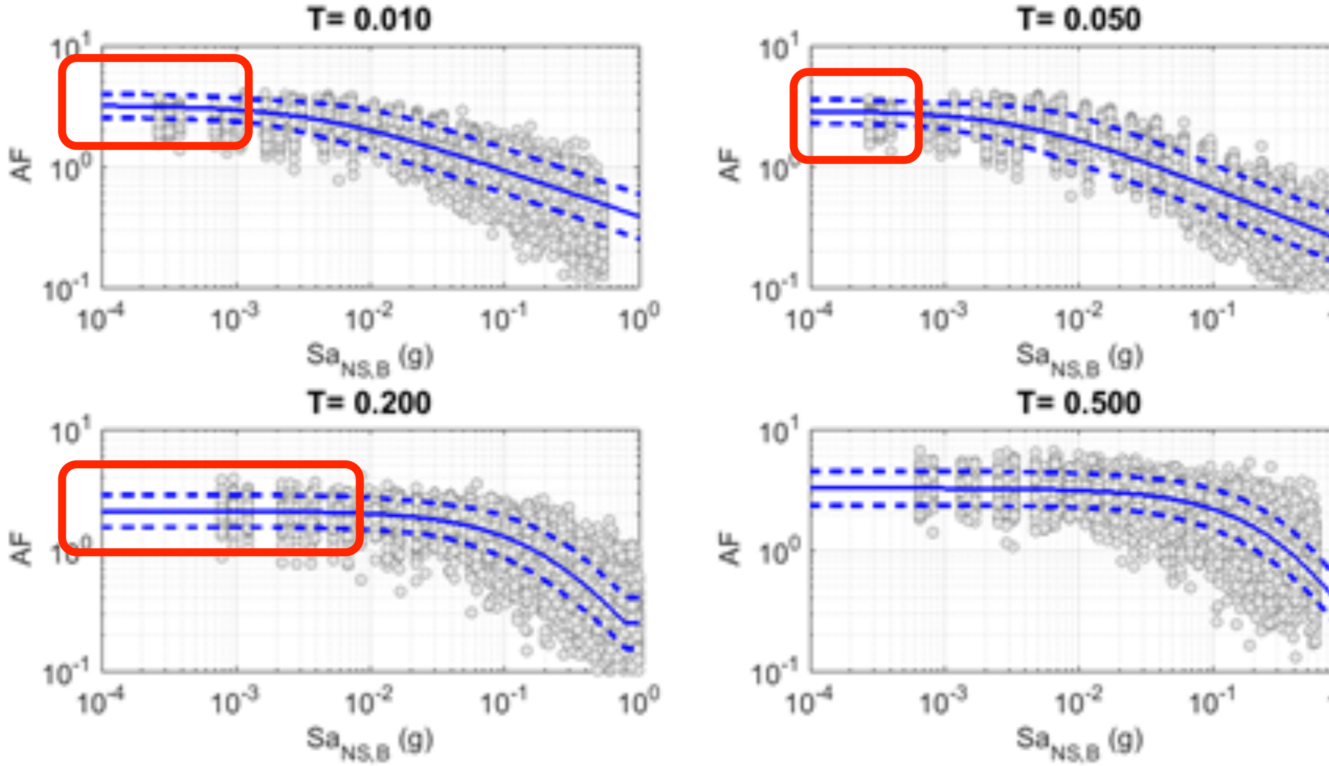

Rodriguez-Marek *et al.* (

Horizontal Component Definition

Predictive model expressed in terms of geometric mean horizontal component

Fragility function derivation based on the rbitrary horizontal component, so in the k calculations an adjustment is needed for the component-to-component variability (Baker & Cornell, 2006)

he model for component-to-component variability is a function of distance and onverges to standard tectonic models at larger magnitudes

Many near-source Groningen recordings obtained show strong polarisation

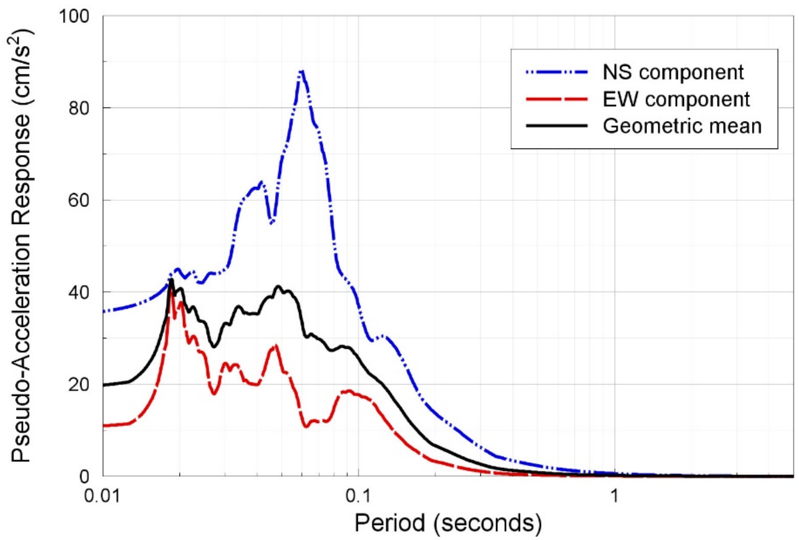

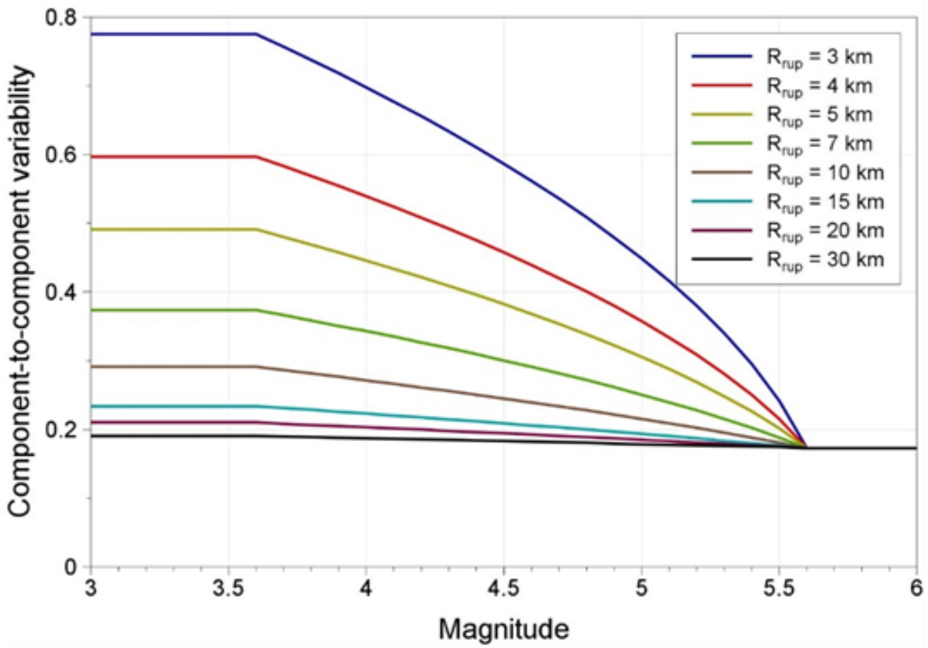

Duration Prediction Model

The Groningen ground motions display very short durations close to the source and grow rapidly with distance, features not well captured by existing duration GMPEs

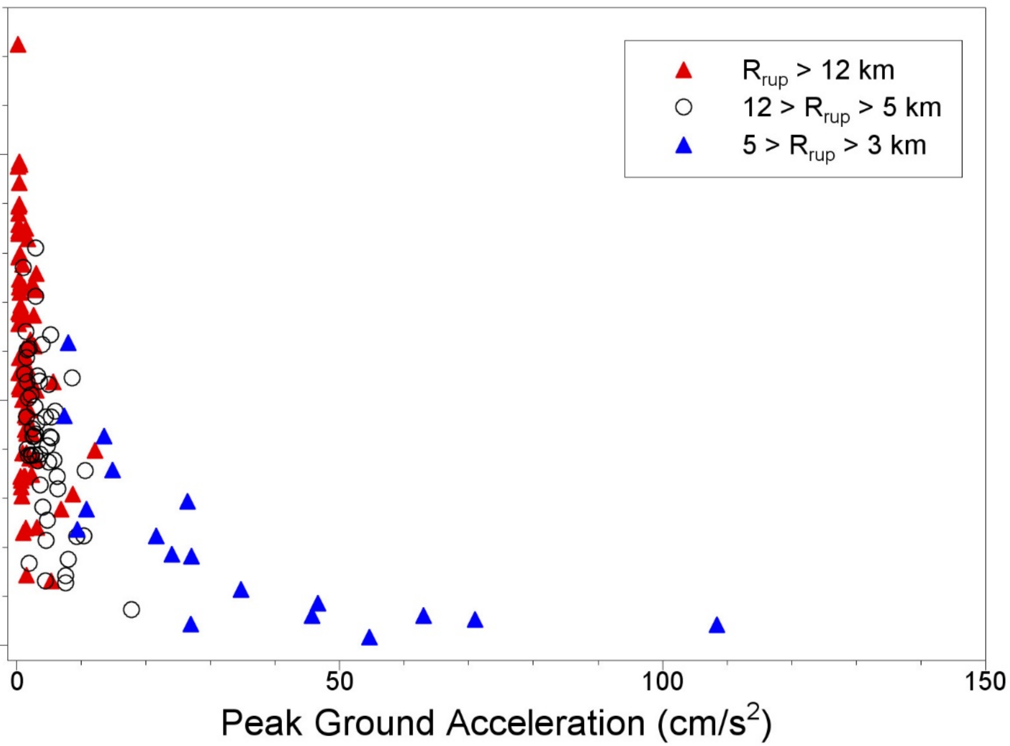

Groningen-specific model derived from EXSIM time-histories at NS_B horizon combined with V_{S30}-based site factors from model of Afshari & Stewart (2016)

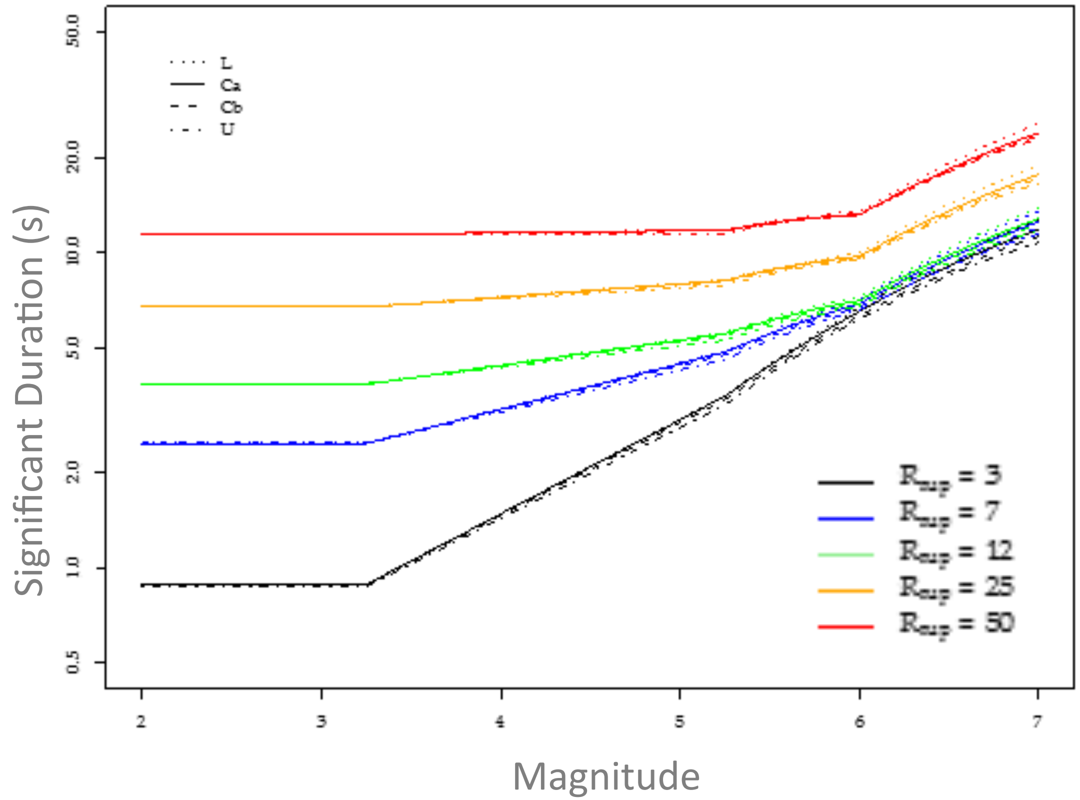

Peer Review

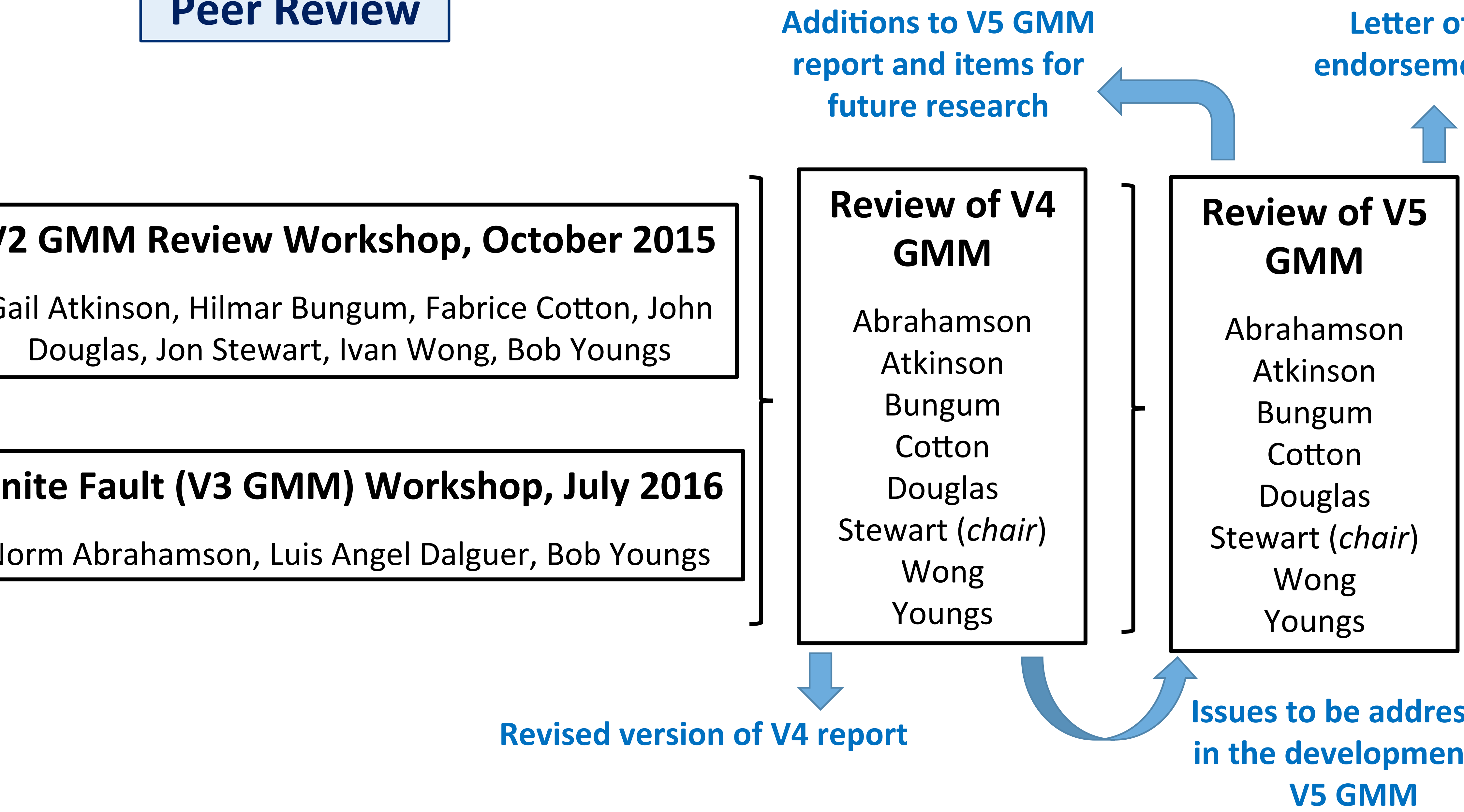

Additions to V5 GMM report and items for future research
Letter of endorseme
/2 GMM Review Workshop, October 2015
Gail Atkinson, Hilmar Bungum, Fabrice Cotton, John Douglas, Jon Stewart, Ivan Wong, Bob Youngs
nite Fault (V3 GMM) Workshop, July 2016
Norm Abrahamson, Luis Angel Dalguer, Bob Youngs
Review of V4 GMM
Abrahamson
Atkinson
Bungum
Cotton
Douglas
Stewart (chair)
Wong
Youngs
Review of V5 GMM
Abrahamson
Atkinson
Bungum
Cotton
Douglas
Stewart (chair)
Wong
Youngs
Revised version of V4 report
Issues to be addres in the developmen V5 GMM

uary 15 2018

Jan van Elk
lerlandse Aardolie Maatschappij B.V. (NAM)
epersmaat 2,
5 TA Assen, The Netherlands

r Mr. van Elk:

undersigned are members of an international panel of experts in earthquake ground tion modelling, which was engaged at various intervals since July 2015 to review the elopment of ground motion models for the Groningen field. Panel reports presenting our essments have been submitted for the Version 4 model (May 2017) and the Version 5 model uary 2018).

overall assessment of the modeling effort to date is that it has produced a state-of-the-art del that is well suited for its purpose of regional ground motion prediction to support hazard risk studies in the Groningen field. While our most recent review of the draft Version 5 ort resulted in some technical and editorial comments, these issues do not impact the damental viability of the model that has been developed.

pectfully submitted,

athan P. Stewart (Chair)	Norman A. Abrahamson	Gail M. Atkinson
har Bungum	Fabrice Cotton	John Douglas
Wong	Robert R Youngs	

"Our overall assessment of the modelling effort to date is that it ha produced a state-of-the-art model that it well suited for its purpose of regional ground motion prediction t support hazard and risk studies in th Groningen field."

References

, K. & J.P. Stewart (2016). Physically parameterized prediction equations for significant duration in active crustal regions. *Earthquake Spectra* **32**(4), 2057-2081

J.W. & C.A. Cornell (2006). Which spectral acceleration are you using? *Earthquake Spectra* **22**(2), 293-312.

er, J.J., B. Dost, B. Edwards, P.J. Stafford, J. van Elk, D. Doornhof & M. Ntinalexis (2016). Developing an application-specific ground-motion model for induced city. *Bulletin of the Seismological Society of America* **106**(1), 158-173.

er, J.J., P.J. Stafford, B. Edwards, B. Dost, E. van Dedem, A. Rodriguez-Marek, P. Kruiver, J. van Elk, D. Doornhof & M. Ntinalexis (2017). Framework for a grou model for induced seismic hazard and risk analysis in the Groningen gas field, The Netherlands. *Earthquake Spectra* **33**(2), 481-498.

er, J.J., B. Dost, B. Edwards, P.P. Kruiver, M. Ntinalexis, A. Rodriguez-Marek, P.J. Stafford & J. van Elk (2017). Developing a model for the prediction of ground earthquakes in the Groningen gas field. *Netherlands Journal of Geoscience* **96**(5), s203-s213.

., B. Edwards & J.J. Bommer (2018). The relationship between **M** and M_L - a review and application to induced seismicity in the Groningen gas field, the Nether *ed for publication in Seismological Research Letters*.

., E. Ruigrok & J. Spetzler (2018). Development of probabilistic seismic hazard assessment for the Groningen gas field. *Netherlands Journal of Geoscience* **96** 245.

, P. P., E. van Dedem, E. Romijn, G. de Lange, M. Korff, J. Stafleu, J.L. Gunnink., A. Rodriguez-Marek, J.J. Bommer, J. van Elk & D. Doornhof (2017). An integr wave velocity model for the Groningen gas field, The Netherlands. *Bulletin of Earthquake Engineering* **15**(9), 3555-3580.

ndt, R.P., P.P. Kruiver, M.P.E. de Kleine, M. Karaoulis, G. de Lange, A. Di Matteo, J. von Ketelhodt, E. Ruigrok, B. Edwards, A. Rodriguez-Marek, J.J. Bommer, J . Doornhof (2018). Characterisation of ground-motion recording stations in the Groningen gas field. *Journal of Seismology* DOI: 10.1007/s10950-017-9725-6.

uez-Marek, A., P.P. Kruiver, P. Meijers, J.J. Bommer, B. Dost, J. van Elk & D. Doornhof (2017). A regional site-response model for the Groningen gas field. *Bulle ological Society of America* **107**(5), 2067-2077.

d, P.J., Rodriguez-Marek, A., B. Edwards, P.P. Kruiver & J.J. Bommer (2017). Scenario dependence of linear site effect factors for short-period response spectra es. *Bulletin of the Seismological Society of America*, **107**(6), 2859-2872.

Probabilistic Seismic Hazard Analysis Seismic ground motion hazards associated with the 24 bcm/year Groningen gas production scenario

Stephen Bourne[1], Steve Oates[1], Assaf Mar-Or[1], Tomas Storck[2], Pourya Omidi[2], Julian Bommer[3]

[1] Projects & Technology, Shell Global Solutions International
[2] Alten Nederland, Rotterdam
[3] Imperial College, London

Assurance meeting for Exposure, Fragility and Fatality Models for the Groningen building stock
World Trade Center, Schiphol, 21st February, 2018

Probabilistic seismic hazard model

- Two stochastic simulation models are sampled in the hazard model:

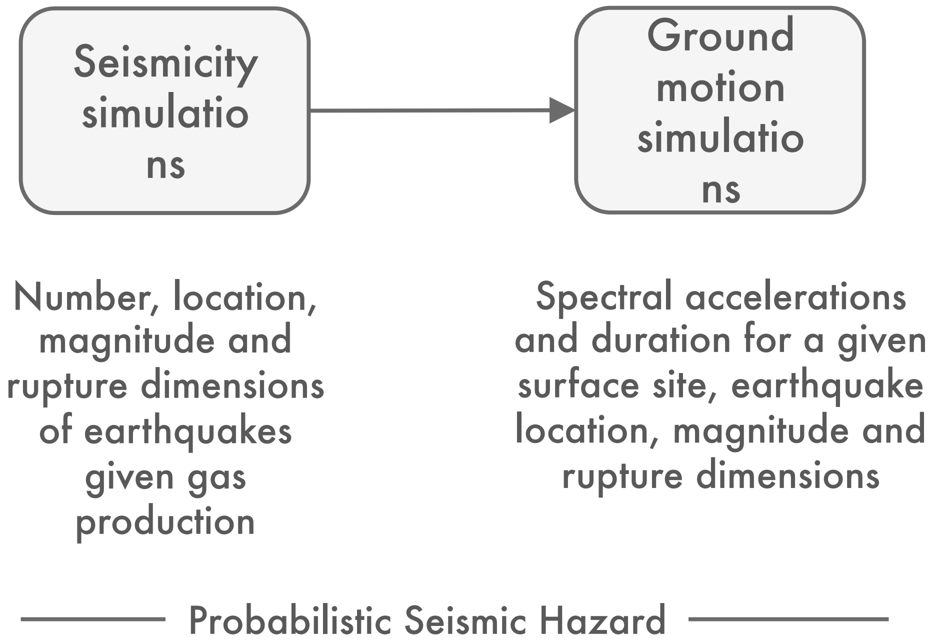

Probabilistic seismic hazard model – unpacked

- Seismological model comprises 5 sequential stochastic elements
- Ground motion model comprises 2 sequential

Reservoir deformation	Fault failures	Induced mainshocks	Triggered aftershocks	Finite ruptures	Base rock motions	Near-surface amplifications
Reservoir stress-strain states given pore pressure depletions	Fault failure probabilities given reservoir stress-strain states	Mainshock locations and magnitudes given fault failure probabilities	Aftershock locations and magnitudes given prior mainshocks and aftershocks	Finite rupture geometries given event locations and magnitudes	Base rock spectral accelerations and duration given base-rock site, event location, magnitude and rupture din	Surface spectral accelerations and duration given surface site, base-rock motions, earthquake location, magnitude and

Seismological Model — Ground Motion Model

Probabilistic Seismic Hazard

Probabilistic seismic hazard model – further unpacked

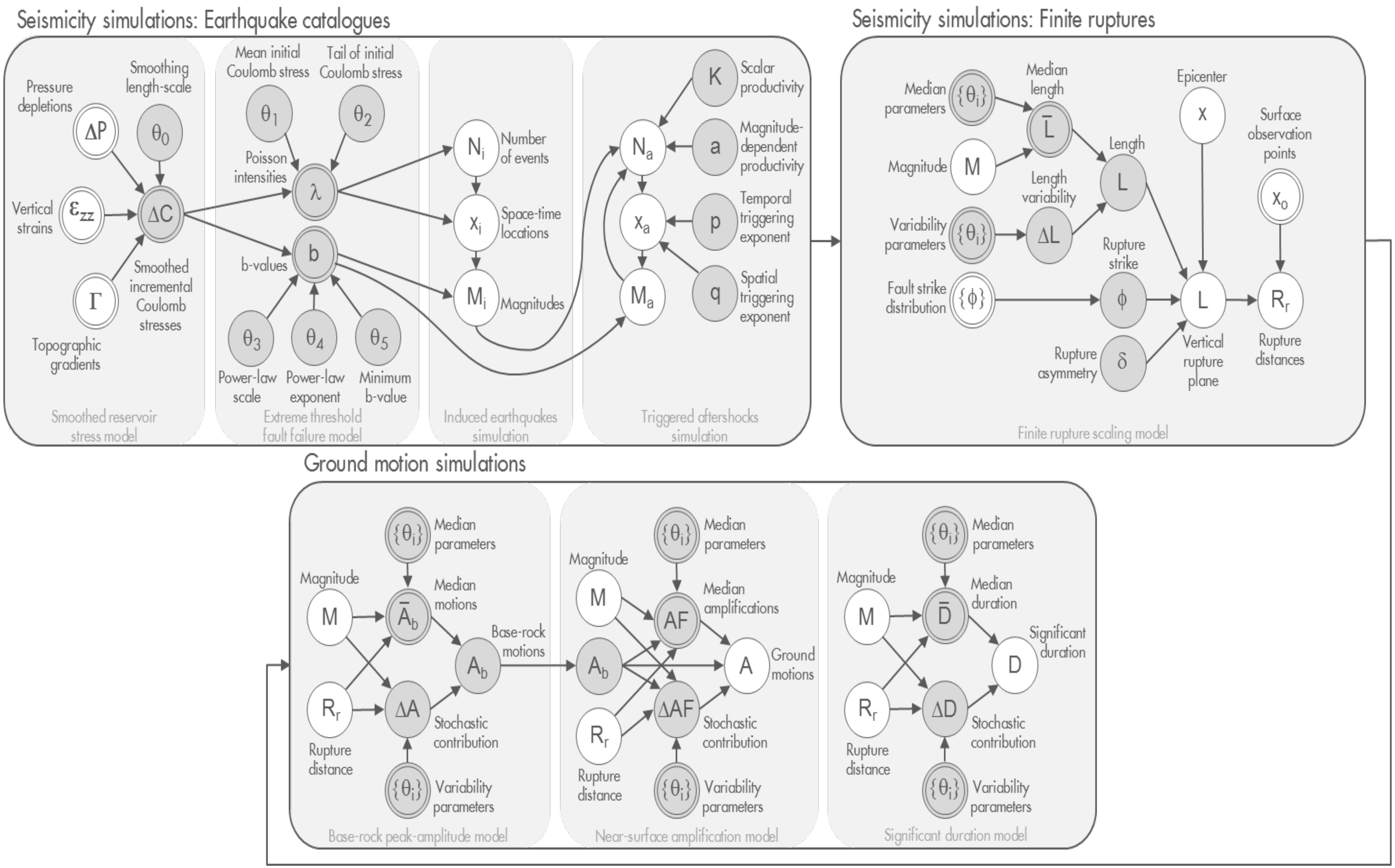

Logic tree description of epistemic uncertainties

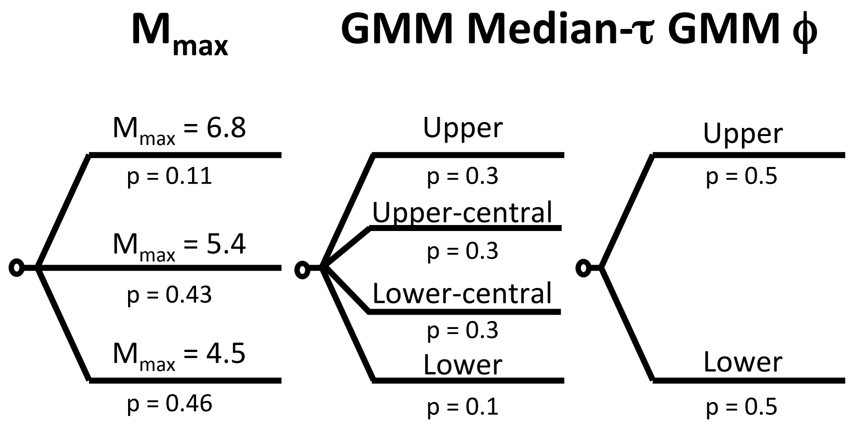

- 3 factors
- 3 x 4 x 2 levels
- 24 full-factorial combinations

Hazard curves

- Assessment period: 1-1-2017 to 1-1-2022
- Production scenario: 24 bcm/year

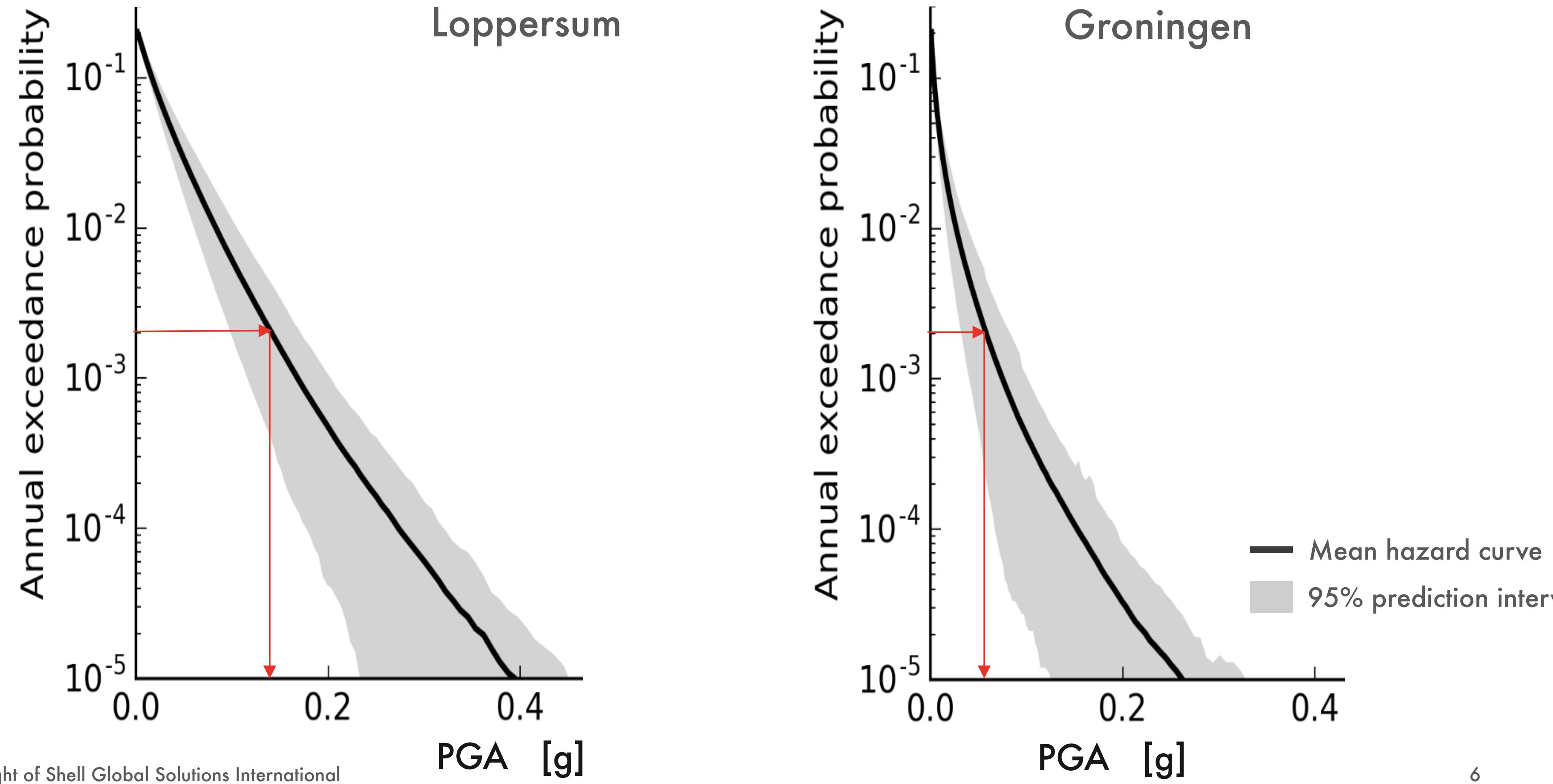

Hazard verification – comparison of C and Python code output

- Assessment period: 1-1-2017 to 1-1-2022
- Production scenario: 24 bcm/year
- Exceedance probability: 0.21%/year
- Single logic tree branch

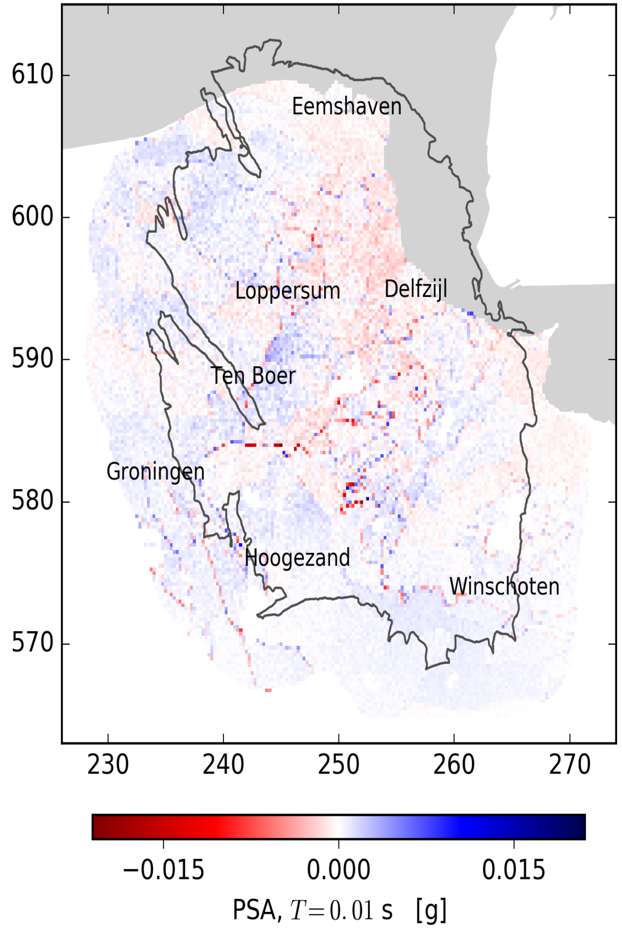

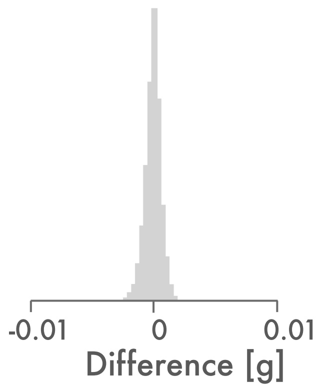

Mean hazard maps

- Assessment period: 1-1-2017 to 1-1-2022
- Production scenario: 24 bcm/year
- Exceedance probability: 0.21%/year

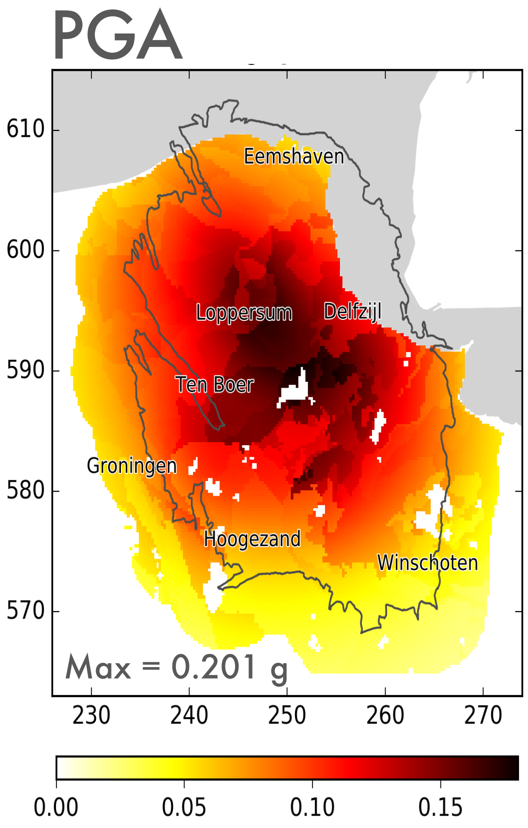

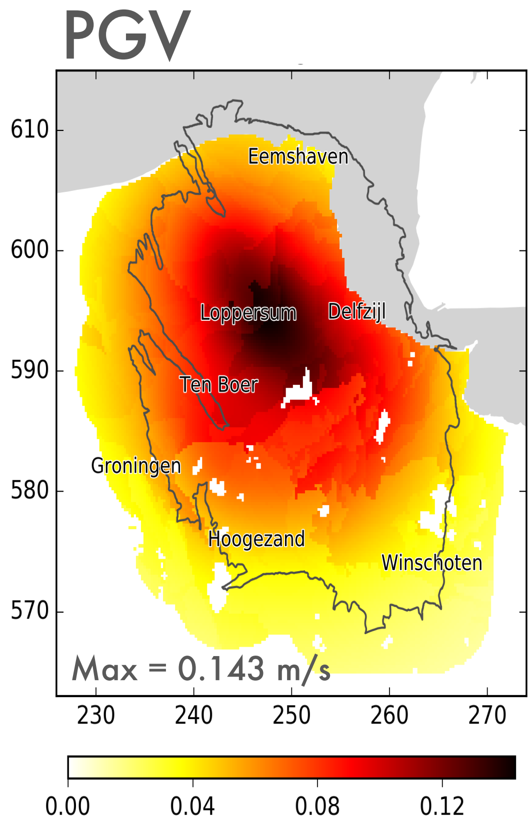

Mean spectral hazard maps

- Assessment period: 1-1-2017 to 1-1-2022
- Production scenario: 24 bcm/year
- Exceedance probability: 0.21%/year
- Colour bar: maps individually auto-scaled to maximum value
- Spatial distribution varies from period to period

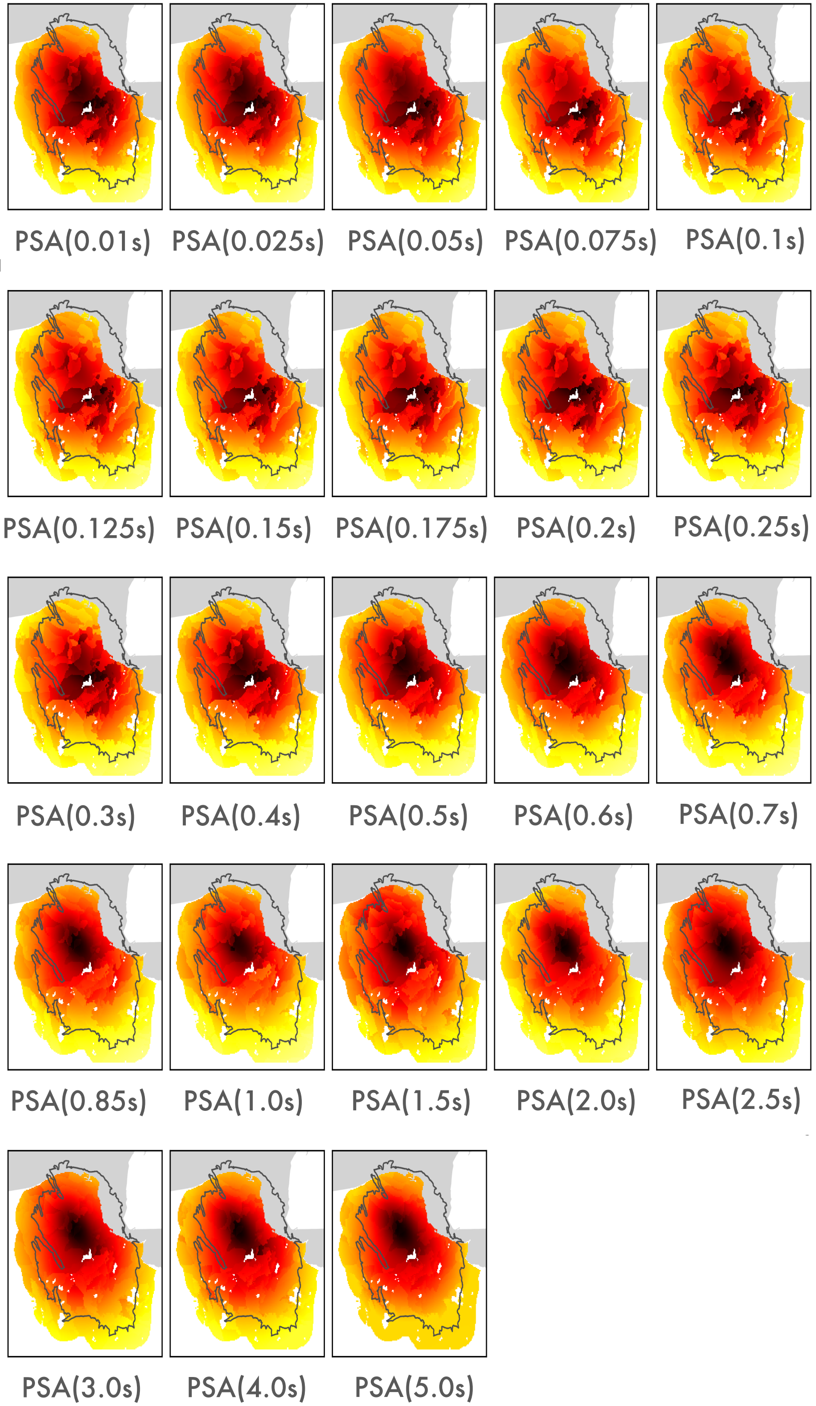

Uniform hazard spectra

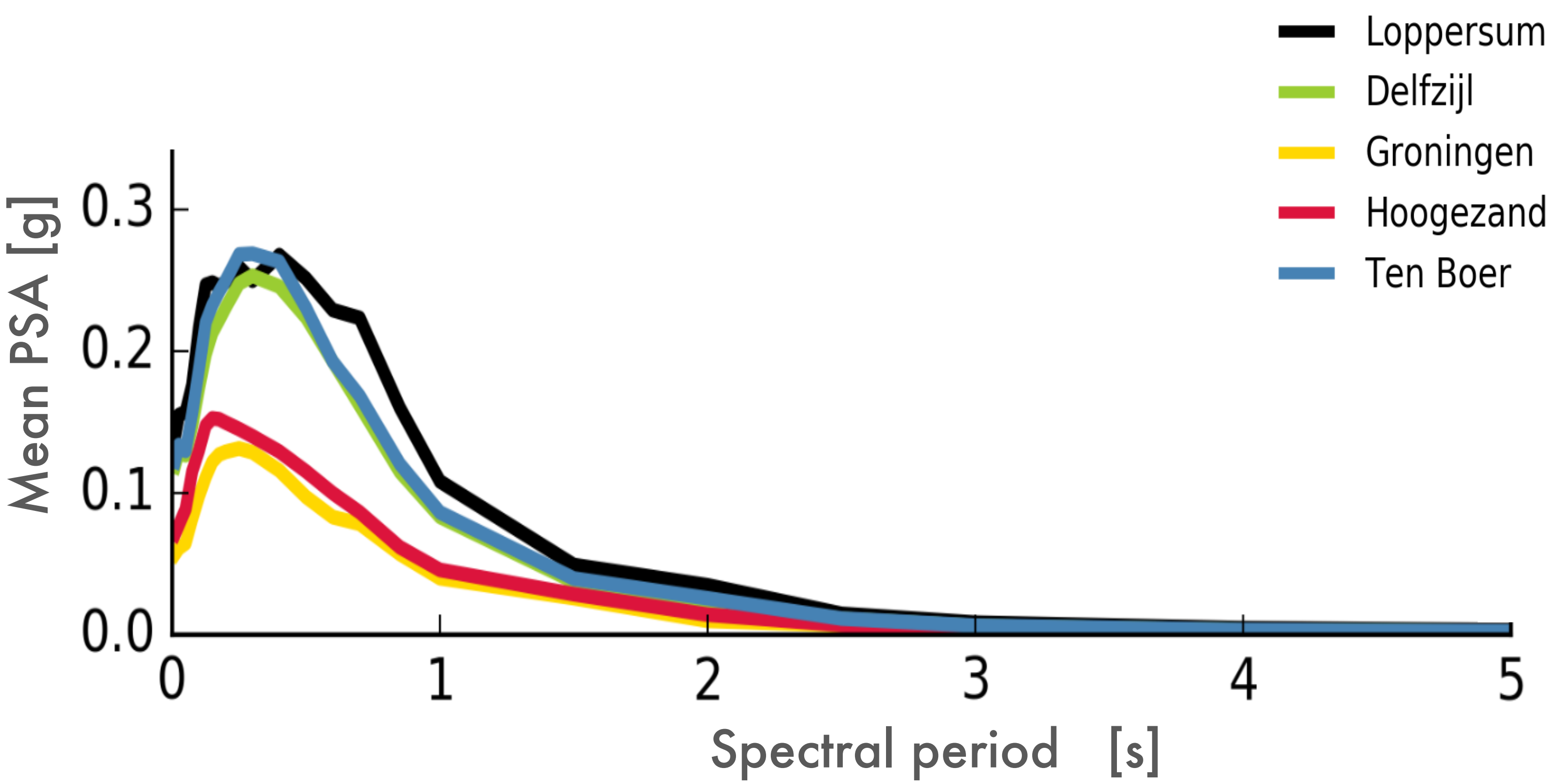

Uniform hazard spectra with 95% prediction intervals

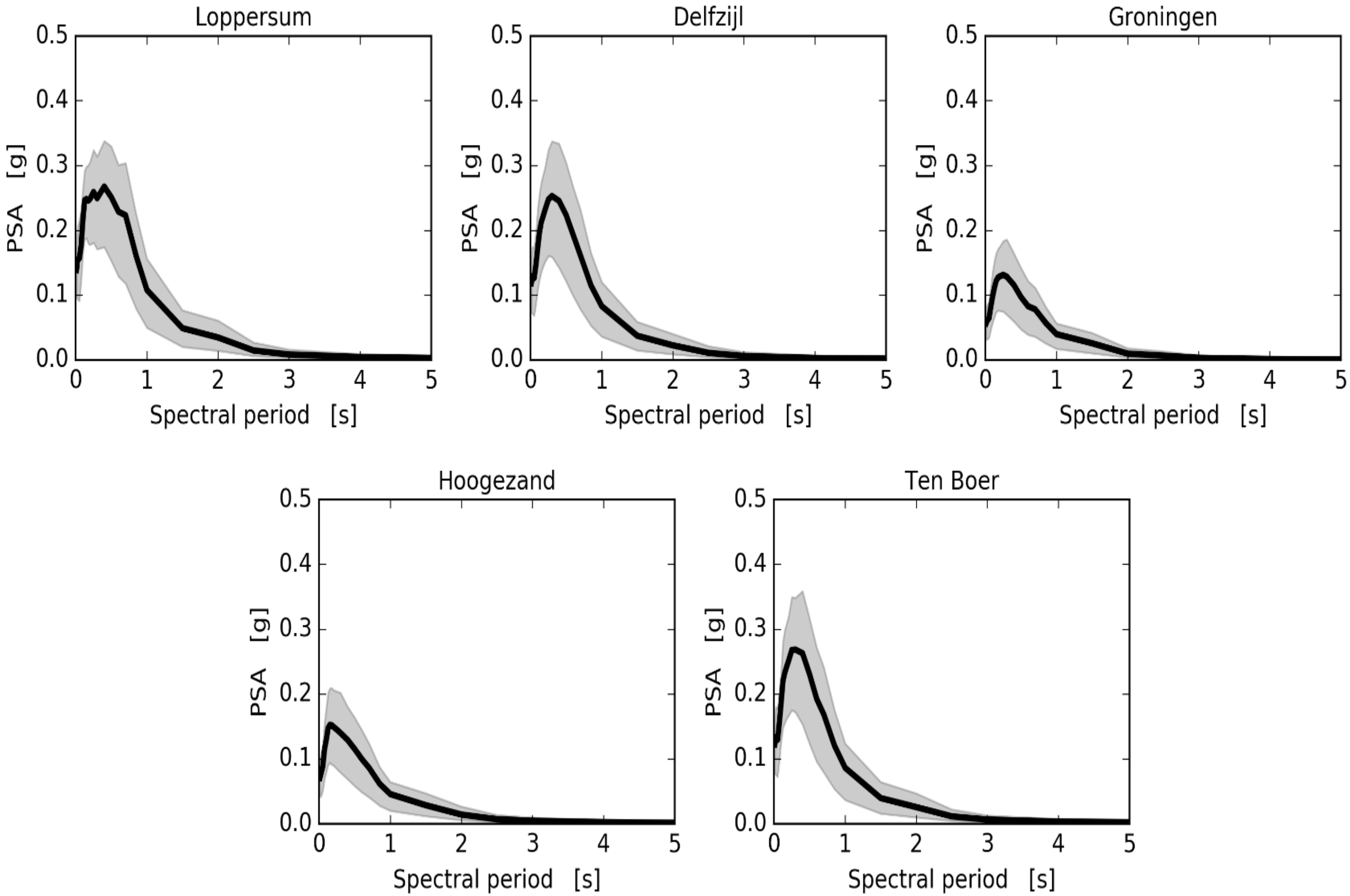

Sensitivity to epistemic uncertainty is dominated by M_{max}

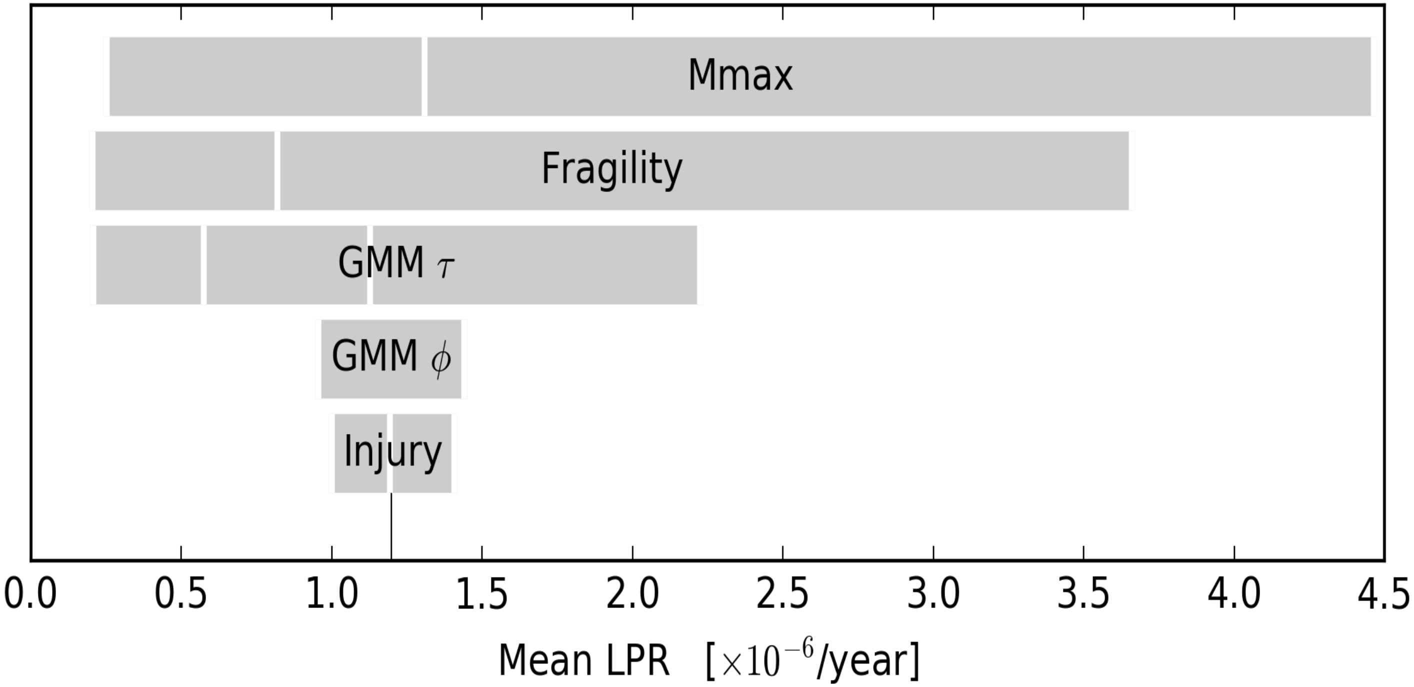

Summary

- Seismic hazard updated to include the V5 seismological and ground motion models
- Hazard verification through replication by independent Python and C codes
- Optimization of MC PSHA code enables 250m resolution, full logic tree simulations overnight
- Maximum PGA at 0.21%/year exceedance is 0.201 g (for 2017 – 2022)
- Development of Probabilistic Liquefaction Hazard Analysis is ongoing

Groningen Building Stock and Exposure Database

21st of February 2018

ARUP

1 // Introduction
2 // Process
3 // Results

ARUP

1 // Introduction

ARUP

Exposure Database V5

- The Exposure Database V5 is an extract of a project database and contains information specific to the Hazard and Risk Modelling. It consists mainly of the building typology classifications and several other building related attributes.

- This is the fifth update of the exposure database and supersedes V0 (July 2014), V1 (March 2015), V2 (September 2015) and V3 (March 2016).

Extract

Exposure Database Extract

Category Name	Column Name
Building ID	BAG_BUILDING_ID
Address coordinates (RD New)	POINT_X
	POINT_Y
Building year	BLDG_YEAR
Footprint Area	FOOTPRINT_AREA
Building addresses	NUMBER_ADDRESSES
Building footprint length exposed	EXPOSED_FOOTPRINT_LENGTH
Building gutter height	GUTTER_HEIGHT
Building use	MAIN_USE
	SECONDARY_USE
	SPECIAL_USE
Structural Layout	STRUCTURAL_LAYOUT
	SL_FLAG
Structural Systems	SYSTEM_n
	S_PROBABILITY_n
	S_CONFIDENCE
Strengthening Flag	UPGRADING_FLAG
Potential Failure Mechanisms	SOFT_STOREY
Opening Percentage	GROUND_OPENING_FRONT
	GROUND_OPENING_BACK
	GROUND_OPENING_LEFT
	GROUND_OPENING_RIGHT

Category Name	Column Name
Adjacency Flags	END_BUILDING
	BLOCK_PART_FLAG
	BLOCK_PART_UNITS
	BLOCK_FLAG
	BLOCK_UNITS
Population	SUM_POP_IN_DAY
	SUM_POP_IN_NIGHT
	SUM_POP_OUT_PAS_DAY
	SUM_POP_OUT_PAS_NIGHT
	SUM_POP_RUNNERS_OUT_DAY
	SUM_POP_RUNNERS_OUT_NIGHT

Structural System Reference Extract

Column name	Description
INDEX	Unique index string for each GEM taxonomy string.
GEM_TAXONOMY	GEM taxonomy description.
SUM_OF_PROBABILITIES	(Expected) number of buildings per taxonomy string based on the sum of individual building probabilities.

Scope Area

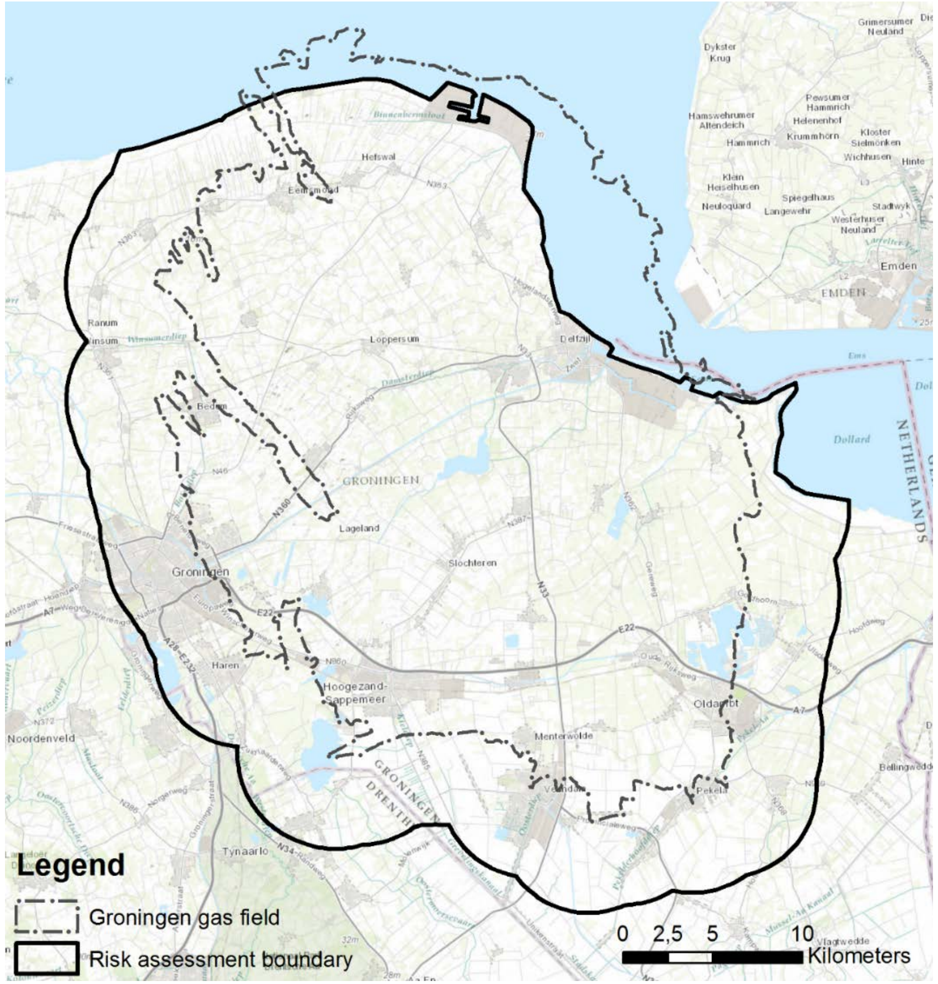

The area of interest for the Hazard and Risk analysis is based on the Slochteren gas field outline. The extract boundary for the EDB V5 is a 5 km buffer around the gas field outline.

Total amount of buildings: **257 174**.

Total amount of buildings with addresses *(with population)*: **164 032**.

Building Stock

2 // Process

ARUP

Available data

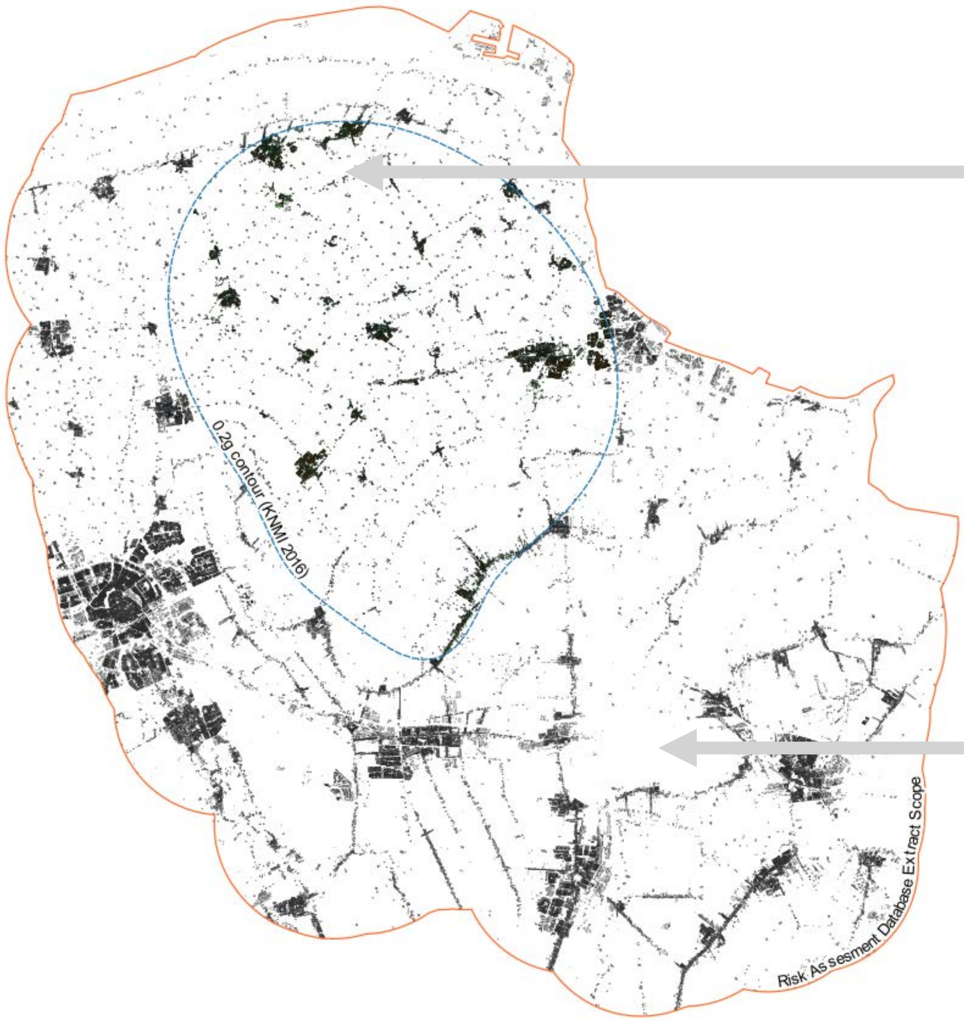

Structural System
Inspection data

- RVS Inspection Data
- EVS Inspection Data
- Drawing Data (TBDB)
- Visual Inspections (JBG)
- Arup Expert

Building Data Mining

- BAG
- Dataland
- Parcel
- AHN
- Rijksmonumenten
- Nationale Atlas Volksgezondheid
- Basisregister Instellingen

Classification: Building Use

Classification: Overview of Classification Process

Geometrical class	Structural Layout class	Structural Systems (GEM)

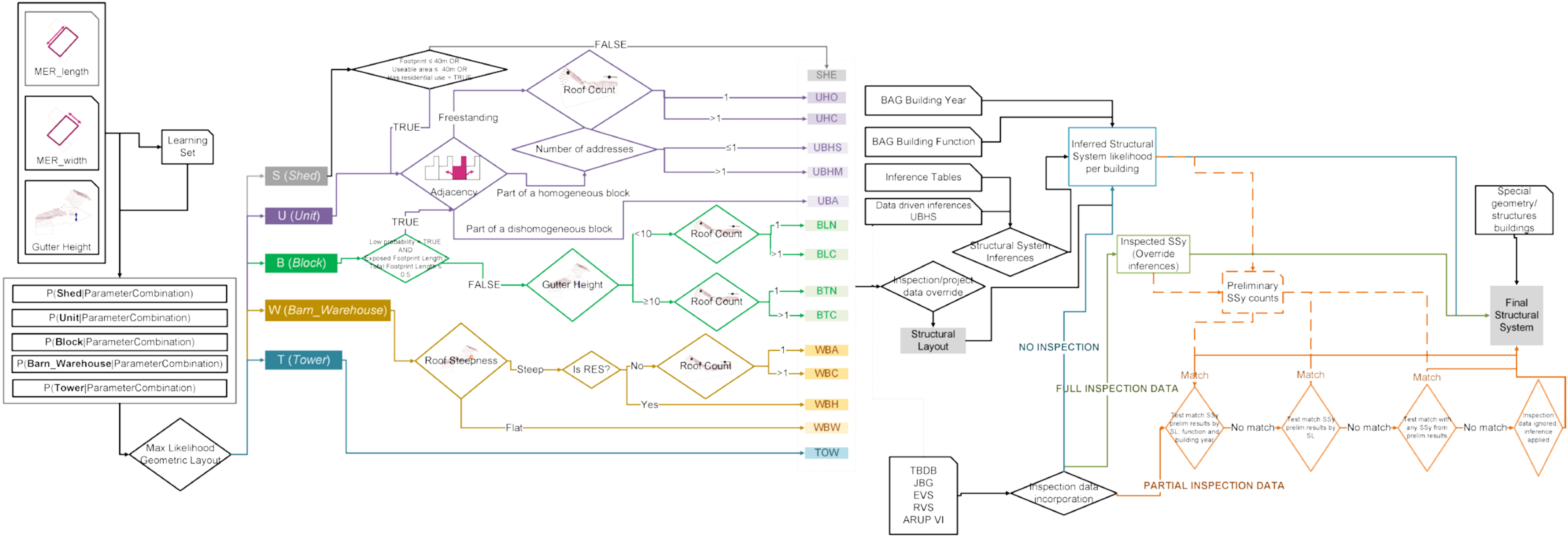

Classification: Main Phases

- Building data-mining and geometrical characterization
- Classification into Structural Layouts
- Structural System Inference
- Incorporation of available Inspection Data
- Final Structural System Assignment

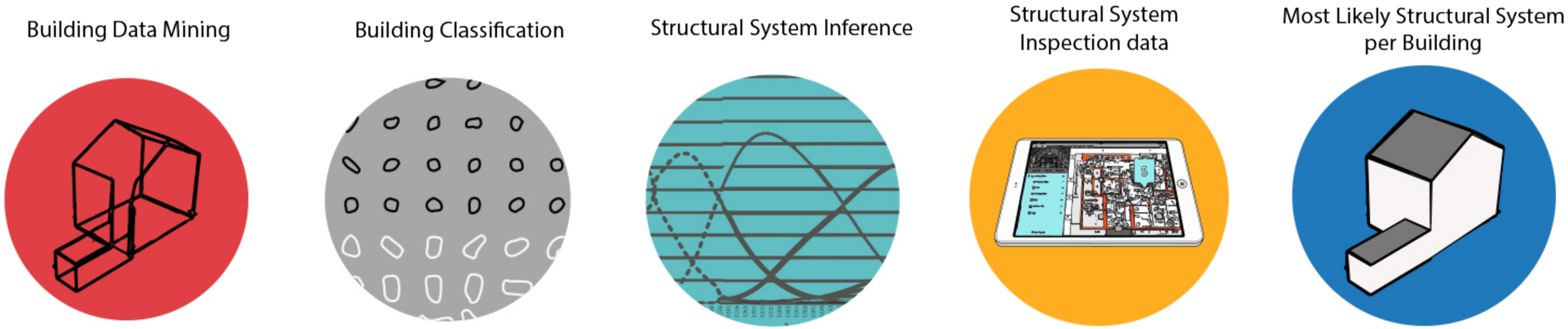

Classification: Building Data Mining & Geometrical Characterization

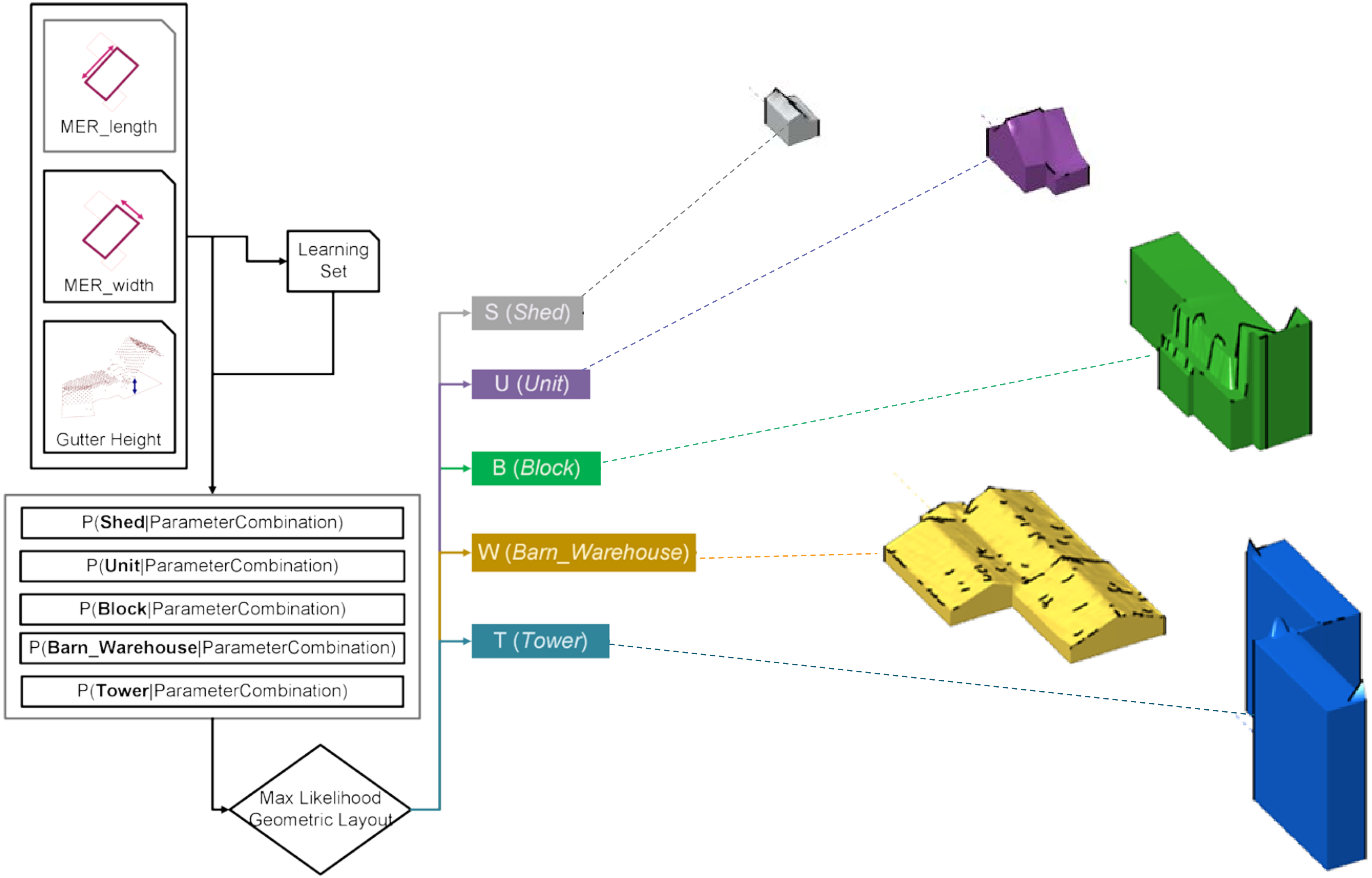

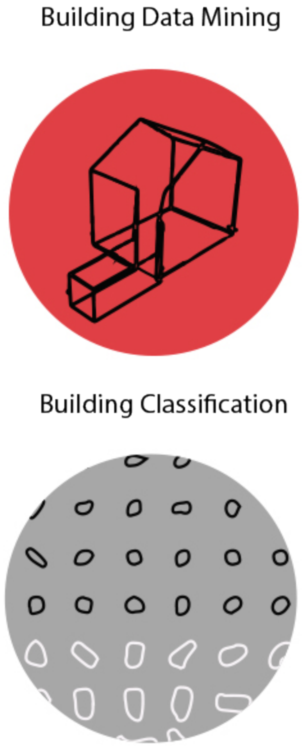

Classification: Data Mining

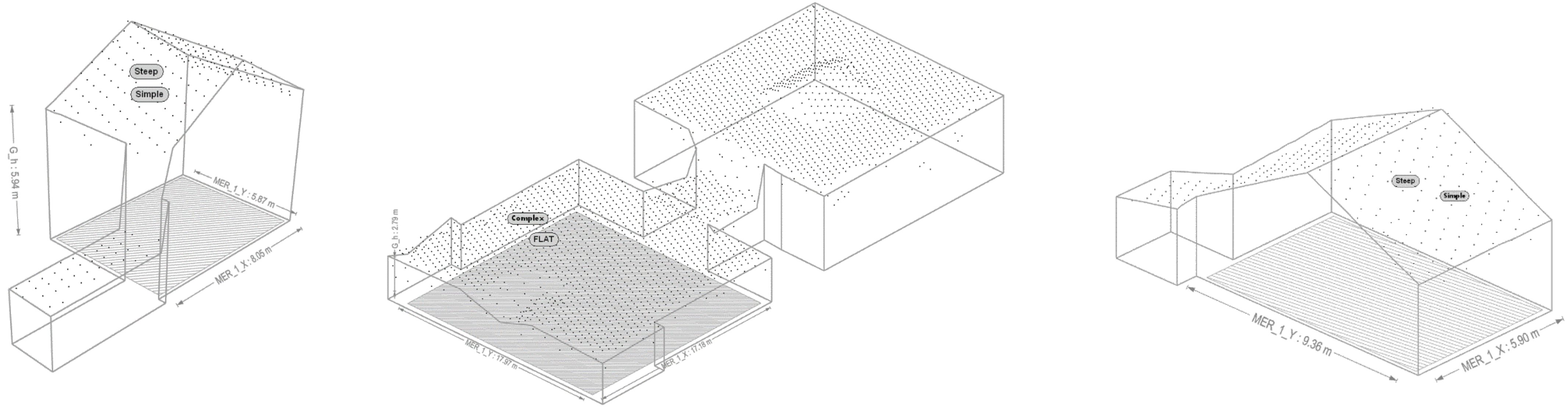

1. Width of Maximum Enclosed Rectangle within the footprint outline
2. Length of Maximum Enclosed Rectangle within the footprint outline
3. Gutter Height

Building Data Mining

Classification: Learning Set

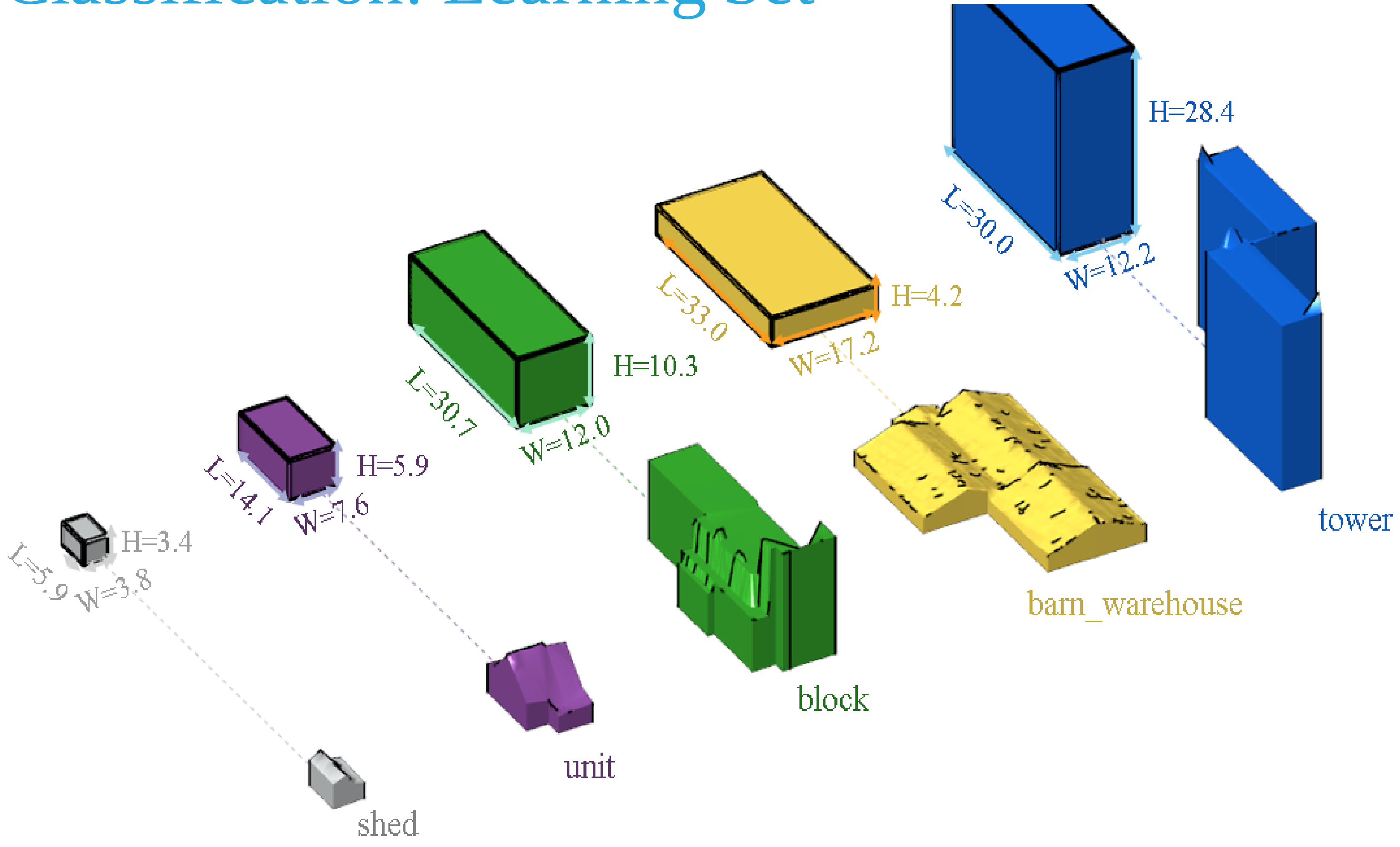

Building Data Mining

Classification: Classification Maps

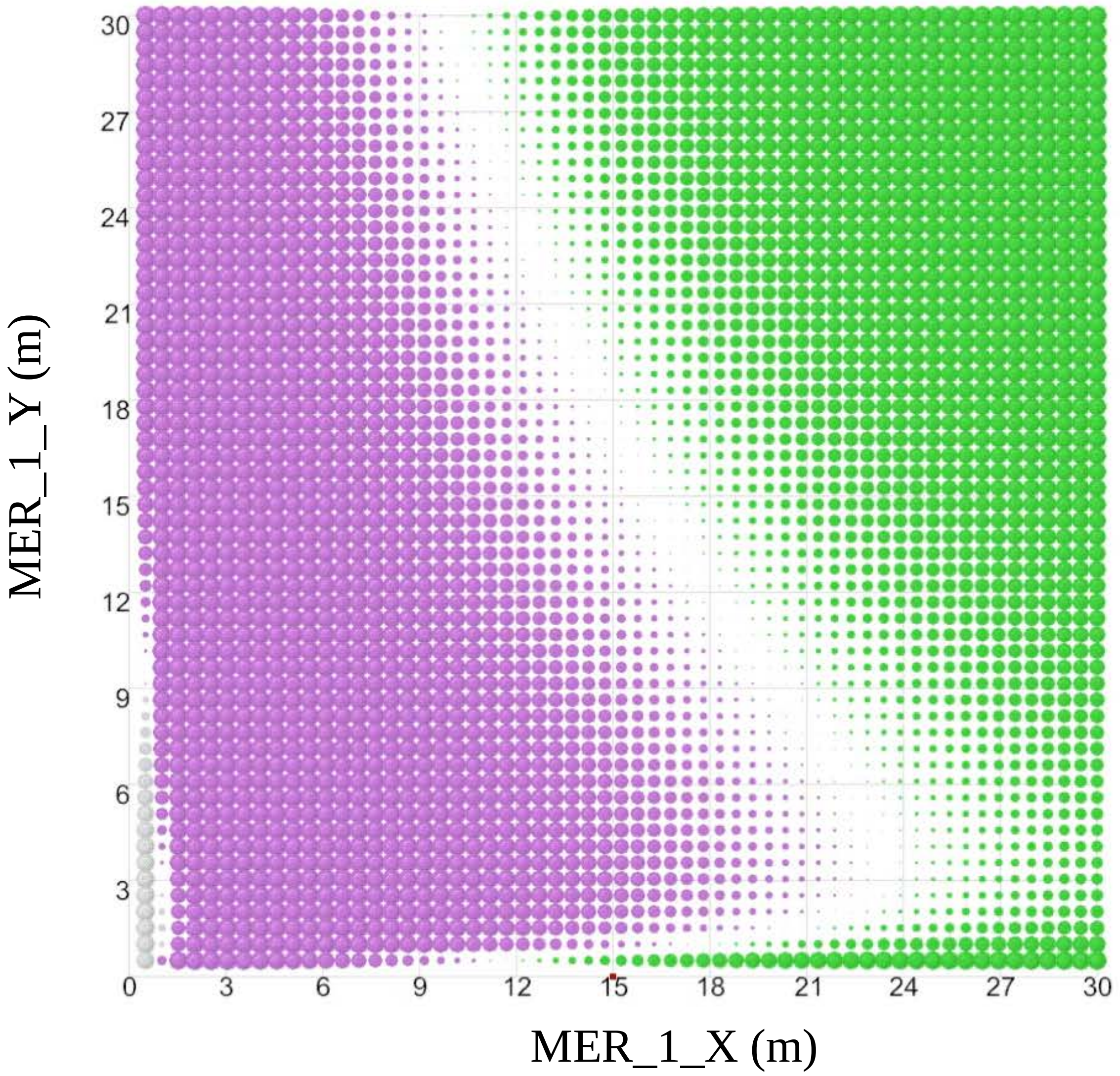

Sphere Diameter = Confidence

GUTTER HEIGHT [M]:0.5

barn_warehouse
tower
block
unit
shed

Building Classification

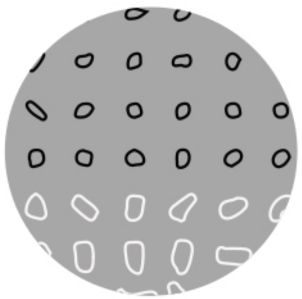

Classification: Geometrical Characterization

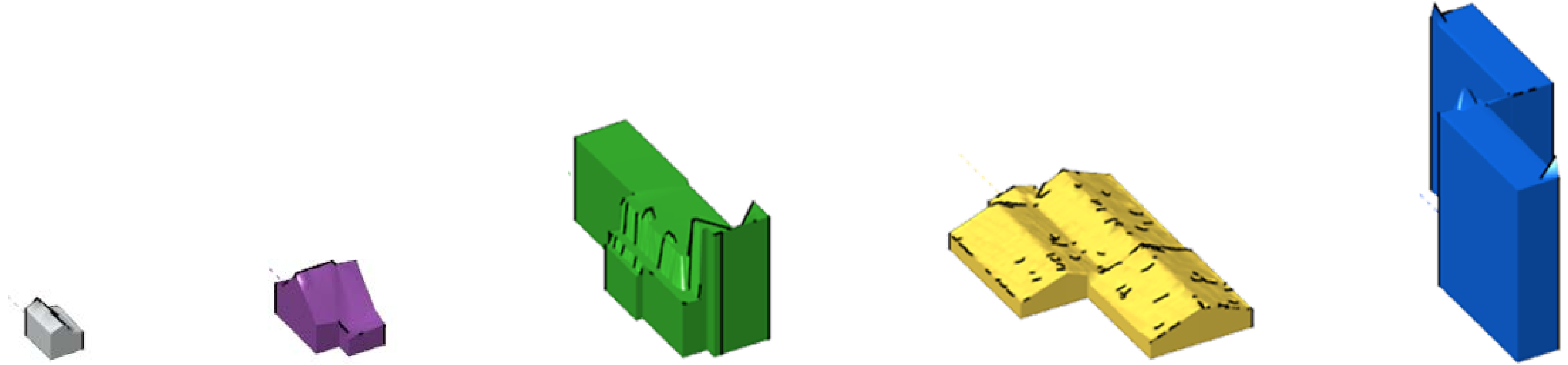

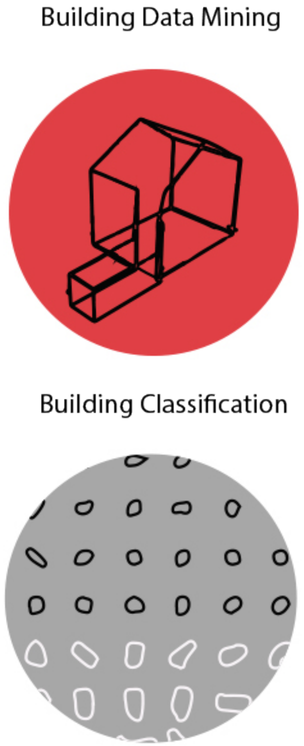

Classification: Structural Layout Class

The Geometric Layouts are further subdivided into Structural Layouts using the following classification parameters:

- Gutter Height
- Roof Steepness and Count
- Footprint Area
- Exposed Footprint Length
- Footprint Length
- Adjacency
- Number of Addresses
- Building Function

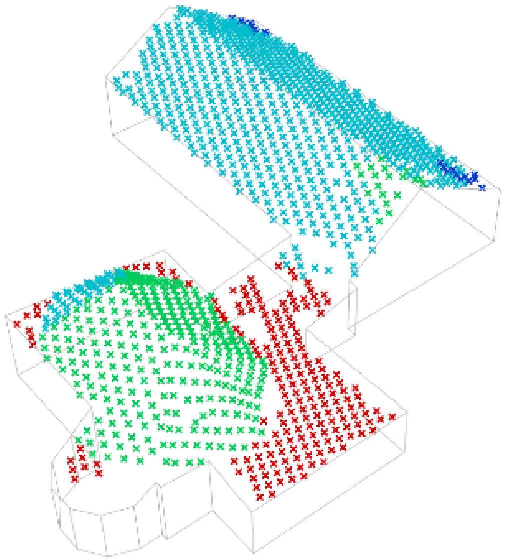

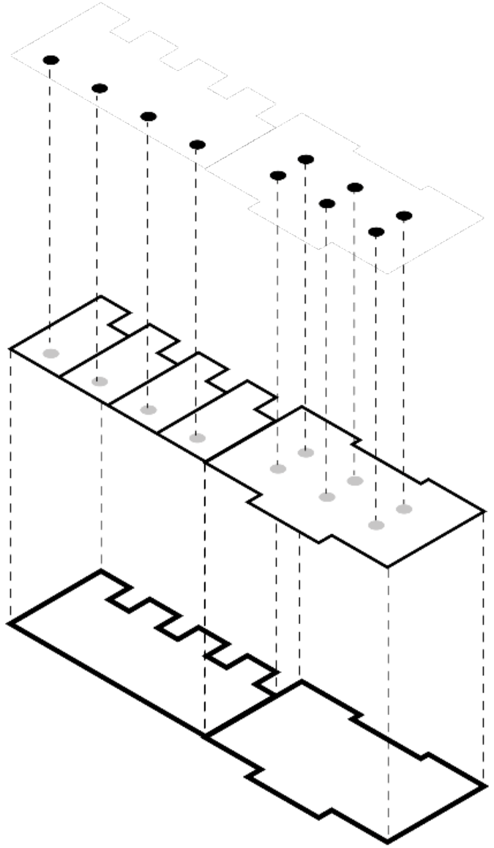

Building Classification

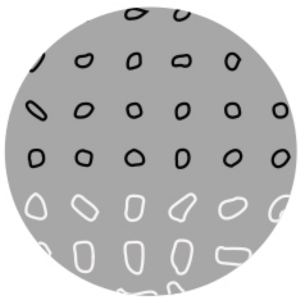

ARUP

Classification: Structural Layout Class

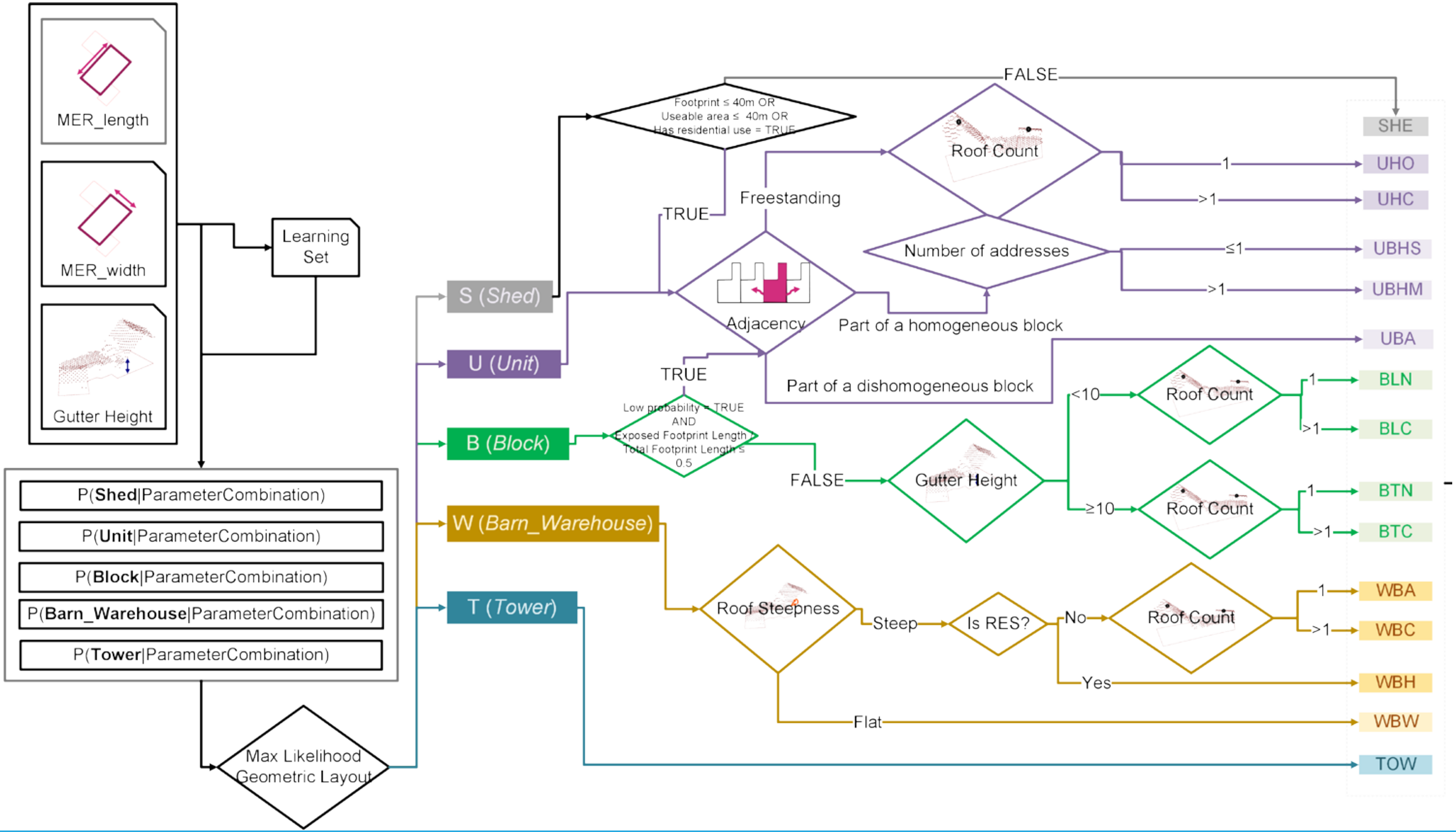

Building Classification

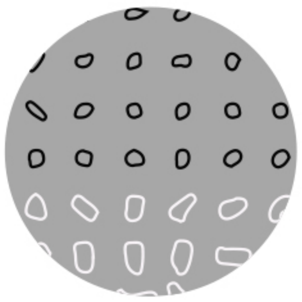

Classification: Structural Layout Overview

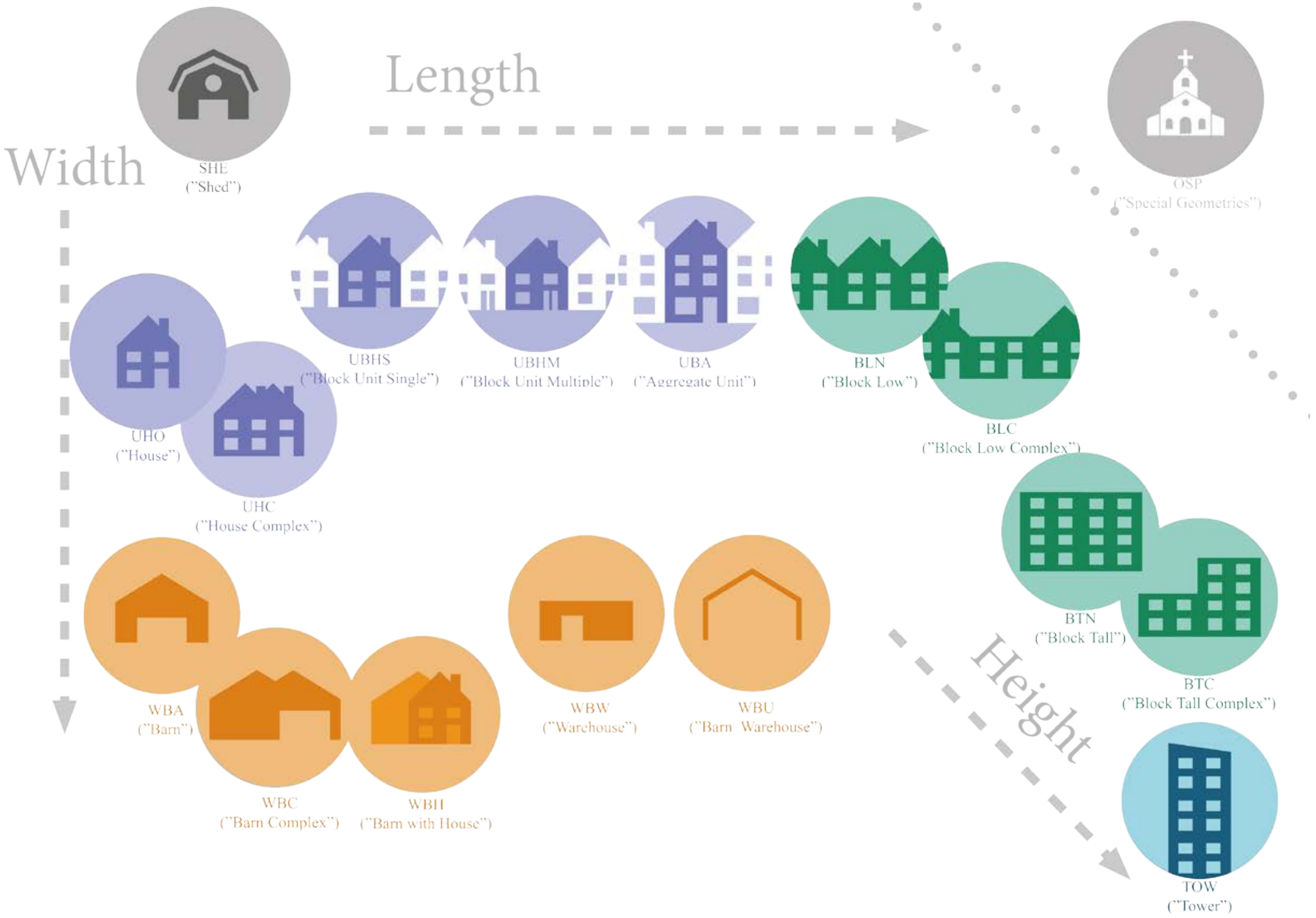

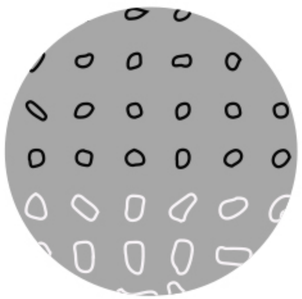

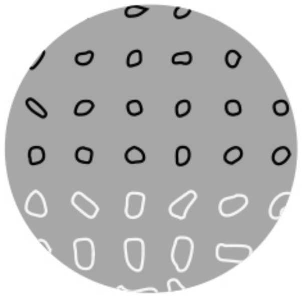

Classification: Structural Layout Project Data Verification

The assigned structural layout are verified against the following project datasets:

- Drawing data *(technical building database)*, Arup
- Farm houses, Dataland
- Special geometries, Arup
- Arup desk study data, Arup
- Desk study data, JBG

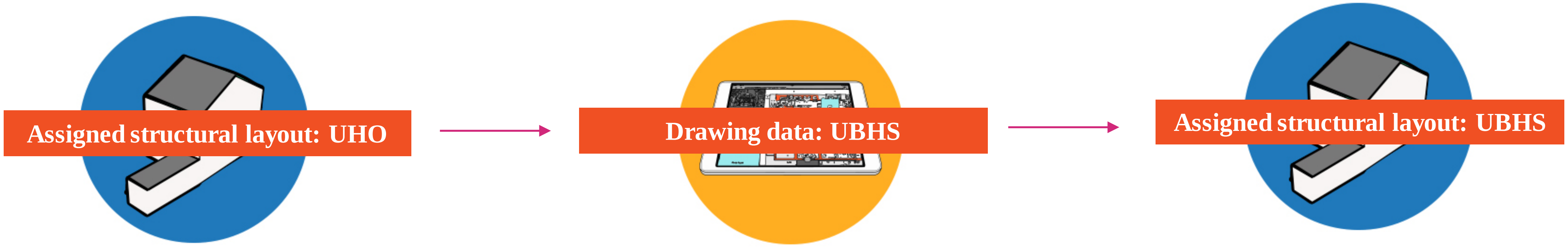

Classification: Example Structural Layout process

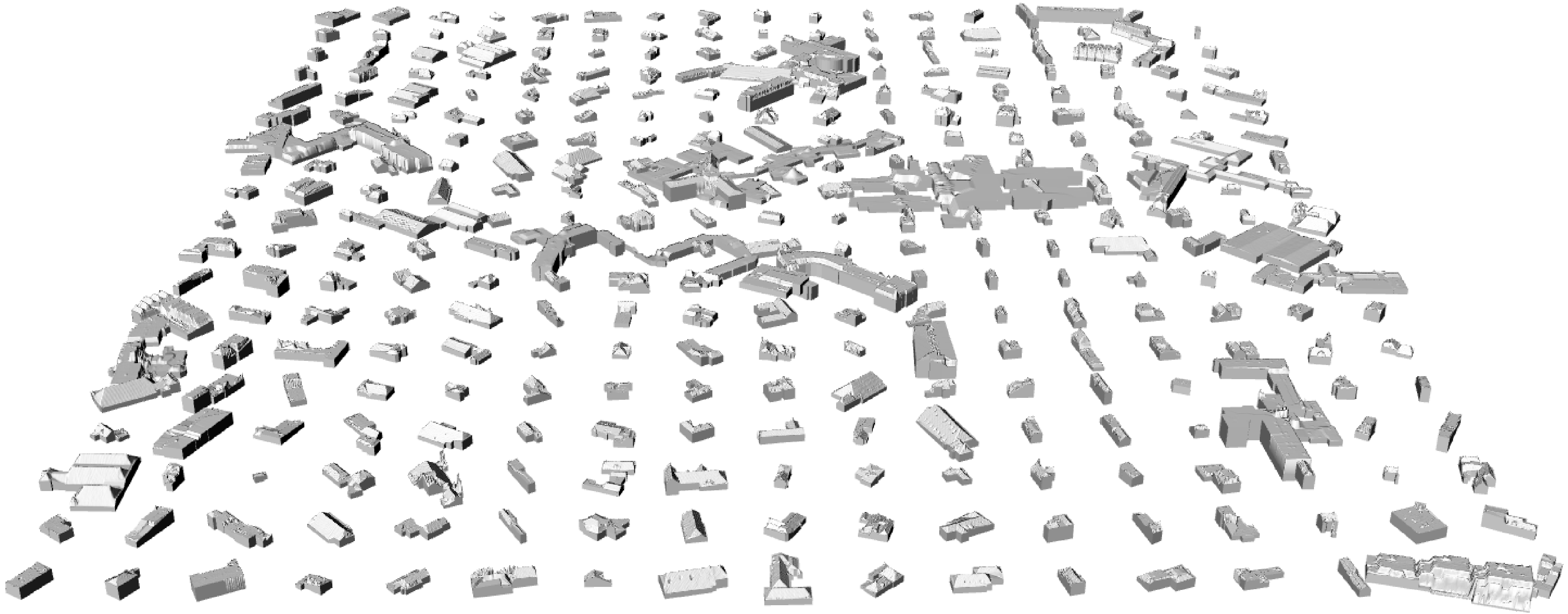

Building Classification

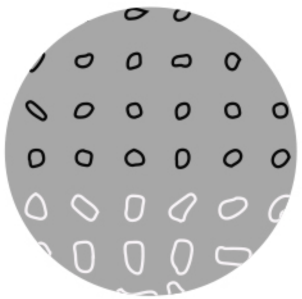

Classification: Example Structural Layout process

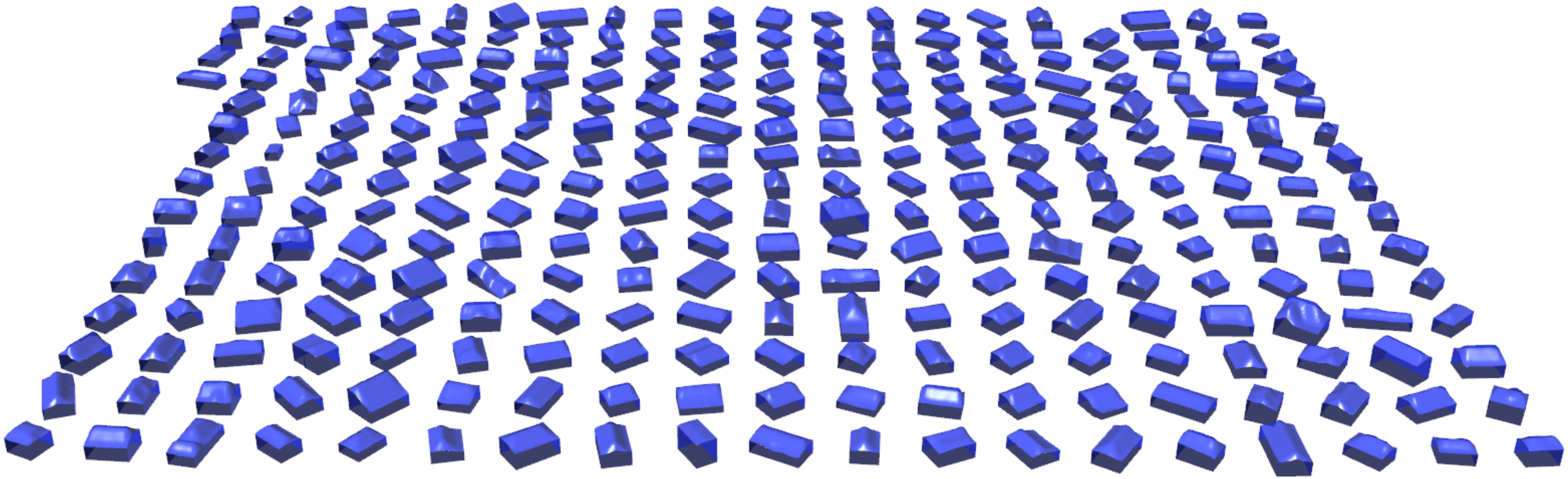

Building Classification

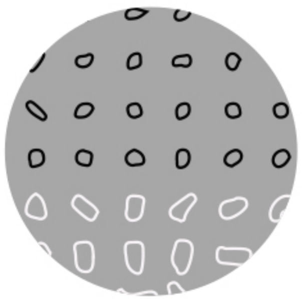

Classification: Final Structural System Assignment GEM

GLOBAL EARTHQUAKE MODEL
working together to assess risk

OPENQUAKE
calculate share explore

Mat_X / Ssy_X / Mat_Y / Ssy_Y / Ext_Wall / Floor_Mat

MAT99
MATO
CR
CR+PC
CR+CIP
MUR
MUR+CLBRS
MUR+CSBRS
MUR+MO
MUR+CB99
MUR+ST99
W
S

L99
LO
LN
LDUAL
LPB
LFM
LFBR
LH
LWAL

EW99
EWO
EWN
EW

F99
FO
FN
FC
FM
FW
FME

Structural System Inference

Structural System Inspection data

Most Likely Structural System per Building

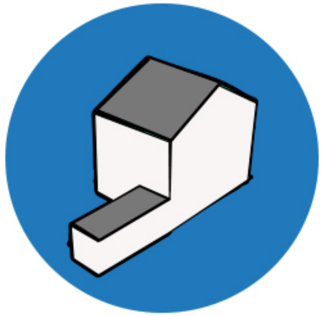

Classification: Structural System

- Inference based Structural System assignment:
  - Structural Systems are assigned through judgement-based inferences based on the Structural Layout and building year with a function modifier.
  - For buildings assigned a UBHS Structural Layout, data-driven inferences are applied.

- Inspection data Structural System assignment:
  - Assignment using full inspection data.
  - Assignment using partial inspection data.

- Special geometry Structural System assignment.

Structural System Inference

Structural System Inspection data

Most Likely Structural System per Building

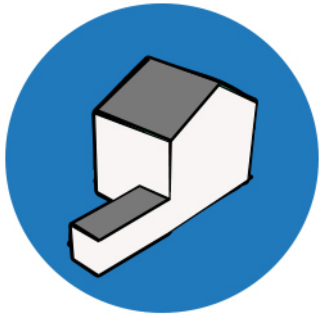

Classification: Final Structural System Assignment

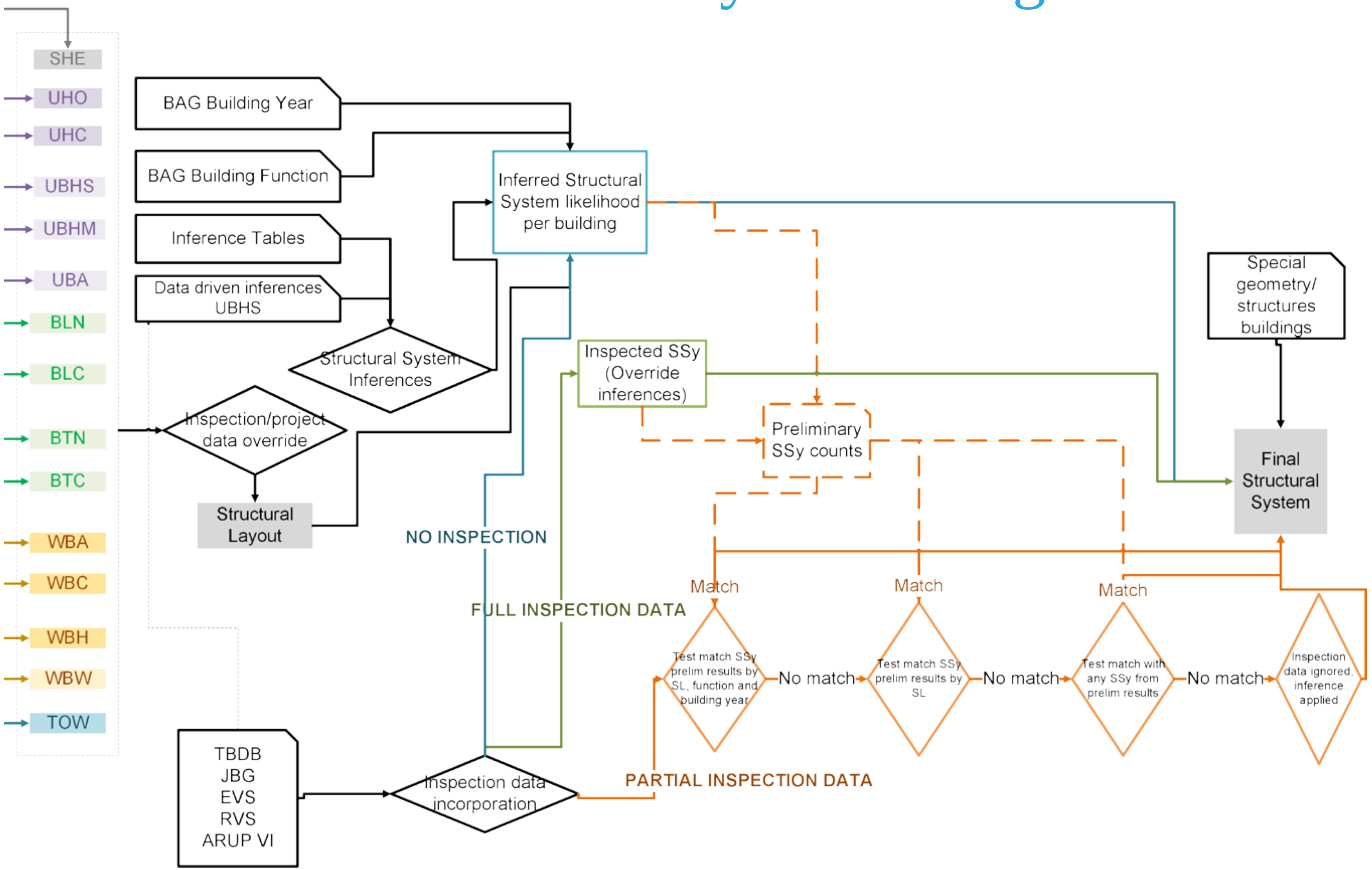

Structural System Inference

Structural System Inspection data

Most Likely Structural System per Building

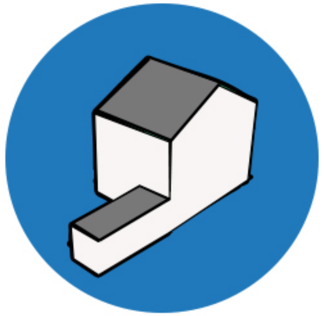

ARUP

Classification: Determination of Structural System

Creation of Expert Judgment inferences using:

- Online surveys with Dutch Engineers and related evaluation workshops.
- Literature studies on Dutch Structural Systems.
- Investigation on changes in Dutch legislation.

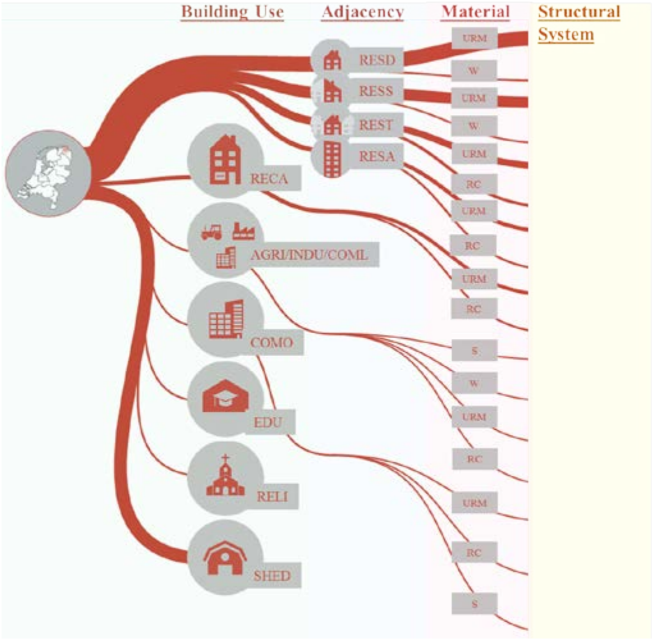

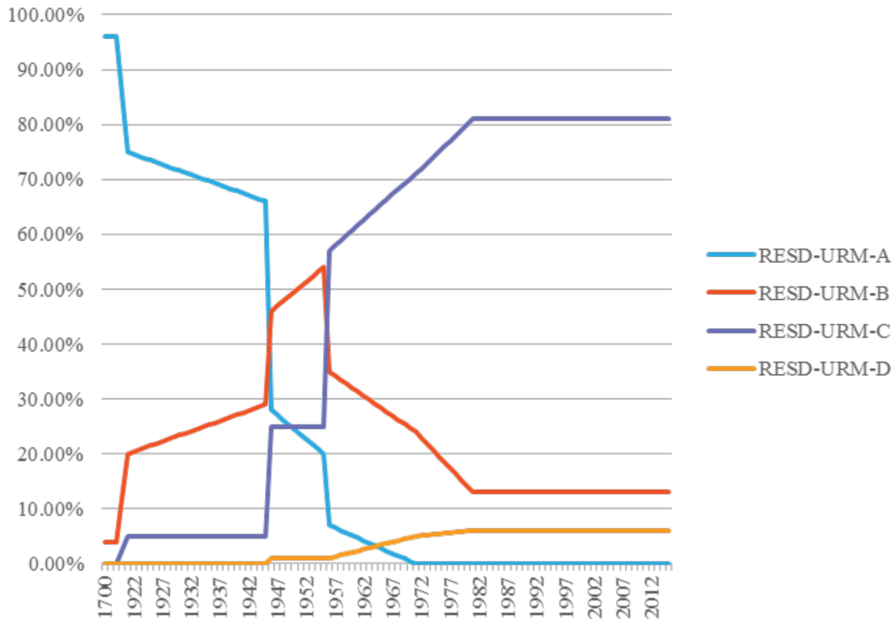

Structural System Inference

Building Classification

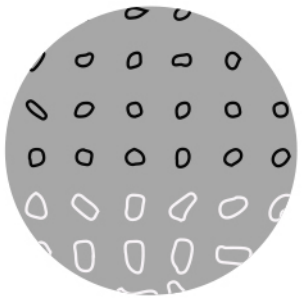

Classification: Structural System judgment based inferences

Structural System Inference for buildings in the UH Structural Layout class

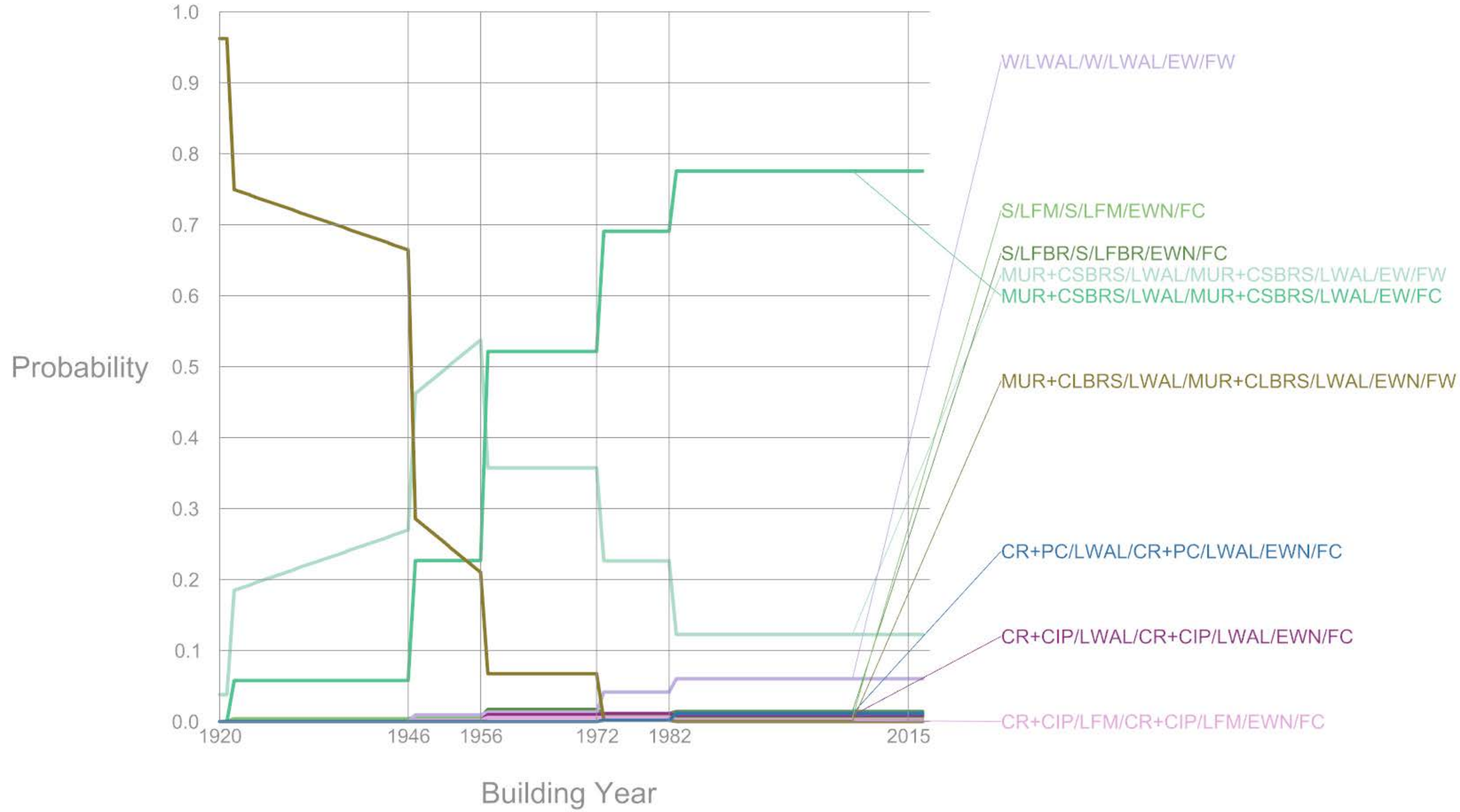

Structural System Inference

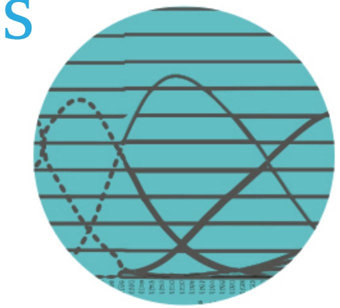

Most Likely Structural System per Building

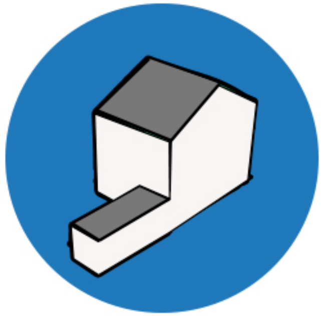

Classification: Structural System data driven inferences

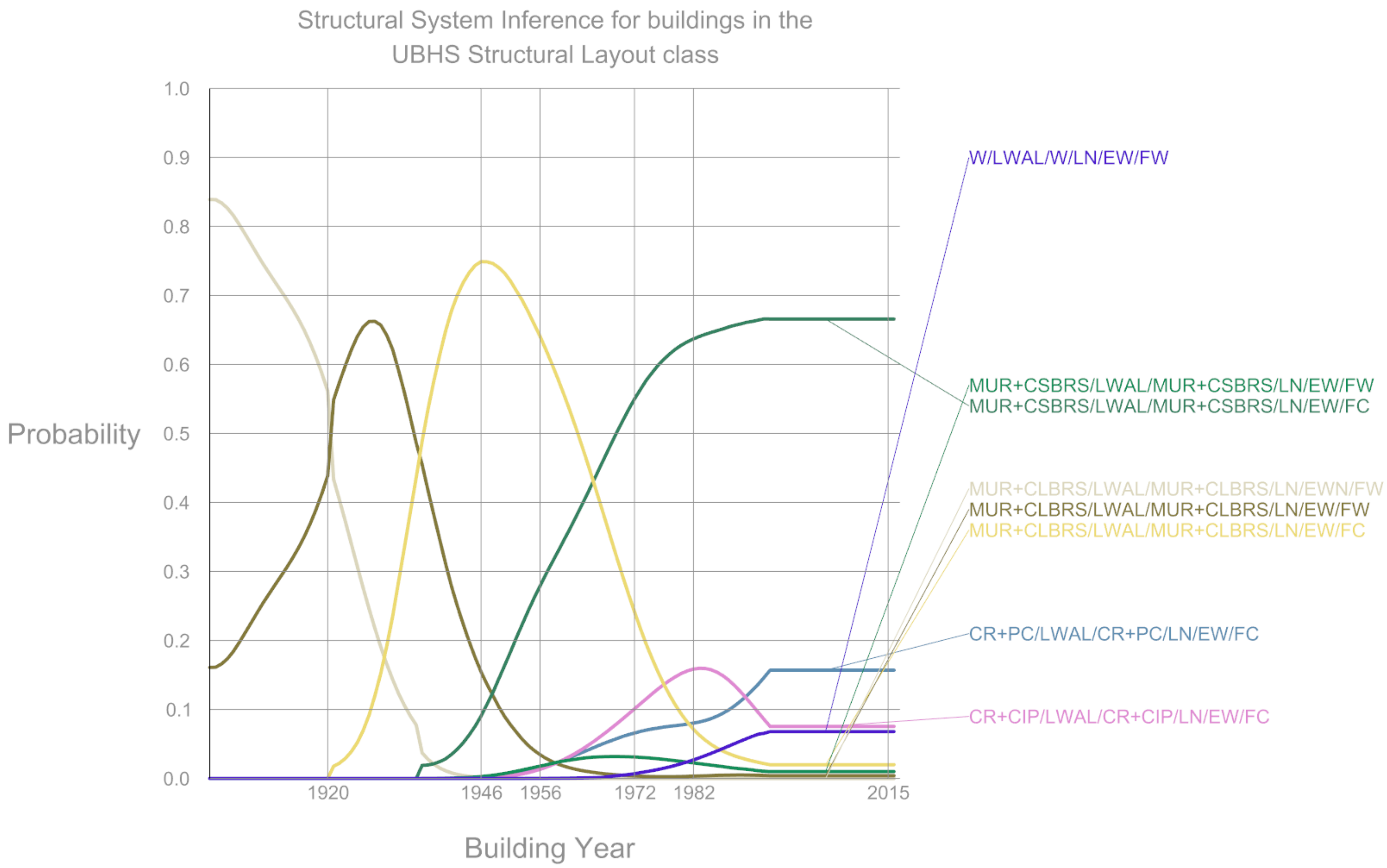

Structural System Inference

Most Likely Structural System per Building

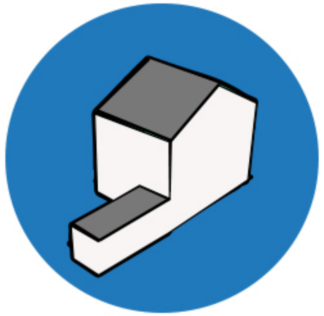

Classification Check: Inspections vs Data driven comparison

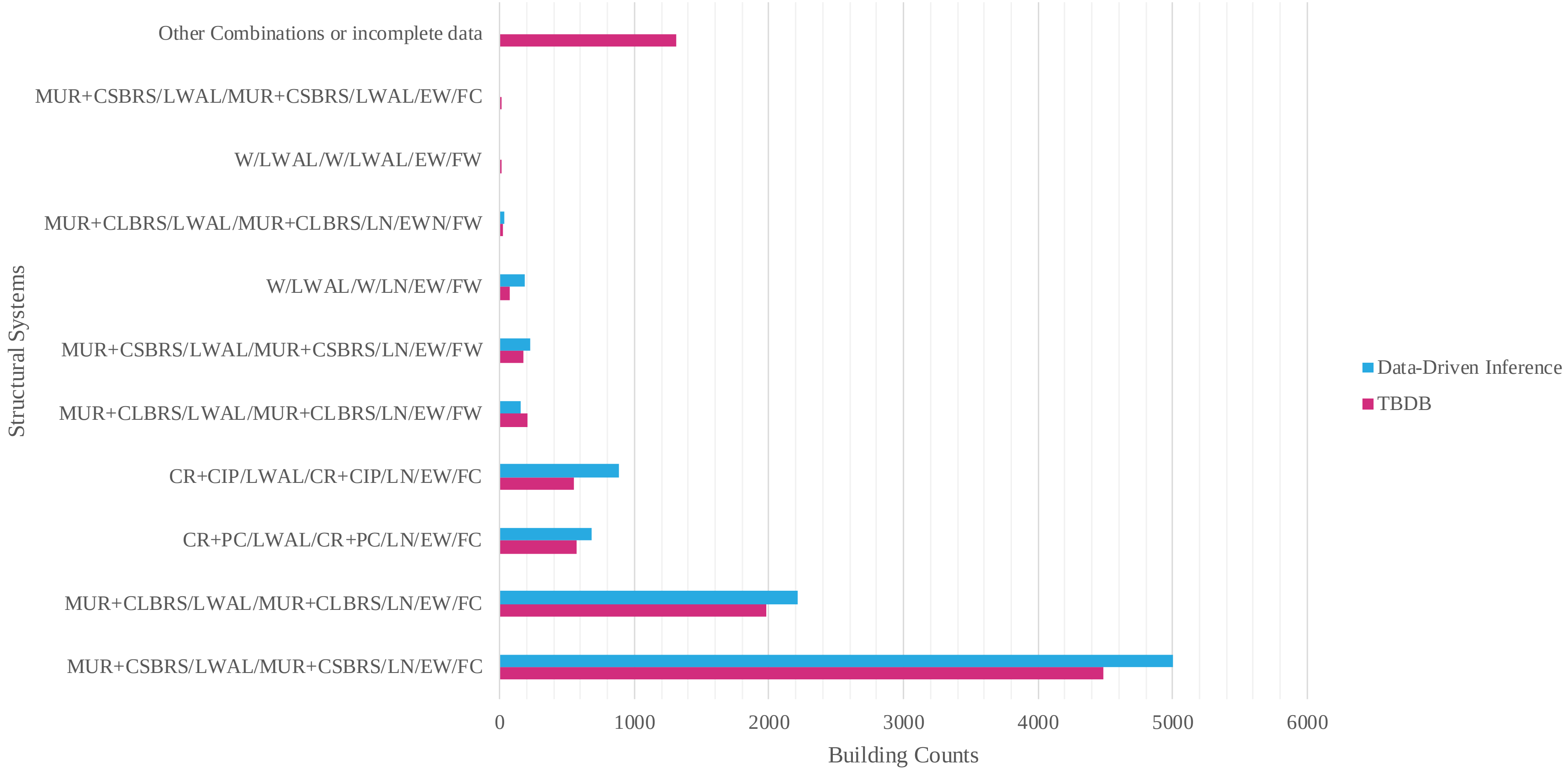

Classification: Available Inspection Data

Total amount of buildings with inspection: **26 847**.

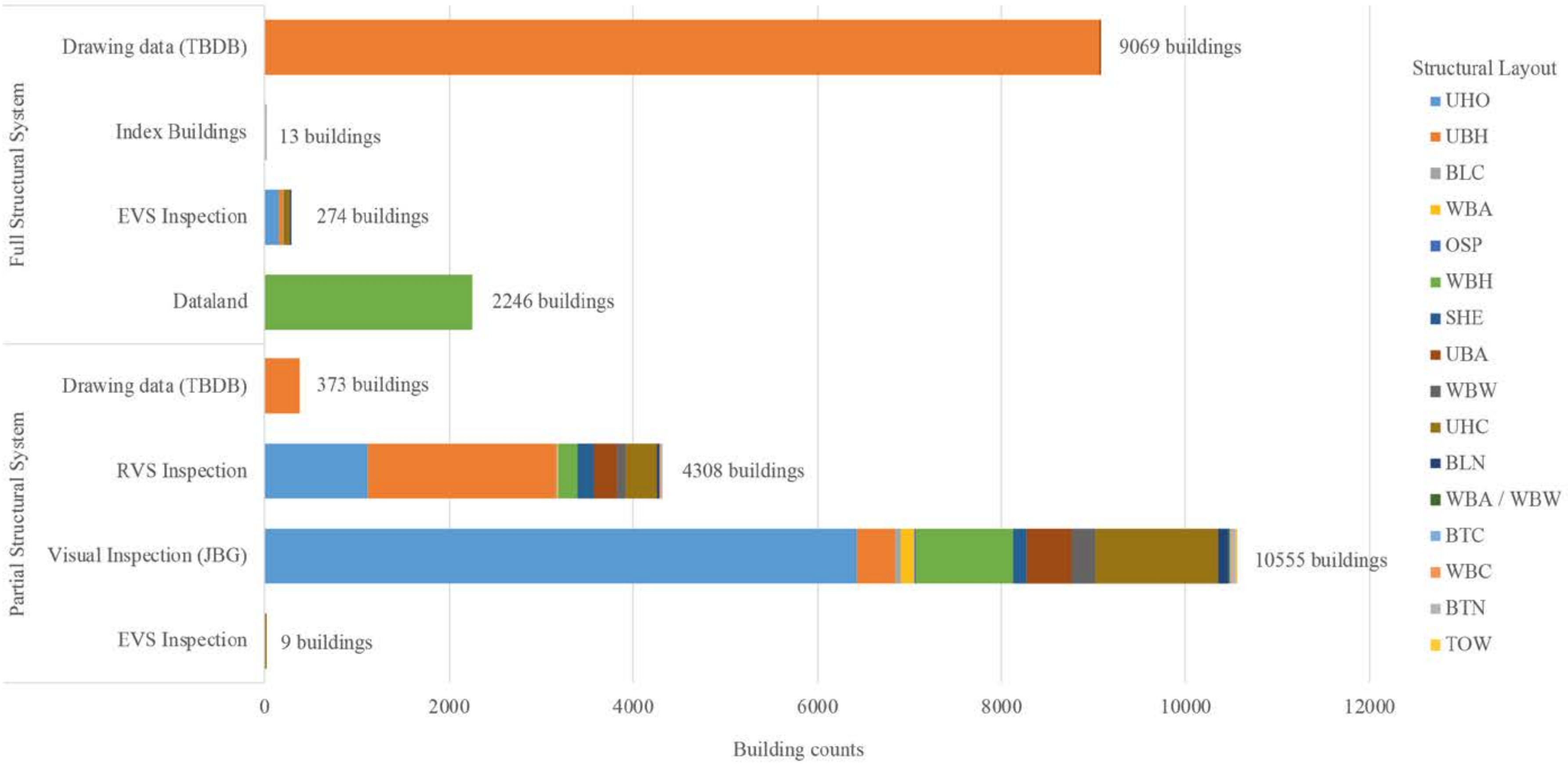

Structural System Inspection data

Most Likely Structural System per Building

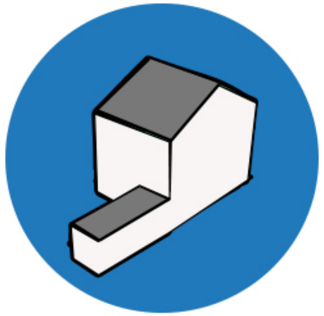

Process

ARUP

Classification: Example GEM Strings using Inspection Data

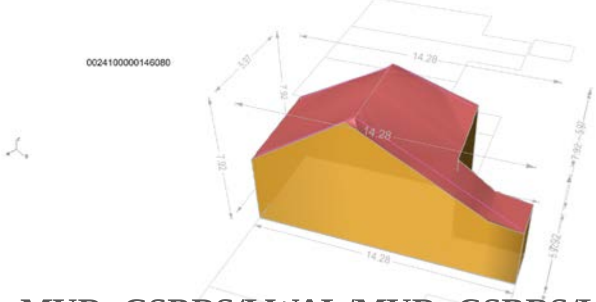

MUR+CSBRS/LWAL/MUR+CSBRS/LN/EW/FC – 65%
MUR+CSBRS/LWAL/MUR+CSBRS/LWAL/EW/FC – 11%
MUR+CLBRS/LWAL/MUR+CLBRS/LN/EW/FW – 10%
CR+CIP/LWAL/CR+CIP/LWAL/EWN/FC – 5%
CR+CIP/LWAL/CR+CIP/LN/EW/FC – 4%
MUR+CLBRS/LWAL/MUR+CLBRS/LWAL/EWN/FW – 2%
MUR+CSBRS/LWAL/MUR+CSBRS/LN/EW/FC – 1%
CR+PC/LWAL/CR+PC/LN/EW/FC – 1%
W/LWAL/W/LWAL/EWN/FW – 1%

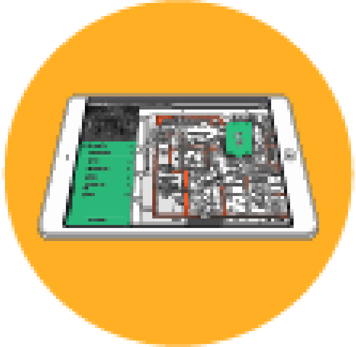

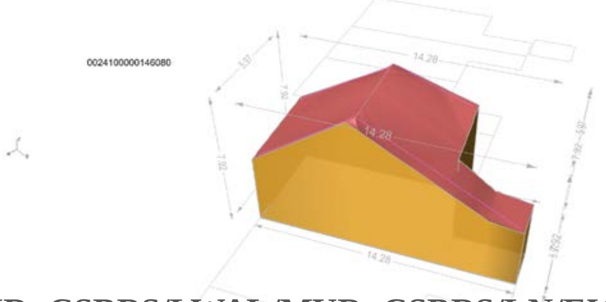

MUR+CSBRS/LWAL/MUR+CSBRS/LN/EW/FC – 100%
~~MUR+CSBRS/LWAL/MUR+CSBRS/LWAL/EW/FC – 0%~~
~~MUR+CLBRS/LWAL/MUR+CLBRS/LN/EW/FW – 0%~~
~~CR+CIP/LWAL/CR+CIP/LWAL/EWN/FC – 0%~~
~~CR+CIP/LWAL/CR+CIP/LN/EW/FC – 0%~~
~~MUR+CLBRS/LWAL/MUR+CLBRS/LWAL/EWN/FW – 0%~~
~~MUR+CSBRS/LWAL/MUR+CSBRS/LN/EW/FC – 0%~~
~~CR+PC/LWAL/CR+PC/LN/EW/FC – 0%~~
~~W/LWAL/W/LWAL/EWN/FW – 0%~~

Most Likely Structural System per Building

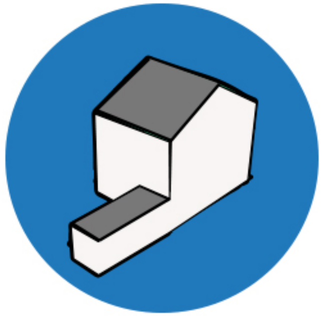

MUR+CSBRS / LWAL / MUR+CSBRS / LN/ / FC

Process

ARUP

Classification: Special Geometries

We also have a number of buildings which have special / unique geometries.
The total amount of special geometries: **1031** buildings.
Of the 1031 building, 149 or ~ 14% have addresses *(i.e. may be populated)*.

Most Likely Structural System per Building

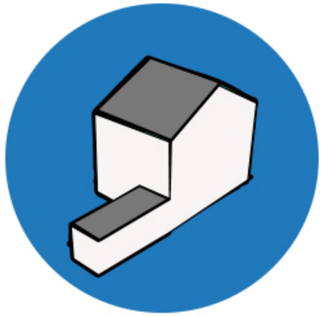

Classification: Confidence Flag

Confidence coefficient	Description
0	Assigned a Structural System only through its building year as no layout or function data was available.
1	Assigned a Structural System through function related inferences. This occurs when data is missing for the building's Structural Layout.
2	Assigned a Structural System through Structural-Layout- based inferences. This occurs when data is missing for the building's function.
3	Assigned a Structural System through Structural-Layout-based inferences and function related inferences, from data driven inferences or through special geometries.
4	Assigned a Structural System partially through inspection data.
5	Assigned a full Structural System through inspection data.

Structural System
Inspection data

Most Likely Structural System
per Building

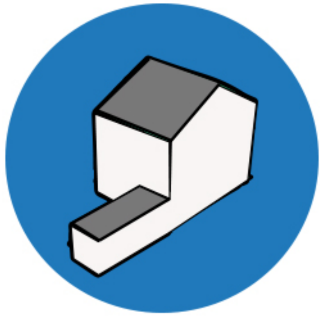

Building Data Mining

Process
ARUP

1900
1985
2007
1970
1975
2006
1973
1973
1883
1961
1987
1876
1954
1972
1972
1972
1972
1975
1972
1989
1989
1989
1989
1985
1972
1972
1972
1996
1985
1922
1978
1972
1972
1919
1923
1920
1934
1974
1974
1974
1974
Structural System Inference

Process


MUR+CSBRS/LWAL
MUR+CLBRS/LWAL
MAT99/LN
MUR+CSBRS/LWAL
MUR+CSBRS/LN
MUR+CSBRS/LN
MUR+CSBRS/LWAL
MUR+CLBRS/LWAL
MUR+CSBRS/LN
MAT99/LN
MUR+CSBRS/LN
MUR+CSBRS/LN
MUR+CSBRS/LN
MUR+CLBRS/LWAL
MUR+CSBRS/LH
MAT99/LN
MUR+CSBRS/LN
MUR+CSBRS/LWAL
MUR+CSBRS/LN
MUR+CSBRS/LN
W/LWAL
MUR+CSBRS/LN
MUR+CSBRS/LWAL
MAT99/LN
MUR+CLBRS/LWAL
MUR+CSBRS/LN
MUR+CLBRS/LWAL
MUR+CSBRS/LN
MUR+CLBRS/LWAL
MUR+CLBRS/LWAL
MUR+CSBRS/LWAL
MUR+CSBRS/LN
MUR+CSBRS/LN
MUR+CSBRS/LN
MUR+CSBRS/LN
Most Likely Structural System
per Building


0
1
2
3
4
5
Structural System
Inspection data


Legend
Inspections
Dataland - Full Structural System
EVS - Full Structural System
EVS - Partial Structural System
Index buildings - Full Structural System
Visual Inspections - Partial Structural System
RVS - Partial Structural System
Drawing Data (TBDB) - Full Structural System
Drawings Data (TBDB) - Partial Structural System
Buildings

3 // Results

ARUP

Results Geometric Layout

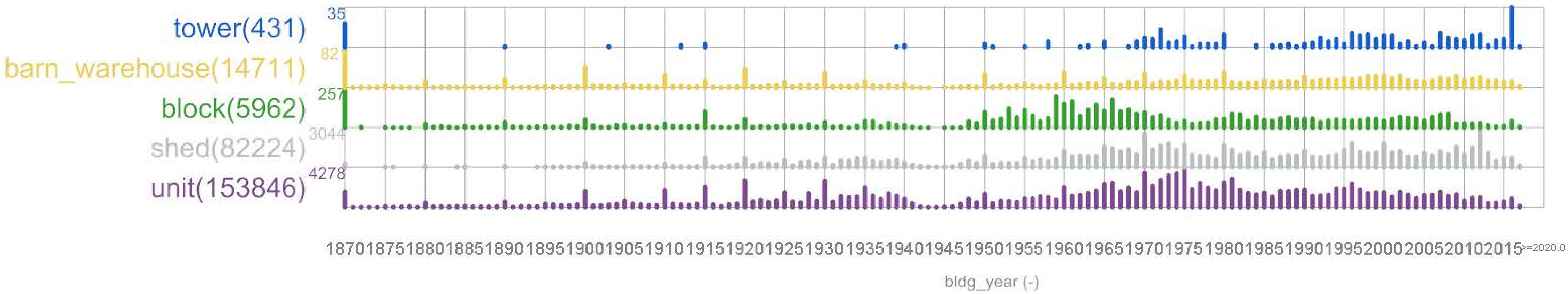

Results Structural Layout

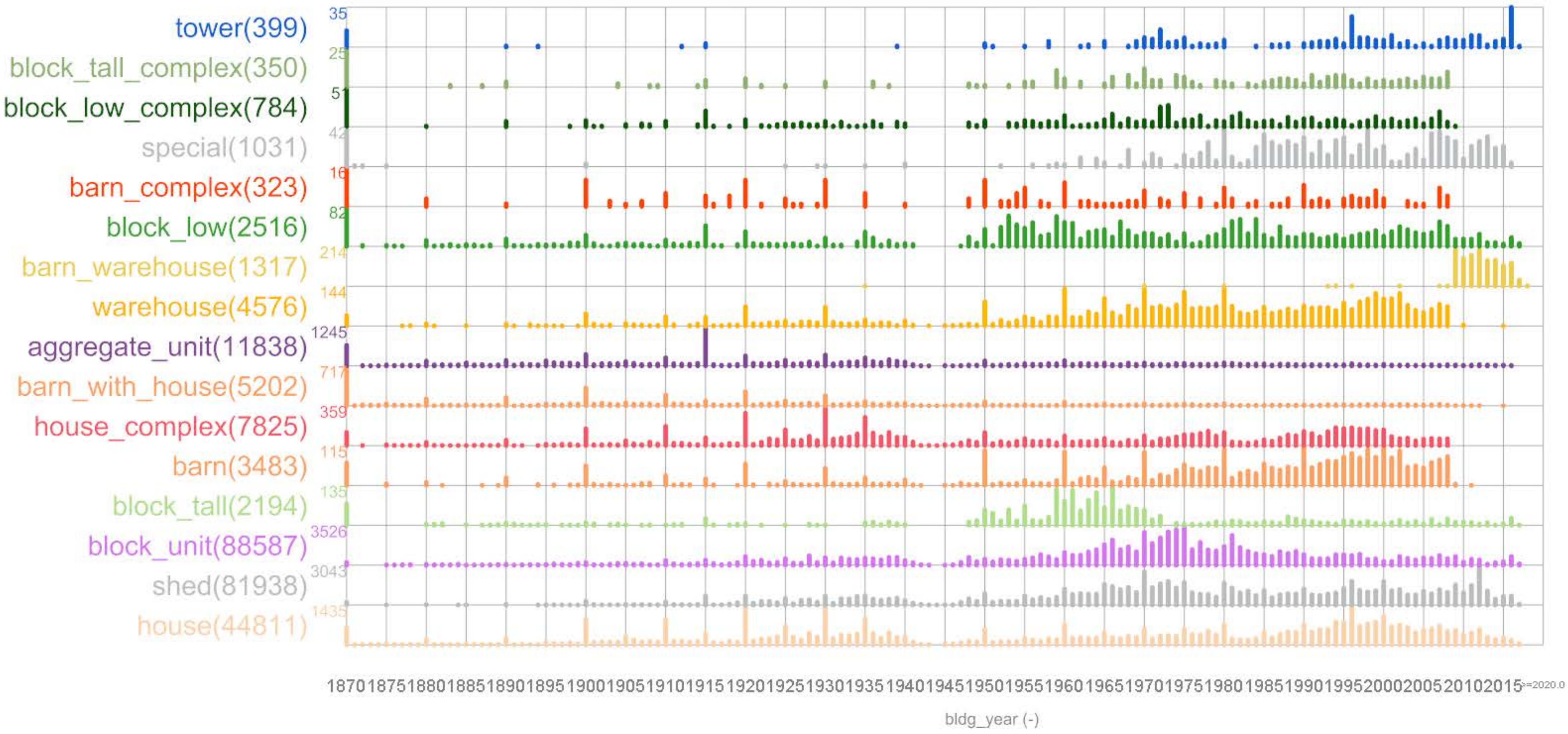

Results Structural Layout

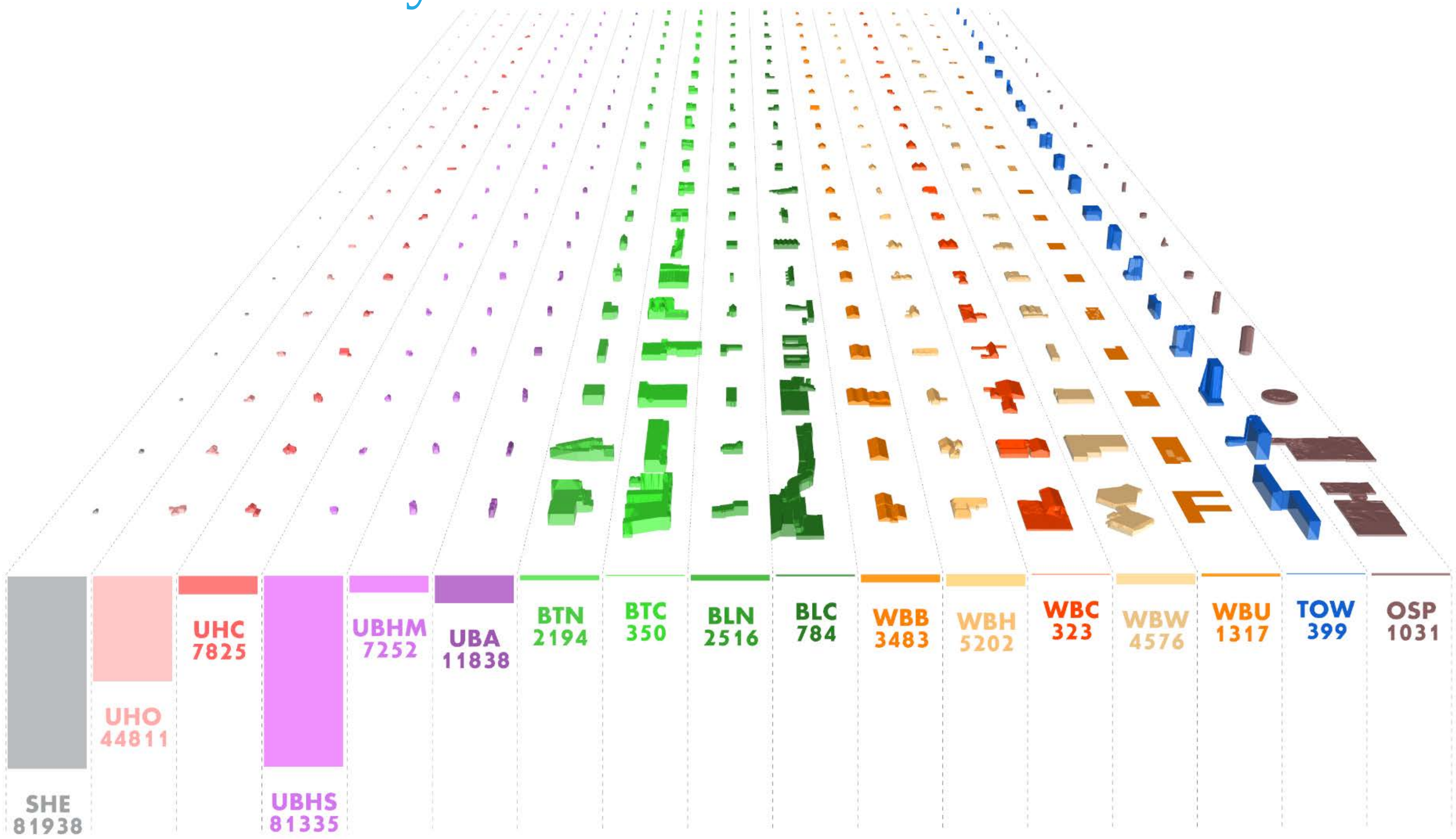

Results Structural System

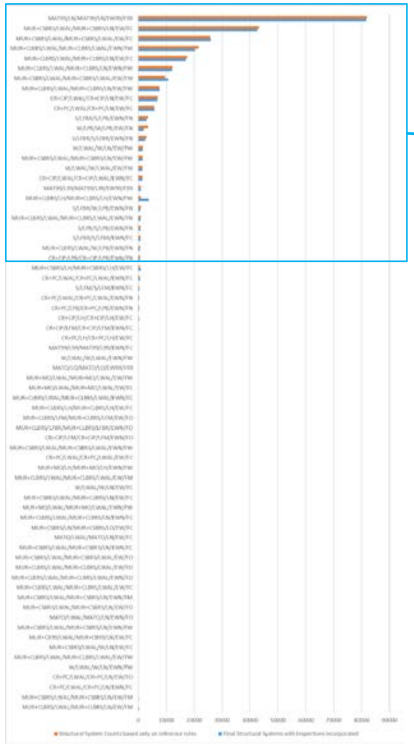

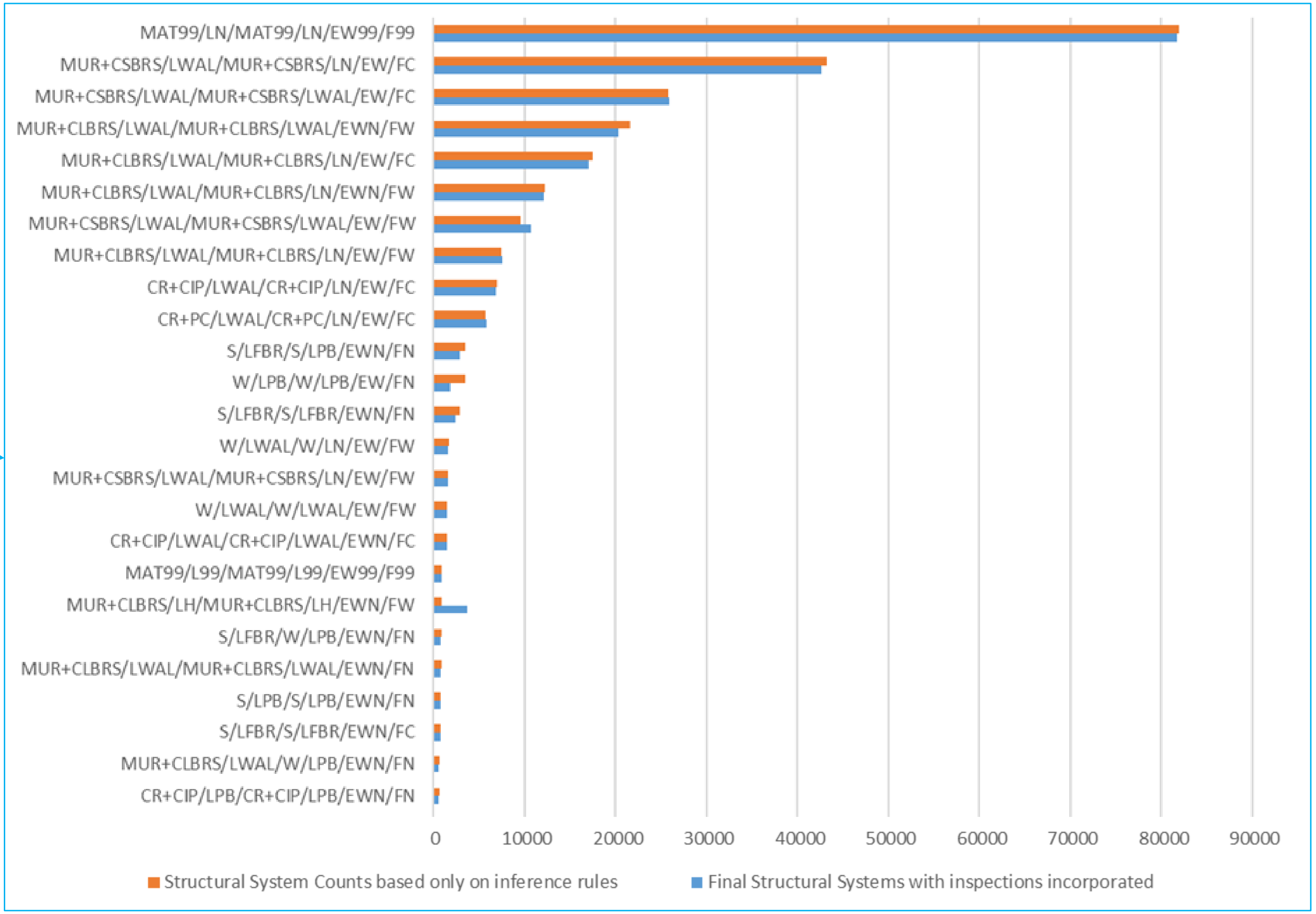

Results Structural System

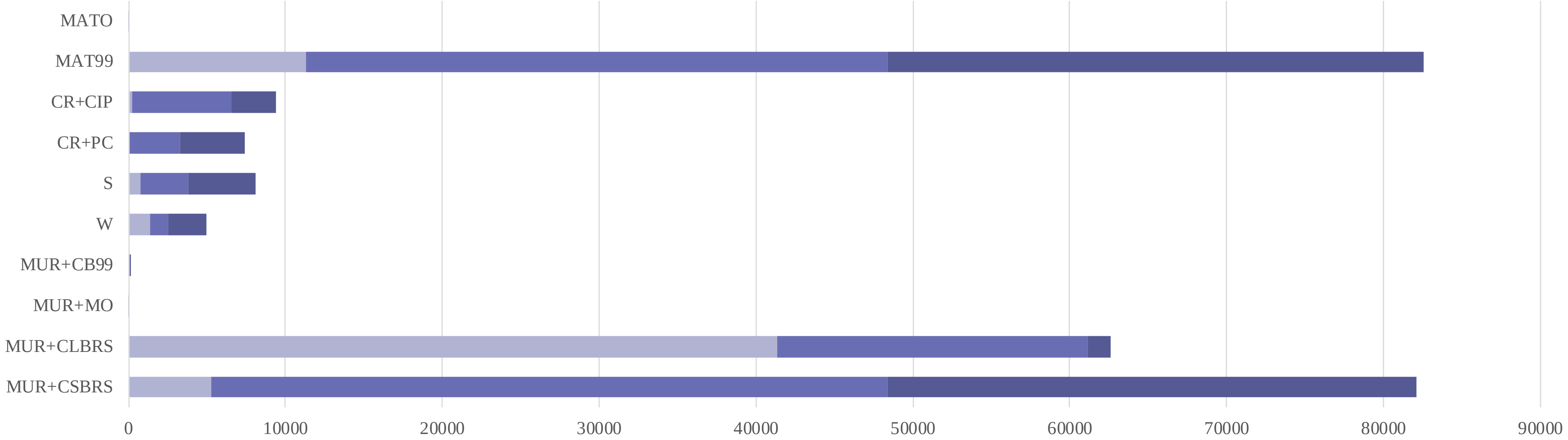

	MUR+CSBRS	MUR+CLBRS	MUR+MO	MUR+CB99	W	S	CR+PC	CR+CIP	MAT99	MATO
building_year<1945	5292	41325	5	0	1340	749	57	234	11270	3
1945<=building_year<=1985	43088	19802	2	39	1139	3041	3224	6339	37101	20
building_year>1985	33717	1446	1	0	2478	4295	4111	2853	34199	6

Population: Input Data

- Population data (NCG, November 2016): number of residents per BAG_VBO_ID
- School data (DUO, oktober 2016): number of pupils/students per educational institute
- Day Care data (https://www.landelijkregisterkinderopvang.nl oktober 2016)
- Time use report ‘Met het oog op de tijd’ (Sociaal Cultureel Planbureau, 2013): specification how people in The Netherlands spend their time
- Footfall data for a selection of buildings (Tony Taig, October 2015): number of passers-by per BAG_BUILDING_ID, during day and night
- Calculation factor for runners-out (Tony Taig, February 2016): multiplication factor times people inside, during day and night
- Mapping table (NAM, February 2016): identify buildings with guests/customers/patients (specified per Dataland object code).

Population

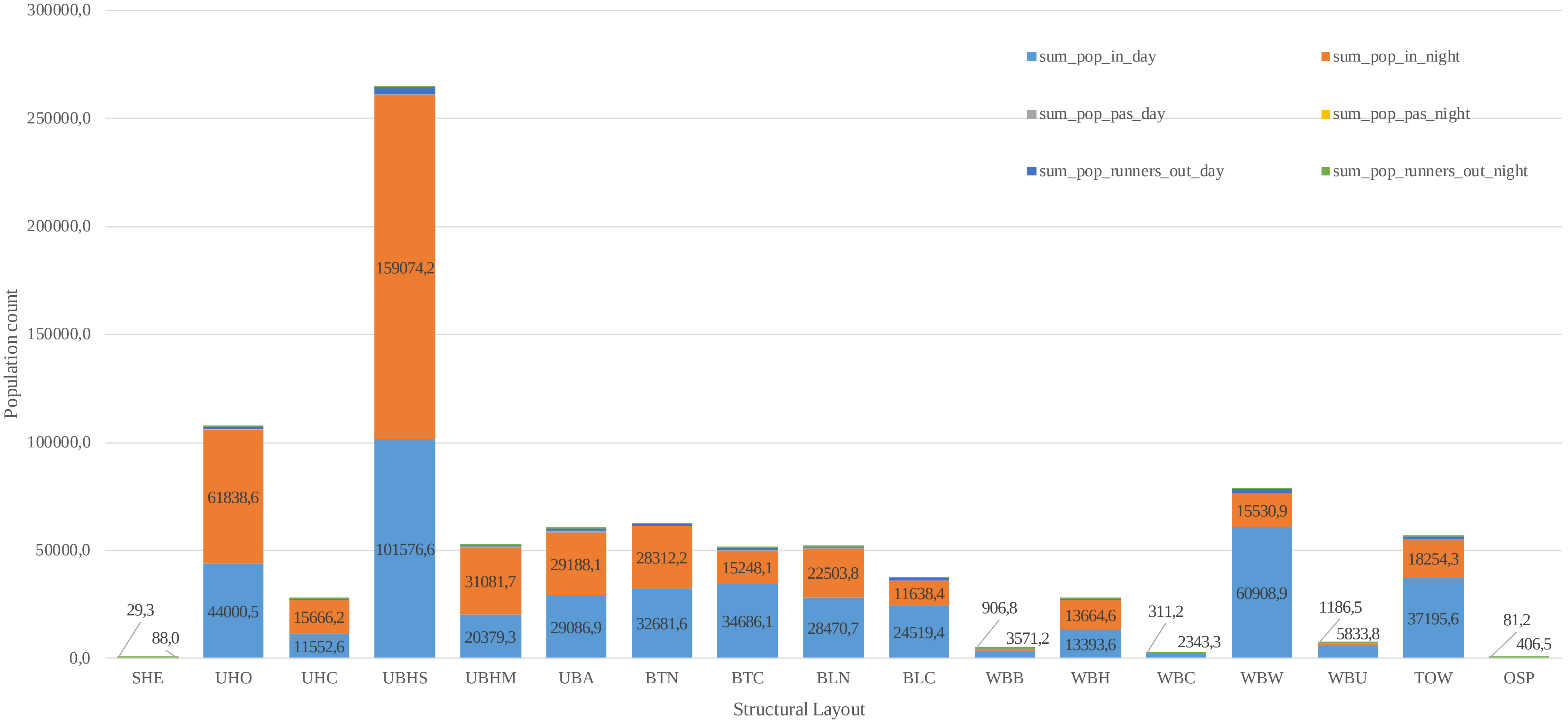

300000,0
250000,0
200000,0
150000,0
100000,0
50000,0
0,0
Population count
sum_pop_in_day
sum_pop_in_night
sum_pop_pas_day
sum_pop_pas_night
sum_pop_runners_out_day
sum_pop_runners_out_night
29,3
88,0
61838,6
44000,5
15666,2
11552,6
159074,2
101576,6
31081,7
20379,3
29188,1
29086,9
28312,2
32681,6
15248,1
34686,1
22503,8
28470,7
11638,4
24519,4
906,8
3571,2
13664,6
13393,6
311,2
2343,3
15530,9
60908,9
1186,5
5833,8
18254,3
37195,6
81,2
406,5
SHE
UHO
UHC
UBHS
UBHM
UBA
BTN
BTC
BLN
BLC
WBB
WBH
WBC
WBW
WBU
TOW
OSP
Structural Layout

Exposure Database Status Monitor dashboard

ARUP

edb_structural_layout ▾

enter pand id

Building attribute	Value
Pand id	0003100000125453
BAG view	Go to webpage
Streetview	Go to webpage
Geometry class	unit
Missing geometry parameter	false
Structural layout	block_unit
Missing descision-tree parameter	false
Low probability	false
Overwrite	true
Structural System confidence	4
MUR+CSBRS/LWAL/MUR+CSBRS/LN/EW/FC	0.26
CR+CIP/LWAL/CR+CIP/LN/EW/FC	0.24
MUR+CSBRS/LWAL/MUR+CSBRS/LWAL/EW/FC	0.24
CR+PC/LWAL/CR+PC/LN/EW/FC	0.24
MUR+CLBRS/LWAL/MUR+CLBRS/LN/EW/FC	0.01

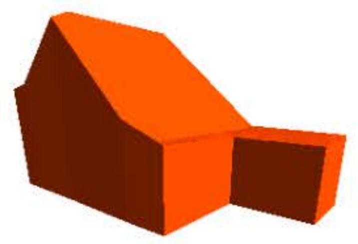

Thank You

ARUP

Experimental testing programme for URM materials characterisation at TU Delft

Assurance meeting Hazard & Risk, Schiphol, 21-22 February 2018

- *Samira Jafari, Rita Esposito, Jan Rots et al., TU Delft*
- *Collaboration with Beatriz Zapico-Blanco, Arup, and with EU Centre and TU/e*

Aim and scope

- To feed constitutive/computational masonry models in ELS and LS-Dyna with representative materials input parameters, so that – after validation against structural tests – the models can be projected towards H&R fragility
- Strength, stiffness and toughness (softening, complete stress-strain laws)
- Tension, shear and compression
- Orthotropy included
- Applicable to continua and discontinua
- Lab and in-situ
- Existing and replicated masonry

(Indirect) tension

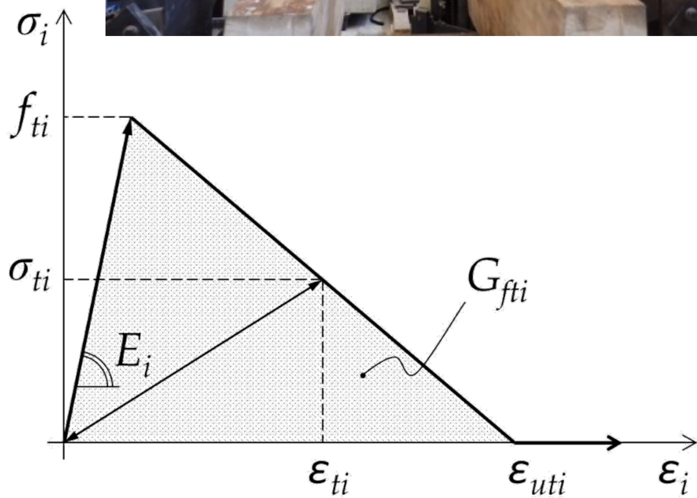

Flexural and bond wrench tests

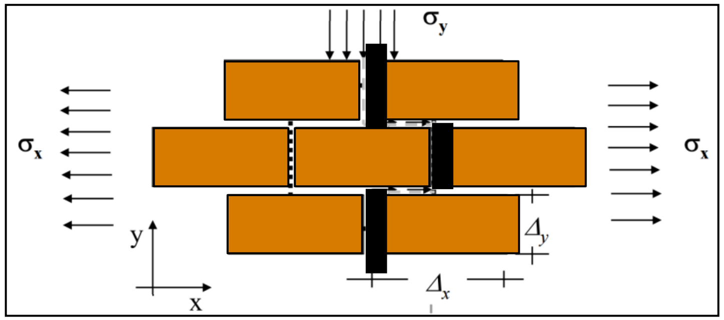

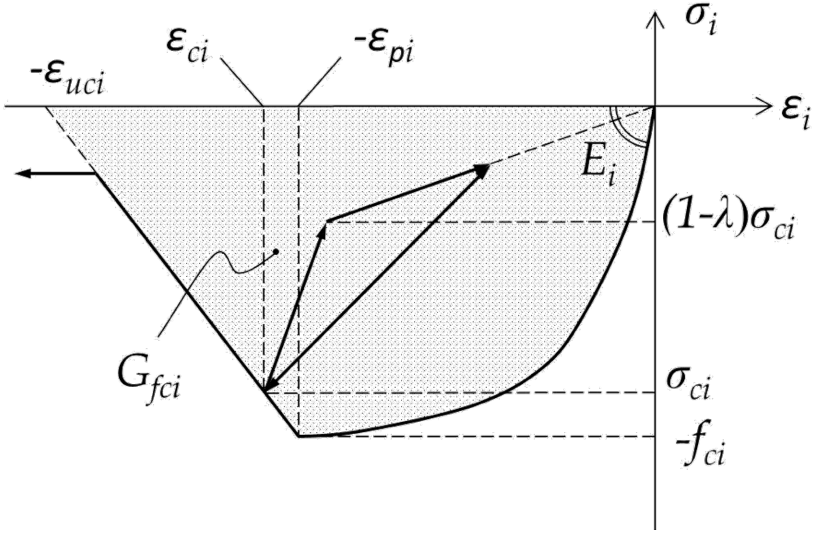

Compression

Shear

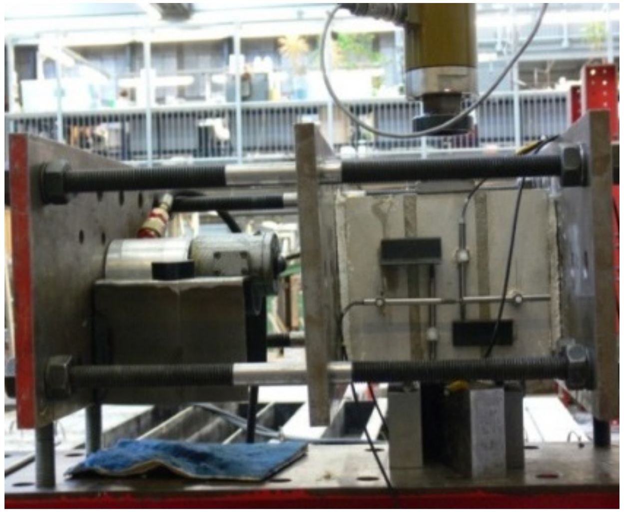

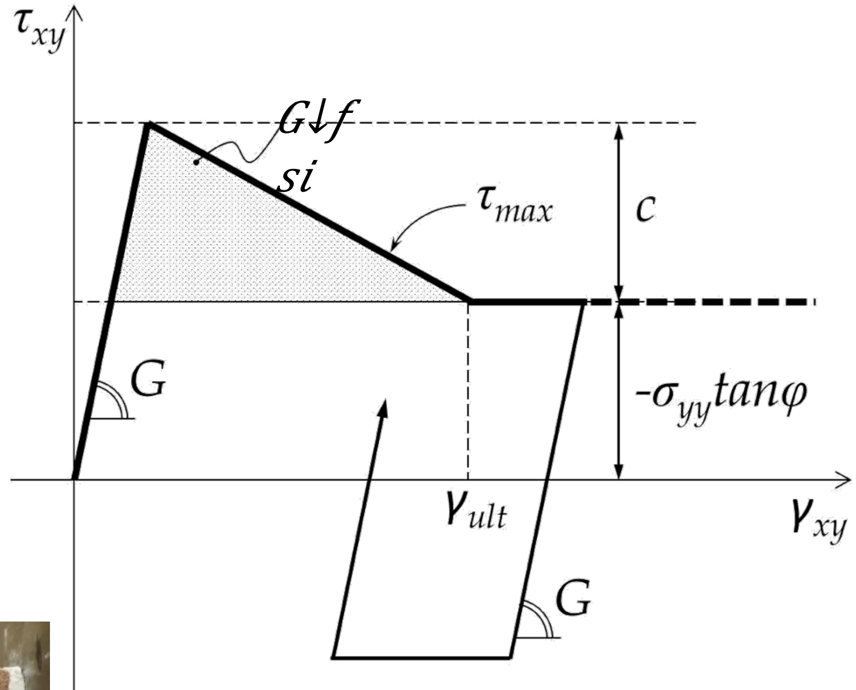

Triplet tests

Building stock in Groningen

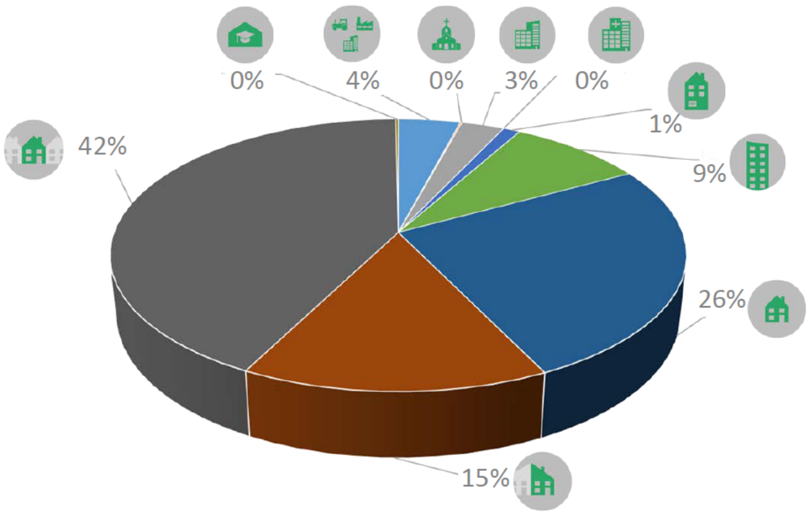

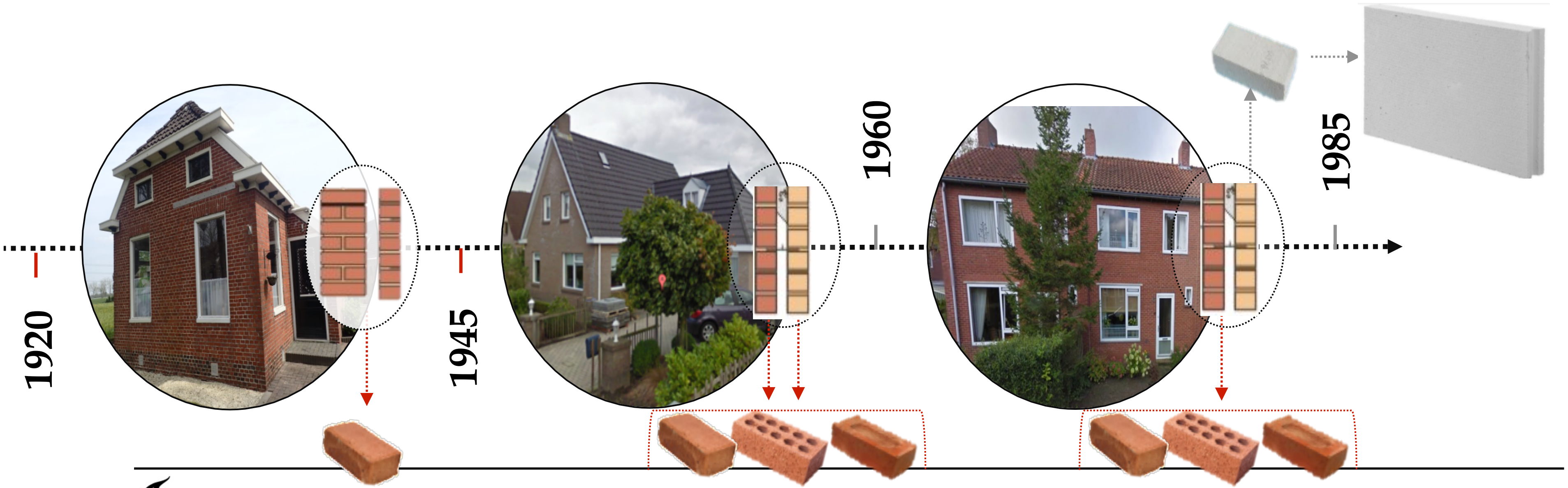

TU Delft

Source pie chart: TU Delft Open Course Ware, Introduction to Seismic Essentials in Groningen

Existing masonry tested 2014-2017

Lab tests

In – situ tests

Source : EU Centre Arup TU Delft report – Material characterisation v1.3

Overview of the houses tested in 2014-2017





	Type	Code	Y.o.C.	Quality	Compression		Four-point-bending			Shear	Bond wrench	Brick	
					Vert.	Horiz.	OOP1	OOP2	IP			Comp.	Bending
Clay brick masonry	Solid	HOG-H1	1912	Poor	-	-	-	1	-	-	7	6	6
	Solid	WIR-H1	1920	Good	3	2	-	3	3	9	6	6	12
	Solid	MID-H1.1	1920	Good	3	-	-	-	-	9	-	-	6
	Solid	MID-H1.2	1920	Good	3	-	-	-	-	9	-	-	-
	Solid	ROE-S1.1	1922	Good	5	-	-	-	3	9	6	6	6
	Solid	ROE-S1.2	1922	Good	-	-	-	-	3	9	6	-	6
	Solid	MOL-H1	1932	Poor	3	-	-	-	-	9	-	5	6
	Solid	MOL-H2	1932	Poor	3	-	-	-	-	9	-	-	-
	Solid	WIL-H2	1952	Good	3	6	-	3	3	9	6	-	6
	Solid	ROE-S2	1955	Good	5	-	-	3	3	9	6	-	6
	Solid	BEA-S1	1955	Poor	5	-	-	3	3	9	6	6	5
	Solid	KWE-H2	1958	Good	4	-	-	1	3	9	6	6	6
	Solid	ROE-S3	1985	Good	2	-	-	2	2	9	6	6	5
	Perforated	TRIA-S2	1984	Poor	6	-	3	4	3	6	4	-	-
	Solid	ROE-S3-I	1988	Poor	4	-	-	2	2	9	-	-	-
	Perforated	TIL-H2	1990	Good	-	-	3	3	3	-	13	6	6
	perforated	BEA-S2	2001	Good	8	-	-	3	2	10	5	-	6
	Frogged	HOO-H2	2013	Poor	5	-	-	-	2	9	3	6	6
CS brick masonry		WIL-H1	1952	Poor	2	3	-	-	-	10	-	4	12
		BEA-H1	1958	Poor	2	2	-	-	-	9	2	6	12
		ZIJL-H1	1976	Poor	6	-	2	1	-	7	6	-	11
		LAG-H1	1978	Good	3	3	-	-	2	9	5	6	12
		SCH-H1	1978	Good	5	-	-	-	3	9	2	6	6
		TRIA-S1	1984	Poor	5	-	1	-	3	6	8	-	-
		TIL-H1	1990	Poor	3	3	-	-	-	5	-	6	6
		KWE-H1	1995	Poor	-	-	-	-	-	-	-	6	6

Lab inspection | In-situ inspection

Overview of the houses tested in 2014/2017





					sion		Four-point-bending			Shear	Bond wrench	Brick	
						Horiz.	OOP1	OOP2	IP			Comp.	Bending
Clay brick masonry						-	-	1	-	-	7	6	6
						2	-	3	3	9	6	6	12
						-	-	-	-	9	-	-	6
						-	-	-	-	9	-	-	-
						-	-	-	3	9	6	6	6
						-	-	-	3	9	6	-	6
						-	-	-	-	9	-	5	6
						-	-	-	-	9	-	-	-
						6	-	3	3	9	6	-	6
	Solid	BEA-S1	1955	Poor									
	Solid	KWE-H2	1958	Good									
	Solid	ROE-S3	1985	Good									
	Perforated	TRIA-S2	1984	Poor									
	Solid	ROE-S3-I	1988	Poor									
	Perforated	TIL-H2	1990	Good									
	perforated	BEA-S2	2001	Good									
	Frogged	HOO-H2	2013	Poor									
CS brick masonry		WIL-H1	1952	Poor	2	3	-	-	-	10	-	4	12
		BEA-H1	1958	Poor	2	2	-	-	-	9	2	6	12
		ZIJL-H1	1976	Poor	6	-	2	1	-	7	6	-	11
		LAG-H1	1978	Good	3	3	-	-	2	9	5	6	12
											2	6	6
											8	-	-
											-	6	6
											-	6	6

Lab inspection

Overview of the houses tested in 2014/2017

Poor quality

	Frogged	HOO-H2	2013	Poor	5	-	-	-	2	9	3	6	6
CS brick masonry		WIL-H1	1952	Poor	2	3	-	-	-	10	-	4	12
		BEA-H1	1958	Poor	2	2	-	-	-	9	2	6	12
		ZIJL-H1	1976	Poor	6	-	2	1	-	7	6	-	11
		LAG-H1	1978	Good	3	3	-	-	2	9	5	6	12
		SCH-H1	1978	Good	5	-	-	-	3	9	2	6	6
		TRIA-S1	1984	Poor	5	[illegible]	1	[illegible]	3	6	8	-	-
											-	6	6
											-	6	6

In-situ inspection

TU Delft

Overview of the houses tested in 2014/2017

Good quality

CS brick masonry	WIL-H1	1952	Poor	2	3	-	-	-	10	-	4	12
	BEA-H1	1958	Poor	2	2	-	-	-	9	2	6	12
	ZIJL-H1	1976	Poor	6	-	2	1	-	7	6	-	11
	LAG-H1	1978	Good	3	3	-	-	2	9	5	6	12
	SCH-H1	1978	Good	5	-	-	-	3	9	2	6	6
	TRIA-S1	1984	Poor	5		1		3	6	8	-	-
										-	6	6
										-	6	6

In-situ inspection

Overview of the houses tested in 2014-2017

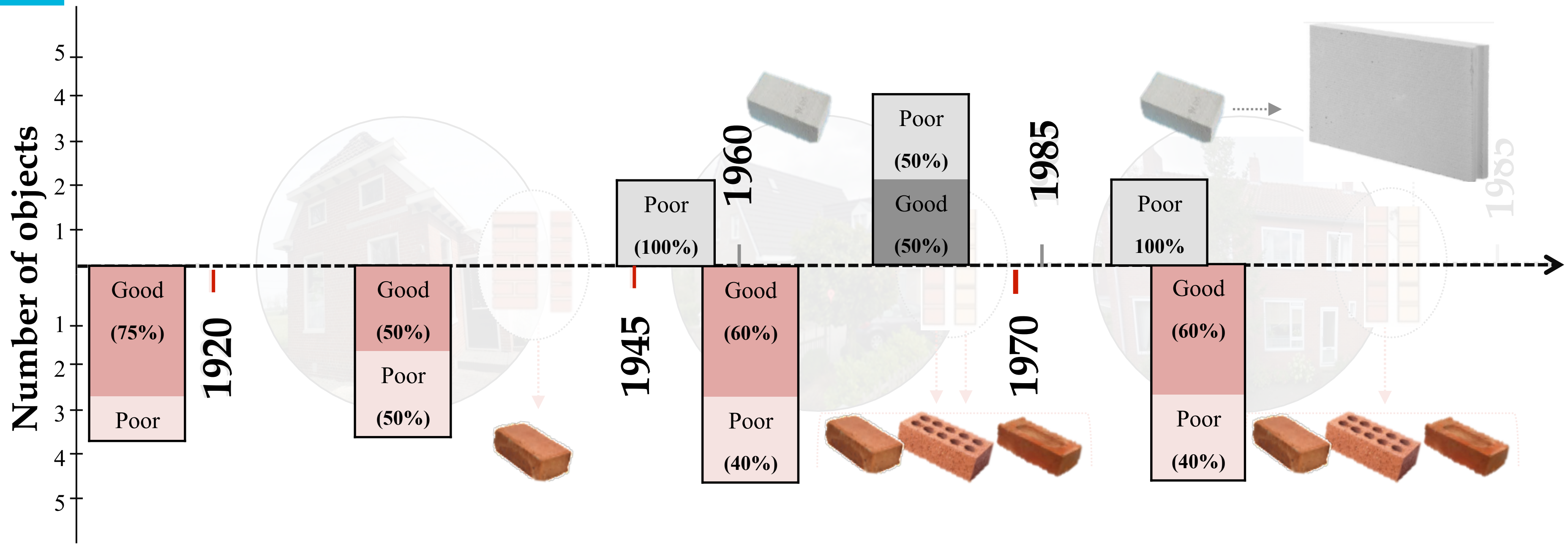

TU Delft

Concrete outcomes of material tests

Table F.2 — Mean values of material properties for different types of masonry

Symbol	Material property	Masonry (strength and stiffness values in N/mm², fracture energy values J/m²)			
		Clay brickwork (pre 1945) [d]	Clay brickwork (post 1945)	Calcium-silicate brickwork with general purpose mortar (typical approx. 1960-present)	Calcium-silicate blocks/elements with thin layer mortar (typical approx. [illegible] present)
f'_m	Compressive strength	8,5	10,0	7,0	[illegible]
E_m	Young's modulus	5 000	6 000	4 000	[illegible]
G_m	Shear modulus	2 000	2 500	1 650	[illegible]
f_{x1}	Bending strength for plane of failure parallel to the bed joints [a]	0,15	0,3	[illegible]	0,6
f_{x2}	Bending strength for plane of failure perpendicular to the bed joints [a]	0,55	[illegible]	[illegible]	1,0
$f_{mt\perp}$	Uniaxial tensile strength perpendicular to the bed joint	[illegible]	[illegible]	0,1	0,4
$f_{mt//}$	Uniaxial tensi[illegible] parallel to [illegible]	[illegible]	0,55	0,35	0,65
f_{v0}	[illegible]	0,3	0,4	0,25	0,8
[illegible]	[illegible] friction	0,75	0,75	0,6	0,8
[illegible]	[illegible]acture energy [b] in tension perpendicular to the bed joints	10	10	10	20
$G_{ft//}$	Fracture energy [b] in tension parallel to the bed joints	35	35	20	20
G_{fc}	Fracture energy [c] in compression	20 000	15 000	15 000	20 000
G_{fs}	Fracture energy [b] in shear (bed joint)	100	200	100	200

[a] Not to be used in combination with softening
[b] To be used in combination with a crack band width, in case of smeared finite element models
[c] To be used in combination with a crush band width, in case of smeared finite element models
[d] When clay brickwork pre 1945 is of a clearly poor quality in terms of mortar quality, mortar ageing, filling of joints, layout and bond pattern, the mean values of strength, stiffness and fracture energy properties in this column are advised to be reduced by approximately 40%

Compressive behaviour

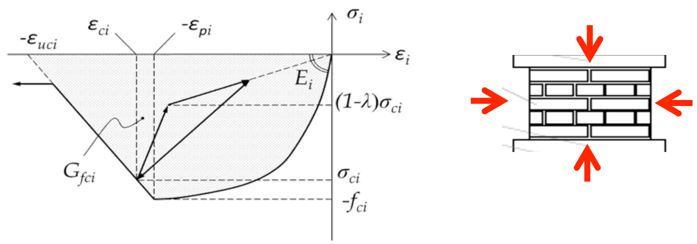

Tensile behaviour

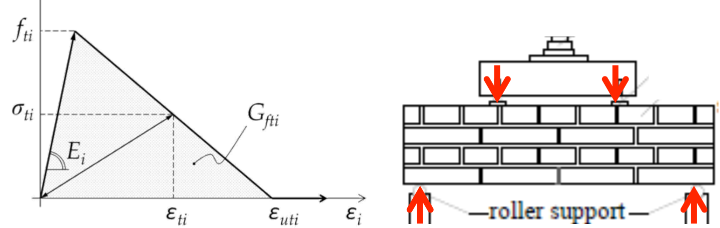

Shear behaviour

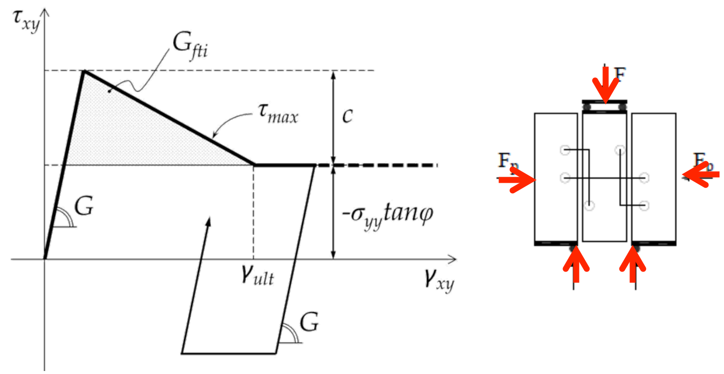

Overview test results
Compared with mean values tabulated in NEN-NPR 9998:2017

Material properties of Clay brick masonry		Unit	**Clay masonry pre 1945**				**Clay masonry post 1945**			
			All	Poor quality	Good quality	**NPR 2017**	All	Poor quality	Good quality	**NPR 2017**
Compressive strength of masonry in the	Vertical	MPa	10	4	12	**8.50**	15	11	20	**10.00**
	Horizontal	MPa	11	-	11		11	-	11	
Elastic chord modulus of masonry	Vertical	GPa	5	3	8	**5.00**	8	5	10	**6.00**
	Horizontal	GPa	9	-	9		5	-	5	
Fracture energy in compression	Vertical	N/mm	12	8	19	**20.00**	21	15	26	**15.00**
	Horizontal	N/mm	31	-	31		32	-	32	
Masonry bending strength with the moment vector parallel to the bed joints and in the plane of the wall		MPa	-	-	-	**0.15**	0.43	0.33	0.52	**0.3**
Masonry bending strength with the moment vector orthogonal to the bed joint and in the plane of the wall		MPa	0.62	0.41	0.83	**0.55**	1.18	1.01	1.24	**0.85**
Masonry (bed joint) initial shear strength		MPa	0.31	0.21	0.34	**0.30**	0.47	0.39	0.53	**0.40**
Masonry (bed joint) shear friction coefficient		-	0.80	0.59	0.90	**0.75**	0.76	0.71	0.79	**0.75**

Overview test results
Compared with mean values tabulated in NEN-NPR 9998:2017

Material properties of CS brick masonry		Unit	CS brick masonry pre 1985			
			All	Poor quality	Good quality	**NPR 2017**
Compressive strength of masonry in the	Vertical	MPa	9	8	14	**7.0**
	Horizontal	MPa	7	6	7	
Elastic chord modulus of masonry	Vertical	GPa	7	6	9	**4.00**
	Horizontal	GPa	4	5	3	
Fracture energy in compression	Vertical	N/mm	18	14	25	**15.00**
	Horizontal	N/mm	18	18	19	
Masonry bending strength with the moment vector parallel to the bed joints and in the plane of the wall		MPa	0.13	0.13	-	**0.15**
Masonry bending strength with the moment vector orthogonal to the bed joint and in the plane of the wall		MPa	0.59	0.59	-	**0.55**
Masonry (bed joint) initial shear strength		MPa	0.26	0.28	0.28	**0.25**
Masonry (bed joint) shear friction coefficient		-	0.79	0.77	0.82	**0.60**

TU Delft

Overview test results
Compared with mean values tabulated in NEN-NPR 9998:2017

Replicated masonry

Material properties of CS brick masonry		Unit	CS brick masonry pre 1985				CS element masonry post 1985			
			All	Poor quality	Good quality	**NPR 2017**	All	Poor quality	Good quality	**NPR 2017**
Compressive strength of masonry in the	Vertical	MPa	9	8	14	**7.0**	13.93	-	13.93	**10.00**
	Horizontal	MPa	7	6	7		9.42	-	9.42	
Elastic chord modulus of masonry	Vertical	GPa	7	6	9	**4.00**	8313	-	8313	**7.50**
	Horizontal	GPa	4	5	3		7701	-	7701	
Fracture energy in compression	Vertical	N/mm	18	14	25	**15.00**	20.9	-	20.9	**20.00**
	Horizontal	N/mm	18	18	19		12.8	-	12.8	
Masonry bending strength with the moment vector parallel to the bed joints and in the plane of the wall		MPa	0.13	0.13	-	**0.15**	0.58	-	0.58	**0.6**
Masonry bending strength with the moment vector orthogonal to the bed joint and in the plane of the wall		MPa	0.59	0.59	-	**0.55**	0.73	-	0.73	**1.0**
Masonry (bed joint) initial shear strength		MPa	0.26	0.28	0.28	**0.25**	0.83	-	0.83	**0.80**
Masonry (bed joint) shear friction coefficient		-	0.79	0.77	0.82	**0.60**	1.48	-	1.48	**0.80**

Example: indication of distribution, compressive strength clay brick masonry

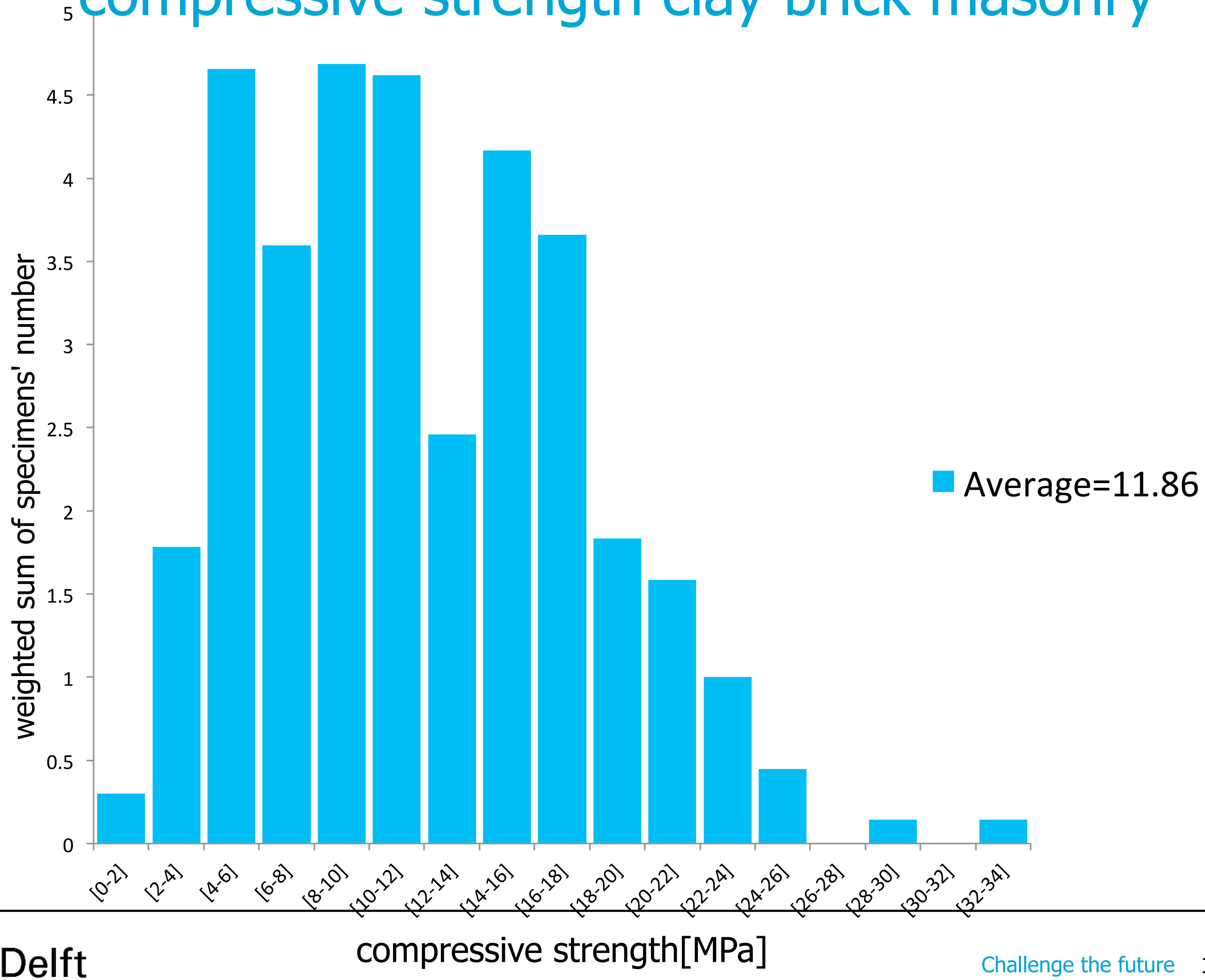

Example: indication of distribution, according to age, compressive strength clay brick masonry

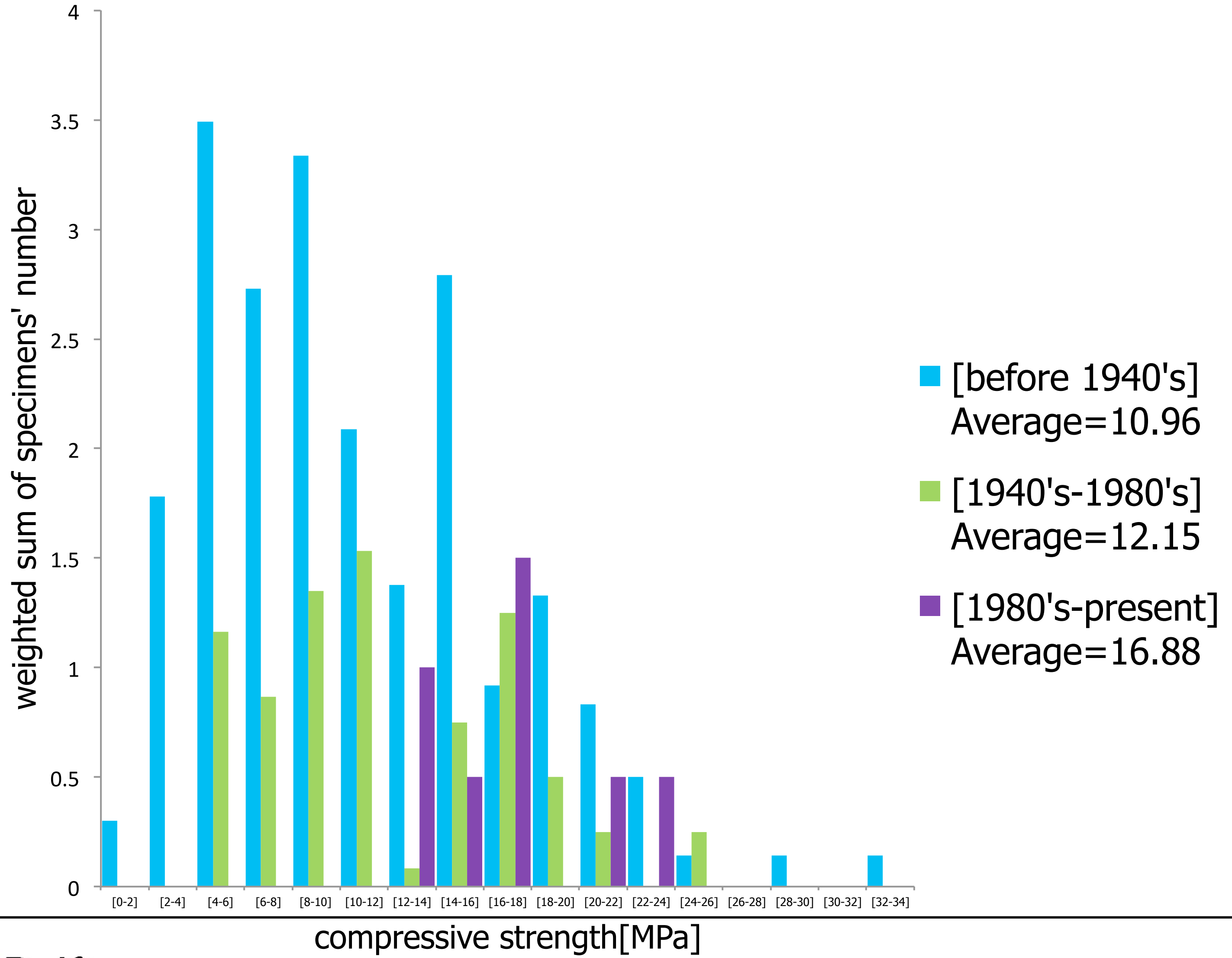

Details compressive tests

Symbol	Material property	Masonry (strength and stiffness values in N/mm², fracture energy values J/m²)			
		Clay brickwork (pre 1945) d	Clay brickwork (post 1945)	Calcium-silicate brickwork with general purpose mortar (typical approx. 1960-present)	Calcium-silicate blocks/elements with thin layer mortar (typical approx. 1985-present)
f'_m	Compressive strength	8,5	10,0	7,0	10,0
E_m	Young's modulus	5 000	6 000	4 000	7 500
G_m	Shear modulus	2 000	2 500	1 650	3 000
f_{x1}	Bending strength for plane of failure parallel to the bed joints a	0,15	0,3	0,15	0,6
f_{x2}	Bending strength for plane of failure perpendicular to the bed joints a	0,55	0,85	0,55	1,0
$f_{mt\perp}$	Uniaxial tensile strength perpendicular to the bed joint	0,1	0,2	0,1	0,4
$f_{mt//}$	Uniaxial tensile strength parallel to the bed joint	0,35	0,55	0,35	0,65
f_{v0}	Initial bed joint shear strength	0,3	0,4	0,25	0,8
tan φ	Bed joint shear friction coefficient	0,75	0,75	0,6	0,8
$G_{ft\perp}$	Fracture energy b in tension perpendicular to the bed joints	10	10	10	20
$G_{ft//}$	Fracture energy b in tension parallel to the bed joints	35	35	20	20

Compressive behaviour

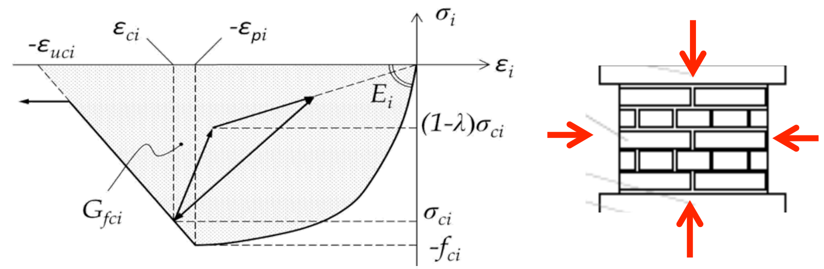

- Compressive strength
- Young's modulus
- Shear modulus
- Fracture energy in compression

Compression test -Existing masonry 2014-2017

Vertical compression test

Horizontal compression test

Vertical compression test - Replicated masonry 2014-2017

Horizontal compression test - Replicated masonry 2014-2017

    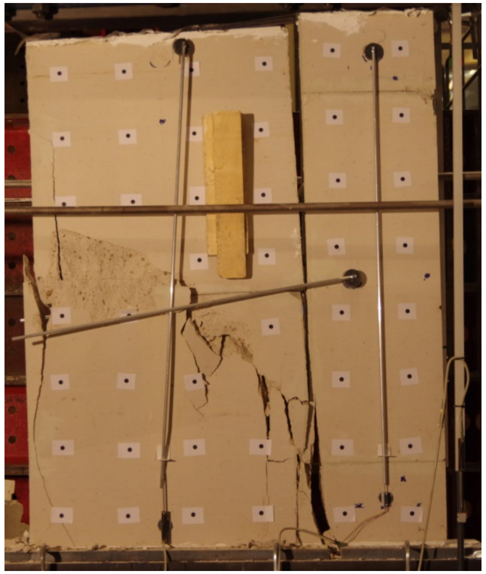

Vertical compression test – CS element masonry

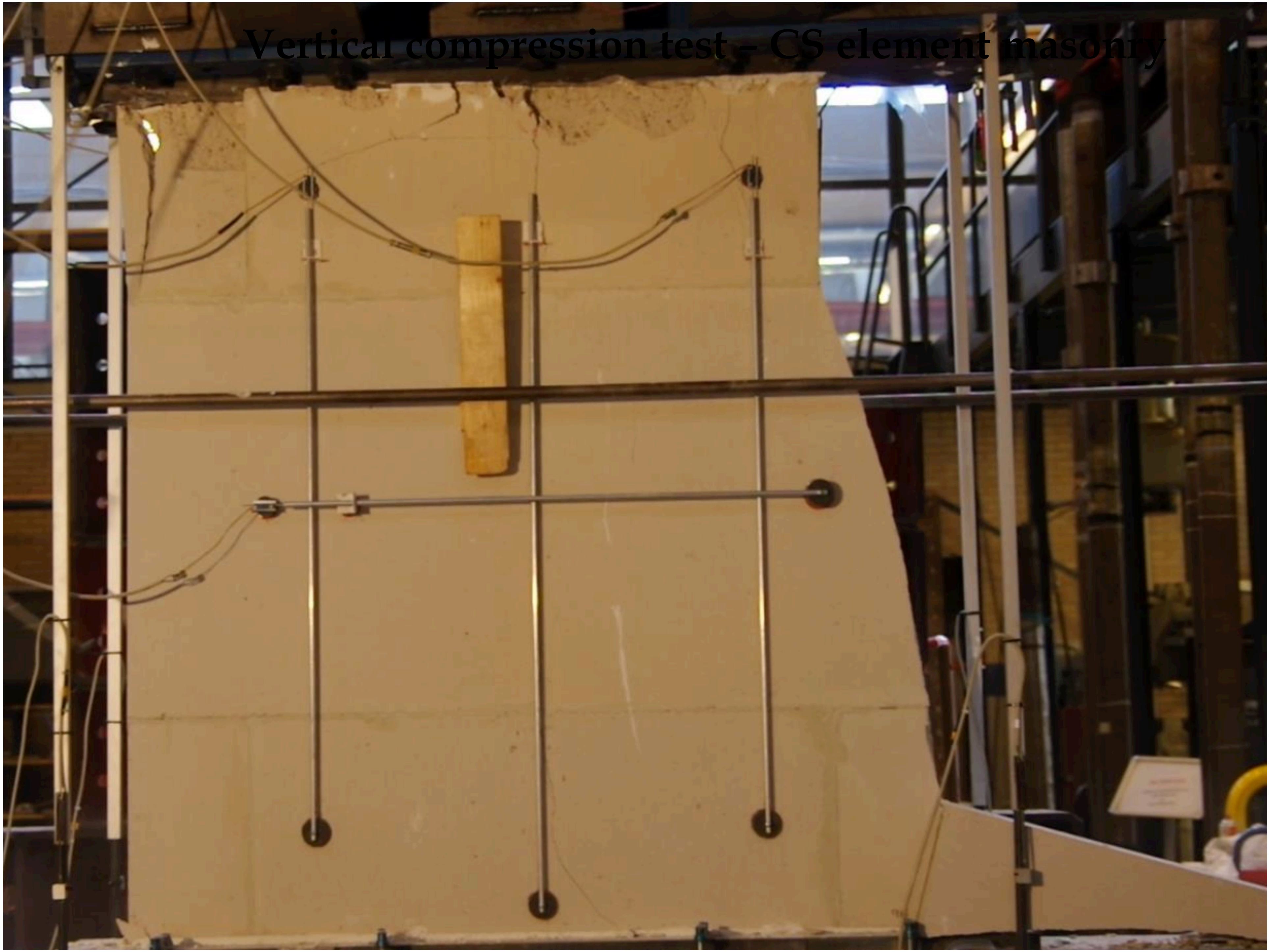

Estimation of the Young's modulus

- E_1 is the secant elastic modulus evaluated at 1/3 of the maximum stress;
- E_2 is the secant elastic modulus evaluated at 1/10 of the maximum stress;
- E_3 is the chord elastic modulus evaluated between 1/10 and 1/3 of the maximum stress.

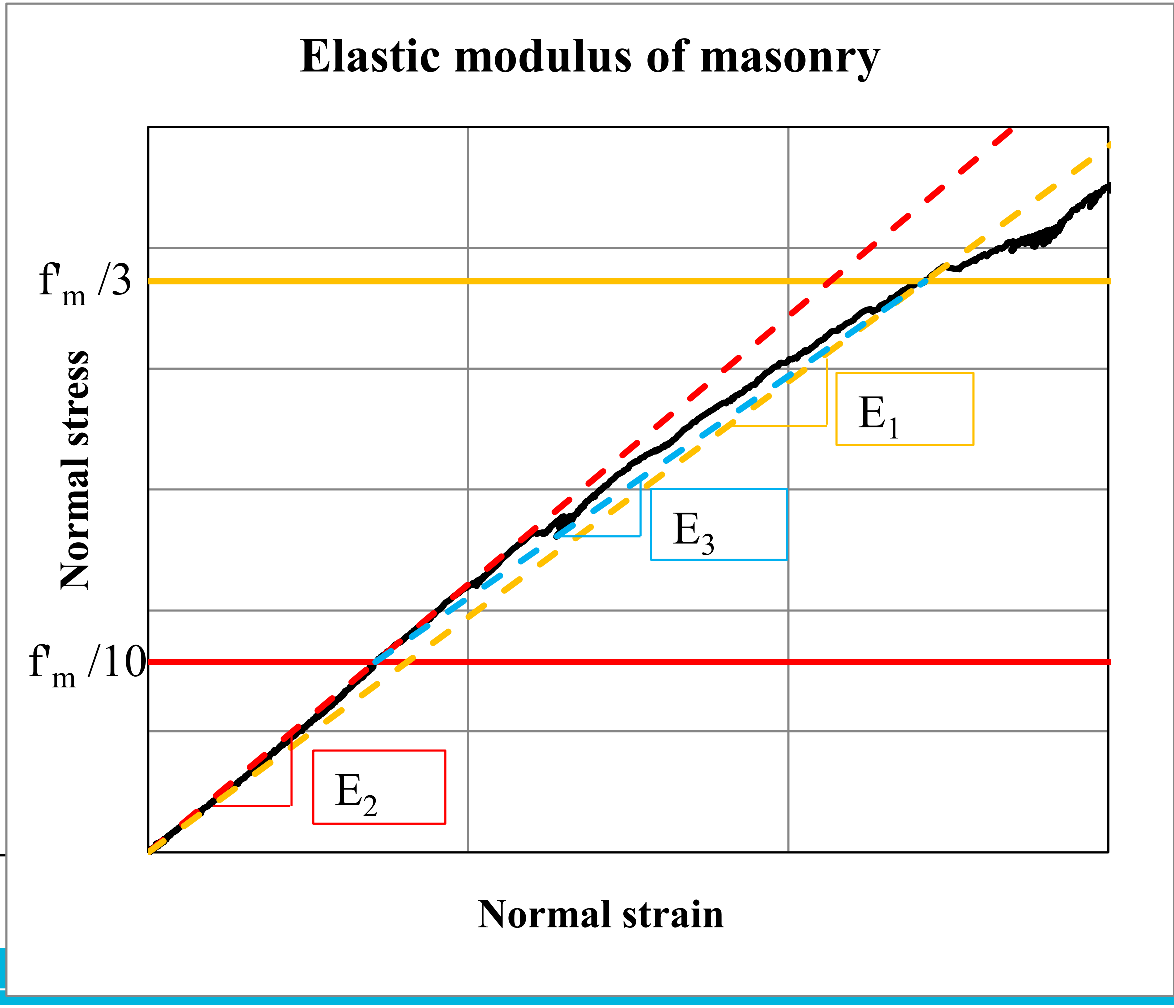

Evaluation of Poisson ratio

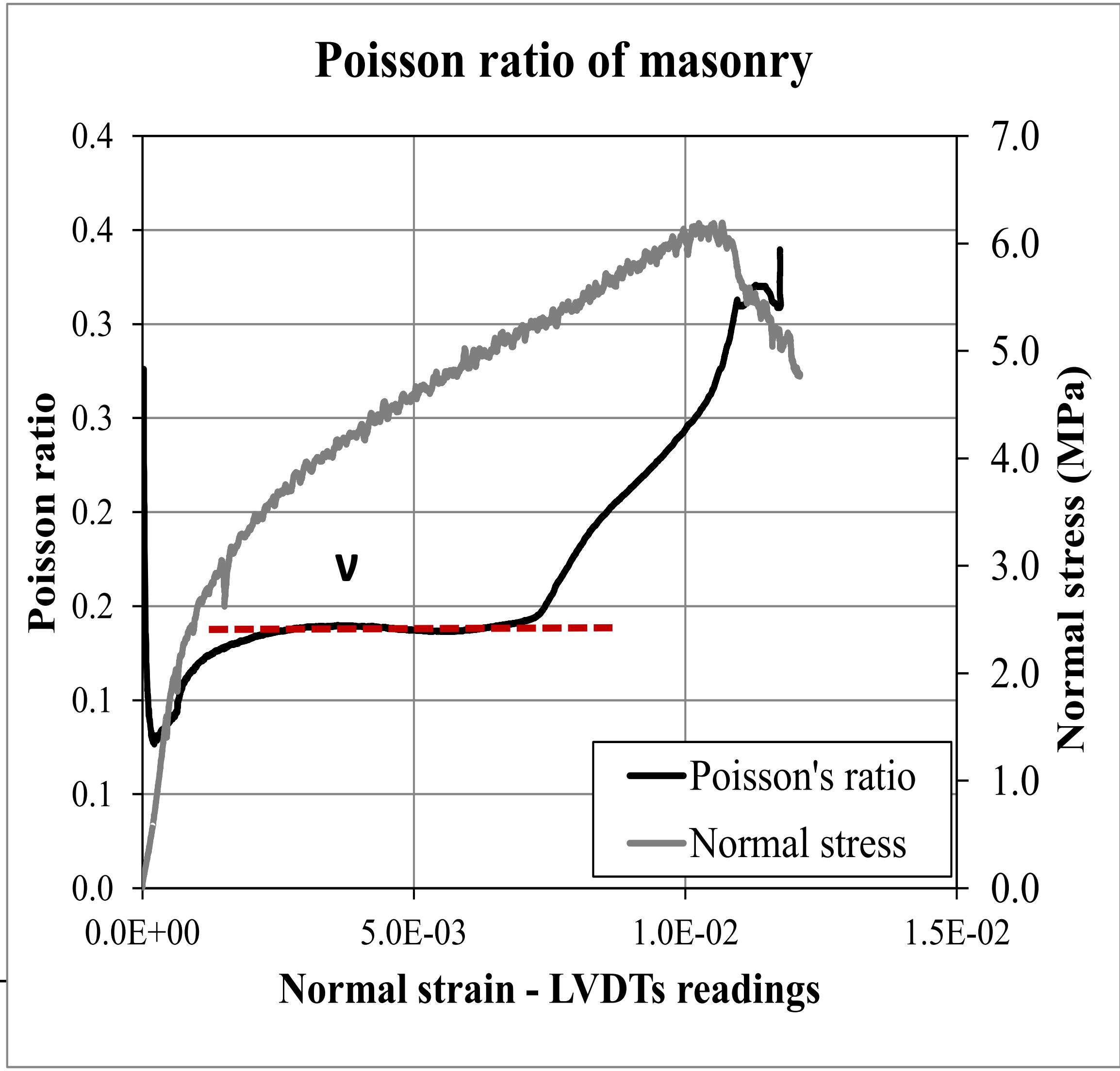

Evaluation of the fracture energy in compression

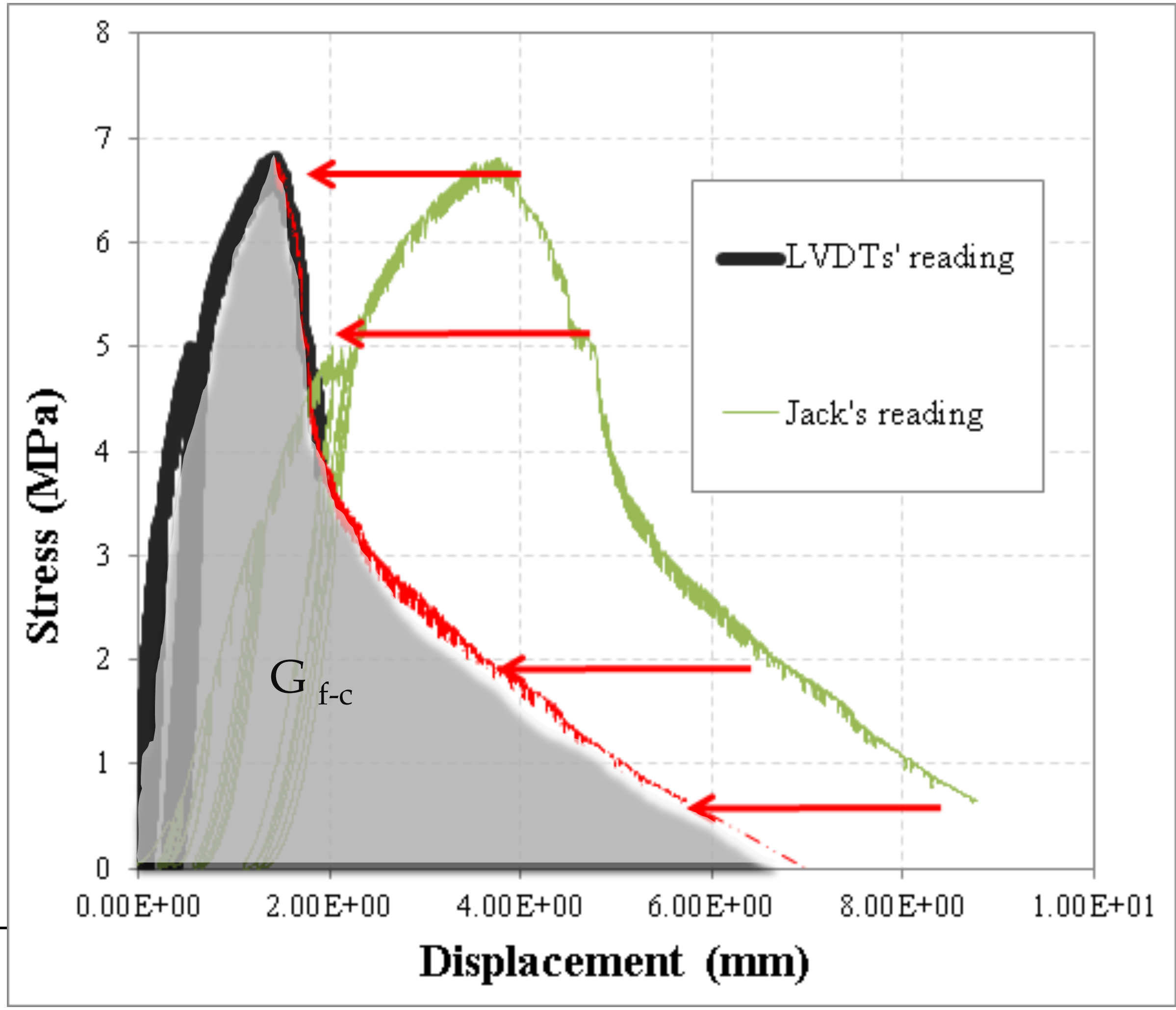

Finding the mean curve in compression

3. Finding the mean values

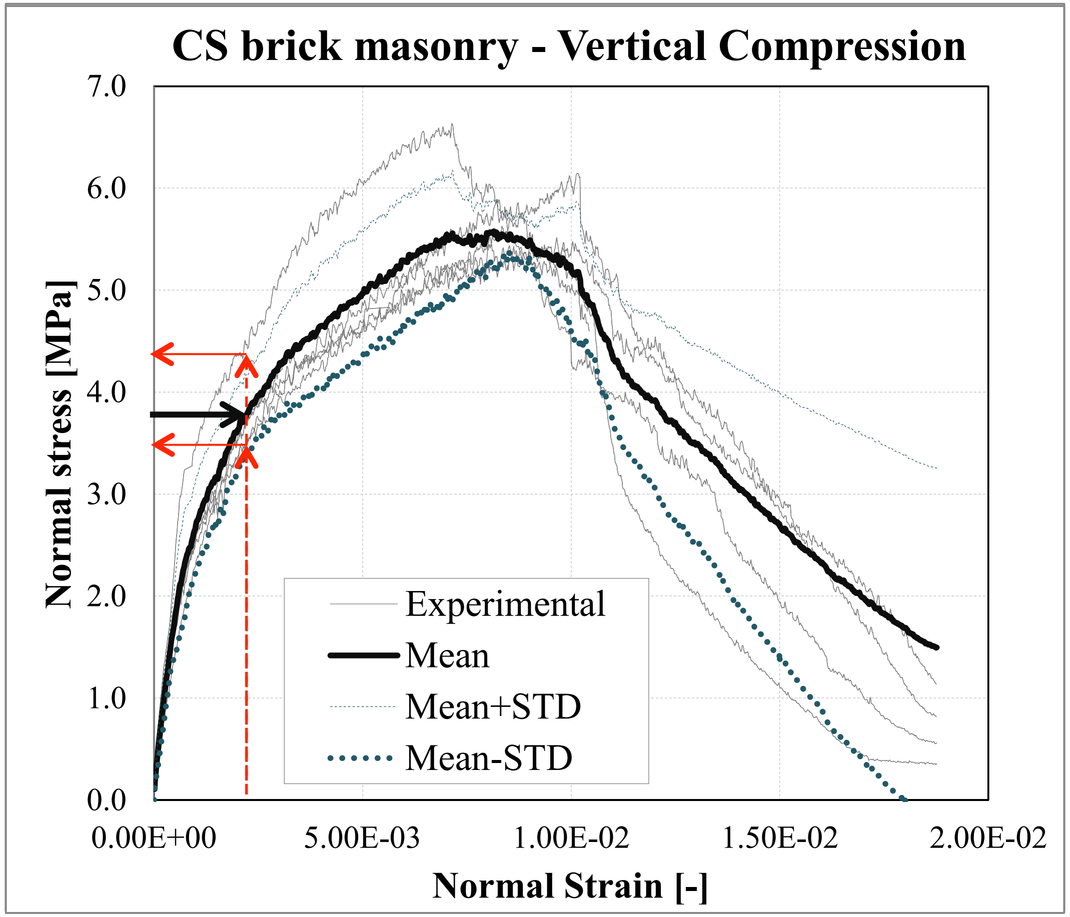

Histogram representation of compressive strength

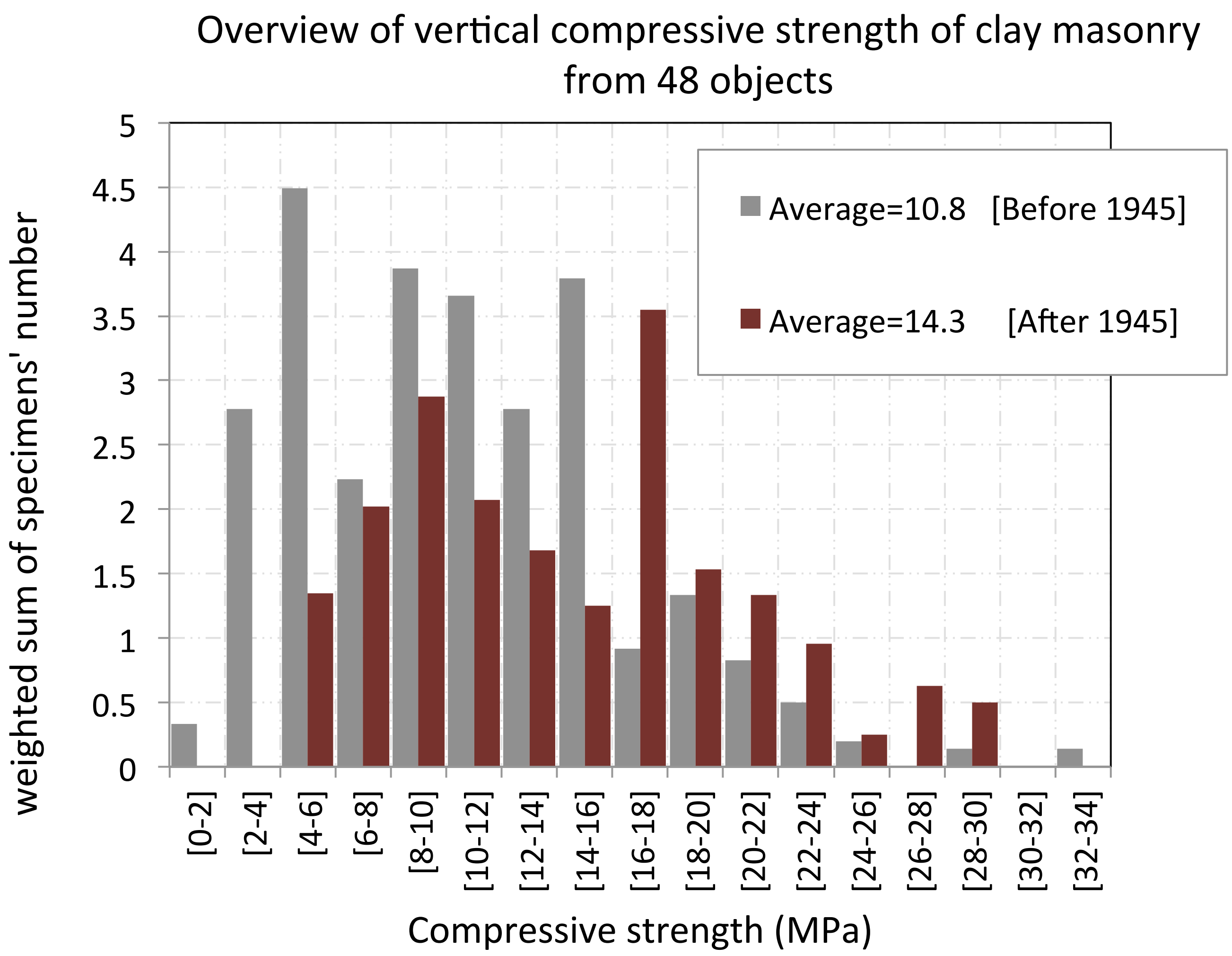

Histogram representation of compressive strength

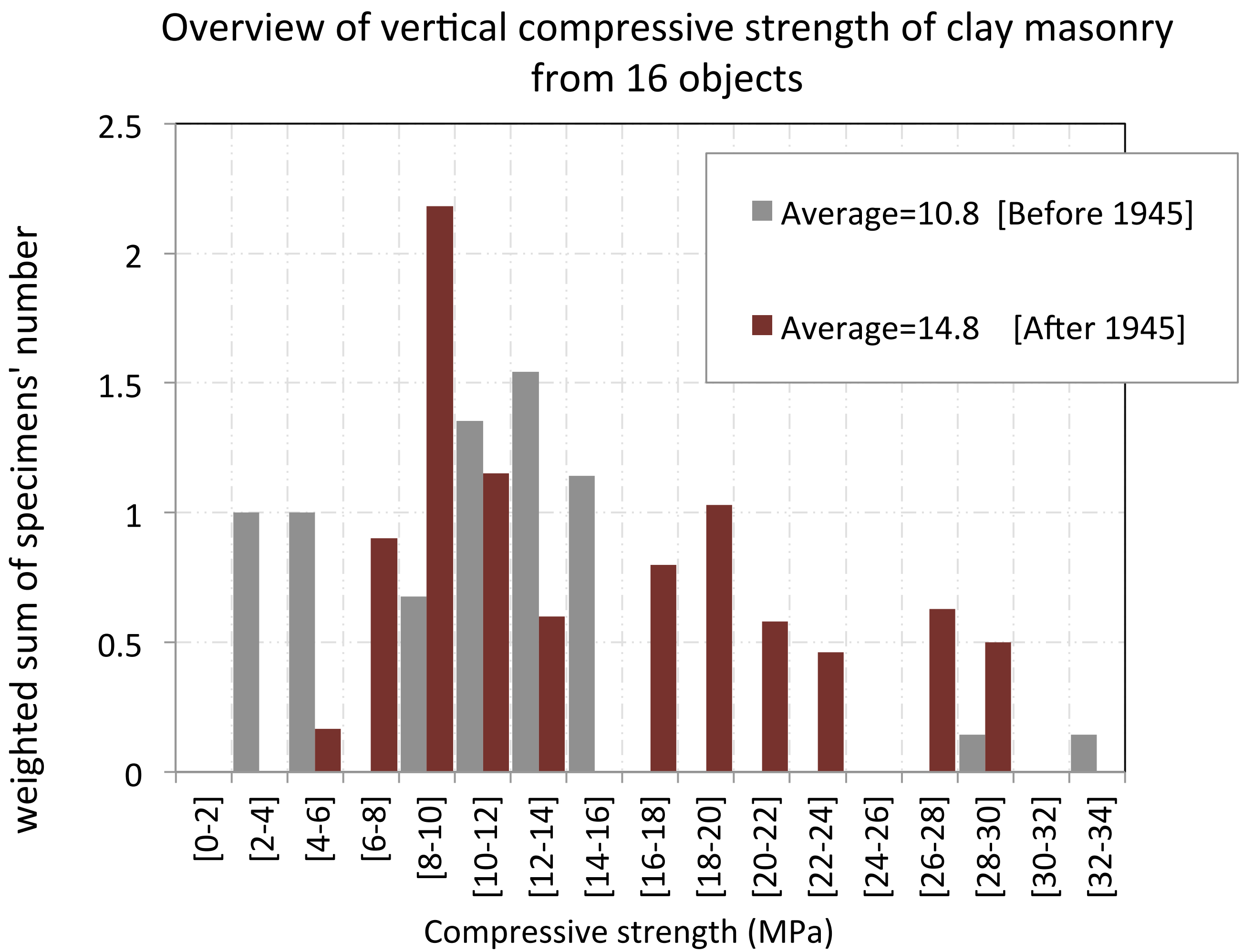

Correlations between compression properties

$$E = 600\, f_k$$
$$f_k = 1.645\, f_m - \sigma$$

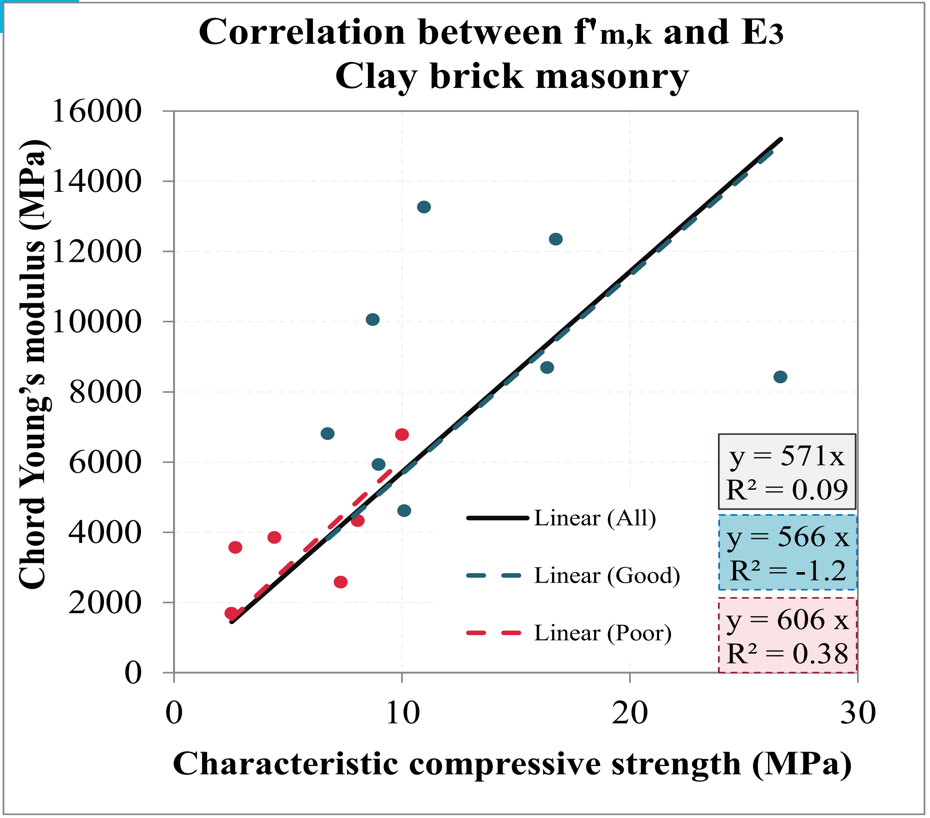

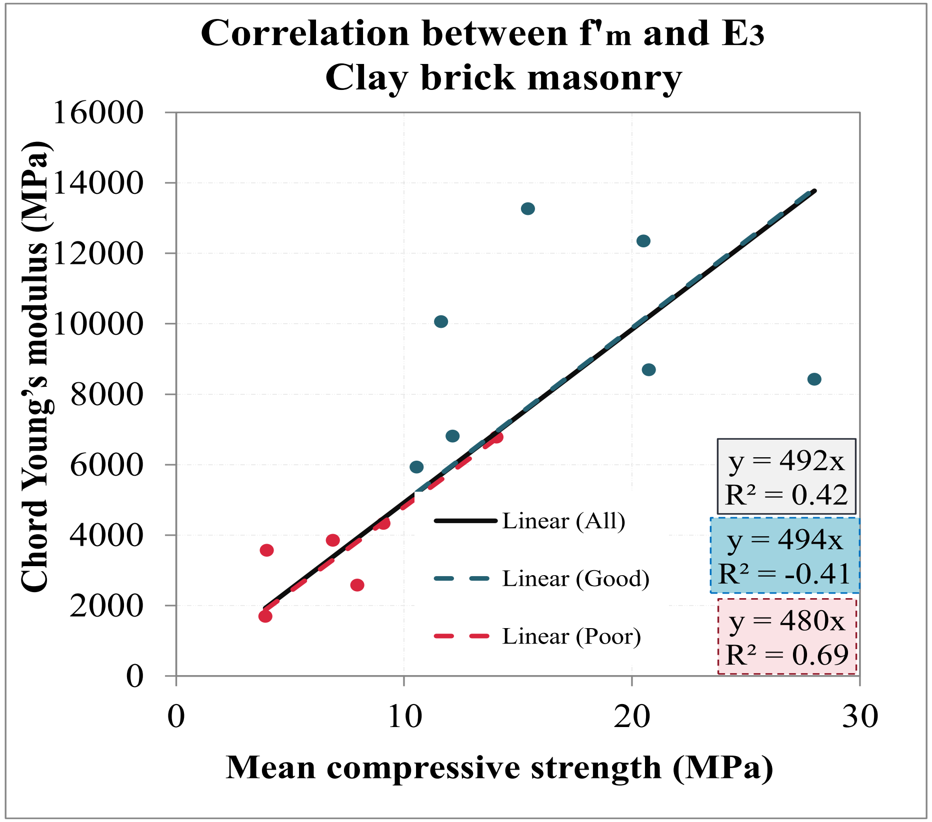

Orthotropic behaviour in compression

Masonry type			$f'_{m,v}/ f'_{m,h}$	$E_{3,v}/ E_{3,h}$	$G_{f\text{-}c,v}/ G_{f\text{-}c,h}$
Clay brick masonry	Existing	<1945	1.33	-	-
		1945>	1.87	2.26	0.60
	Replicated	Perforated	1.97	1.74	1.50
		Solid-single wythe	1.07	1.43	0.81
		Solid-double wythe	1.17	0.69	1.20

Solid brick

Perforated brick

Frogged brick

Single and double wythe

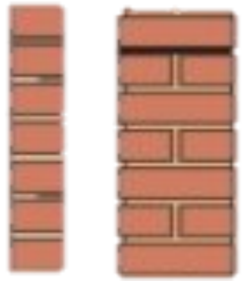

TU Delft

Orthotropic behaviour in compression

Masonry type			$f'_{m,v}/ f'_{m,h}$	$E_{3,v}/ E_{3,h}$	$G_{f\text{-}c,v}/ G_{f\text{-}c,h}$
CS masonry	Existing-*Brick masonry*	<1985	1.53	1.62	1.26
		1985>	1.17	1.28	0.58
	Replicated	*Brick masonry*	0.78	1.32	0.73
		Element masonry	1.48	1.08	1.63

CS brick masonry

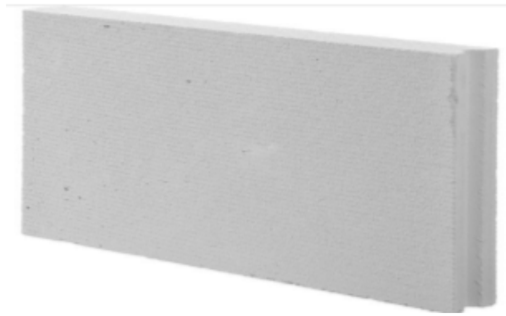

CS element masonry

Details tensile (bending) tests

Table F.2 — Mean values of material properties for different types of masonry

Symbol	Material property	Masonry (strength and stiffness values in N/mm², fracture energy values J/m²)			
		Clay brickwork (pre 1945)[d]	Clay brickwork (post 1945)	Calcium-silicate brickwork with general purpose mortar (typical approx. 1960-present)	Calcium-silicate blocks/elements with thin layer mortar (typical approx. [illegible] present)
f'_m	Compressive strength	8,5	10,0	7,0	[illegible]
E_m	Young's modulus	5 000	6 000	4 000	[illegible]
G_m	Shear modulus	2 000	2 500	1 650	[illegible]
f_{x1}	Bending strength for plane of failure parallel to the bed joints[a]	0,15	0,3	[illegible]	0,6
f_{x2}	Bending strength for plane of failure perpendicular to the bed joints[a]	0,55	[illegible]	[illegible]	1,0
$f_{mt\perp}$	Uniaxial tensile strength perpendicular to the bed joint	[illegible]	[illegible]	0,1	0,4
$f_{mt//}$	Uniaxial tensi[illegible] parallel to [illegible]	[illegible]	0,55	0,35	0,65
f_{v0}	[illegible]	0,3	0,4	0,25	0,8
[illegible]	[illegible] friction	0,75	0,75	0,6	0,8
[illegible]	[illegible]cture energy[b] in tension perpendicular to the bed joints	10	10	10	20
$G_{ft//}$	Fracture energy[b] in tension parallel to the bed joints	35	35	20	20
G_{fc}	Fracture energy[c] in compression	20 000	15 000	15 000	20 000
G_{fs}	Fracture energy[b] in shear (bed joint)	100	200	100	200

[a] Not to be used in combination with softening
[b] To be used in combination with a crack band width, in case of smeared finite element models
[c] To be used in combination with a crush band width, in case of smeared finite element models
[d] When clay brickwork pre 1945 is of a clearly poor quality in terms of mortar quality, mortar ageing, filling of joints, layout and bond pattern, the mean values of strength, stiffness and fracture energy properties in this column are advised to be reduced by approximately 40%

Compressive behaviour

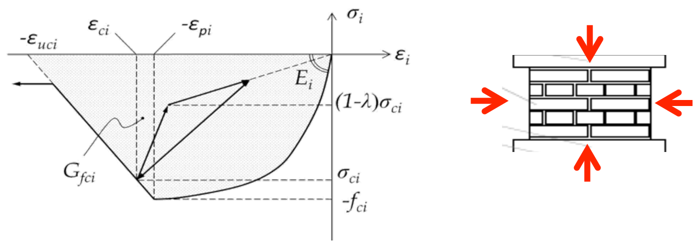

Tensile behaviour

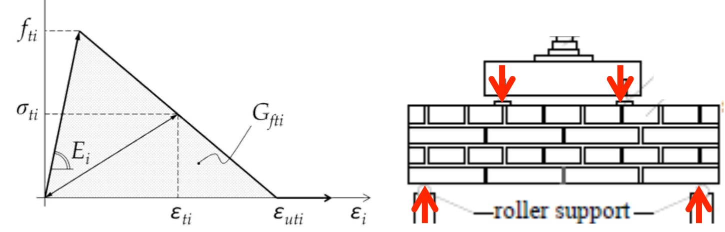

Shear behaviour

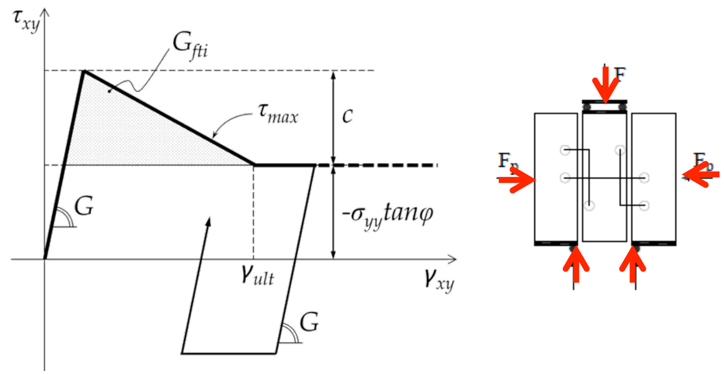

Tensile behaviour

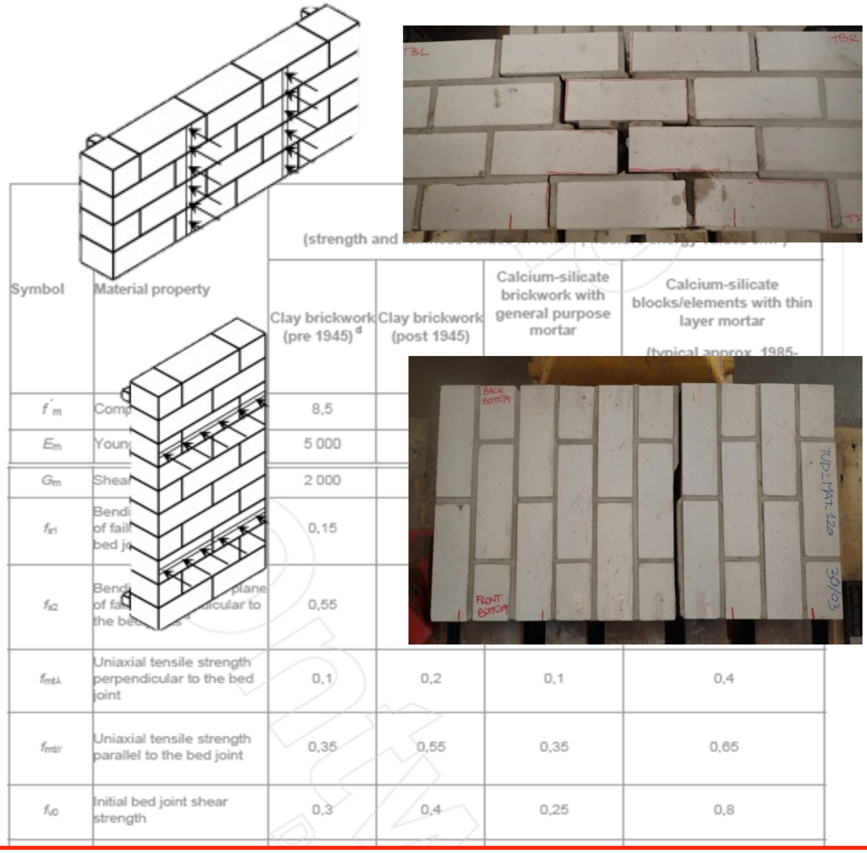

Tensile behaviour

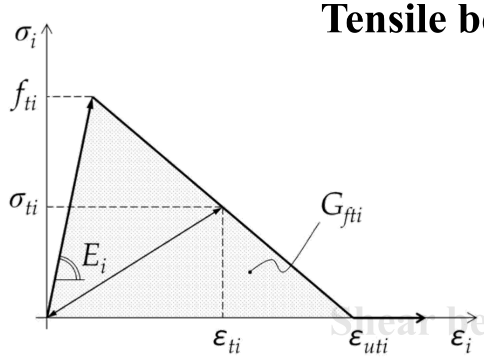

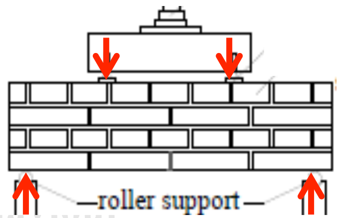

- Bending strength for plane of failure parallel to the bed joints
- Bending strength for plane of failure perpendicular to the bed joints
- Uniaxial tensile strength parallel to the bed joints
- Uniaxial tensile strength perpendicular to the bed joints
- Fracture energy in tension parallel to the bed joints
- Fracture energy in tension perpendicular to the bed joints

Tensile behaviour

TU Delft

Out-of-plane vertical bending tests – OOP1

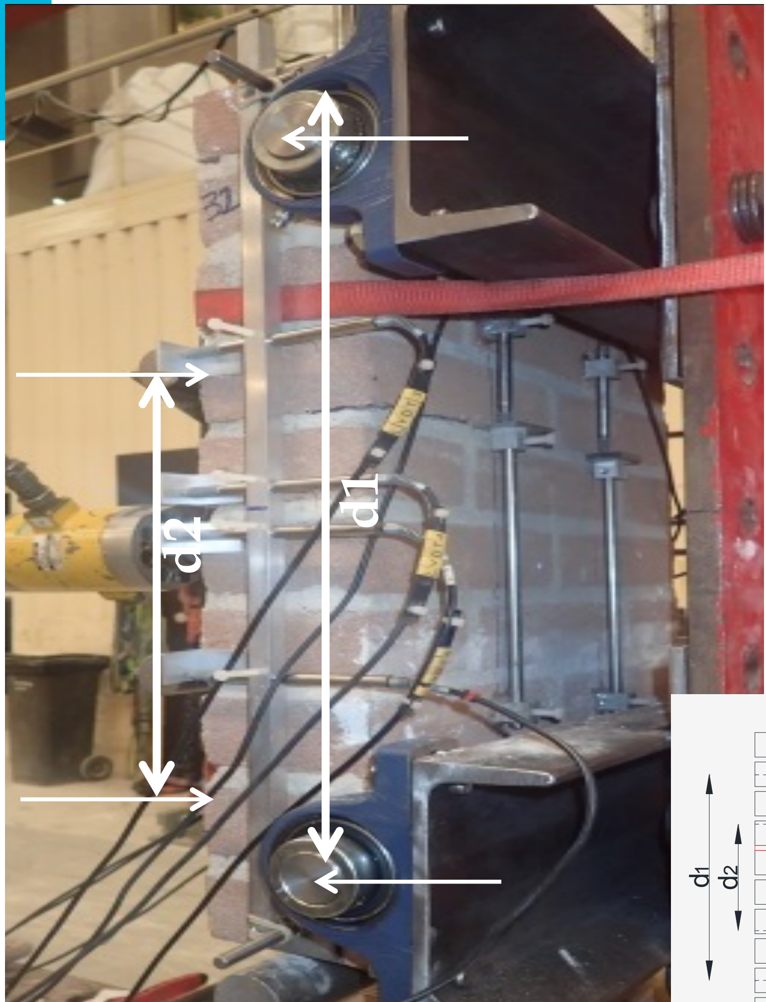

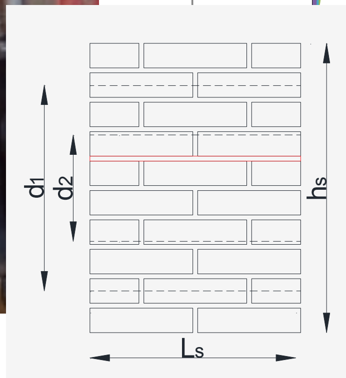

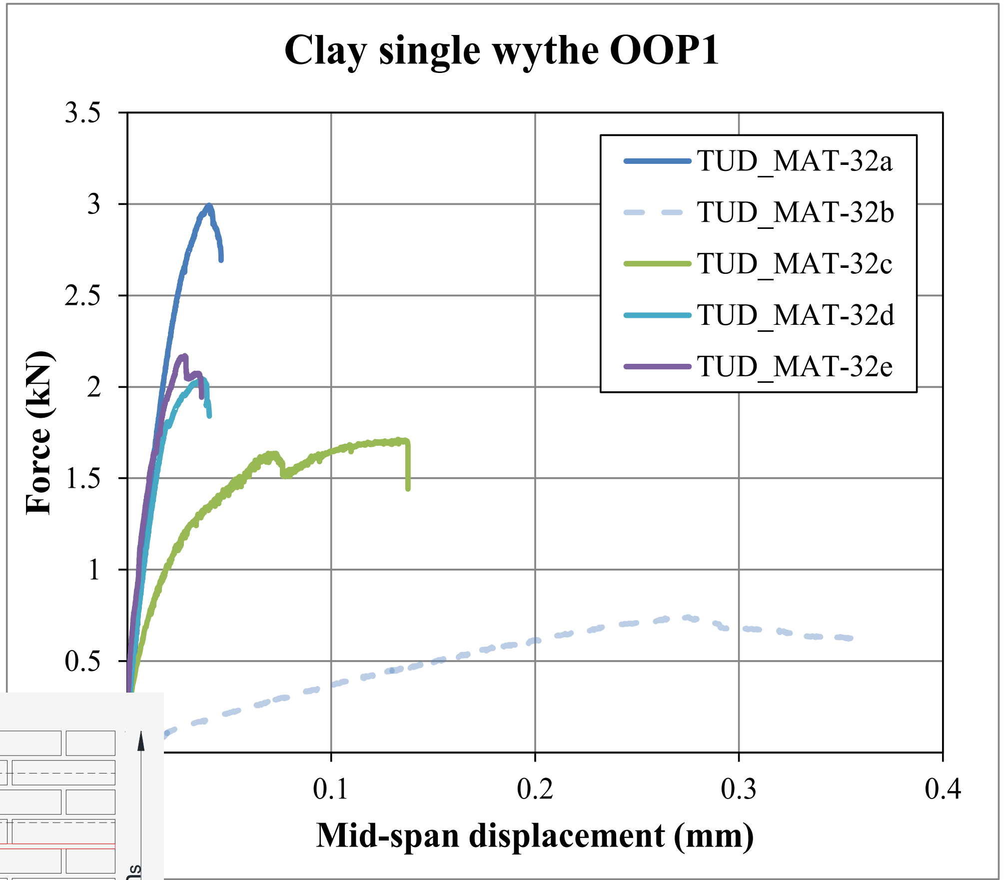

Tensile behaviour

Out-of-plane horizontal bending test – OOP2

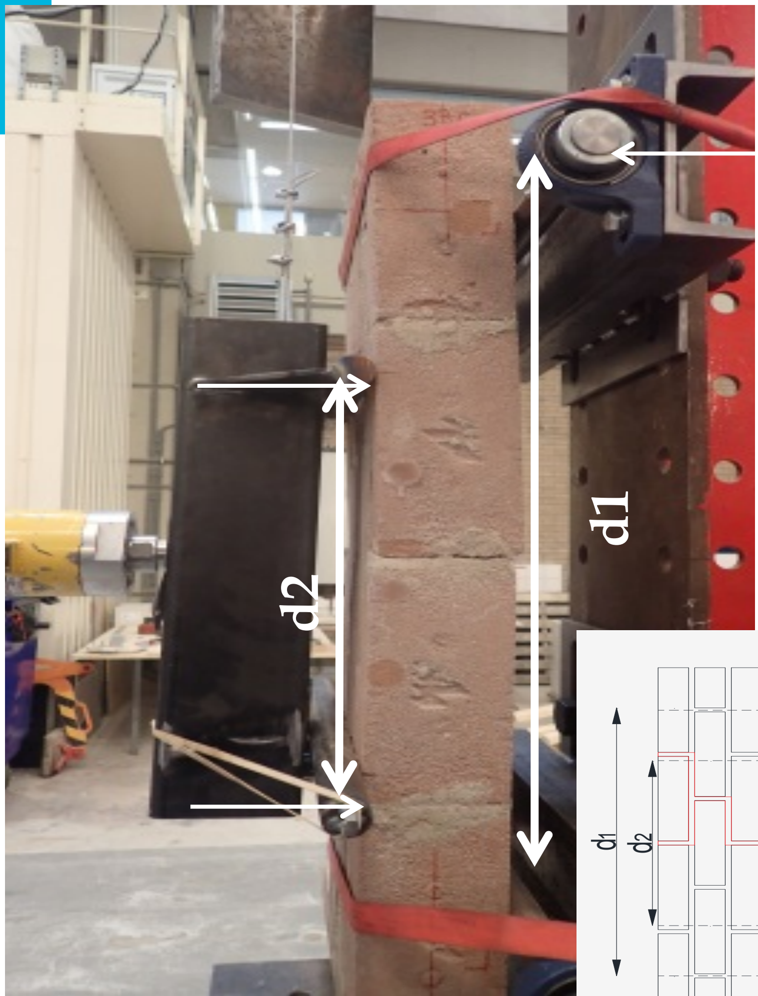

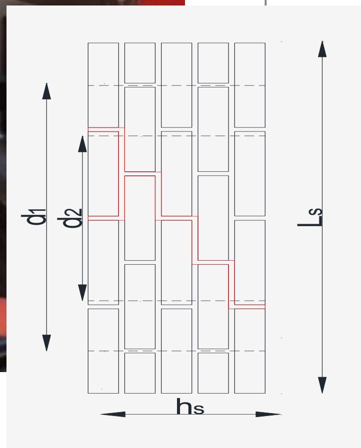

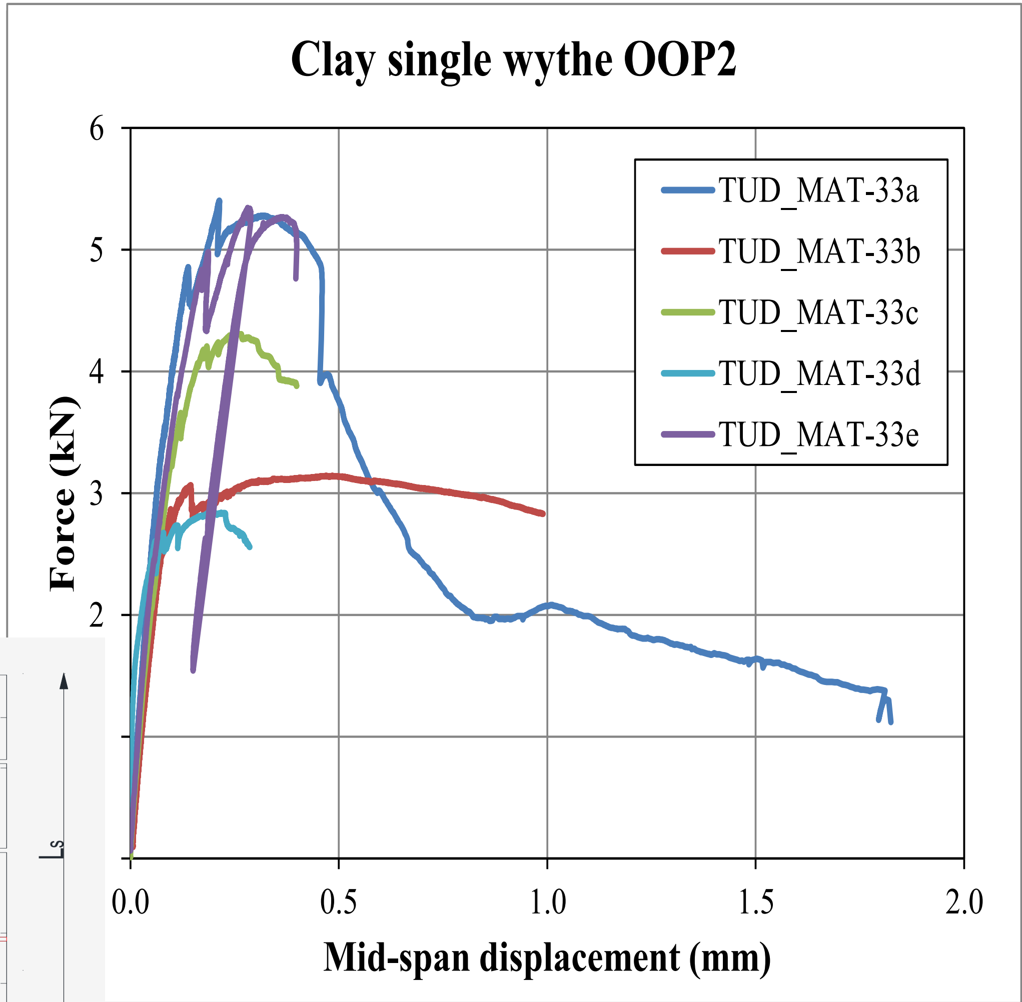

Tensile behaviour

In plane bending test – IP

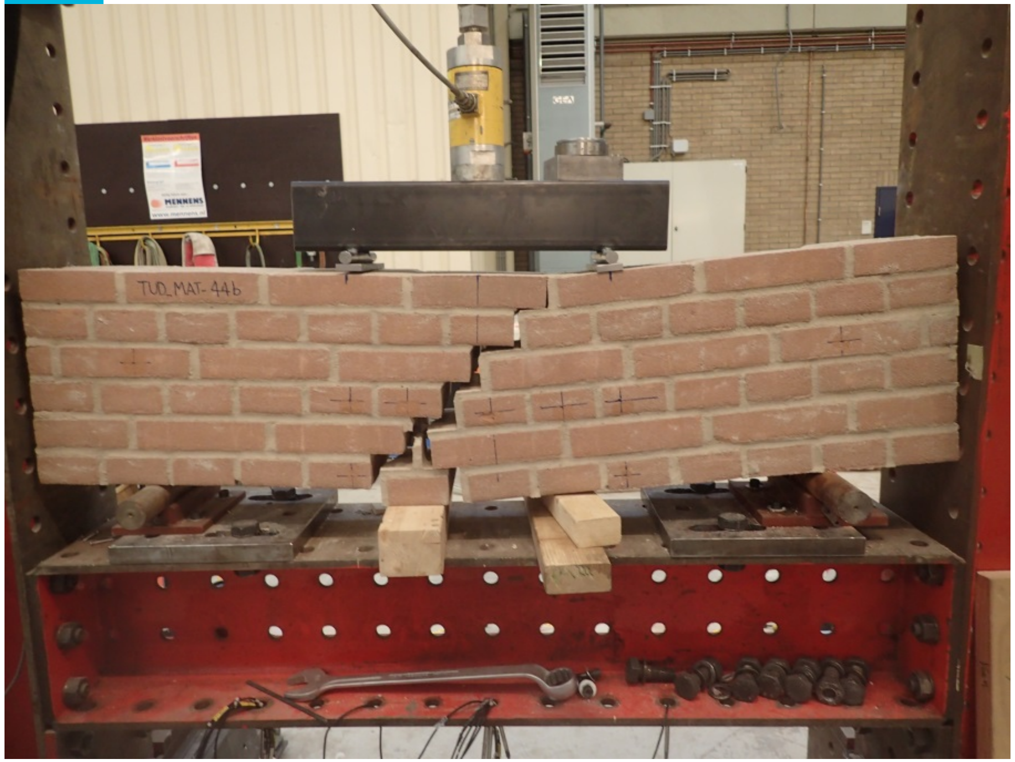

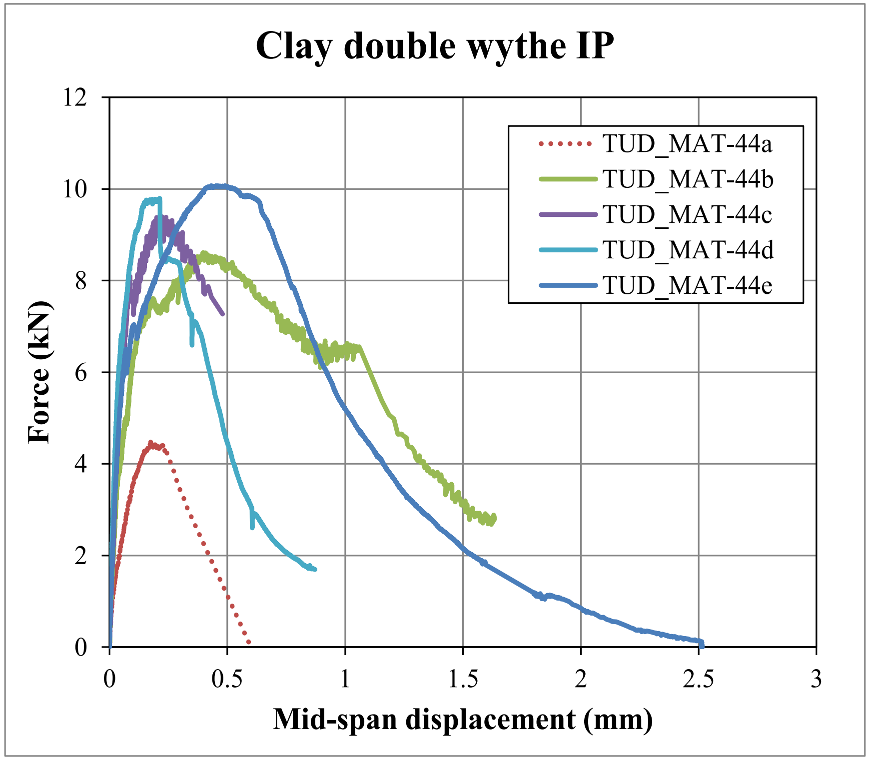

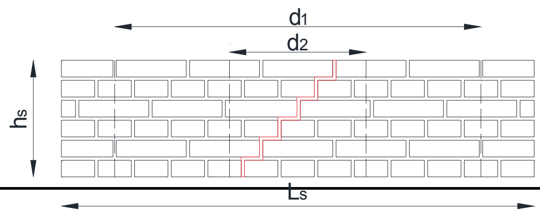

Tensile behaviour

Bondwrench test

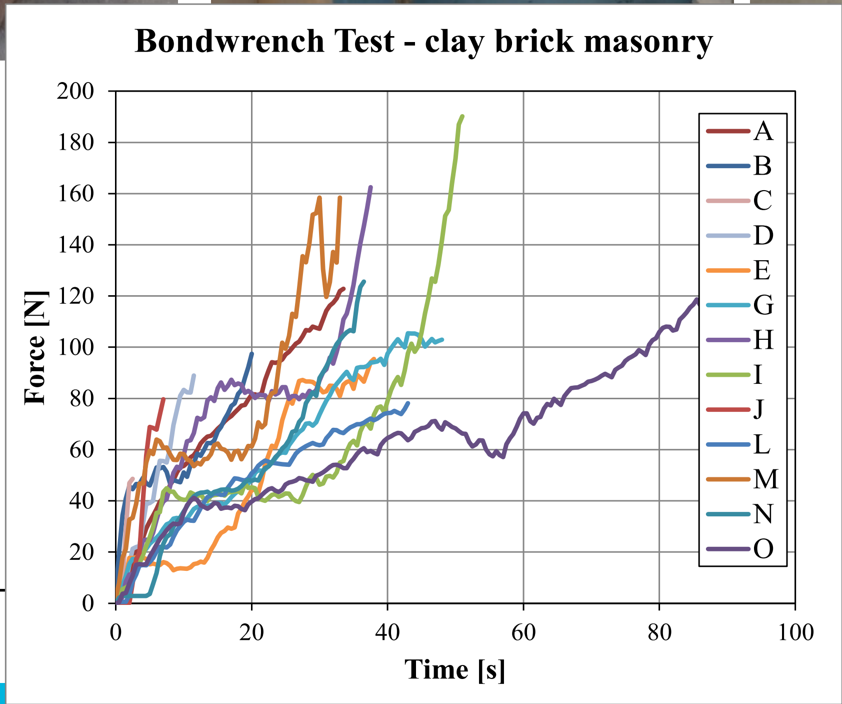

Orthotropic behaviour in bending

Masonry type			Orthogonality ratio in bending		
			f_{x1}	f_{x2}	f_{x2}/f_{x1}
			MPa	MPa	-
CS masonry	Existing (brick)	<1985	0.13	0.59	4.2
		1985>	-	-	-
	Replicated	Brick masonry	0.21	0.76	3.6
		Element masonry	0.58	0.73	1.3
	NPR 2017	CS brick	0.15	0.55	3.7
		CS element	0.60	1.0	1.7

CS brick masonry

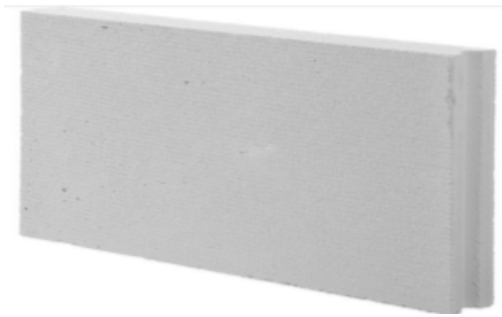

CS element masonry

Orthotropic behaviour in bending

Masonry type			Orthogonality ratio in bending		
			f_{x1}	f_{x2}	f_{x2}/f_{x1}
			MPa	MPa	-
Clay brick masonry	Existing	<1945	-	0.62	-
		>1945	0.43	1.18	2.9
	Replicated	Perforated	0.40	1.12	2.8
		Solid-single wythe	0.16	0.65	4.1
		Solid-double wythe	0.14	0.41	2.9
	NPR 2017	<1945	0.15	0.55	3.7
		>1945	0.30	0.85	2.8

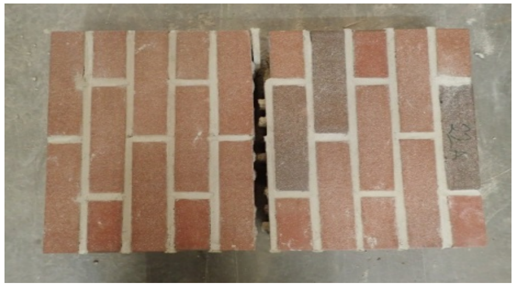

Solid brick

Perforated brick

Frogged brick

Single and double wythe

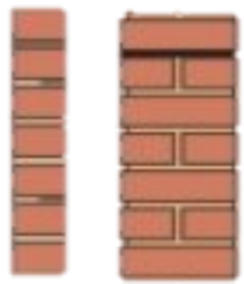

Correlation between f_{x1} and f_w

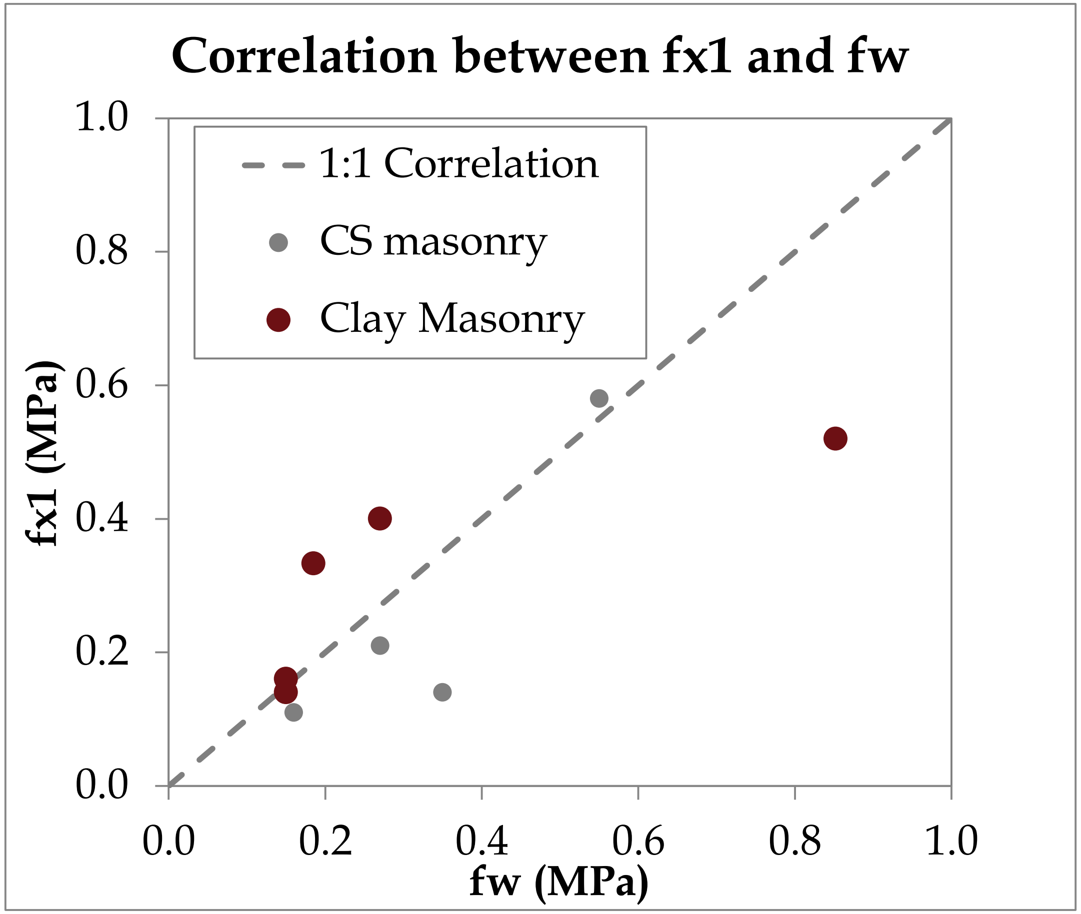

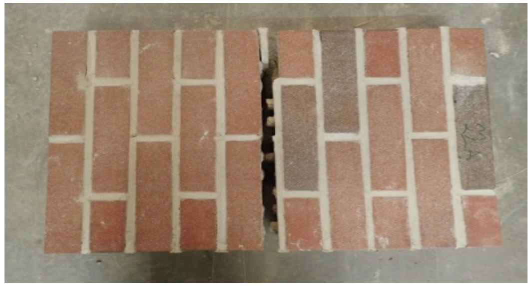

Flexural bond strength (f_w)
Flexural strength subjecting to vertical out-of-plane strength (f_{x1})

Mode I fracture energy

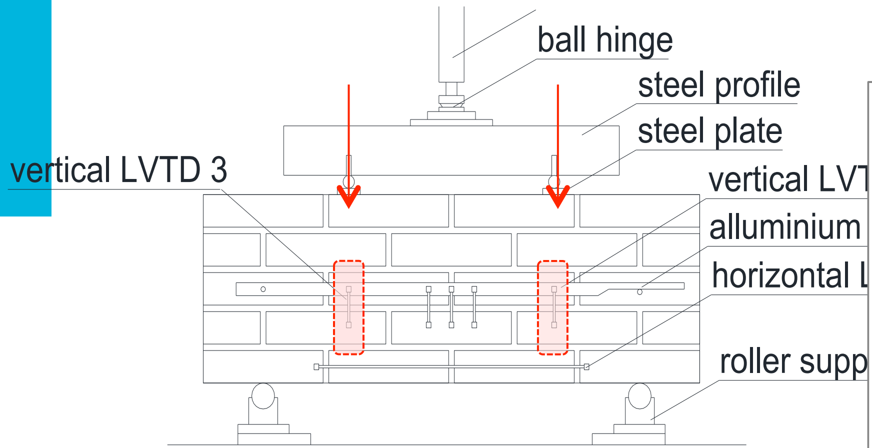

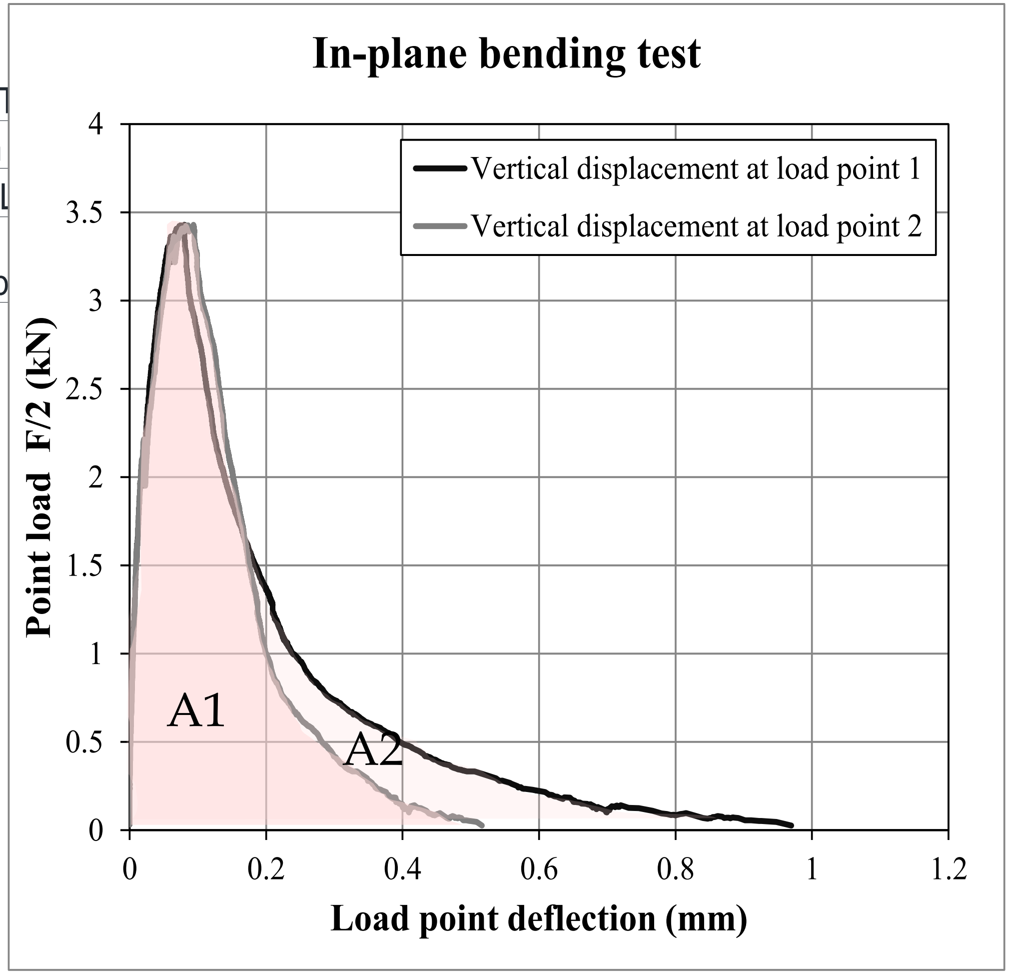

$$G_{f\text{-}I} = (A1 + A2)/\ \text{Cross section}$$

Details shear tests

Table F.2 — Mean values of material properties for different types of masonry

Symbol	Material property	Masonry (strength and stiffness values in N/mm², fracture energy values J/m²)			
		Clay brickwork (pre 1945)[d]	Clay brickwork (post 1945)	Calcium-silicate brickwork with general purpose mortar (typical approx. 1960-present)	Calcium-silicate blocks/elements with thin layer mortar (typical approx. 1[illegible] present)
f'_m	Compressive strength	8,5	10,0	7,0	[illegible]
E_m	Young's modulus	5 000	6 000	4 000	[illegible]
G_m	Shear modulus	2 000	2 500	1 650	[illegible]
f_{x1}	Bending strength for plane of failure parallel to the bed joints[a]	0,15	0,3	[illegible]	0,6
f_{x2}	Bending strength for plane of failure perpendicular to the bed joints[a]	0,55	[illegible]	[illegible]	1,0
$f_{mt\perp}$	Uniaxial tensile strength perpendicular to the bed joint	[illegible]	[illegible]	0,1	0,4
$f_{mt//}$	Uniaxial tensi[illegible] parallel to [illegible]	[illegible]	0,55	0,35	0,65
f_{v0}	[illegible]	0,3	0,4	0,25	0,8
[illegible]	[illegible] friction	0,75	0,75	0,6	0,8
[illegible]	[illegible]cture energy[b] in tension perpendicular to the bed joints	10	10	10	20
$G_{ft//}$	Fracture energy[b] in tension parallel to the bed joints	35	35	20	20
G_{fc}	Fracture energy[c] in compression	20 000	15 000	15 000	20 000
G_{fs}	Fracture energy[b] in shear (bed joint)	100	200	100	200

[a] Not to be used in combination with softening
[b] To be used in combination with a crack band width, in case of smeared finite element models
[c] To be used in combination with a crush band width, in case of smeared finite element models
[d] When clay brickwork pre 1945 is of a clearly poor quality in terms of mortar quality, mortar ageing, filling of joints, layout and bond pattern, the mean values of strength, stiffness and fracture energy properties in this column are advised to be reduced by approximately 40%

Compressive behaviour

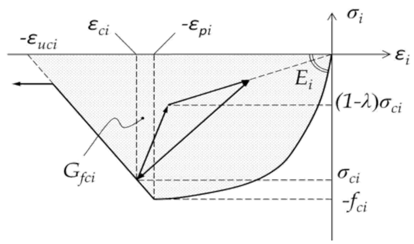

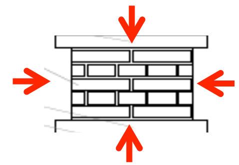

Tensile behaviour

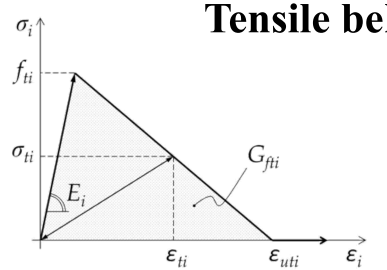

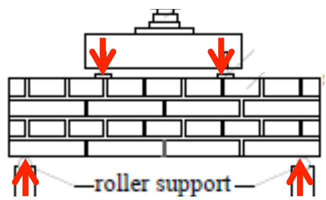

Shear behaviour

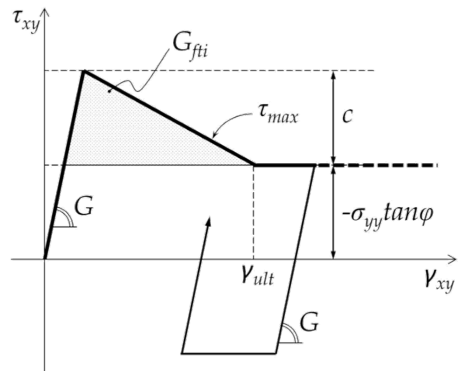

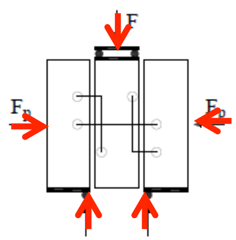

Shear tests for different confinement

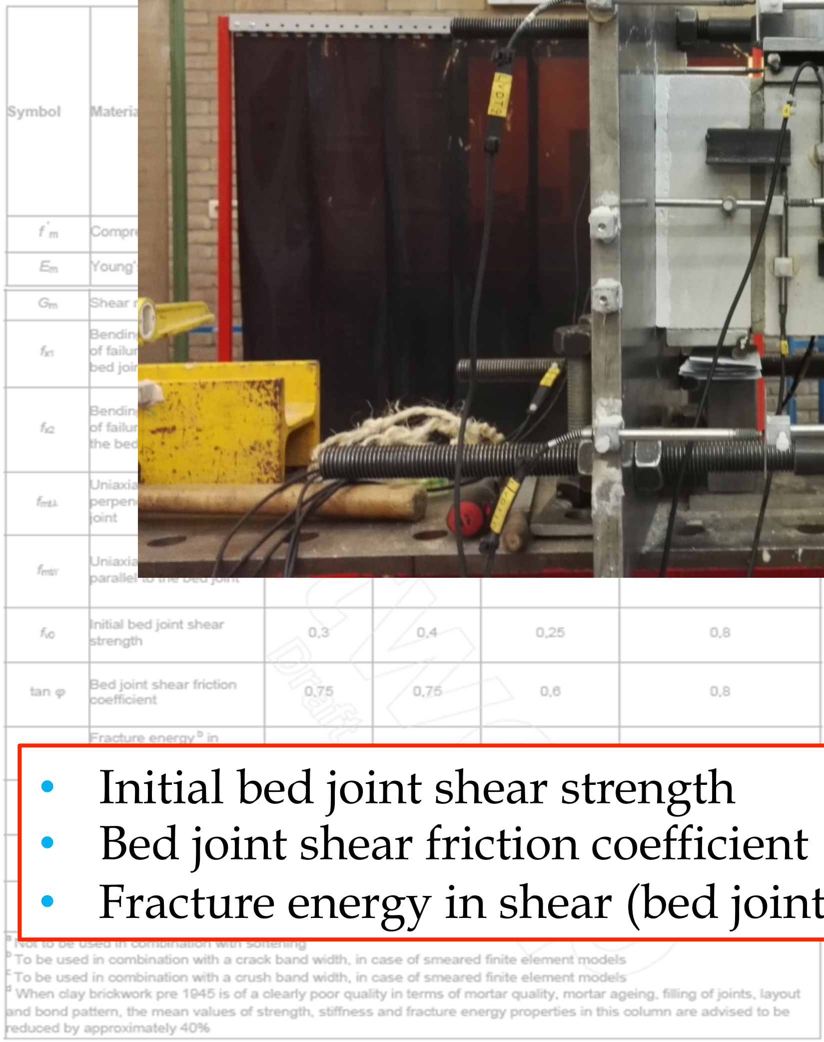

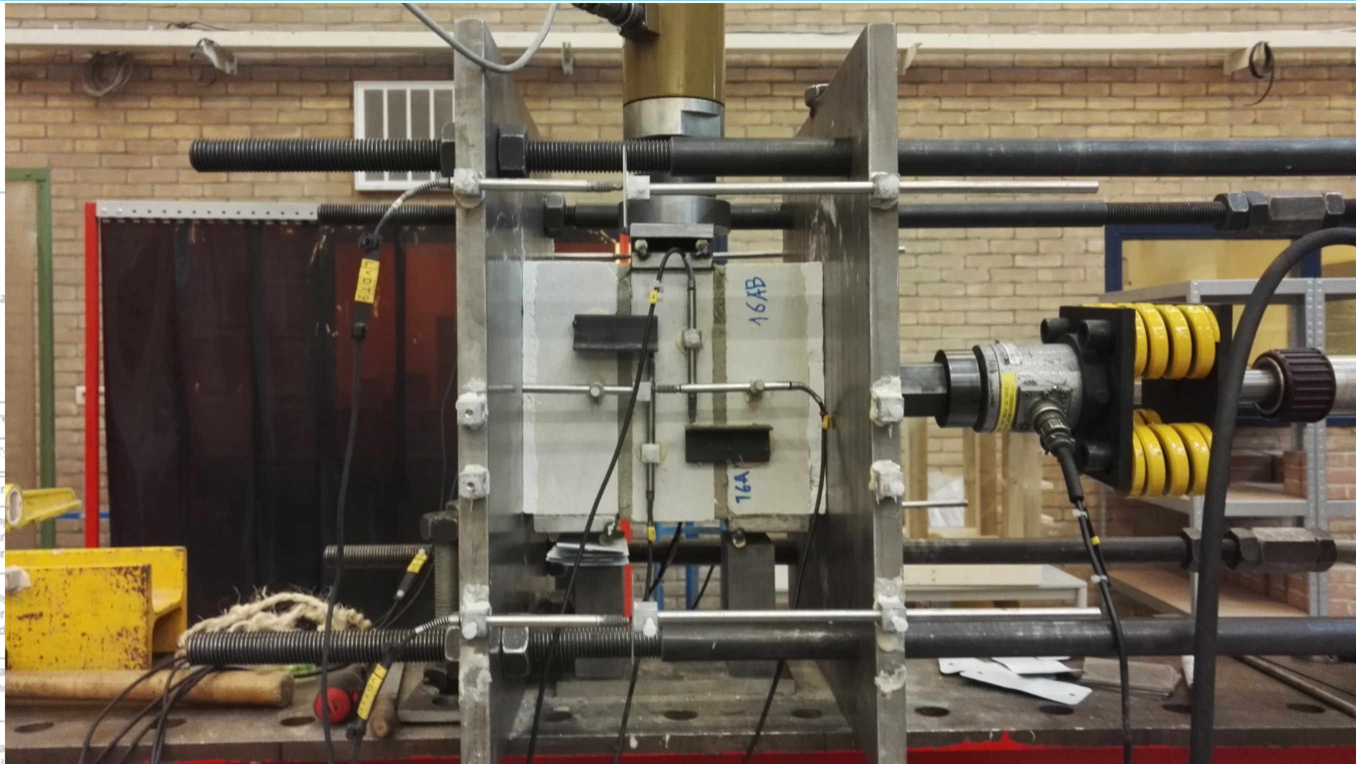

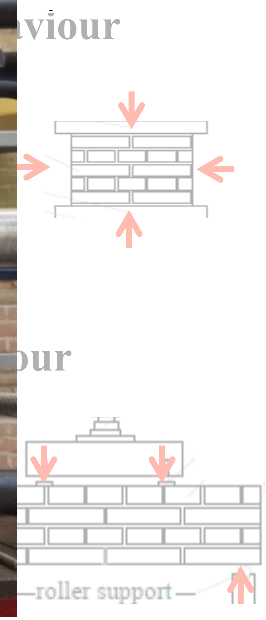

- Initial bed joint shear strength
- Bed joint shear friction coefficient
- Fracture energy in shear (bed joint)

Shear behaviour

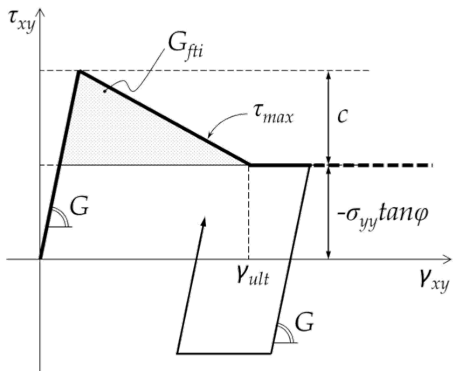

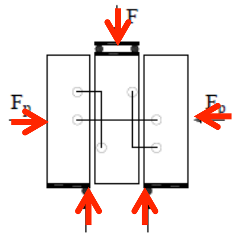

Shear tests

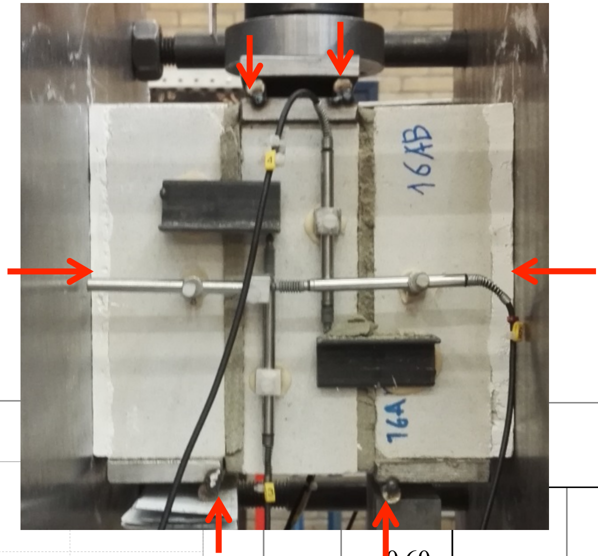

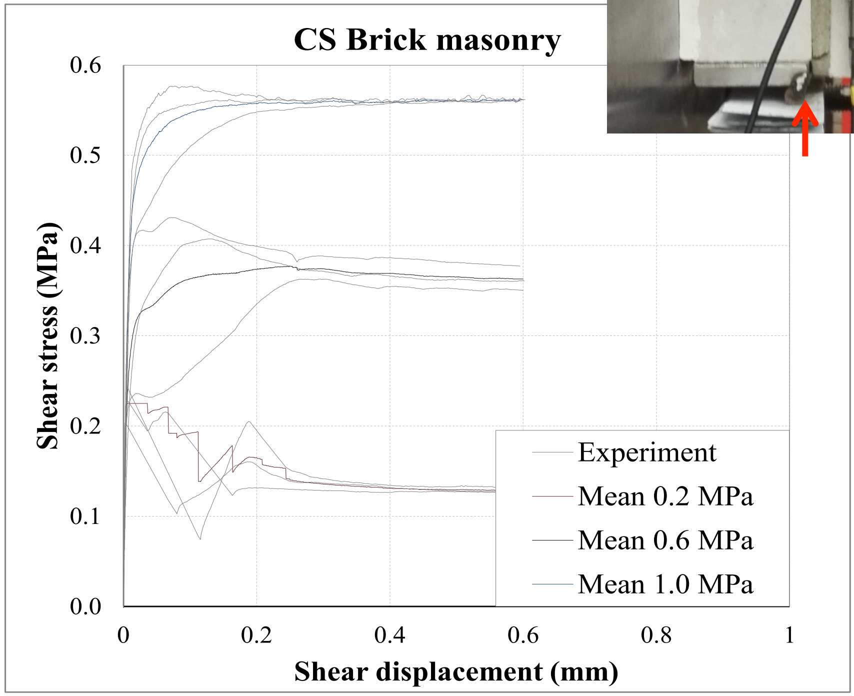
CS Brick masonry
Shear stress (MPa)
Shear displacement (mm)
0.0
0.1
0.2
0.3
0.4
0.5
0.6
0
0.2
0.4
0.6
0.8
1
Experiment
Mean 0.2 MPa
Mean 0.6 MPa
Mean 1.0 MPa

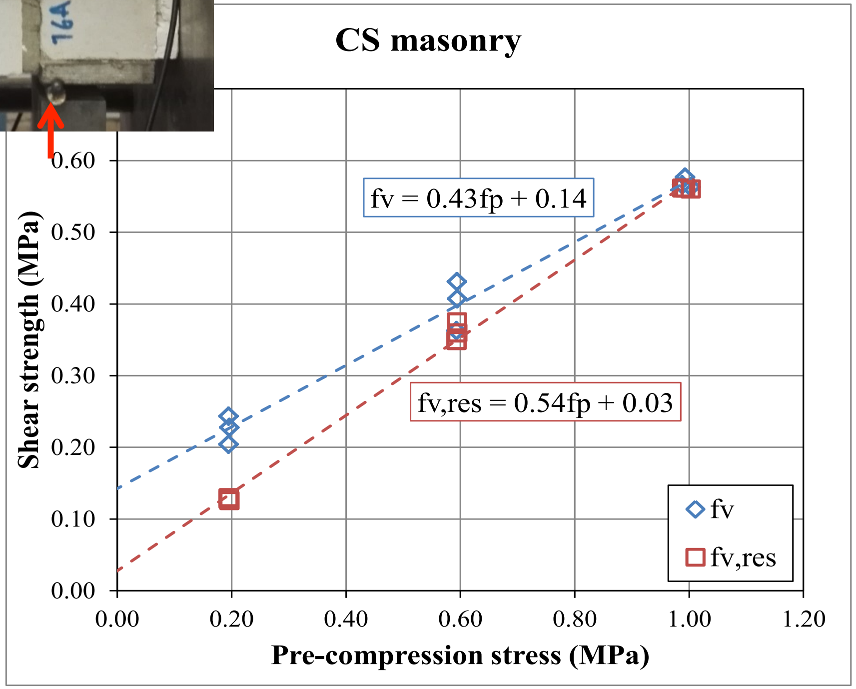
CS masonry
fv = 0.43fp + 0.14
fv,res = 0.54fp + 0.03
Shear strength (MPa)
Pre-compression stress (MPa)
0.00
0.10
0.20
0.30
0.40
0.50
0.60
0.00
0.20
0.40
0.60
0.80
1.00
1.20
fv
fv,res

Shear tests

Masonry type			f_{v0}	μ
			MPa	-
CS masonry	Existing (brick)	<1985	0.28	0.79
		1985>	0.11	0.70
	Replicated	Brick masonry	0.14	0.48
		Element masonry*	0.83	1.48
	NPR 2015	CS brick	0.25	0.60
		CS element	0.80	0.80

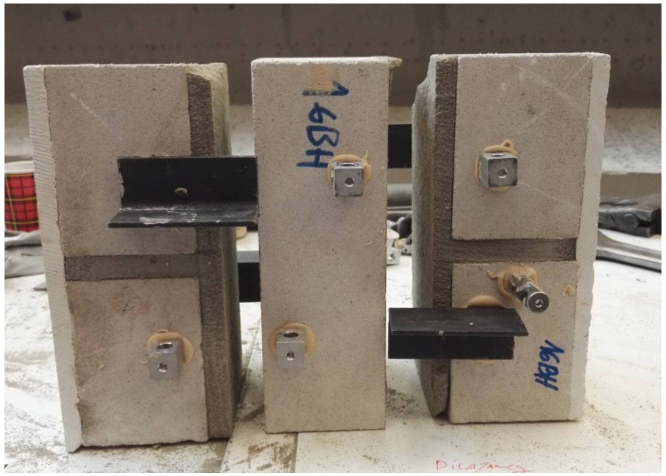

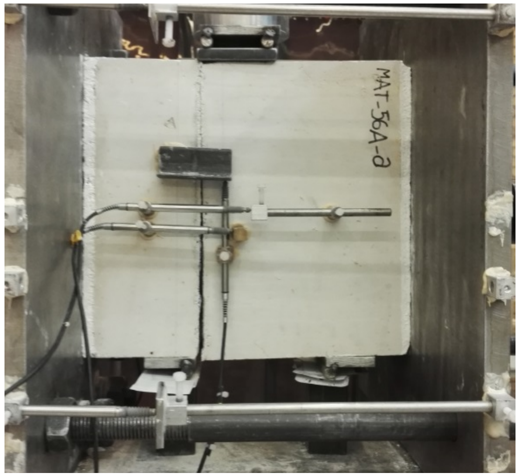

Shear tests

Masonry type			f_{v0}	μ
			MPa	-
Clay masonry	Existing (brick)	<1945	0.30	0.80
		1945>	0.47	0.76
	Replicated	Perforated	0.15	0.48
		Solid-single wythe*	0.20	0.69
		Solid-double wythe*		
	NPR 2015	<1945	0.30	0.75
		>1945	0.40	0.75

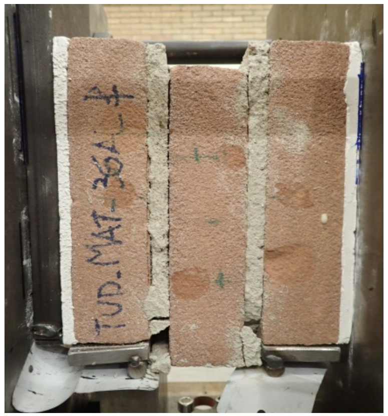

Mode II fracture energy in shear

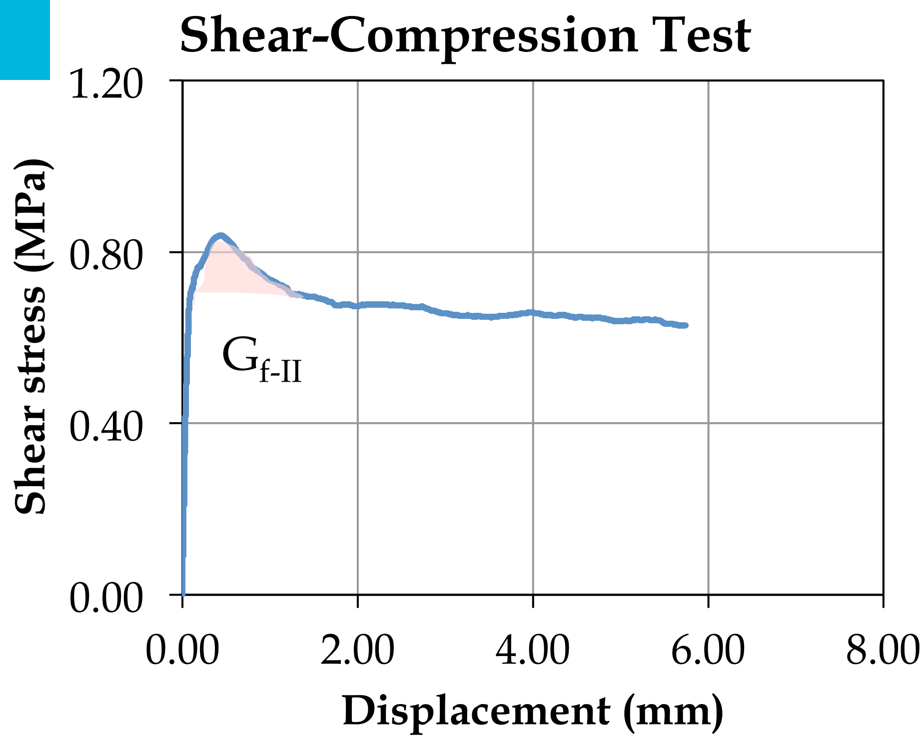

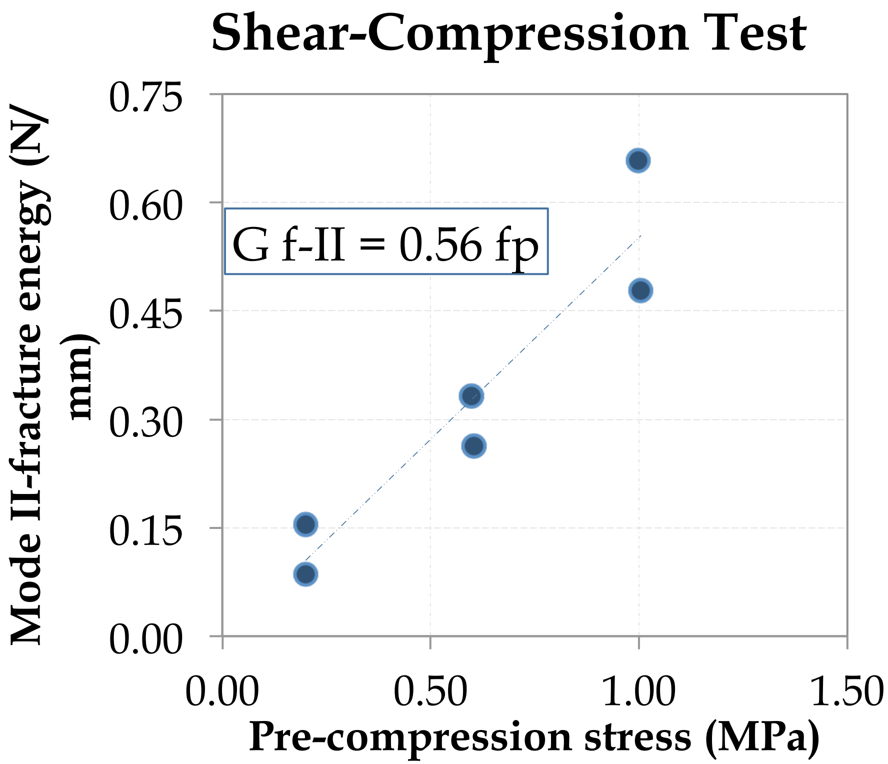

Correlation between cohesion and bond flexural strength

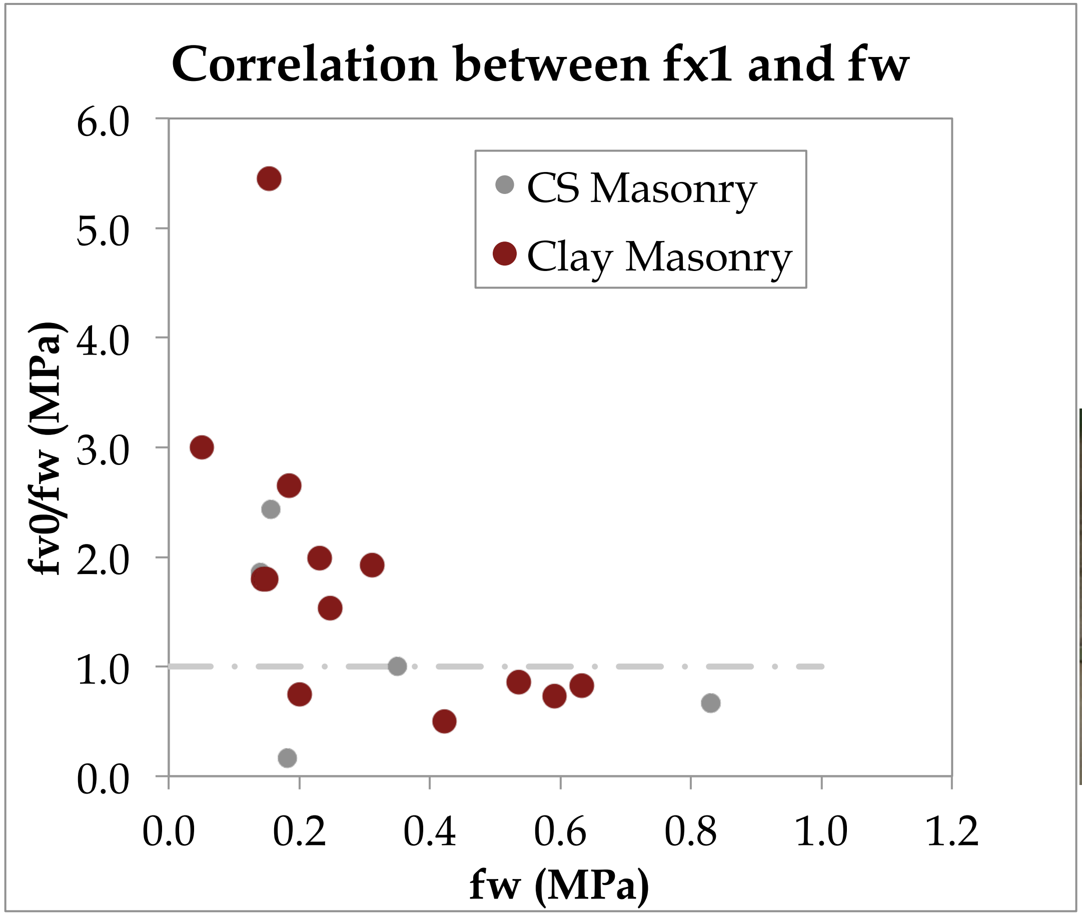

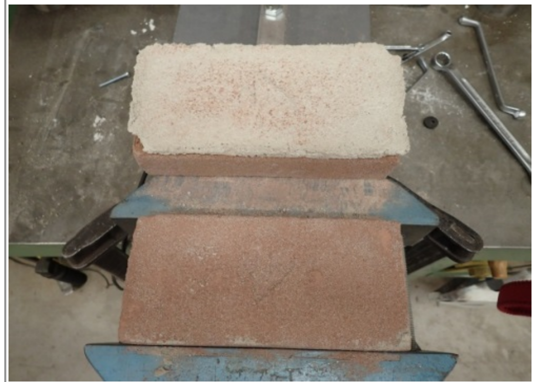

Initial shear strength or cohesion (f_{v0})
Flexural bond strength (f_w)

In-situ investigations 2015, E-modulus correlation, double-flat jack tests and lab compression tests

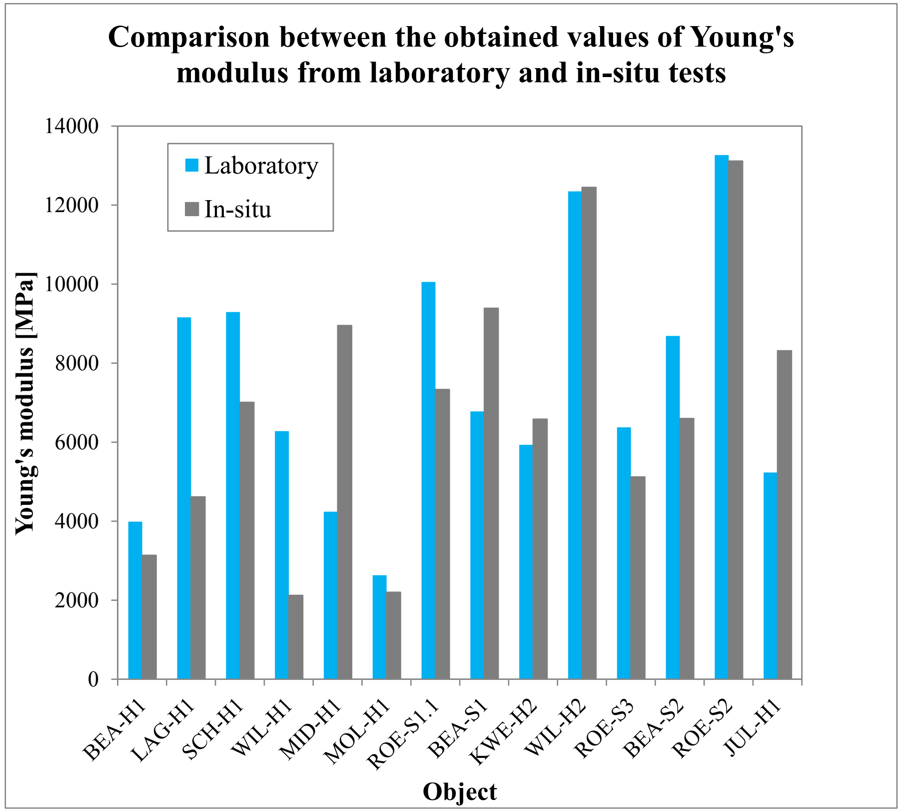

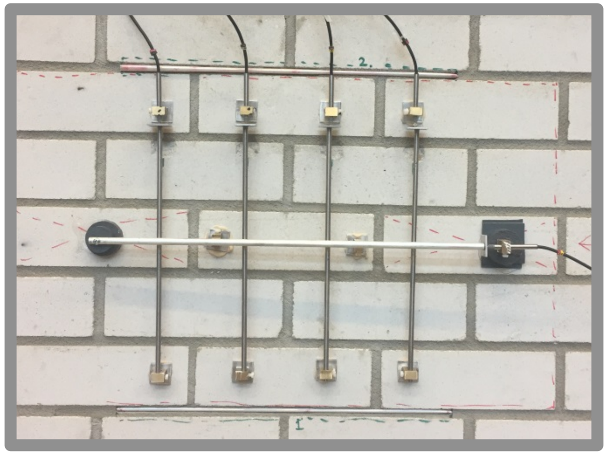

In-situ investigations 2015, cohesion correlation, shove tests and triplet tests

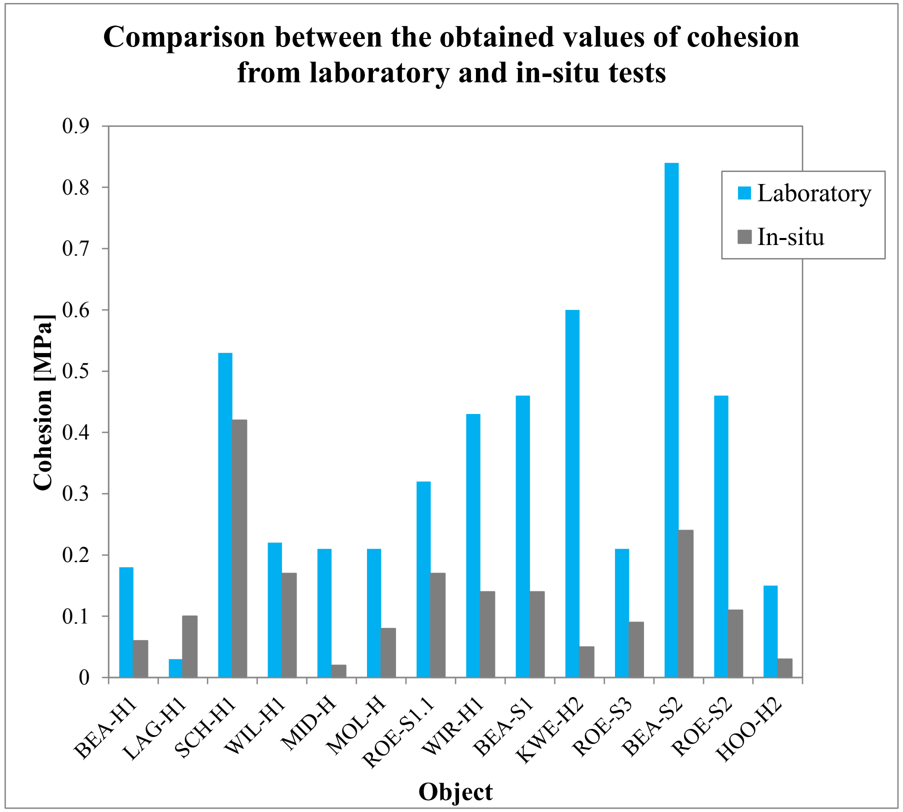

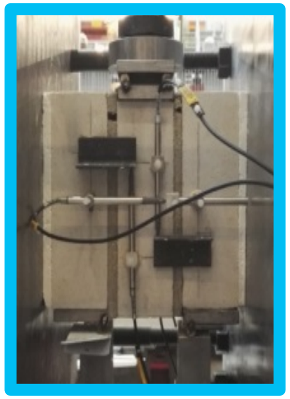

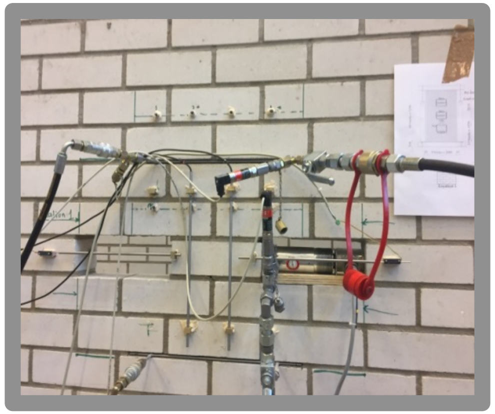

Weak correlation between DT and SDT

Further research is ongoing

Validation shove and flat-jack tests 2017

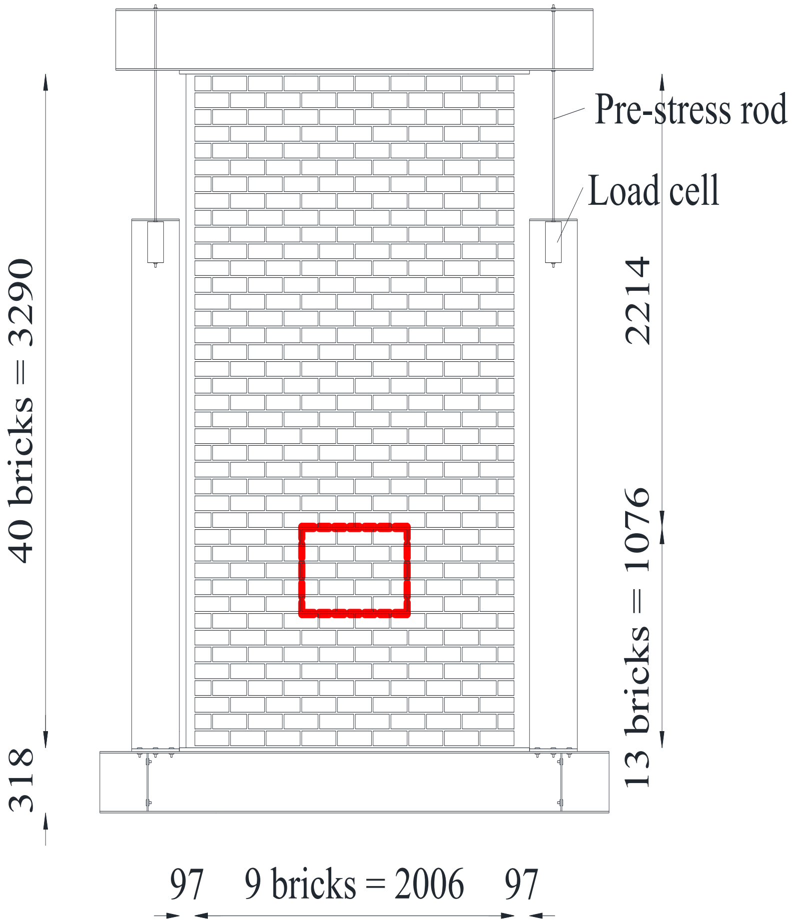

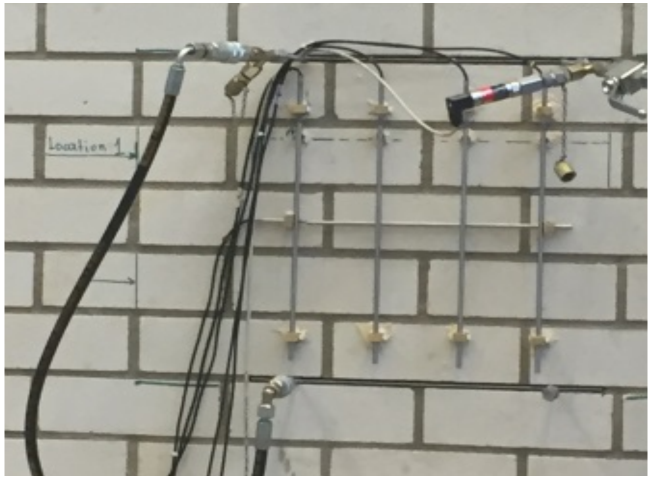

TU Delft

Other slightly destructive tests: tests on cores

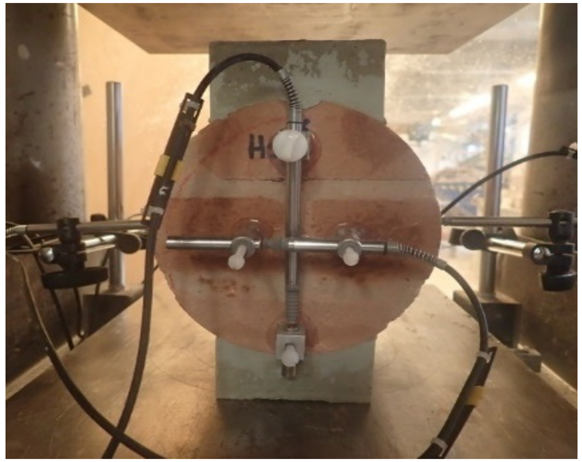

TUDelft

New slightly destructive test method: tests on cores

Replicated clay brick masonry

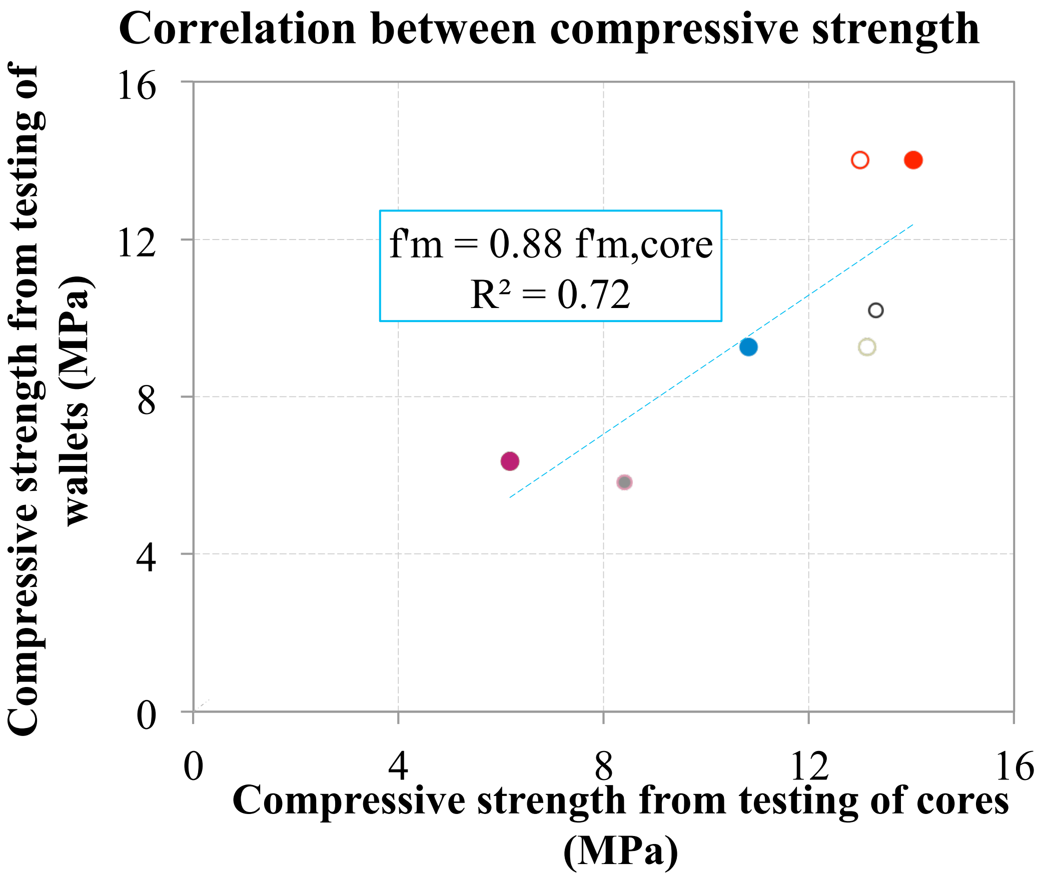

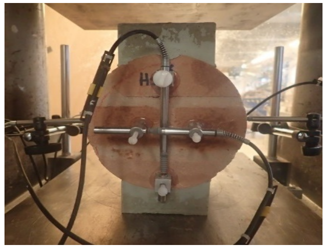

Thank you for your attention

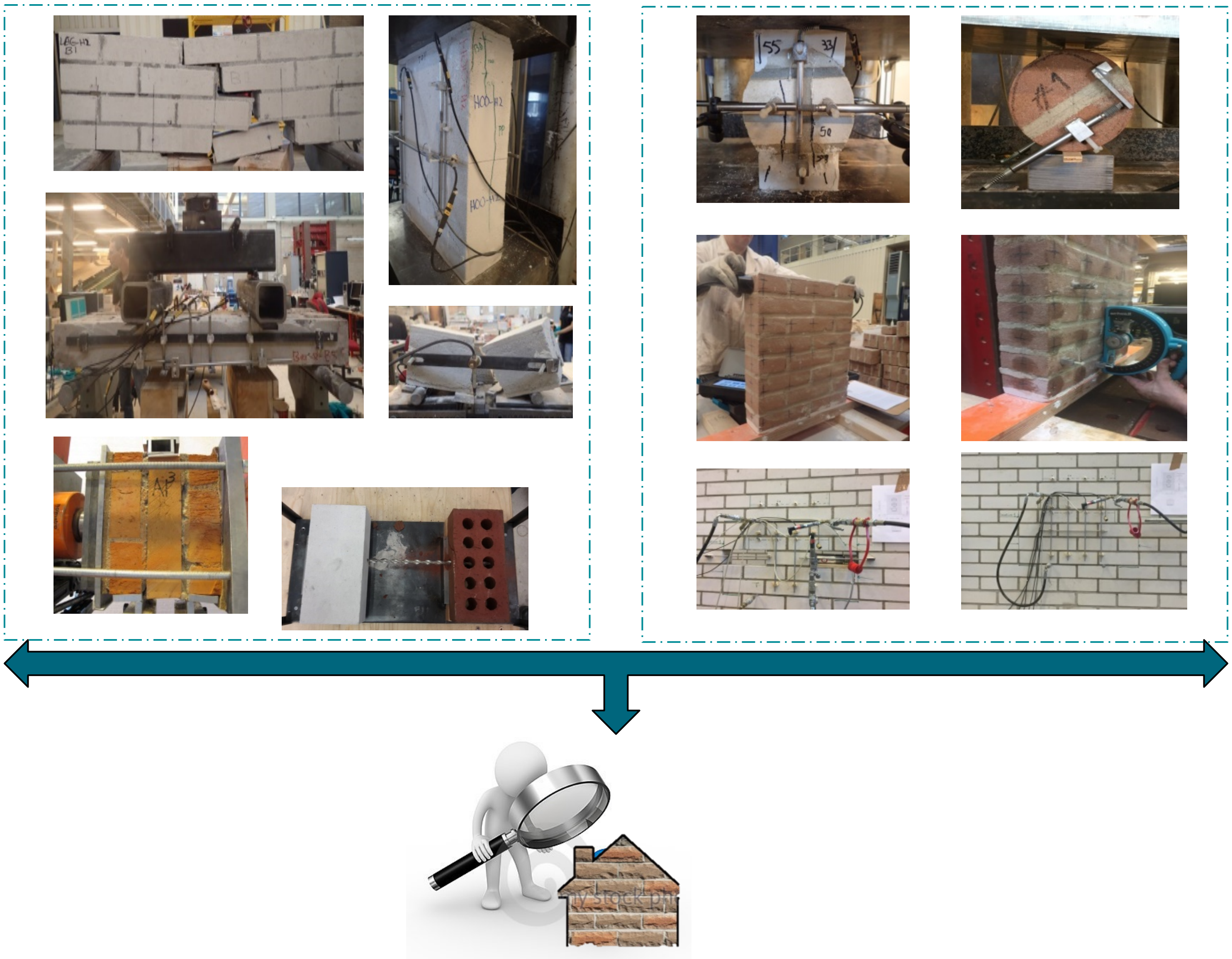

NEN-NPR2017

Symbol	Material property	Masonry (strength and stiffness values in N/mm², fracture energy values J/m²)			
		Clay brickwork (pre 1945) [d]	Clay brickwork (post 1945)	Calcium-silicate brickwork with general purpose mortar (typical approx. 1960-present)	Calcium-silicate blocks/elements with thin layer mortar (typical approx. 1985-present)
f'_m	Compressive strength	8,5	10,0	7,0	10,0
E_m	Young's modulus	5 000	6 000	4 000	7 500
G_m	Shear modulus	2 000	2 500	1 650	3 000
f_{x1}	Bending strength for plane of failure parallel to the bed joints [a]	0,15	0,3	0,15	0,6
f_{x2}	Bending strength for plane of failure perpendicular to the bed joints [a]	0,55	0,85	0,55	1,0
$f_{mt\perp}$	Uniaxial tensile strength perpendicular to the bed joint	0,1	0,2	0,1	0,4
$f_{mt//}$	Uniaxial tensile strength parallel to the bed joint	0,35	0,55	0,35	0,65
f_{v0}	Initial bed joint shear strength	0,3	0,4	0,25	0,8
$\tan\varphi$	Bed joint shear friction coefficient	0,75	0,75	0,6	0,8
$G_{ft\perp}$	Fracture energy [b] in tension perpendicular to the bed joints	10	10	10	20
$G_{ft//}$	Fracture energy [b] in tension parallel to the bed joints	35	35	20	20
G_{fc}	Fracture energy [c] in compression	20 000	15 000	15 000	20 000
G_{fs}	Fracture energy [b] in shear (bed joint)	100	200	100	200

[a] Not to be used in combination with softening
[b] To be used in combination with a crack band width, in case of smeared finite element models
[c] To be used in combination with a crush band width, in case of smeared finite element models
[d] When clay brickwork pre 1945 is of a clearly poor quality in terms of mortar quality, mortar ageing, filling of joints, layout and bond pattern, the mean values of strength, stiffness and fracture energy properties in this column are advised to be reduced by approximately 40%

Properties of masonry unit

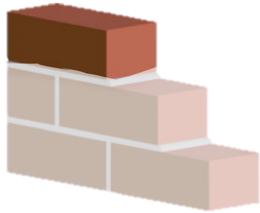

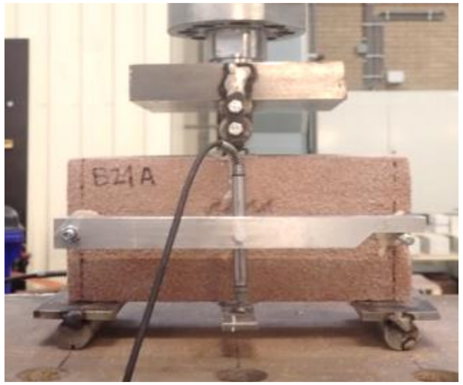

- Flexural strength
- Elastic modulus
- Stress-strain relationship in bending

- Compressive strength
- Stress-strain relationship in compression

- Young's modulus
- Stress-strain relationship in compression

Properties of mortar

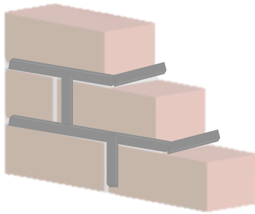

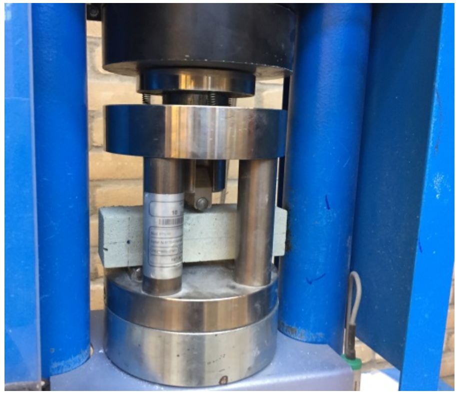

- Flexural strength

- Compressive strength

- Young's modulus
- Stress-strain relationship in compression

Characterising the material behaviour of existing masonry

Destructive test	Slightly-destructive test	Non-destructive test

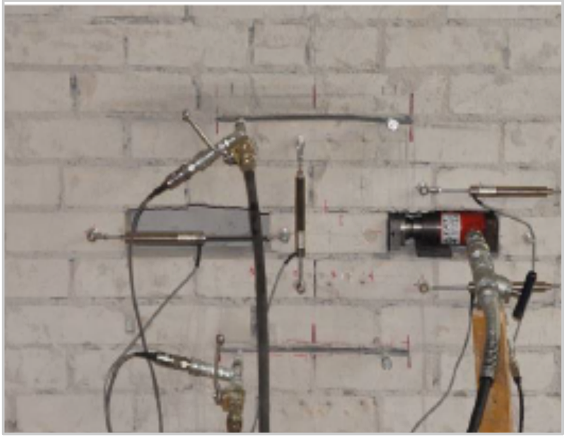

Characterising the material behaviour of existing masonry

Destructive test	Slightly-destructive test	Non-destructive test
• Compression tests in two orthogonal directions • Out-of-plane bending tests in two orthogonal directions • In-plane bending test • Bond wrench test • Shear-compression test	• Single flat jack test • Double flat jack test • Shove test	• Rebound hammer on brick • Rebound hammer on mortar • Ultrasonic tests on masonry/brick
• Directly providing properties + • Invasive − • Costly − • Technical challenges −	• Slightly destructive + • Reliability method − • Skilled technician − • Accurate acquisition system −	• Non-destructive + • Technically efficient + • Reliability method −

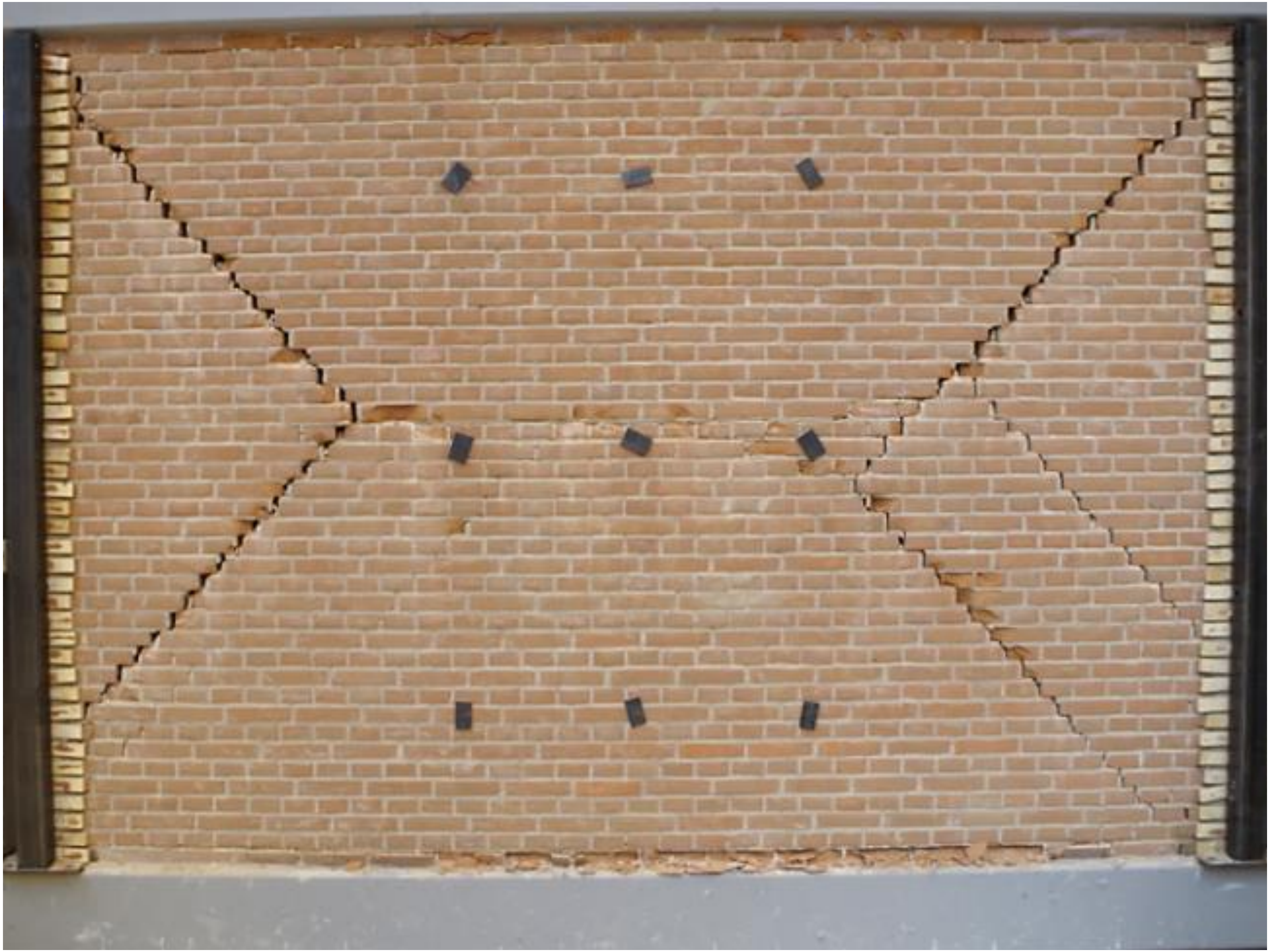

Assurance Meeting on Exposure, Fragility and Fatality Models for the Groningen Building Stock

EUCENTRE
FOR YOUR SAFETY.

Experimental Testing Programme for URM Components and Structures at EUCENTRE and LNEC

21-22 February 2018, Schiphol Airport, Amsterdam

NAM's seismic risk model for the Groningen Field

Seismicity Model * **GMPE** * **Exposure Model** * **Fragility Curves** * **Risk/Scenario Analysis**

Seismicity Model	GMPE	Exposure Model	Fragility Curves	Risk/Scenario Analysis
Number, magnitude, mechanism and location of earthquakes	Log-normal distribution of PGA values for a given earthquake	Location and classification of buildings in and around the gas field	Probability, for each building class, reaching a damage state DS_i as a function of seismic shaking	Probability of reaching a loss SL_i as a function of DS

EUCENTRE's involvement

Seismic Hazard

Building Risk

Injury or Loss Risk

(courtesy of Stephen Bourne)

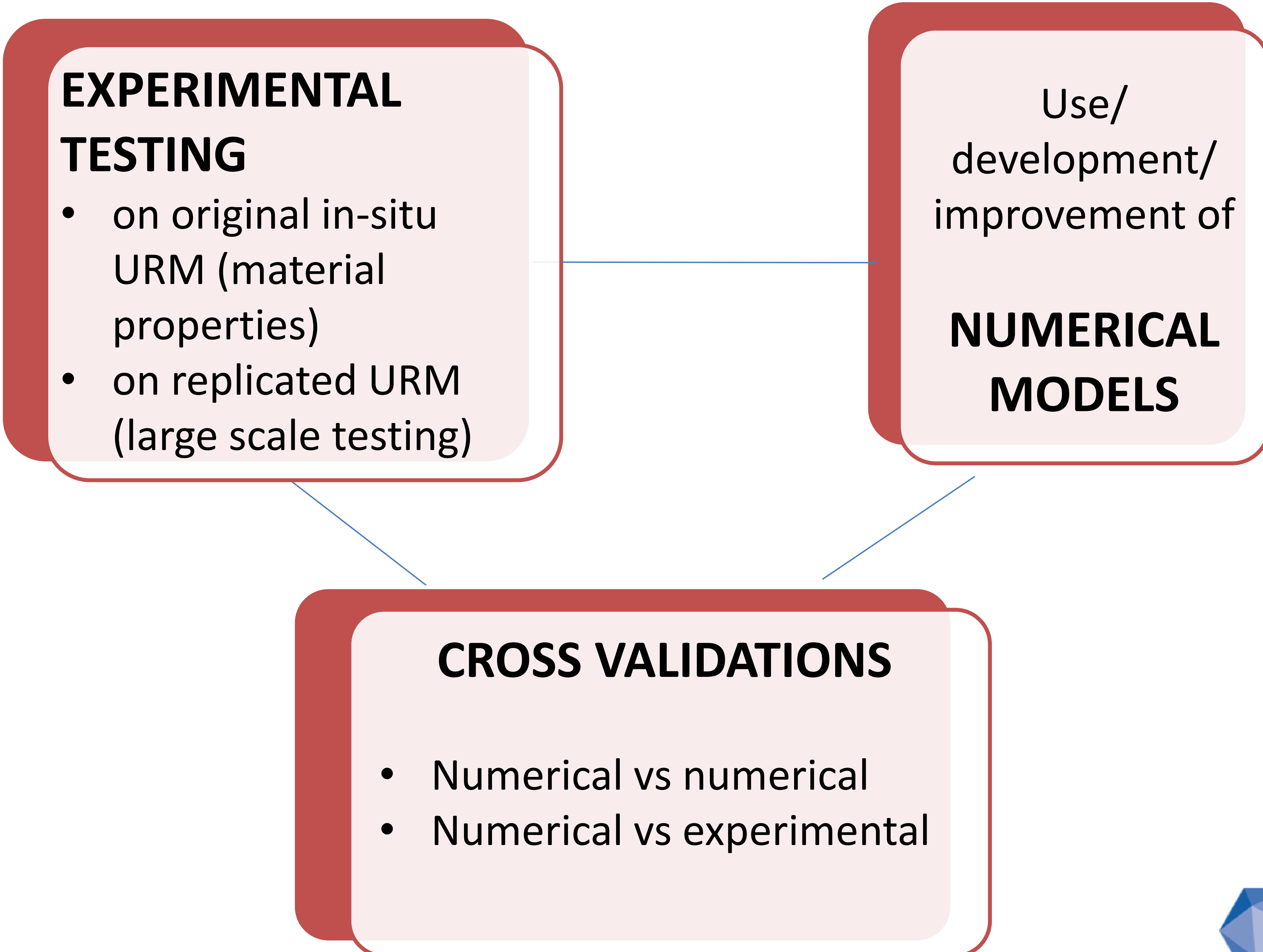
EXPERIMENTAL TESTING
• on original in-situ URM (material properties)
• on replicated URM (large scale testing)
Use/ development/ improvement of
NUMERICAL MODELS
CROSS VALIDATIONS
• Numerical vs numerical
• Numerical vs experimental

Research on the seismic behaviour of URM buildings

- Mechanical properties of materials (components and assemblage of components)

- Numerical modelling

- In-plane behaviour on masonry structural elements

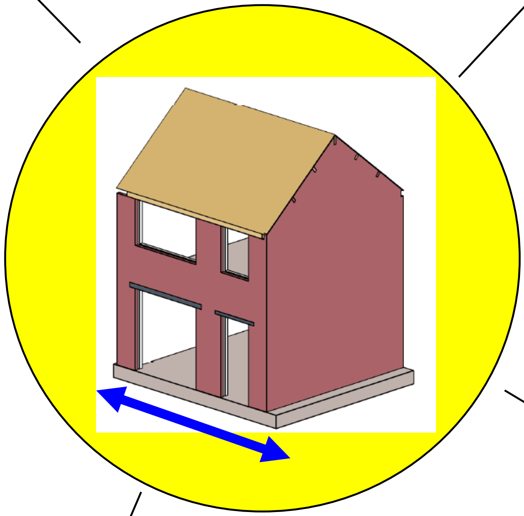

- Structural layout (geometry, floor and roof typology…)

- Out-of-plane behaviour of structural elements

- Mechanical behaviour of connections (floor-to-wall, wall-to-wall…)

The experimental campaign

Project aiming at assessing the vulnerability of Groningen buildings subjected to induced seismicity.
Experimental campaign:

- Characterization tests on materials, components and small assemblages (laboratory & in-situ);
- **8** In-Plane cyclic tests;
- **9** OOP shaking table tests on full-scale URM piers;
- **3** shaking table tests on full-scale URM buildings;
- **1** collapse test of a roof structure.



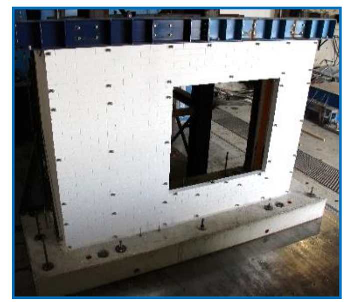





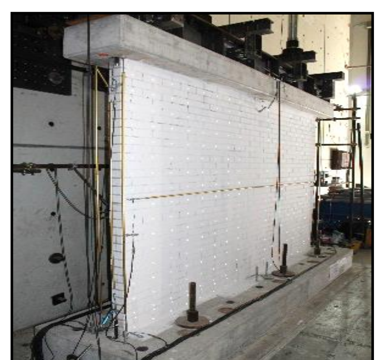


Material Characterization

Laboratory and In-situ

Complementary Laboratory Tests

All campaigns accompanied by complementary material characterization tests:

- **Units**:
  - Compression;
  - Flexural Tension.
- **Mortar**:
  - Compression;
  - Flexural Tension.
- **Masonry** (assemblages):
  - Compression;
  - OOP flexural strength;
  - Bond strength;
  - Direct shear strength;
  - Torsional.

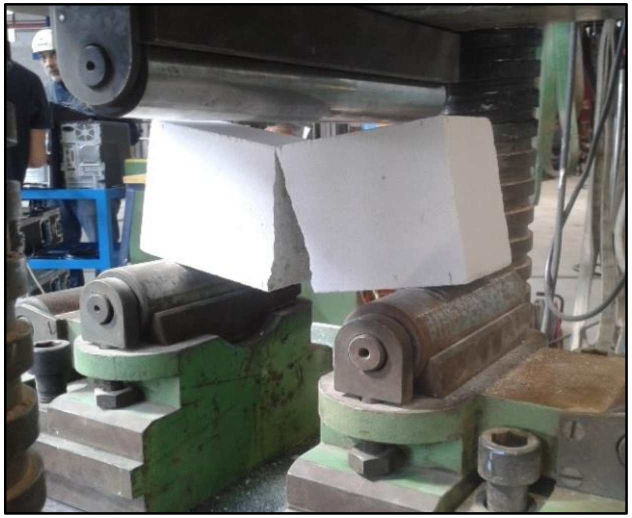

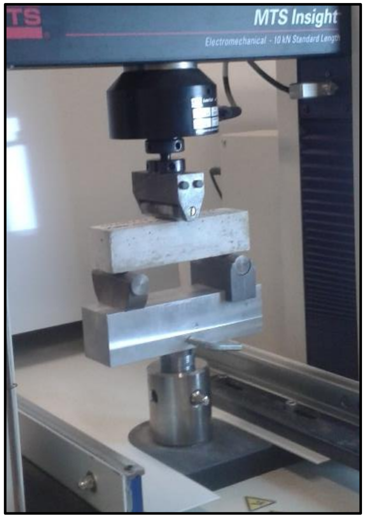

Laboratory Tests

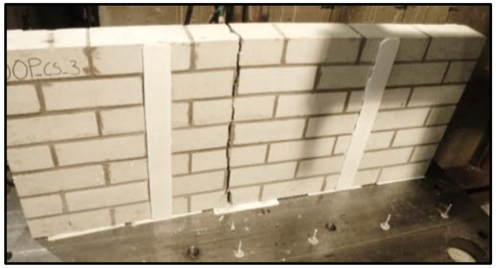

Torsional Shear Test

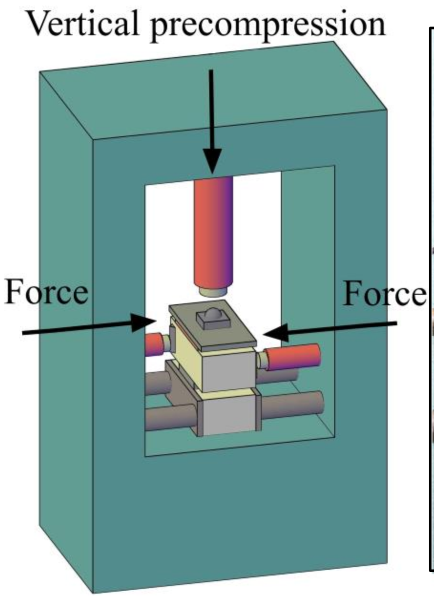

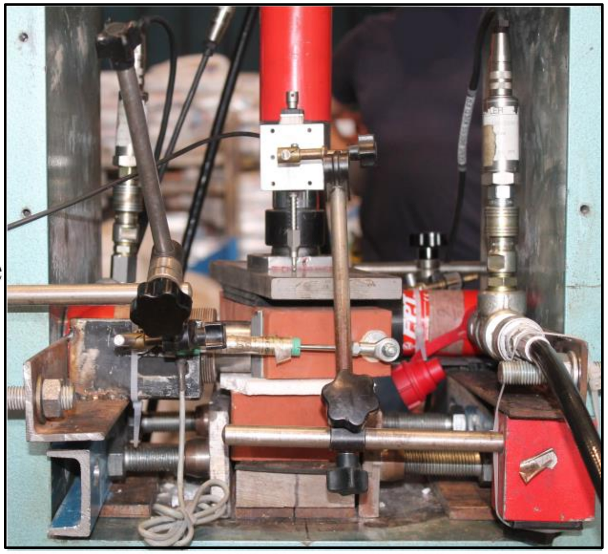

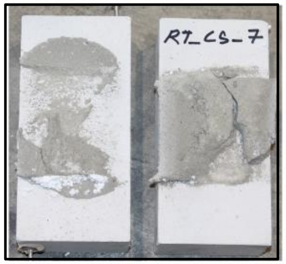

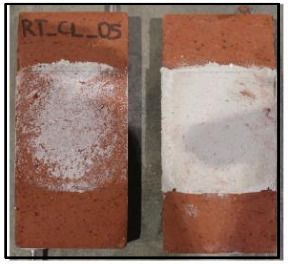

In-situ Tests

TYPICAL URM TERRACED HOUSES

In-situ characterization of materials and portion of URM, by means of mildly invasive tests:

Single Flatjack Test

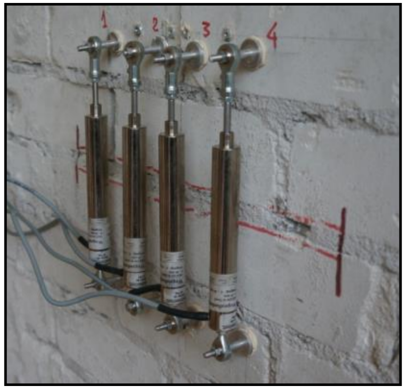

Compressive stress state

Double Flatjack Test

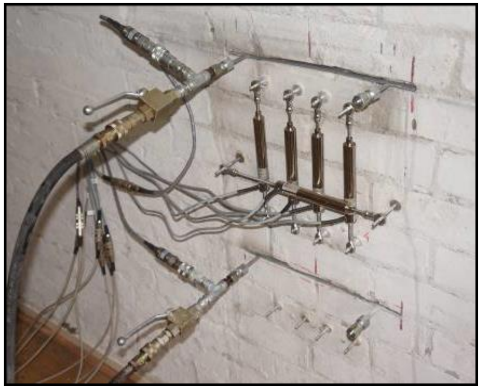

Masonry Elastic Modulus

Shove Test

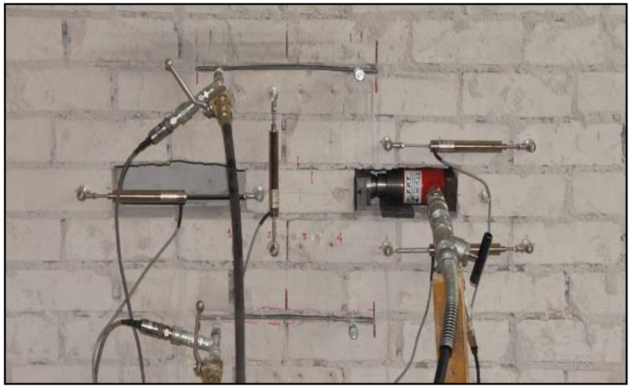

Shear Strength at brick/mortar interface

In-situ Tests

Ultrasonic Test

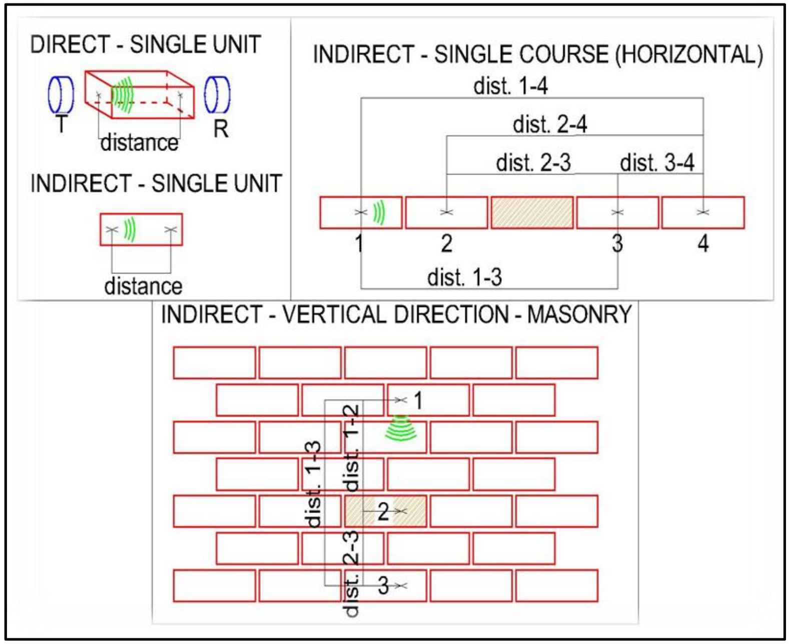

Indications on the quality of the bricks and the masonry

Rebound Hammer Test
&
Penetrometric Test on Mortar

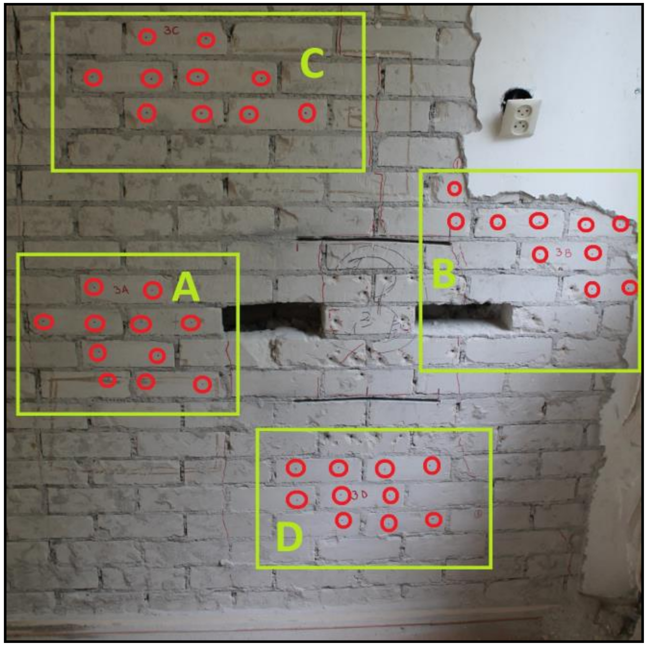

Indications on the quality of the bricks and mortar

In-situ Tests

Dynamic Identification

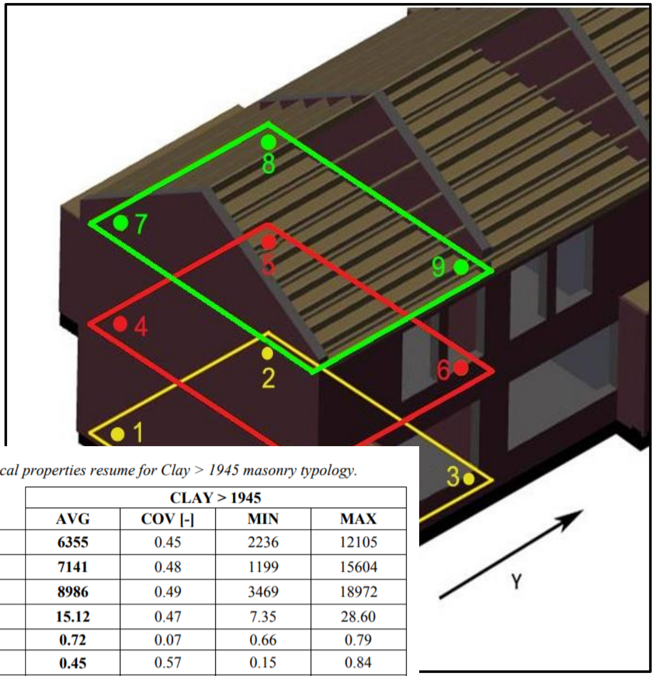

Table 62. Mechanical properties resume for Clay > 1945 masonry typology.

		CLAY > 1945			
		AVG	COV [-]	MIN	MAX
$E_{m,v(30-70)}$	[MPa]	**6355**	0.45	2236	12105
$E_{m,v(LIN)}$	[MPa]	**7141**	0.48	1199	15604
$E_{m,v(IS)}$	[MPa]	**8986**	0.49	3469	18972
$f_{m,v}$	[MPa]	**15.12**	0.47	7.35	28.60
μ	[-]	**0.72**	0.07	0.66	0.79
$\tau_{0,(LAB)}$	[MPa]	**0.45**	0.57	0.15	0.84
$\tau_{0,(IS)}$	[MPa]	**0.11**	0.85	0.00	0.38
$f_{bu,c}$	[MPa]	**22.06**	0.40	9.40	48.10
$f_{mu,t}$	[MPa]	**4.69**	0.4	1.75	8.79
$f_{m,h}$	[MPa]	**11**	0.23	7.41	14.23
$G_{f\text{-}c,h}$	[N/mm]	**47.59**	0.3	29.22	70.96
f_{x2}	[MPa]	**1.22**	0.28	0.59	1.68
f_{x3}	[MPa]	**0.76**	0.44	0.25	1.4
$f_{b,bj}$	[MPa]	**0.43**	0.51	0.12	0.95

es of the
it

Thermography
&
Video Endoscopy

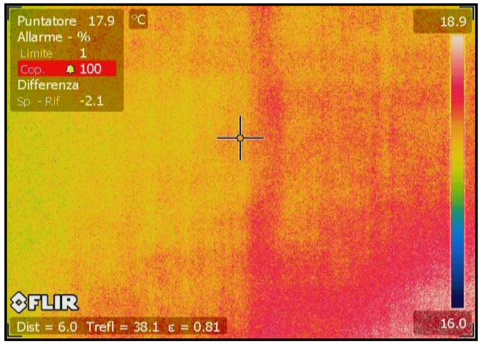

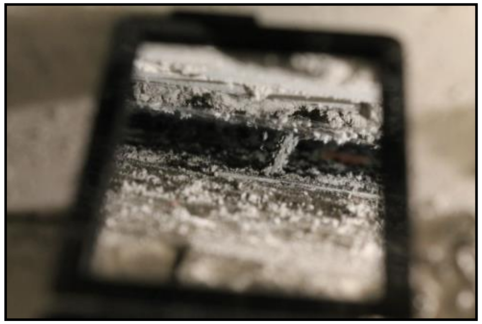

To better understand the geometry, the discontinuities and the position of steel ties

In situ mechanical properties database

Structural Component Tests

In-plane Cyclic Tests

Calcium Silicate and Clay

In-plane Tests - Calcium Silicate

2 Slender Piers Double Fixed:

EC_COMP_1

$\sigma_v = 0.52$ MPa

EC_COMP_2

$\sigma_v = 0.70$ MPa

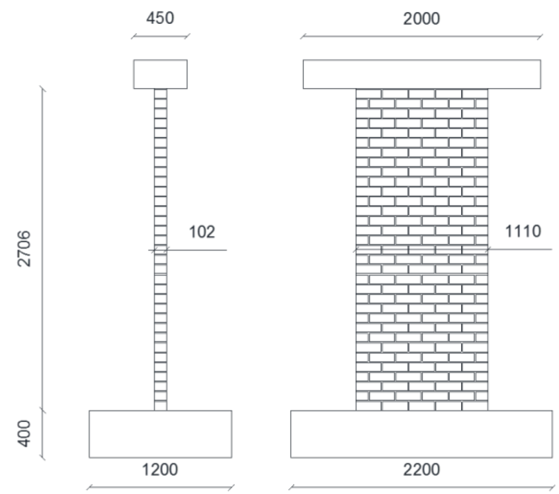

1 Pier Cantilever:

EC_COMP_3

$\sigma_v = 0.30$ MPa

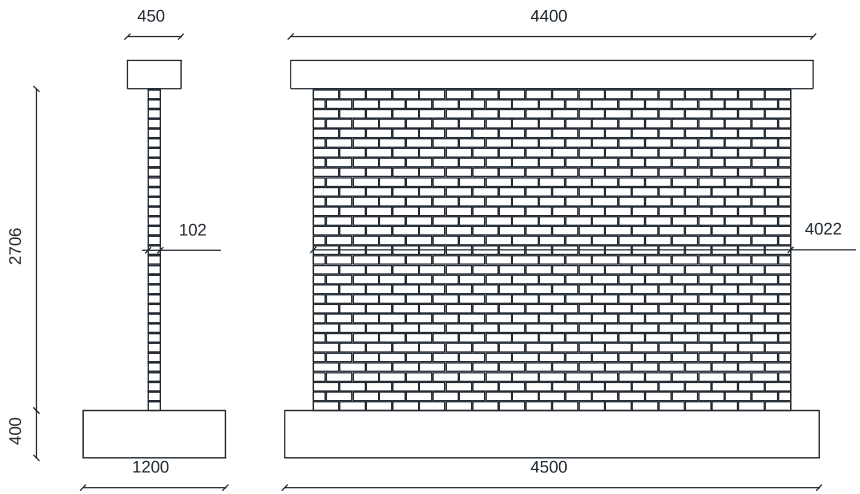

Test Set-up

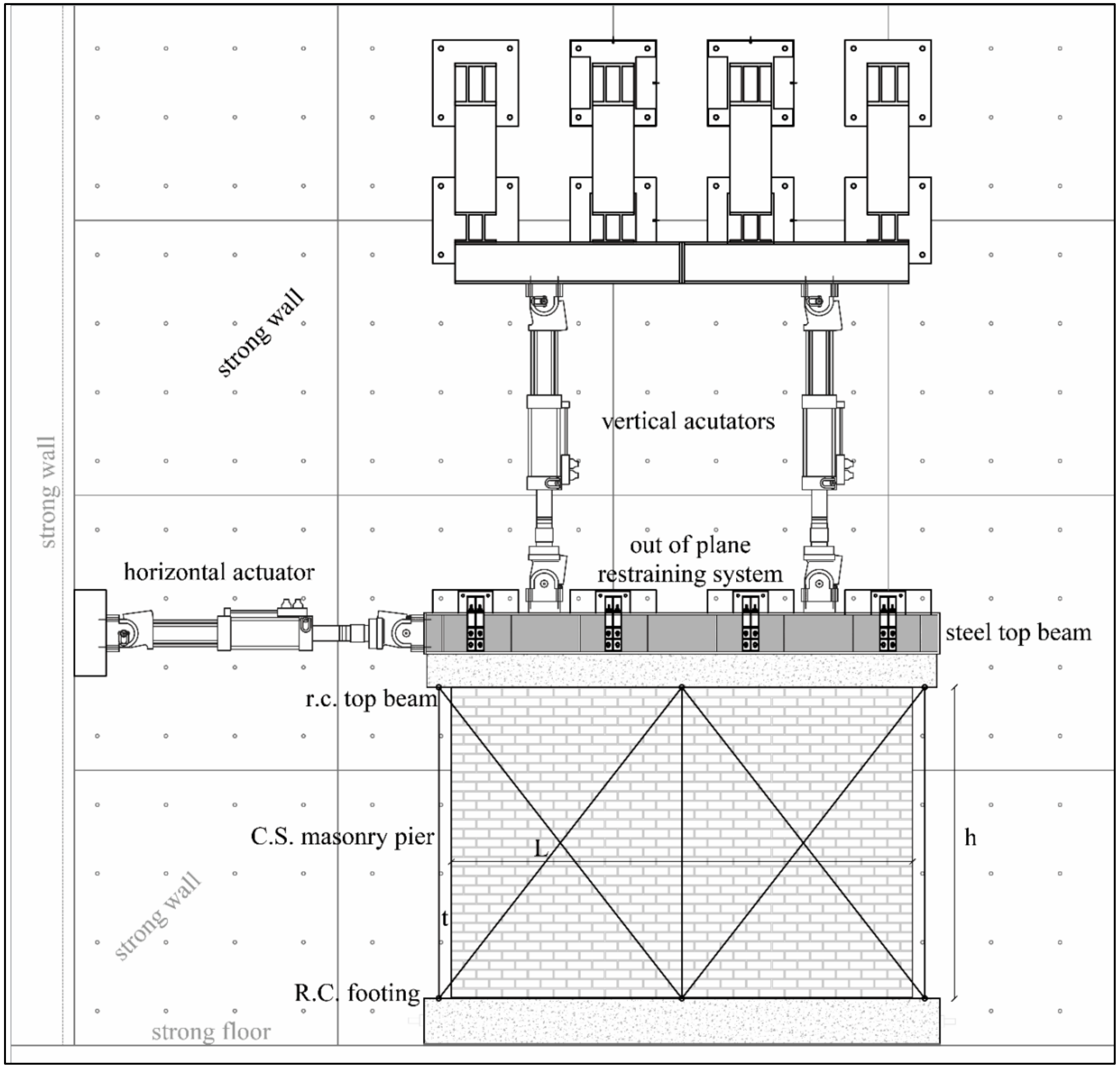
strong wall
strong wall
strong wall
vertical acutators
horizontal actuator
out of plane
restraining system
steel top beam
r.c. top beam
C.S. masonry pier
L
t
h
R.C. footing
strong floor

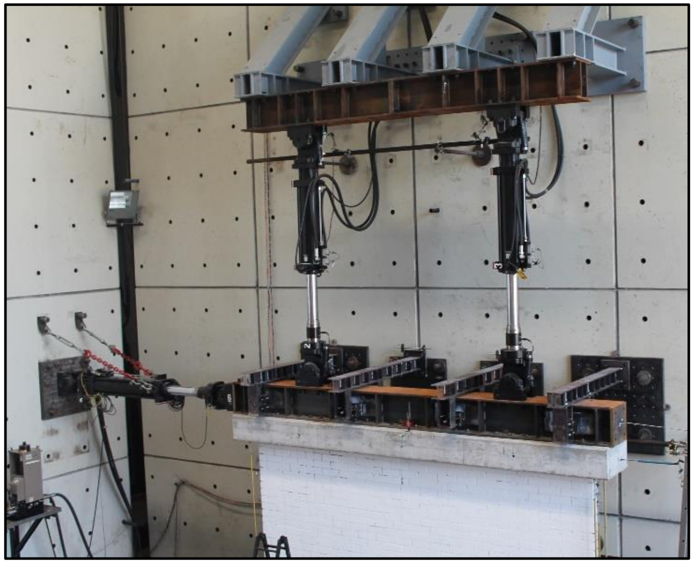

Failure Mechanisms

EC_COMP_1

First cracking
0.20% of drift

Failure
2% of drift

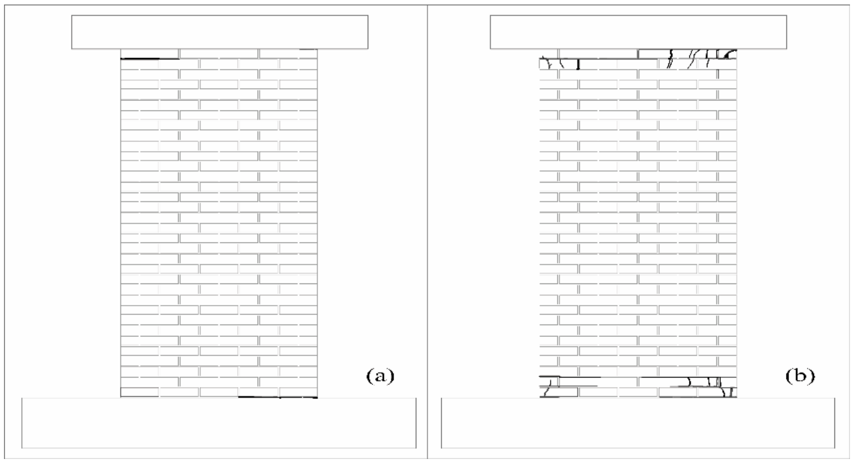

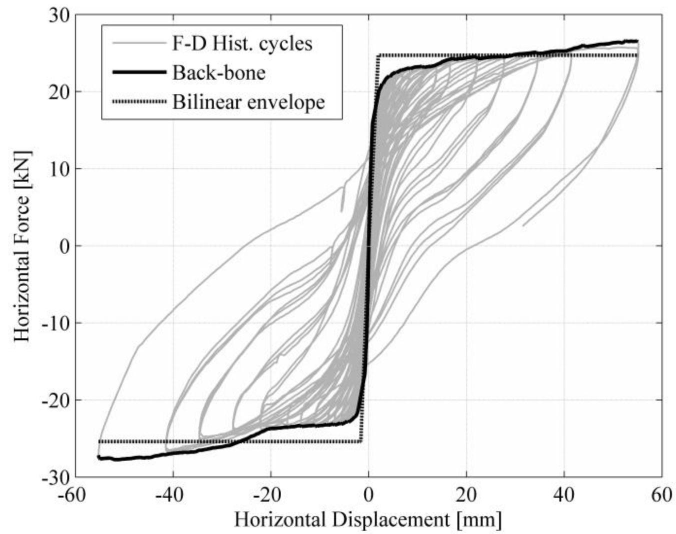

EC_COMP_2

Failure
0.25% of drift

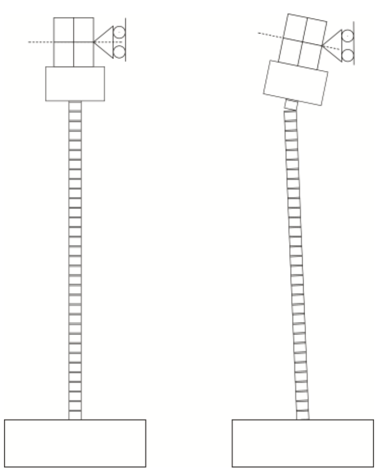

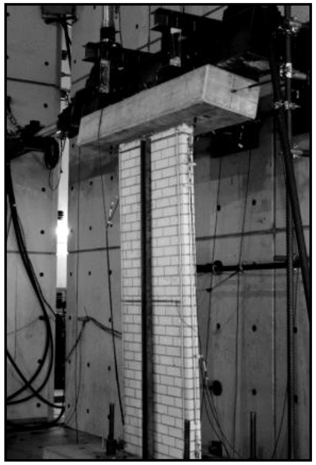

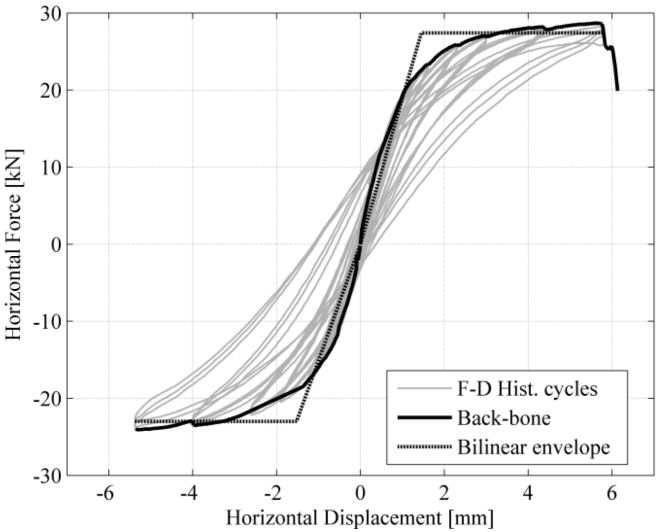

Failure Mechanisms

EC_COMP_3

First cracking 0.05% of drift

Failure 0.30% of drift

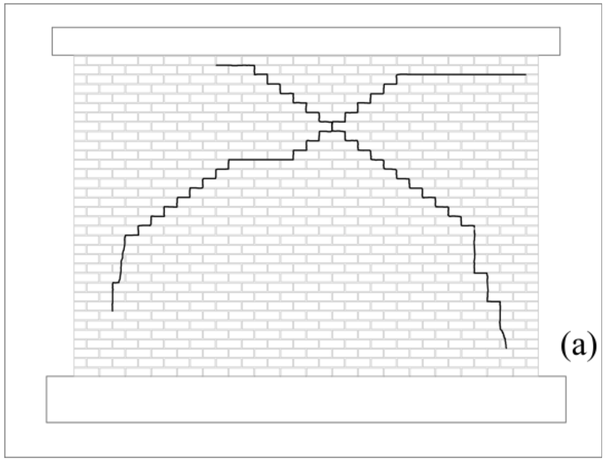

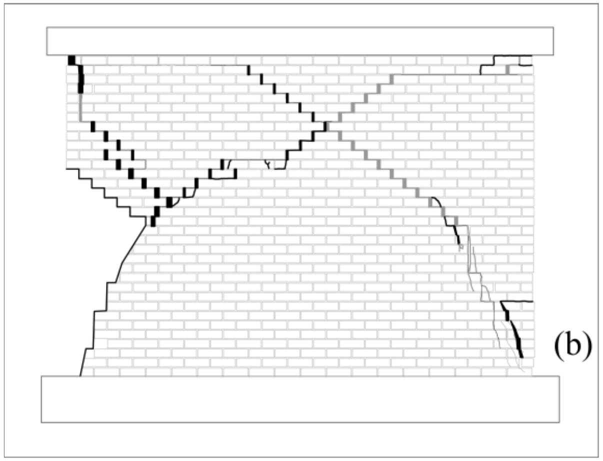

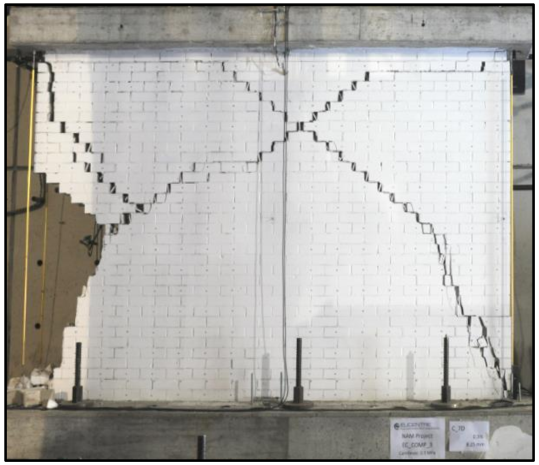

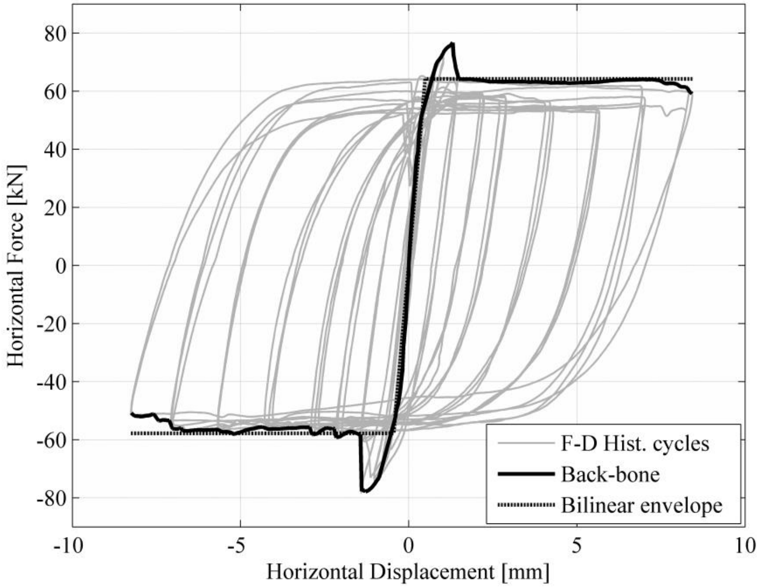

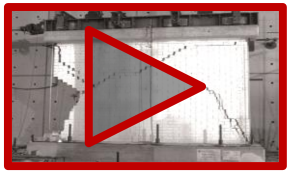

In-plane Tests - Clay

3 Slender Piers Double Fixed:

- **EC_COMP_1**, $\sigma_v = 0.52$ MPa;
- **EC_COMP_2**, $\sigma_v = 1.2$ MPa;
- **EC_COMP_3**, $\sigma_v = 0.86$ MPa.

2 Squat Piers Double Fixed:

- **EC_COMP_4**, $\sigma_v = 0.3$ MPa;
- **EC_COMP_5**, $\sigma_v = 0.3$ MPa.

Built with the Dutch cross brickwork bond

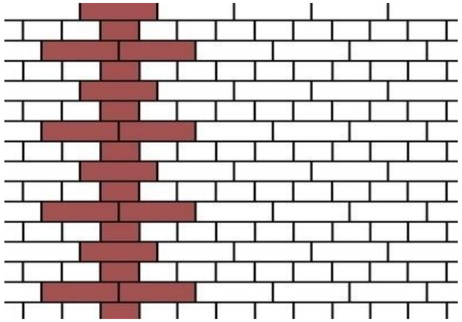

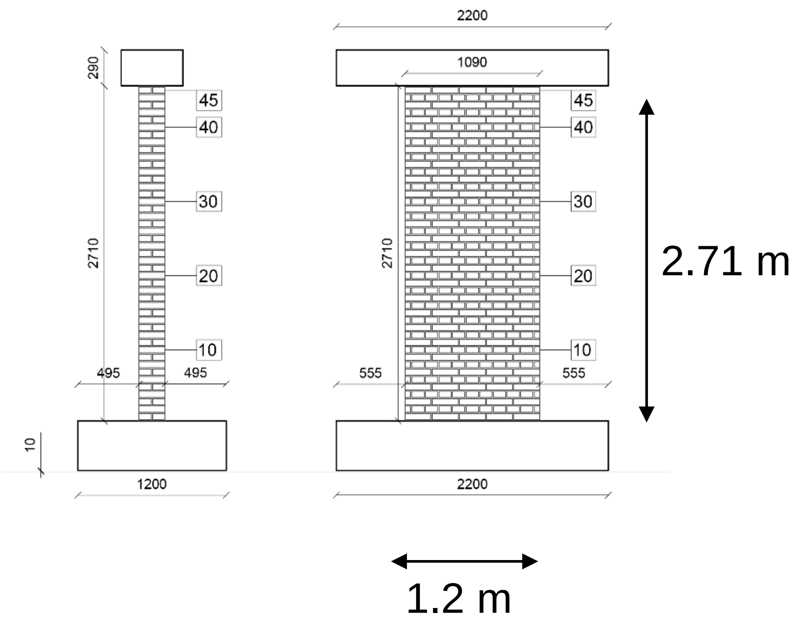

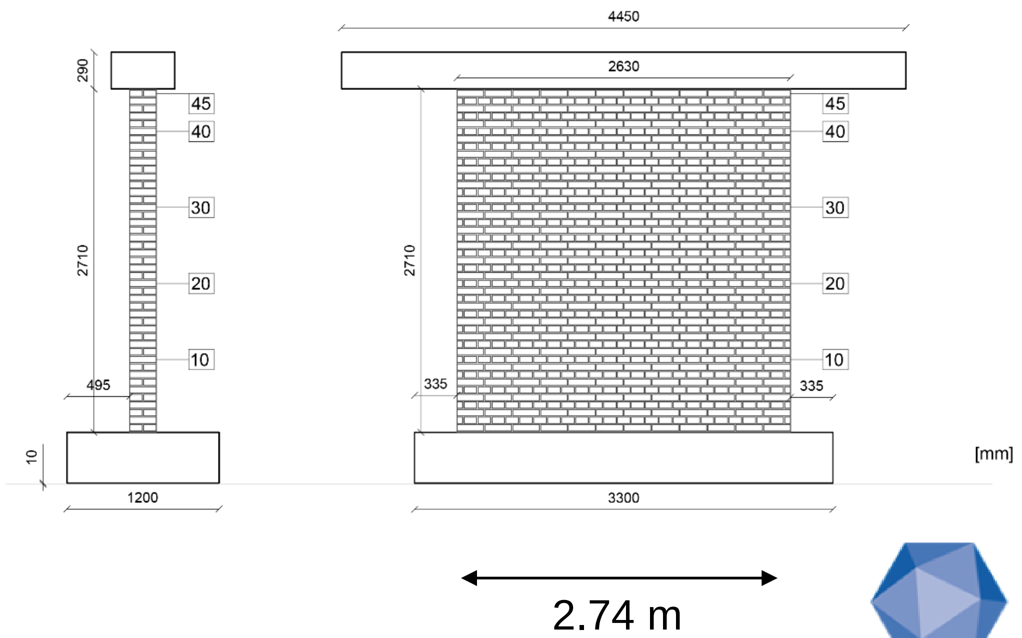

Failure Mechanisms

EC_COMP_1 (0.5 MPa)

- Pure rocking response;
- First crack for 0.2% wall-drift ratio;
- Ultimate drift capacity of 3%;
- No shear damage.

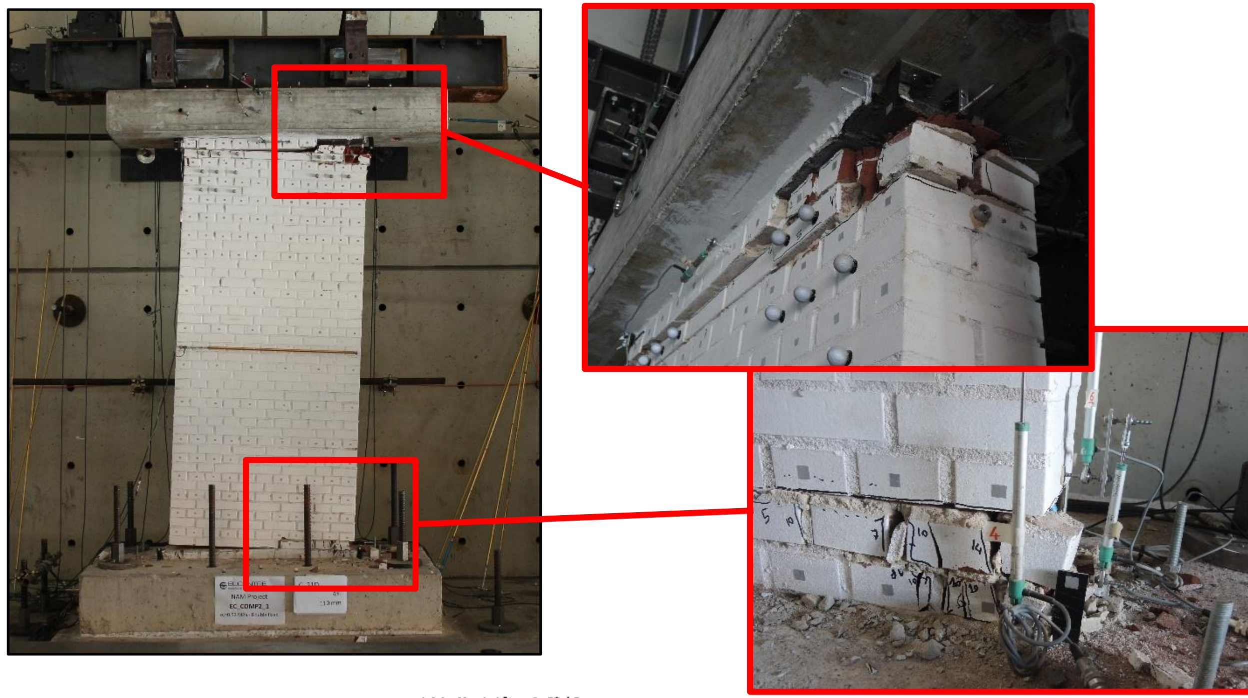

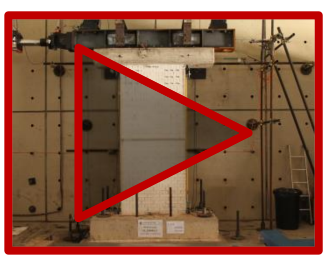

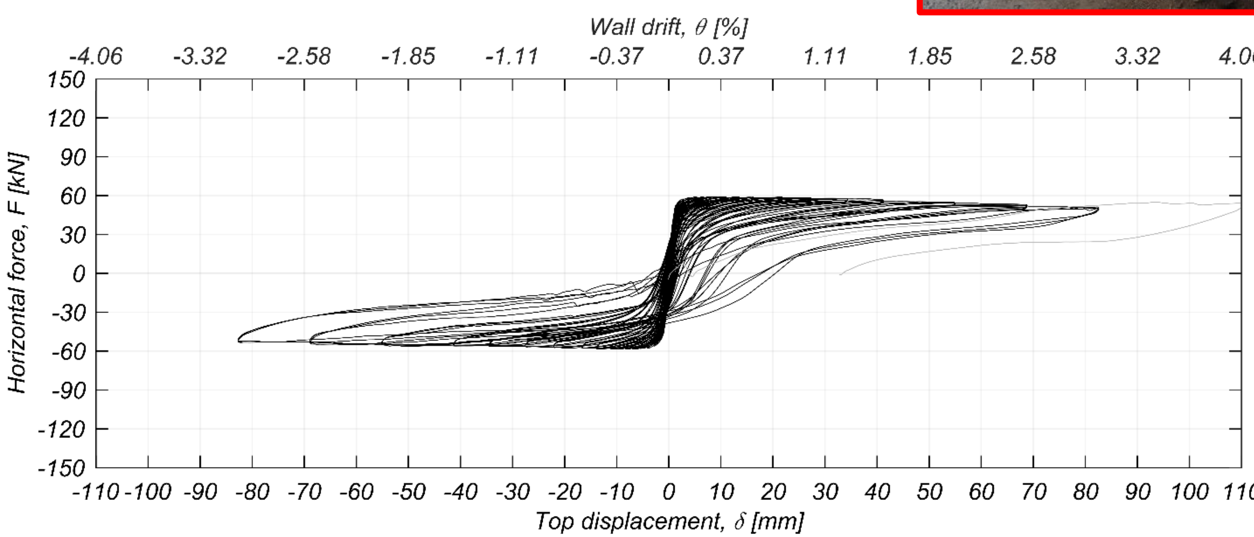

Failure Mechanisms

EC_COMP_2 (1.2 MPa)

- Hybrid rocking-shear behavior;
- First flexural cracks for 0.2% drift ratio;
- Toe crushing at 0.5%;
- Shear damage at 1% (diagonal crack at 45°);
- Ultimate drift of 1.25%.

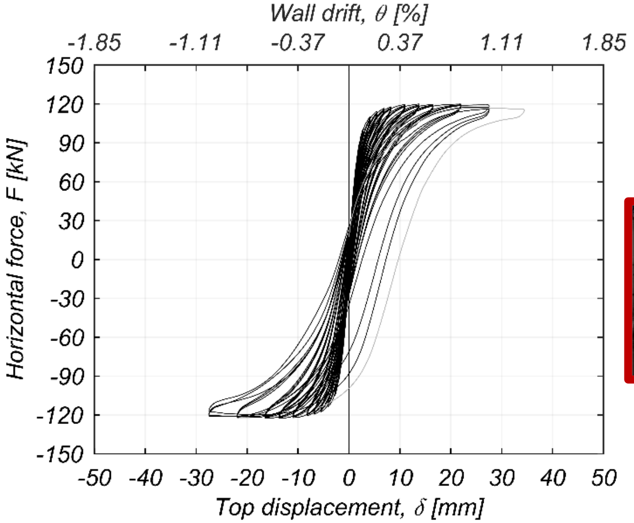

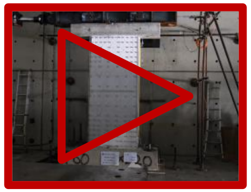

EC_COMP_3 (0.86 MPa)

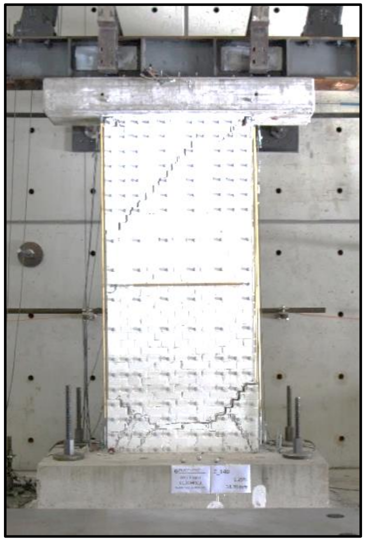

- Hybrid rocking-shear behavior;
- First flexural cracks for 0.15% drift ratio;
- Shear damage at 1%;
- Ultimate drift of 1.25% (unable to sustain any vertical loads).

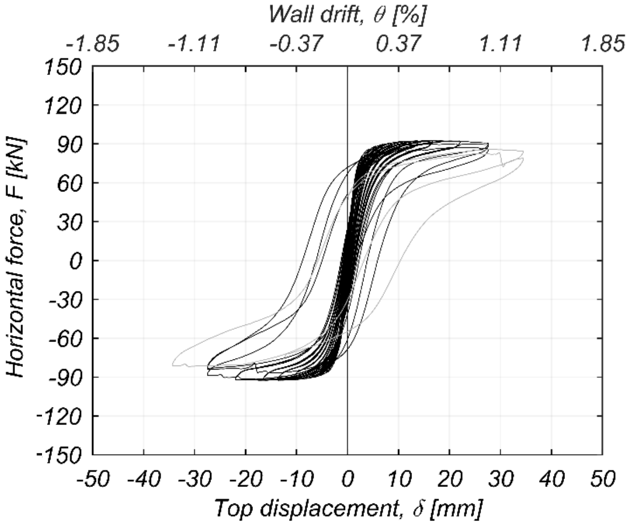

Failure Mechanisms

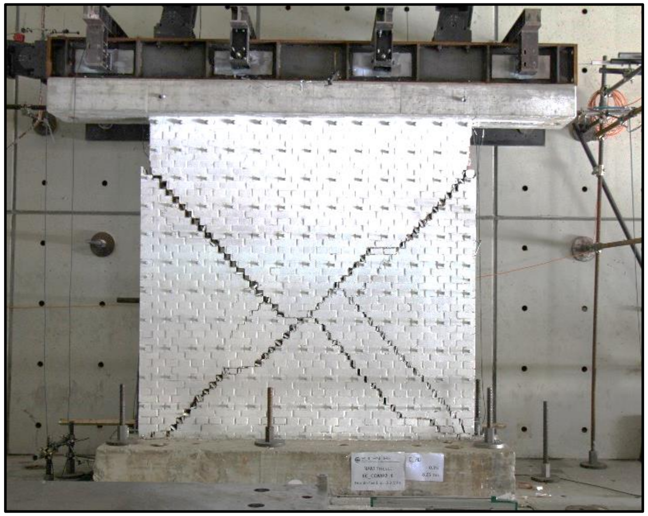

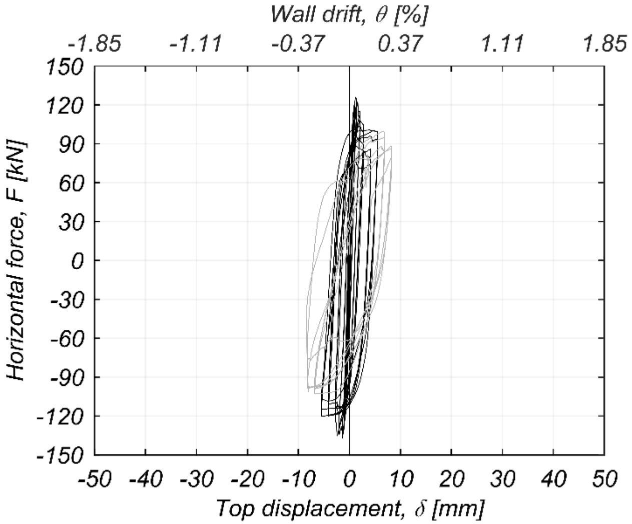

EC_COMP_4 (0.3 MPa)

- First flexural crack at drift ratio 0.02%;
- First diagonal shear crack at 0.05%;
- Ultimate drift of 0.32% with typical shear damage.

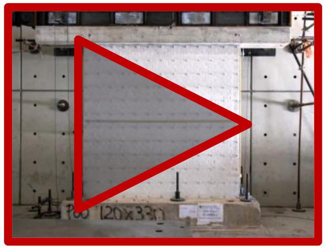

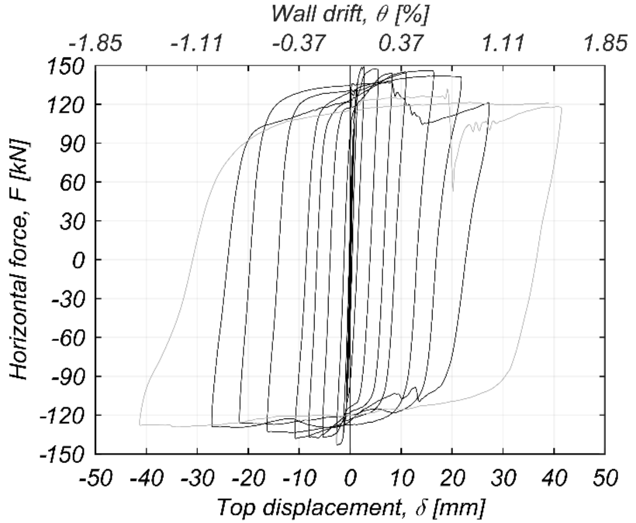

EC_COMP_5 (0.3 MPa)

- First shear crack at 0.05% due to sliding;
- Ultimate drift of 1.5% with typical shear failure and partial collapse.

Identification of the Local Damage Levels (LDLs)

- ϑ_{CR}: first visible crack (structural crack, no plaster's crack)
- ϑ_{Vmax}: maximum value of lateral strength
- ϑ_{U}: strength degradation equal to 20%
- ϑ_{NC}: end of the test (before the collapse of the specimen)

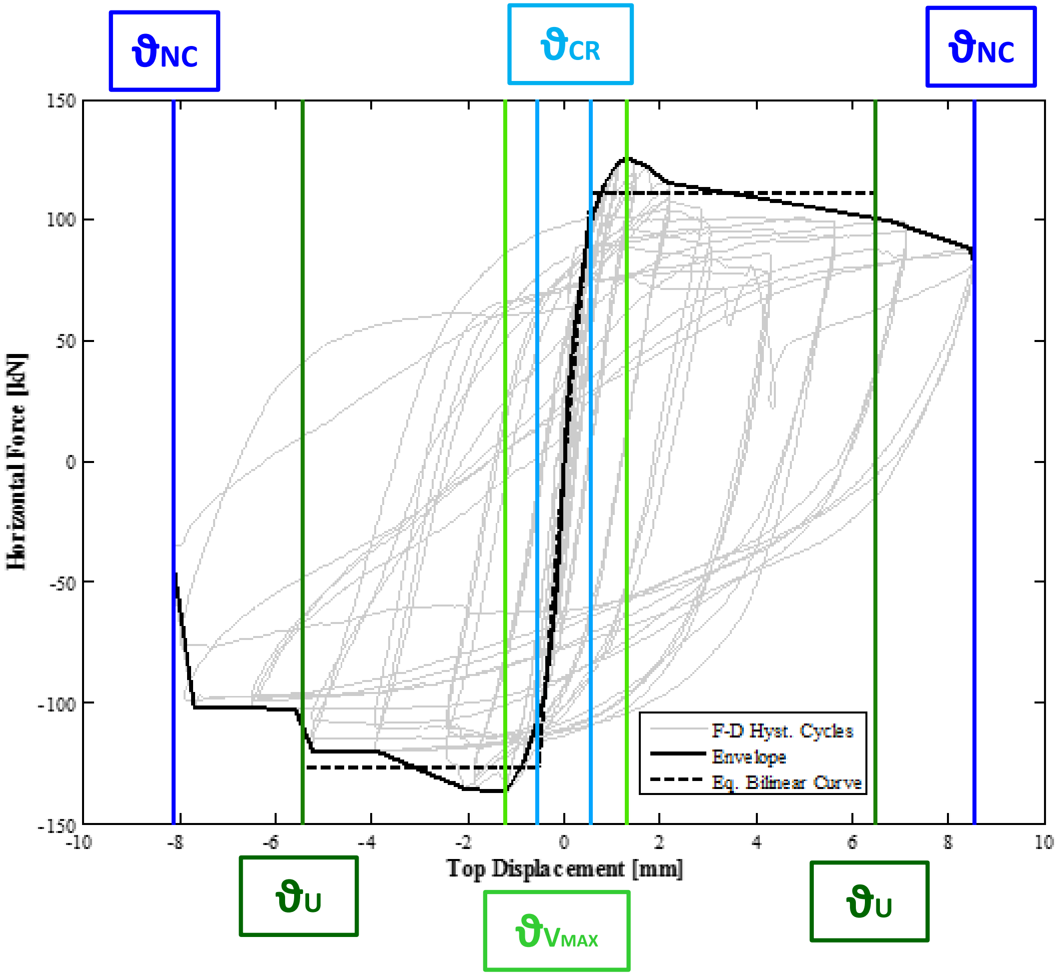

EC COMP2_4 – Clay

h=2.71m, L=2.74m, t=0.208 m, σ_v=0.3MPa, double fixed

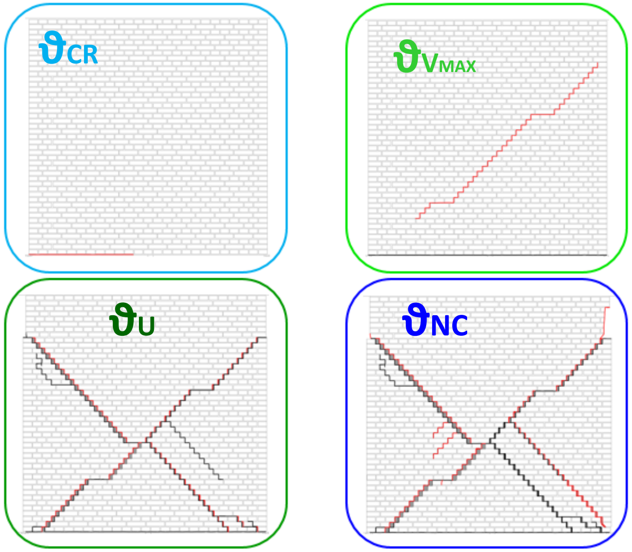

Summary of the LDLs in relation to the failure modes

ϑ_{CR}: first visible crack (structural crack, no plaster's crack)

ϑ_{Vmax}: maximum value of lateral strength

ϑ_{U}: strength degradation equal to 20%

ϑ_{NC}: end of the test (before the collapse of the specimen)

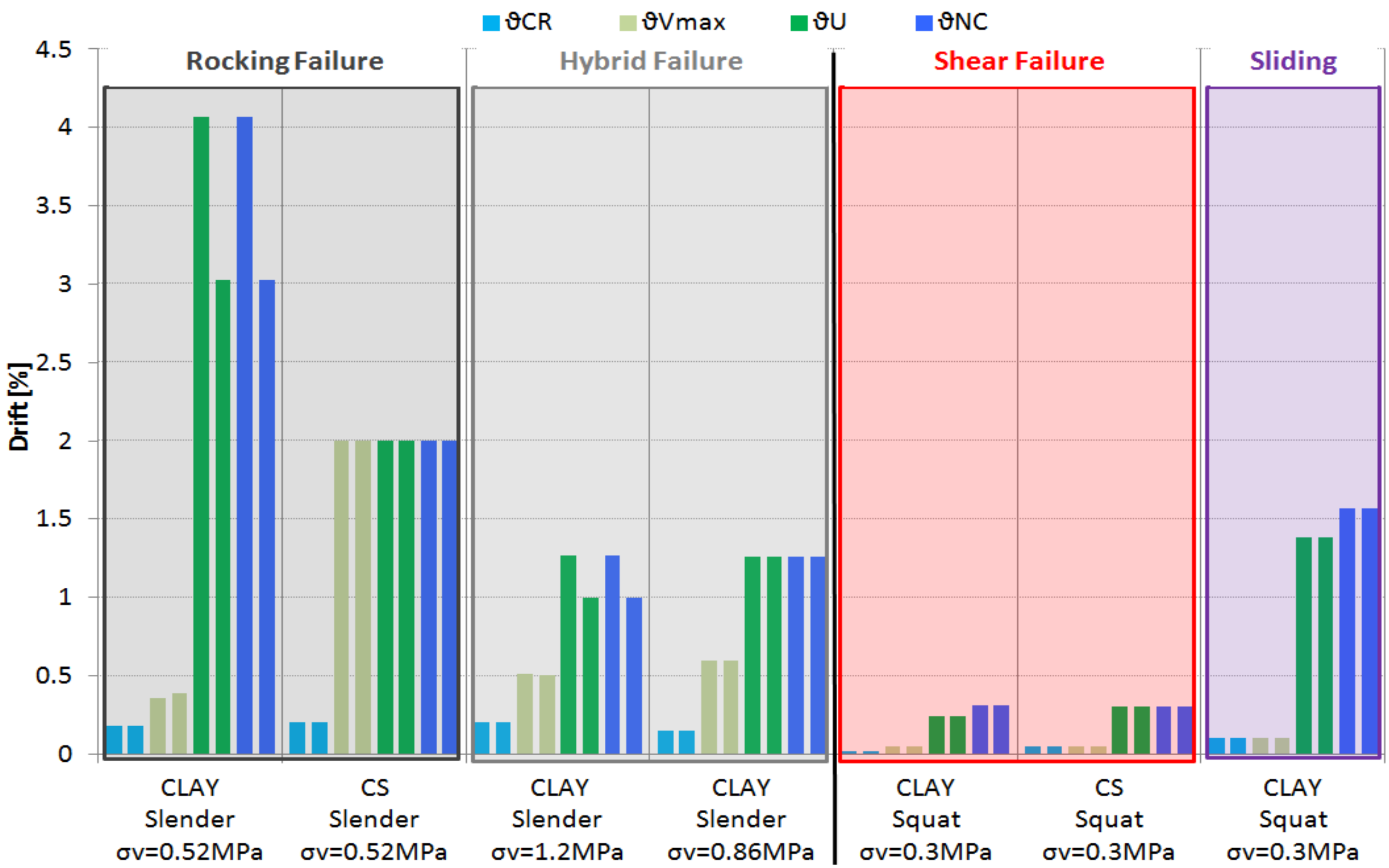

Summary of the LDLs

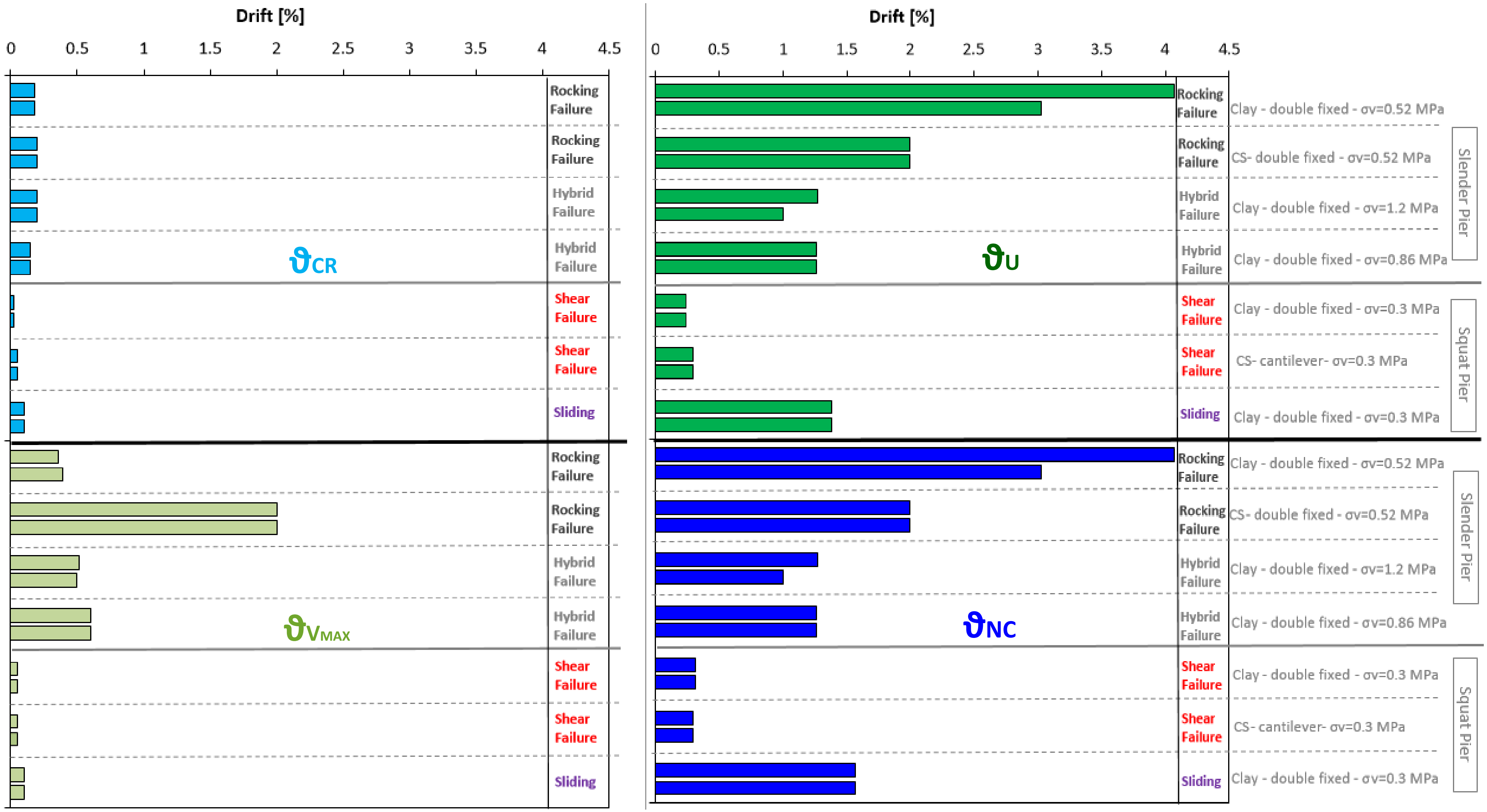

Out-of-plane Shaking Table Tests

One-Way and Two-Way Bending

Out-of-Plane Failures

One-way Bending

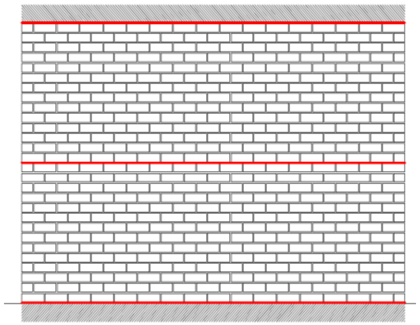

Two-way Bending

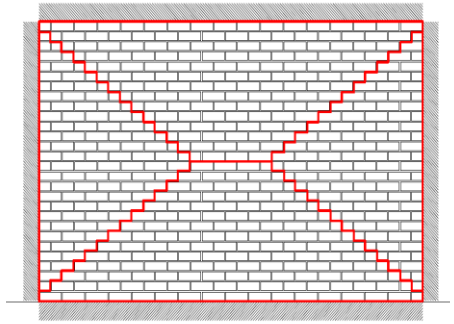

Top portion Cantilever

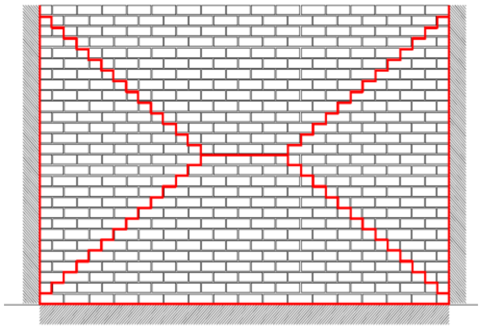

Cavity wall buildings could be particularly vulnerable:

- High slenderness of the masonry leaves;
- Possible inefficiency of the anchoring system (deteriorated and too widely spaced);
- Low level of acting axial load;
- Lack of wall to floor and wall to roof connection.

OOP One-way Bending

Incremental dynamic tests on full-scale specimens:

- 2 CS single leaf walls;
- 3 cavity walls: two (2 ties/m^2) and one (4 ties/m^2).

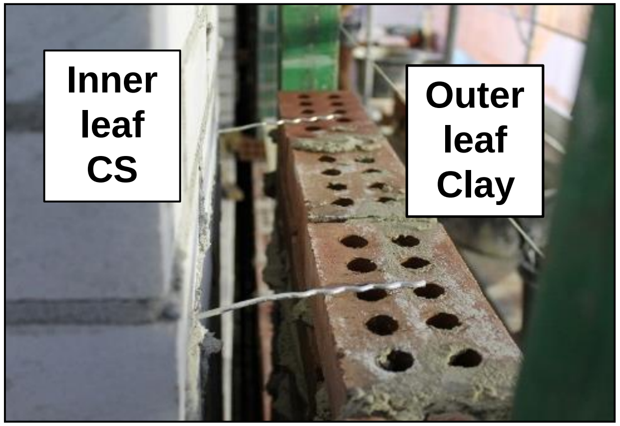

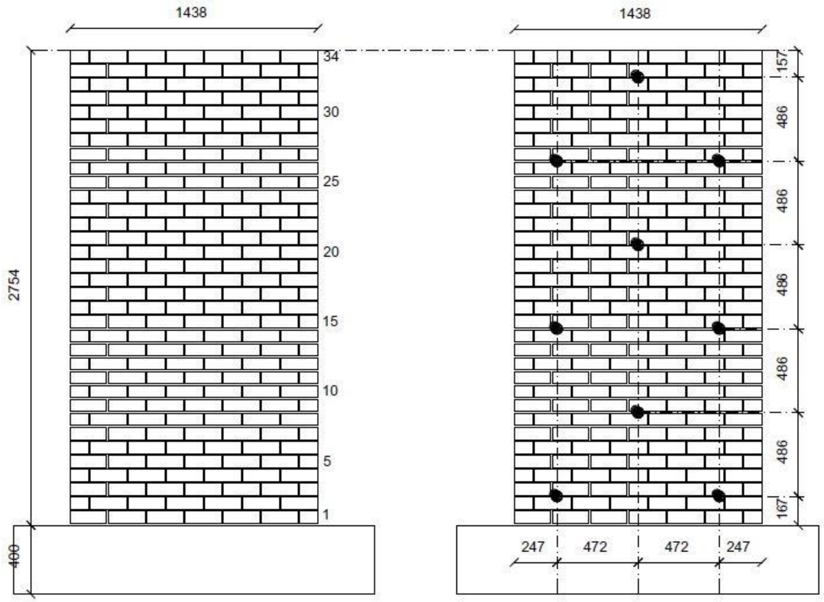

Connection detail

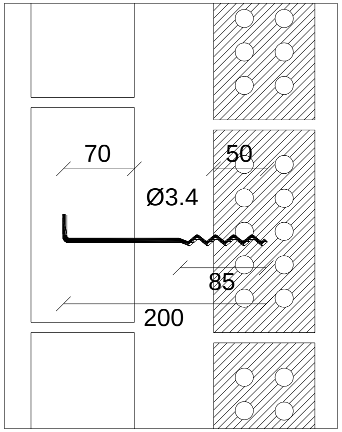

Test Set-up

Uni-directional shaking table test inducing pure OOP one-way bending action in specimens:

- Inner leaf loaded through the top steel beam pulled down by means of steel rods in series with a spring system;
- Mechanical braces transferring the dynamic input and allowing the wall uplift;
- Adjustable safety system to prevent the specimen collapse.

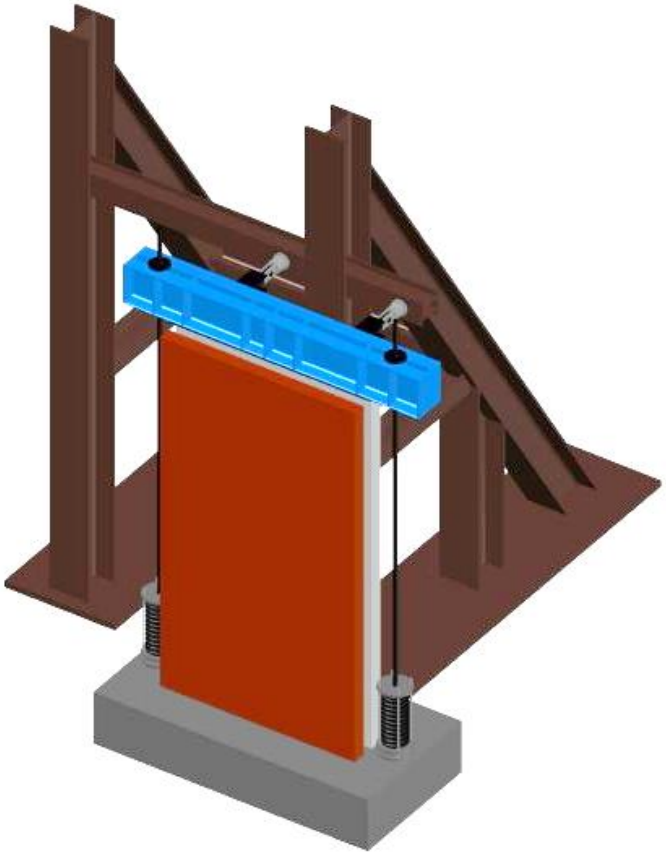

Instrumentation

- Accelerometers;
- Potentiometers;
- Wire Potentiometers.

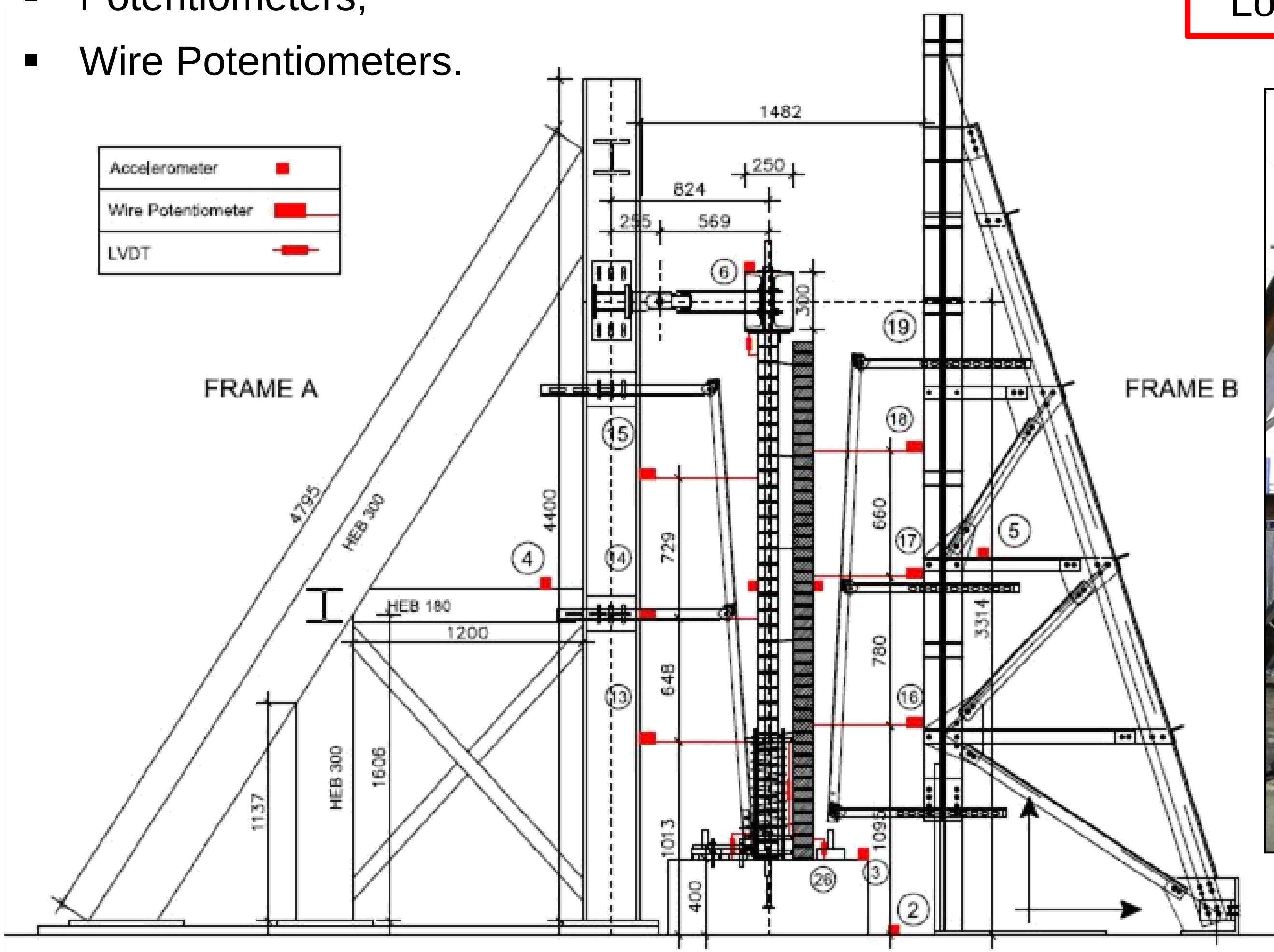

CS Leaf Loaded

Clay Leaf Unloaded

Input Signals

TreMuri

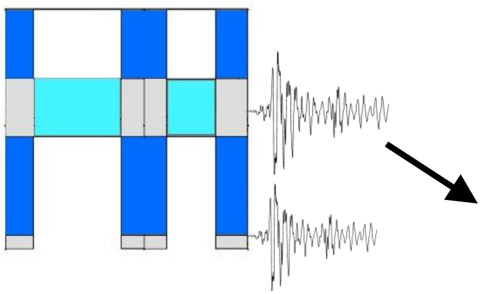

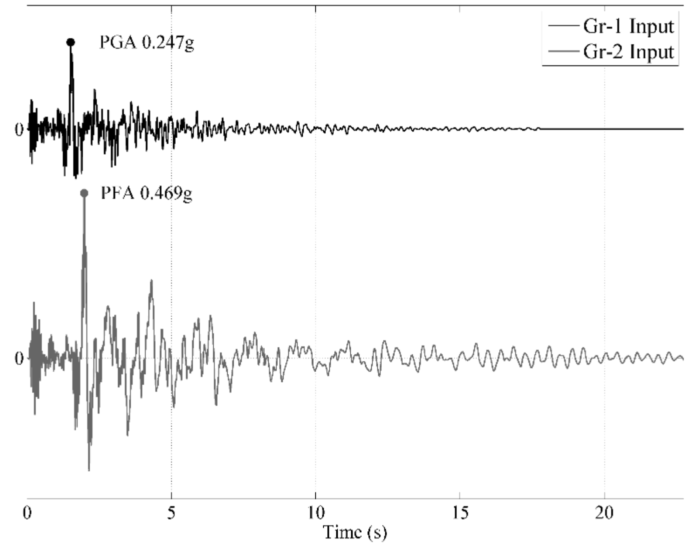

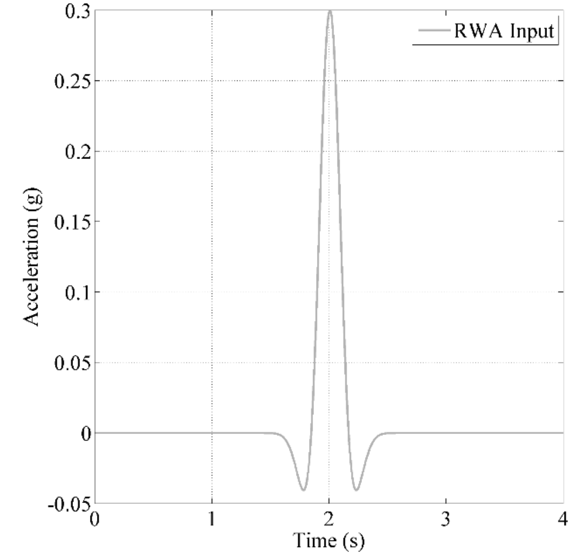

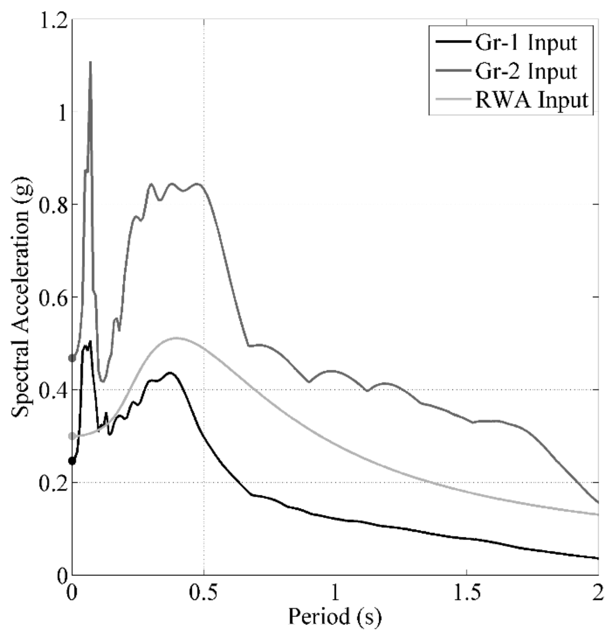

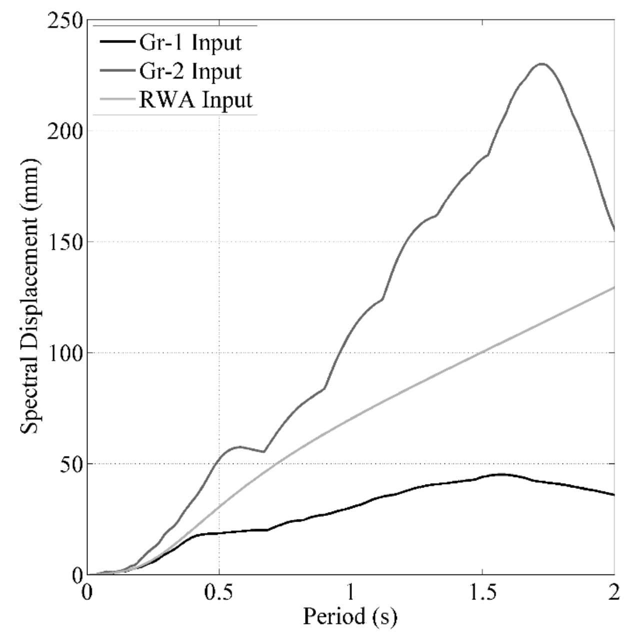

Failure Mechanisms

SINGLE LEAF
0.1 and 0.3 MPa

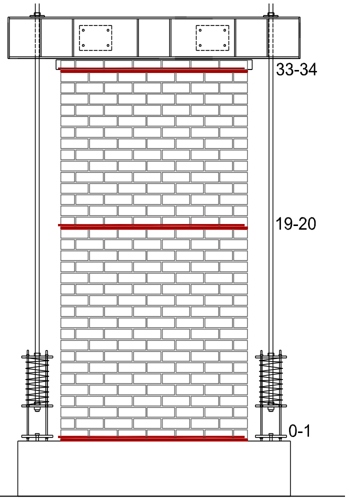

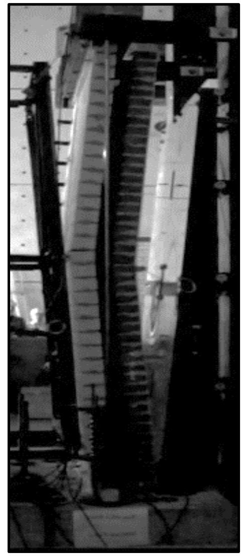

CAVITY
0.1 MPa, 4 ties/m^2

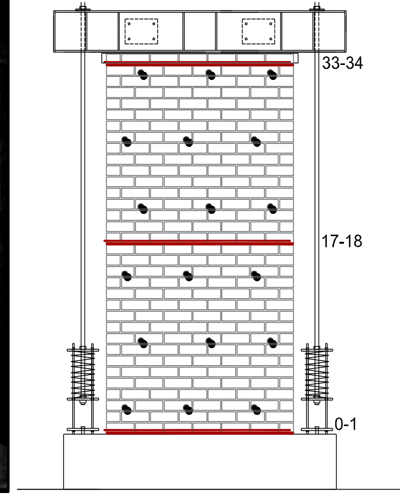

CAVITY 0.1 MPa
4 ties/m^2

RWA (0.5 g)

Gr-2 (0.7 g)

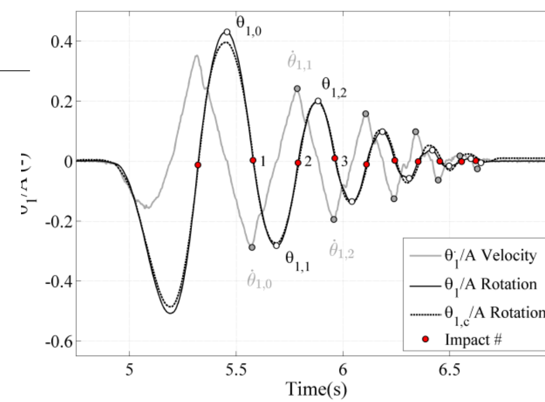

CAVITY
0.3 MPa, 2 ties/m^2

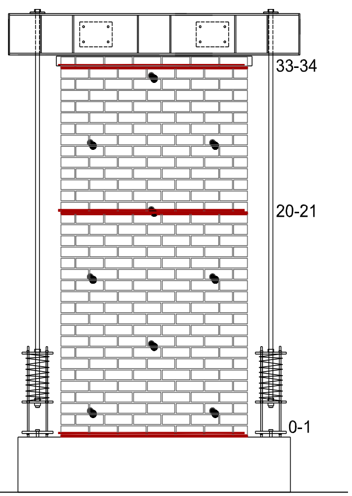

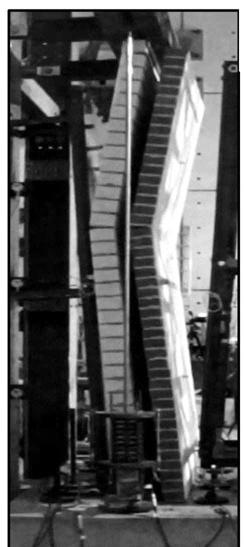

CAVITY
0.1 Mpa, 2 ties/m^2

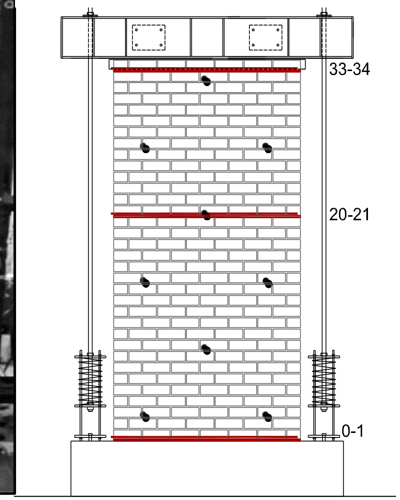

Force - Displacement

CAVITY 0.1 MPa, 2 ties/m^2

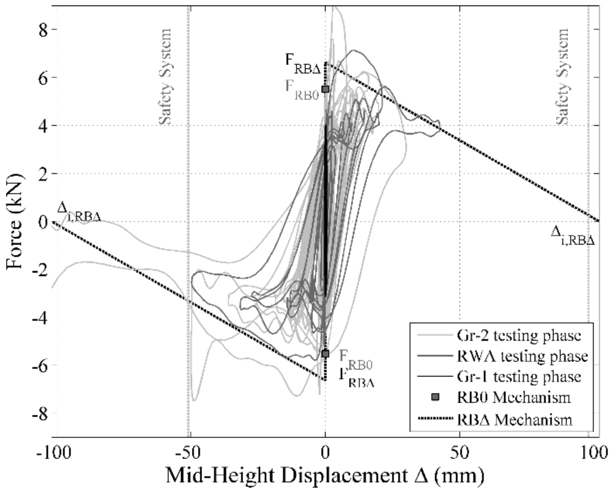

CAVITY 0.1 MPa, 4 ties/m^2

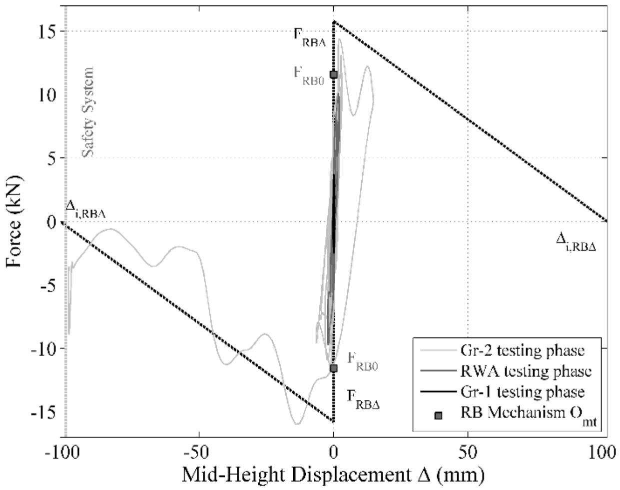

CAVITY 0.3 MPa, 2 ties/m^2

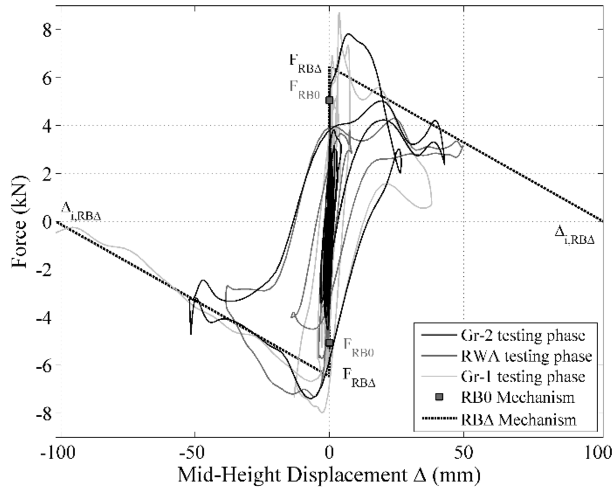

SINGLE LEAF, 0.3 MPa

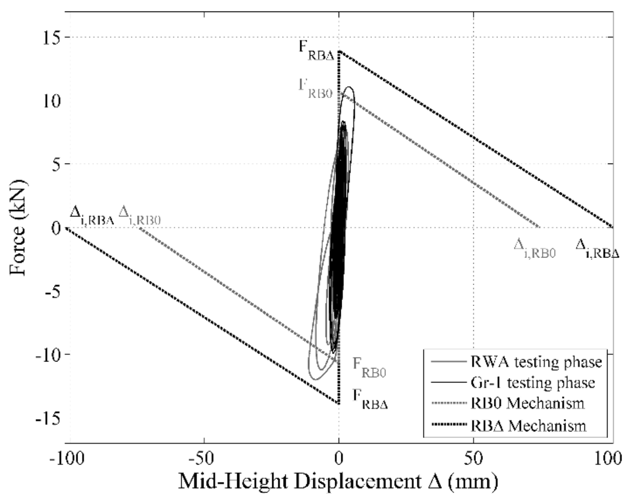

SINGLE LEAF, 0.1 MPa

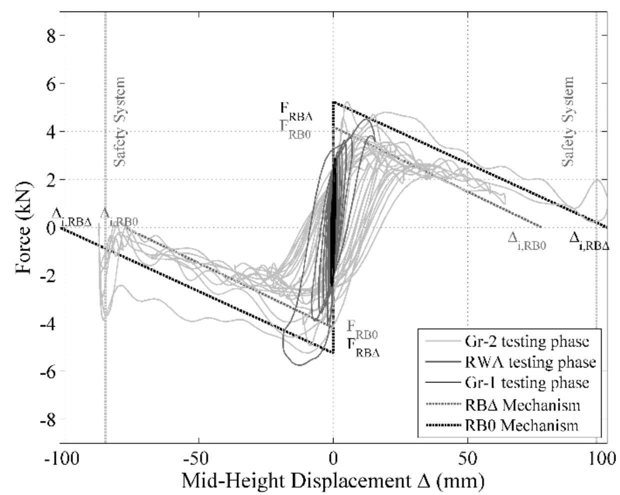

OOP Two-way Bending

Incremental dynamic tests on full-scale specimens:

- 3 CS single leaf U-shaped walls;
- 1 Clay single leaf U-shaped wall;
- 1 Cavity U-shaped wall (2 ties/m^2).

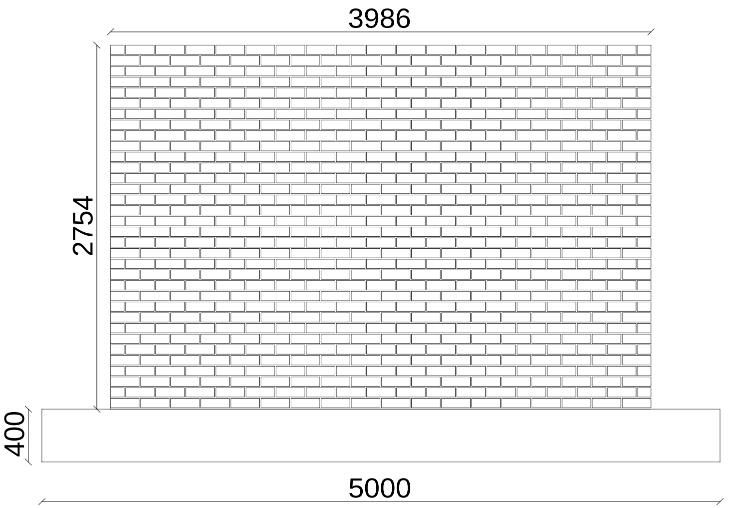

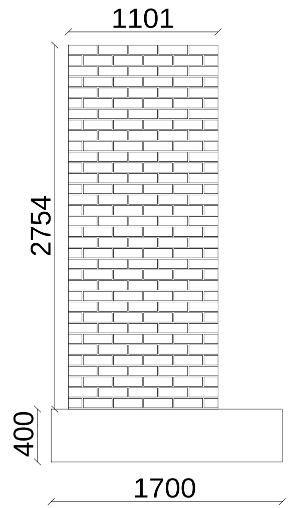

Boundary Conditions

CS
FIXED ON TOP
σ_v = 0.05 MPa

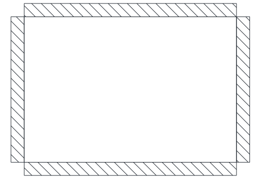

CS
FREE ON TOP

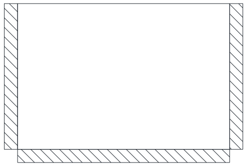

CS
WINDOW
FREE ON TOP

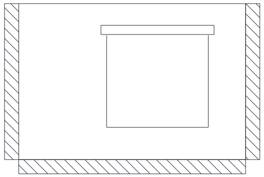

CLAY
FREE ON TOP

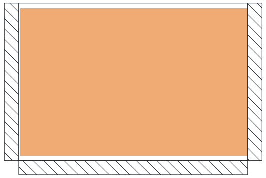

CAVITY
FREE ON TOP

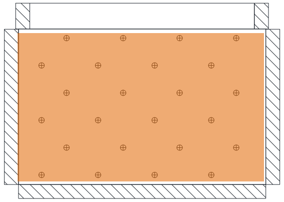

Masonry Behaviour

Calcium Silicate: Line cracks

Clay: Stepped cracks

Out-of-plane Flexural Strength Test

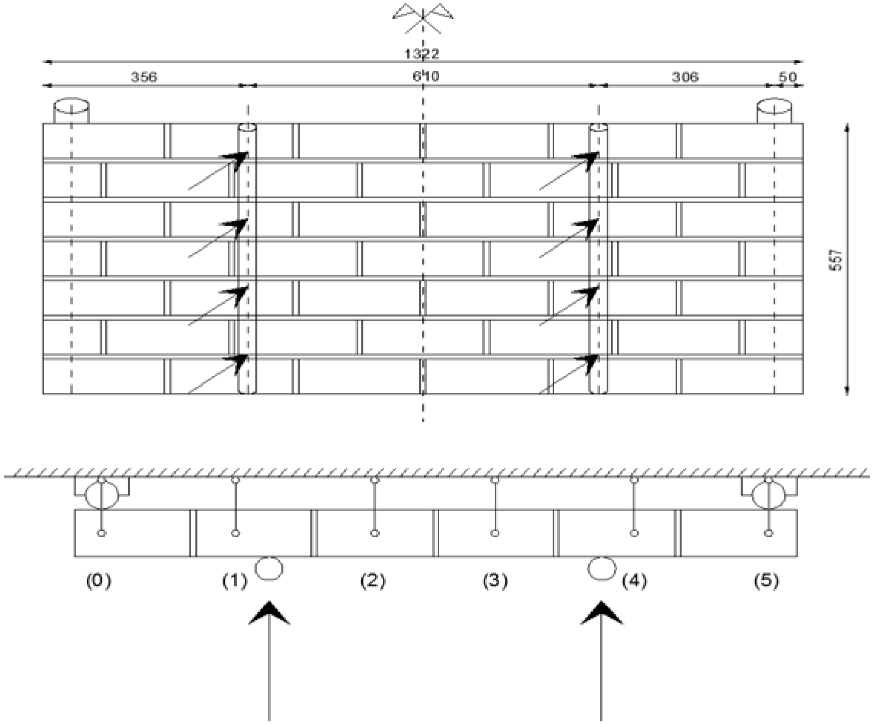

Test Set-up

Uni-directional shaking table test inducing pure OOP two-way bending action in specimens:

- Adapted version of one-way bending set-up;
- Return walls;
- Spring system;
- Top beam: fixed and free.

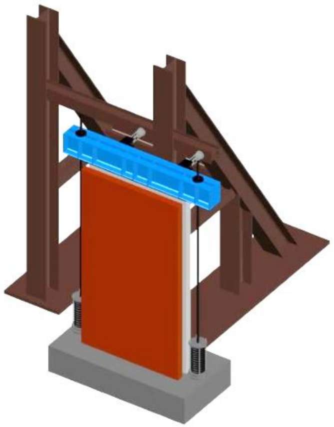

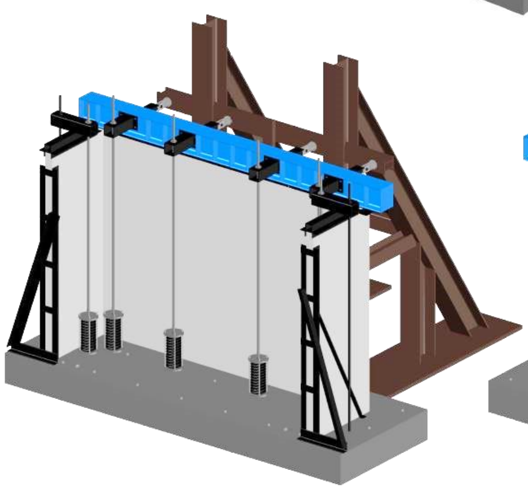

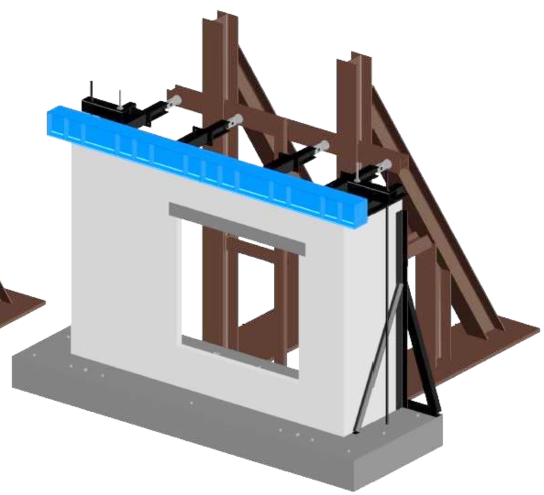

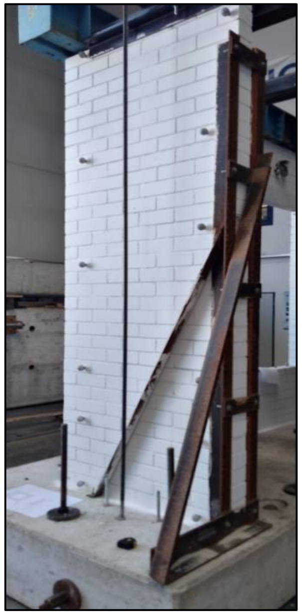

Instrumentation

Accelerations and displacements

- Accelerometers;
- Potentiometers;
- Wire Potentiometers;
- Optical acquisition.

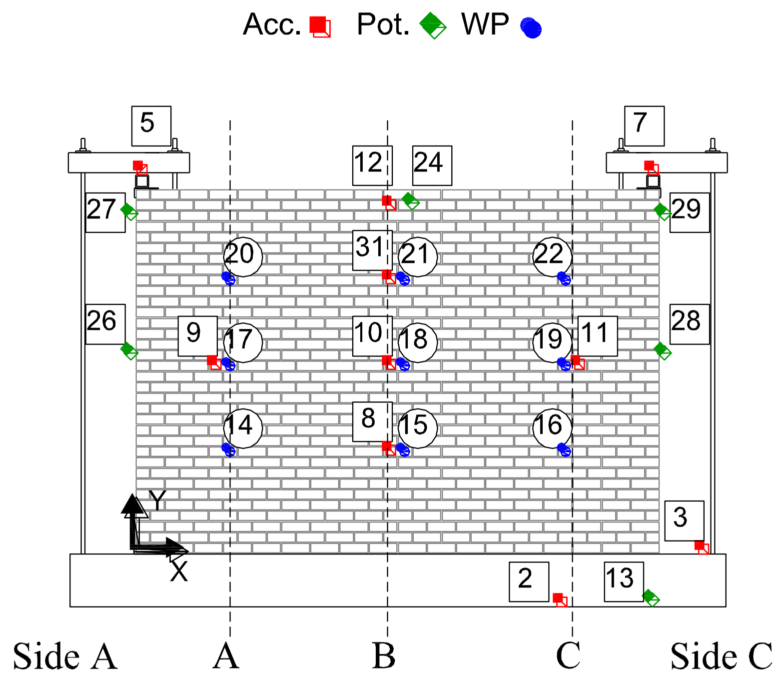

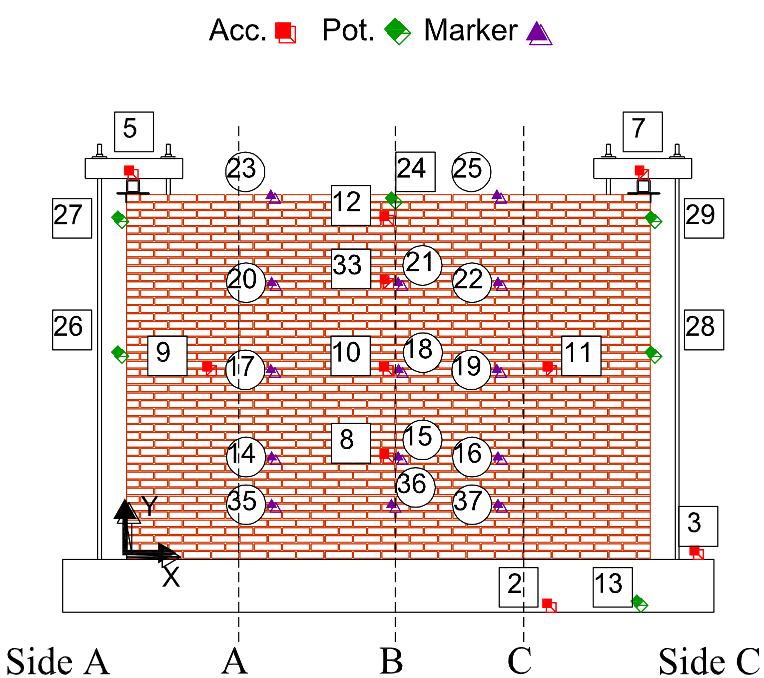

Input Signals

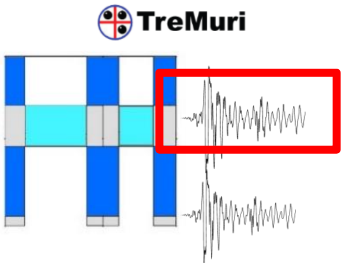

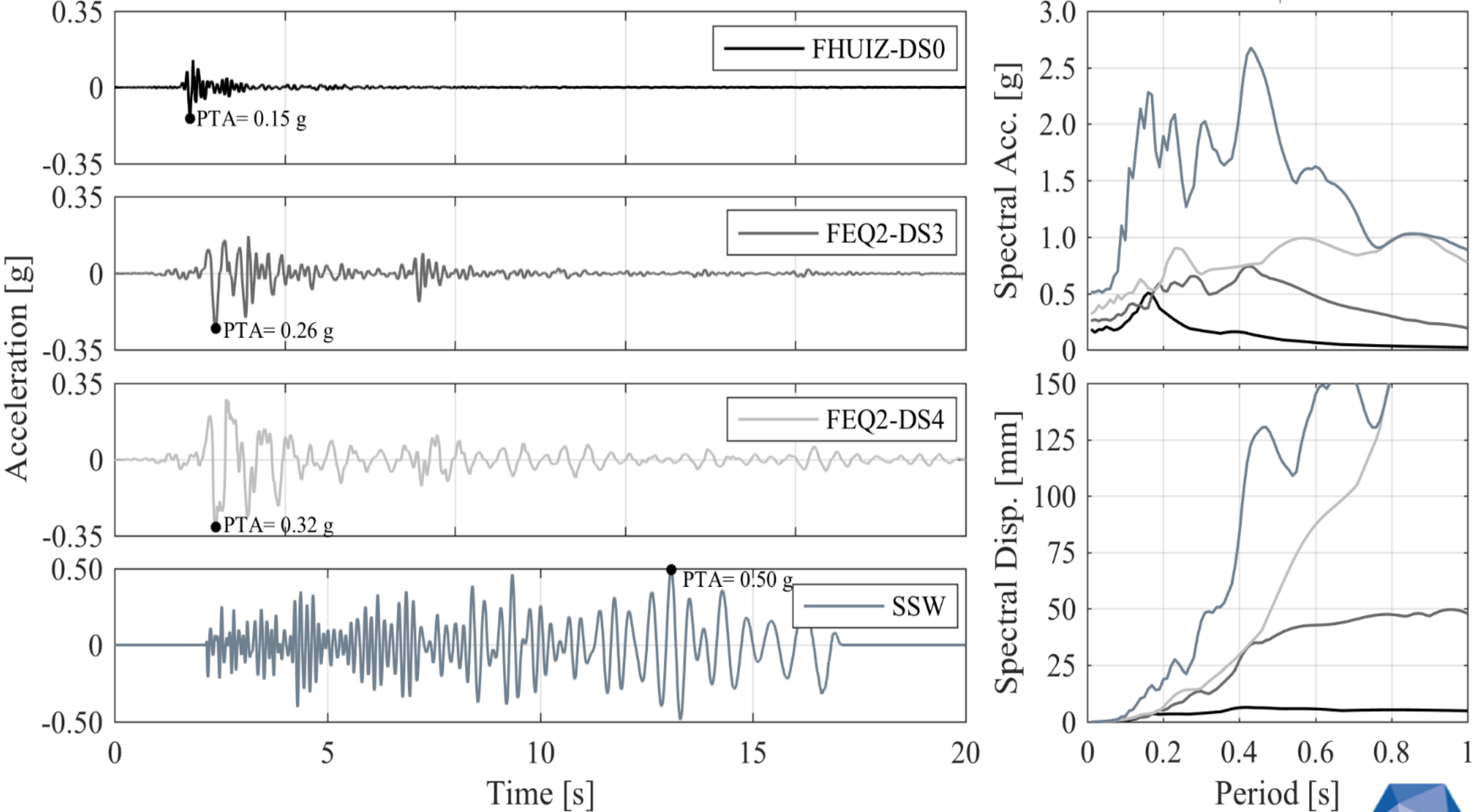

Failure Mechanisms

CS
FIXED ON TOP
σ_v = 0.05 MPa

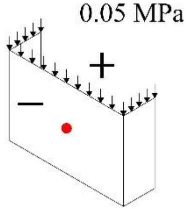

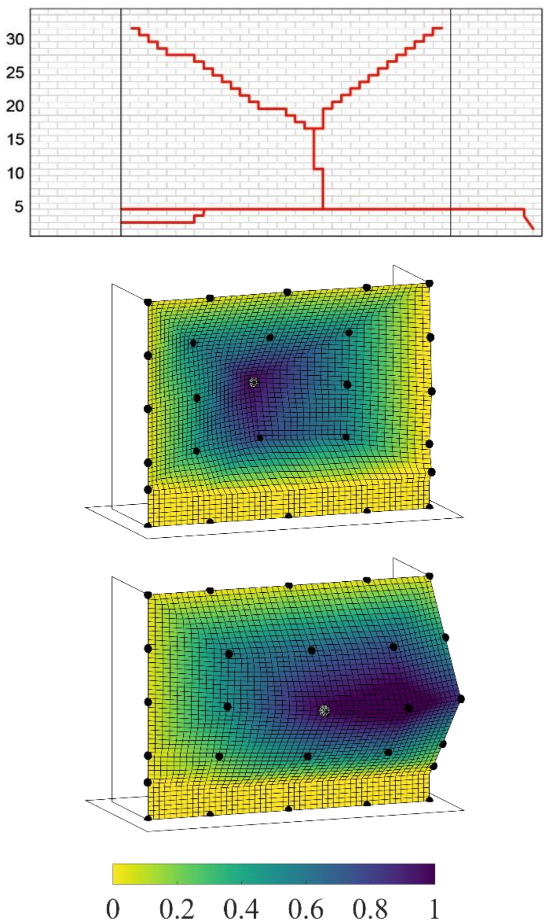

CS
FREE ON TOP

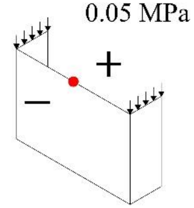

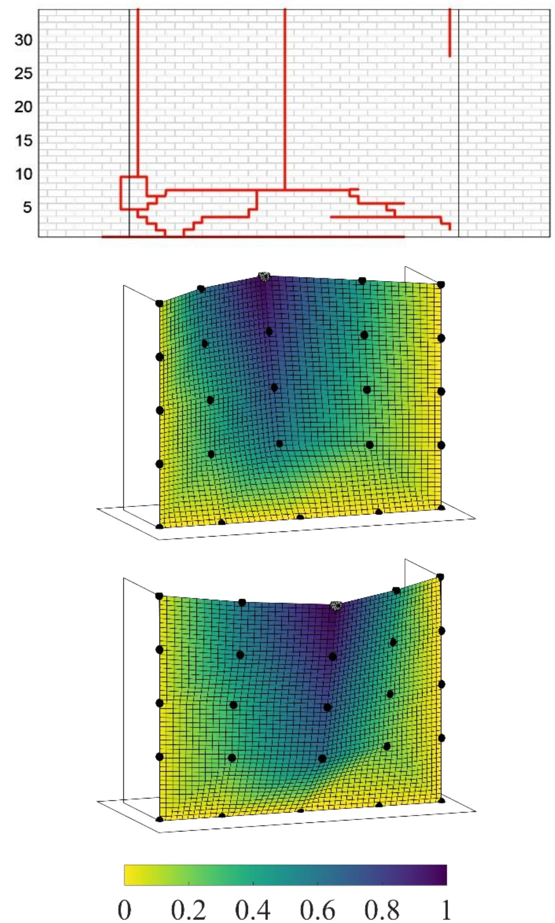

CS
WINDOW
FREE ON TOP

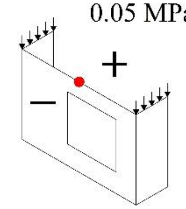

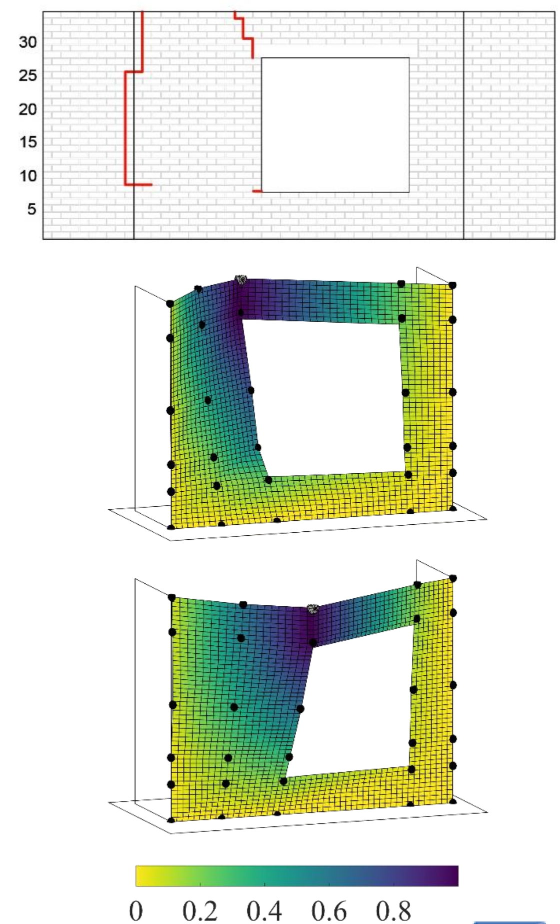

SSW 300%
(1.42 g)

FEQ2-DS4 200%
(0.62 g)

Failure Mechanisms

CLAY FREE ON TOP

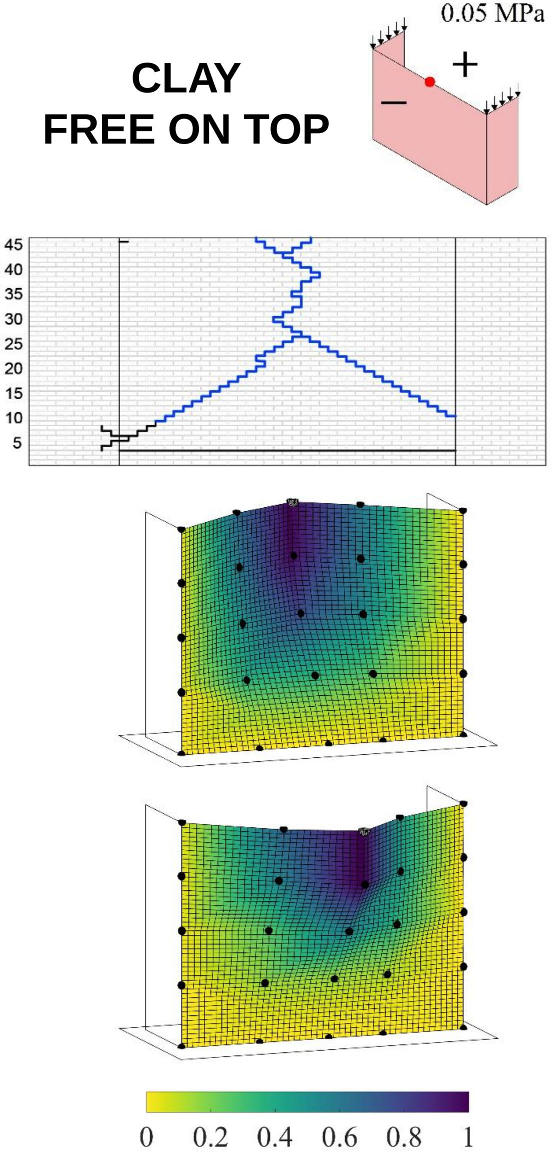

CAVITY FREE ON TOP (CS)

CAVITY FREE ON TOP (CLAY)

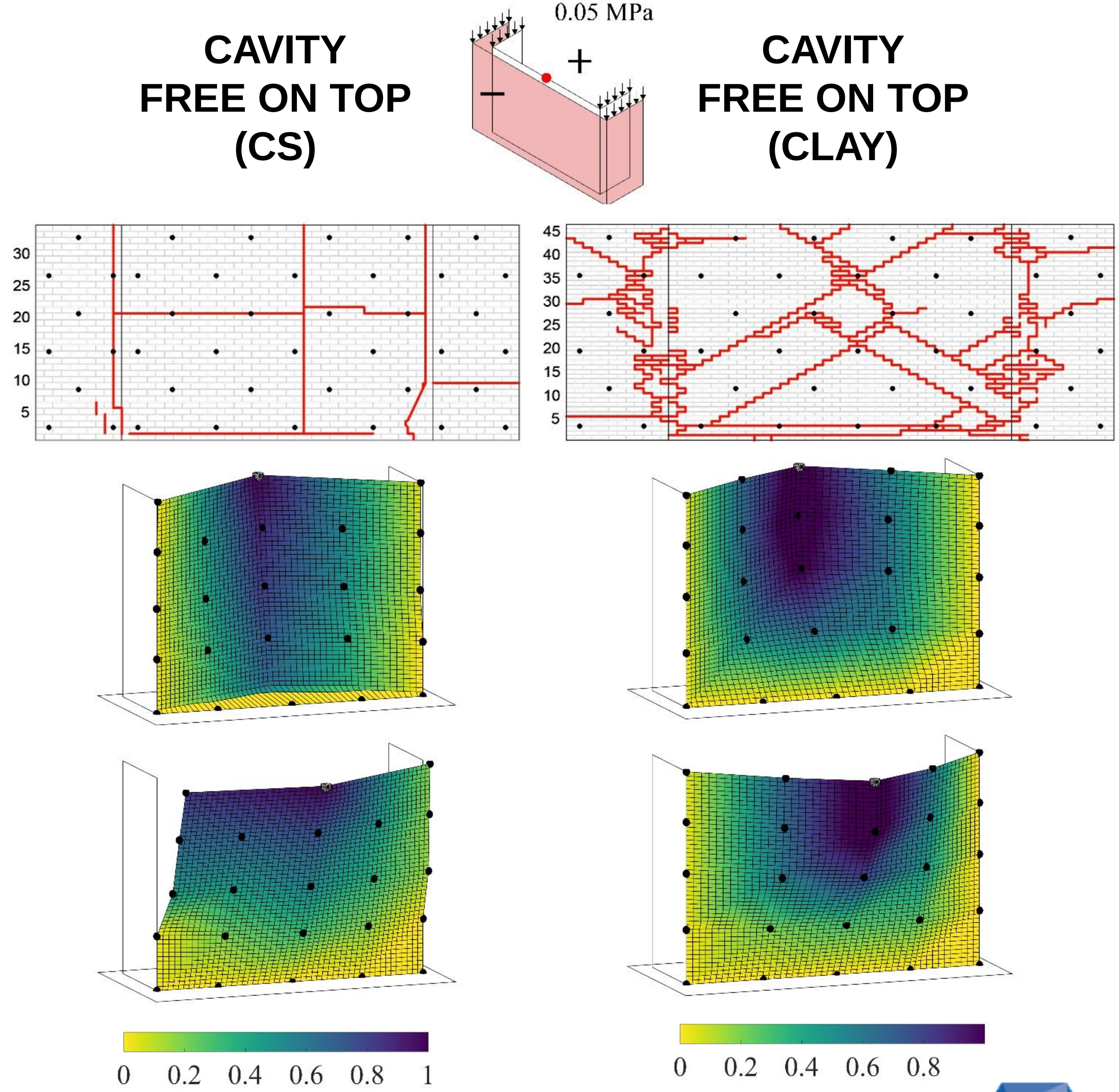

FEQ2-DS4 500% (1.71 g)

Incremental Dynamic Response

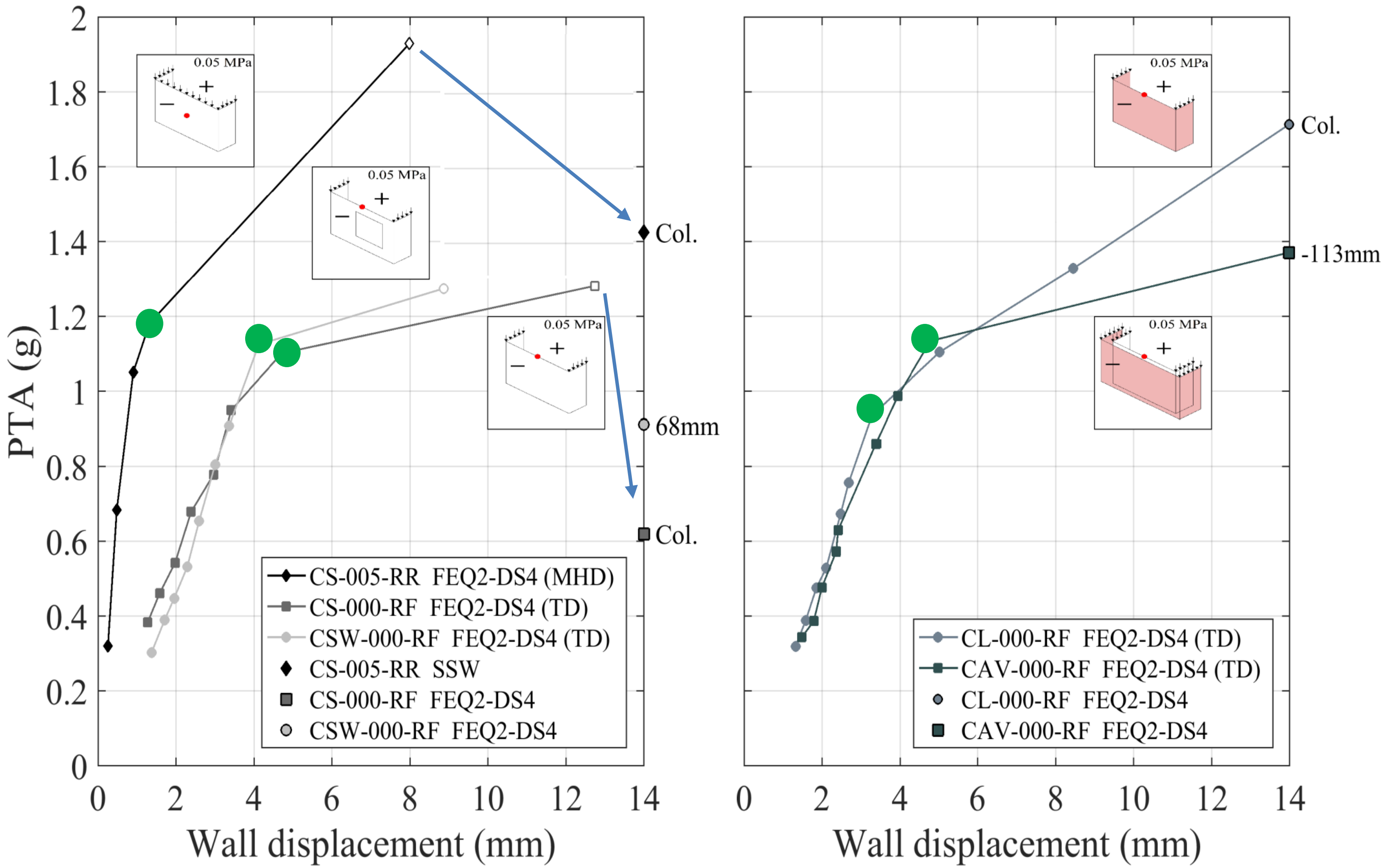

- Relatively brittle behavior, if compared to quasi-static tests in literature;
- Higher vulnerability for longer duration motions.

Force - Displacement

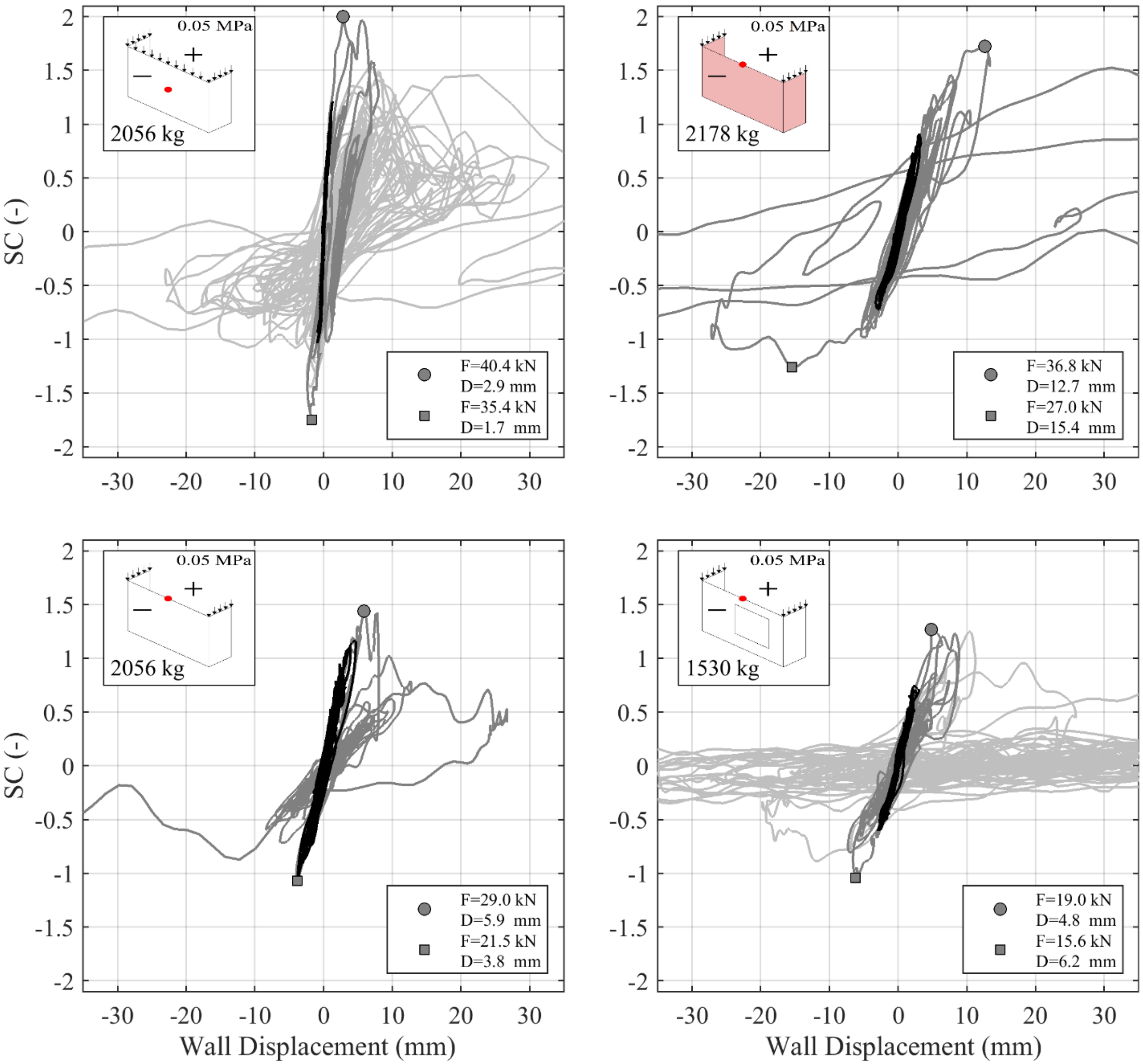

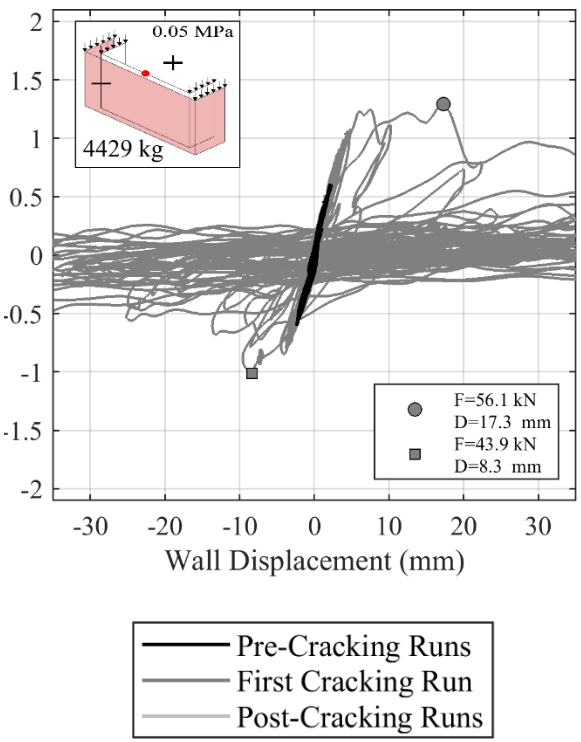

Willis 2004

Griffith & Vaculik 2007

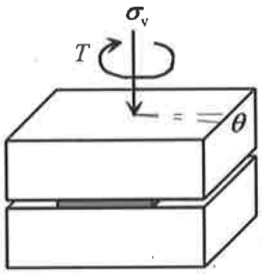

Analytical Treatment

- **VG**, **mVG**: both use mechanical model developed in Willis 2004, Vaculik 2007;
- **mVG**: different only in terms of t_u ($t_u = t_{tor}$ i.e. experimentally obtained results);
- **AS 3700**: Empirical model.

Very good agreement with shake table results.

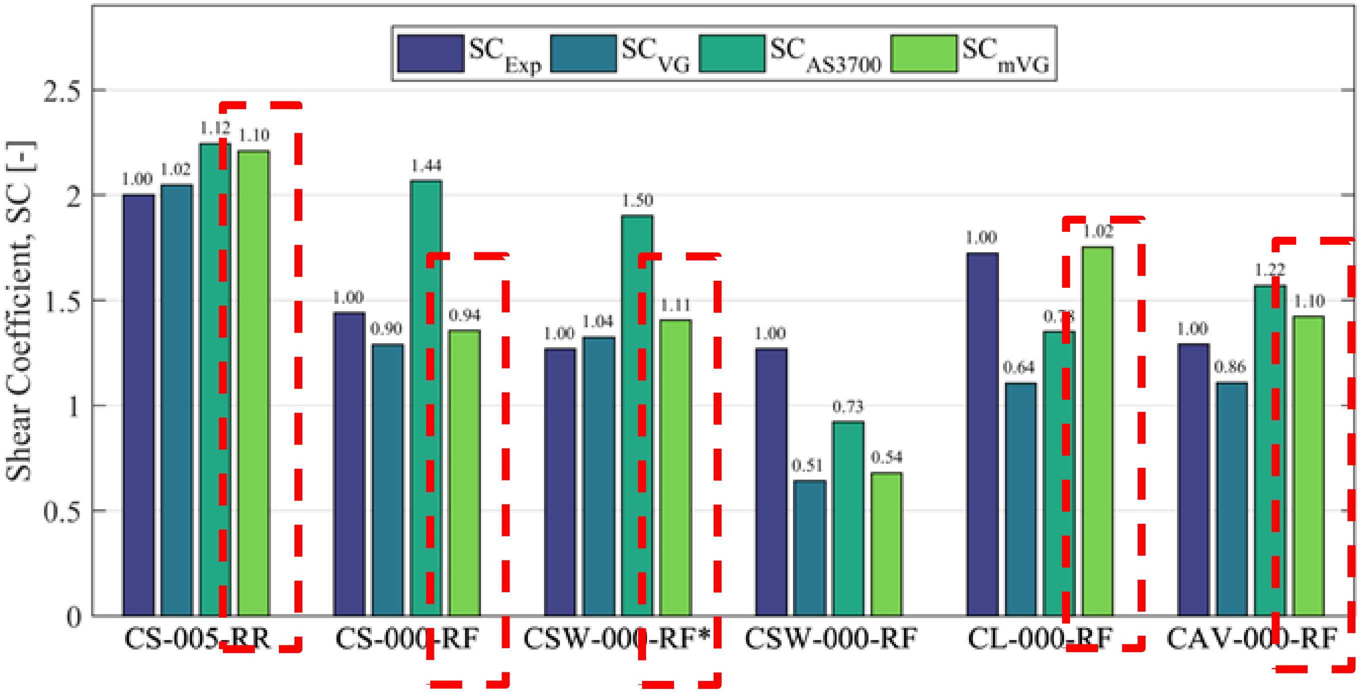

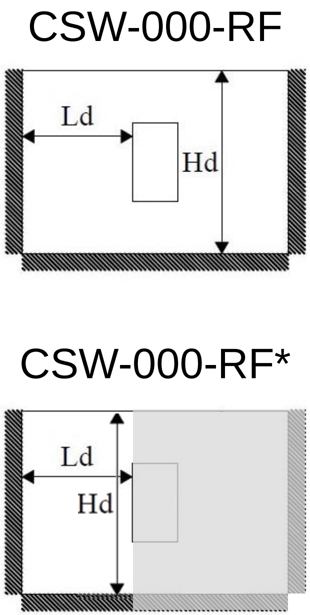

On going investigations:

- Parametric studies on torsional shear strength of masonry.
- Correlation with other standardized characterisation tests?

Torsional tests

Line Cracks

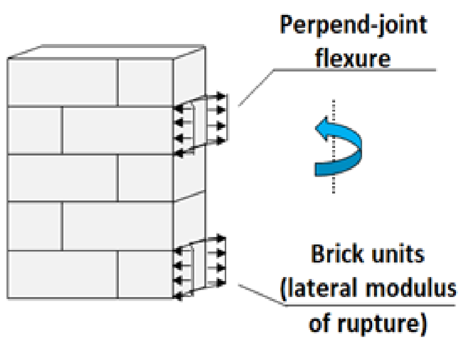

Stepped Cracks

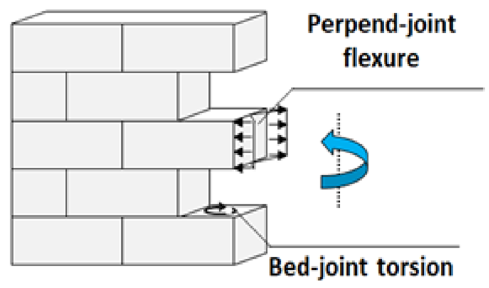

Diagonal Cracks

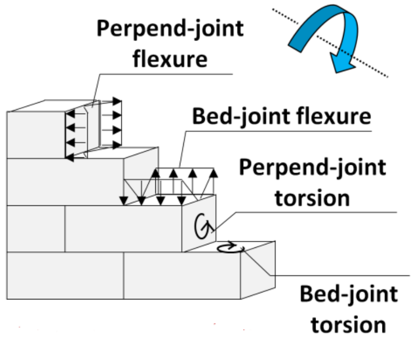

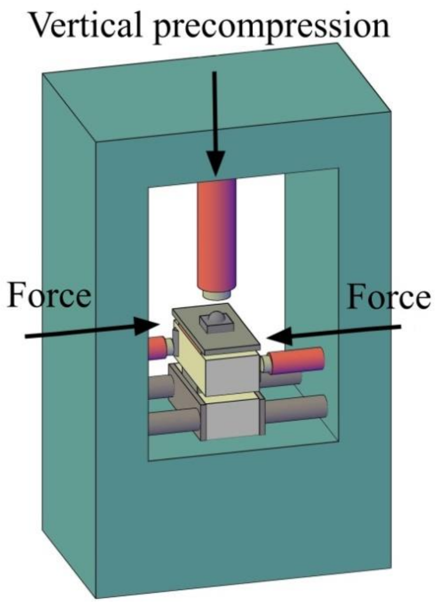

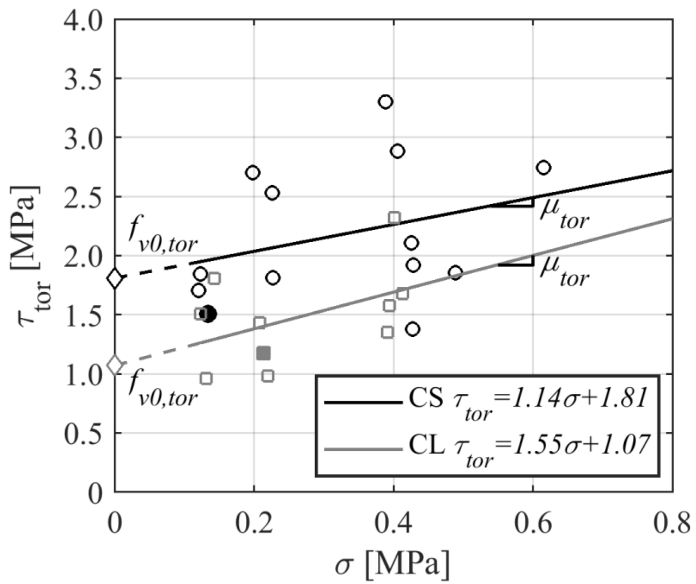

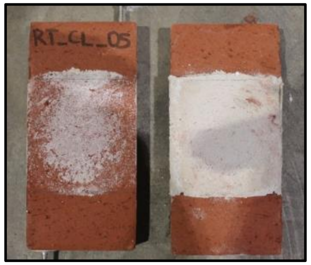

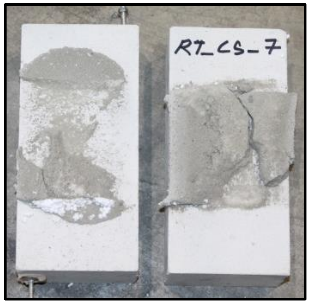

CS $f_{mt} \approx 1$ MPa
Clay $f_{mt} \approx 0.4$ MPa

Higher values than Willis, 2004 $\tau_u = 1.6 f_{mt} + 0.9\sigma_v$

Full-Scale Buildings

EUC_Build 1 - 2

LNEC_Build 1 - 2 - 3

EUC_Build1

FULL-SCALE CAVITY-WALL BUILDING

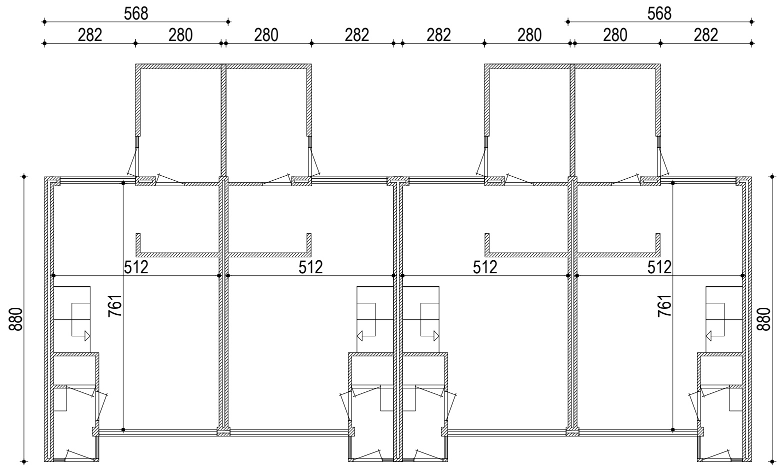

Construction Phases

Walls of first storey

Laying of the R.C. slab above the first storey

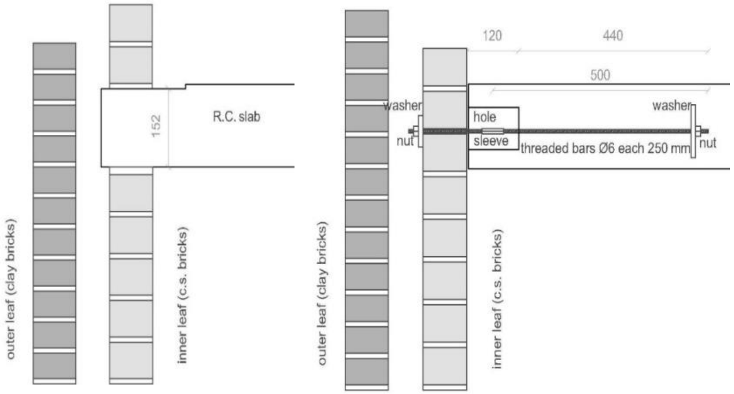

South side

East and West side

Construction Phases

Veneer and Timber Roof

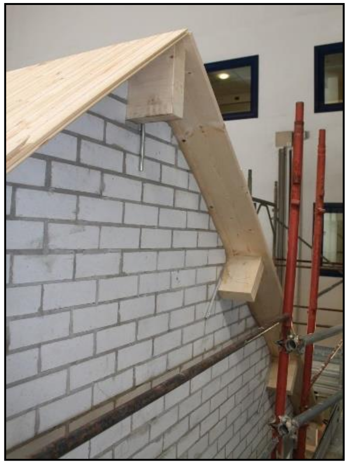

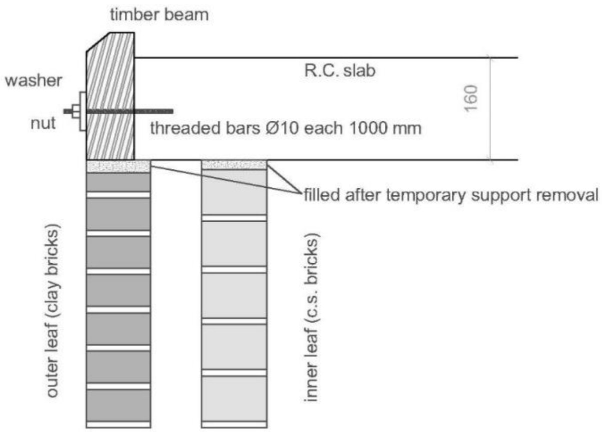

East and West side

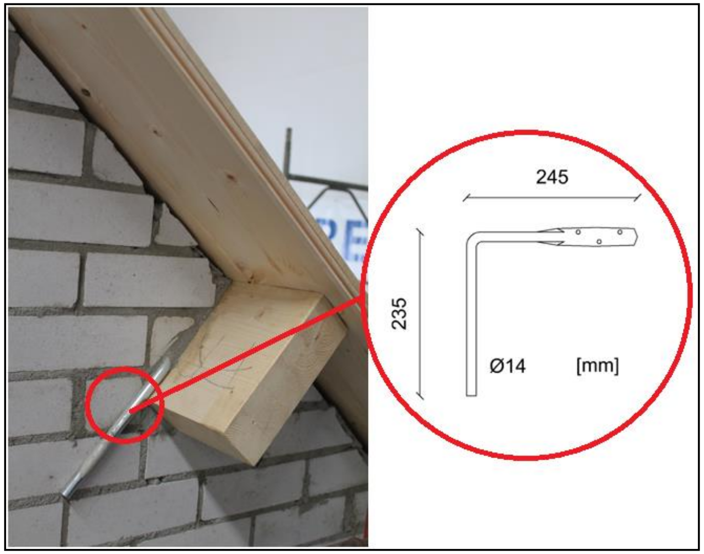

Instrumentation

Accelerometers:

- Mono-directional;
- Bi-directional;
- Tri-directional.

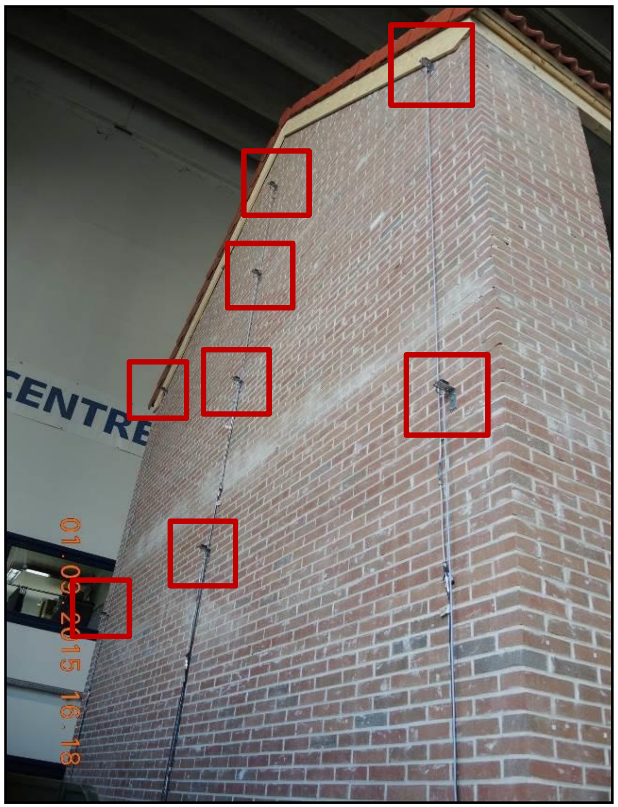

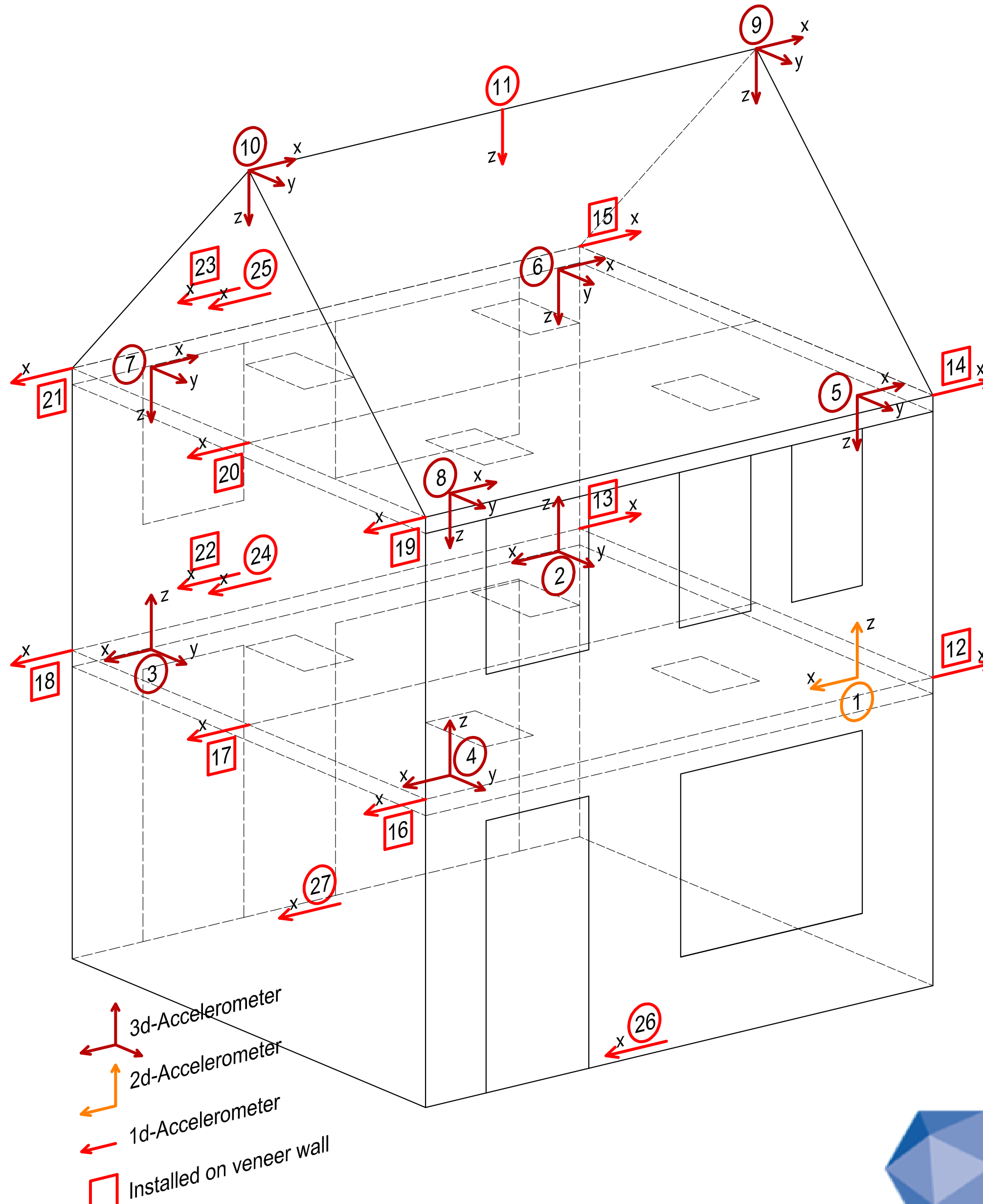

Instrumentation

Traditional and Wire Potentiometers:

- Floor displacements and rotations;
- OOP wall displacements.

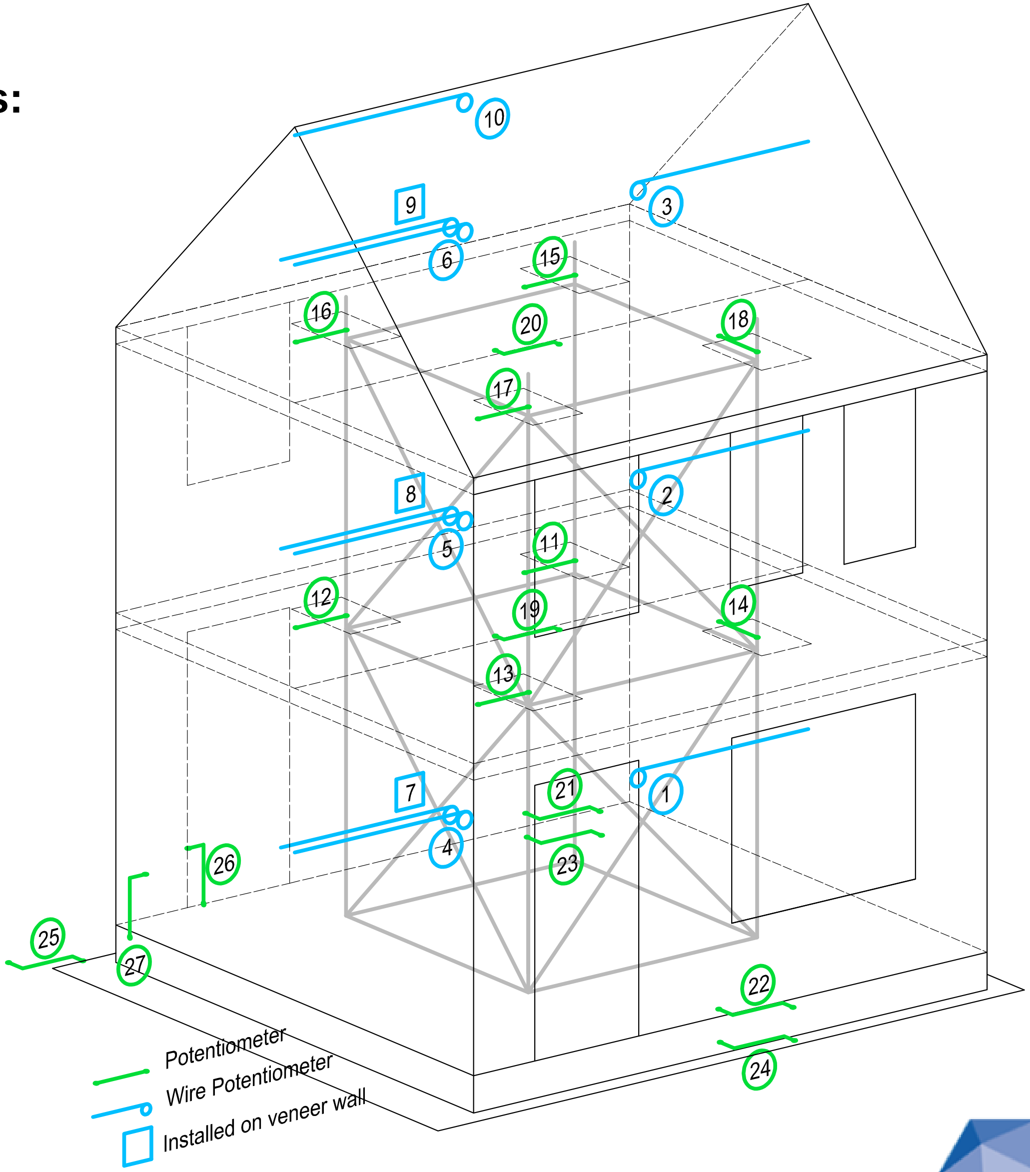

Instrumentation

3D Optical Acquisition

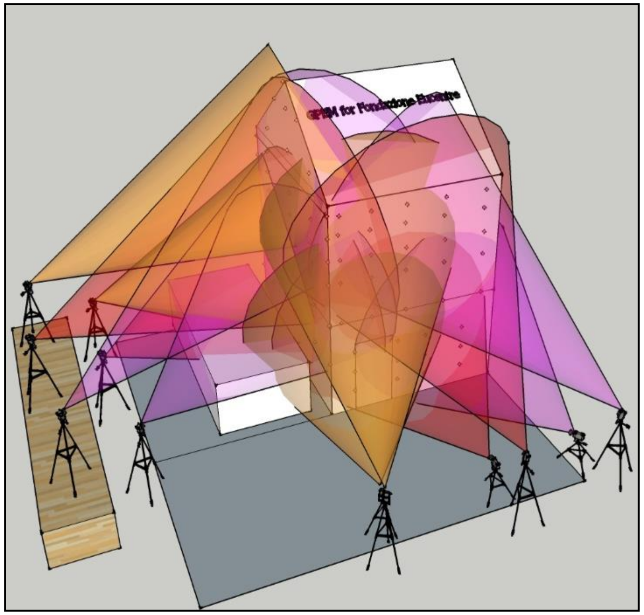

Input Signals

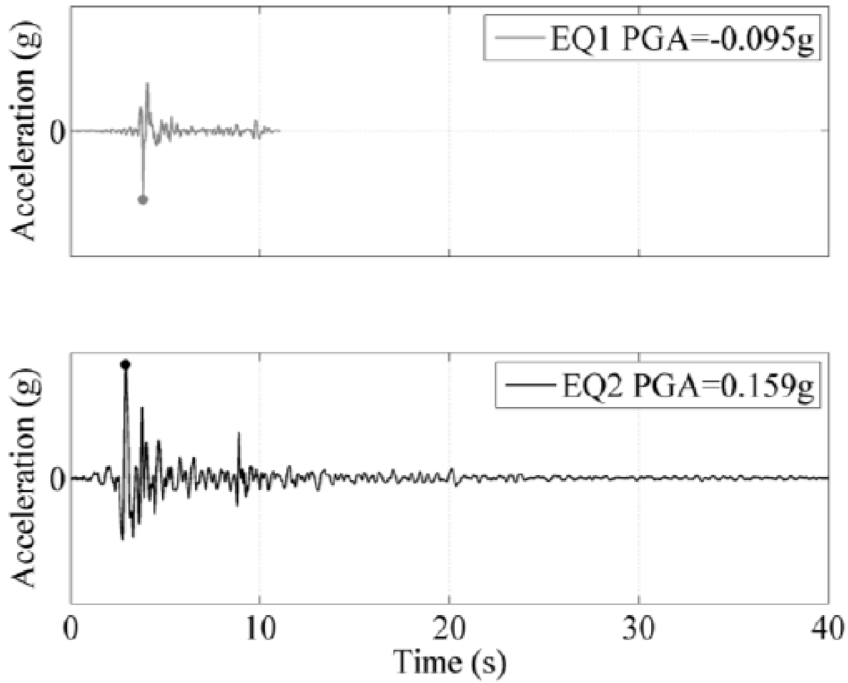

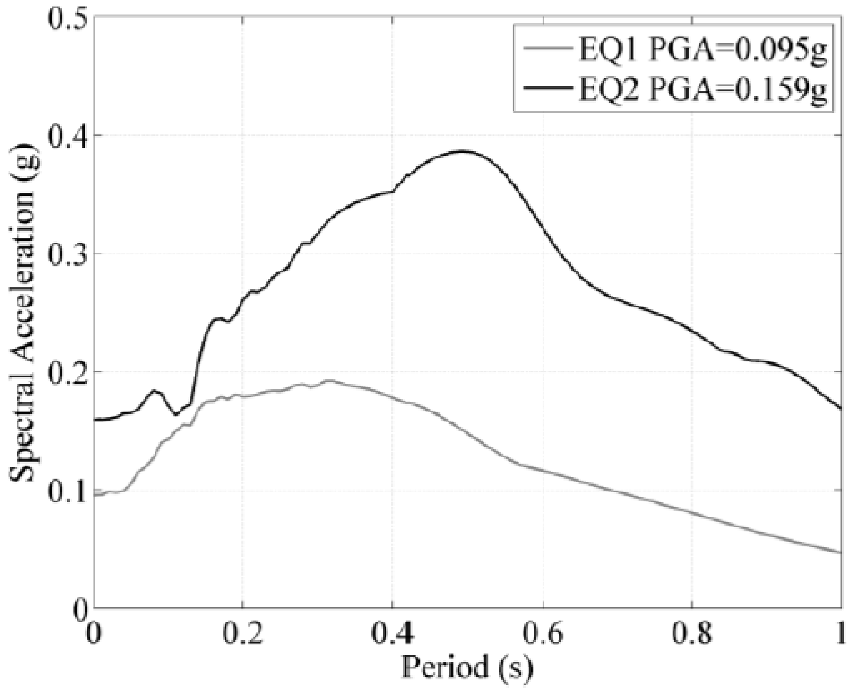

Test Input	*Intensity [%]*	*Nominal PGA [g]*	*Recorded PGA [g]*	*Recorded PGV [m/s]*
EQ1	25%	0.024	0.023	0.015
EQ1	50%	0.051	0.050	0.031
EQ1*	100%	0.102	0.097	0.056
EQ1	150%	0.153	0.138	0.077
EQ2*	50%	0.082	0.085	0.067
EQ2*	100%	0.163	0.166	0.123
EQ2*	125%	0.204	0.192	0.133
EQ2	150%	0.245	0.241	0.164
EQ2	200%	0.326	0.305	0.218

*Shaking table excitations preceded by tests of the same typology but with reduced intensity for shake table calibration purpose

Deformed Shapes

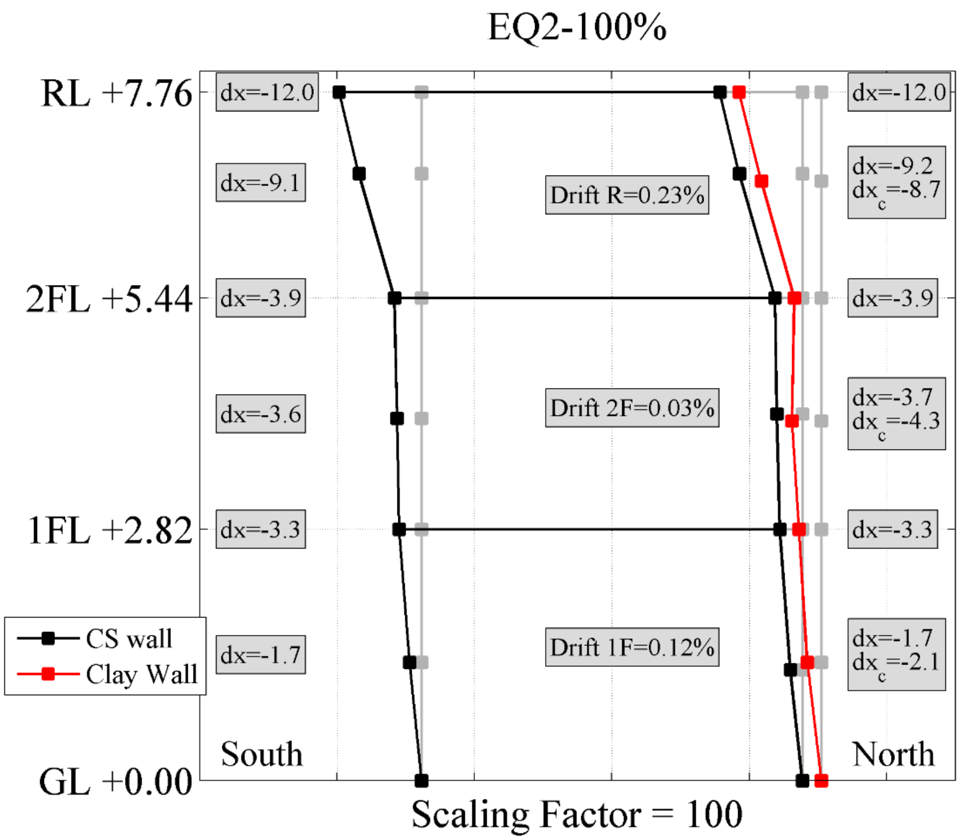

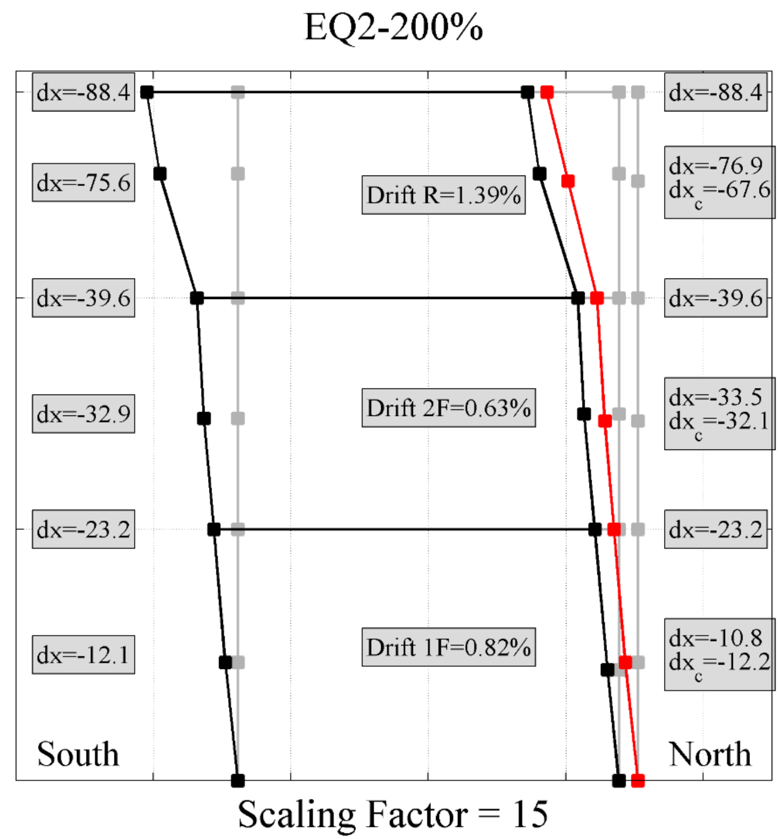

EQ2-200% (0.305 g)

4 views

1 view

Failure Mechanisms

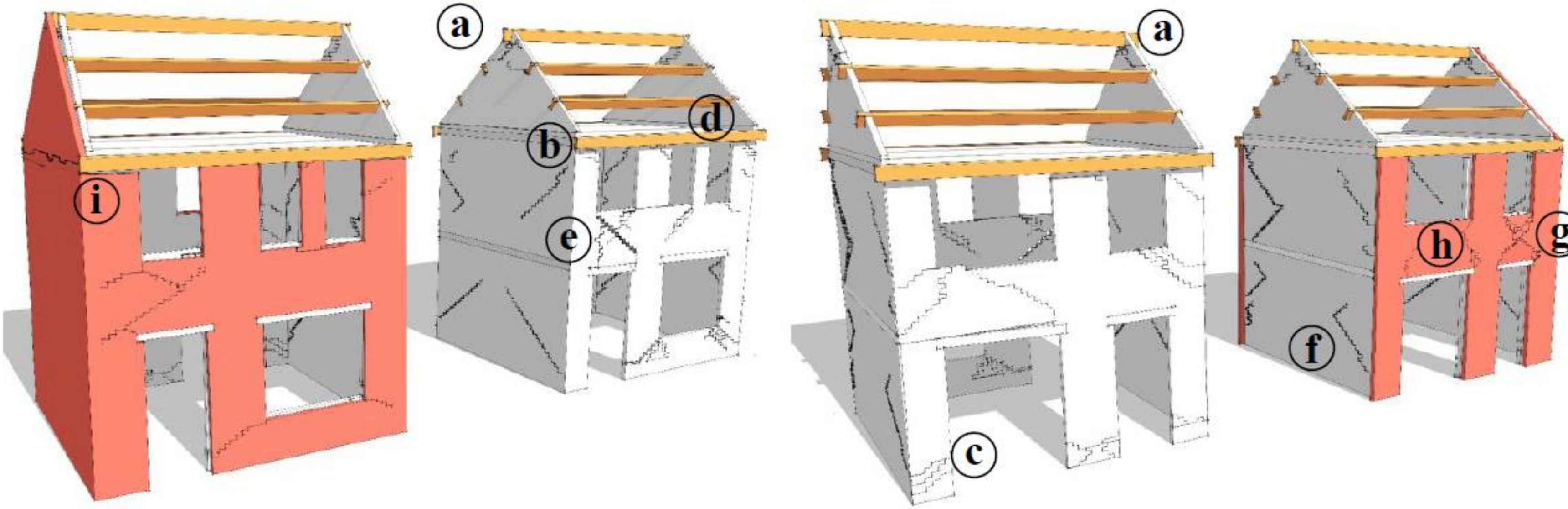

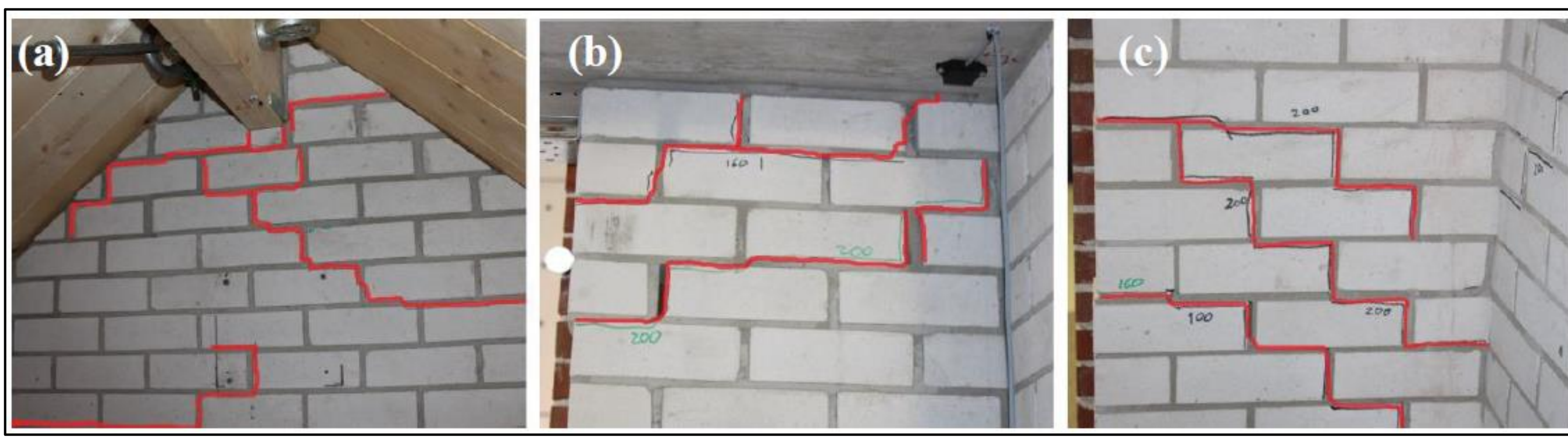

Failure Mechanisms

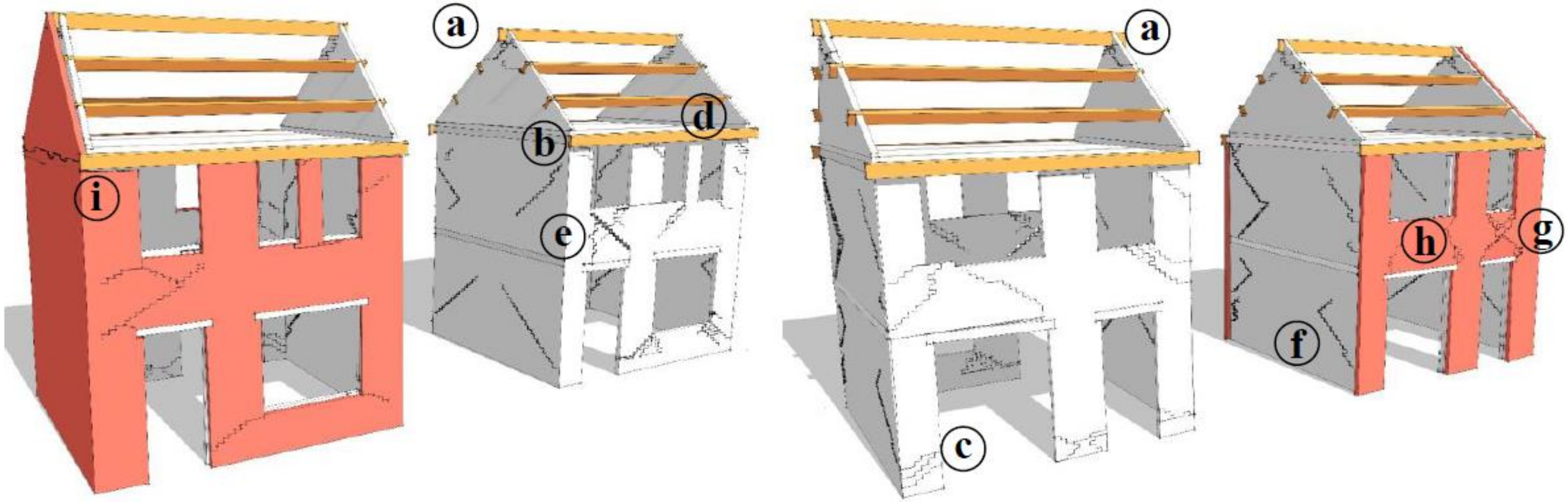

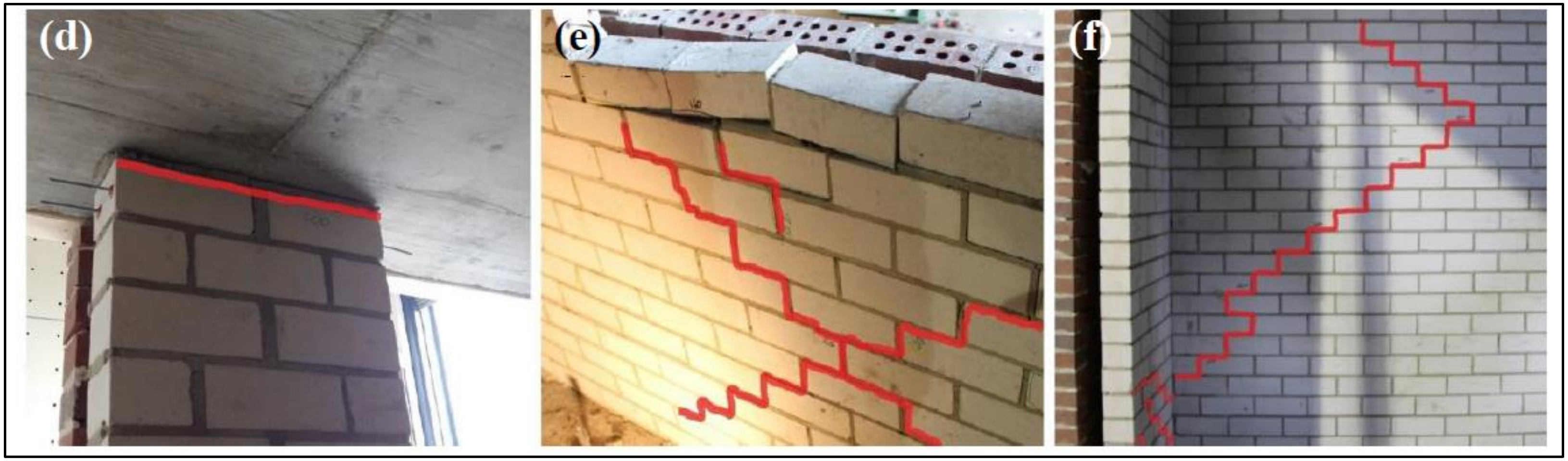

Failure Mechanisms

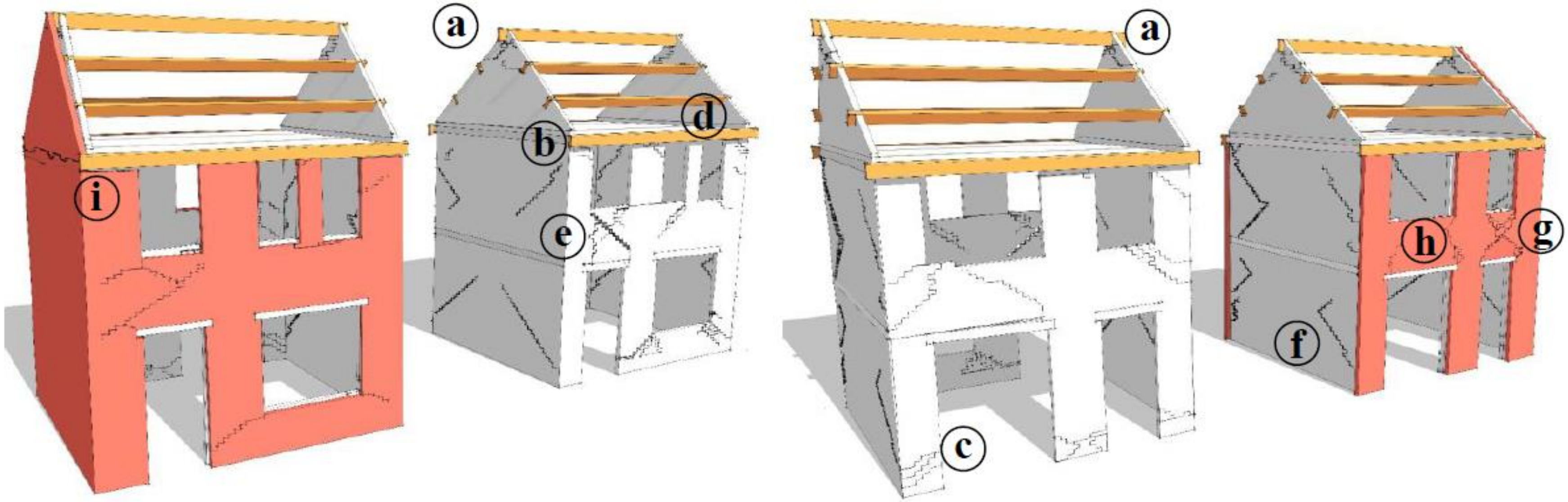

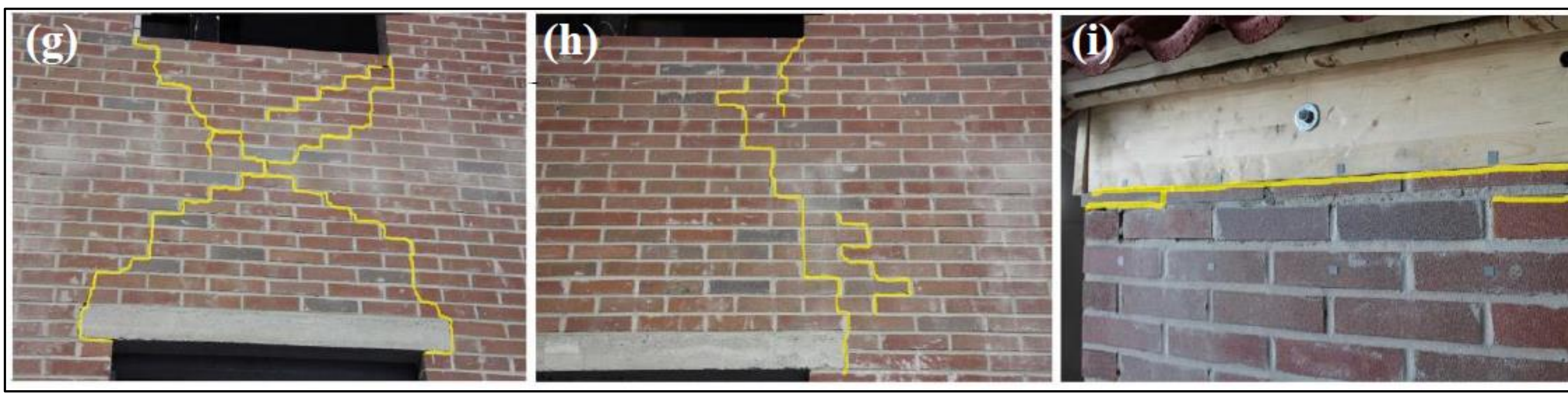

Force - Displacement

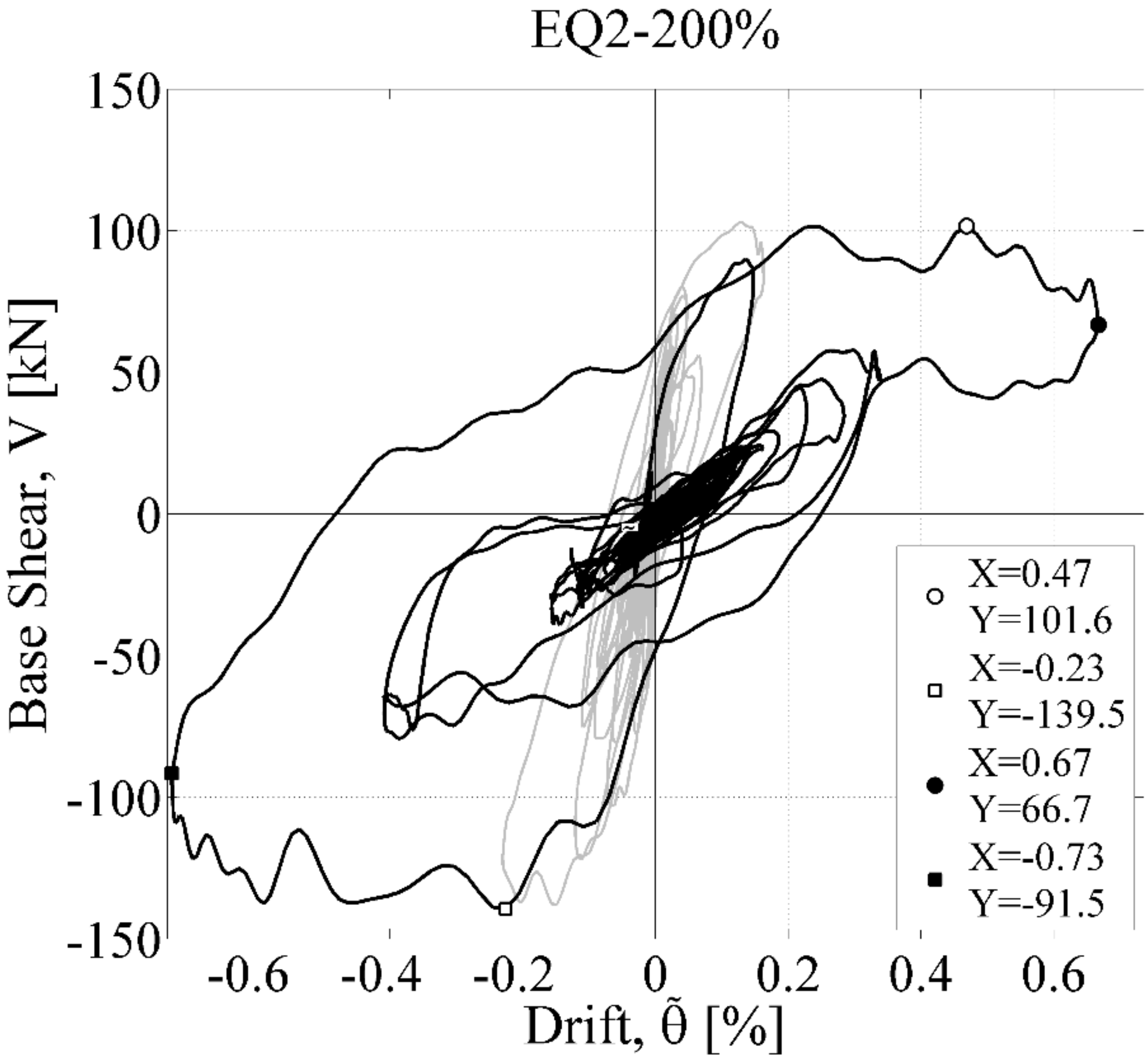

Identification of Performance Limits

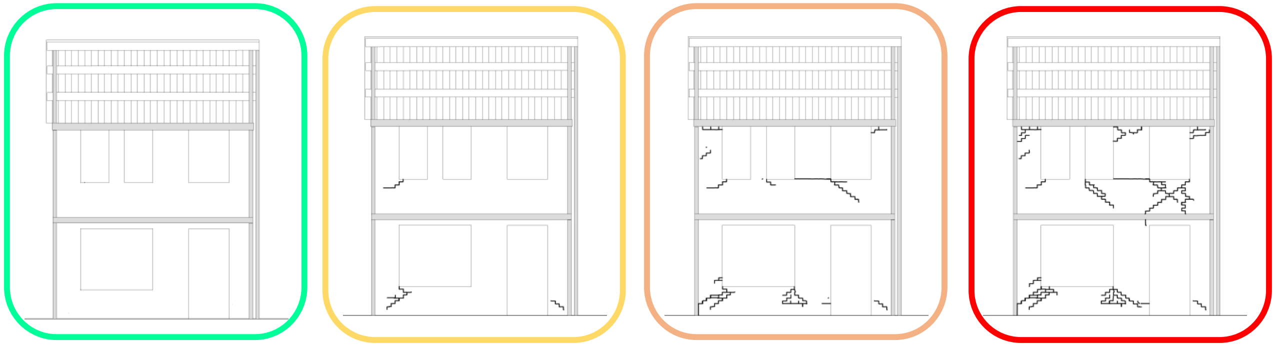

- Envelope curve
- Damage accumulation
- Finite number of test

	Scale	Variable	*DL1*	*DL2*	*DL3*	*DL4*
Calvi (1999)	Sub-system	θ_i	0.10%		0.30%	0.50%
Lagomarsino & Cattari (2015)		θ_i	0.05-0.10%	0.15-0.3%	0.35-0.50%	0.55-0.70%
Experimental		θ_1	0.07%	0.12%	0.34%	0.88%
Lagomarsino & Cattari (2015)	Global	V/V_{max}	≥0.50	0.95-1.0	0.80-0.9	0.60-0.7
Experimental		V/V_{max}	0.57	0.76	1	0.66
		$\tilde{\theta}$	0.047%	0.073%	0.23%	0.73%

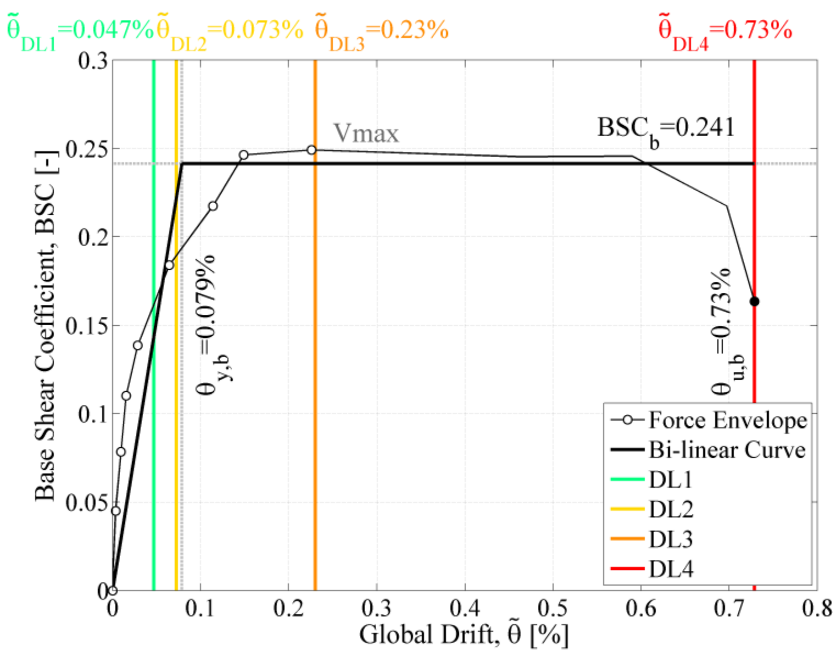

- **DS1**, no structural damage;
- **DS2**, minor structural damage;
- **DS3**, moderate structural damage;
- **DS4**, heavy structural damage;
- **DS5**, very heavy structural damage with partial or total collapse.

Evolution of the Building Performance

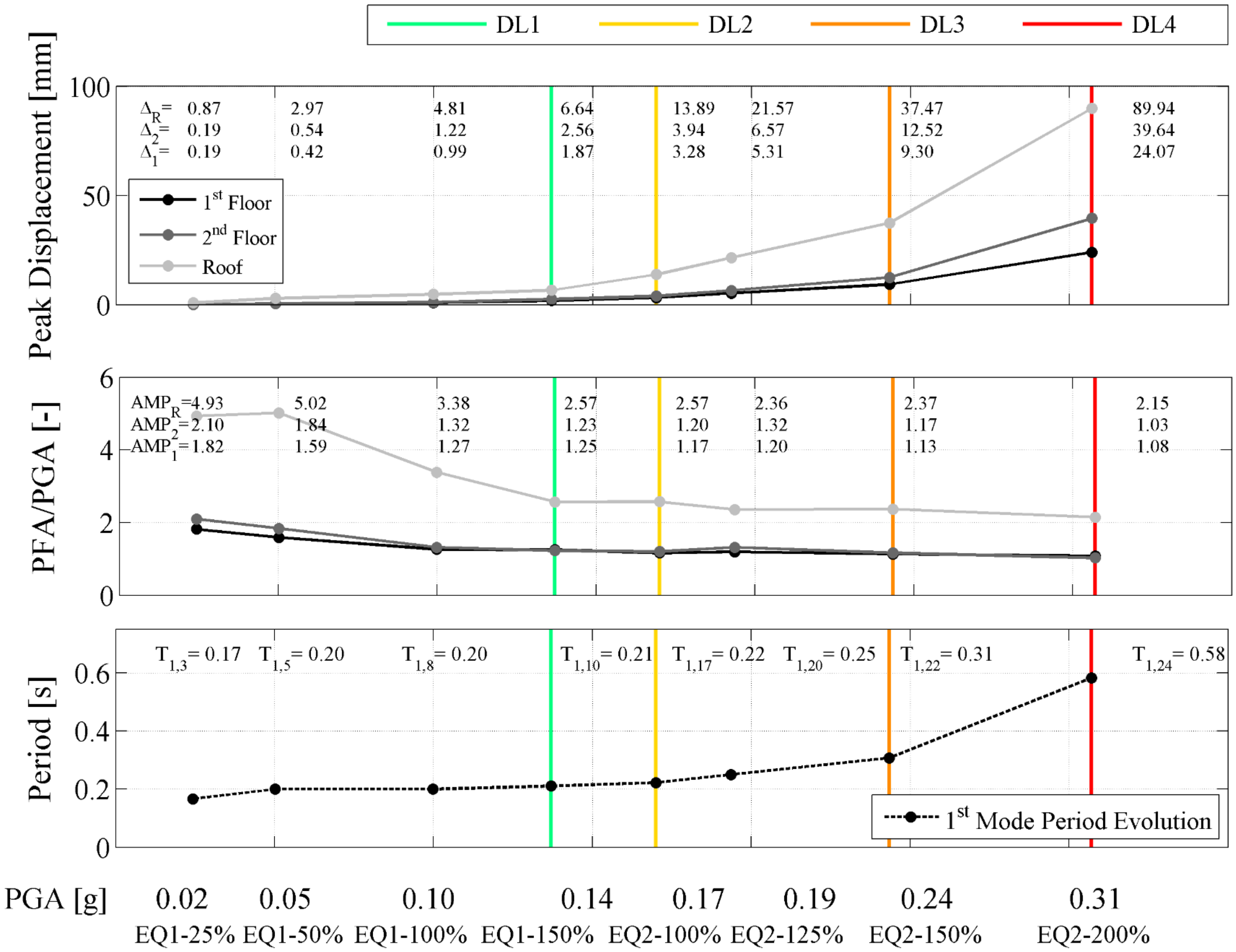

Damage State

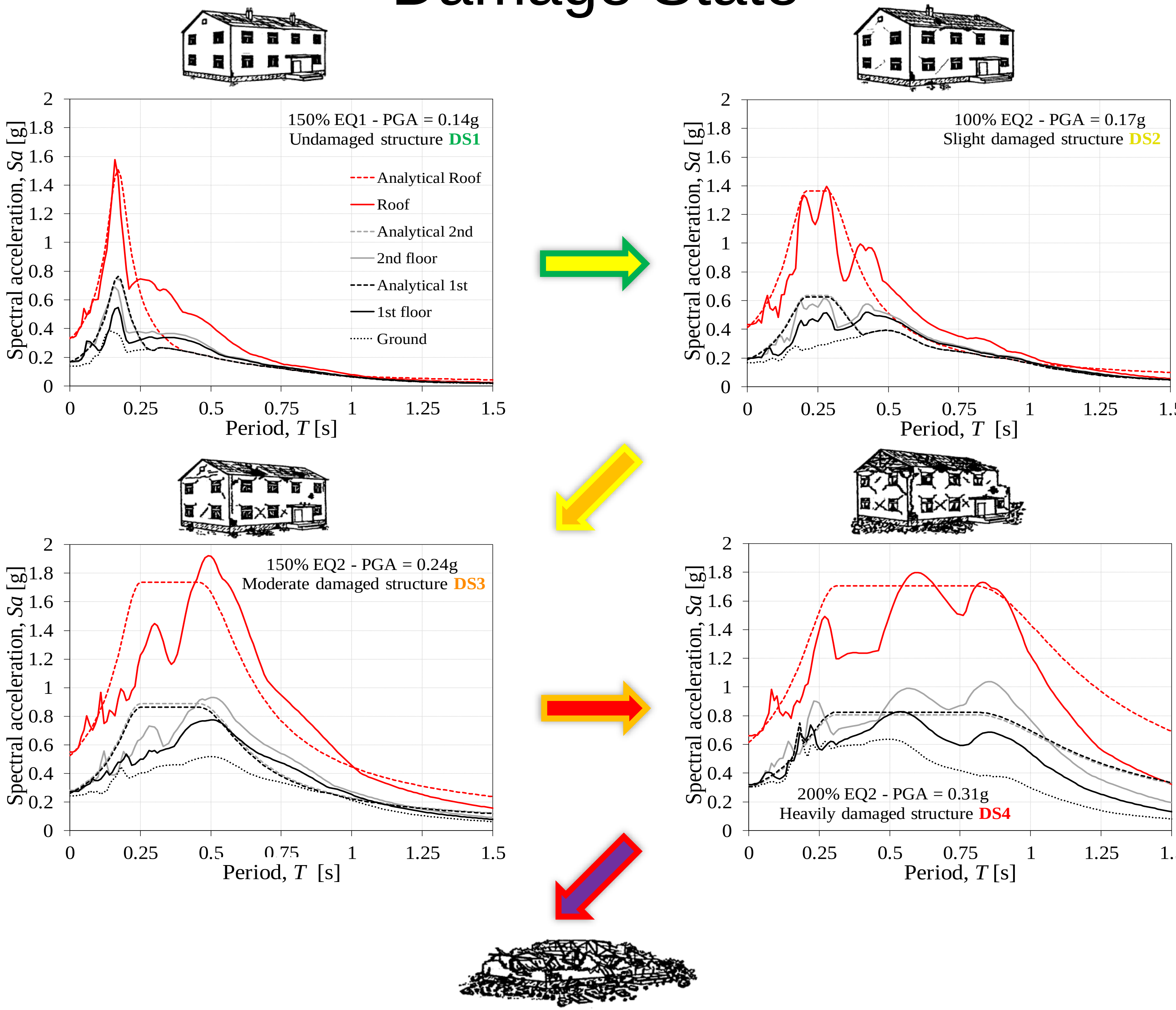

LNEC_Build1

FULL-SCALE CAVITY BUILDING

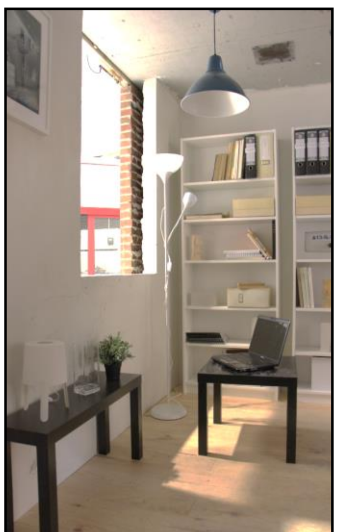

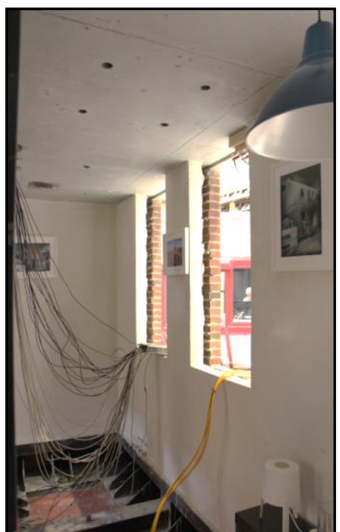

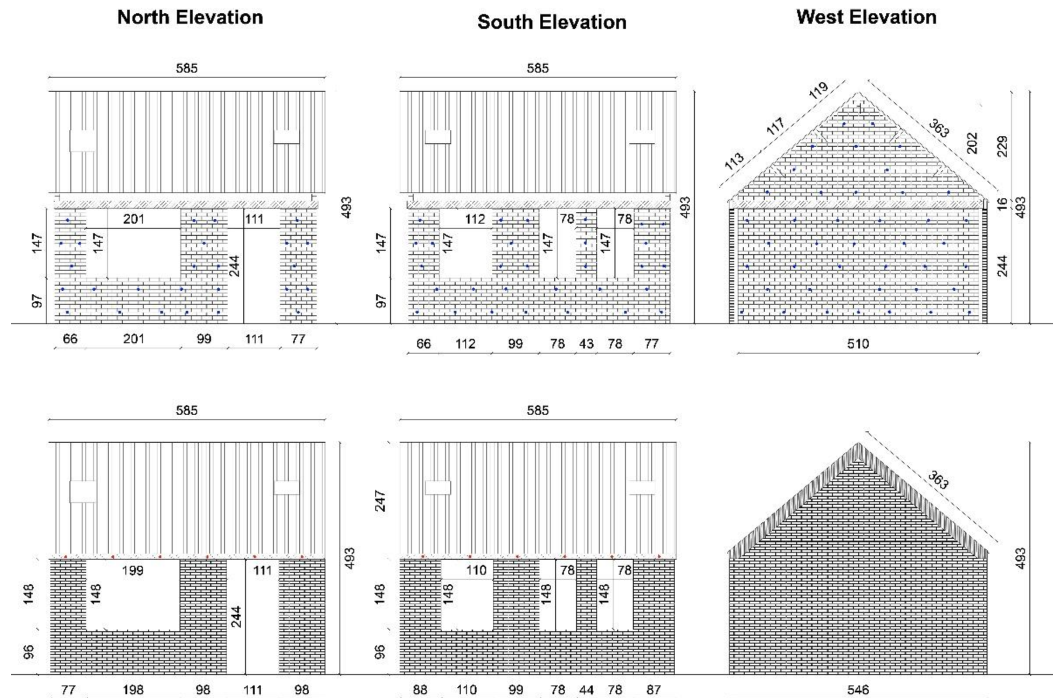

Equal to the 1st floor of EUC_Build1

Instrumentation

Traditional and Wire Potentiometers

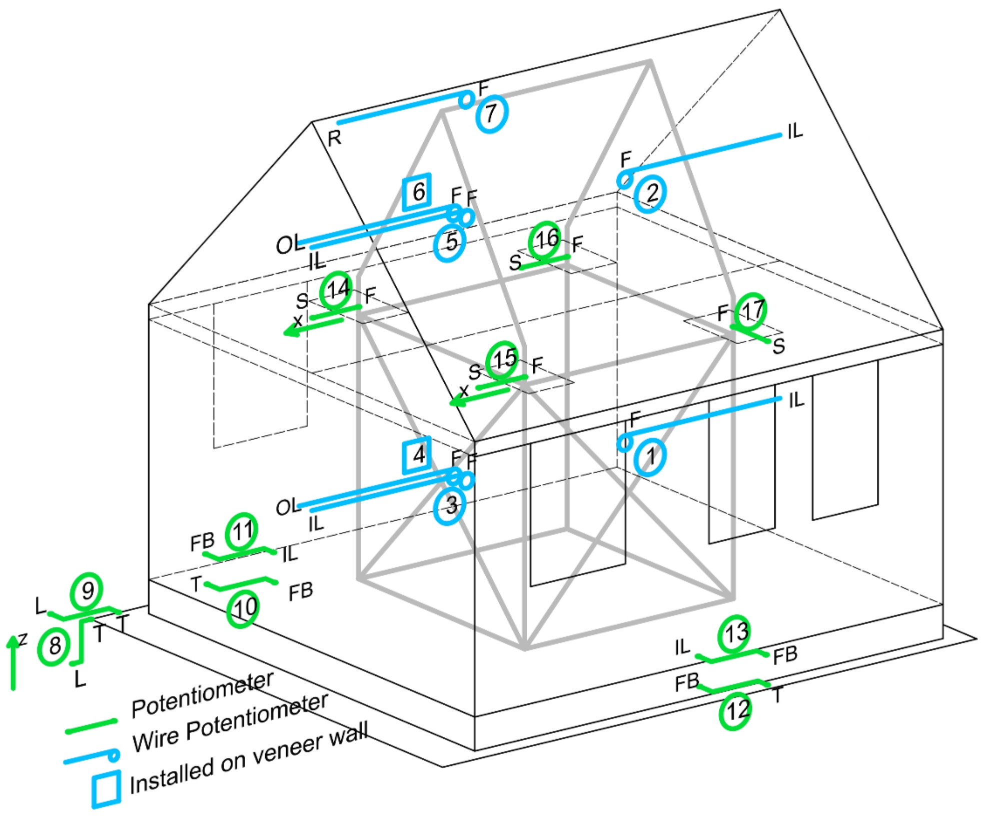

Accelerometers

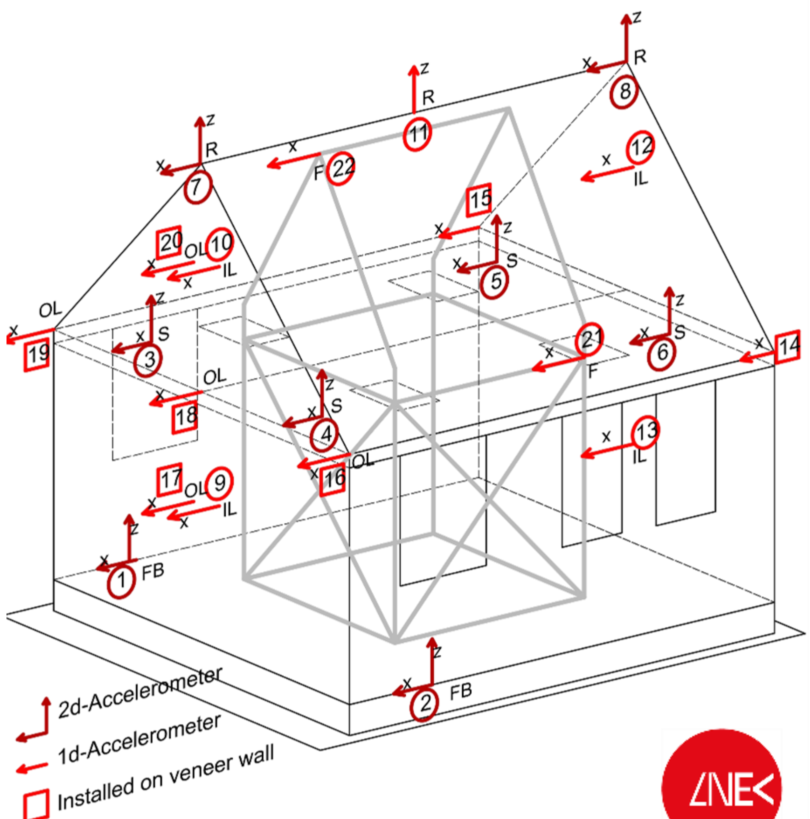

Input Signals

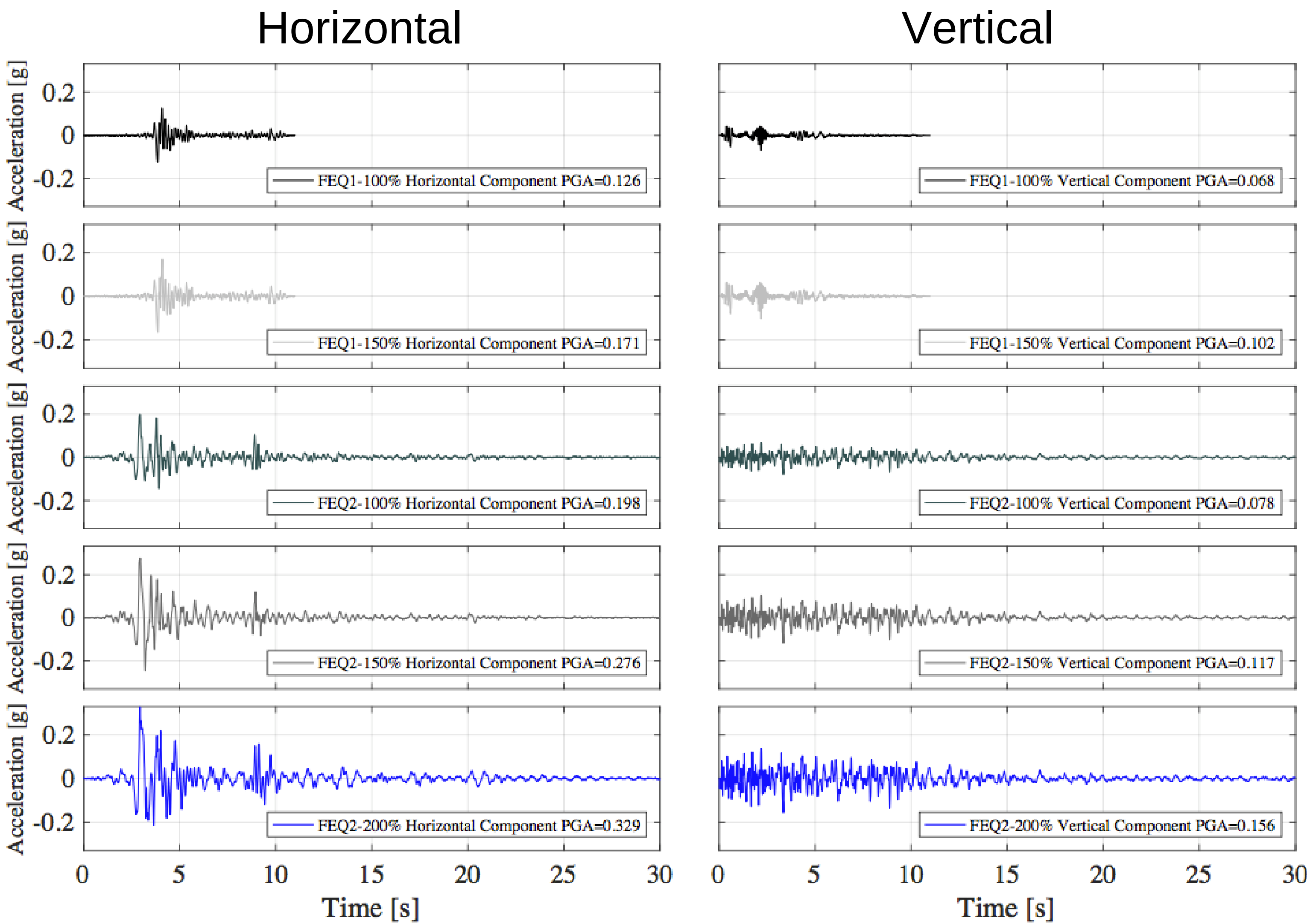

Failure Mechanisms

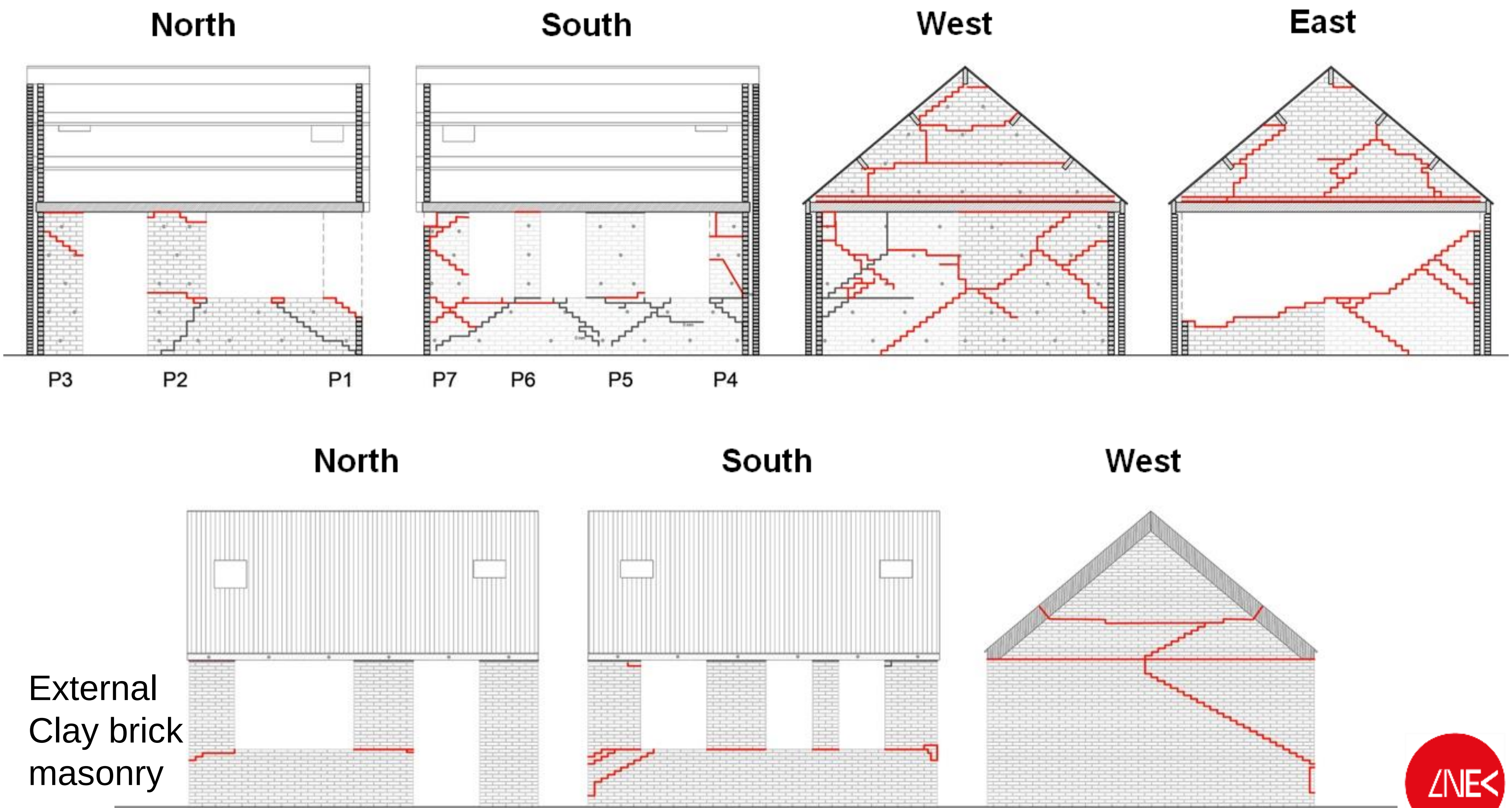

External
Clay brick
masonry

Failure Mechanisms

FEQ2-300% (0.630g): Collapse Mechanism

Outside

Inside

Failure Mechanisms

Partial Collapse in Two-way Bending

FEQ2-300% (H-PTA = 0.495 g, V-PTA = 0.234 g)

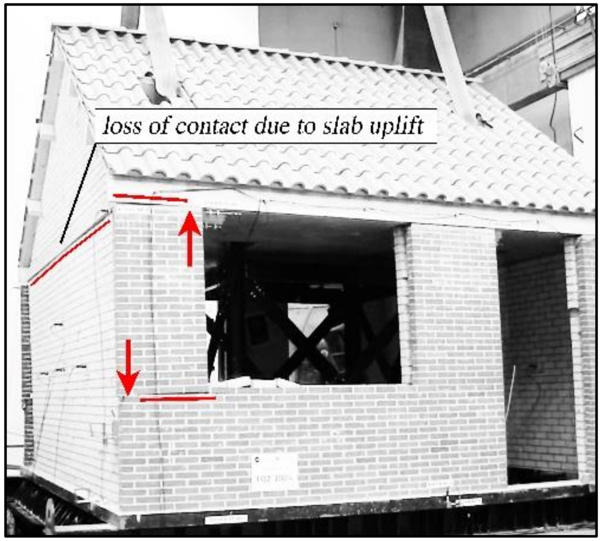

First negative response peak

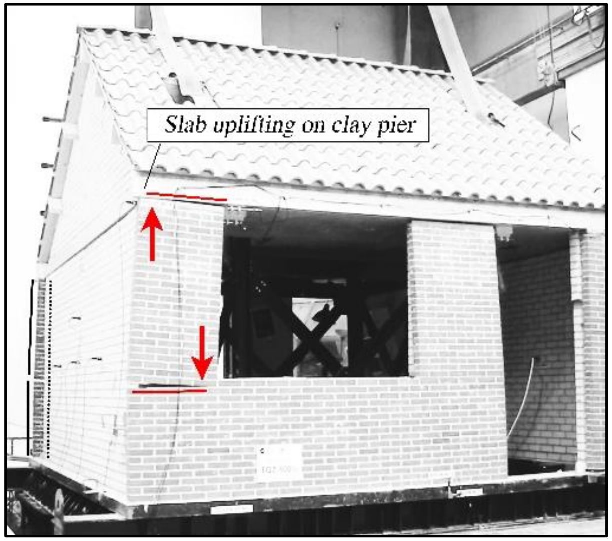

Positive response peak

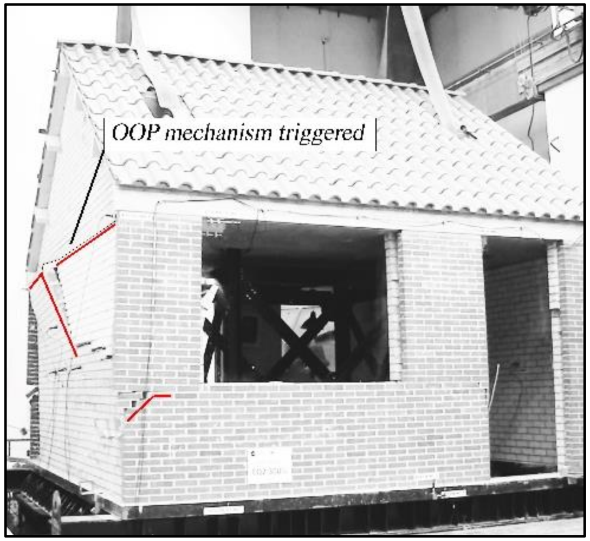

Triggering of the failure mechanism

Failure Mechanisms

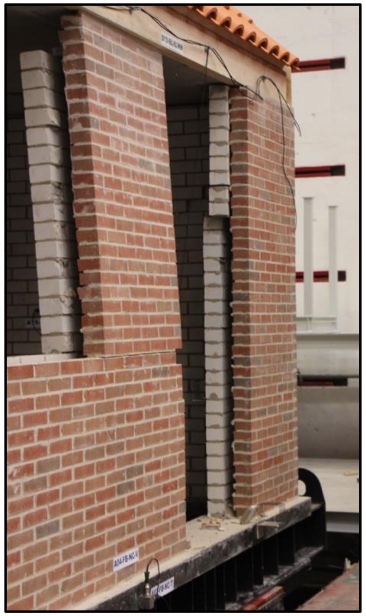

Force - Displacement

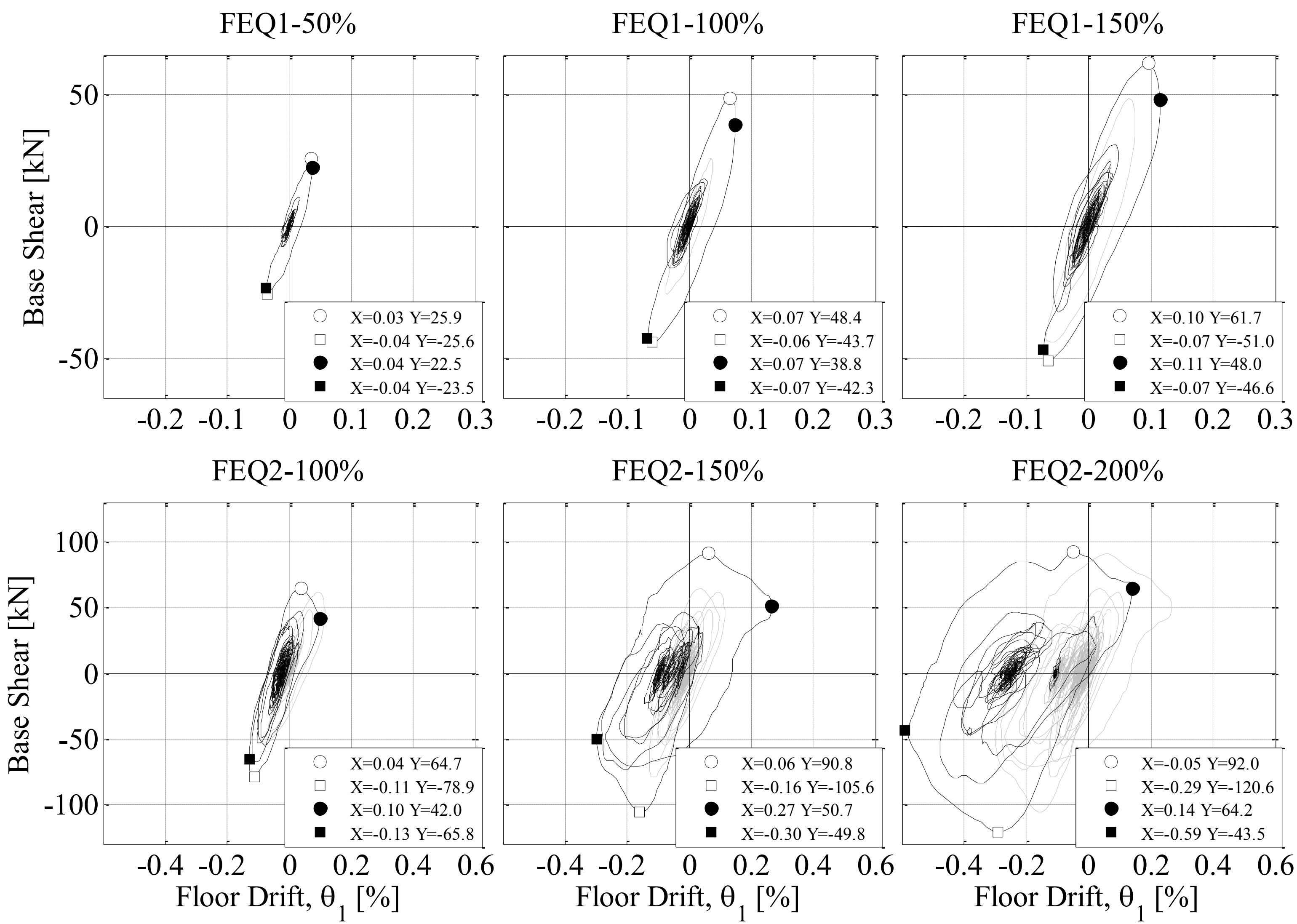

Force - Displacement

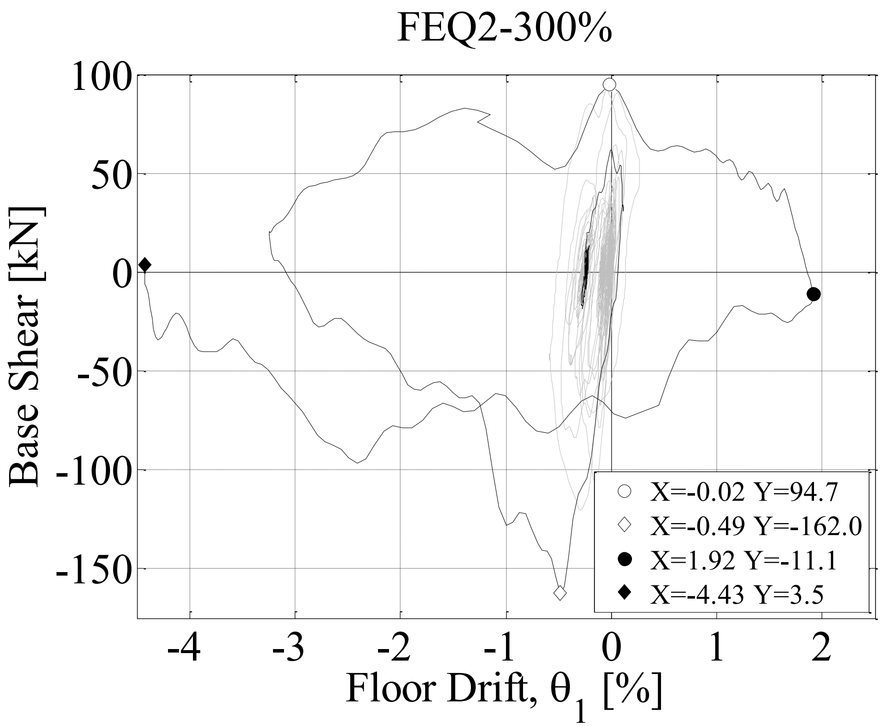

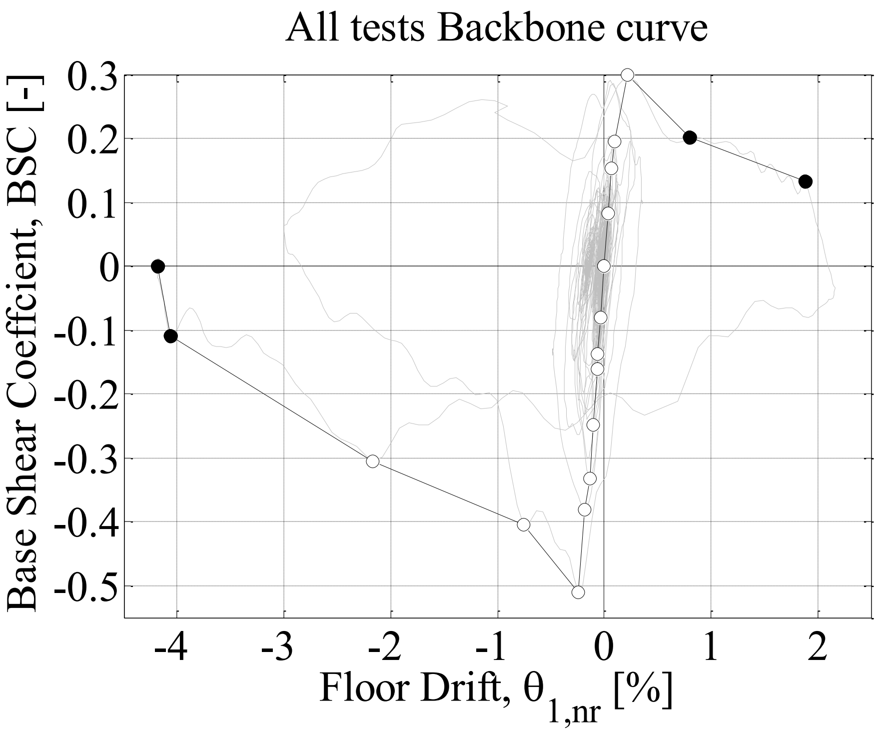

Damage States

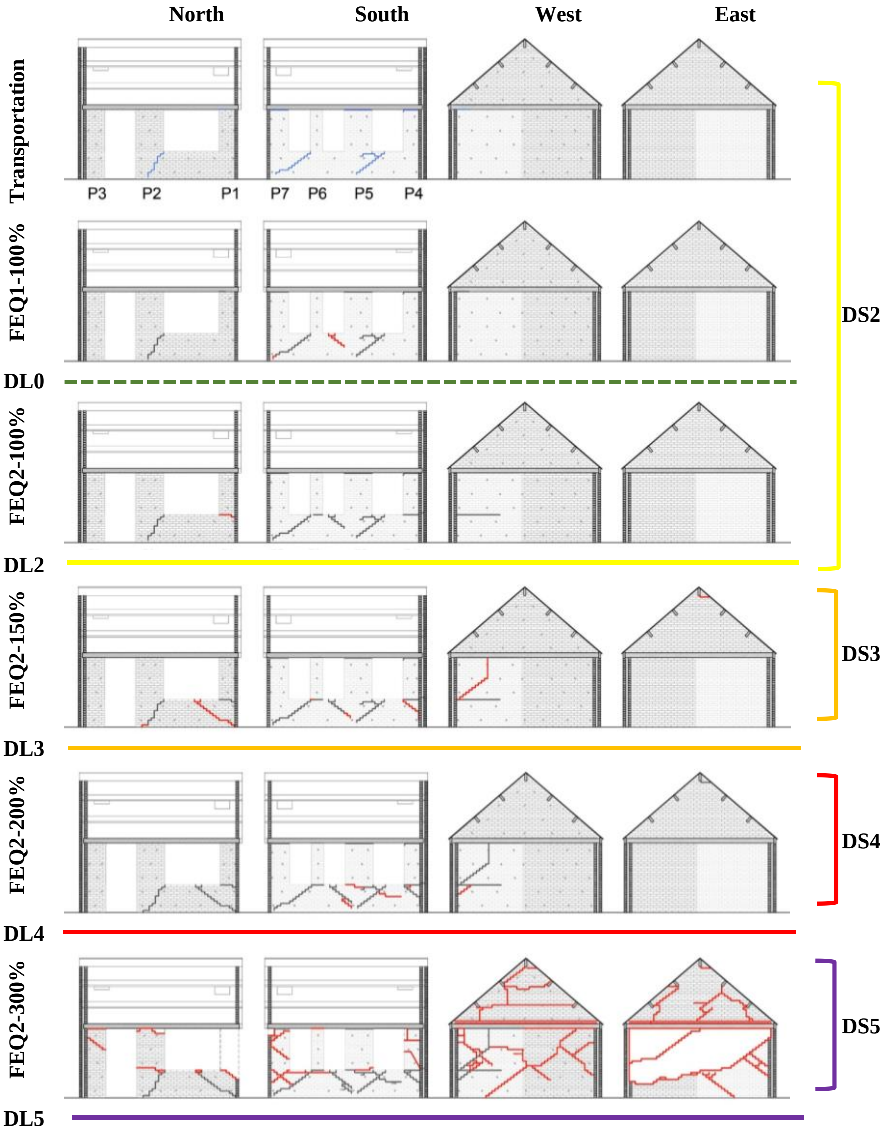

Qualitative definition of damage states (DS):

- **DS0**, no damage;
- **DS1**, no structural damage;
- **DS2**, minor structural damage;
- **DS3**, moderate structural damage;
- **DS4**, heavy structural damage;
- **DS5**, very heavy structural damage with partial or total collapse.

Performance Levels

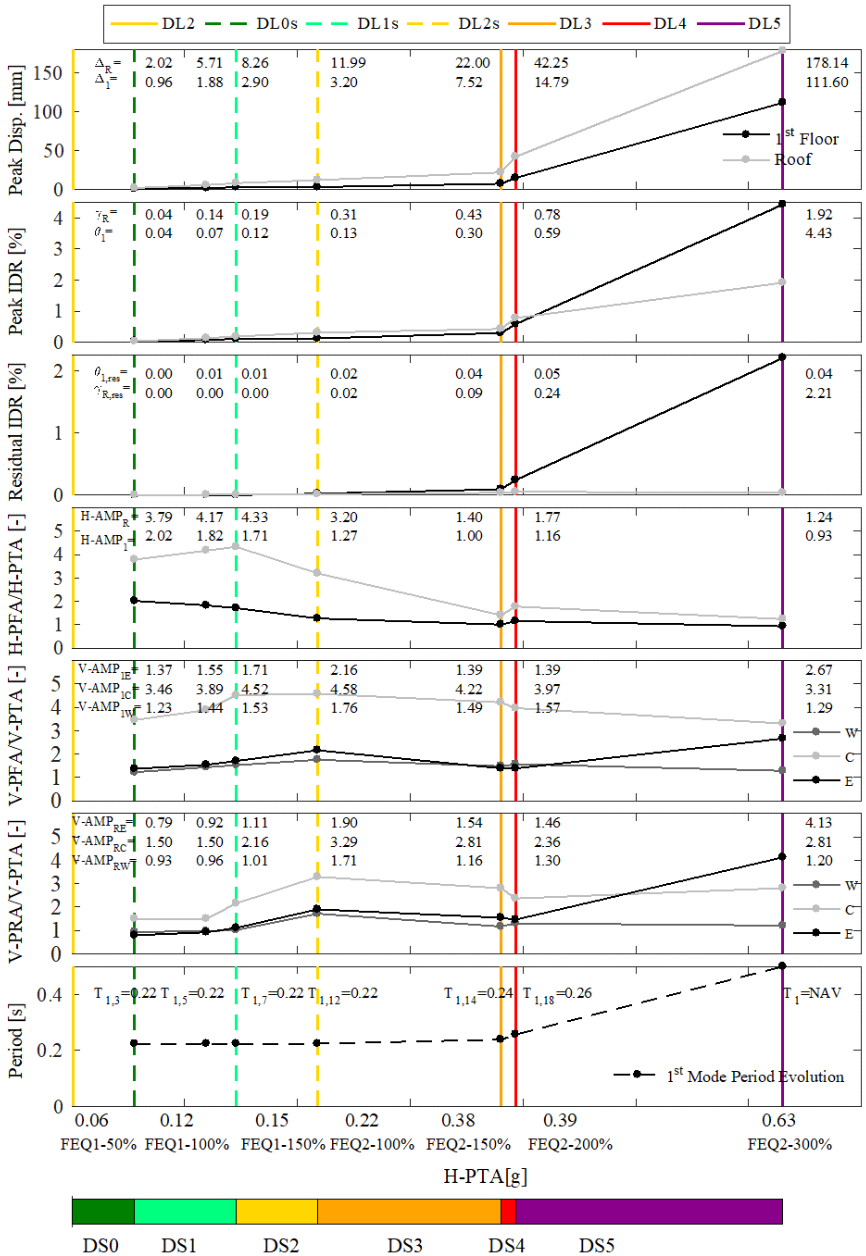

Damage limits were associated to quantitative **EDPs** defined in each sub-system and the overall building:

- Accelerations;
- Displacements/drift (peak and residual).

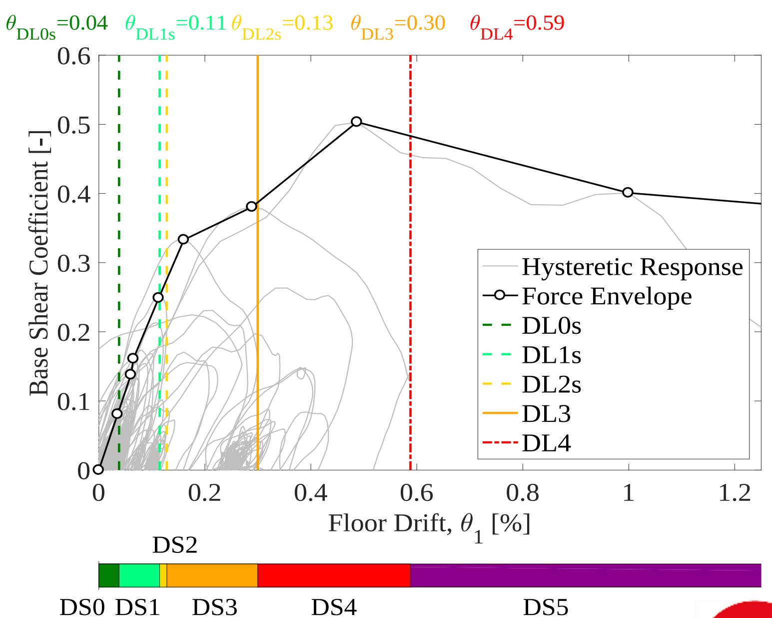

LNEC_Build2

ROOF SUBSTRUCTURE

One gable made with CS single leaf (plastered) and the other made with cavity wall.

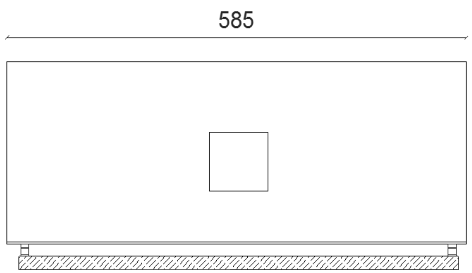

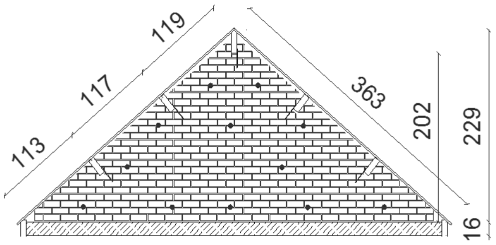

Equal to the roof of EUC_Build1

Failure Mechanisms

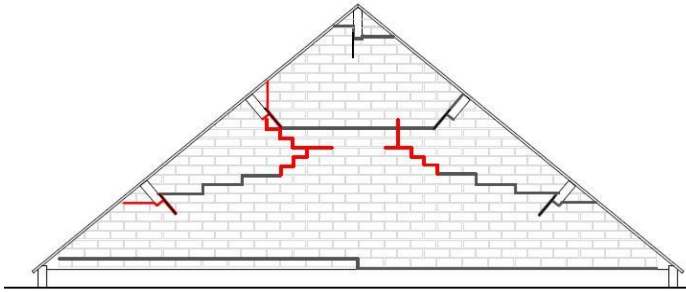

Gable - CS

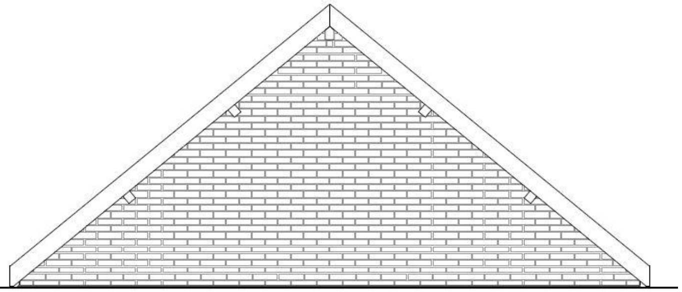

Gable - Clay

FEQ2-600% (1.138 g): Collapse Mechanism

Pushover Tests

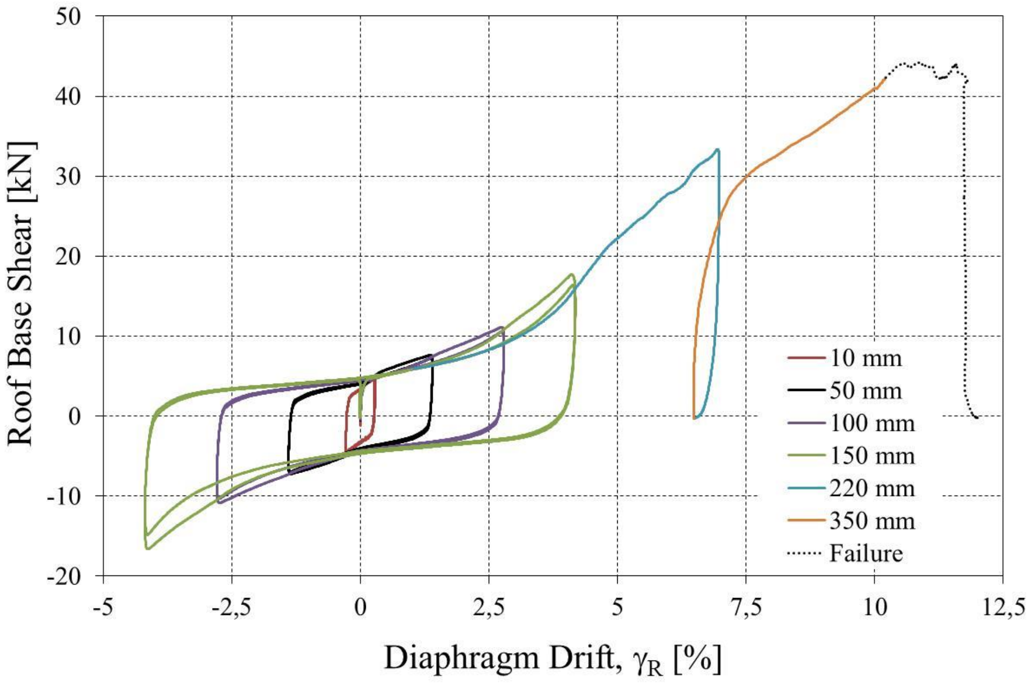

EUC_Build2

FULL-SCALE PRE 1940s DETACHED HOUSE

- Nearly 50% of URM building stock; date back to before World War II;
- No seismic design or detailing; limited available information on the seismic performance;
- Irregular plan configurations; wide openings; flexible floors; and steep pitched roofs.

EUC_Build2

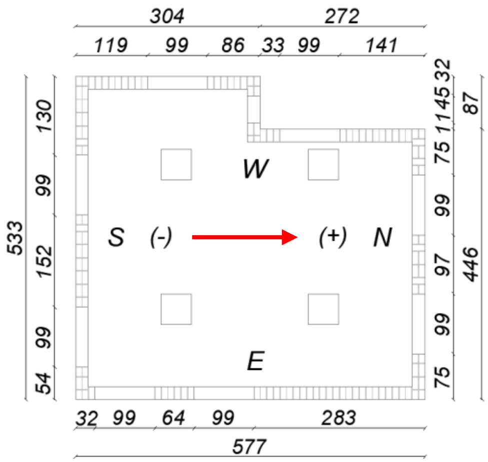

Specimen overview:

- Dimensions: 5.8 x 5.3 x 6.2 m;
- Weight: 33 t;
- Double-wythe solid clay-brick walls, 200-mm thick;
- 1 story (2.9 m) plus an attic (3.3 m), large asymmetrical openings, reentrant corners;
- Flexible timber diaphragms.

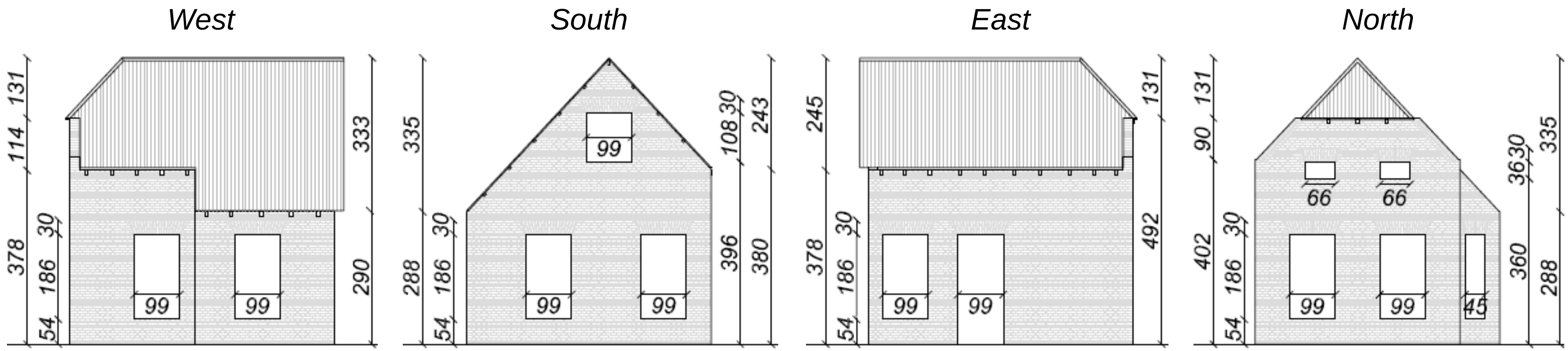

Construction Details

- Contractors from the Groningen area;
- Materials shipped from the Netherlands;
- The Dutch cross brickwork bond was adopted;
- 208×100×50 mm solid clay bricks;
- 10-mm-thick fully mortared head and bed joints;
- Lintels above all openings.

The Dutch cross bond

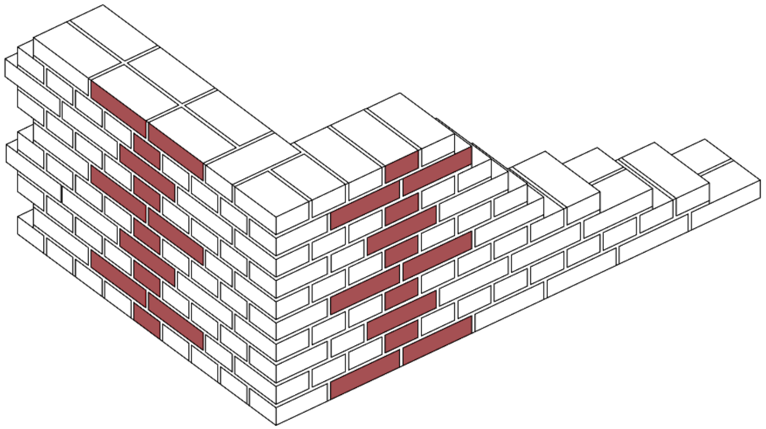

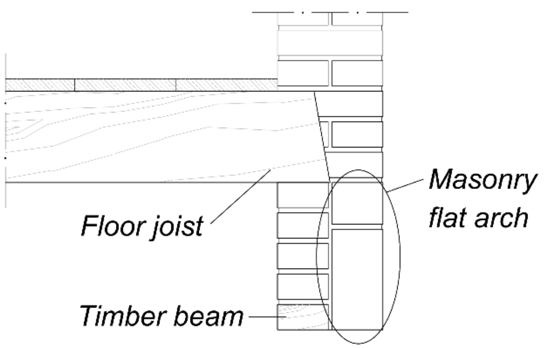

300-mm-deep brick flat arch (below the exterior wythe)

timber beam (below the interior masonry wythe)

Construction Details

Floor Diaphragm

Flexible timber diaphragm:

- spruce timber floorboards;
- timber joists.

Steel ties between walls and diaphragm

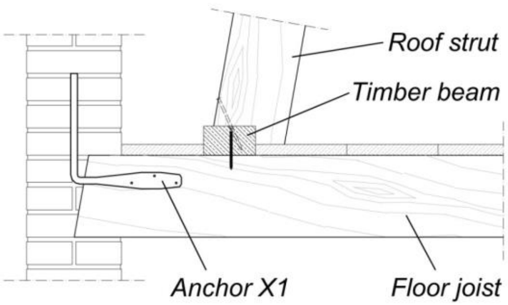

Connection between every other diaphragm joist and **longitudinal** walls

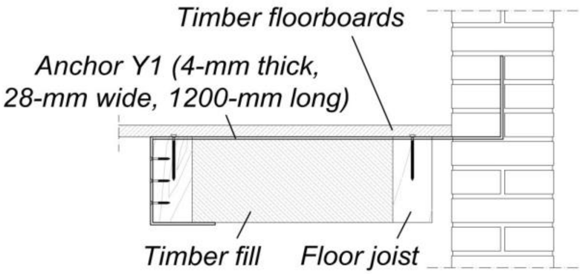

Connection between diaphragm end joists and **transverse** walls

Construction Details

Pitched Roof

- Timber roof supported on trusses resting on longitudinal walls;
- Gables unloaded, not intentionally restrained against overturning.

Construction Timelapse (Duration: 4 weeks)

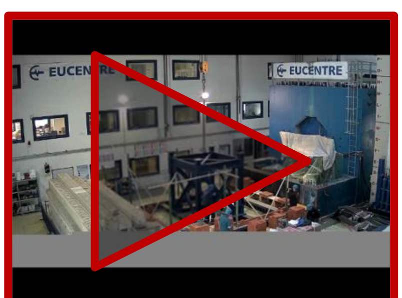

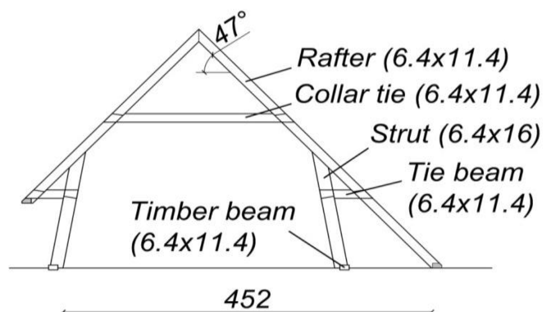

Roof trusses spanning between the E and outermost W wall

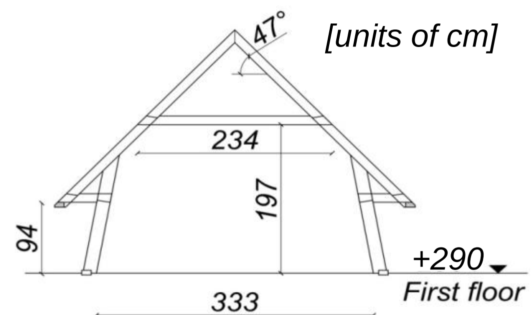

Roof trusses spanning between the E and reentrant W wall

Instrumentation

- Accelerometers;
- Potentiometers;
- 3D optical acquisition system.

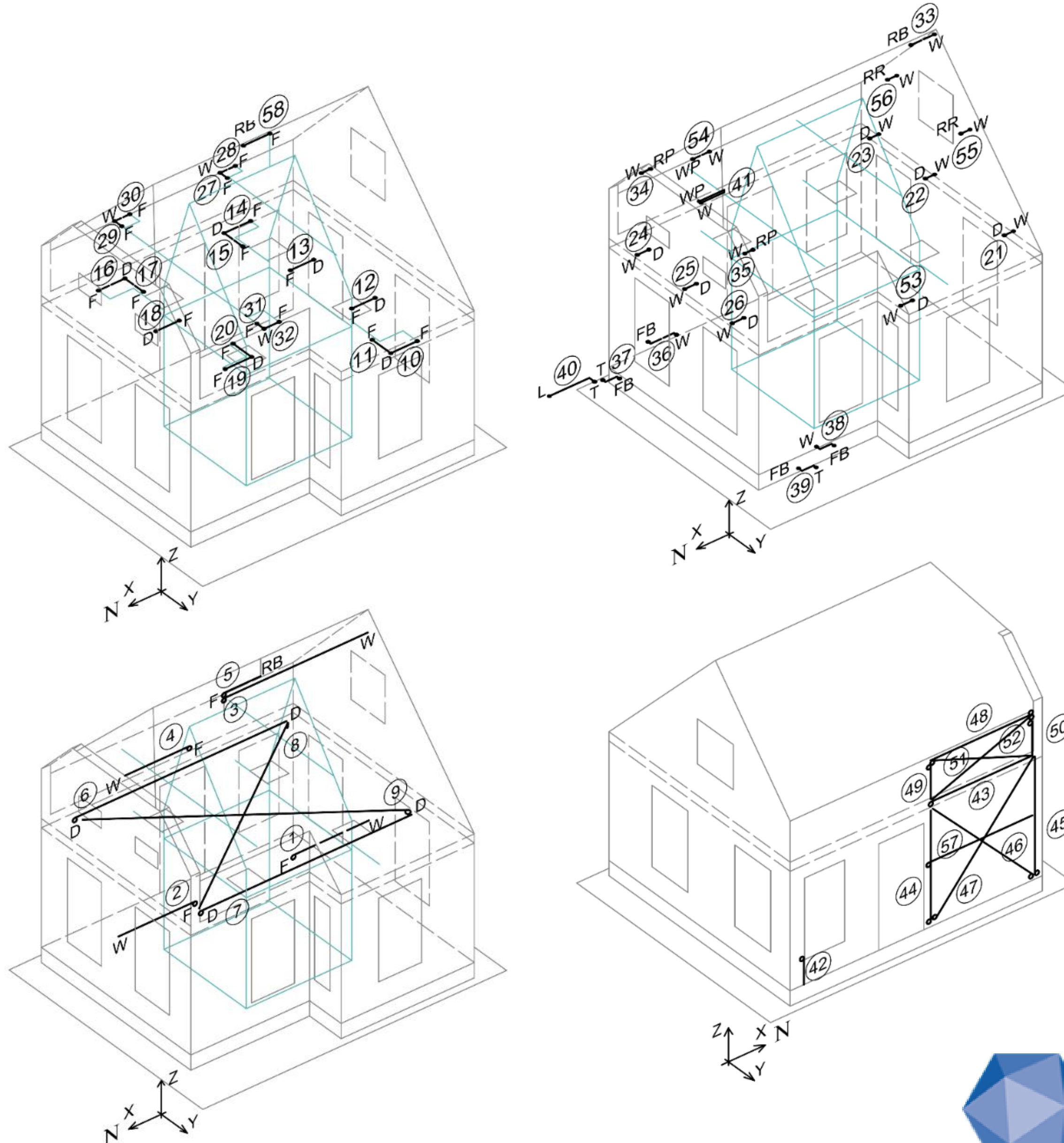

Input Signals

2 realistic seismic scenarios for the Groningen region:

- SC1: scenario #1, comparable to the 2012 Huizinge event
  5-75% significant duration = 0.39 s, PGA = 0.096 g;
- SC2: scenario #2, maximum expected event
  5-75% significant duration = 1.73 s, PGA = 0.155 g.

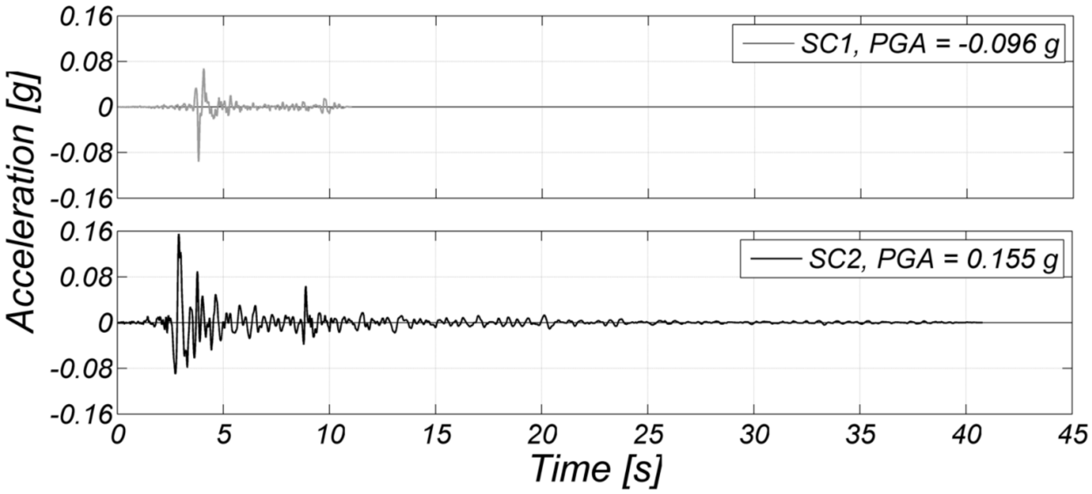

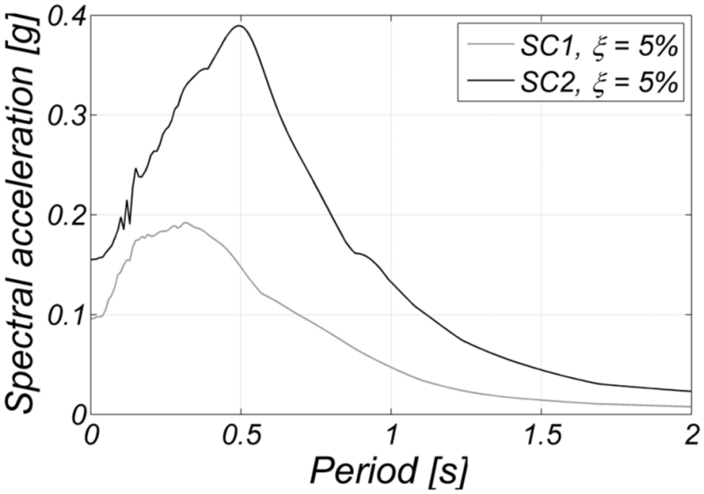

Hysteretic Response and Deformed Shapes

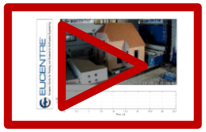

SC2 - 400%
(0.68g)

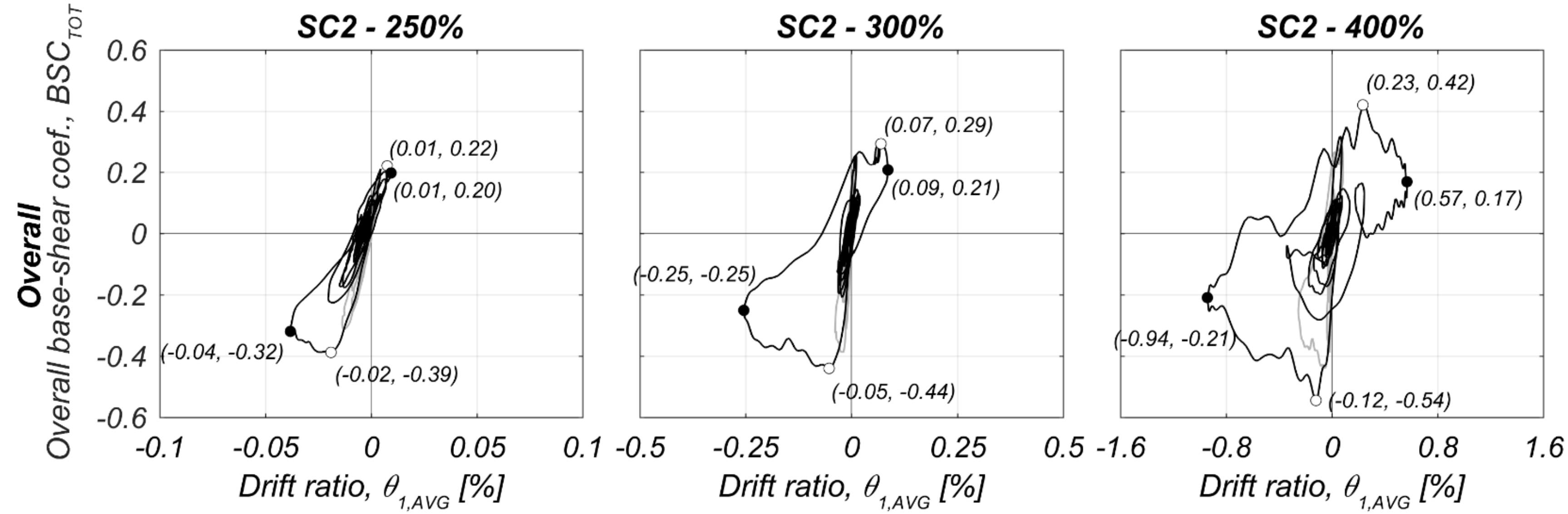

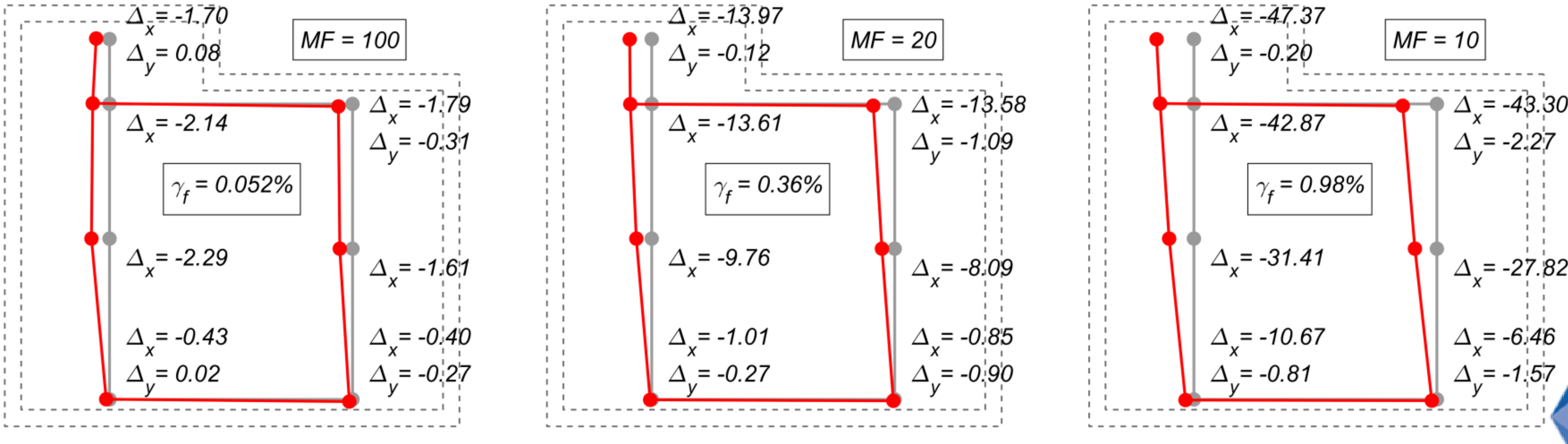

Damage Observation

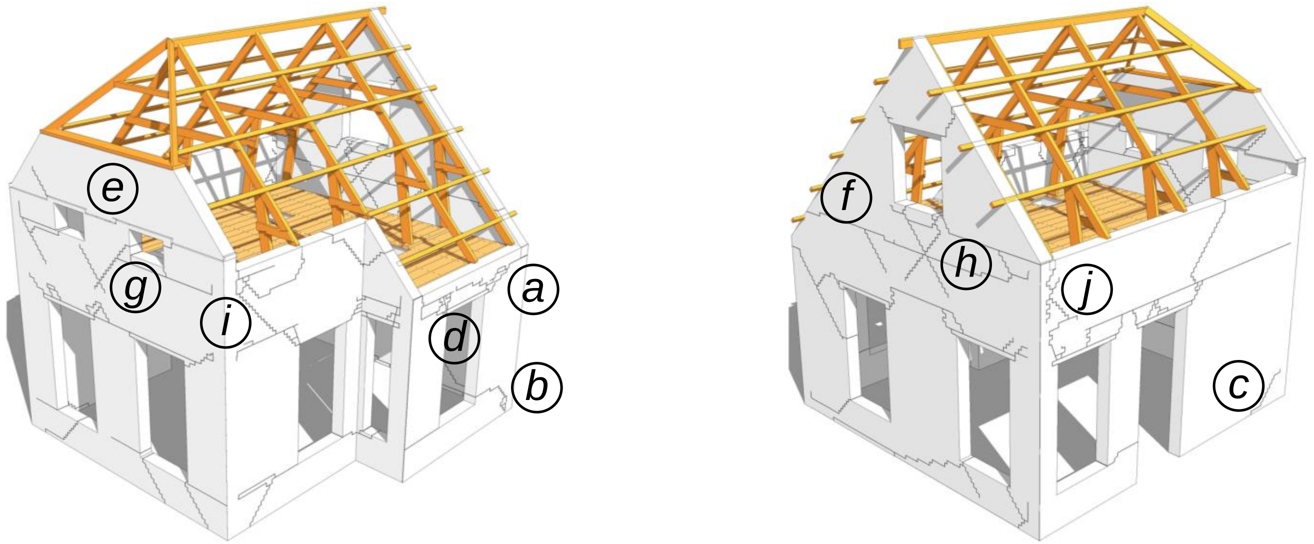

- **Slender piers (West and East walls):** flexural cracks at both ends (a, b);
- **Squat pier (East wall):** flexural cracks at base and sliding (c);
- **Lintels:** diffuse cracks and block de-cohesion (d);
- **North gable:** horizontal crack above openings, residual sliding, and block de-cohesion due to out-of-plane response (e);
- **South gable:** horizontal cracks at base due to overturning (f);
- **Transverse walls:** X cracks due to steel ties restraining out-of-plane mech. (g, h);
- **Participation** of longitudinal walls to transverse walls out-of-plane mech.(i, j).

Failure Mechanisms

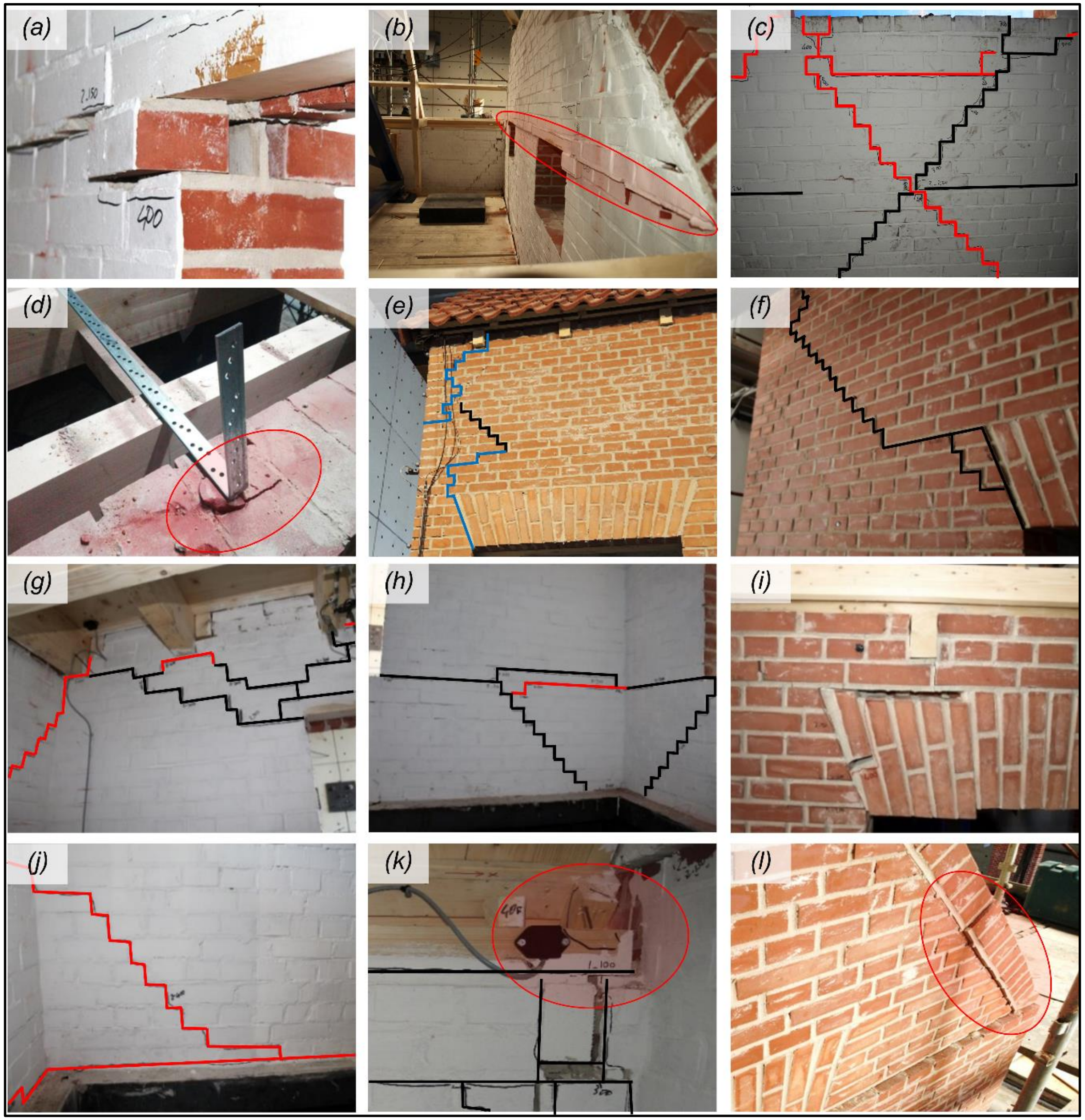

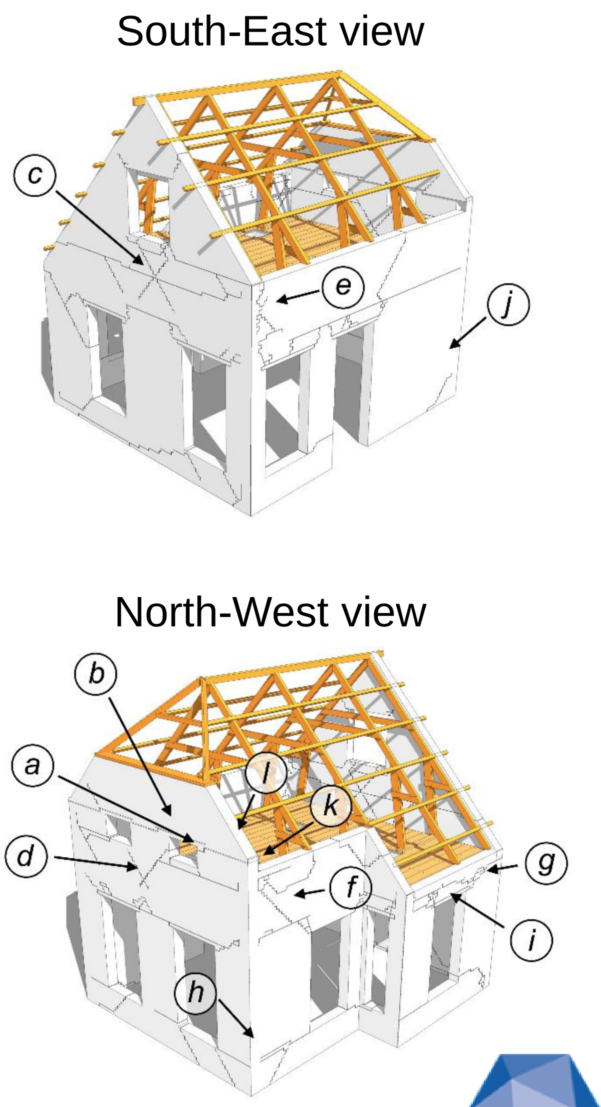

Damage States

Qualitative definition of damage states (DS):

- **DS1**, no structural damage;
- **DS2**, minor structural damage;
- **DS3**, moderate structural damage;
- **DS4**, heavy structural damage;
- **DS5**, very heavy structural damage with partial or total collapse.

Three sub-systems:

- Gables-roof assembly;
- East wall;
- West wall.

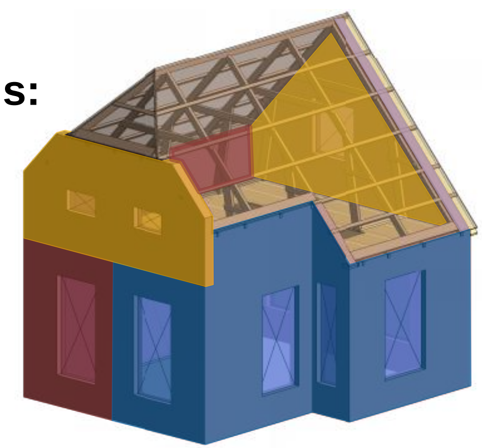

Performance Levels

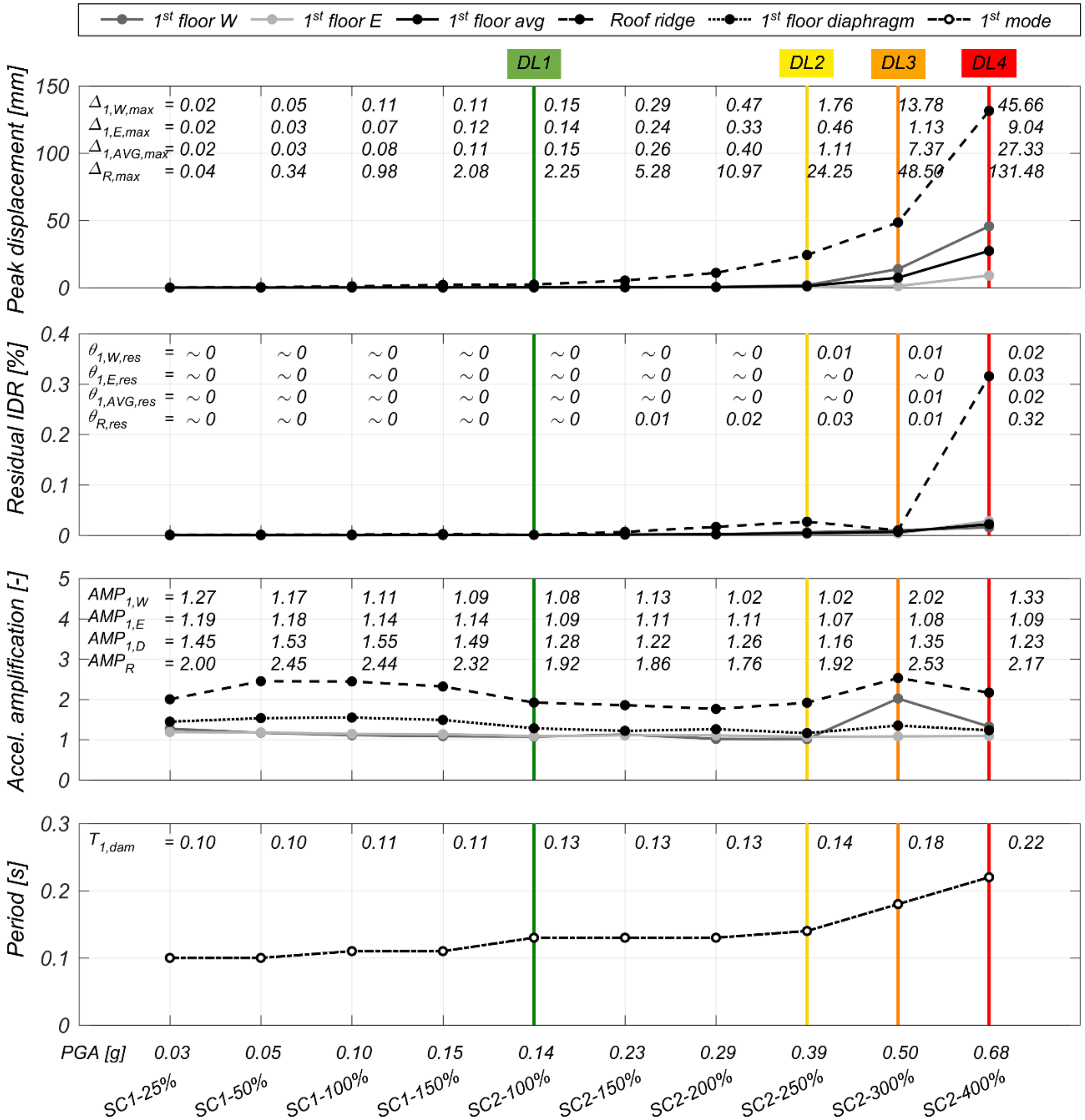

Damage limits were associated to quantitative **EDPs** defined in each sub-system and the overall building:

- Accelerations;
- Displacements/drift (peak and residual).

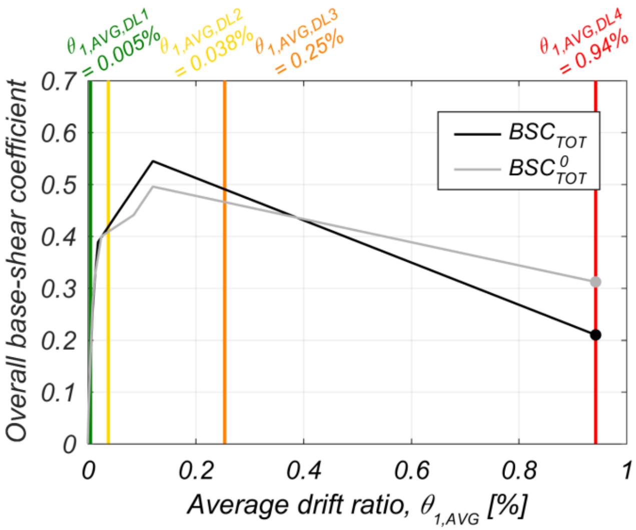

Critical Remarks

- Incremental dynamic excitations, with input representative of induced seismicity scenarios for the Groningen region in the Netherlands:
    - no structural damage for input comparable to the 2012 event (PGA ≈ 0.1 g);
    - the building suffered only minor damage up to PGA of 0.23 g;
    - reached its near-collapse state at a PGA of 0.68 g.

- Gable walls are the most vulnerable components of this type of structures:
    - out-of-plane overturning;
    - significant residual dislocation of the North half-hipped gable.

- The two longitudinal façades exhibited different vulnerabilities and independent response due to the flexible floor diaphragm.

Full-scale Buildings Comparison

EUC_Build1

	DL0 No Damage	DL1 No Structural Damage	DL2 Minor Structural Damage	DL3 Moderate Structural Damage	DL4 Extensive Structural Damage	DL5 Collape
θ [%]	-	0.07	0.12	0.34	0.88	-
PGV [mm/s]	-	77	123	164	218	-
PGA [g]	-	0.137	0.170	0.243	0.307	-

LNEC_Build1

θ [%]	0.04	0.11	0.13	0.30	0.60	4.43
PTV [mm/s]	33	86	141	200	272	419
Est. PGV [mm/s]	31	77	123	164	218	327
PTA [g]	0.056	0.170	0.270	0.276	0.330	0.490
Est. PGA [g]	0.050	0.137	0.170	0.243	0.307	0.460

EUC_Build2

θ [%]	-	0.01	0.04	0.25	0.94	-
PGV [mm/s]	-	110	297	346	444	-
PGA [g]	-	0.140	0.392	0.500	0.942	-

LNEC_Build3

TYPICAL DETACHED HOUSE OF THE GRONINGEN REGION (LOPPERSUM)

The prototype incorporates two additional distinctive features:

- An internal wall;
- Two slender chimneys.

UNDER CONSTRUCTION

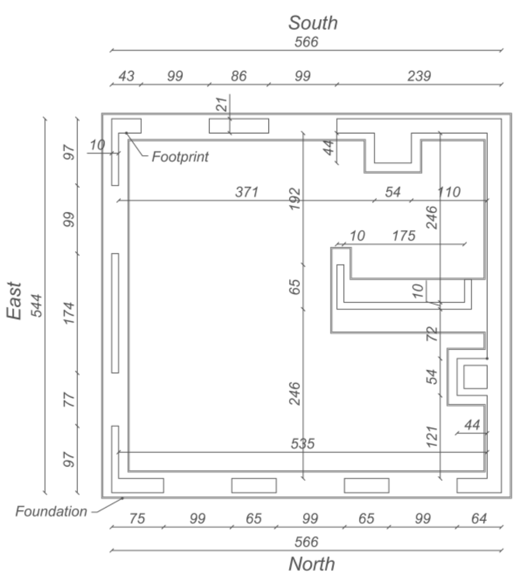

LNEC_Build3

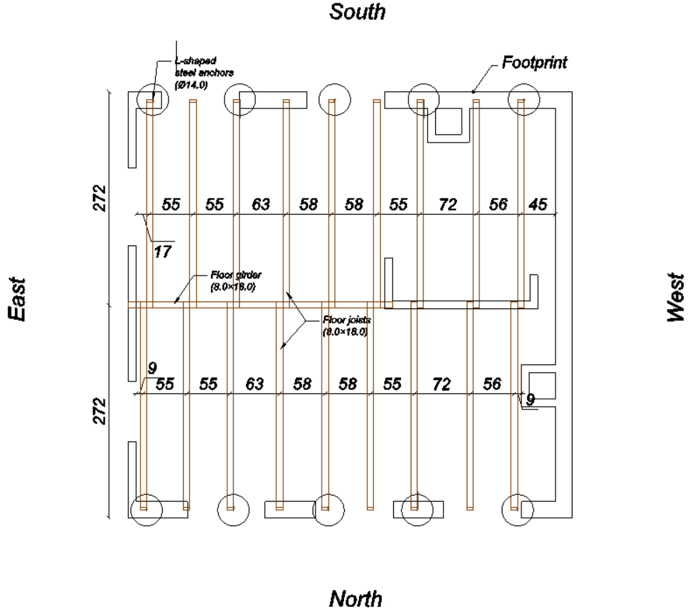

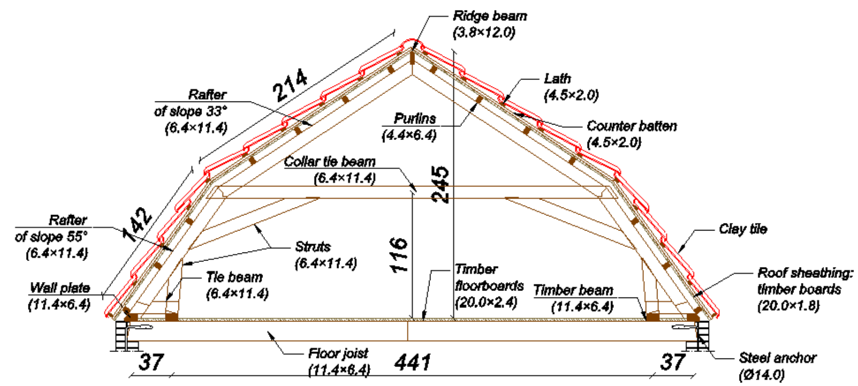

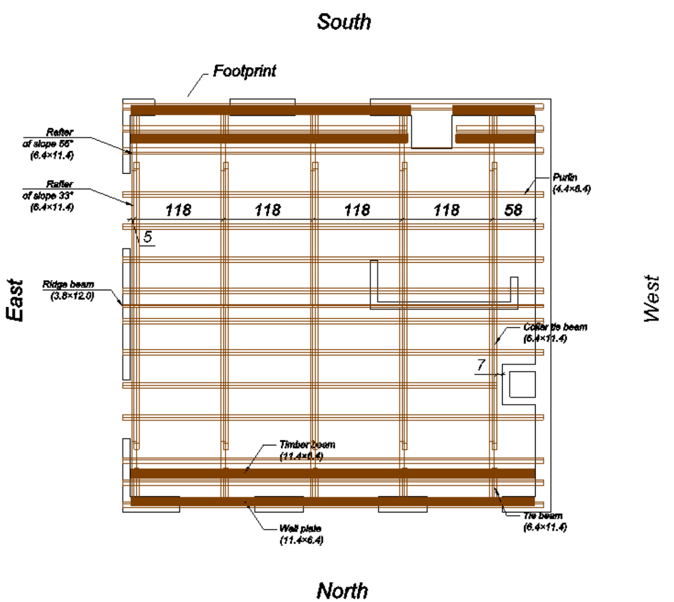

Numerical Model

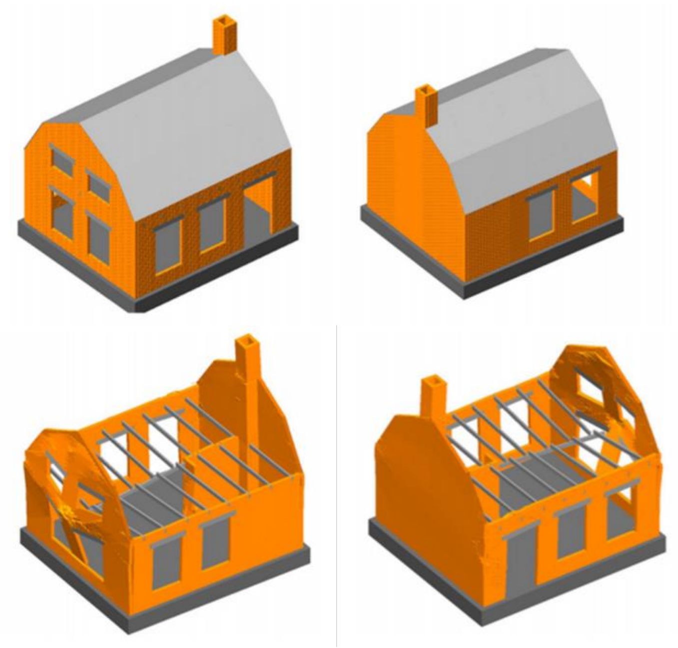


20.02.2018 17:56


Metsel en
10.02.2018 16:2

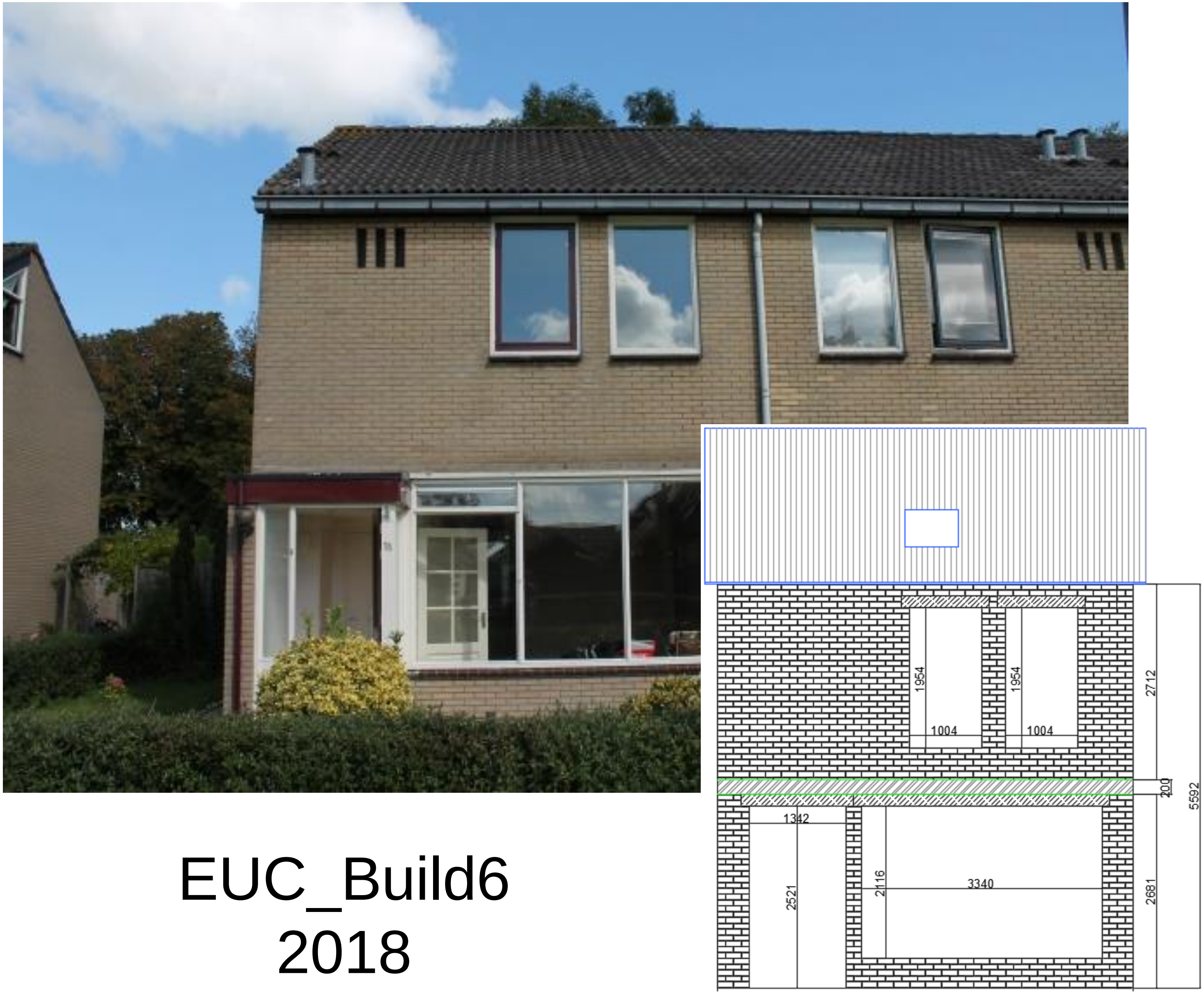

EUC_Build6
2018

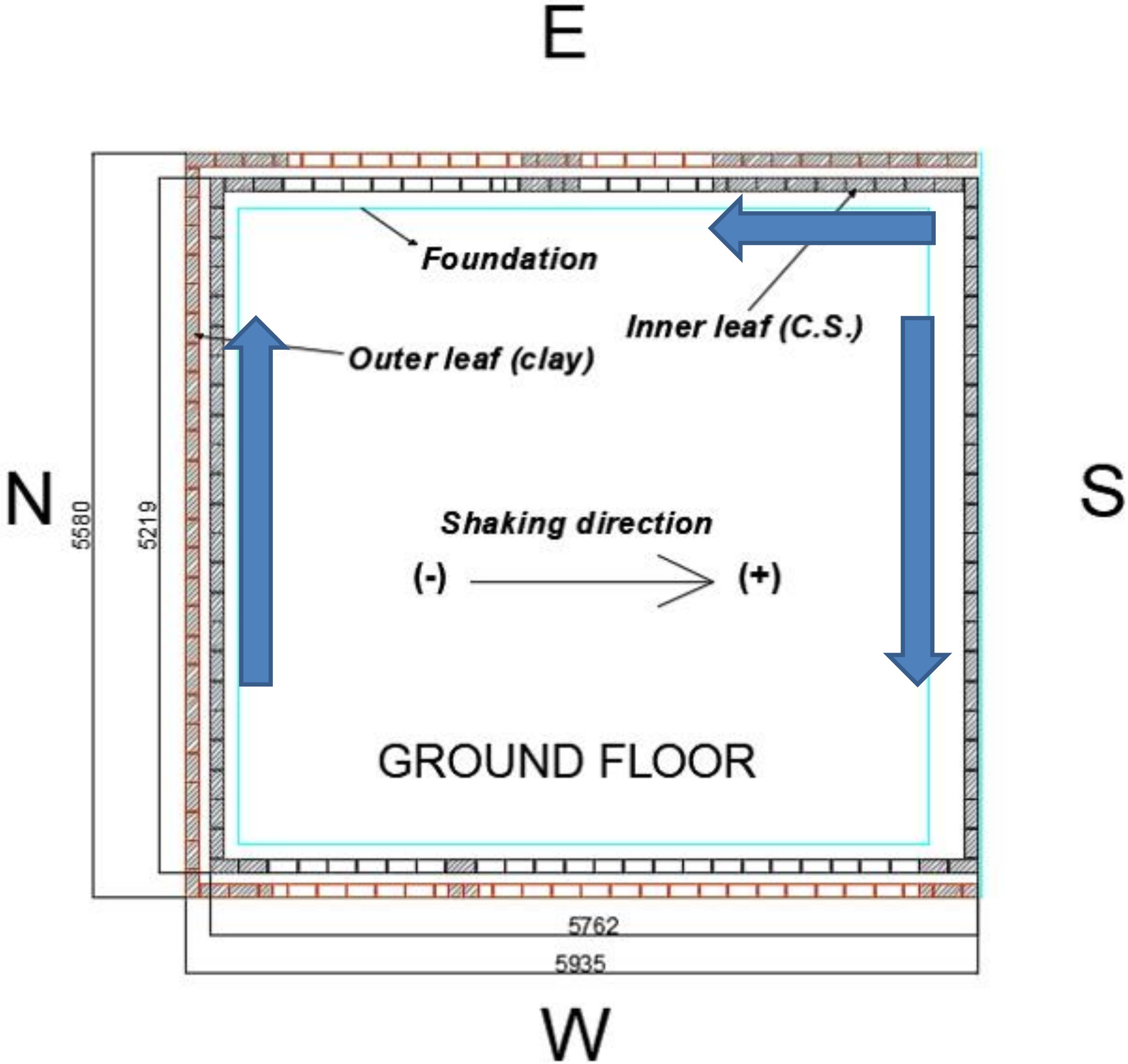
E
Foundation
Inner leaf (C.S.)
Outer leaf (clay)
N
5580
5219
Shaking direction
(-)
(+)
S
GROUND FLOOR
5762
5935
W

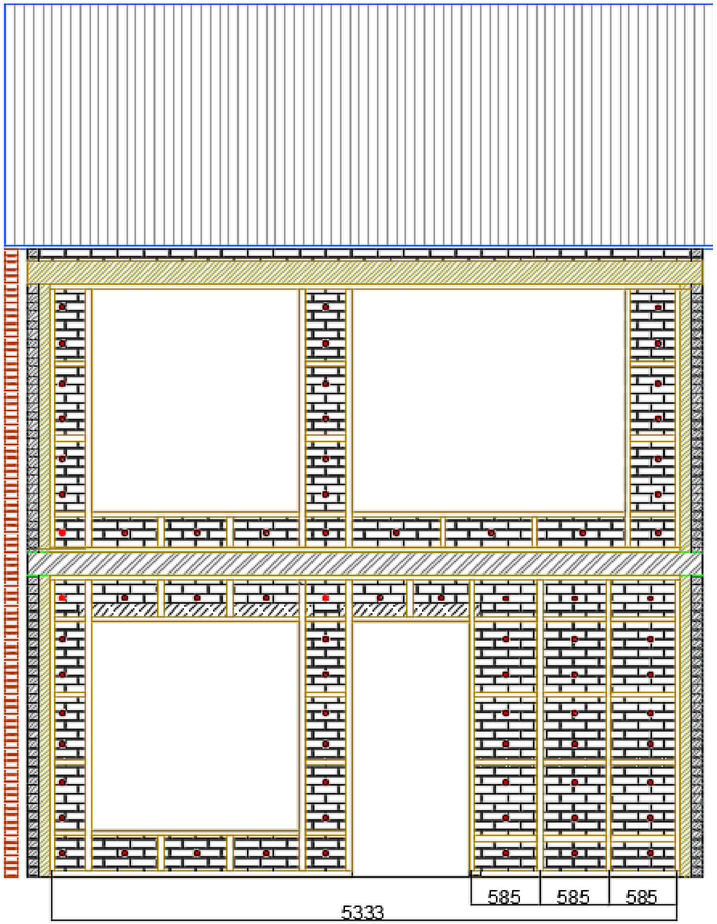

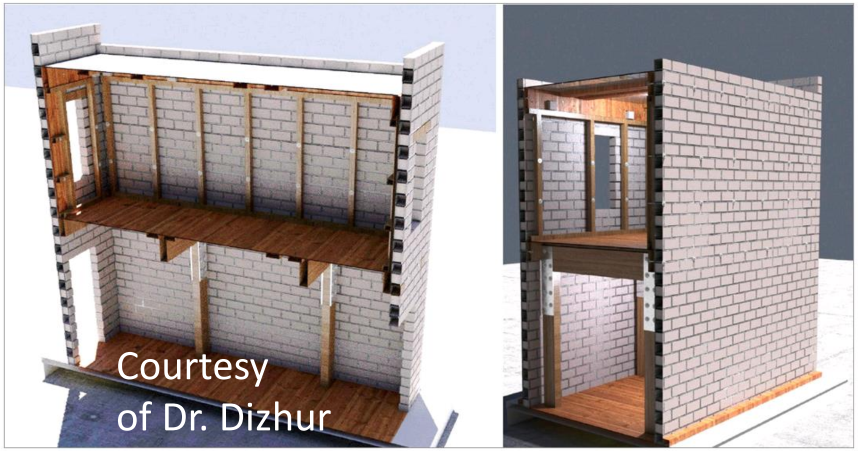

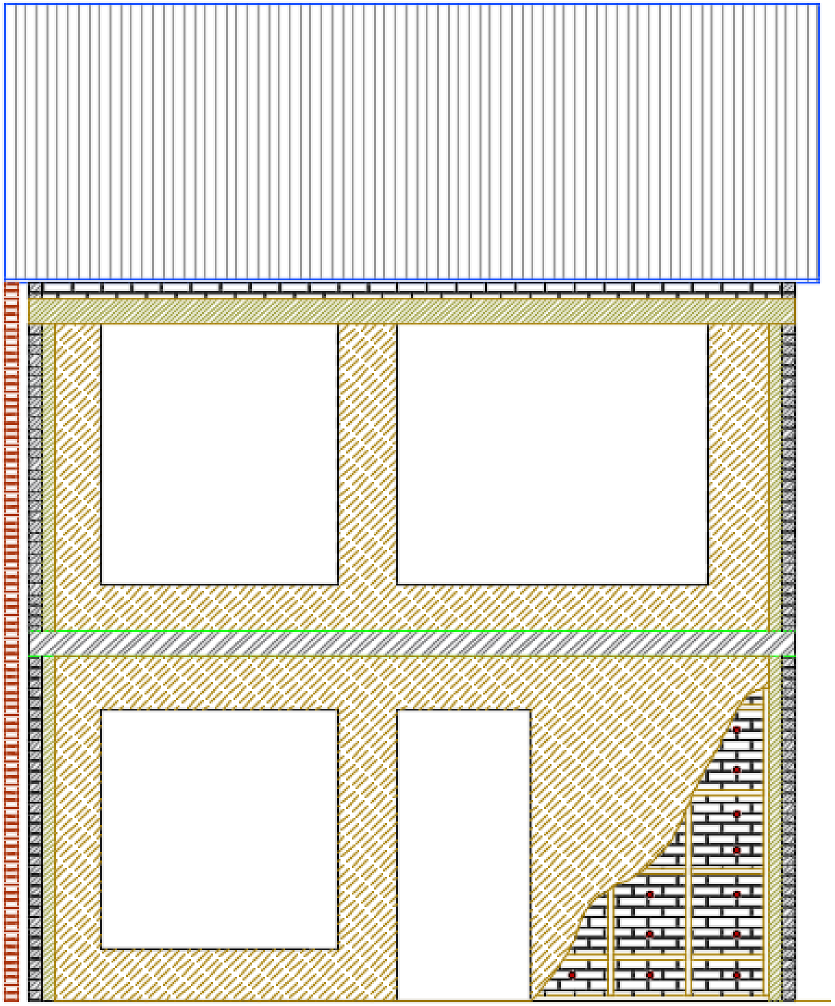

Seismic behaviour of ‘light-retrofitted’ terrace house http://www.eucentre.it/nam-project

NAM Project

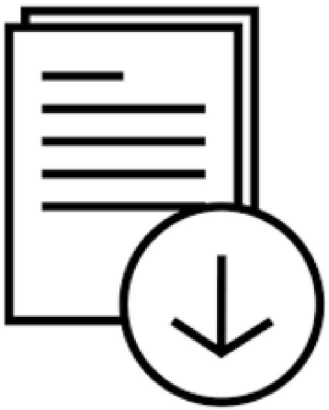

The project's main objective is that of increasing the knowledge on the seismic response of unreinforced masonry (URM) and precast buildings typically found in the province of Groningen, in the north of the Netherlands, which in recent years has been hit by earthquakes of relatively low magnitude (M2 to M4) related to gas extraction activities.
To this end, the following combined set of experimental and numerical activities has been planned:

1. Validation against experimental benchmarks, as well as through comparison with numerical models developed by other research groups, of macro-element models of URM buildings typical of the Groningen region
2. Development of detailed finite element models of precast panels, and its connections, typical of precast construction in the Groningen region
3. Experimental in situ-testing of URM buildings in the Groningen region
4. Cyclic and dynamic laboratory testing of URM and precast components and sub-assemblages
5. Shake-table testing of full-scale URM houses (terraced and detached)

The project started on May 2014 and is currently envisaged to be completed by the end of 2017. A number of deliverables have been produced, in the form of numerical models, research reports and experimental tests, some of which can be accessed below:

- Videos of URM terraced house shake-table testing.
- Videos of URM detached house shake-table testing.
- Videos of URM walls out-of-plane dynamic testing.
- Videos of cyclic testing of URM wall and precast panel.
- Report on precast panels testing.
- Report on in-situ URM material testing.
- Report on URM terraced house shake-table testing.
- Report on URM detached house shake-table testing.
- Paper on URM walls out-of-plane dynamic testing.

If you are interested in gaining access to the aforementioned experimental data, please fill-in the following form:

Name:

Email address:

RESEARCH

- Aerospace
- Computational Mechanics
- Design Methods
- Environmental Health and Safety (EHS)
- Geotechnical Earthquake Engineering
- Multi-risk assessment and Copernicus services
- Masonry Structures
- Non-Structural Elements
- Risk Governance
- Structural Analysis
- ...ological Innovation

Journal Papers

Characterisation:

- Andreotti G., Graziotti F., Magen
of brick masonry specimens: the

One-way Bending:

- Graziotti F., Tomassetti U., Penn
URM single leaf and cavity walls

Two-way Bending:

- Tomassetti U., Sharma S., Grott ... ic
behavior of URM single leaf and

EUCENTRE Building 1:

- Graziotti F., Tomassetti U., Kallic
full scale URM cavity wall buildir

LNEC Building 1:

- Tomassetti U., Correia A. A., Gra
structural collapse induced by a
URM building via shake table tes

EUCENTRE Building 2:

- Kallioras S., Guerrini G., Tomass
seismic performance of a full-sca
timber diaphgrams, *Engineering Structures*.

Engineering Structures
Volume 161, 15 April 2018, Pages 231–249

Experimental seismic performance of a full-scale unreinforced clay-masonry building with flexible timber diaphragms

Stylianos Kallioras[a], Gabriele Guerrini[b, c], Umberto Tomassetti[b, c], Beatrice Marchesi[c], Andrea Penna[b, c], Francesco Graziotti[b, c], Guido Magenes[b, c]
Show more

https://doi.org/10.1016/j.engstruct.2018.02.016
Get rights and content

Highlights

- Full-scale shake-table test on a clay URM building specimen with flexible diaphragms.
- Detailed information about geometry and mechanical properties.
- Input motions selected to be compatible with gas-field induced seismicity hazard.
- Damage mechanisms evolution, limit states, hysteretic and dynamic response.
- Full data available at www.eucentre.it/nam-project.

Abstract

This paper presents the results of a unidirectional shake-table test performed on a full-scale, single-storey unreinforced masonry building. The specimen represented a typical detached house of the Groningen region of the Netherlands, consisting of double-wythe clay-brick unreinforced masonry walls, without any specific seismic detailing. The building prototype included large openings and a reentrant corner, causing a

Technical Reports

Two-way Bending:

- Graziotti F., Tomassetti U., Sharma S., Grottoli L., Dainotti S., Scherini S., Penna A., Magenes G., 2017. Out-of-plane two-way bending shaking table tests on single leaf and cavity walls, EUCENTRE, Pavia, Italy.

EUCENTRE Building 1

- Graziotti F., Tomassetti U., Rossi A., Kallioras S., Mandirola M., Cenja F., Penna A., Magenes G., 2015. Experimental campaign on cavity-wall systems representative of the Groningen building stock. EUC318/2015U, EUCENTRE, Pavia, Italy.
- Mandirola M., Kallioras S., Tomassetti U., Graziotti F., 2017. Tests on URM clay and calcium silicate masonry structures: identification of damage limit states.

LNEC Building 1:

- Tomassetti U., Correia A. A., Graziotti F., Marques A. I., Mandirola M., Candeias P. X., 2017. Collapse shaking table tests on a URM cavity wall structure representative of a Dutch terraced house.

LNEC Roof:

- Correia A. A., Marques A. I., Bernardo V., Grottoli L., Tomassetti U., Graziotti F., 2017. Shake table test up to collapse on a roof substructure of a Dutch terraced house.

EUCENTRE Building 2

- Graziotti F., Tomassetti U., Rossi A., Marchesi B., Kallioras S., Mandirola M., Fragomeli A., Mellia E., Peloso S., Cuppari F., Guerrini G., Penna A., Magenes G., 2016. Shaking table tests on full-scale clay-brick masonry house representative of the Groningen building stock and related characterization tests. EUC128/2016U, EUCENTRE, Pavia, Italy.

Conference Papers

Characterisation:

- Graziotti F., Guerrini G., Rossi A., Andreotti G., Magenes G., 2018. Proposal for an improved procedure and interpretation of ASTM C1531 for the in-situ determination of brick-masonry shear strength, ASTM Selected Technical Papers: 2018 Masonry Symposium, San Diego, California, United States, (ACCEPTED)
- Bonura V., Jafari S., Zapico Blanco B., Graziotti F., 2018. Interpretation of in-situ shear test for brick masonry: a benchmark study, 16th ECEE Conference, Thessaloniki, Greece;
- Zapico Blanco B., Tondelli M., Jafari S., Graziotti F., Millekamp H., Rots J., Palmieri M., 2018. A masonry catalogue for the Groningen region, 16th ECEE Conference, Thessaloniki, Greece;
- Graziotti F., Rossi A., Mandirola M., Penna A., Magenes G., 2016. Experimental characterization of calcium-silicate brick masonry for seismic assessment, Proc. of 16th IB^{2}MAC, Padua, Italy;
- Rossi A., Graziotti F., Magenes G., 2015. A proposal for the interpretation of the in-situ shear strength index test for brick Masonry, Proc. of XV ANIDIS conference, L'Aquila, Italy.

One-way Bending:

- Tomassetti U., Graziotti F., Penna A., Magenes G., 2017. Energy dissipation involved in the out-of-plane response of unreinforced masonry walls, Proc. COMPDYN 2017 6th ECCOMAS, Rhodes Island, Greece;
- Tomassetti U., Graziotti F., Penna A., Magenes G., 2016. Out-of-plane shaking table test on URM cavity walls, Proc. of 16th IB^{2}MAC, Padua, Italy;
- Tomassetti U., Graziotti F., Penna A., Magenes G., 2015. Single degree of freedom numerical model (SDOF) for the simulation of the out-of-plane response (OOP) of unreinforced masonry (URM) walls, Proc. of XV ANIDIS conference, L'Aquila, Italy.

Conference Papers

Two-way Bending:

- Graziotti F., Tomassetti U., Sharma S., Grottoli L., Penna A., Magenes G., 2018. Out-of-plane shaking table tests on URM single leaf and cavity walls in two-way bending, 10th IMC, Milan, Italy;
- Graziotti F., Tomassetti U., Grottoli L., Penna A., Magenes G., 2018. Full-scale out-of-plane shaking table tests of URM walls in two-way bending, 10th AMC, Sydney, Australia;
- Graziotti F., Tomassetti U., Grottoli L., Dainotti S., Penna A., Magenes G., 2017. Shaking table tests of URM walls subjected to two-way bending out-of-plane seismic excitation, Proc. of XVII ANIDIS conference, paper No. 3092, Pistoia, Italy;
- Tomassetti U., Grottoli L., Penna A., Graziotti F., Magenes G., 2017. Two-way bending out-of-plane shaking table tests on URM walls subjected to seismic excitation, Proc. of IF CRASC '17, Milan, Italy.

EUCENTRE Building 1:

- Graziotti F., Tomassetti U., Rossi A., Kallioras S., Mandirola M., Penna A., Magenes G., 2017. Full scale shaking table test on a URM cavity wall terraced house building, 16th WCEE, Santiago, Chile;
- Kallioras S., Graziotti F., Penna A., Magenes G., 2017. Numerical modeling of cavity-wall URM buildings, Proc. of 13th CMS, Halifax, Canada.

Conference Papers

LNEC Building 1:

- Tomassetti U., Correia A. A., Marques A., Graziotti F., Penna A., Magenes G., 2017. Dynamic collapse testing of a full-scale URM cavity-wall structure, Proc. of XVII ANIDIS conference, paper No. 2876, Pistoia, Italy.

LNEC Roof:

- Correia A. A., Tomassetti U., Campos Costa A., Penna A., Magenes G., Graziotti F., 2018. Collapse shake-table test on URM-timber roof substructure, 16th ECEE Conference, Thessaloniki, Greece.

EUCENTRE Building 2:

- Graziotti F., Guerrini G., Kallioras S., Marchesi B., Rossi A.,Tomassetti U., Penna A., Magenes G., 2017. Shaking table test on a full-scale unreinforced clay masonry building with flexible diaphragms, Proc. of 13th CMS, Halifax, Canada;
- Guerrini G., Graziotti F., Penna A., Magenes G., 2017. Dynamic shake-table tests on two full-scale, unreinforced masonry buildings subjected to induced seismicity, Proc. of EVACES2017, San Diego, California, United States.

NAM-Team

Grottoli

Magenes

Tomassetti

Sharma

Moriconi


Graziotti

Scherini

Mandirola


NAM PROJECT

Guerrini

Fragomeli

Penna


Andreotti

Campos Costa

Dainotti
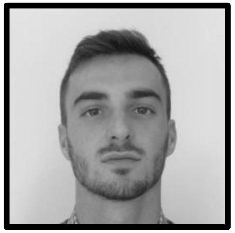
Marchesi

Kallioras

Rossi

Girello


Correia

Marques

Mellia

Tondelli

Peloso

Cenja

Dacarro


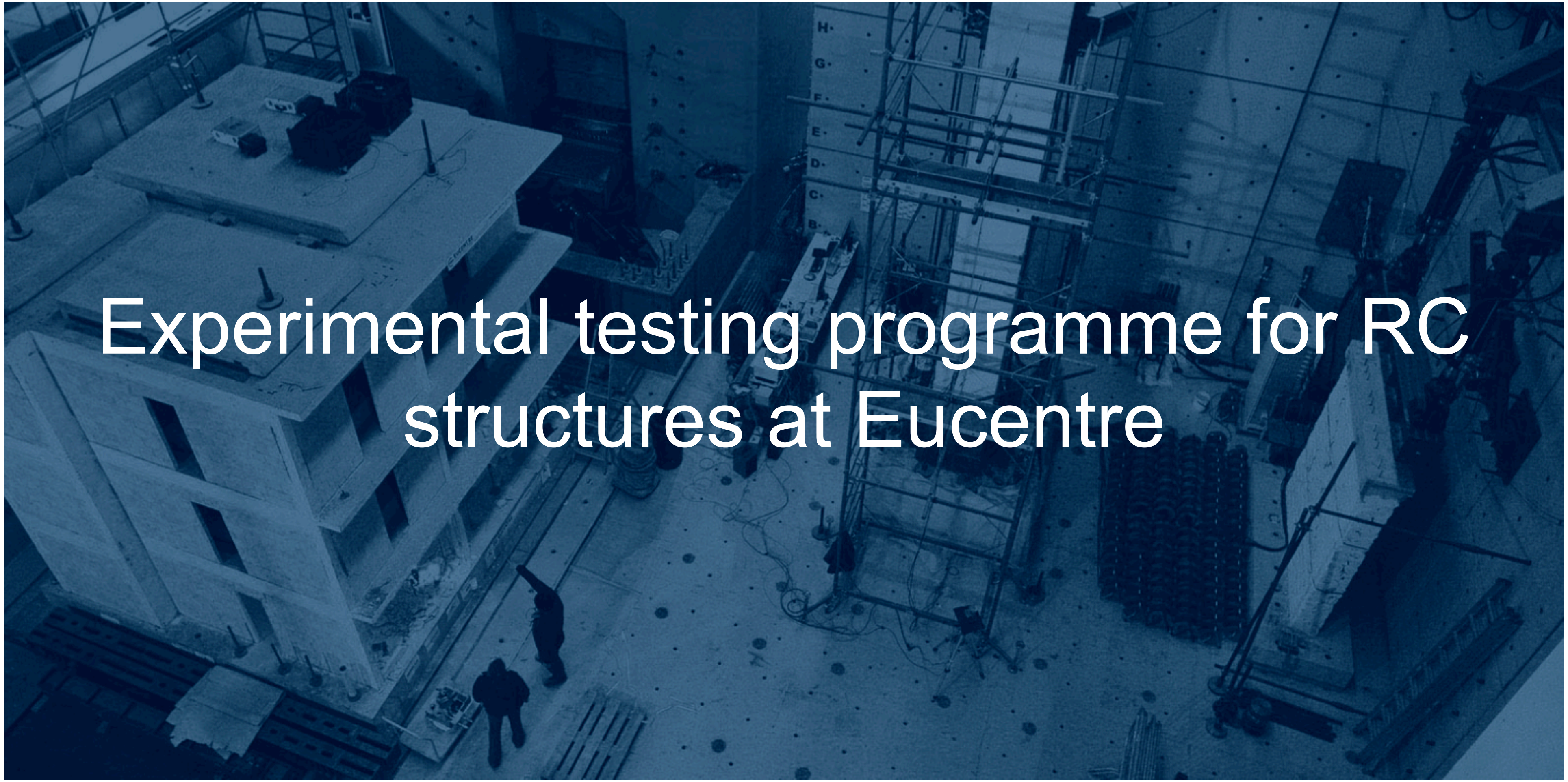

Experimental testing programme for RC structures at Eucentre

Assurance Meeting on Exposure, Fragility and Fatality Models for the Groningen Building Stock

21-22 February 2018, Schiphol Airport, Amsterdam

EUCENTRE
FOR YOUR SAFETY.

Feedback from past review exercises:

- The decision on next structures to be tested should not just consider buildings with highest building count/occupancy, but also what one suspects to be the most fragile building typology (because ILPR is principal risk metric)
- Focus thus further on most fragile building typologies (URM, RC precast and tunnel-form cast-in-place) and their details/connections
- Check modelled ultimate capacities against test data (including under-reinforced RC walls)

Cast-in-place RC structures

(tunnelbouw)

Cast-in-place RC structures

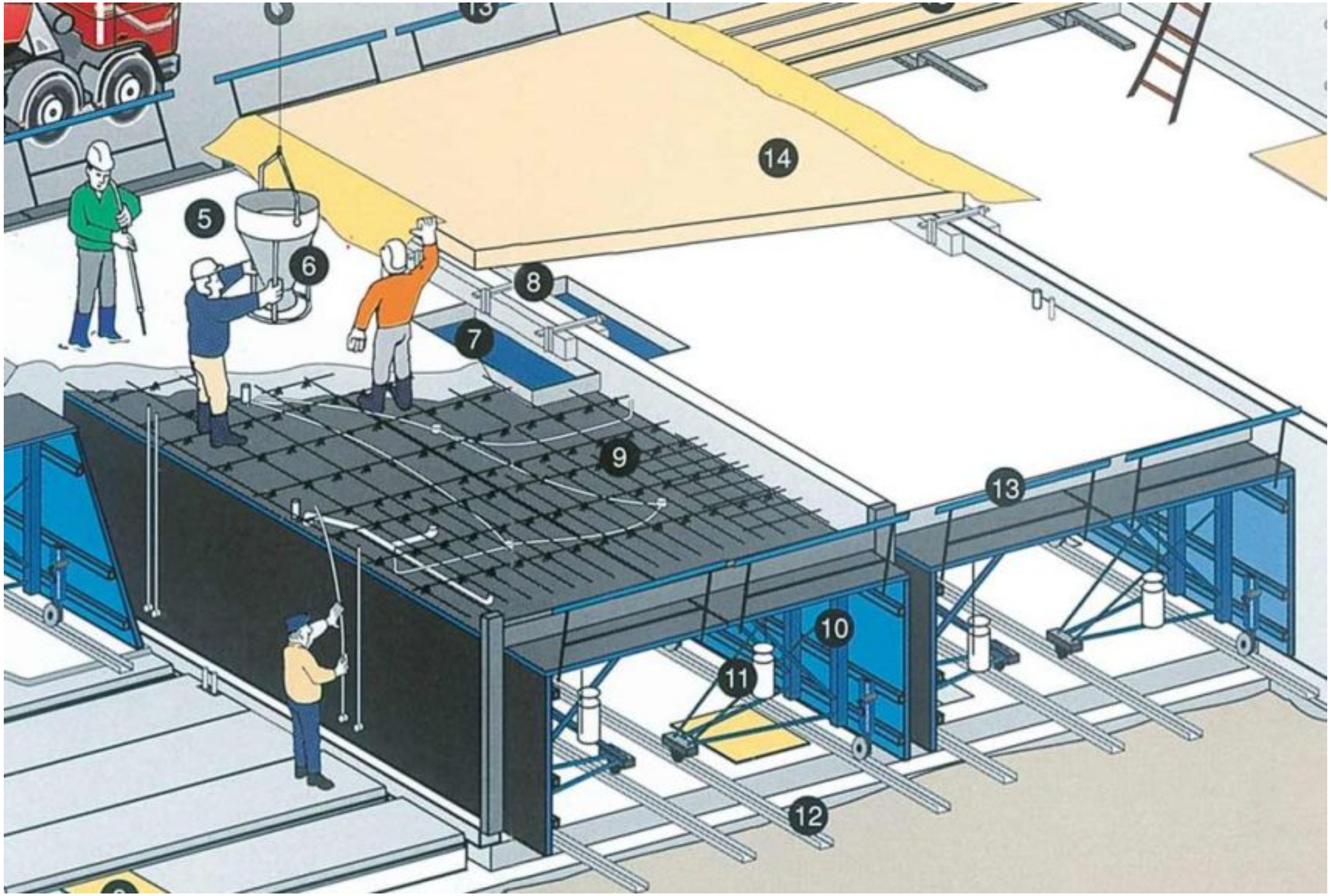

Cast-in-place RC structures

Cast-in-place RC test specimen

Cast-in-place test specimen: construction

Cast-in-place test specimen: construction

Cast-in-place test specimen: construction

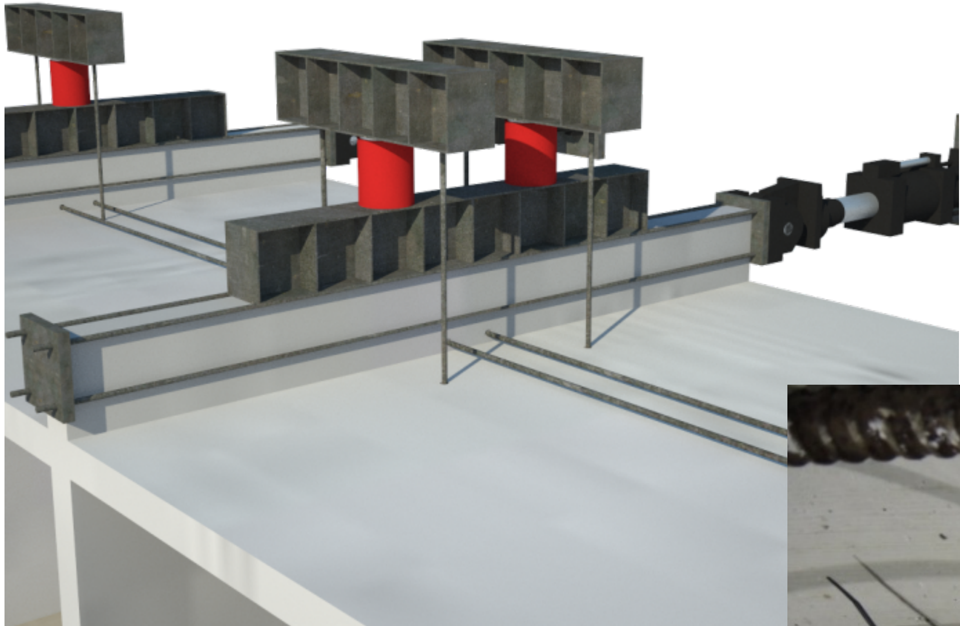

Cast-in-place test specimen: instrumentation

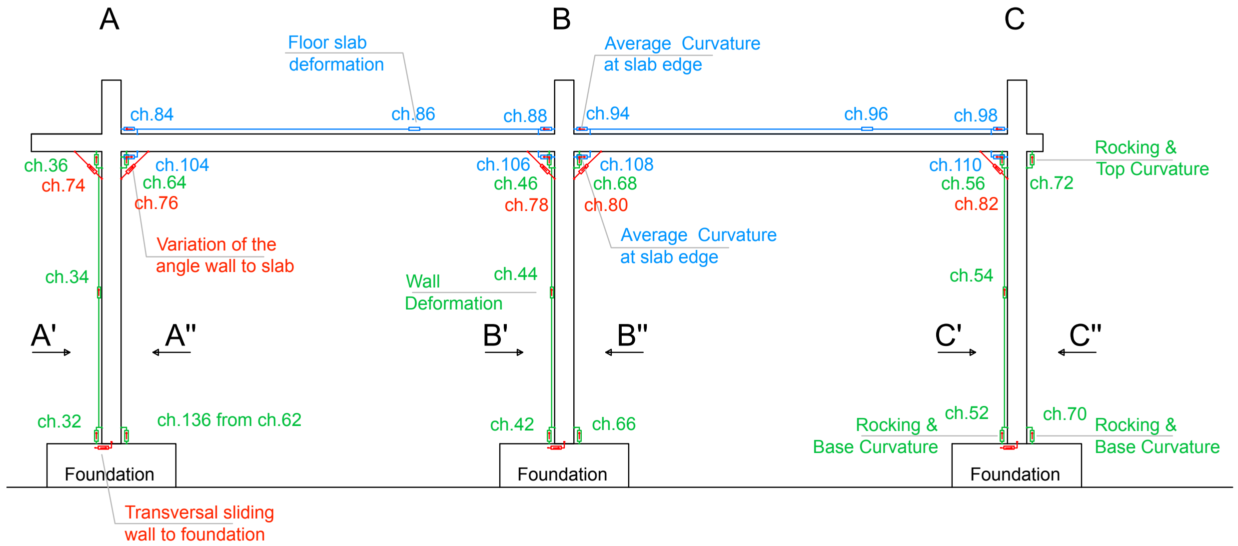

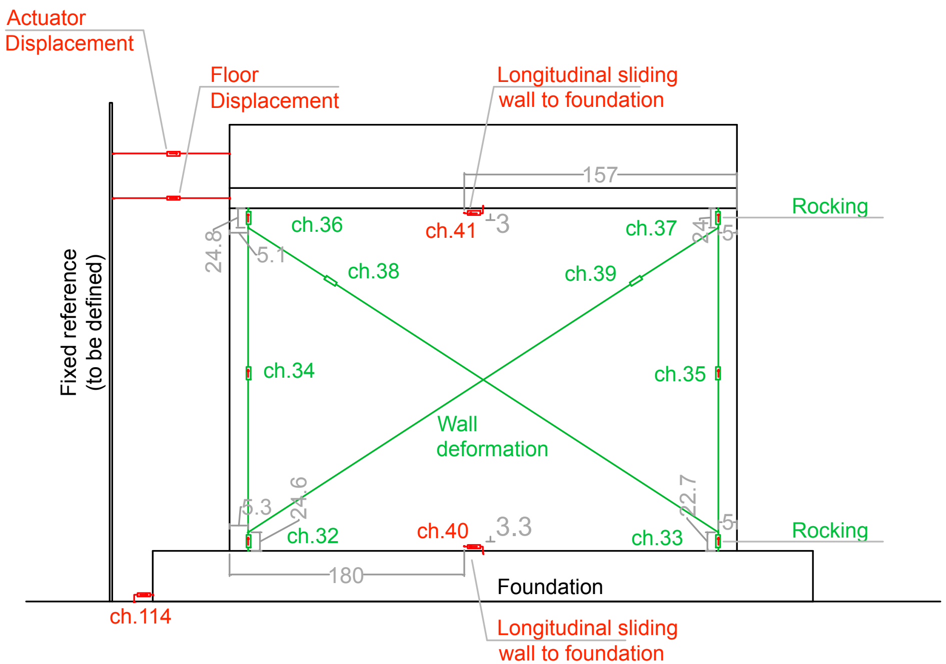

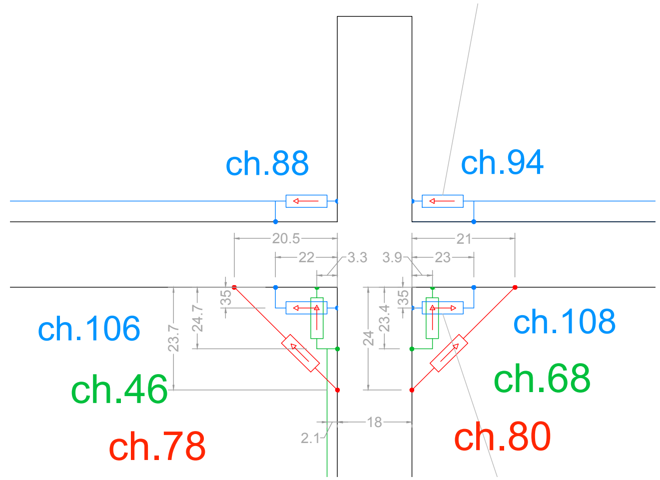

Cast-in-place specimen: testing (longitudinal)

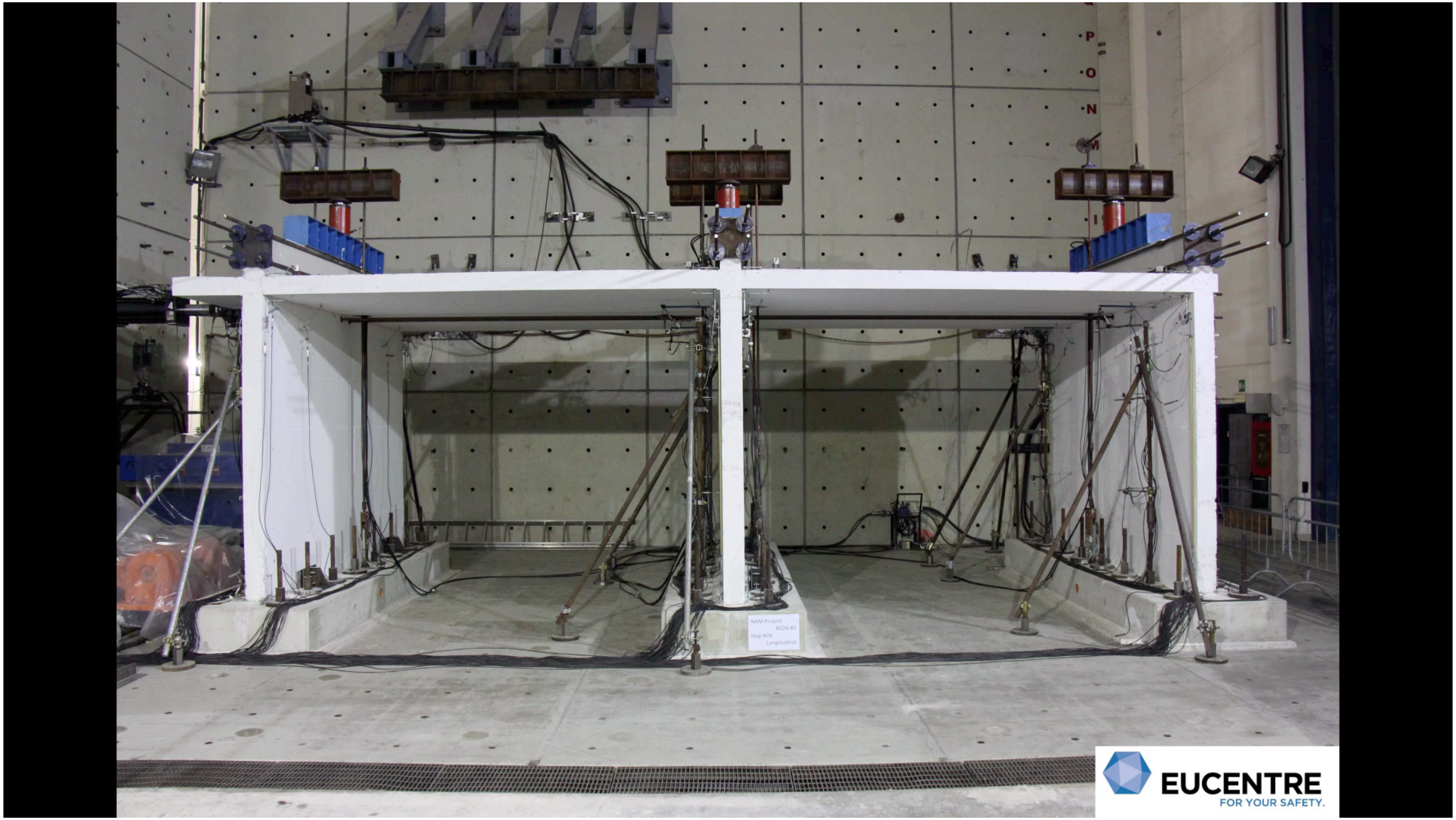

Cast-in-place specimen: testing (longitudinal)

Cast-in-place specimen: testing (longitudinal)

Cast-in-place specimen: testing (longitudinal)

Cast-in-place specimen: testing (longitudinal)

Cast-in-place specimen: testing (longitudinal)

Cast-in-place test specimen: test results
(longitudinal direction)

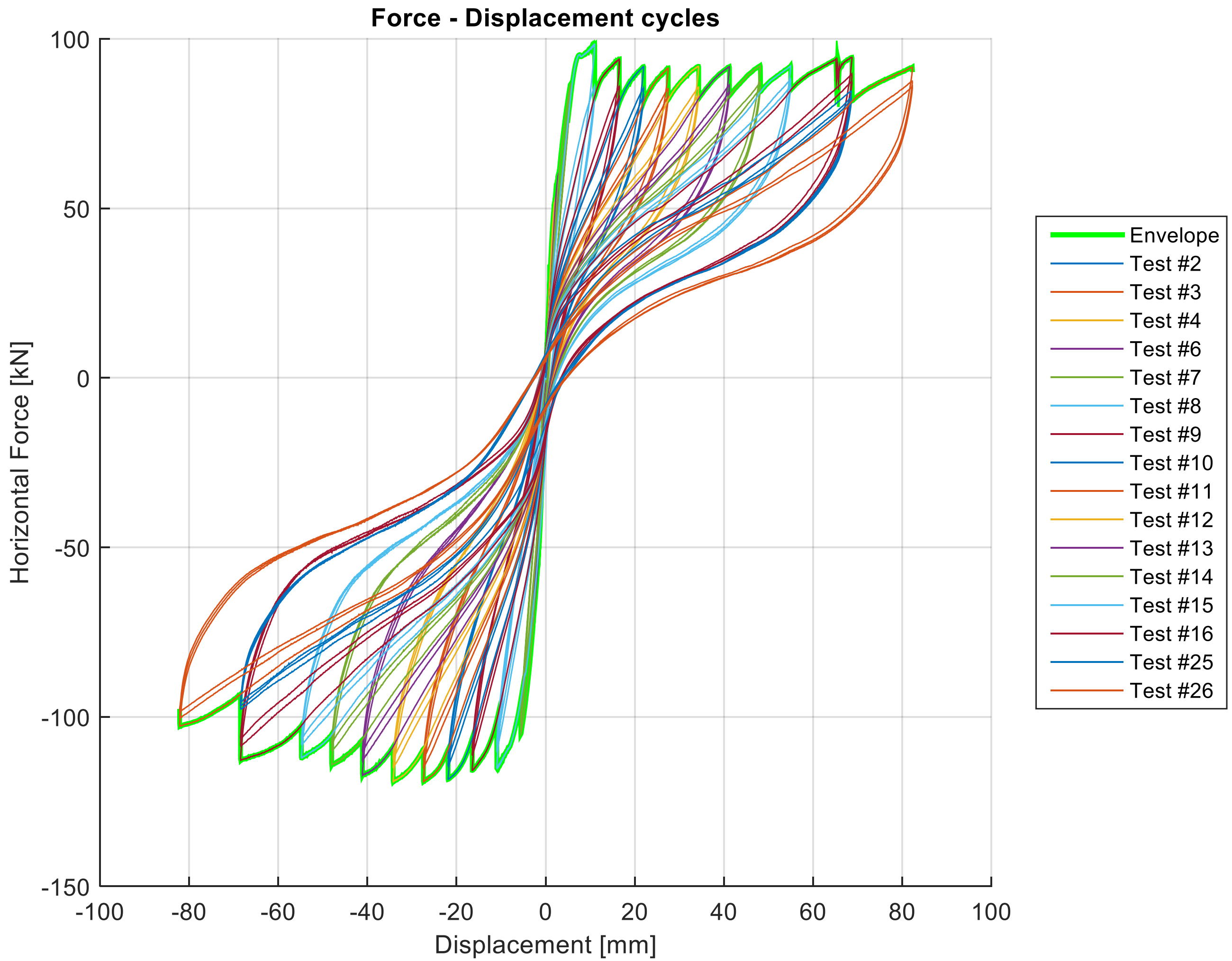

Cast-in-place specimen: testing (transverse)

Cast-in-place test specimen: test results
(transverse direction)

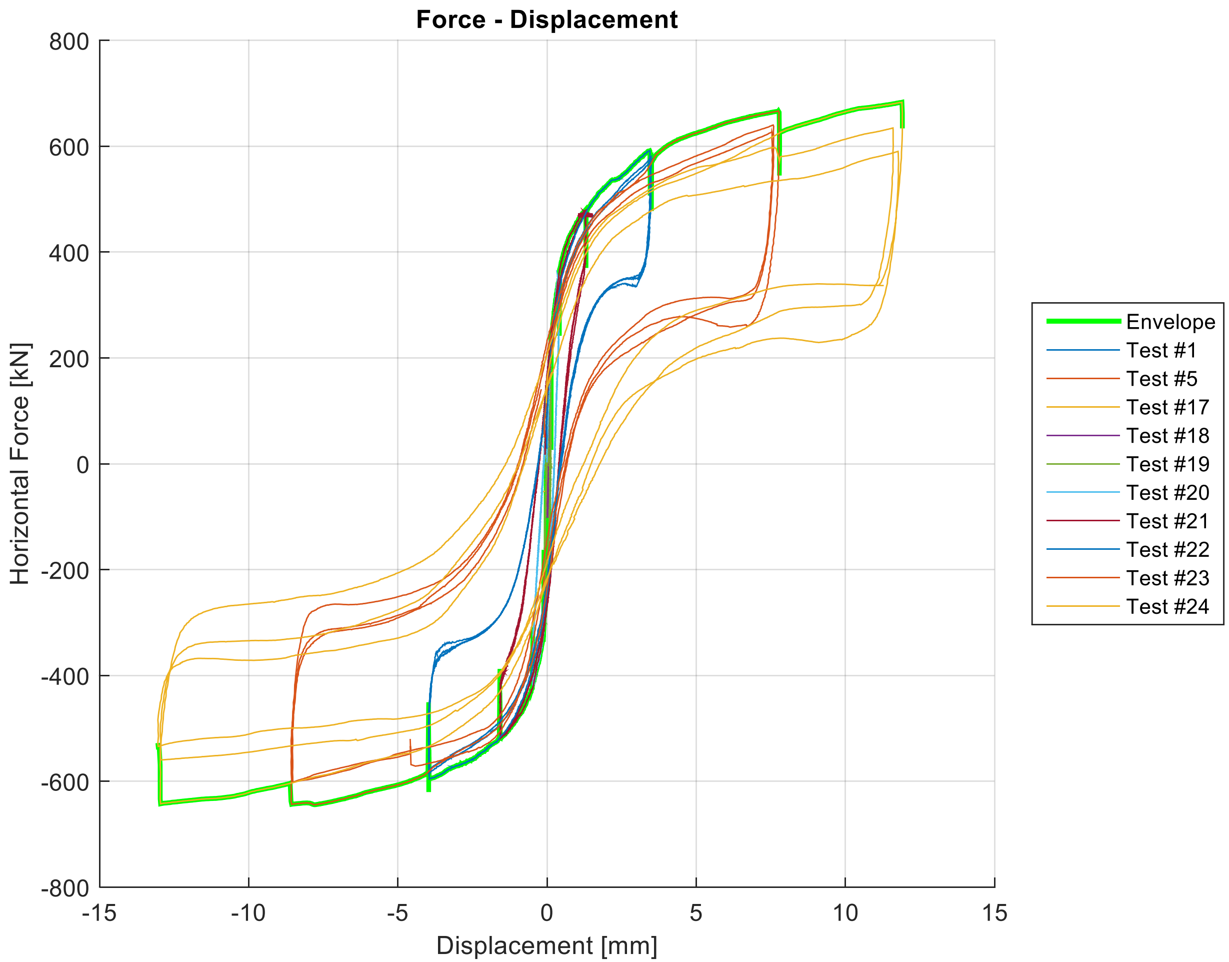

Precast RC structures

Precast RC structures

Precast RC structures

Precast RC structures

Precast RC structures: connections details

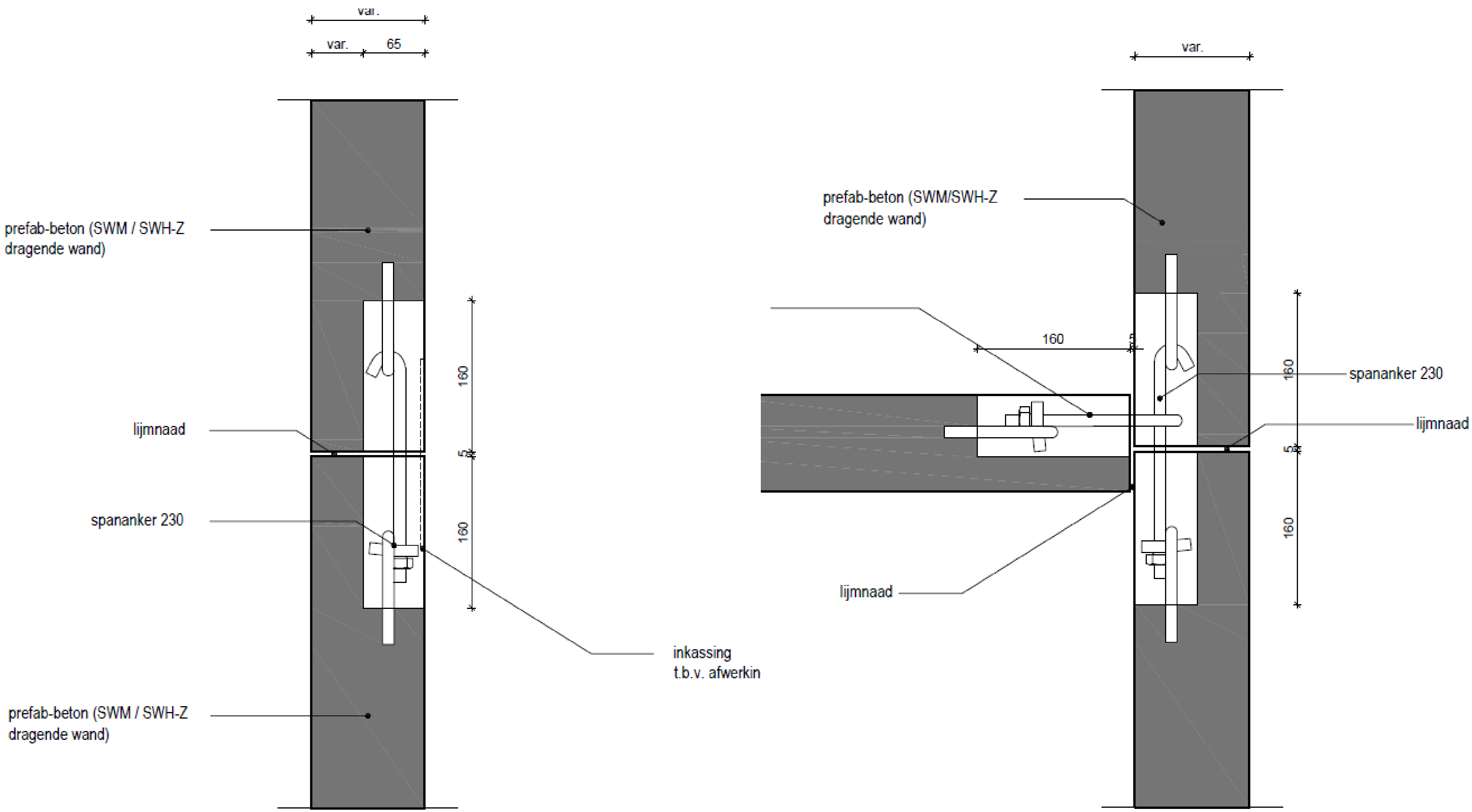

Precast RC test specimens

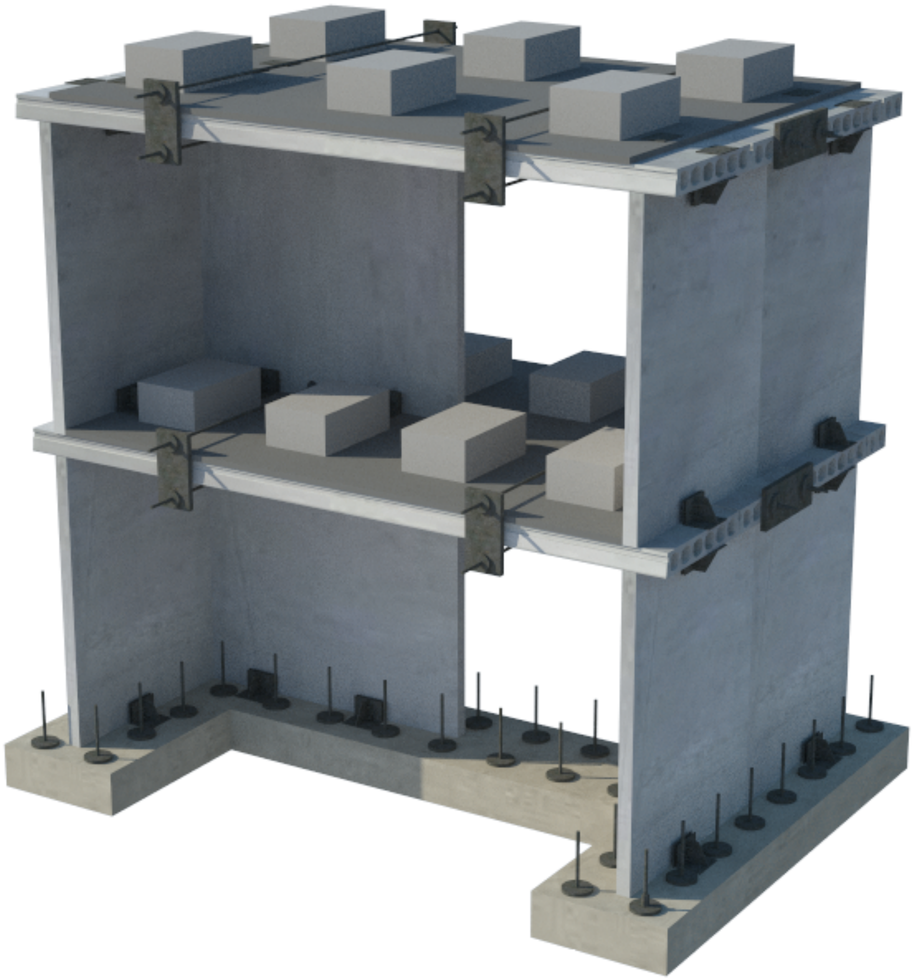

Precast test specimens: construction

Precast test specimens: construction

Precast test specimens: construction

Precast test specimens: construction

Precast test specimens: construction

Precast test specimens: safety restrainers

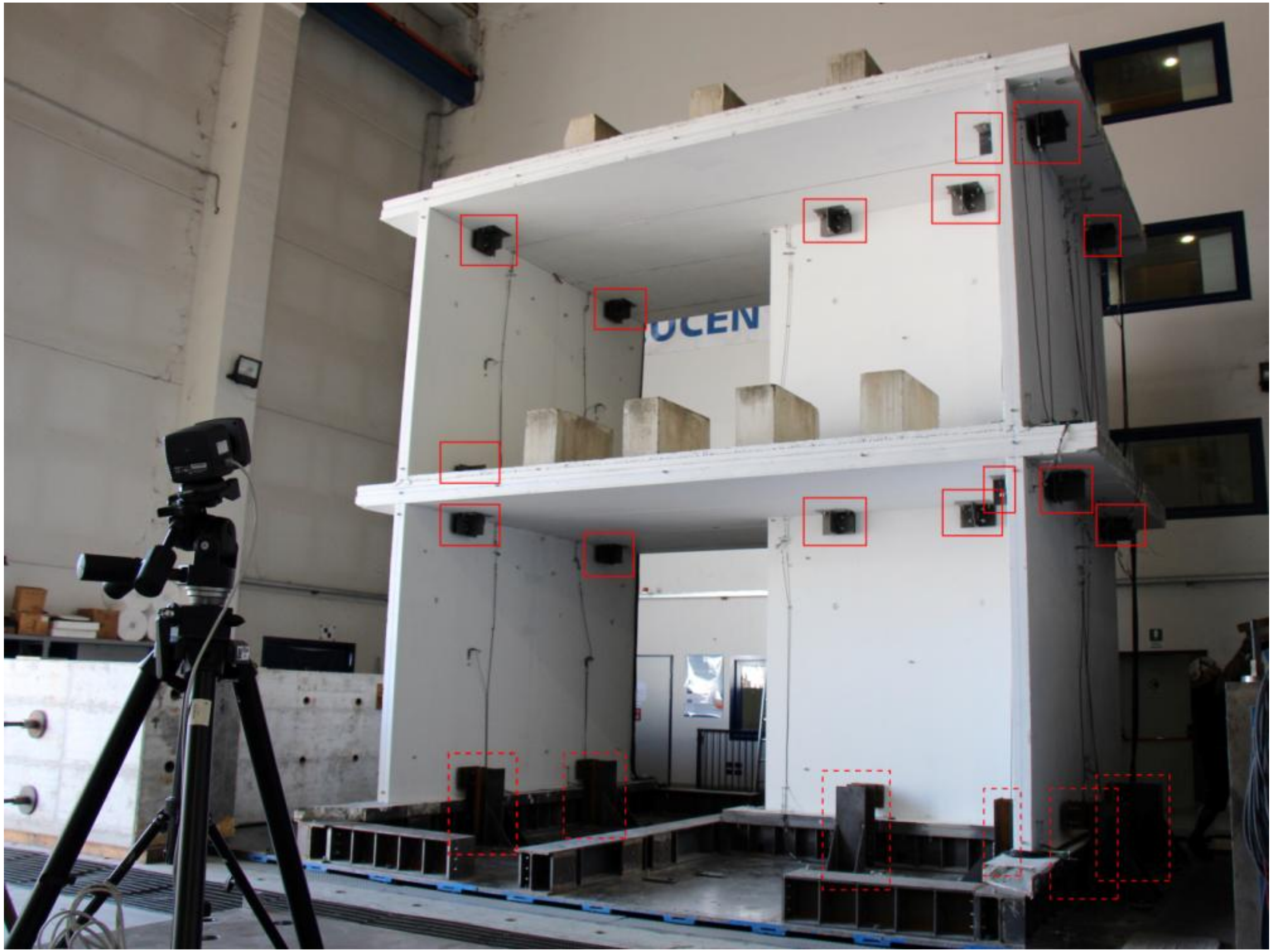

Precast test specimens: stability wall instrumentation

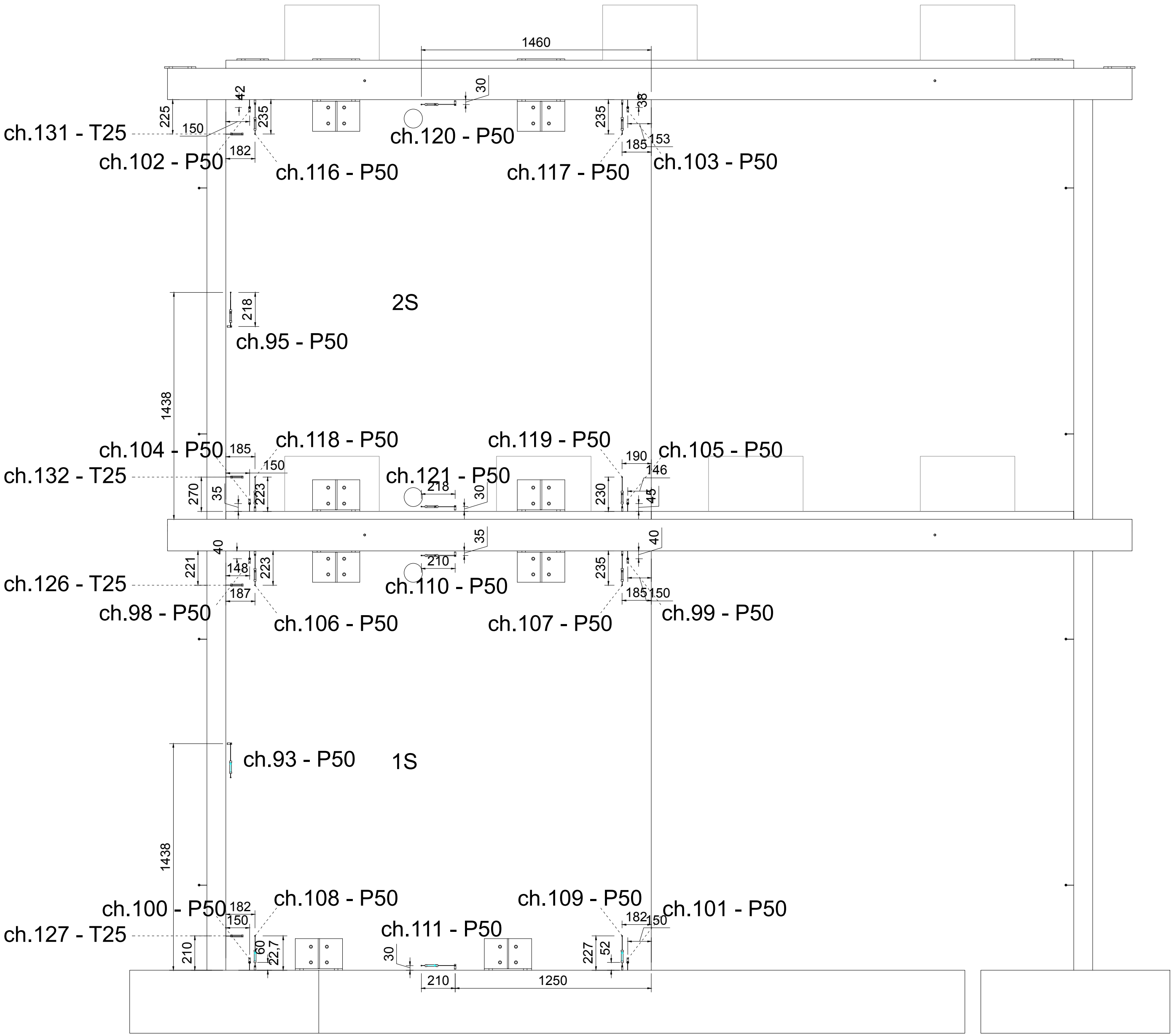

Precast test specimens:
out-of-plane testing of RC wall/slab panels

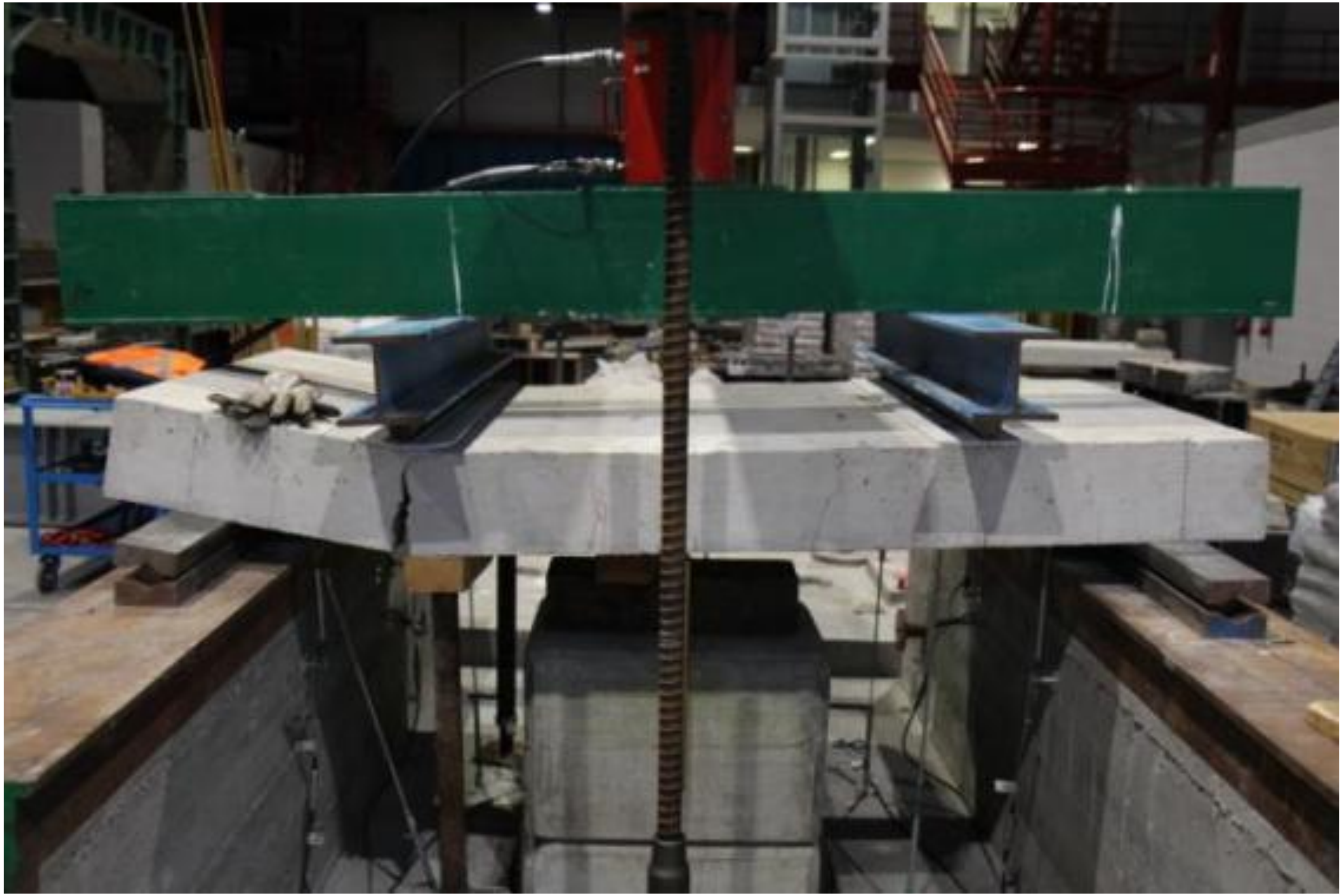

Precast test specimens: out-of-plane testing of RC wall/slab panels

Precast test specimens:
standard mortar characterisation tests

Precast test specimens:
concrete-mortar static friction characterisation tests

Precast test specimens:
concrete-felt cyclic friction characterisation tests

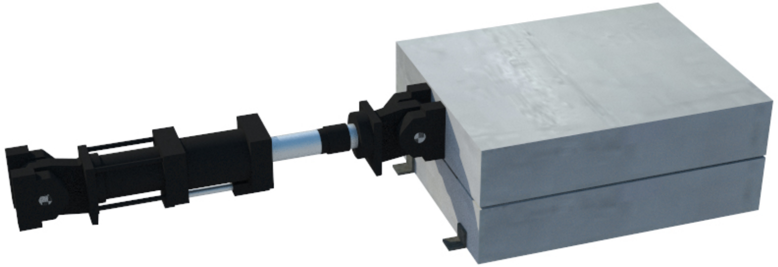

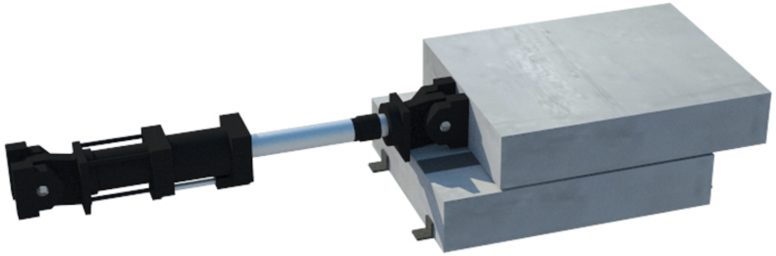

Precast test specimens:
concrete-felt cyclic friction characterisation tests

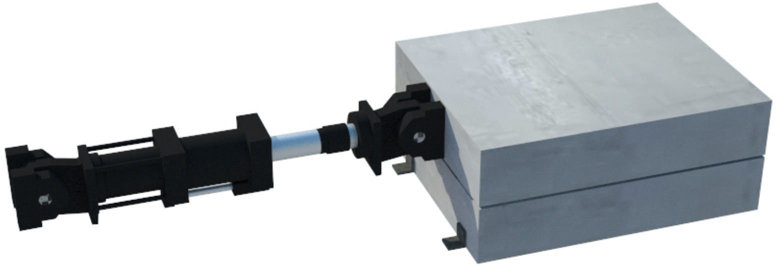

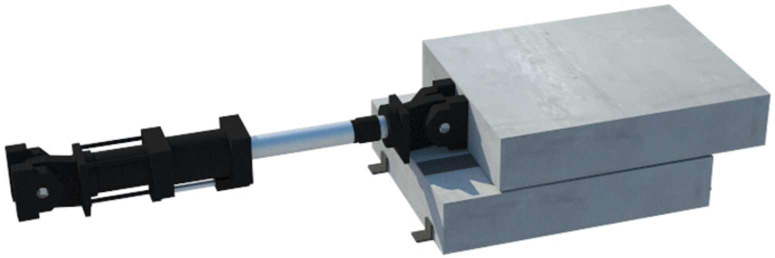

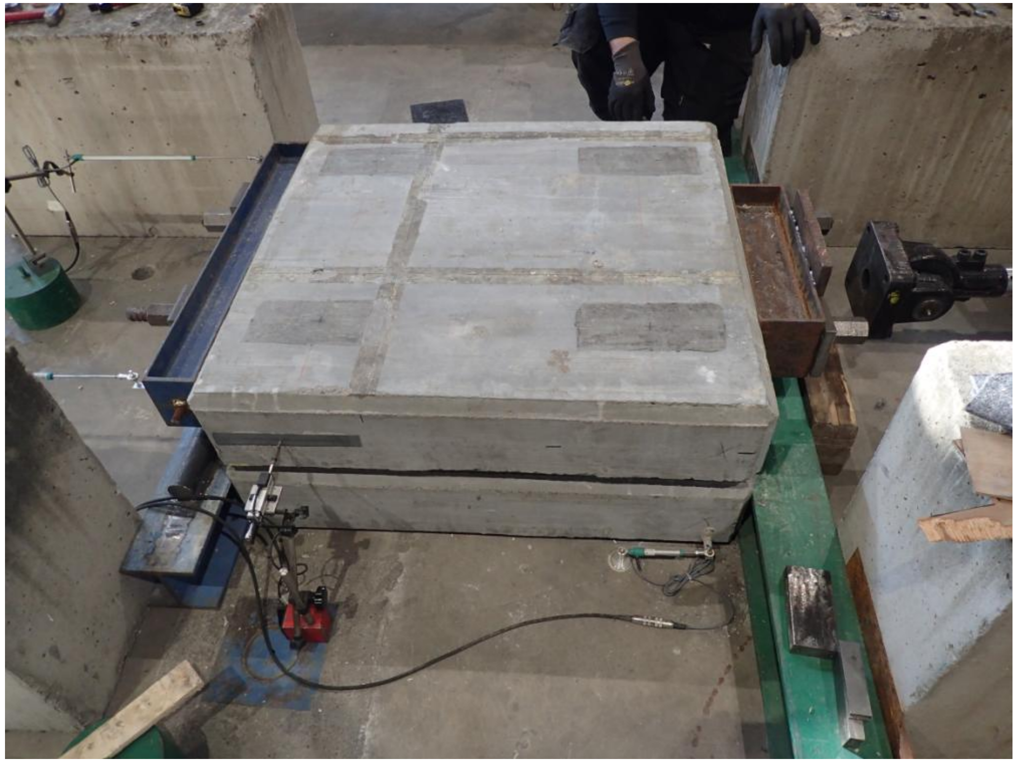

Precast test specimens: concrete-felt cyclic friction characterisation tests

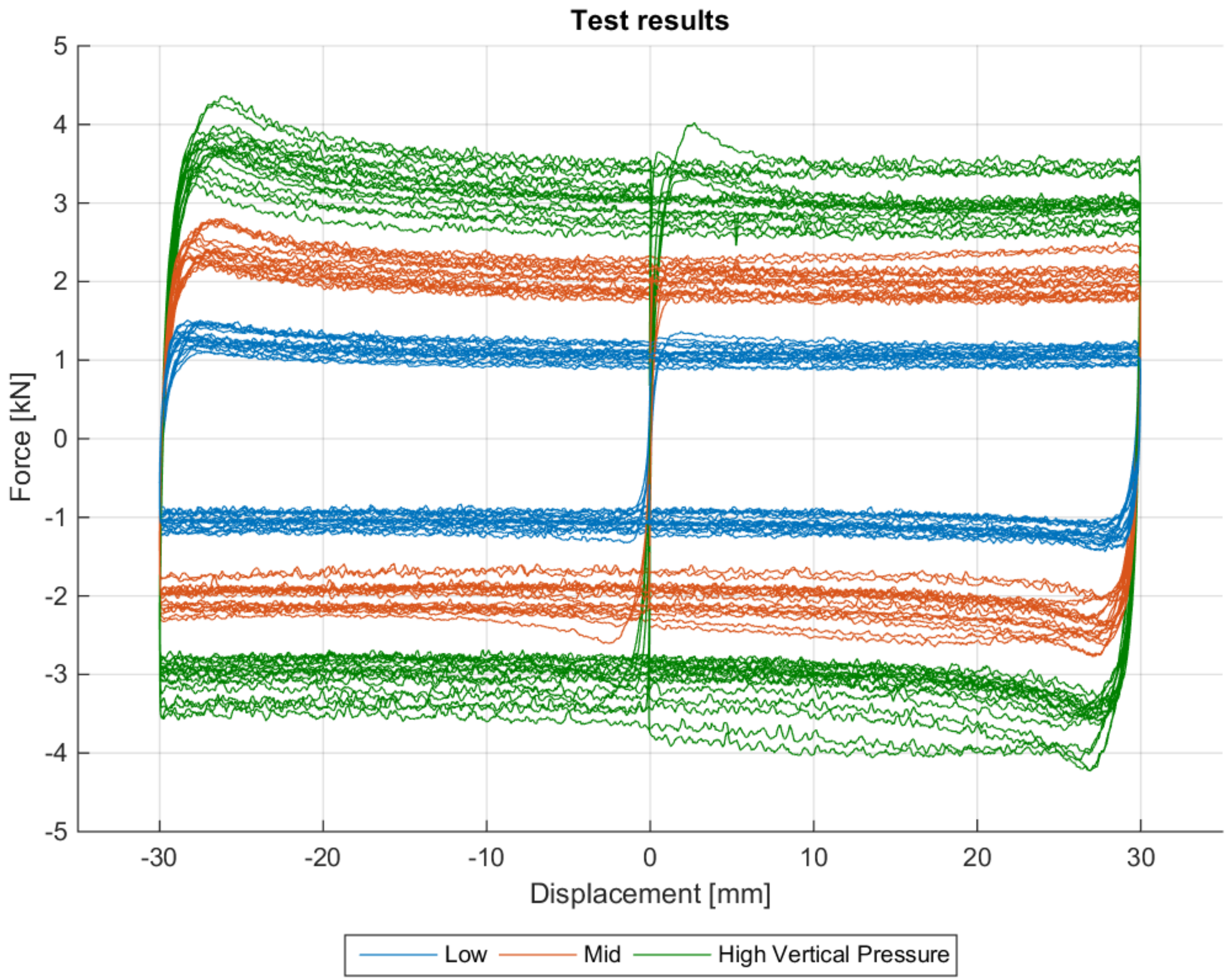

Precast test specimens: cyclic testing of two-wall connectors

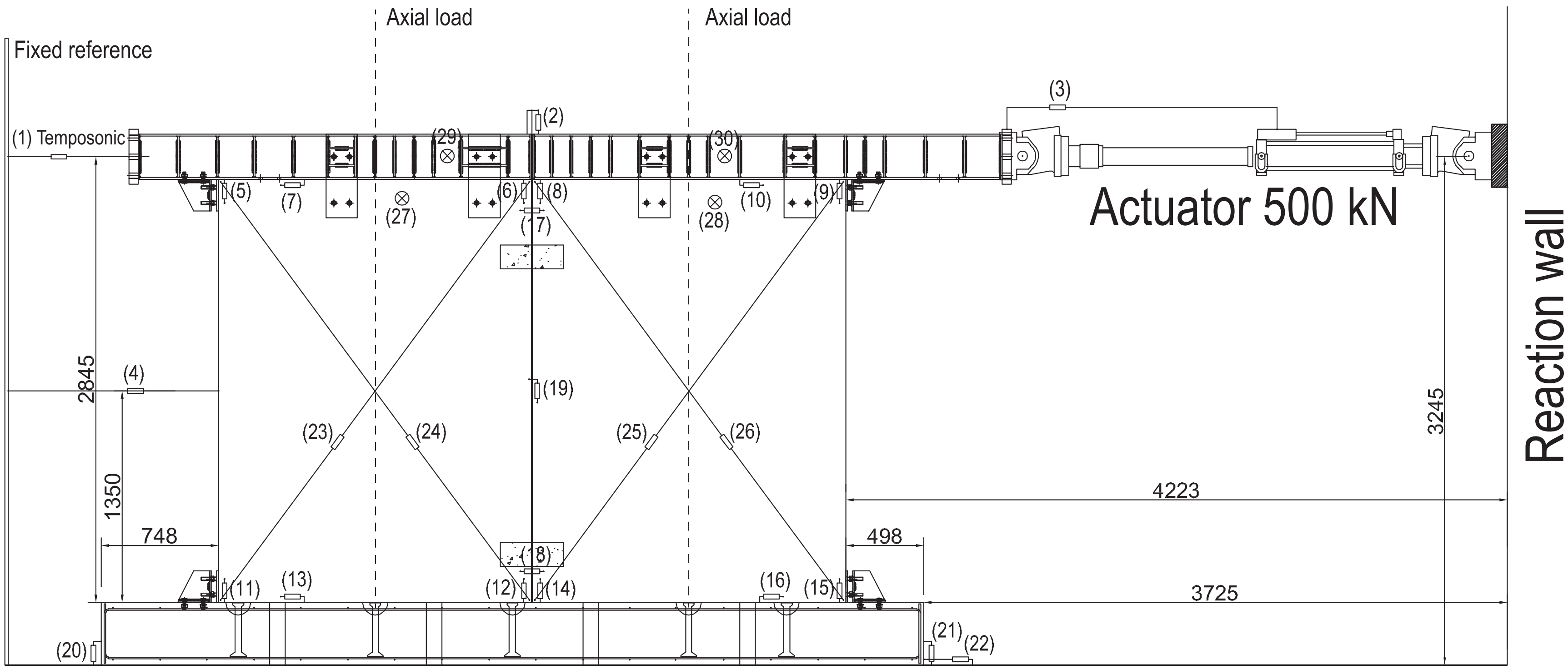

Precast test specimens: cyclic testing of two-wall connectors

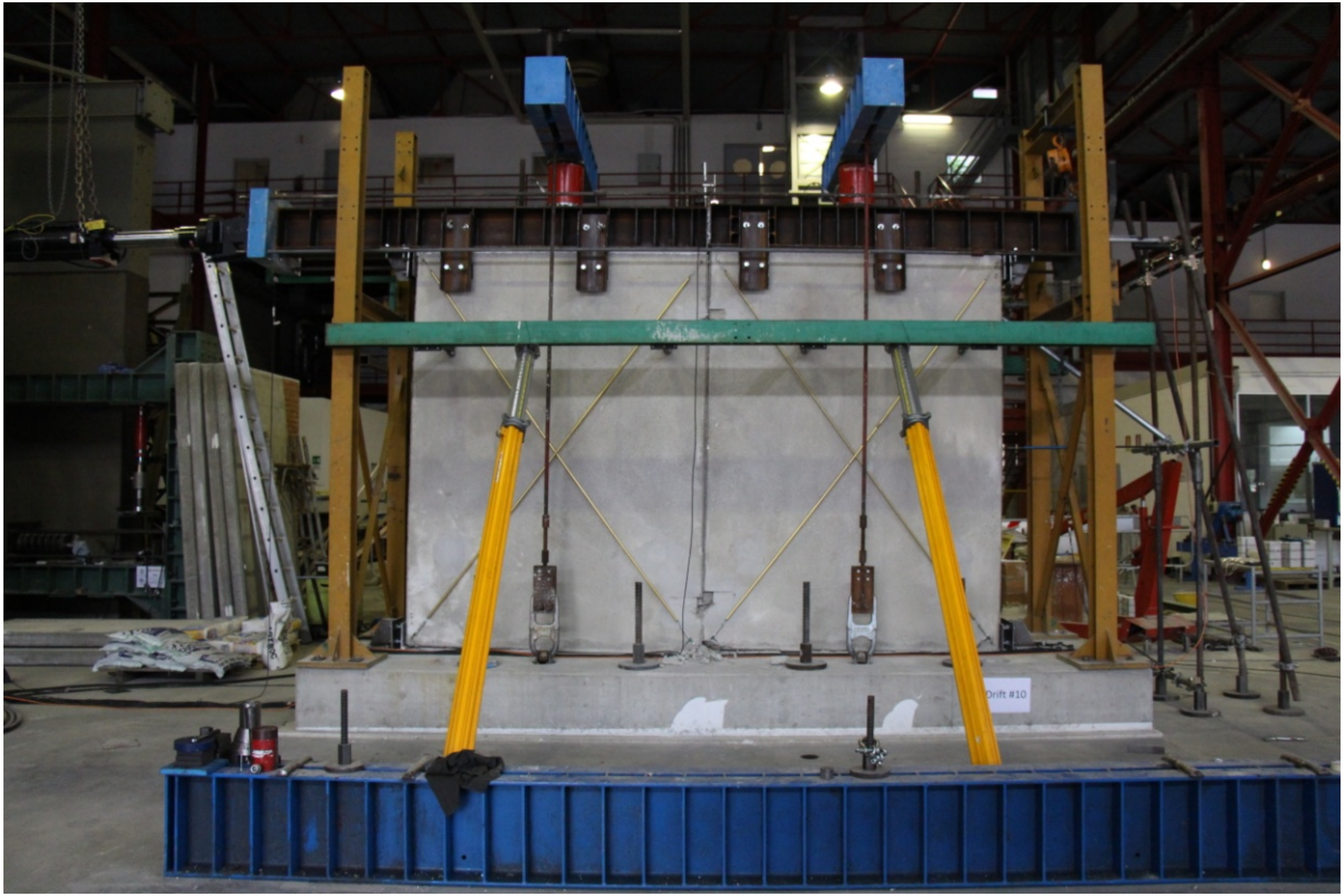

Precast test specimens: cyclic testing of two-wall connectors

Precast test specimens: cyclic testing of two-wall connectors

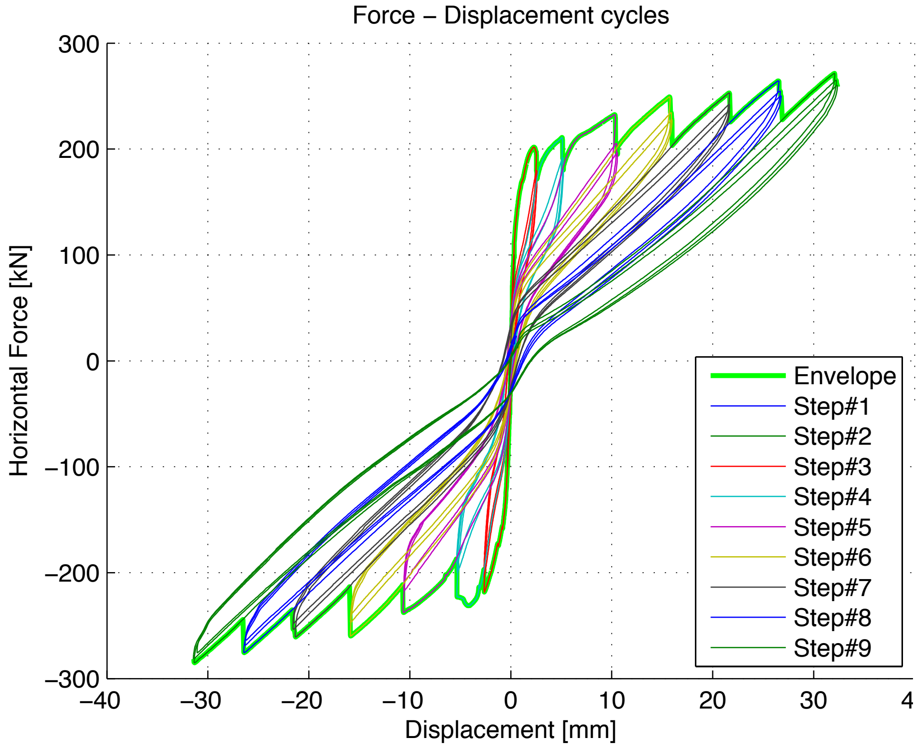

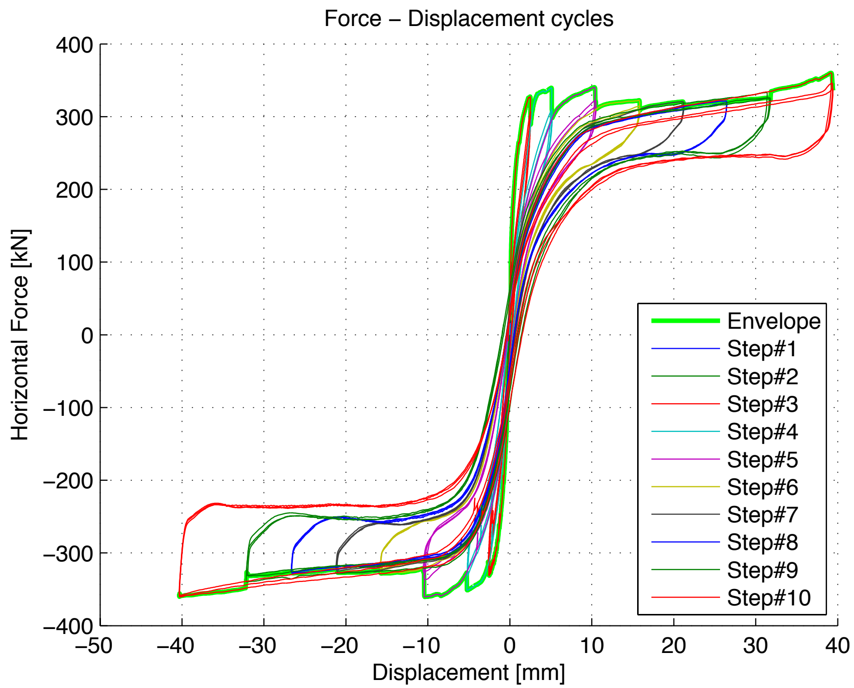

Precast test specimens: cyclic testing of three-wall connectors

Precast test specimens:
cyclic testing of three-wall connectors

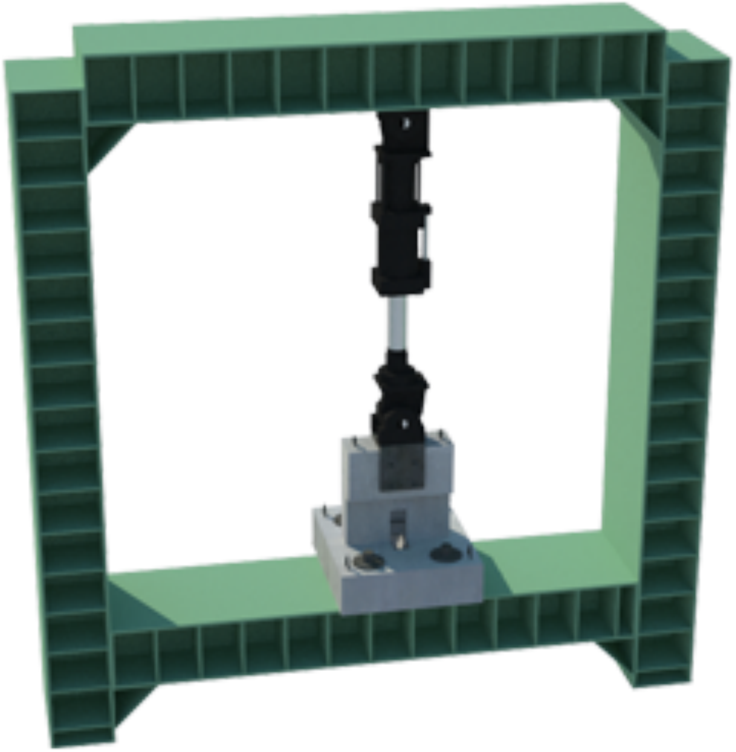

Precast test specimens: cyclic testing of three-wall connectors

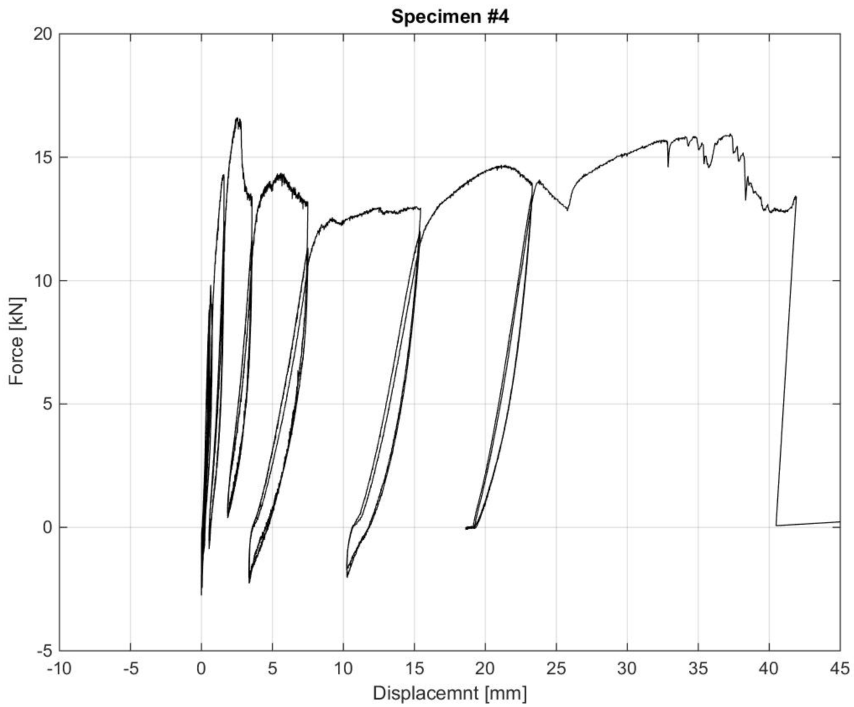

Precast specimen: testing (dynamic)

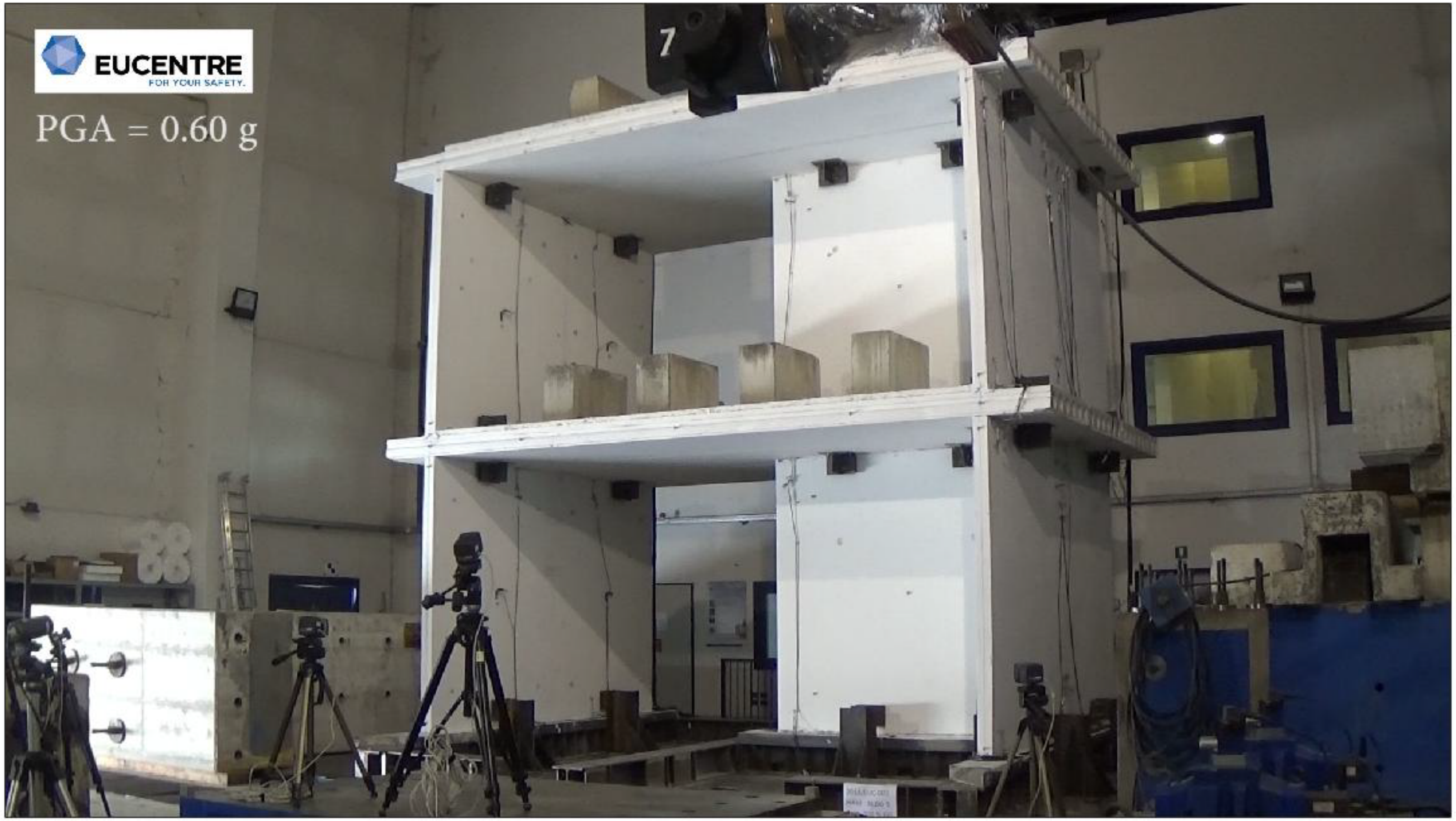

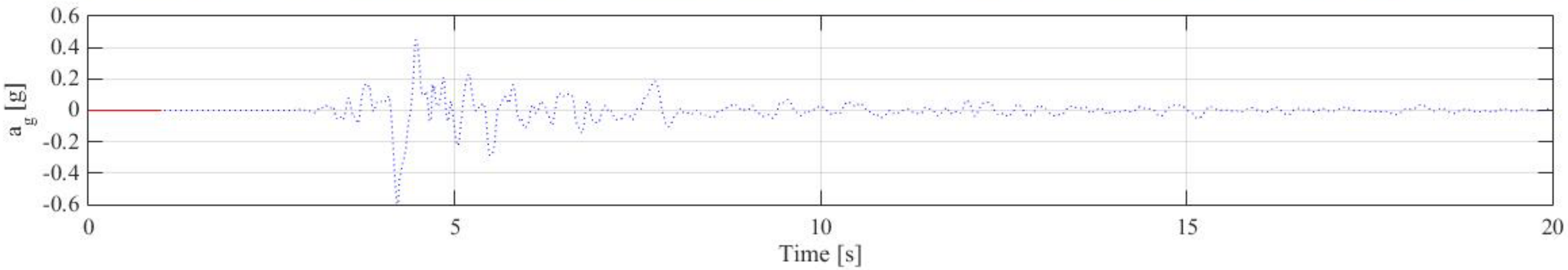

Precast specimen: testing (dynamic)

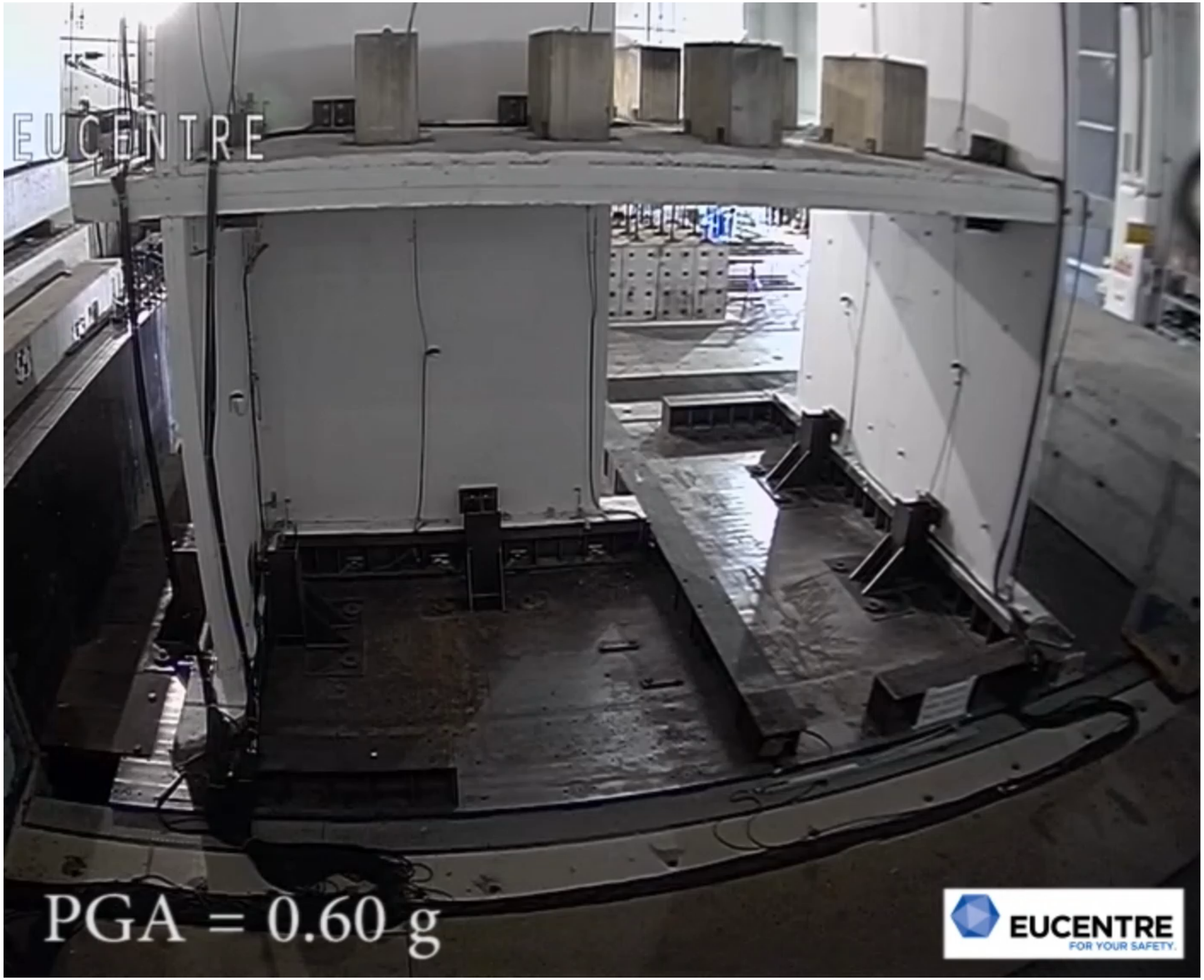

Precast specimen: post-test shoring

Precast specimen: permanent drift

Test run #	Scale factor	Maximum Drift [%]		Residual Drift [%]	
		1st Floor	2nd Floor	1st Floor	2nd Floor
02	50%	0.018	**0.018**	0.002	**0.002**
04	100%	**0.052**	0.038	**0.008**	0.002
06	150%	**0.164**	0.087	**0.037**	0.003
08	200%	**0.534**	0.432	0.275	**0.355**
10	200%	**5.168**	0.581	**5.130**	0.497

Precast specimen: ruptured connections

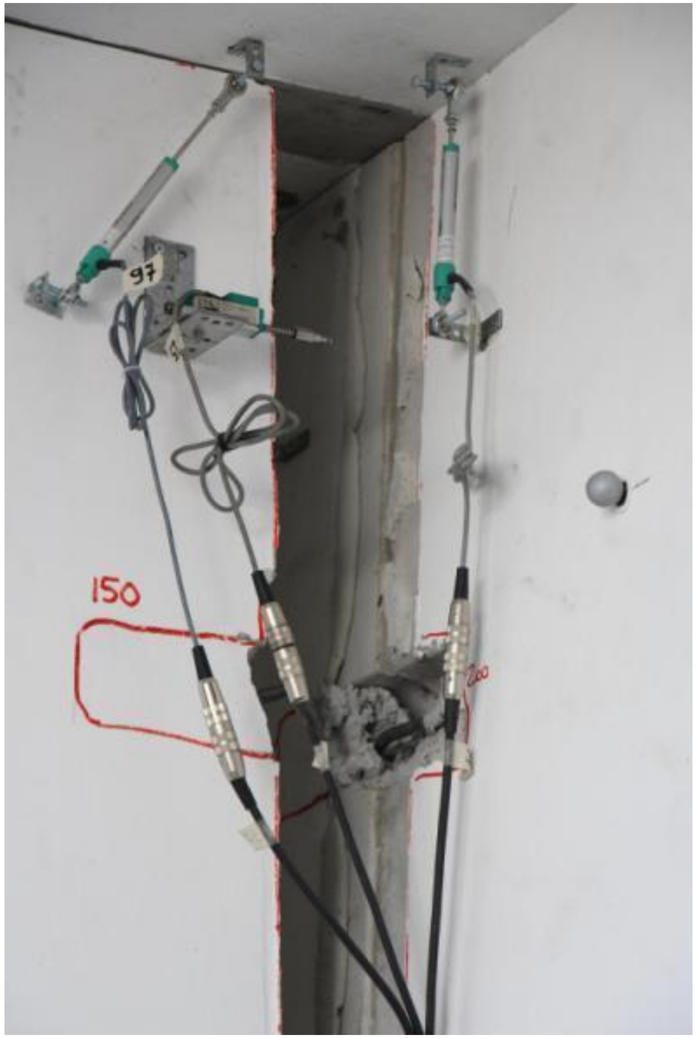

Precast test specimen: response curves

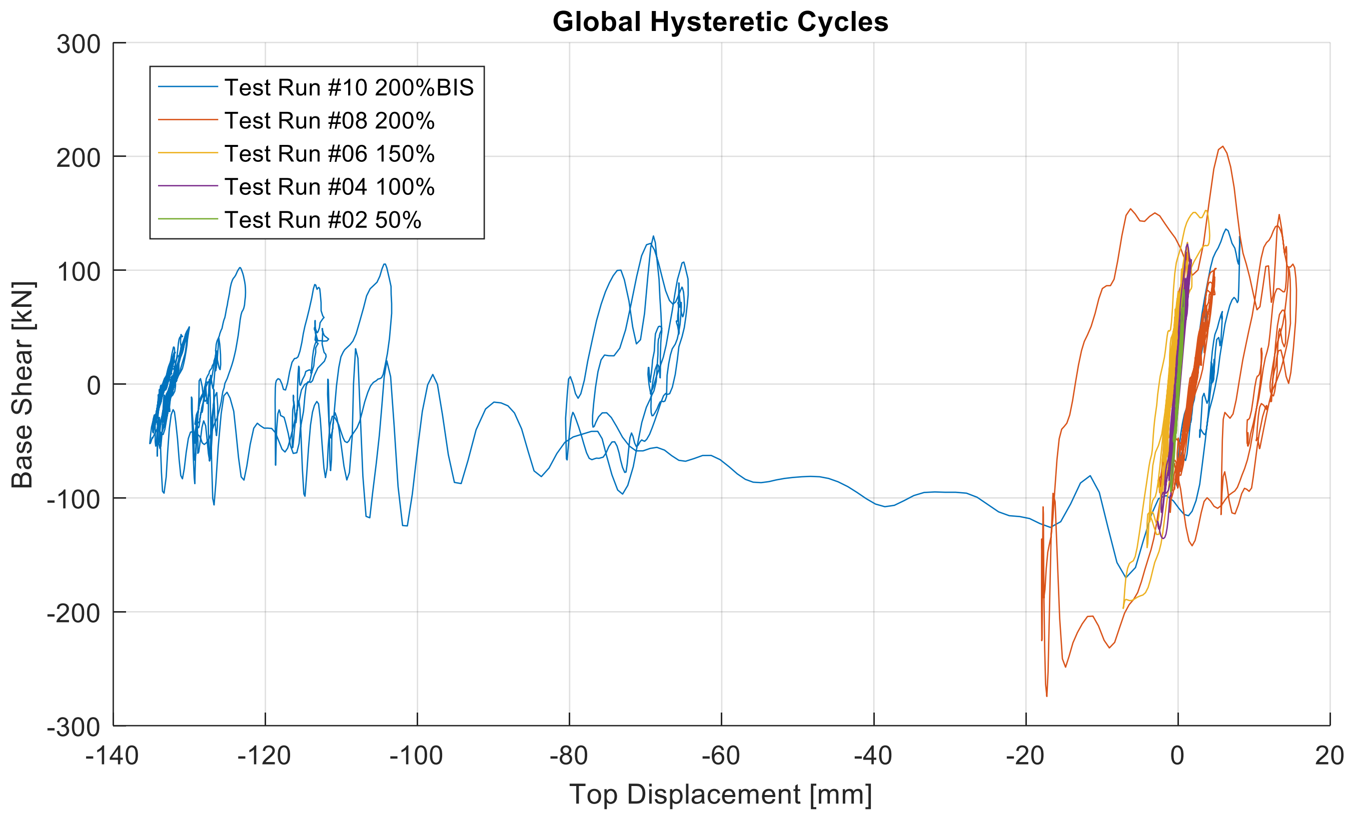

Precast test specimen: “retrofitting” of cyclically tested structure

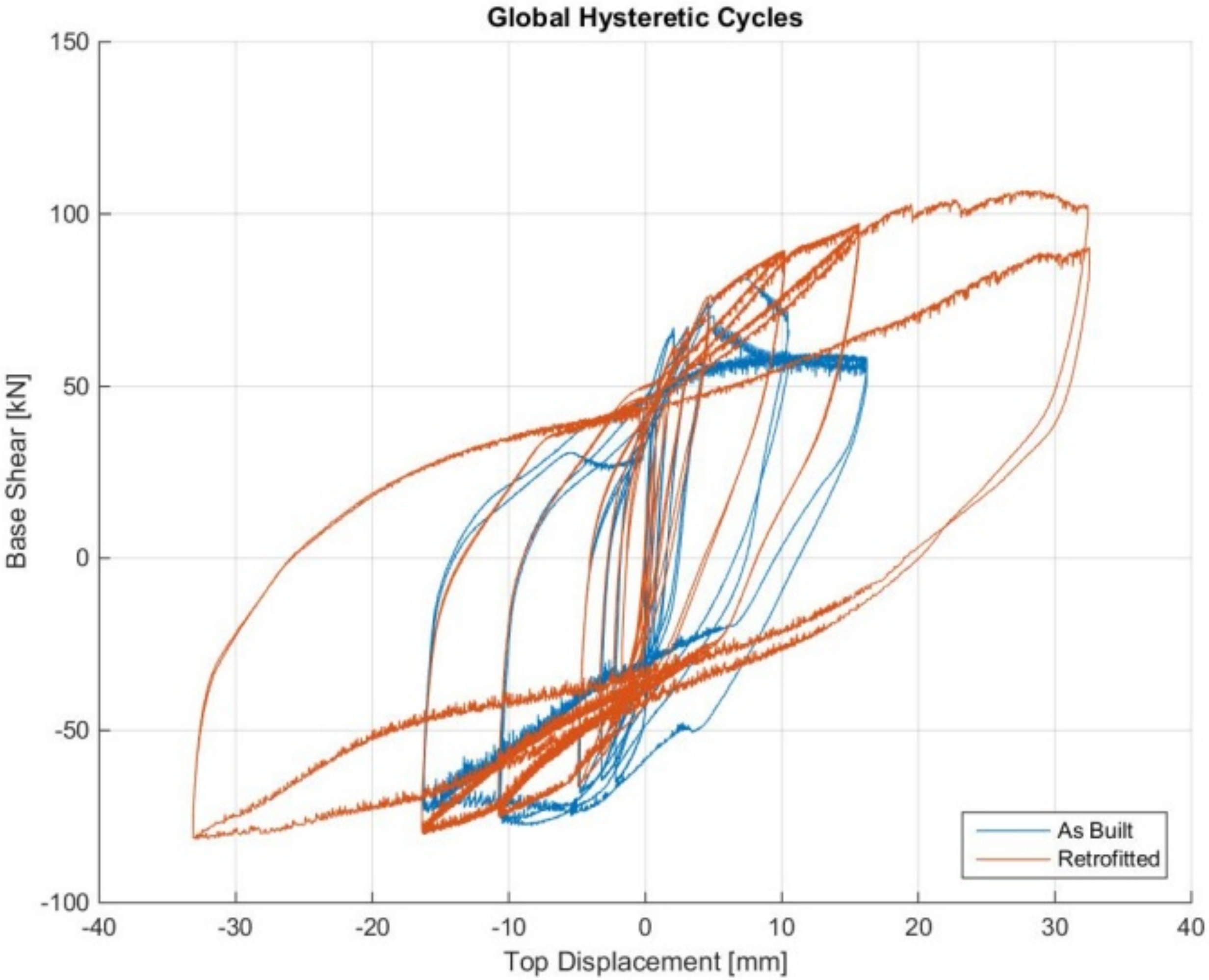

Verification and calibration of numerical models using test data

Several modelling teams involved:

ARUP

EUCENTRE
FOR YOUR SAFETY.

TU Delft

ARCADIS

zonneveld
ingenieurs®

MOSAYK
Modelling and Structural Analysis Konsulting

Different modelling strategies and tools:

LS-DYNA

TreMuri

DIANA

ABAQUS

EXTREME LOADING STRUCTURES

TASK 1: Reproducing existing experimental results

- Kick-start exchange of knowledge/experience between modelling teams
- Identify potential inconsistencies on modelling assumptions (e.g. connections, flange effects, etc.)
- First assessment of capabilities, advantages and limitations of each of the different modelling strategies
- 6 case-studies considered
- LS-Dyna, Tremuri, Diana

Considered literature case-studies

Benchmark test	Behaviour investigated
Ispra wall panel x2 (Anthoine et al., 1995) - **LOWSTA** - **HIGHSTA**	In-plane behaviour of unreinforced clay brick masonry wall panels under quasi-static cyclic loading.
Pavia full building (Magenes et al., 1995)	In-plane behaviour of full-scale two-storey building under quasi-static cyclic loading.
ESECMaSE in-plane cyclic calcium silicate panel (Magenes et al., 2008)	In-plane behaviour of unreinforced calcium silicate block masonry wall panels under quasi-static cyclic loading.
ESECMaSE full-scale calcium silicate half-building (Anthoine & Caperan, 2008)	Behaviour of full-scale calcium silicate brick half-building under pseudo-dynamic loading.
Australia out-of-plane one-way spanning wall (Doherty et al., 2002)	Out-of-plane behaviour of one-way spanning, single-leaf, unreinforced clay brick masonry wall panels under quasi-static and dynamic loading.
Australia out-of-plane two-way spanning wall (Griffith et al., 2007)	Out-of-plane behaviour of two-way spanning, single leaf, unreinforced clay brick masonry wall panels under quasi-static loading.

URM building tested in Pavia (Magenes et al., 1995)

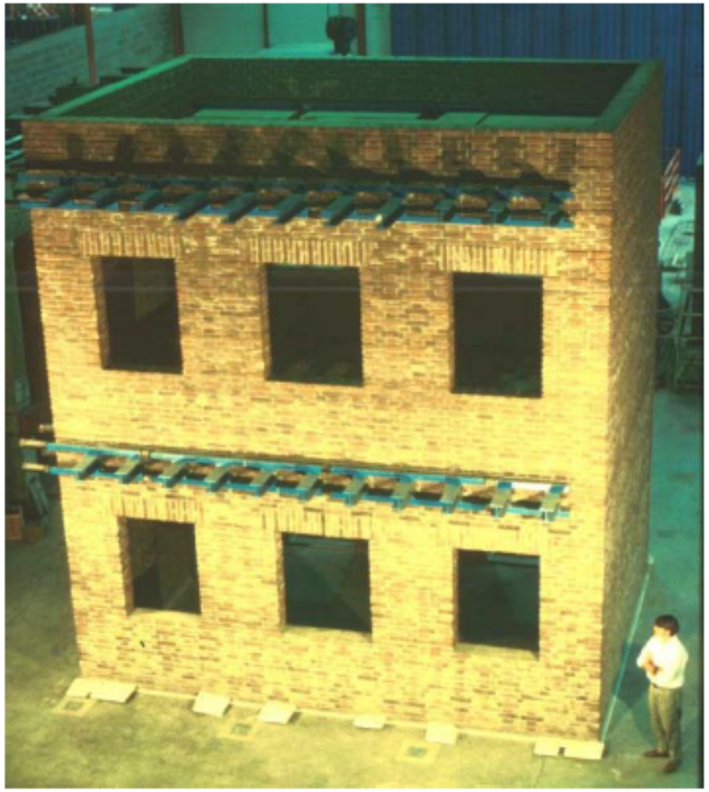

Cyclic testing in longitudinal direction

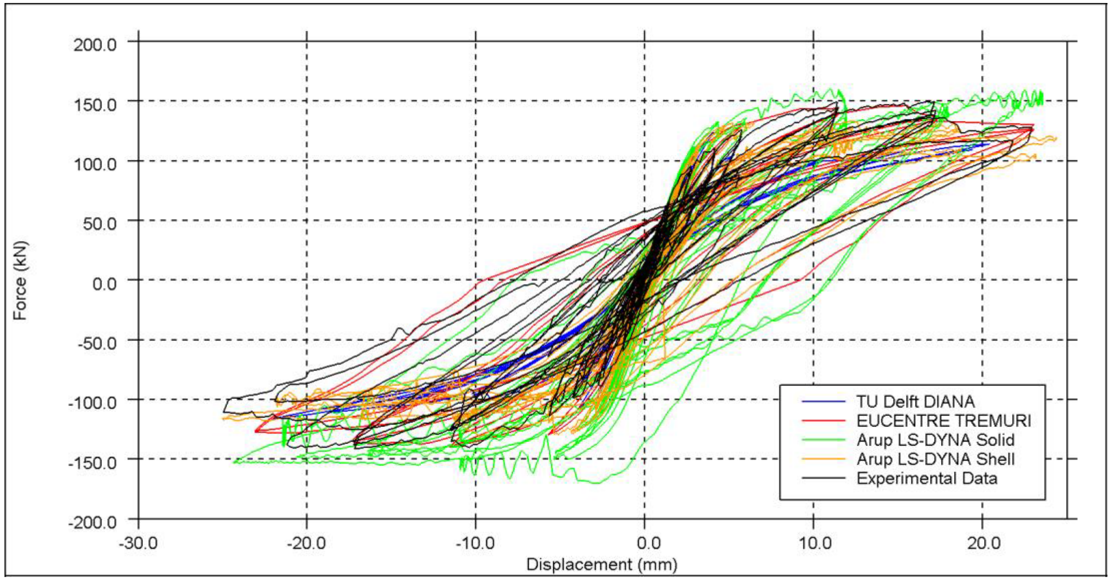

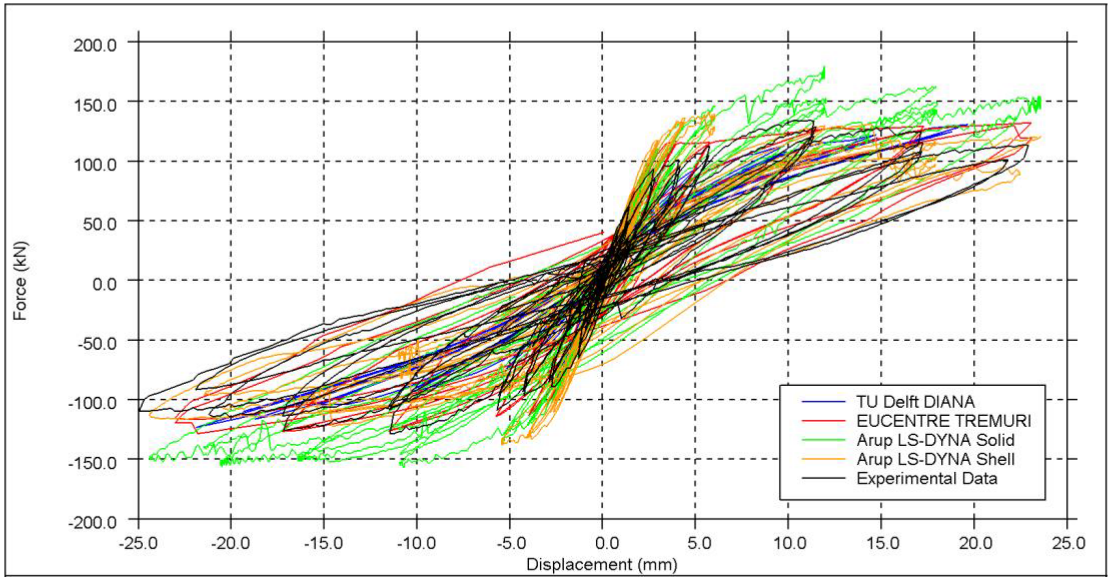

URM building tested in Pavia (Magenes et al., 1995)

Experiment

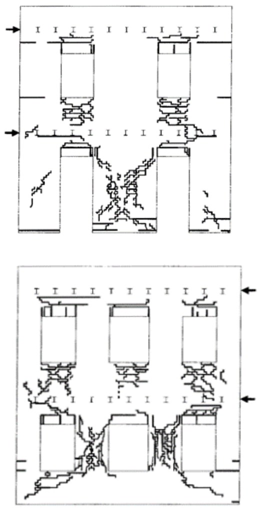

LS-DYNA solid element model

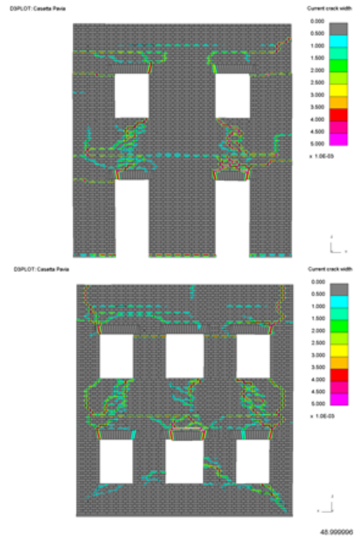

LS-DYNA shell element model

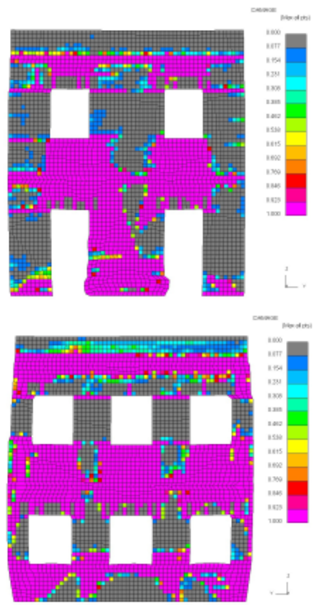

DIANA

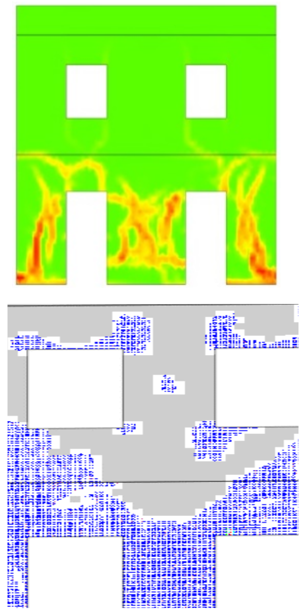

TREMURI

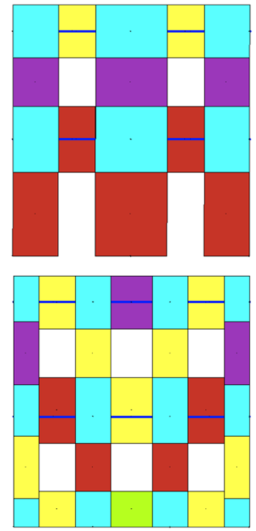

TREMURI damage legend:

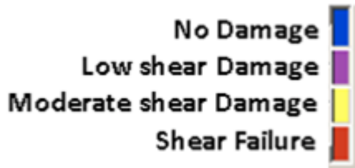

TASK 2: Blind and post-test prediction of Groningen-specific component lab tests

- Calibration or development of constitutive models so as to cater for the specific characteristics of construction materials used in Groningen buildings (e.g. crushing of calcium-silicate brick walls)
- Checking capability of adequately modelling boundary conditions at element level (e.g. links in masonry cavity walls, connectors between precast panels, etc.) and their failure modes (e.g. rupture, punching, sliding, etc.)
- 15 specimens considered
- LS-Dyna, Tremuri, Diana, ELS

URM walls: example blind prediction results

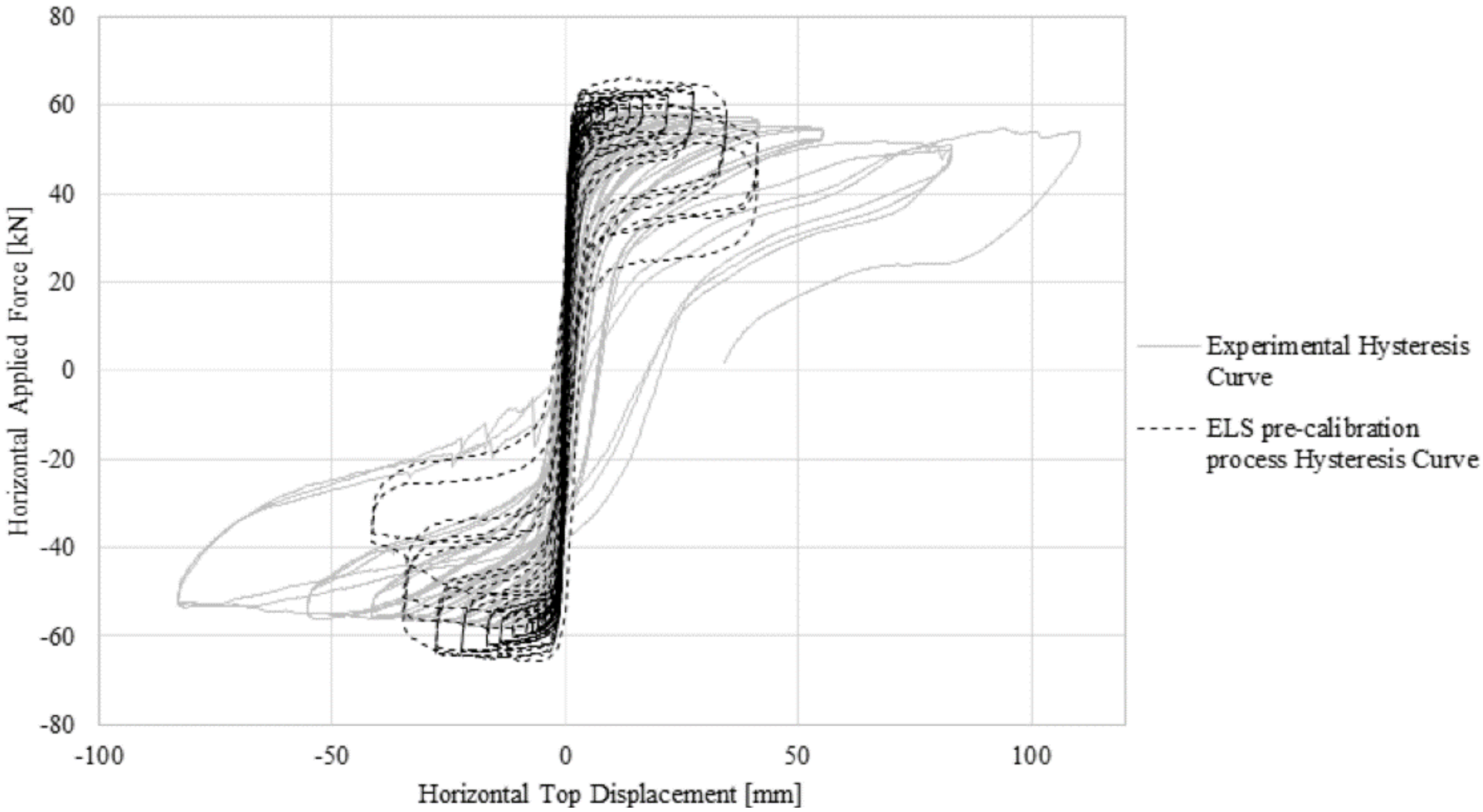

URM walls: example post-diction results

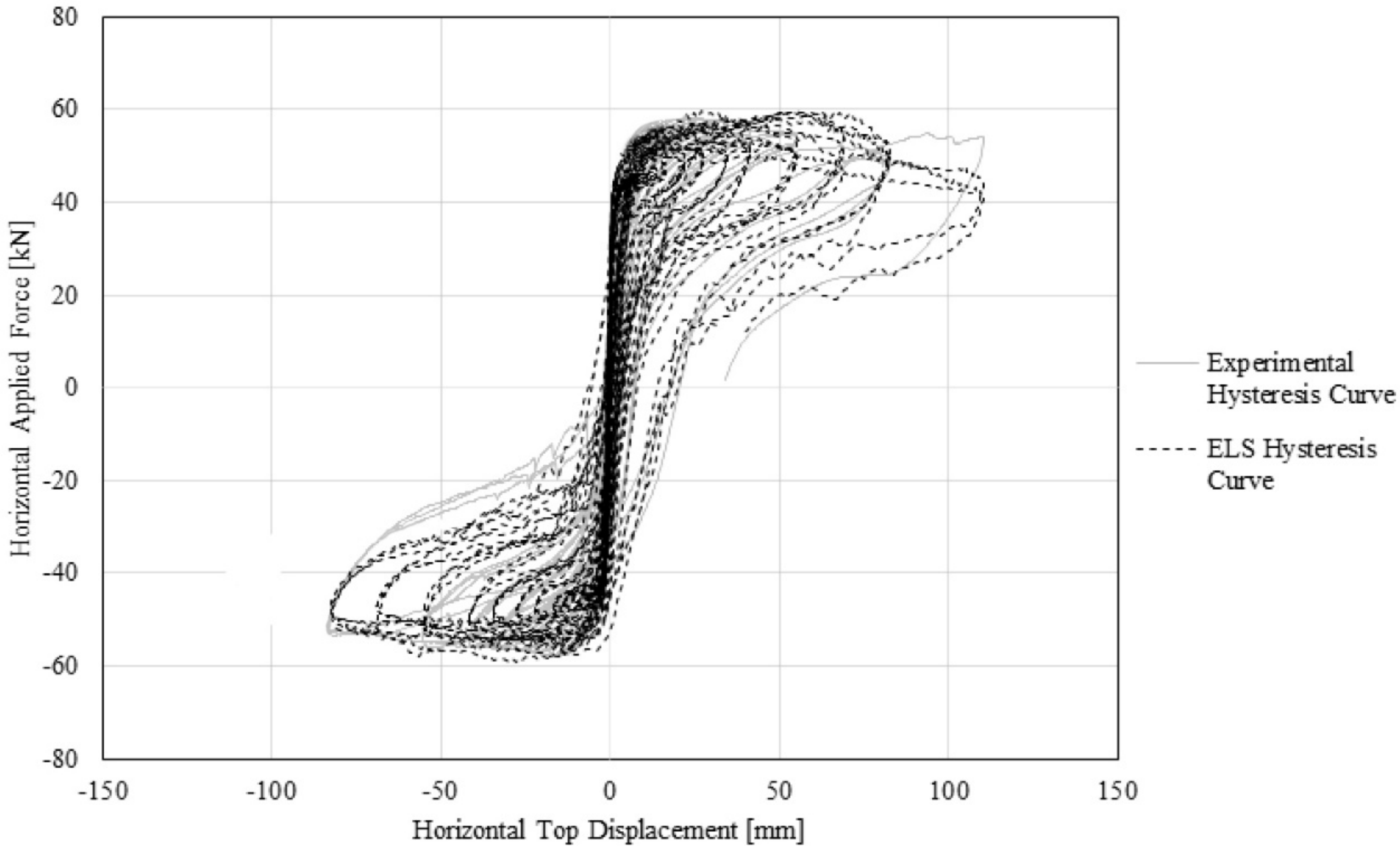

URM walls: cracks pattern modelling

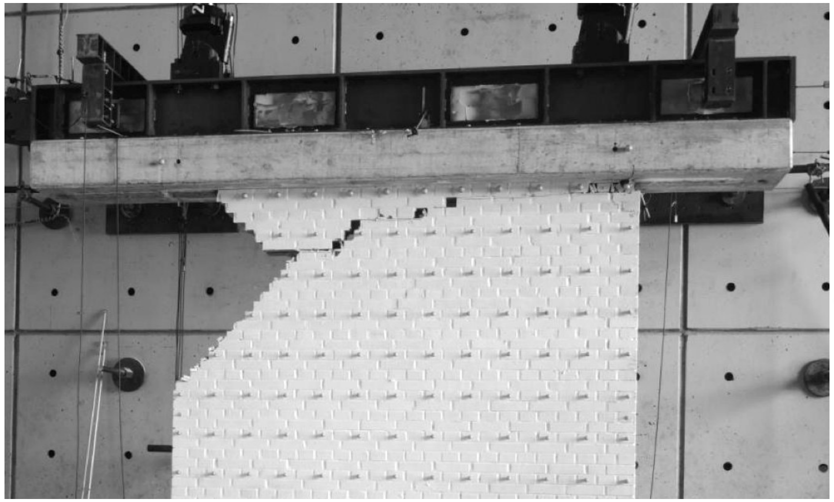

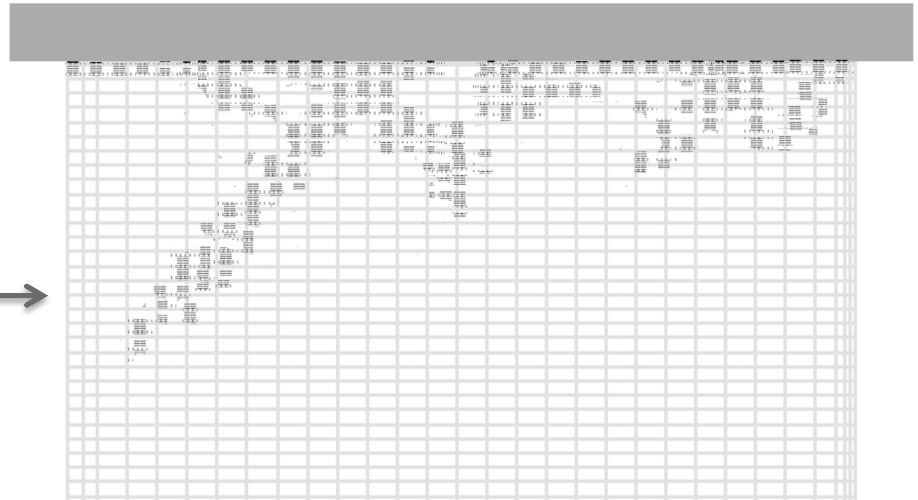

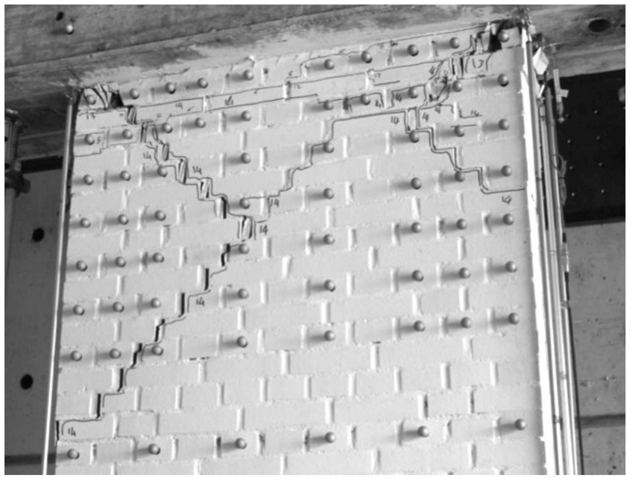

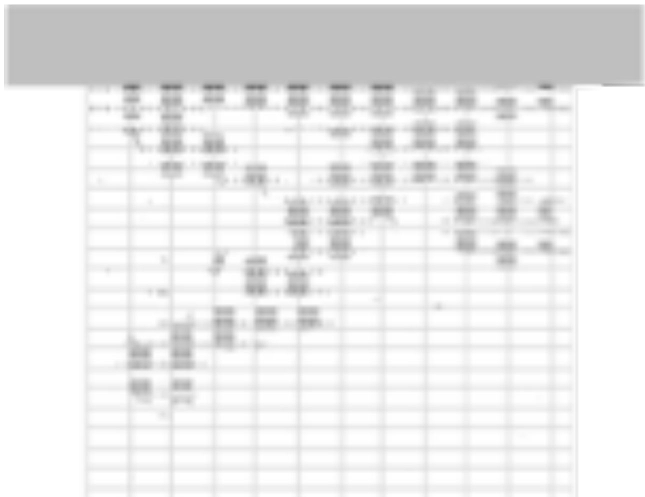

TASK 3: Blind and post-test prediction of Groningen-specific tests of complete structural assemblies

- Check capability in adequately modelling connections between structural elements (e.g. walls, floors, roofs, etc.), mass distribution, load paths, failure modes, shear and displacement capacity, etc.
- 8 full-scale specimens considered
- LS-Dyna, Tremuri, Diana, Abaqus, ELS

Cast-in-place test specimen: blind prediction

(longitudinal direction)

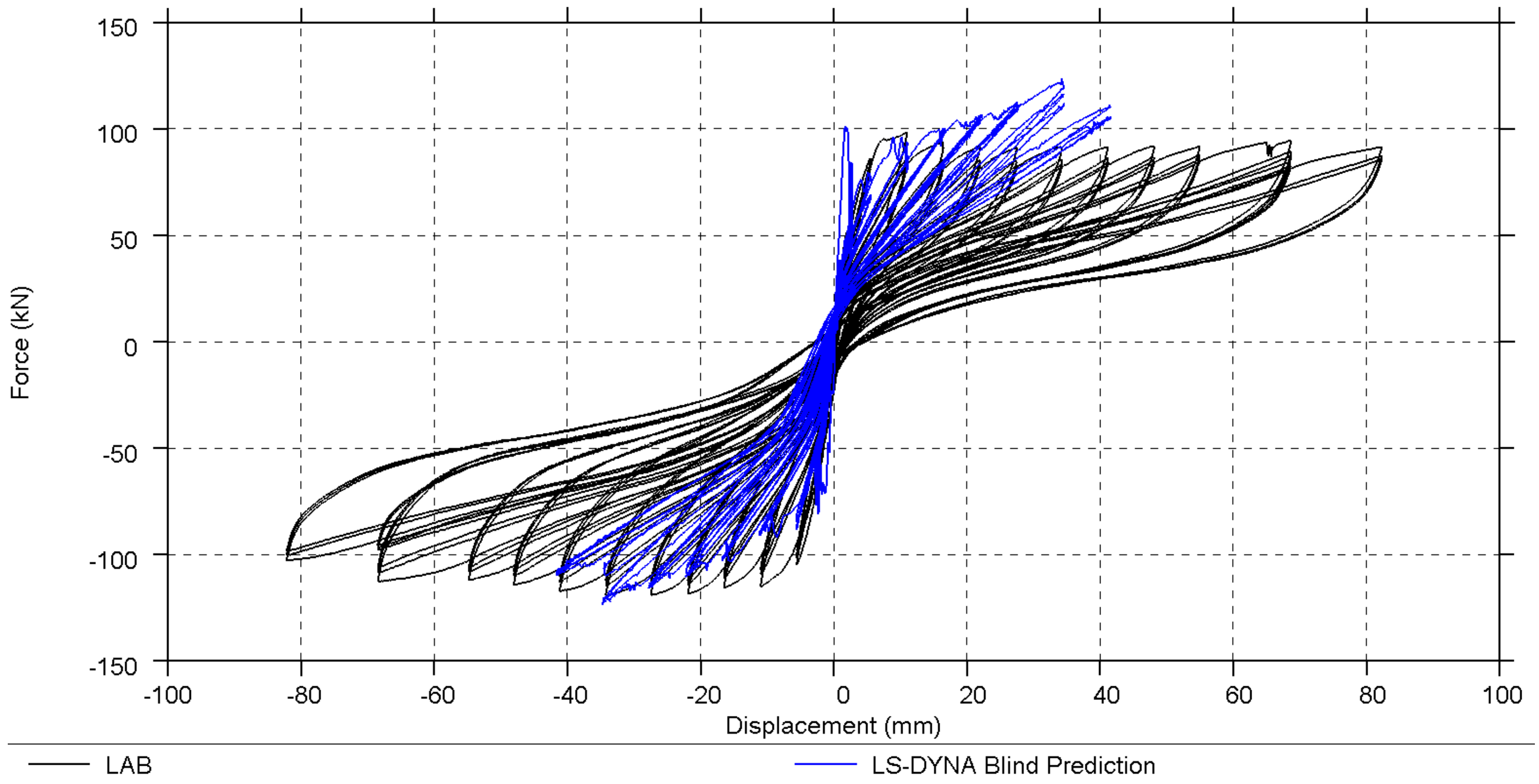

Cast-in-place test specimen: post-diction

(longitudinal direction)

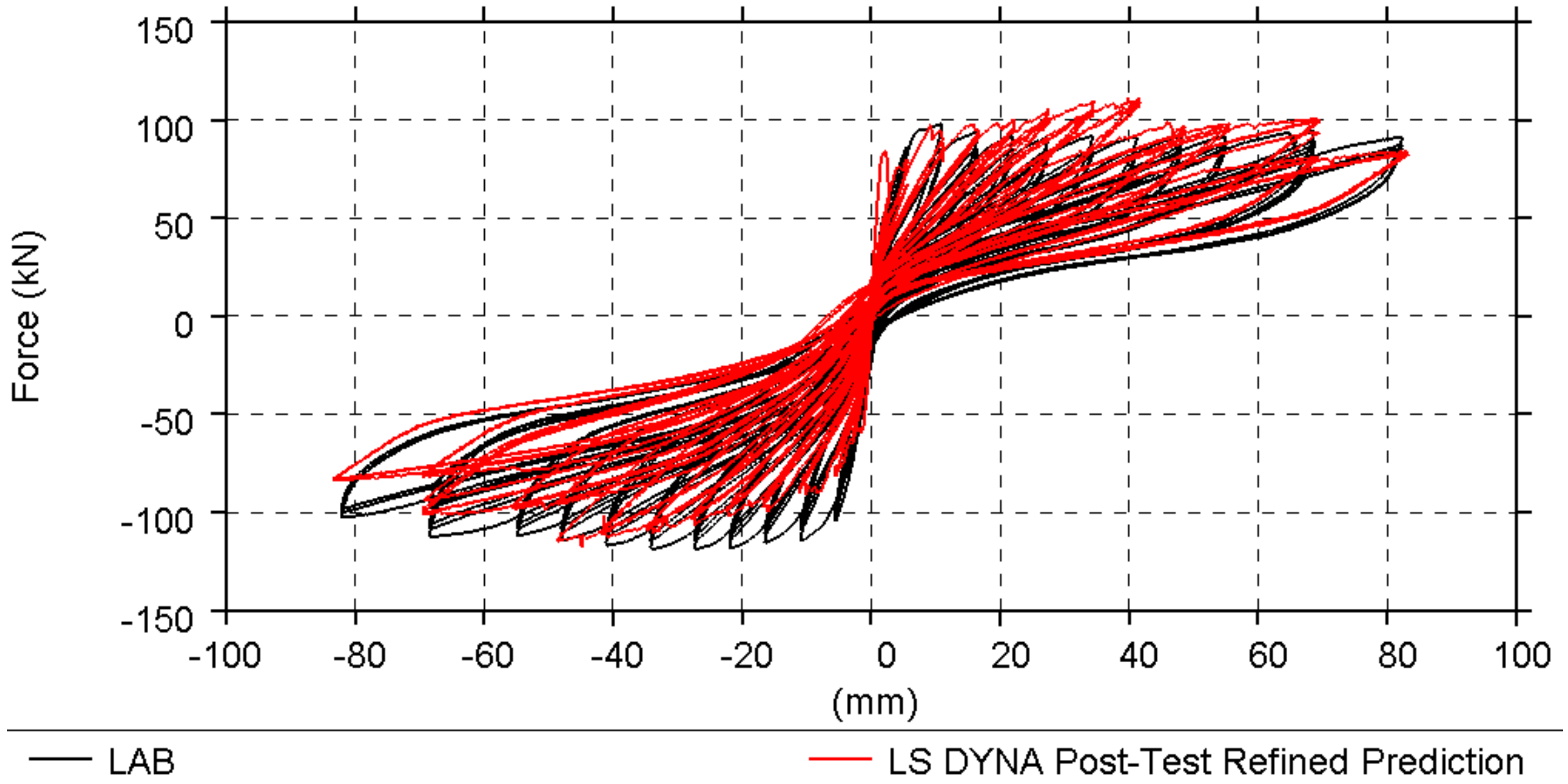

Cast-in-place test specimen: blind prediction
(transverse direction)

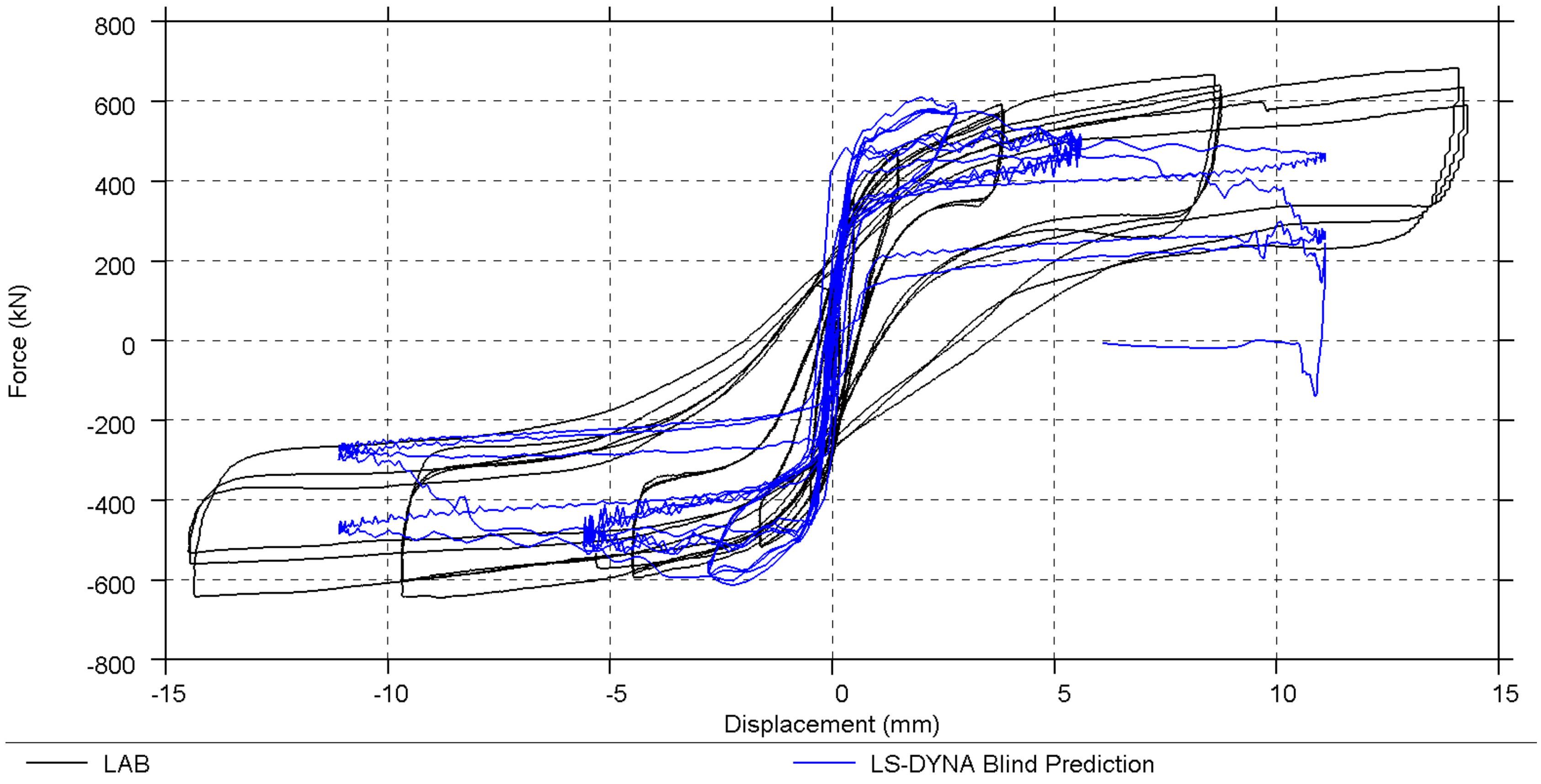

Cast-in-place test specimen: post-diction

(transverse direction)

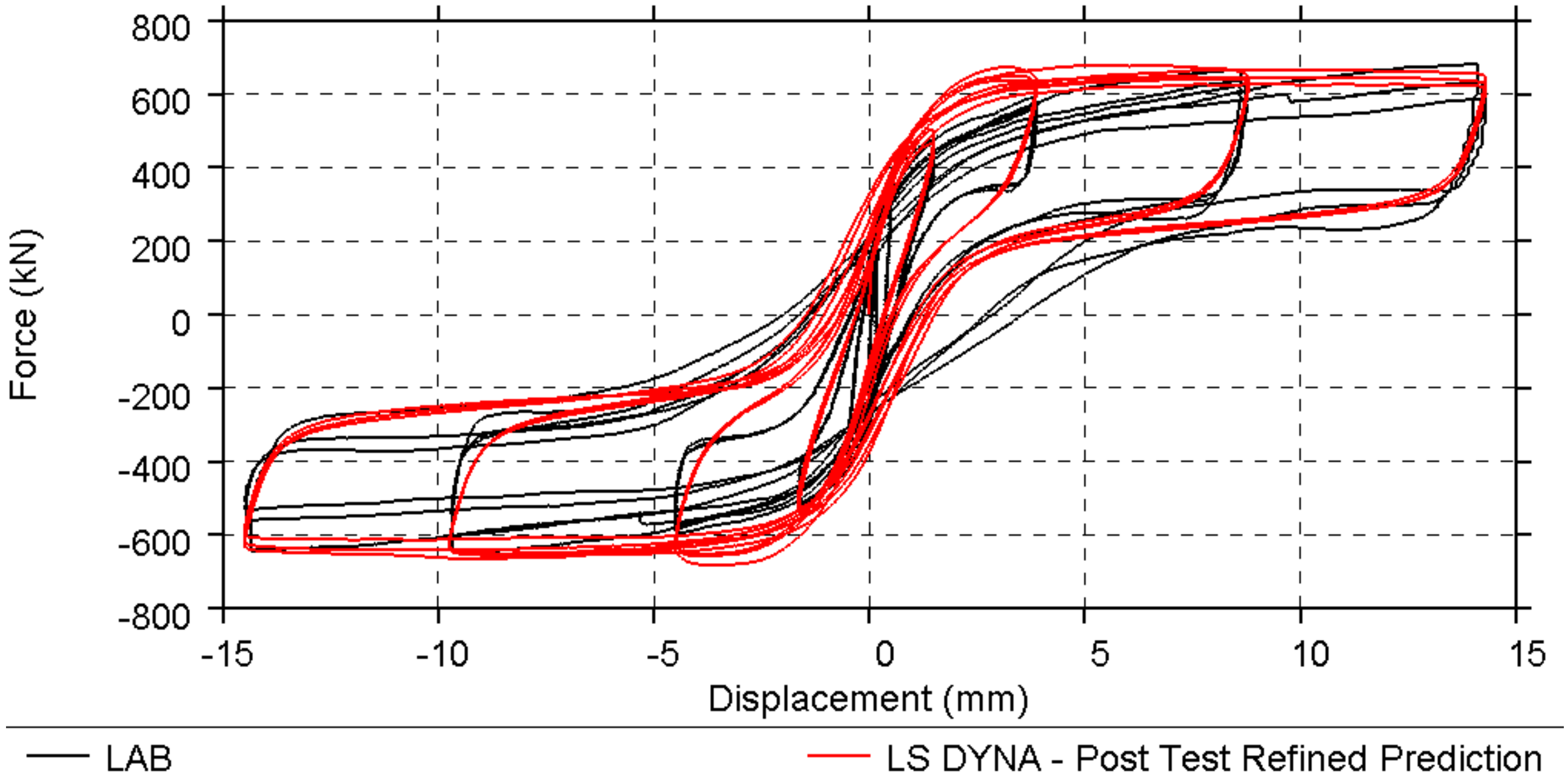

URM detached house specimen: blind prediction

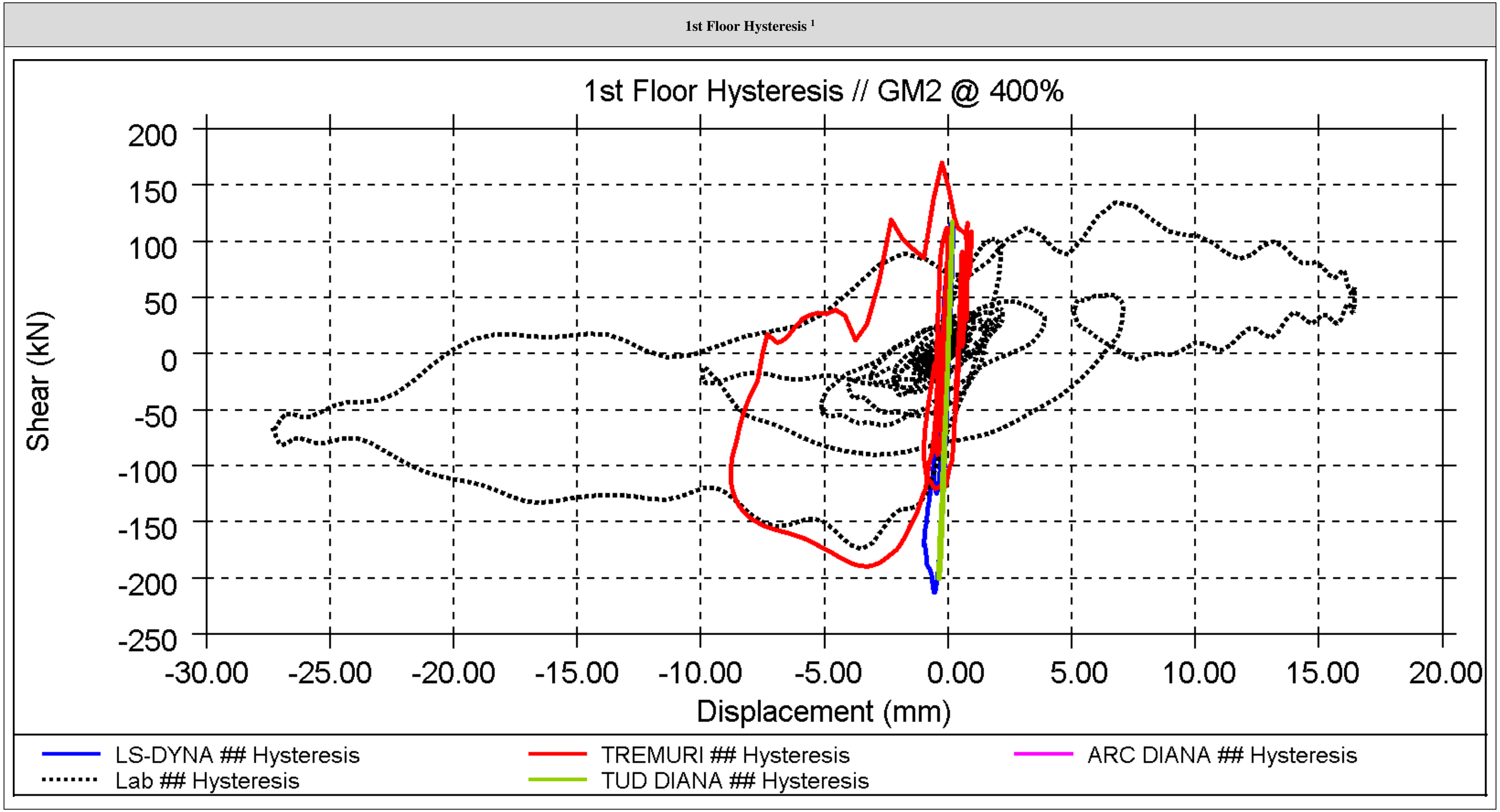

1 1st floor hysteresis is taken as the total base shear vs 1st floor average displacement relative to the base. Displacement is the same as that which is used to produce displacement time history (see Appendix A1.2)

URM detached house specimen: post-diction

1st Floor Hysteresis [1]

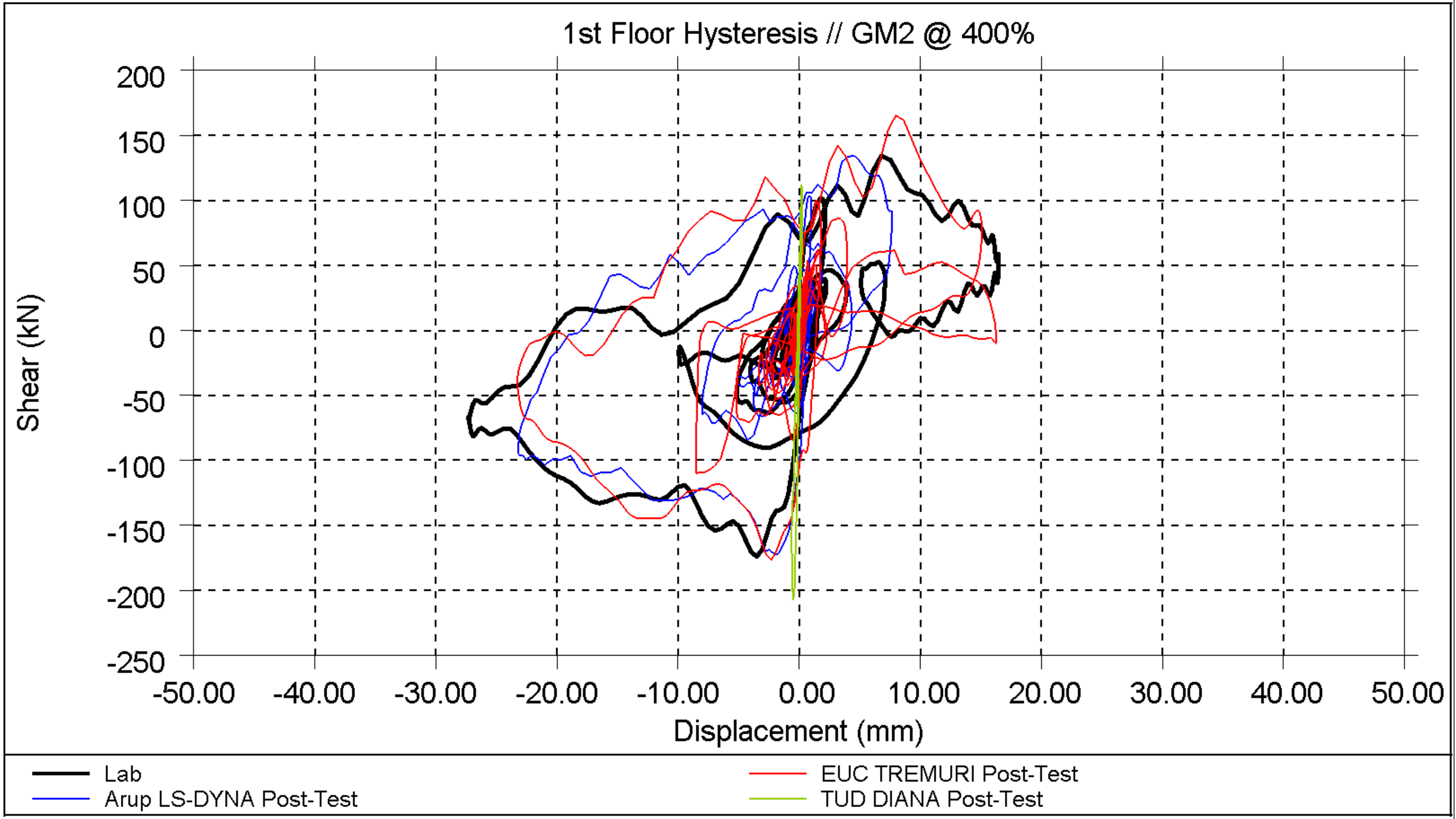

Terraced house collapse testing: blind prediction

Arup / LS-DYNA	Eucentre / TreMuri
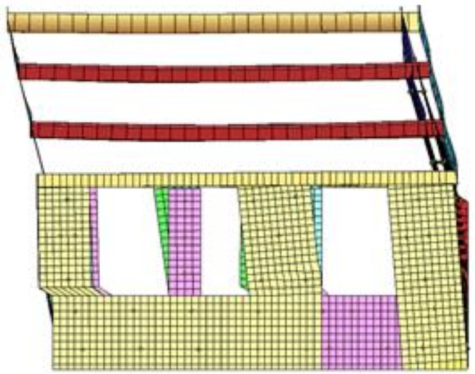 Magnified 5x	NA
TU Delft / DIANA	**Mosayk /ELS**
NA (no collapse)	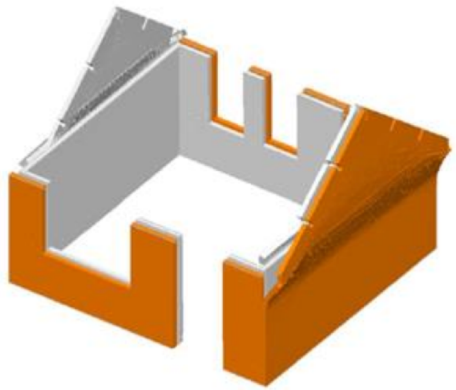 Magnified 2x

Terraced house collapse testing: blind prediction

	LNEC Lab	Arup	Eucentre	TU Delft	Mosayk
Software	---	LS-DYNA	TreMuri	DIANA	ELS
Collapse mechanism	Out-of-plane failure of CaSi [transverse] party wall	Collapse of gables due to out-of-plane rocking	Collapse of roof indicated by relative roof displacement > 100 mm	No collapse	Collapse of gables due to out-of-plane sliding at gable base/top of transverse walls
Collapse Horizontal input motion (PFA)	EQ2-300% (0.63g)	EQ2-400% (0.66g)	EQ2-400% (0.61g)	--- ≥ EQ2-600% (1.03g)	EQ2-250% (0.40g)
Peak floor drift (%) [1]	4.4	0.03[3]	1.4[4]	≥ 0.6	0.9
Peak roof drift (%) [2]	2.0	2.2[3]	2.6[4]	≥ 0.8	3.15
Peak ridge displacement (mm)	170	78[3]	108[4]	≥ 37	124
Base shear (kN)	160	145[3]	124[4]	≥ 188	105

Terraced house collapse testing: post-diction

Arup / LS-DYNA	Eucentre / TreMuri
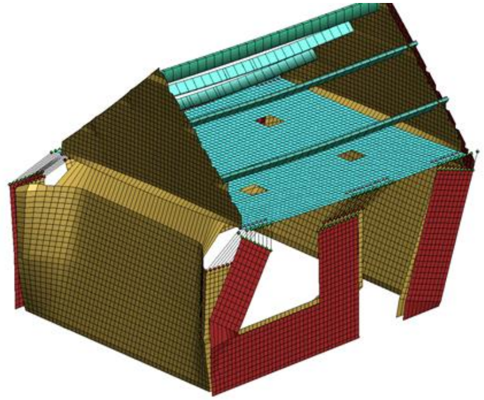 Magnified 10x	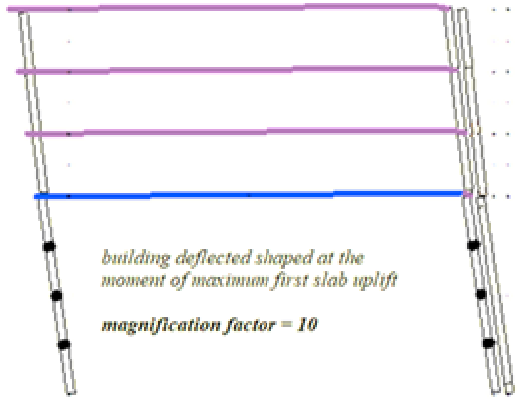
TU Delft / DIANA	**Mosayk /ELS**
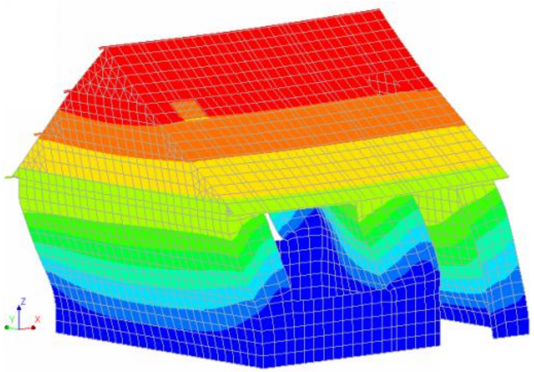 Magnified x25	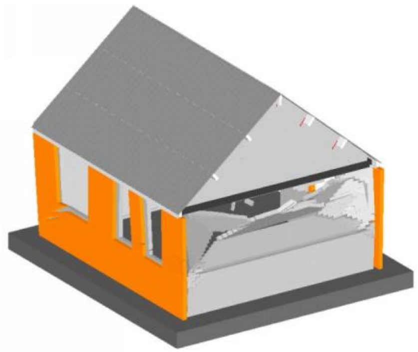 Magnified 2x

Terraced house collapse testing: post-diction

	LNEC Lab	Arup	Eucentre	TU Delft	Mosayk
Software	---	LS-DYNA	TreMuri	DIANA	ELS
Collapse mechanism	Out-of-plane failure of CaSi [transverse] party wall	**No collapse (although visible drop in capacity)**	**No collapse (although visible drop in capacity)**	No collapse	**Out-of-plane failure of CaSi [transverse] party wall**
Collapse Horizontal input motion (PFA)	EQ2-300% (0.63g)	---	---	---	**EQ2-300% (0.63g)**
Peak floor drift (%) [1]	4.4	**4.5**	**2.8**	**≥ 1.2**	**4.8**
Peak roof drift (%) [2]	2.0	1.9	**1.5**	**≥ 0.4**	**3.4**
Peak ridge displacement (mm)	170	**165**	**78**	**≥ 44**	**125**
Base shear (kN)	160	132	136	**≥ 109**	**161**

Terraced house collapse testing: post-diction

Arup / LS-DYNA

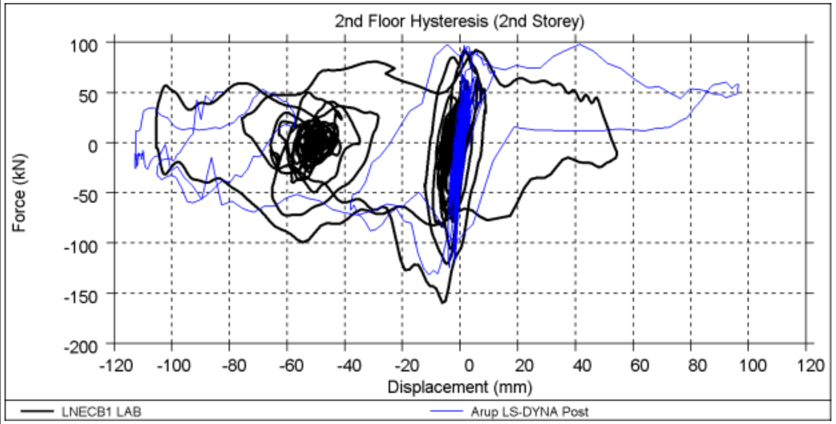

Eucentre TreMuri

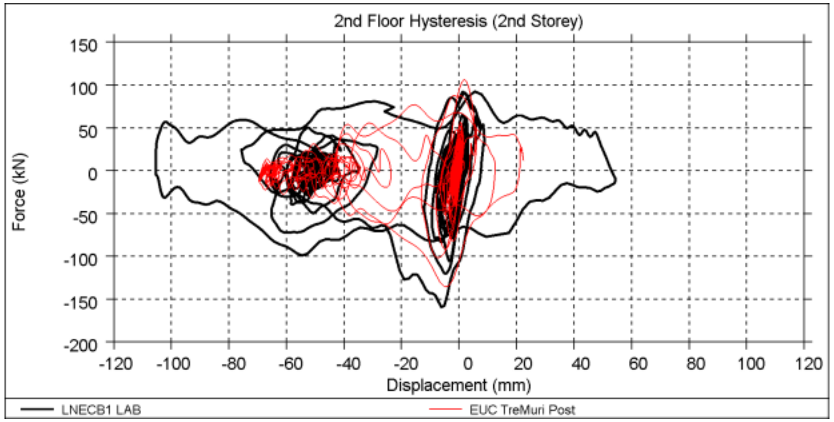

TU Delft / DIANA

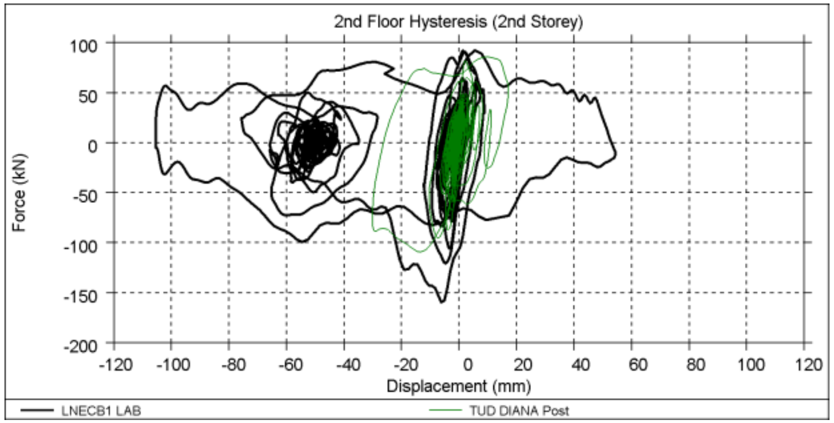

Mosayk / ELS

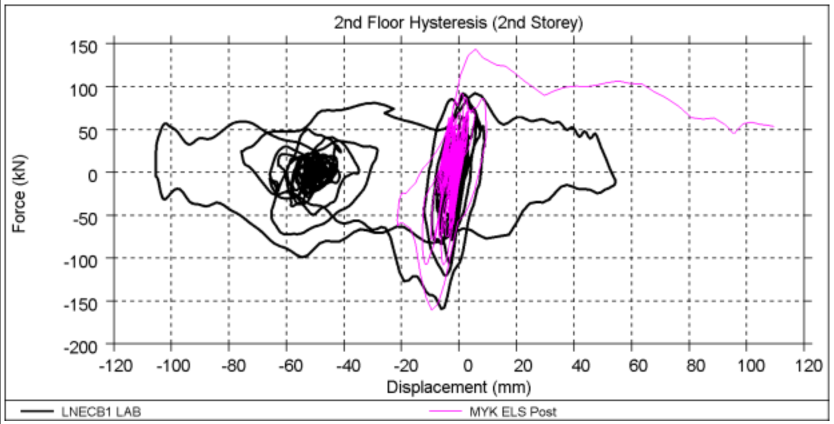

TASK 4: Cross-model validation for actual buildings

- Check modelling assumptions
- 10 existing buildings considered
- LS-Dyna and Tremuri employed (and now also ELS)

Some of the buildings considered in the cross-model validation exercise

Type C house

Julianalaan

Kwelder

Zijlvest

Trial House 1

Trial House 2

Example application of verified numerical tools for collapse mode and debris area estimation

Example building

URM detached house

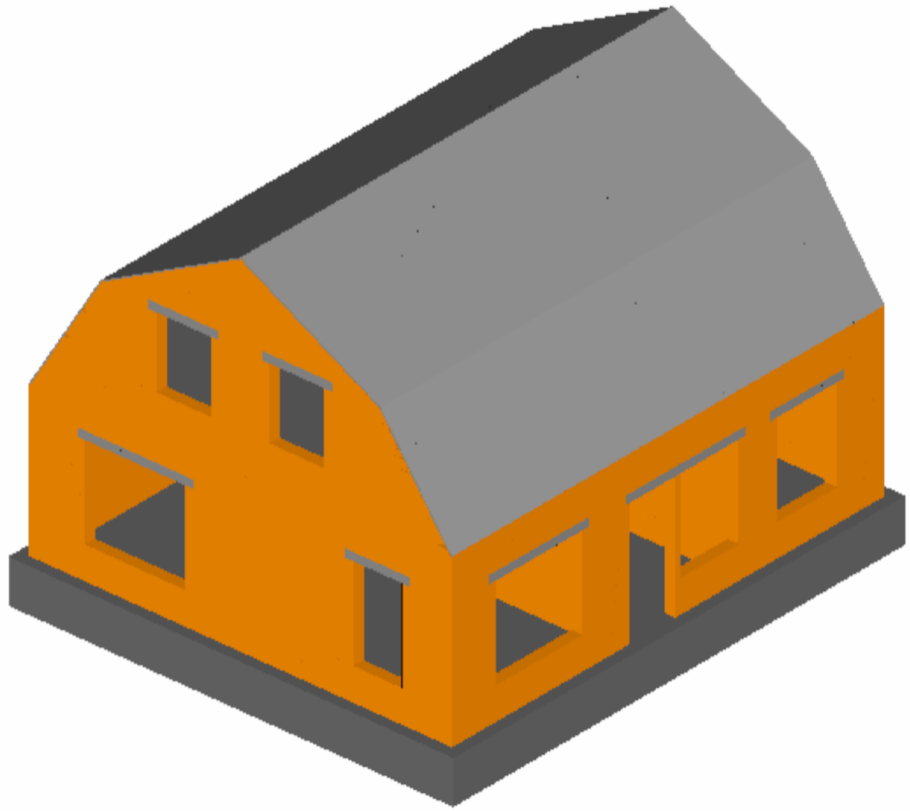

ELS model

Partial collapse modelling (PGA = 0.7g)

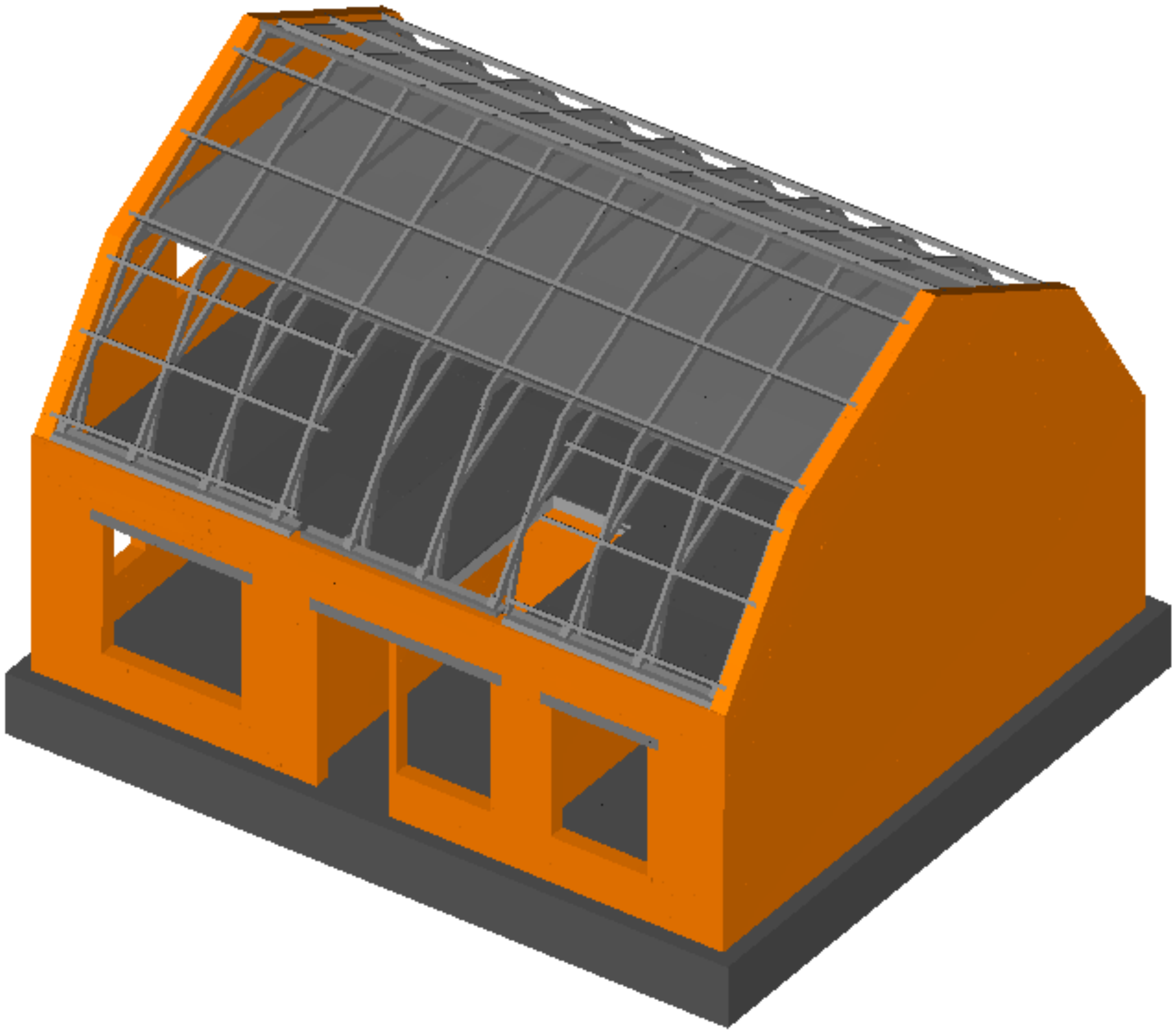

Complete collapse modelling
(three different records with PGA 0.7g to 1.25g)

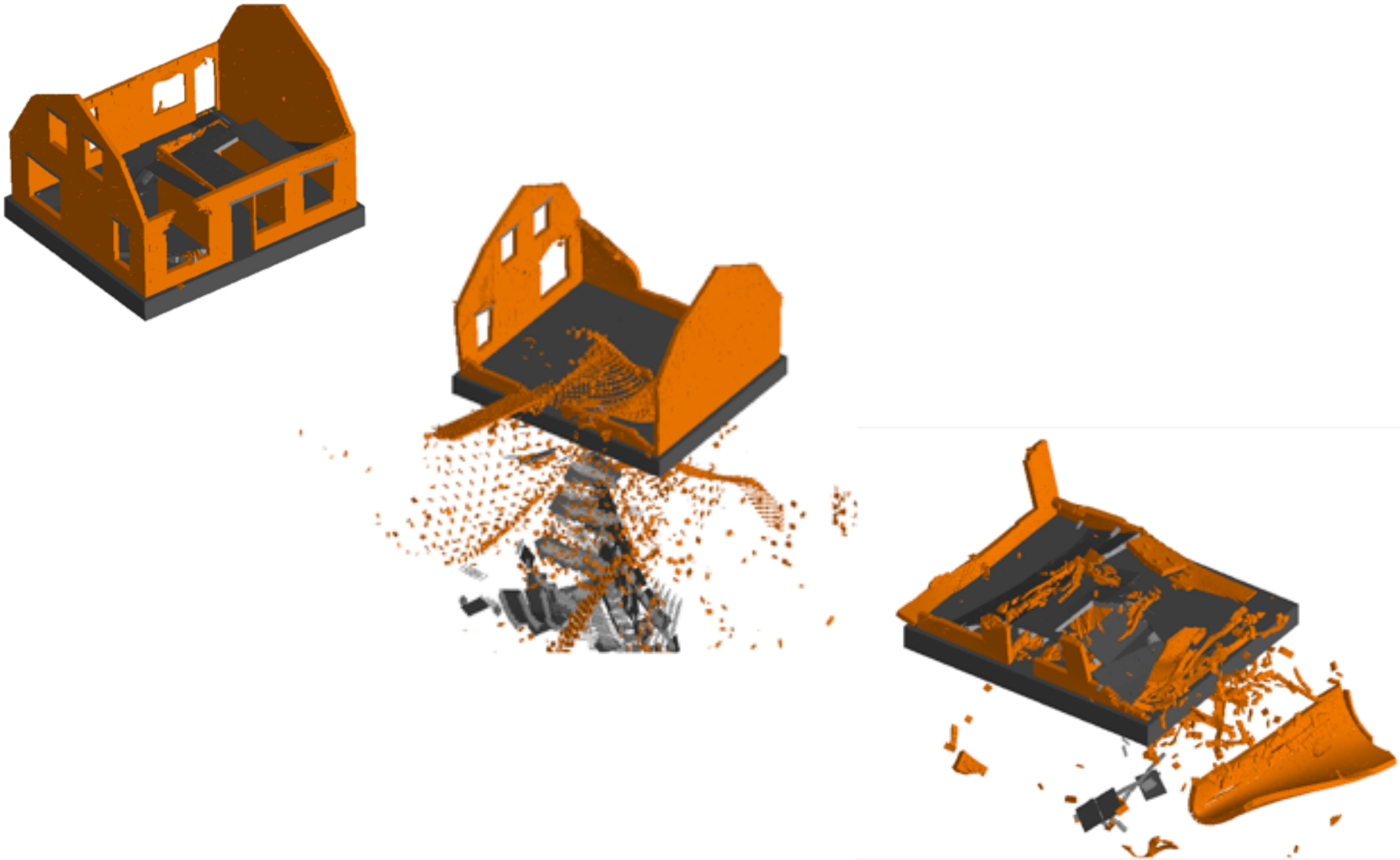

Verification and calibration of numerical models using test data

Several modelling teams involved:

ARUP

EUCENTRE
FOR YOUR SAFETY.

TU Delft

ARCADIS

zonneveld
ingenieurs®

MOSAYK
Modelling and Structural Analysis Konsulting

Different modelling strategies and tools:

TASK 1: Reproducing existing experimental results

- Kick-start exchange of knowledge/experience between modelling teams
- Identify potential inconsistencies on modelling assumptions (e.g. connections, flange effects, etc.)
- First assessment of capabilities, advantages and limitations of each of the different modelling strategies
- 6 case-studies considered
- LS-Dyna, Tremuri, Diana

Considered literature case-studies

Benchmark test	Behaviour investigated
Ispra wall panel x2 (Anthoine et al., 1995) - **LOWSTA** - **HIGHSTA**	In-plane behaviour of unreinforced clay brick masonry wall panels under quasi-static cyclic loading.
Pavia full building (Magenes et al., 1995)	In-plane behaviour of full-scale two-storey building under quasi-static cyclic loading.
ESECMaSE in-plane cyclic calcium silicate panel (Magenes et al., 2008)	In-plane behaviour of unreinforced calcium silicate block masonry wall panels under quasi-static cyclic loading.
ESECMaSE full-scale calcium silicate half-building (Anthoine & Caperan, 2008)	Behaviour of full-scale calcium silicate brick half-building under pseudo-dynamic loading.
Australia out-of-plane one-way spanning wall (Doherty et al., 2002)	Out-of-plane behaviour of one-way spanning, single-leaf, unreinforced clay brick masonry wall panels under quasi-static and dynamic loading.
Australia out-of-plane two-way spanning wall (Griffith et al., 2007)	Out-of-plane behaviour of two-way spanning, single leaf, unreinforced clay brick masonry wall panels under quasi-static loading.

URM building tested in Pavia (Magenes et al., 1995)

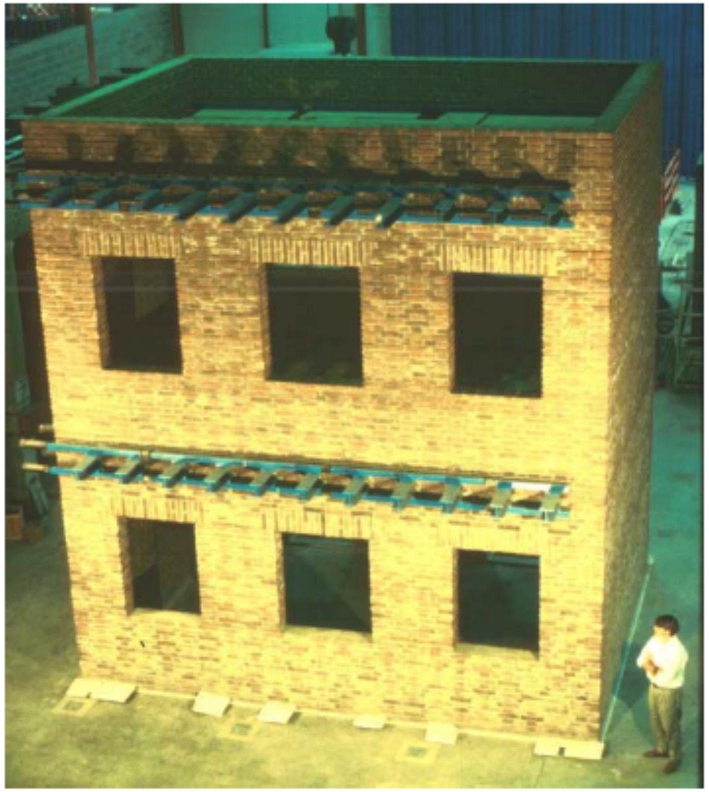

Cyclic testing in longitudinal direction

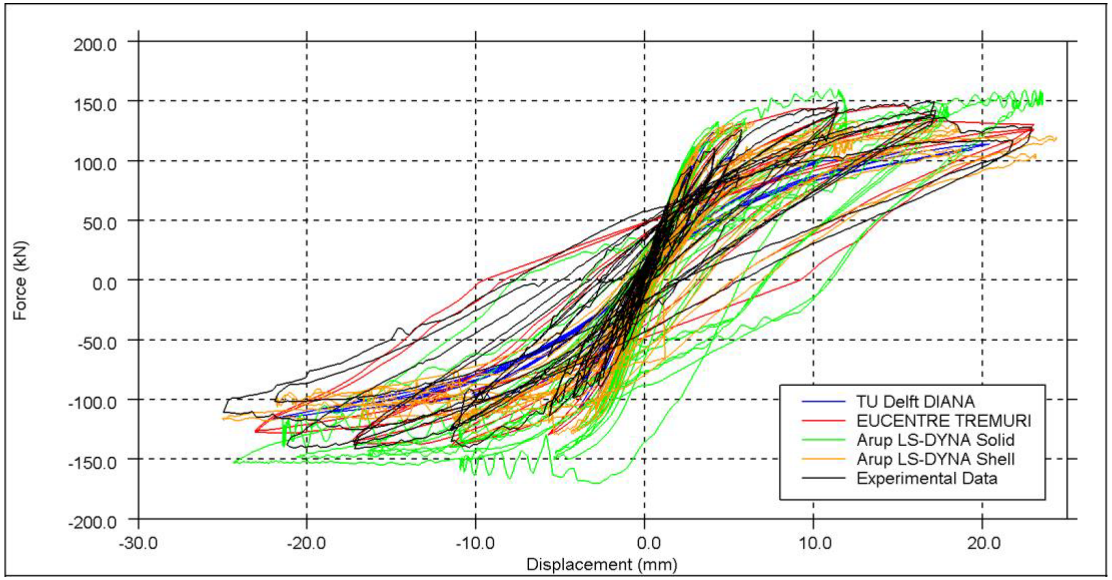

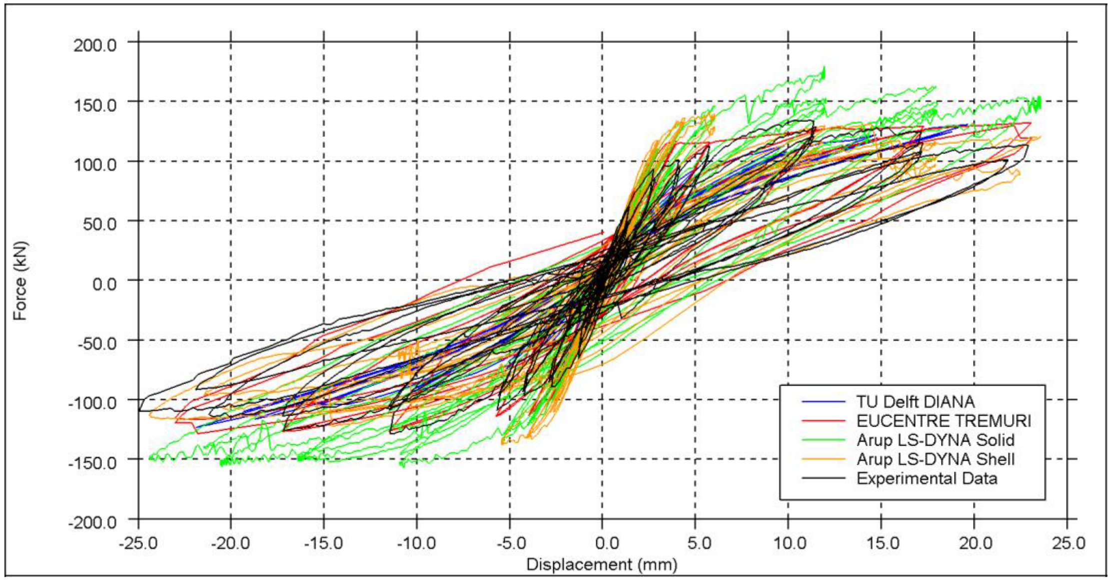

URM building tested in Pavia (Magenes et al., 1995)

Experiment

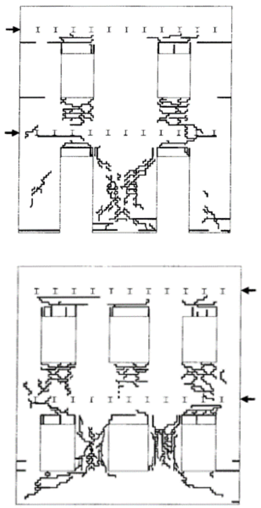

LS-DYNA solid element model

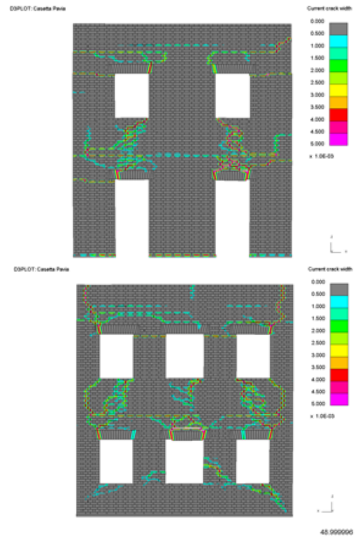

LS-DYNA shell element model

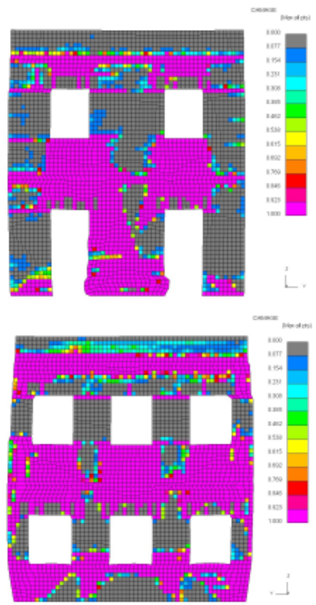

DIANA

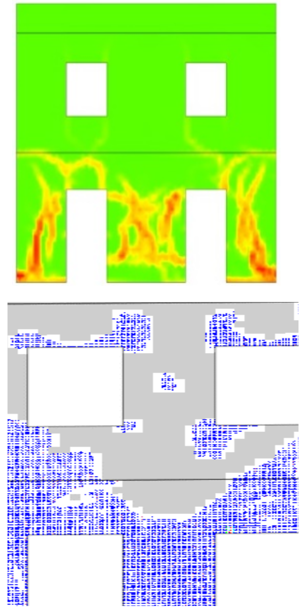

TREMURI

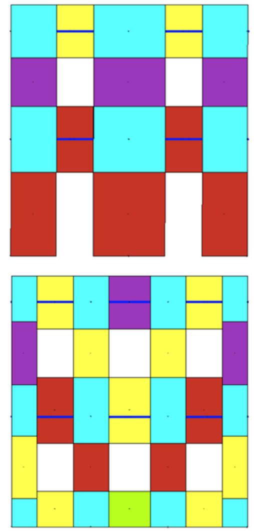

TREMURI damage legend:

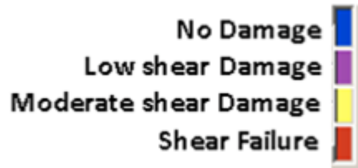

TASK 2: Blind and post-test prediction of Groningen-specific component lab tests

- Calibration or development of constitutive models so as to cater for the specific characteristics of construction materials used in Groningen buildings (e.g. crushing of calcium-silicate brick walls)
- Checking capability of adequately modelling boundary conditions at element level (e.g. links in masonry cavity walls, connectors between precast panels, etc.) and their failure modes (e.g. rupture, punching, sliding, etc.)
- 15 specimens considered
- LS-Dyna, Tremuri, Diana, ELS

URM walls: example blind prediction results

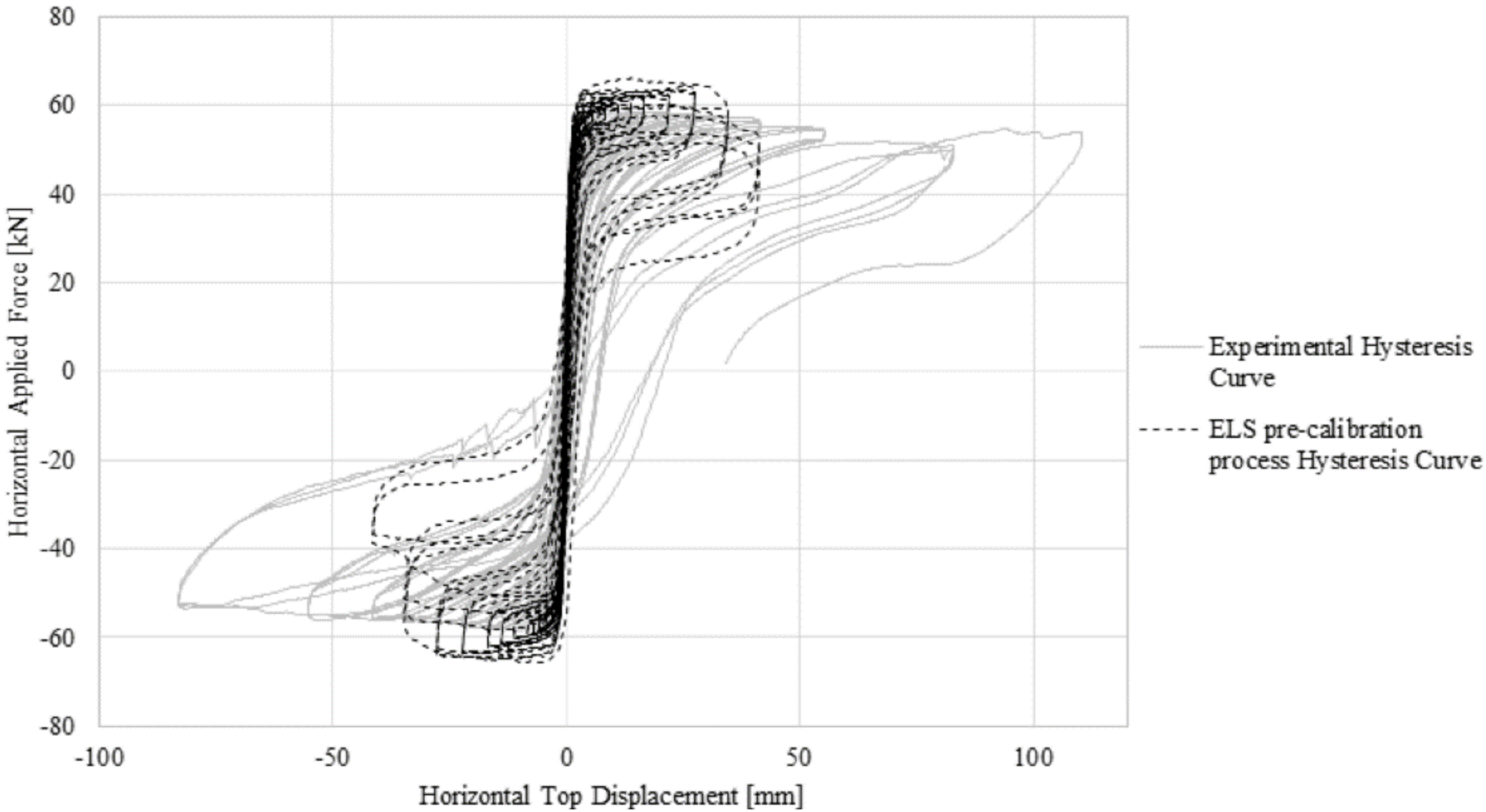

URM walls: example post-diction results

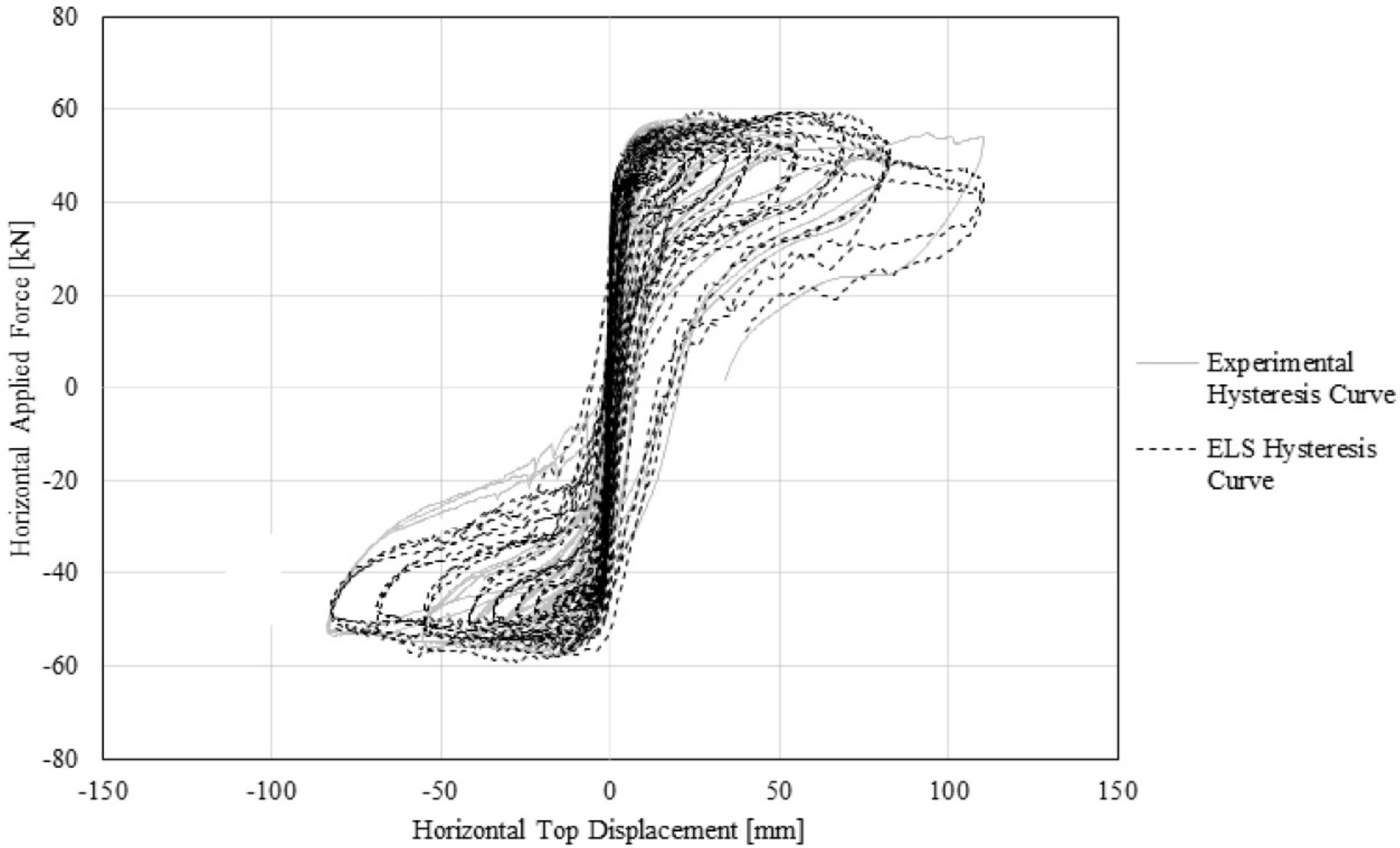

URM walls: cracks pattern modelling

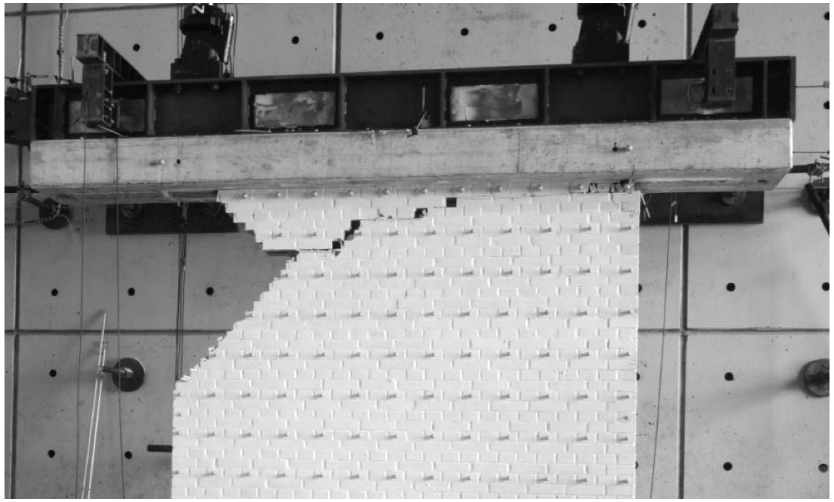

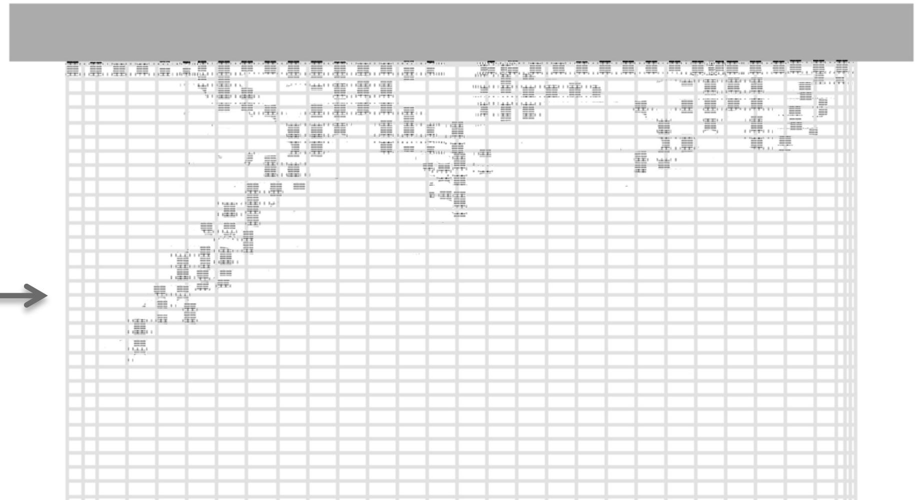

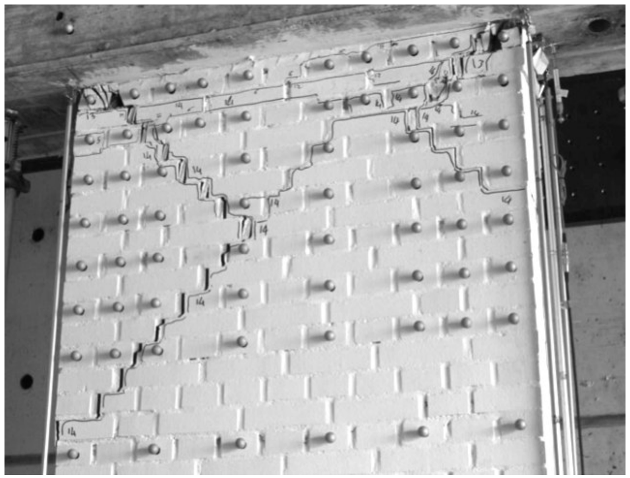

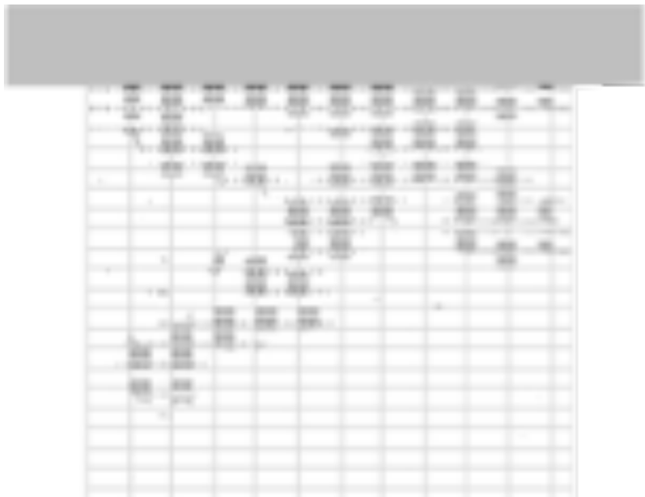

TASK 3: Blind and post-test prediction of Groningen-specific tests of complete structural assemblies

- Check capability in adequately modelling connections between structural elements (e.g. walls, floors, roofs, etc.), mass distribution, load paths, failure modes, shear and displacement capacity, etc.
- 8 full-scale specimens considered
- LS-Dyna, Tremuri, Diana, Abaqus, ELS

Cast-in-place test specimen: blind prediction

(longitudinal direction)

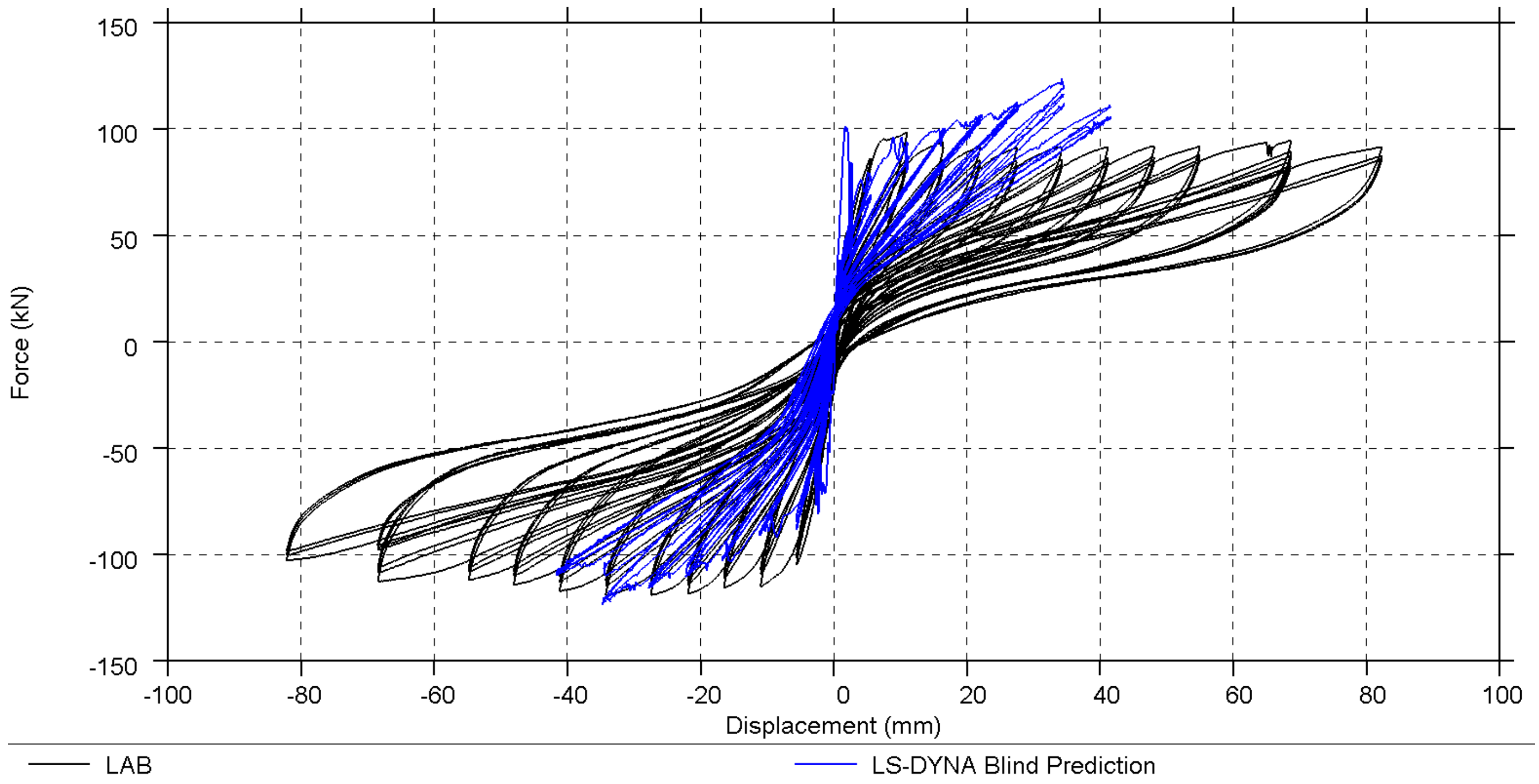

Cast-in-place test specimen: post-diction

(longitudinal direction)

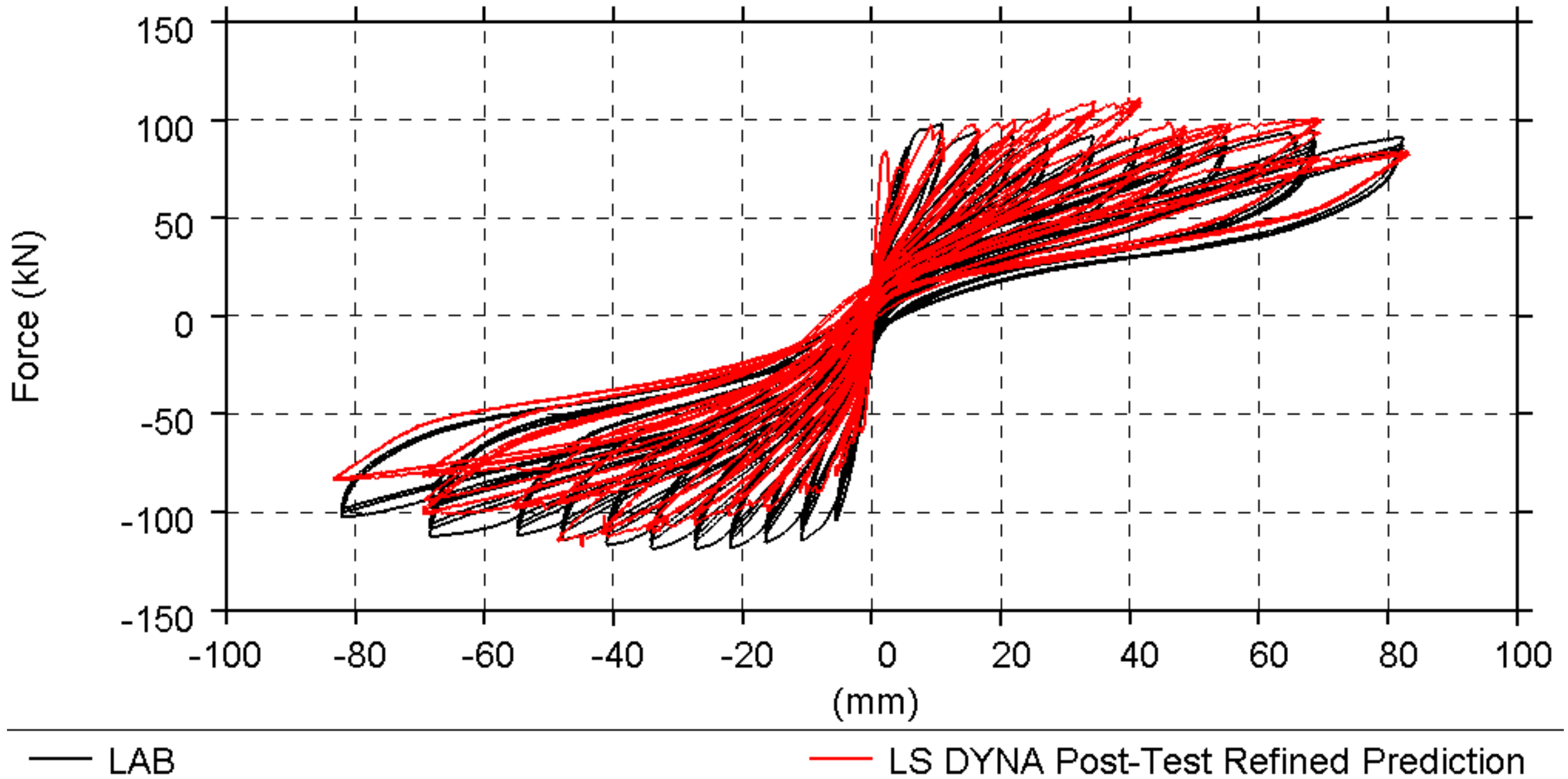

Cast-in-place test specimen: blind prediction
(transverse direction)

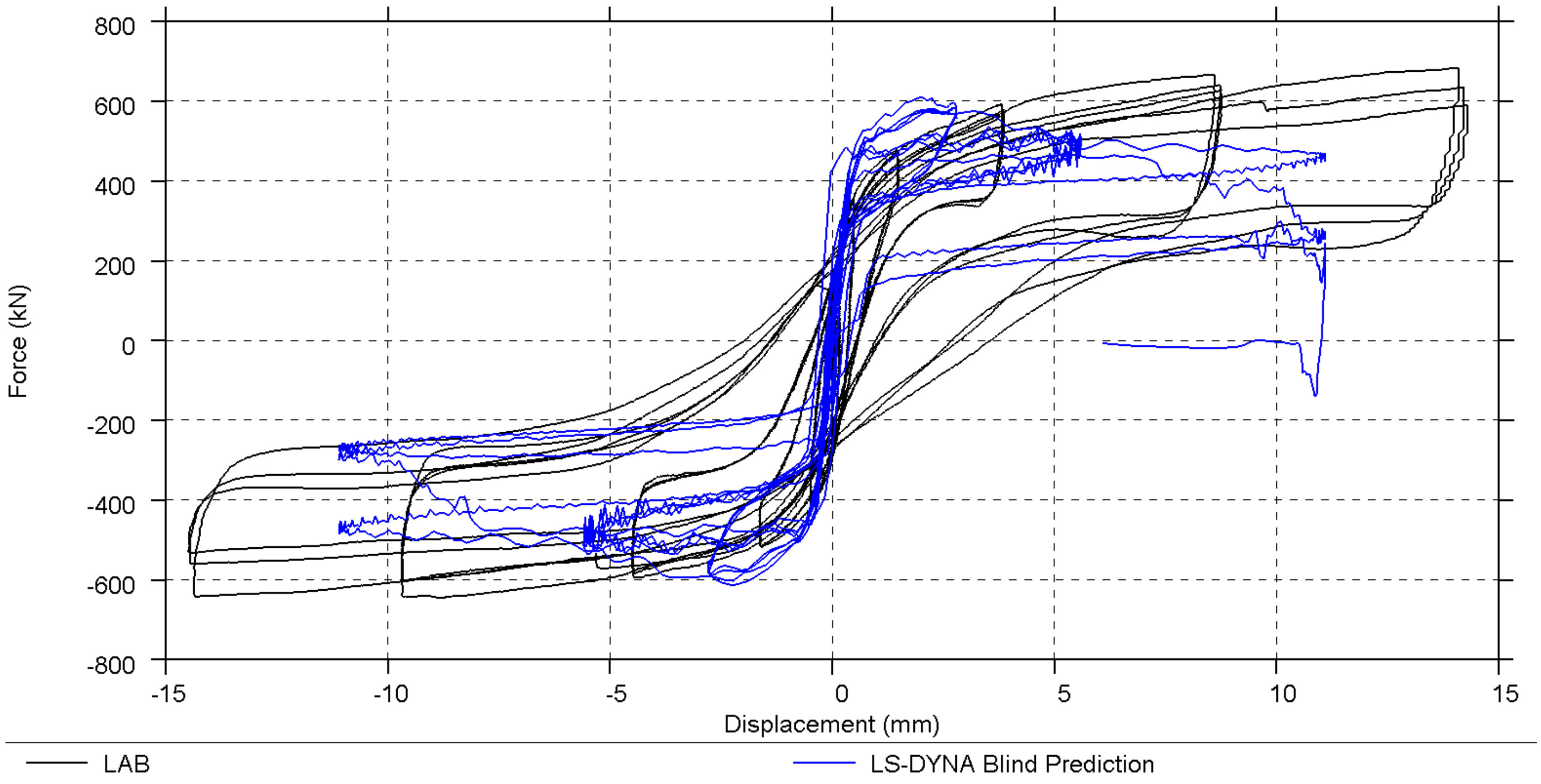

Cast-in-place test specimen: post-diction

(transverse direction)

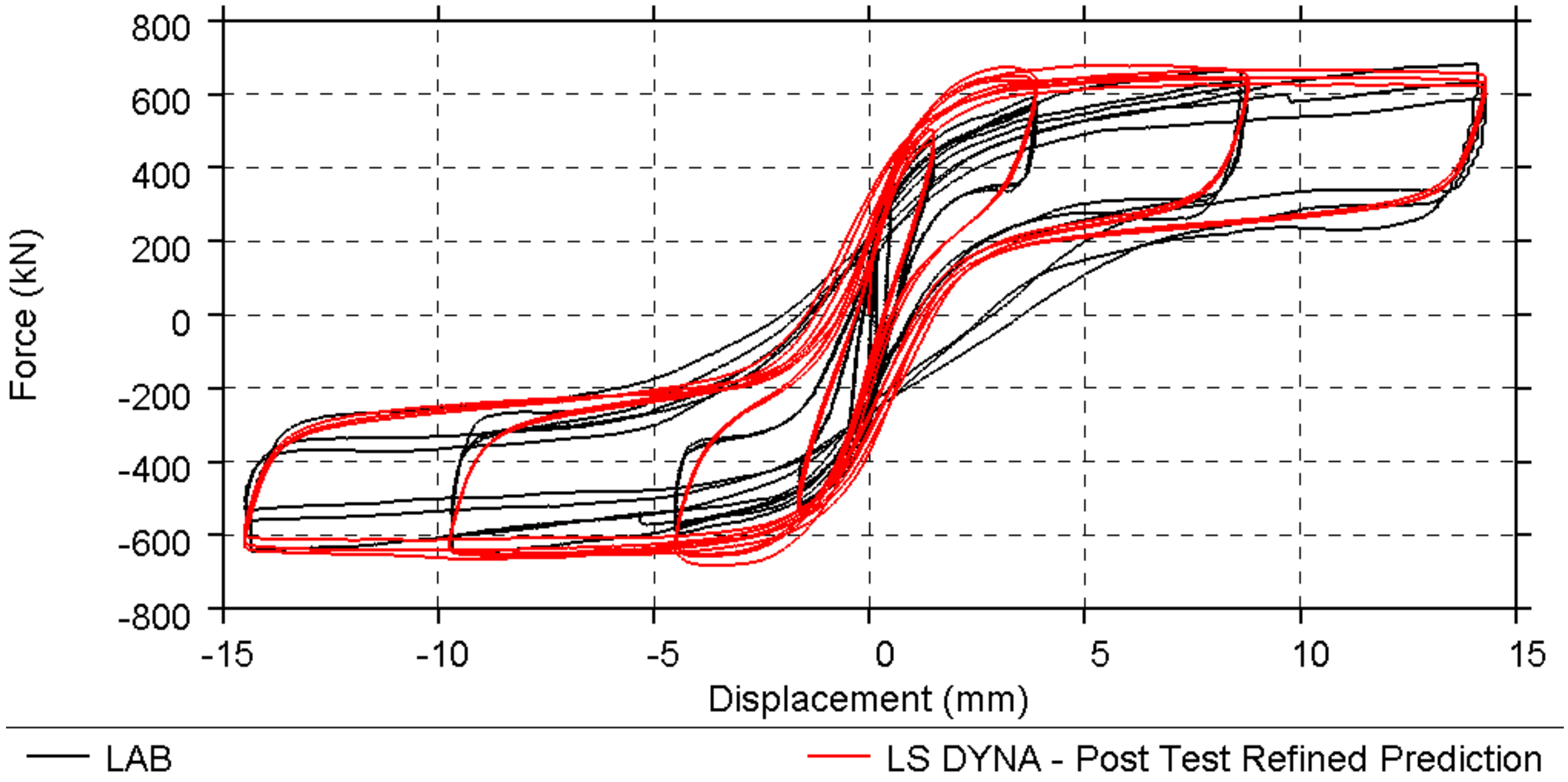

URM detached house specimen: blind prediction

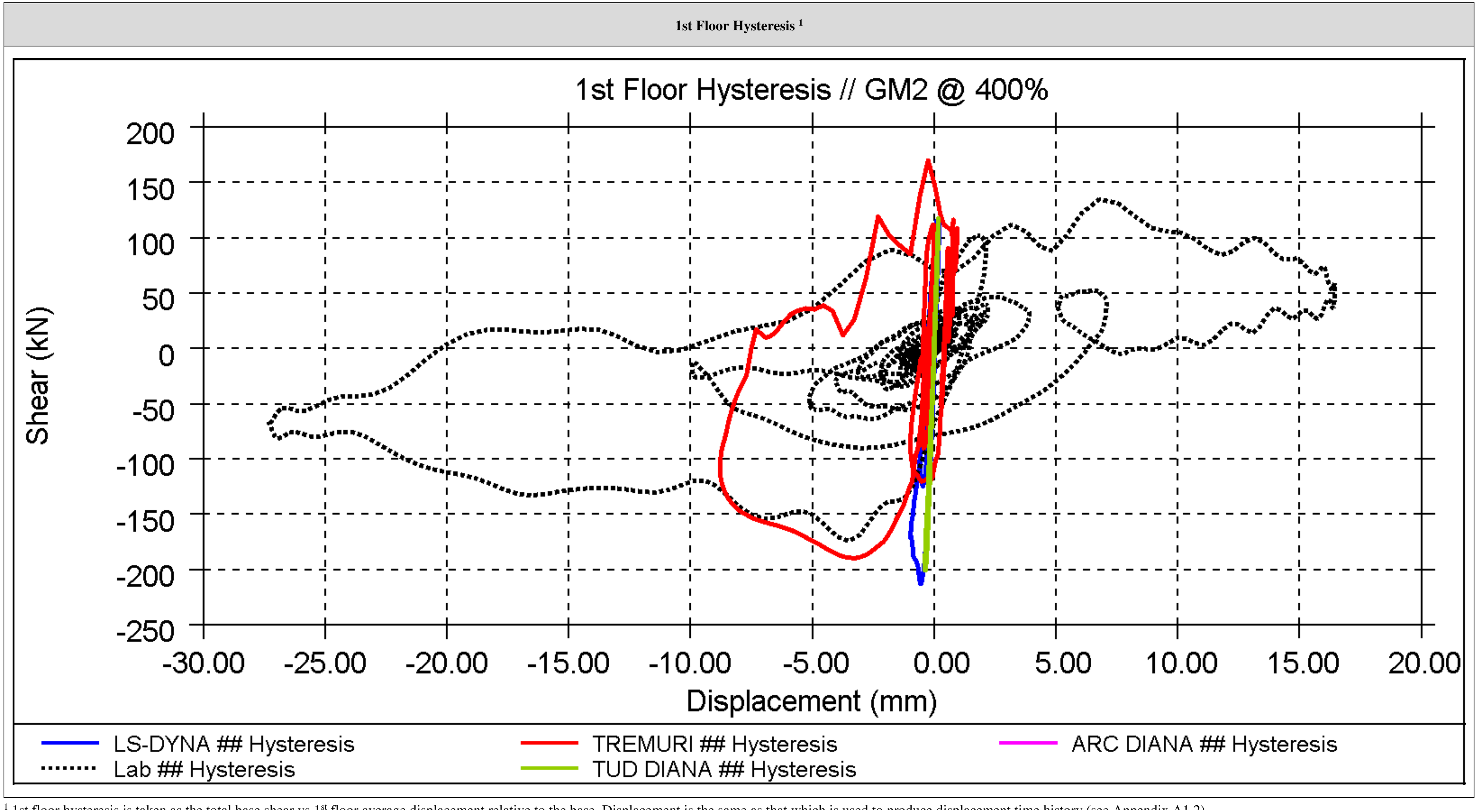

URM detached house specimen: post-diction

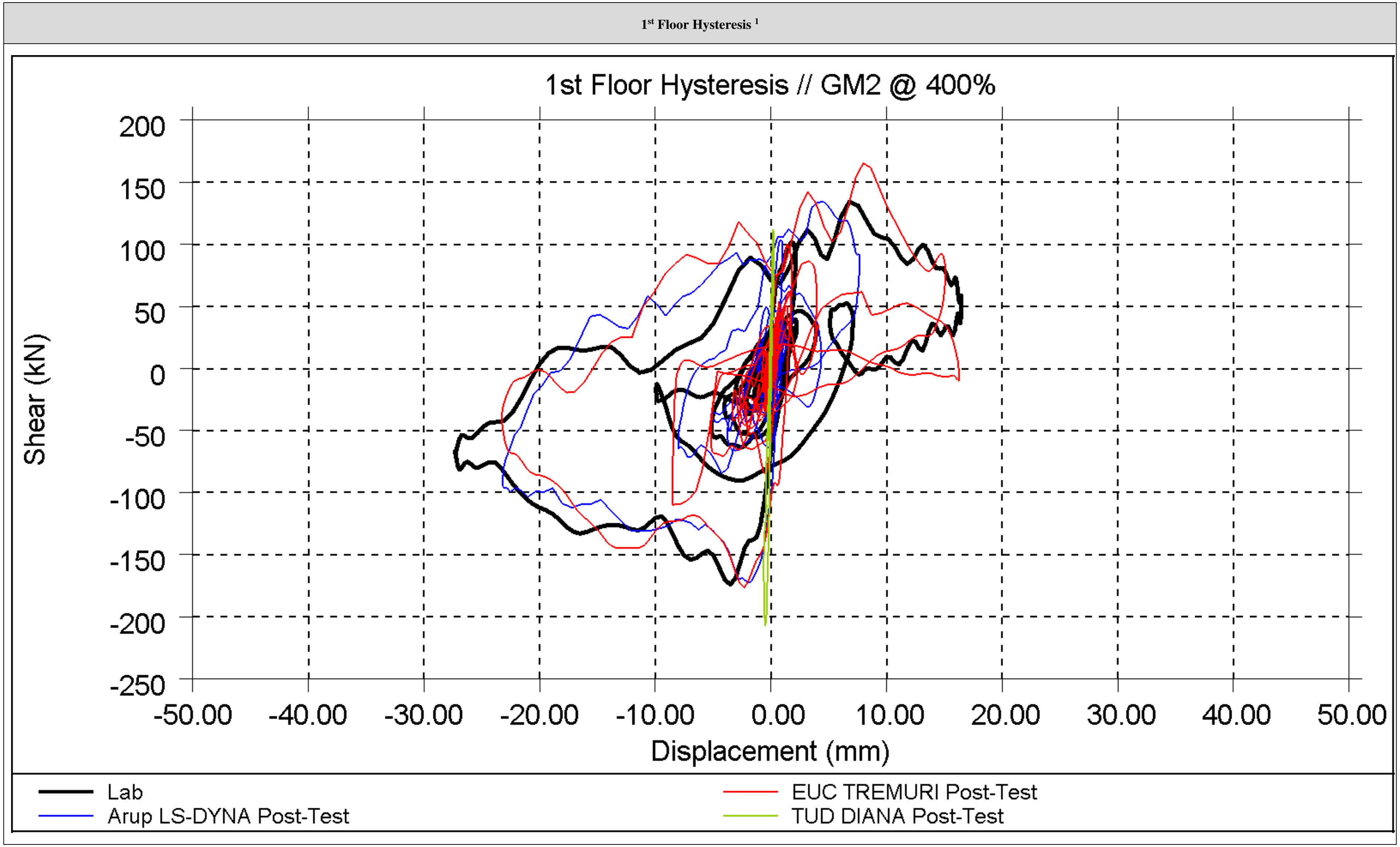

Terraced house collapse testing: blind prediction

Arup / LS-DYNA	Eucentre / TreMuri
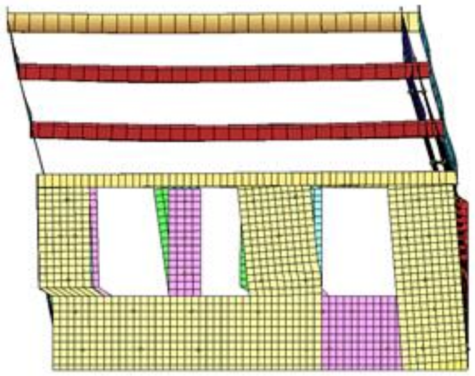 Magnified 5x	NA
TU Delft / DIANA	**Mosayk /ELS**
NA (no collapse)	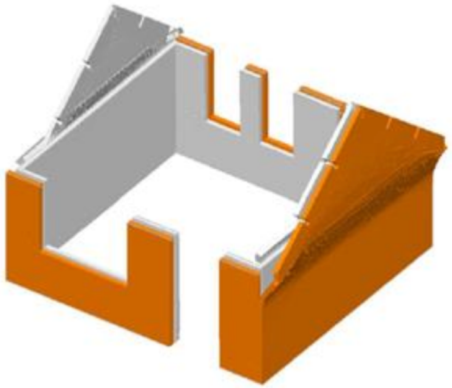 Magnified 2x

Terraced house collapse testing: blind prediction

	LNEC Lab	Arup	Eucentre	TU Delft	Mosayk
Software	---	LS-DYNA	TreMuri	DIANA	ELS
Collapse mechanism	Out-of-plane failure of CaSi [transverse] party wall	Collapse of gables due to out-of-plane rocking	Collapse of roof indicated by relative roof displacement > 100 mm	No collapse	Collapse of gables due to out-of-plane sliding at gable base/top of transverse walls
Collapse Horizontal input motion (PFA)	EQ2-300% (0.63g)	EQ2-400% (0.66g)	EQ2-400% (0.61g)	--- ≥ EQ2-600% (1.03g)	EQ2-250% (0.40g)
Peak floor drift (%) [1]	4.4	0.03[3]	1.4[4]	≥ 0.6	0.9
Peak roof drift (%) [2]	2.0	2.2[3]	2.6[4]	≥ 0.8	3.15
Peak ridge displacement (mm)	170	78[3]	108[4]	≥ 37	124
Base shear (kN)	160	145[3]	124[4]	≥ 188	105

Terraced house collapse testing: post-diction

Arup / LS-DYNA	Eucentre / TreMuri
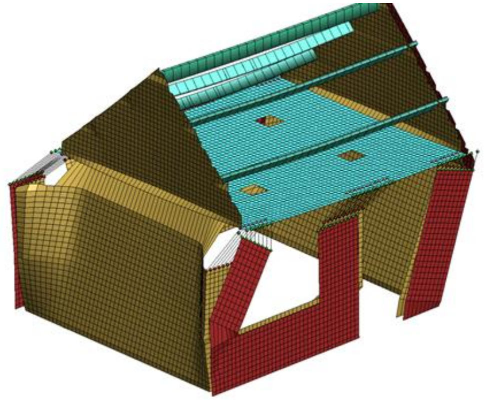 Magnified 10x	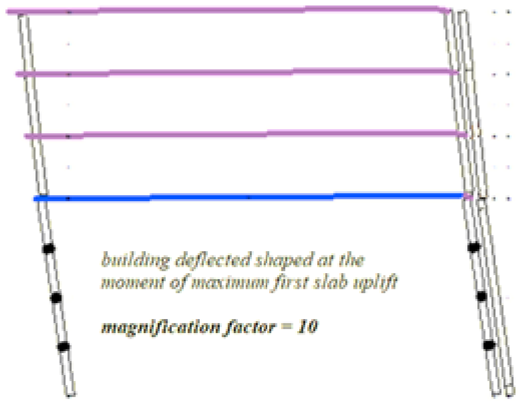
TU Delft / DIANA	**Mosayk /ELS**
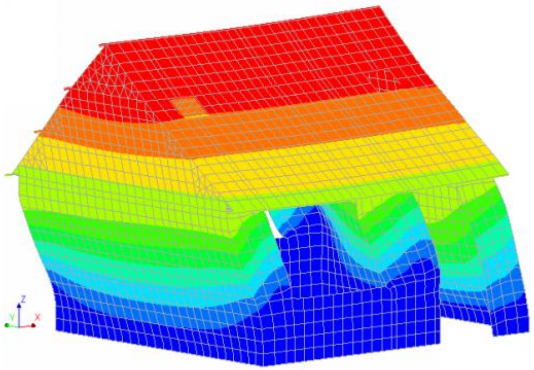 Magnified x25	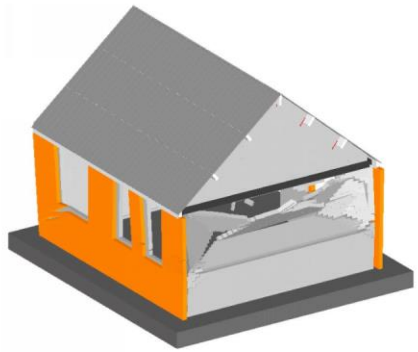 Magnified 2x

Terraced house collapse testing: post-diction

	LNEC Lab	Arup	Eucentre	TU Delft	Mosayk
Software	---	LS-DYNA	TreMuri	DIANA	ELS
Collapse mechanism	Out-of-plane failure of CaSi [transverse] party wall	**No collapse (although visible drop in capacity)**	**No collapse (although visible drop in capacity)**	No collapse	**Out-of-plane failure of CaSi [transverse] party wall**
Collapse Horizontal input motion (PFA)	EQ2-300% (0.63g)	---	---	---	**EQ2-300% (0.63g)**
Peak floor drift (%) [1]	4.4	**4.5**	**2.8**	**≥ 1.2**	**4.8**
Peak roof drift (%) [2]	2.0	1.9	**1.5**	**≥ 0.4**	**3.4**
Peak ridge displacement (mm)	170	**165**	**78**	**≥ 44**	**125**
Base shear (kN)	160	132	136	**≥ 109**	**161**

Terraced house collapse testing: post-diction

Arup / LS-DYNA

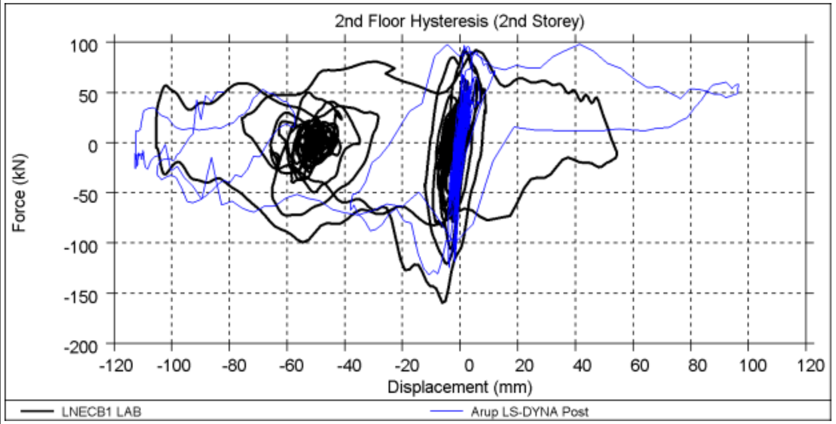

Eucentre TreMuri

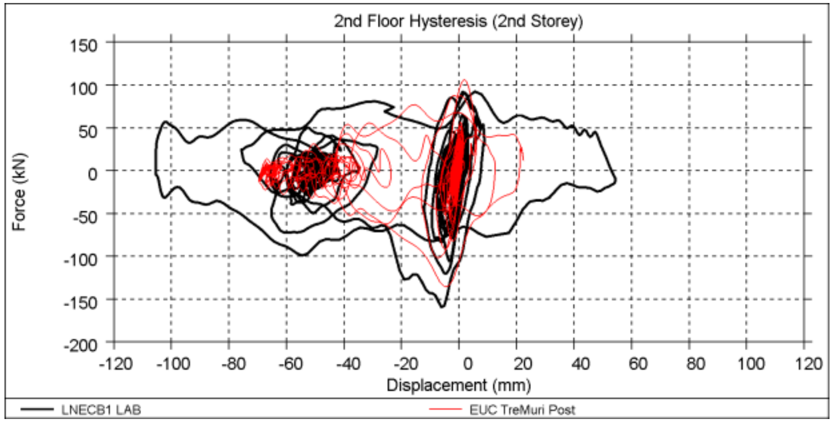

TU Delft / DIANA

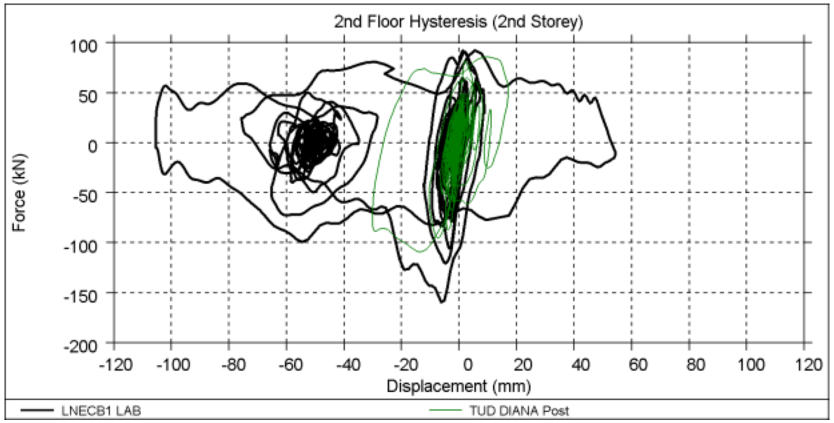

Mosayk / ELS

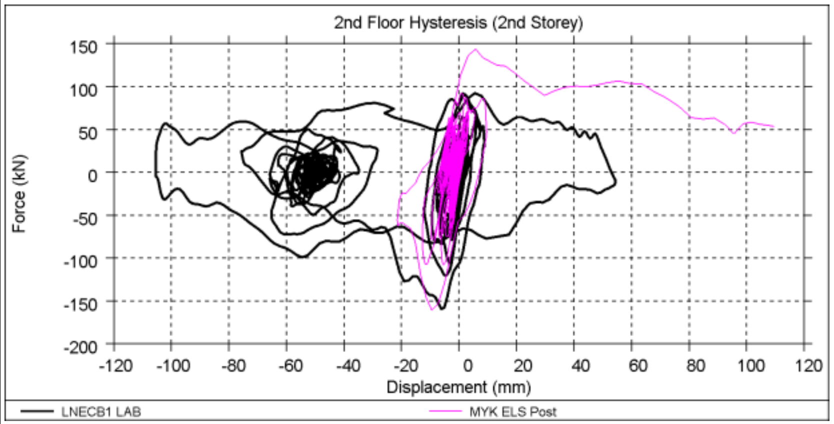

TASK 4: Cross-model validation for actual buildings

- Check modelling assumptions
- 10 existing buildings considered
- LS-Dyna and Tremuri employed (and now also ELS)

Some of the buildings considered in the cross-model validation exercise

Type C house

Julianalaan

Kwelder

Zijlvest

Trial House 1

Trial House 2

Example application of verified numerical tools for collapse mode and debris area estimation

Example building

URM detached house

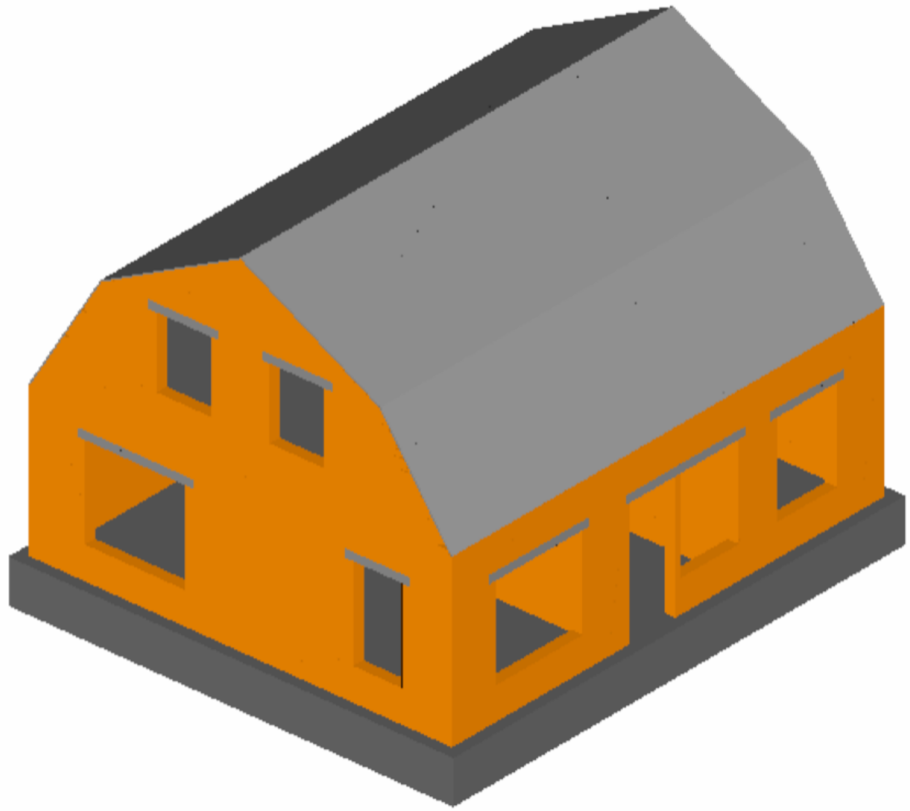

ELS model

Partial collapse modelling (PGA = 0.7g)

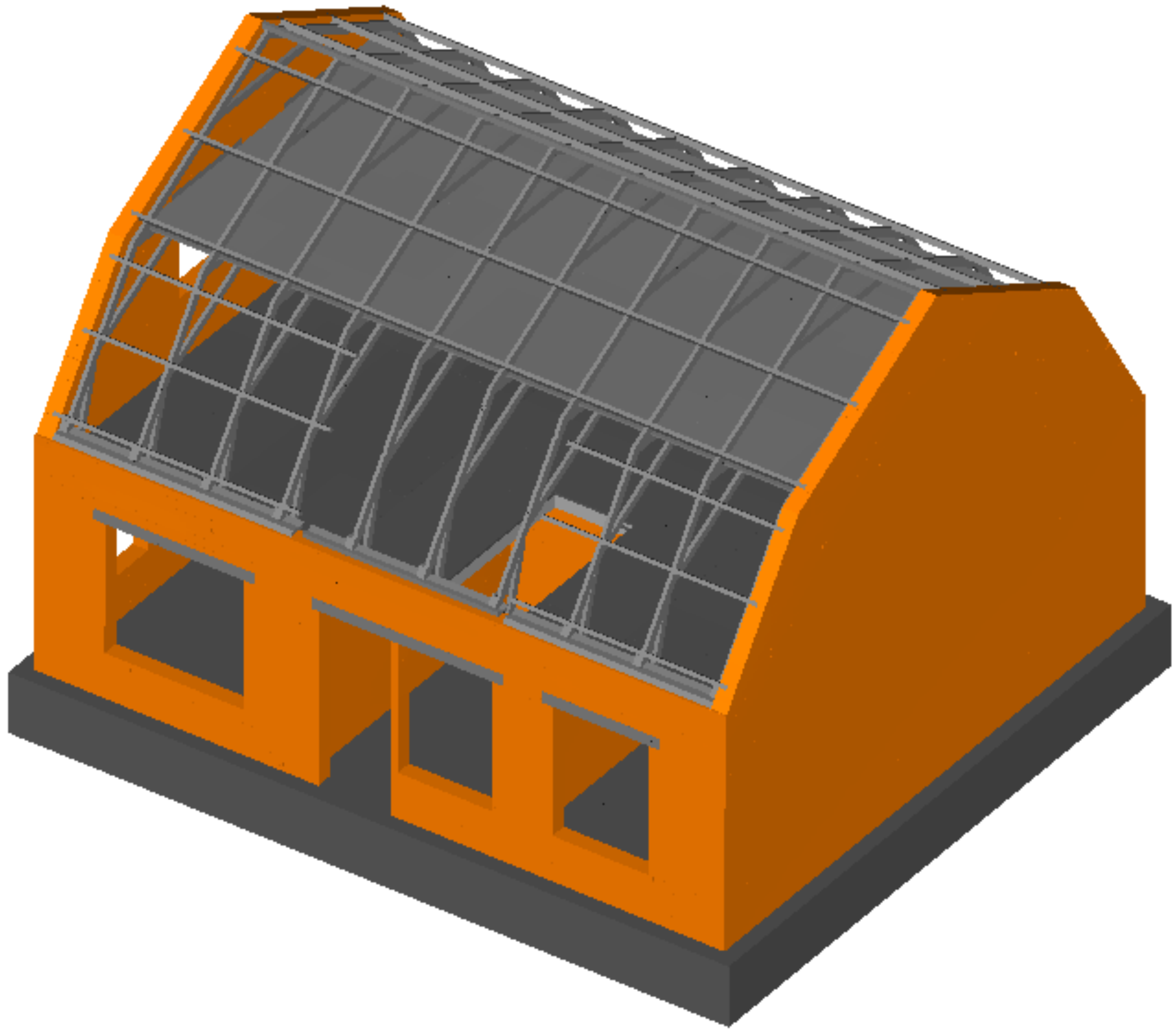

Complete collapse modelling
(three different records with PGA 0.7g to 1.25g)

Assurance Meeting on Exposure, Fragility and Fatality Models
for the Groningen Building Stock

MOSAYK
Modelling and Structural Analysis Konsulting

EUCENTRE
FOR YOUR SAFETY.

UNIVERSITÀ
DI PAVIA

Daniele Malomo, Rui Pinho & Andrea Penna

Numerical modelling of Groningen buildings using the Applied Element Method (AEM)

21-22 February 2018, Schiphol Airport, Amsterdam

Summary

1. Applied Element Method (AEM) overview
2. AEM for masonry structures
3. Modelling of the in-plane cyclic response of URM piers
4. Modelling of the out-of-plane dynamic response of URM piers
5. Numerical results for EUC-BUILD1
6. Numerical results for EUC-BUILD2
7. Numerical results for LNEC-BUILD1
8. Modelling of flexible diaphragms – LNEC-BUILD2
9. Index buildings

Summary

1. Applied Element Method (AEM) overview
2. AEM for masonry structures
3. Modelling of the in-plane cyclic response of URM piers
4. Modelling of the out-of-plane dynamic response of URM piers
5. Numerical results for EUC-BUILD1
6. Numerical results for EUC-BUILD2
7. Numerical results for LNEC-BUILD1
8. Modelling of flexible diaphragms – LNEC-BUILD2
9. Index buildings

1. Applied Element Method (AEM) overview

- Numerical method initially proposed by Meguro & Tagel-Din (2000)
- It could be classified as a rigid body spring model
- Distinct element code according to Cundall & Hart (1992)
  - Automatic detection of element contact/collision
  - Finite displacements and rotations modelling
- Suitable for the modelling of highly nonlinear behaviour, cracks initiation and propagation, element separation and collision
- Implemented in the Extreme Loading for Structures (ELS) commercial software (ASI, 2017)

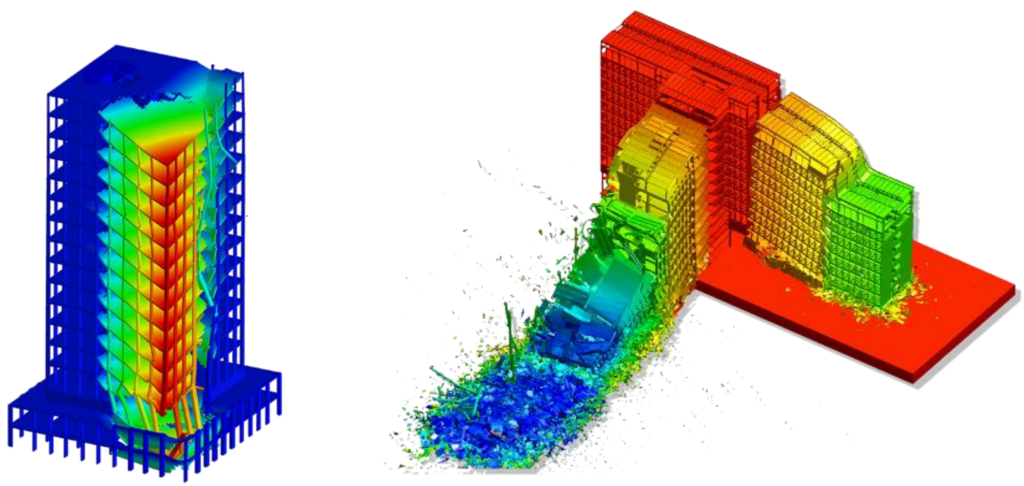

Numerical induced collapse of multi-storeys RC buildings (AEM benchmarks)

1. Applied Element Method (AEM) overview

- Rigid body element assembly
- Rigid blocks connected by linear or nonlinear springs
- Overall behavior deformable
- Normal and Shear springs (K_n, K_s) $k_n = \left(\frac{E\ d\ t_i}{l_i}\right)$, $k_s = \left(\frac{G\ d\ t_i}{l_i}\right)$

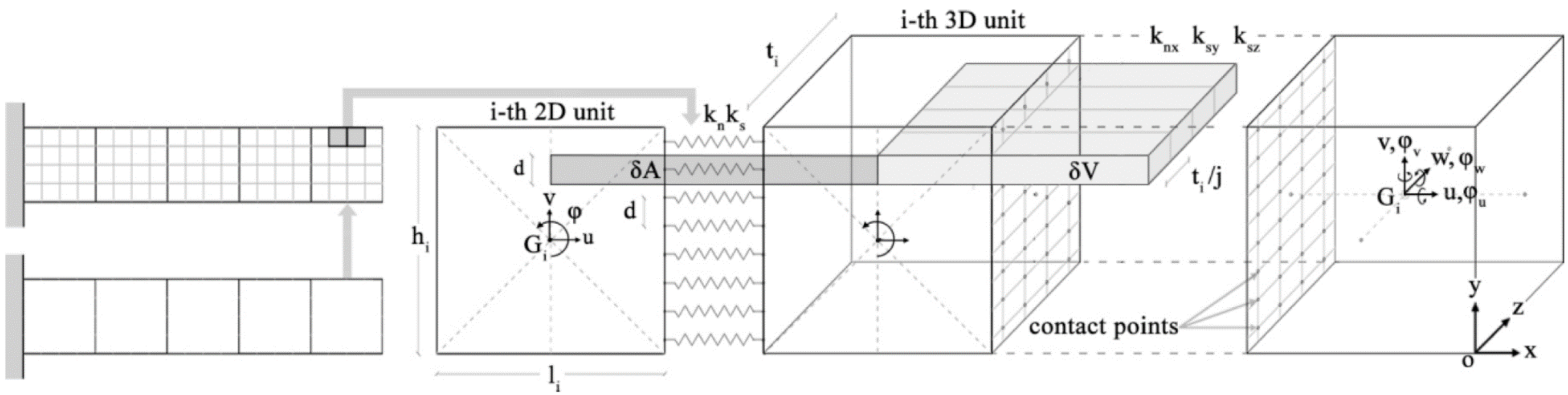

Multi-scale discretisation of a plane element and domain influence
of a set of springs in a 3-D space (Malomo et al., 2018)

Summary

2. AEM for masonry structures

- Simplified micro-modelling approach (as described in Lourenço (2002) [4])
- Dimensionless mortar layers
- Brick and mortar springs in series
- Normal and Shear springs for both brick and mortar (Kbn, Kbs, Kmn, Kms,)

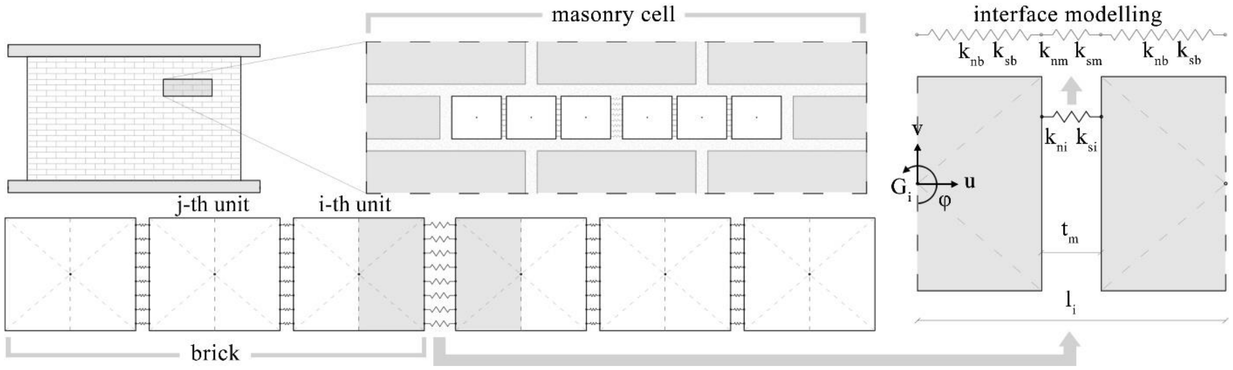

Discretisation of a masonry segment according to the AEM (Malomo et al., 2018)

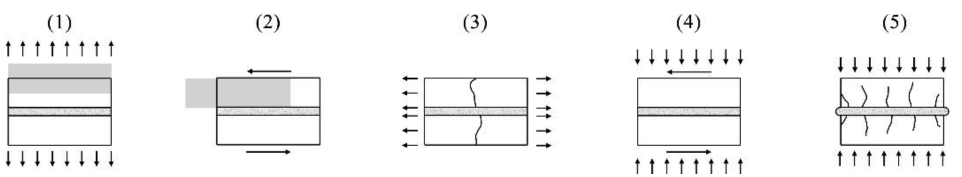

Typical brick-mortar failure mechanisms (Lourenco et al., 1995)

1. Joint cracking (Km)
2. Sliding (Km)
3. Cracking of unit direct tension (Kb)
4. Shear-compression failure (Km, Kb)
5. Brick splitting (Km, Kb)

2. AEM for masonry structures

- Simplified micro-modelling approach (as described in Lourenço (2002))
- Specific mechanical properties of both brick and mortar are needed
- Derivation of material properties through empirical formulae (if no sufficient experimental parameters are available)
- Simplified composite interface cap model (Lourenço et al., 1995)
- Mohr-Coulomb shear slip failure
- Cohesion and bond degradation
- Interlocking phenomena modelling

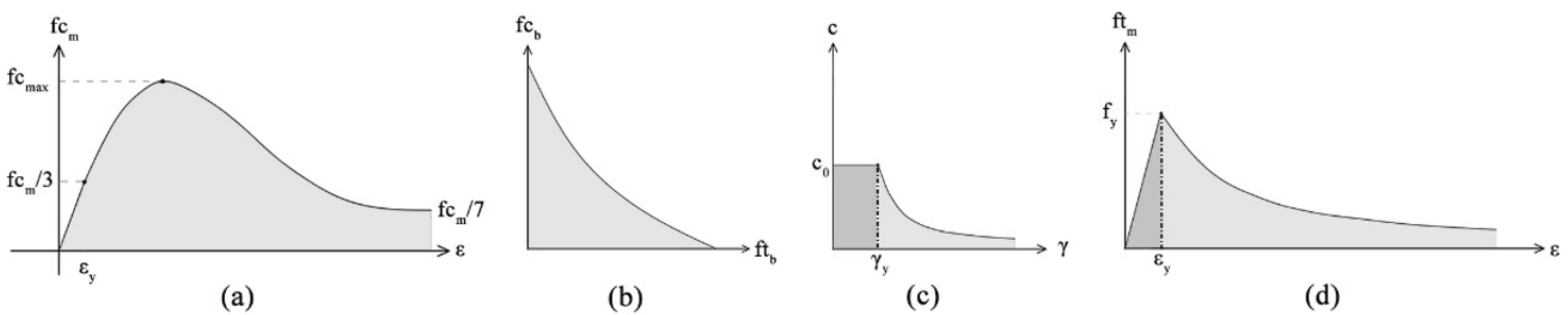

Compressive hardening/softening (a), Khoo-Hendry strength envelope (b) cohesion (c) and bond degradation (d) (Malomo et al., 2018)

Malomo D, Pinho R, Penna A (2018). Using the Applied Element Method for Modelling Calcium-Silicate Brick Masonry Subjected to In-Plane Cyclic Loading, *Earthquake Engineering & Structural Dynamics* (in press)

MOSAYK Modelling and Structural Analysis Konsulting

Summary

MOSAYK
Modelling and Structural Analysis Konsulting

3. Modelling of the in-plane cyclic response of URM piers

Brief description of tests and specimens:

- A total of 3 Calcium Silicate (CS) and 5 Clay (CL) full-scale brick masonry specimens were subjected to cyclic shear-compression loading protocols (Graziotti et al., 2015)
- Different aspect ratios and vertical overburden were considered, as summarised below:

CS

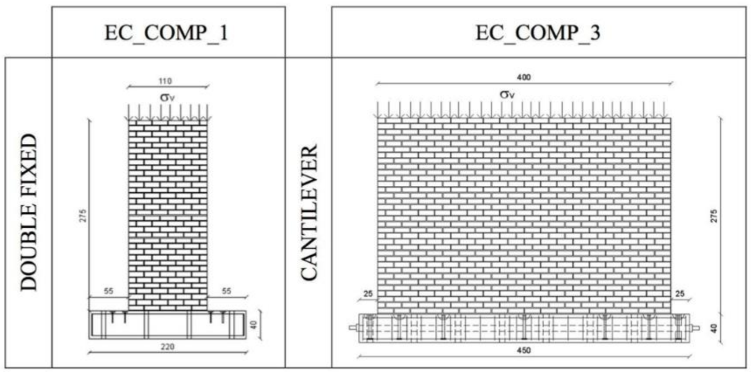

Main Geometric Data	
Brick dimensions [mm]	
212x103x71	
Mortar layer thickness [mm]	
≃1	
Overburden σv [MPa]	
Comp1	Comp3
0.52	0.30

Single-wyhte
Stretcher bond

CL

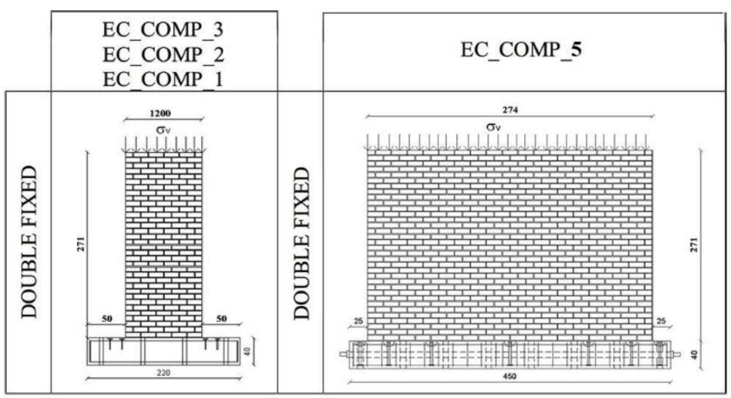

Main Geometric Data	
Brick dimensions [mm]	
208x104x50	
Mortar layer thickness [mm]	
≃1	
Overburden σv [MPa]	
Comp1	Comp2
0.52	1.20
Comp3	Comp5
0.86	0.30

Double-wyhte
Dutch cross bond

3. Modelling of the in-plane cyclic response of URM piers

Brief description of tests and specimens:

- A total of 3 Calcium Silicate (CS) and 5 Clay (CL) full-scale brick masonry specimens were subjected to cyclic shear-compression loading protocols (Graziotti et al., 2015)
- Different aspect ratios and vertical overburden were considered, as depicted below:

CS

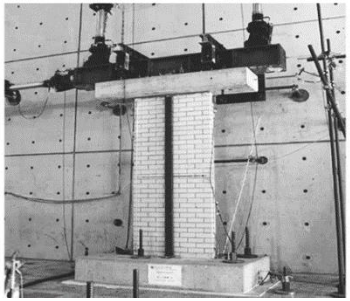

CS-Comp-1-2

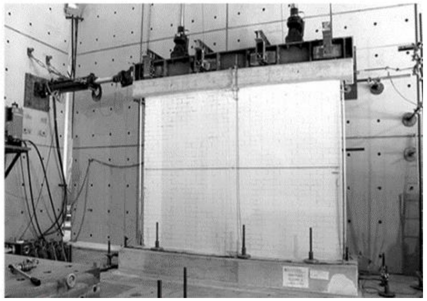

CS-Comp-3

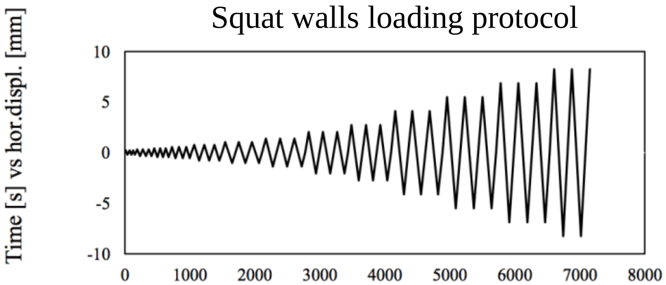

CL

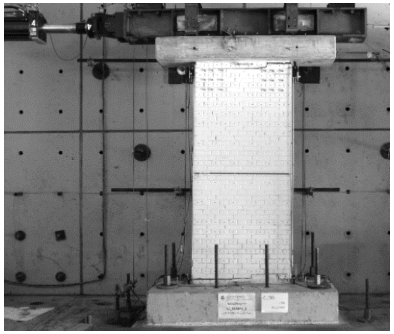

CL-Comp-1-2-3

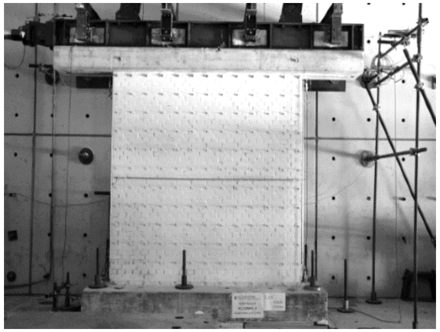

CL-Comp-4-5

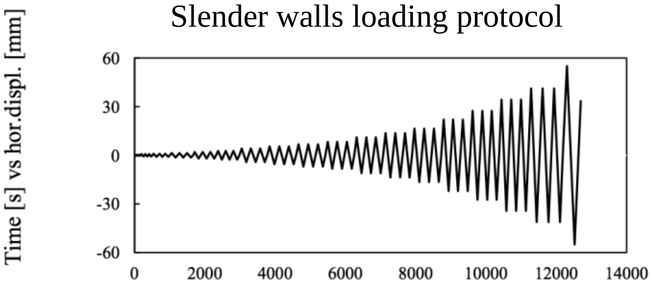

3. Modelling of the in-plane cyclic response of URM piers

Modelling assumptions:

- Actual “brick-texture” meshing for masonry
- Each brick was discretized in two sub-elements, allowing the development flexural and shear cracks in the middle
- The properties of mortar and bricks were inferred by means of empirical formulae (Brooks et al. 1998; Matysek et al. 1996; Cieleski et al. 1999; Uniform Building Code, 1991)
- The loading and foundation RC beams were explicitly modelled and discretised using a coarse mesh since according to the AEM no transition mesh elements are needed, as depicted below:

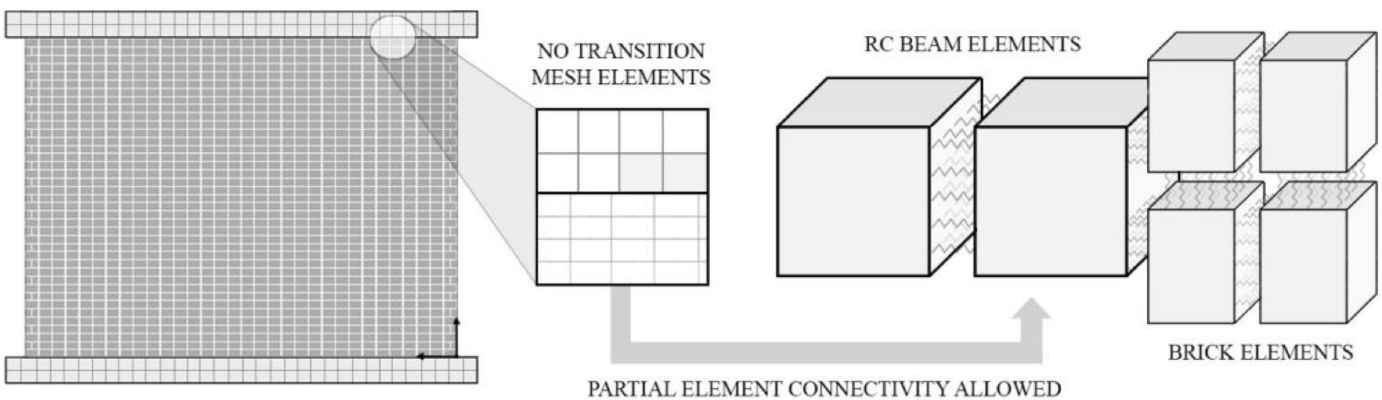

AEM mesh discretisation approach (Malomo et al., 2018)

3. Modelling of the in-plane cyclic response of URM piers

Calcium silicate brick masonry walls - comparisons with experimental results

CS-Comp-1

Fixed-fixed

σ=0.52 MPa

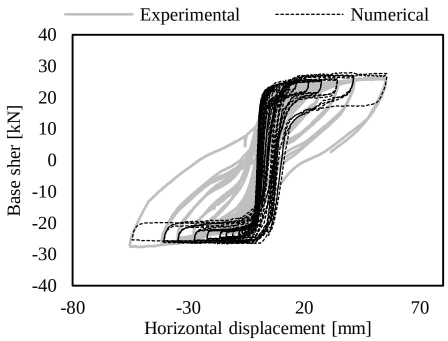

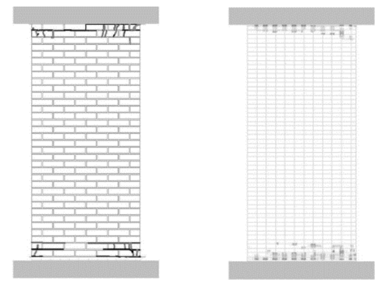

Experimental Numerical

CS-Comp-2

Fixed-fixed

σ=70 MPa

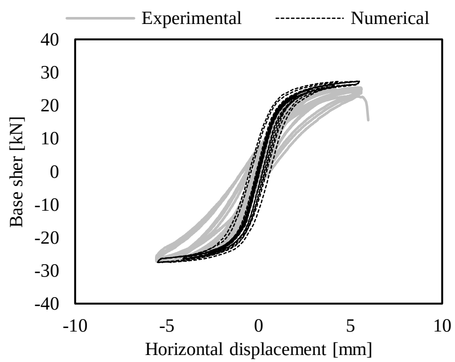

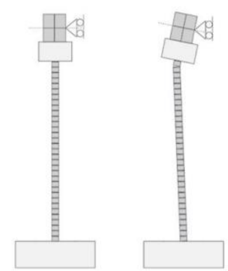

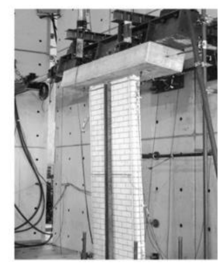

- A spurious OOP mechanism occurred after few cycles and the test was stopped
- No relevant damage occurred up to OOP failure

CS-Comp-3

Cantilevered

σ=0.30 MPa

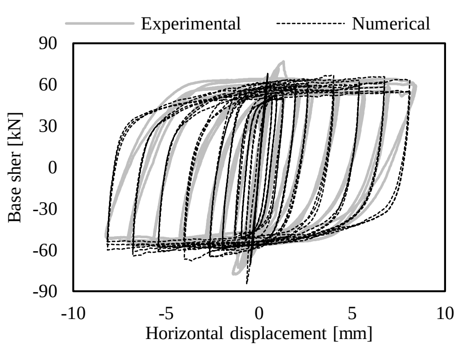

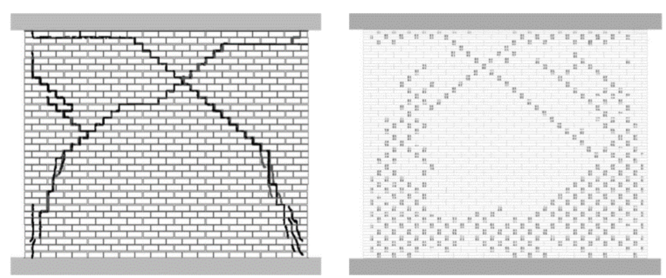

Experimental Numerical

3. Modelling of the in-plane cyclic response of URM piers

Clay brick masonry walls - comparisons with experimental results

CL-Comp-1

Fixed-fixed

σ=0.52 MPa

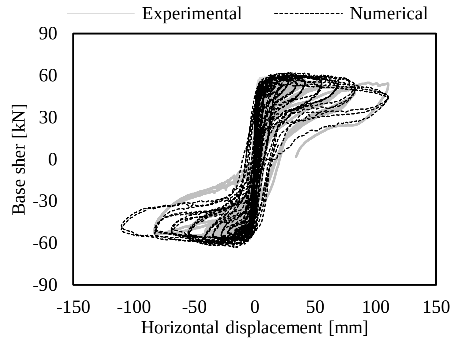

Experimental Numerical

CL-Comp-2

Fixed-fixed

σ=1.20 MPa

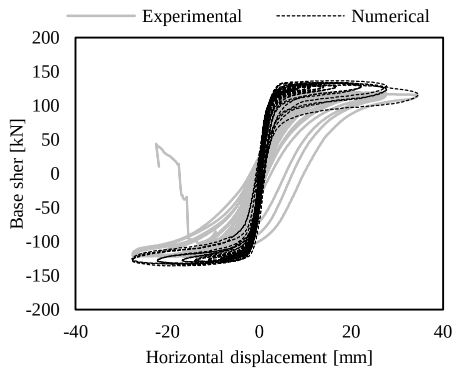

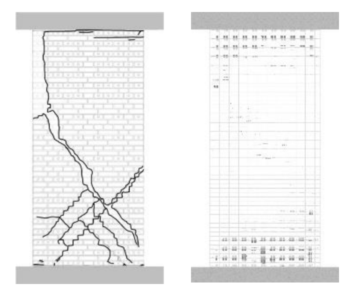

Experimental Numerical

CL-Comp-3

Fixed-fixed

σ=0.86 MPa

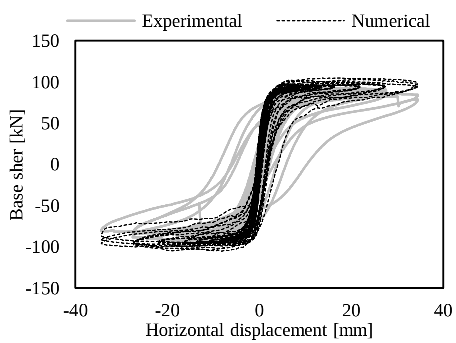

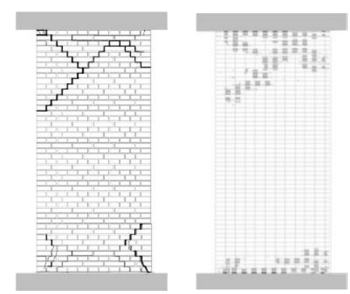

Experimental Numerical

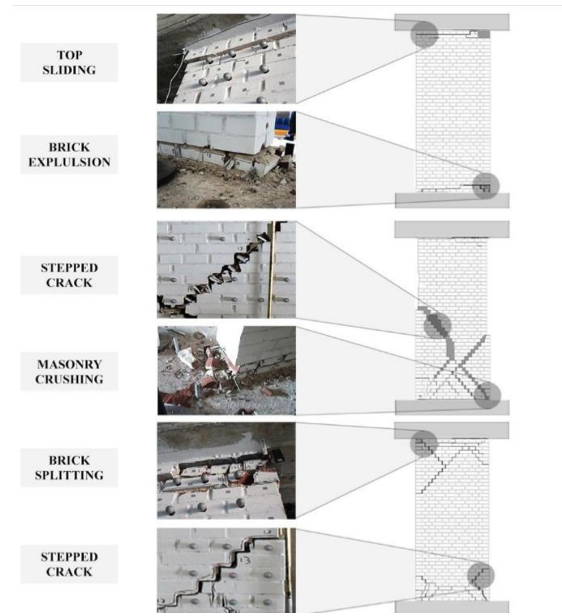

3. Modelling of the in-plane cyclic response of URM piers

Clay brick masonry walls - comparisons with experimental results

CL-Comp-5

Fixed-fixed

σ=0.30 MPa

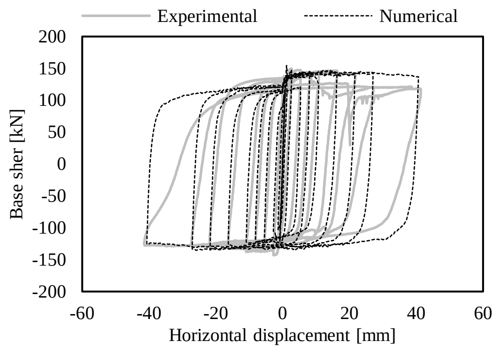

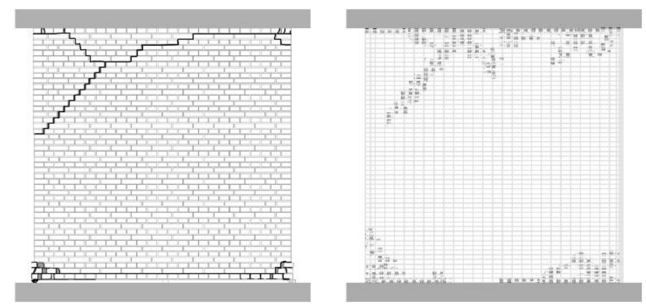

Experimental Numerical

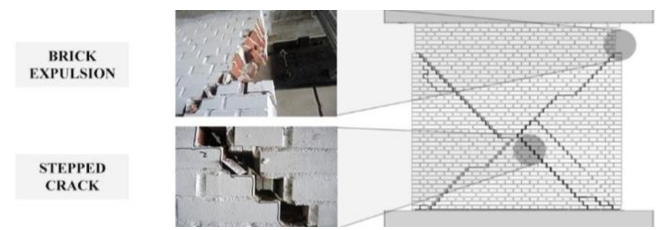

Final considerations:

- The AEM models adequately captured the in-plane response of both CS and CL specimens
- The crack patterns have been reproduced faithfully in most of the cases
- Acceptable numerical results were obtained without altering the experimental material properties
- The toe-crushing mechanism was not captured satisfactorily, leading to an underestimation of the dissipated energy especially for the case of slender piers

Summary

1. Applied Element Method (AEM) overview
2. AEM for masonry structures
3. Modelling of the in-plane cyclic response of URM piers
4. Modelling of the out-of-plane dynamic response of URM piers
5. Numerical results for EUC-BUILD1
6. Numerical results for EUC-BUILD2
7. Numerical results for LNEC-BUILD1
8. Modelling of flexible diaphragms – LNEC-BUILD2
9. Index buildings

4. Modelling of the out-of-plane dynamic response of URM piers

Brief description of tests and specimens:

- Two different types of full-scale specimens (i.e. CS single leaf and cavity walls) were tested dynamically, in their out-of-plane direction at the Eucentre laboratory in Pavia, Italy (Graziotti et al. 2015)
- A different distribution of ties was employed for the cavity walls
- Different types of ground motions were selected, scaled, and incrementally imposed to the full-scale wall specimens (starting from Gr1), where:
    - Gr1: Groningen record (Crowley et al. 2015), representing a potentially realistic excitation of a wall located at the ground floor.
    - Gr2: Floor accelerograms obtained with the software TREMURI, representing a possible dynamic excitation of a wall located at first floor.
    - RWA: pulse excitation with a frequency of 4 Hz.

CS_Comp4 CAV_Comp5 CAV_Comp6 CAV_Comp7

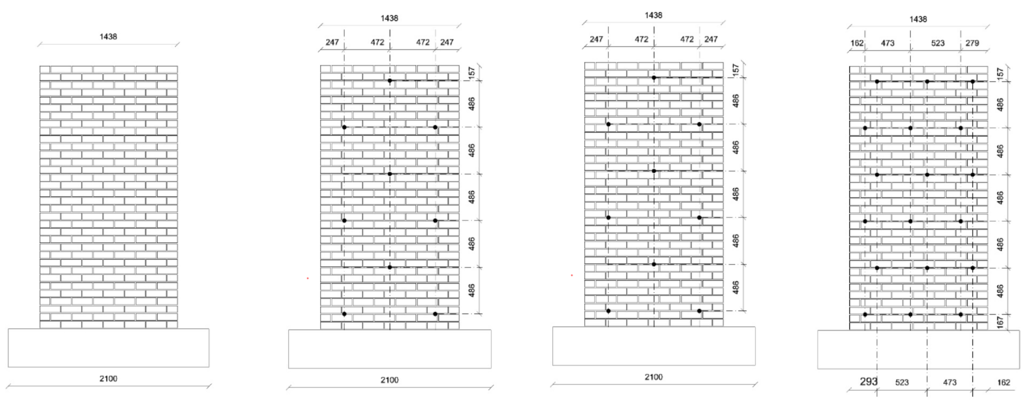

4. Modelling of the out-of-plane dynamic response of URM piers

Brief description of tests and specimens:

- At the bottom of each wall, a reinforced concrete (RC) foundation was anchored to the shake-table with screwed steel rods
- A rigid steel beam connected the CS wall to a rigid steal frame anchored to the shake-table, assuring a negligible amplification in height of the seismic input applied to the shake-table

CS_Comp4

CAV_Comp5

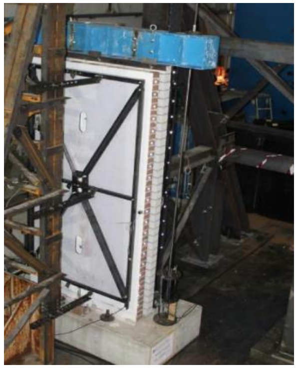

Test-rig setup

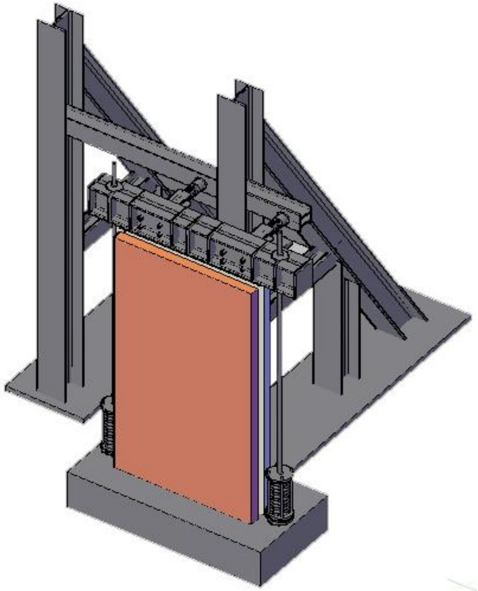

Collapse of CAV_Comp5

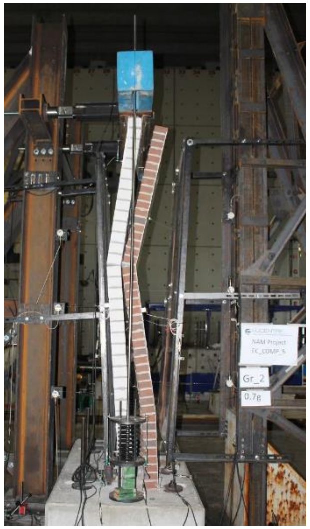

CAV_Comp6

CAV_Comp7

4. Modelling of the out-of-plane dynamic response of URM piers

Modelling assumptions:

- In the ELS framework, a given seismic input can be assigned only if an element is fully fixed. Thus, a slab was seismically excited and the dynamic inputs were consequently transmitted by a rigid link connected to the top beam with negligible amplification
- The vertical compression was assured by two pre-stressed link connecting the top and the foundation beam
- The steel ties were modelled as 3D beam elements with bilinear behaviour, with an ultimate tensile strength equal to the experimentally-recorded one, i.e. 4.3 kN. Moreover, in order to avoid interpenetration between elements, the idealisations reported above were adopted:

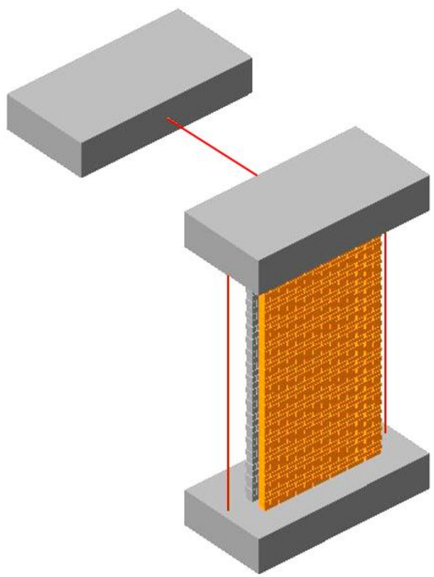

AEM model (Mosayk, 2017a)

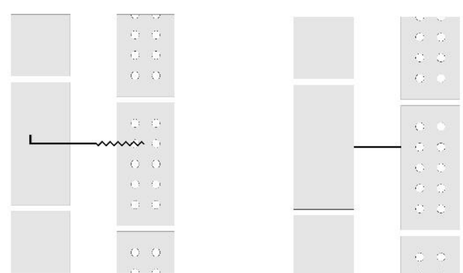

(a) (b)

Experimental cavity wall connector (a) and numerical idealisation (b)

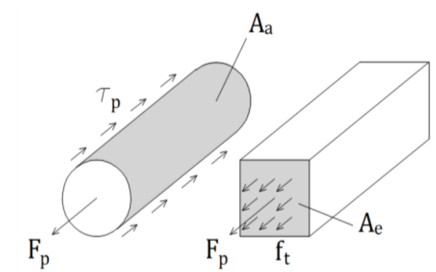

(a) (b)

Experimental stresses along the cavity wall connector (a) and numerical idealisation (b)

4. Modelling of the out-of-plane dynamic response of URM piers

Numerical results:

- The following plot represents a comparison between the experimental (in **grey**) horizontal displacement at the ridge beam [mm] versus base shear [kN] and their numerical counterparts (in **black**)

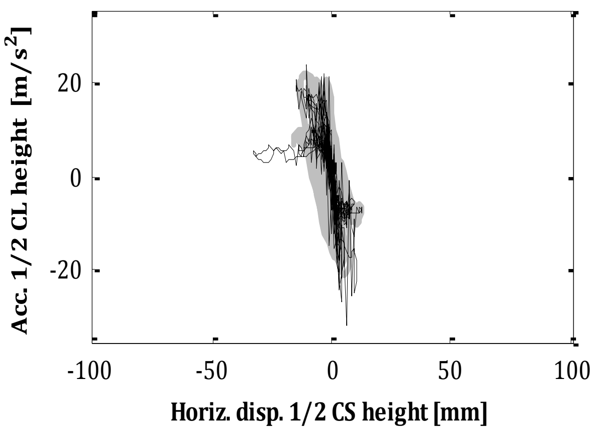

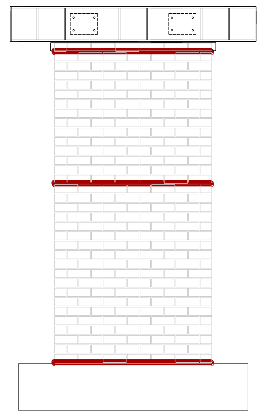

CS-Comp-4

Fixed-fixed

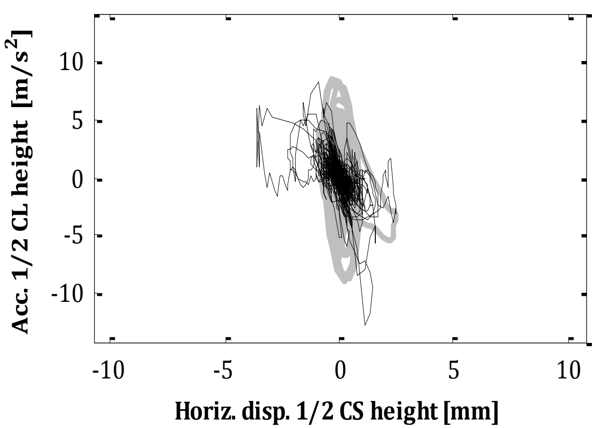

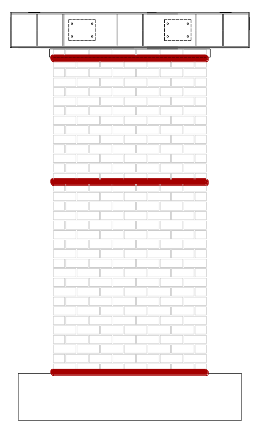

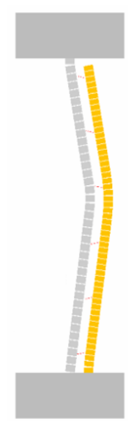

CAV-Comp-5

CS Fixed-Fixed

CL Cantilevered

4. Modelling of the out-of-plane dynamic response of URM piers

Numerical results:

- The following plot represents a comparison between the experimental (in **grey**) horizontal displacement at the ridge beam [mm] versus base shear [kN] and their numerical counterparts (in **black**)

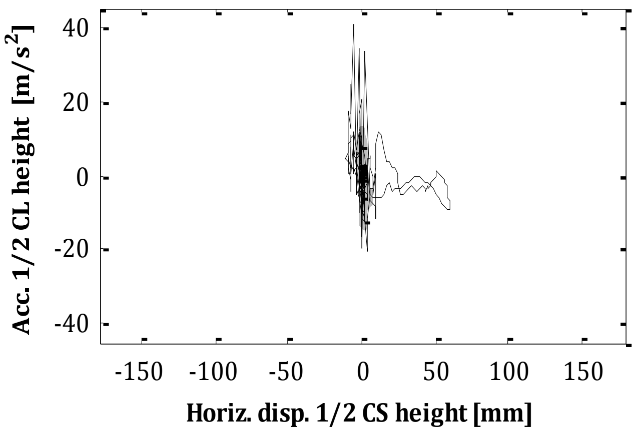

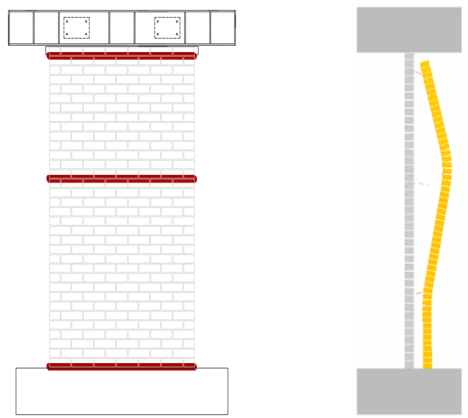

CAV-Comp-6

CS Fixed-fixed

CL Cantilevered

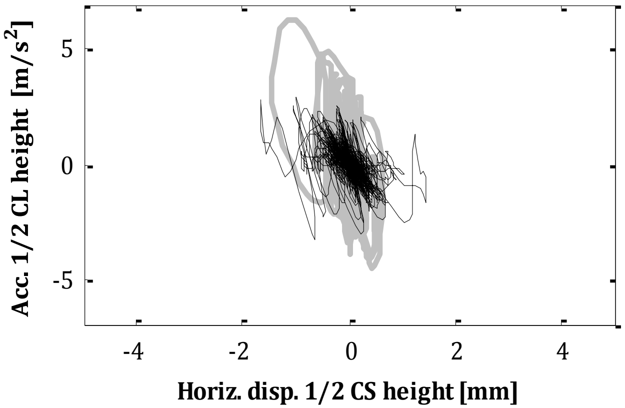

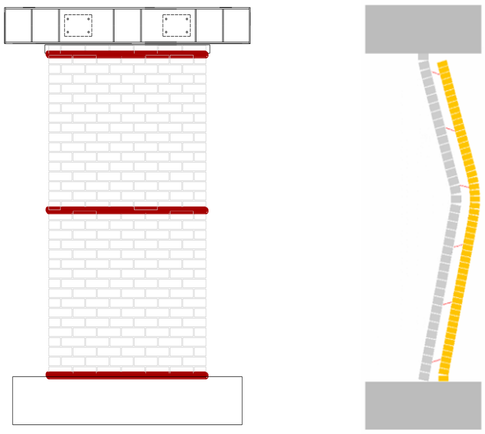

CAV-Comp-7

CS Fixed-Fixed

CL Cantilevered

4. Modelling of the out-of-plane dynamic response of URM piers

Final considerations:

- Out-of-plane one-way bending of masonry walls is a very brittle response mechanism, hence the comparisons previously depicted can be considered as encouraging, with the numerical models producing results that appear to be within the range of their experimental counterparts
- It is worth noting that such numerical results were obtained without altering the experimental material properties (i.e. the latter has been directly employed for the analyses)
- The positive impression on the numerical vs. experimental comparison reported above is further confirmed by the comparisons shown in Table 4 below, where it can be observed that the AEM models estimated values of collapse ground acceleration that feature differences with respect to the tests observations in the range of 7-15%

Specimen Name	Experimental Failure PGA [g]	Numerical Failure PGA [g]
CS-COMP4	0.85	0.96
CAV-COMP5	0.65	0.60
CAV-COMP6	1.17	0.97
CAV-COMP7	0.72	0.66

MOSAYK Modelling and Structural Analysis Konsulting

Summary

1. Applied Element Method (AEM) overview
2. AEM for masonry structures
3. Modelling of the in-plane cyclic response of URM piers
4. Modelling of the out-of-plane dynamic response of URM piers
5. Numerical results for EUC-BUILD1
6. Numerical results for EUC-BUILD2
7. Numerical results for LNEC-BUILD1
8. Modelling of flexible diaphragms – LNEC-BUILD2
9. Index buildings

5. Numerical results for EUC-BUILD1

Brief description of test and specimen:

- The test-house was a full-scale two-storey building, with a timber roof and RC slabs, 5.82 m long, 5.46 m wide and 7.76 m high with a total mass of 56.4 tons
- The walls, supported by a steel-concrete composite foundation, consisted of two URM leaves
- The inner loadbearing leaf was made of CS bricks whereas the external leaf was a clay brick CL veneer without any loadbearing function

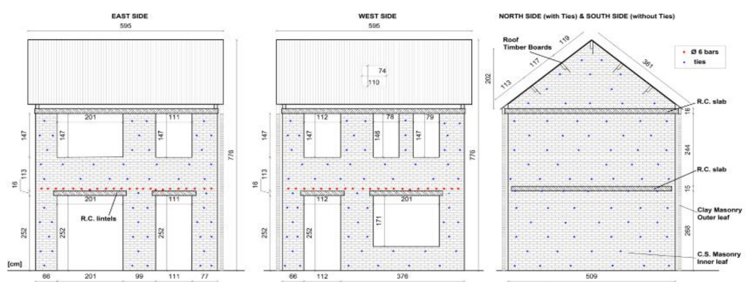

Elevation views of the specimen’s CS inner leaf (Graziotti et al., 2015)

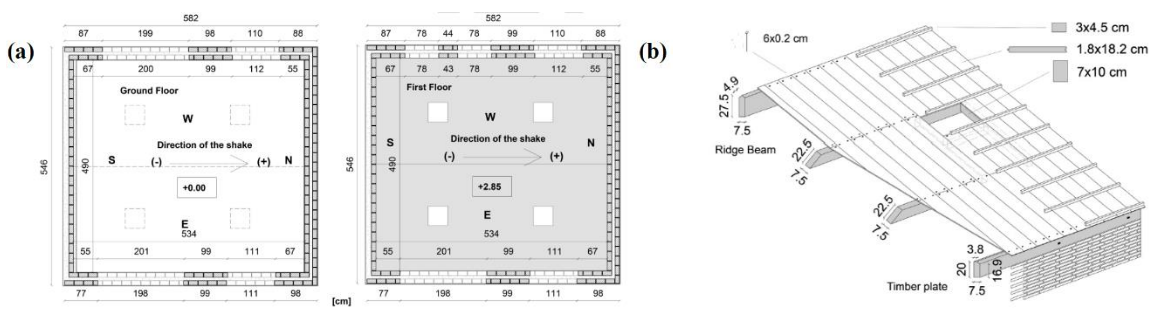

Plan view of the ground floor (left) and details of roof structure (right) (Graziotti et al., 2015)

5. Numerical results for EUC-BUILD1

Brief description of test and specimen:

- The inner CS masonry was continuous along the entire perimeter of the house, while the outer clay brick leaf was not present in the South façade.
- Two different records were imposed: EQ1 (from 25 to 100%) and EQ2 (from 100 to 200%)
- The building experienced a substantial level of damage (compared to that observed under lower intensity shaking) after the test EQ2@200%

Significant damage detected at EQ2@150 and EQ2@200 to the East, West, North and South CS inner walls (Graziotti et al., 2015)

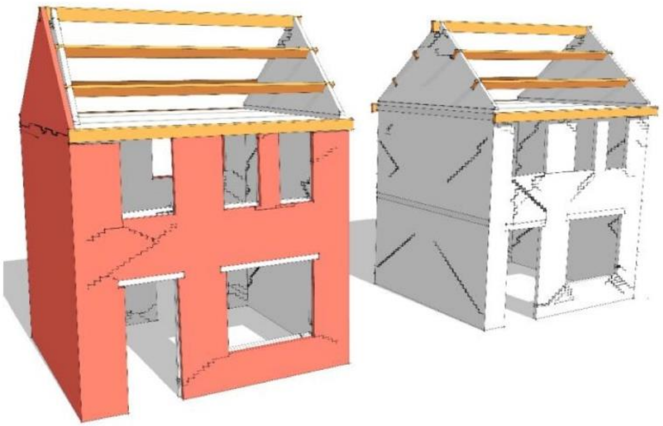

Damage pattern at end of testing (Graziotti et al., 2015)

5. Numerical results for EUC-BUILD1

Modelling assumptions:

Input	Modelling assumption
Boundary condition	Structure connected by mortar interfaces to a fixed slab
Roof diaphragm	Nailed connection between planks and beams modelled as equivalent spring interfaces characterised by an elastic-perfectly-plastic behaviour
Wall ties	Elastic-perfectly-plastic beam elements
First floor slab-front/back inner leaves connection	Mortar interface
Second floor slab-front/back inner leaves connection	Weak mortar interface (since the gap between the slab and the wall was filled after the temporary supports removal, i.e. after RC slab deflection)
Timber beam-front/back outer leaves connection	Weak mortar interface (since the gap between the slab and the wall was filled after the temporary supports removal, i.e. after RC slab deflection)
First and second floor slab and end/party walls connection	Mortar interface
Connection between roof girders and end/party walls	Mortar interface plus elastic-perfectly plastic L-steel anchors
Wall-to-wall connection	45-degrees connections between adjacent walls

5. Numerical results for EUC-BUILD1

Screenshots of the numerical model:

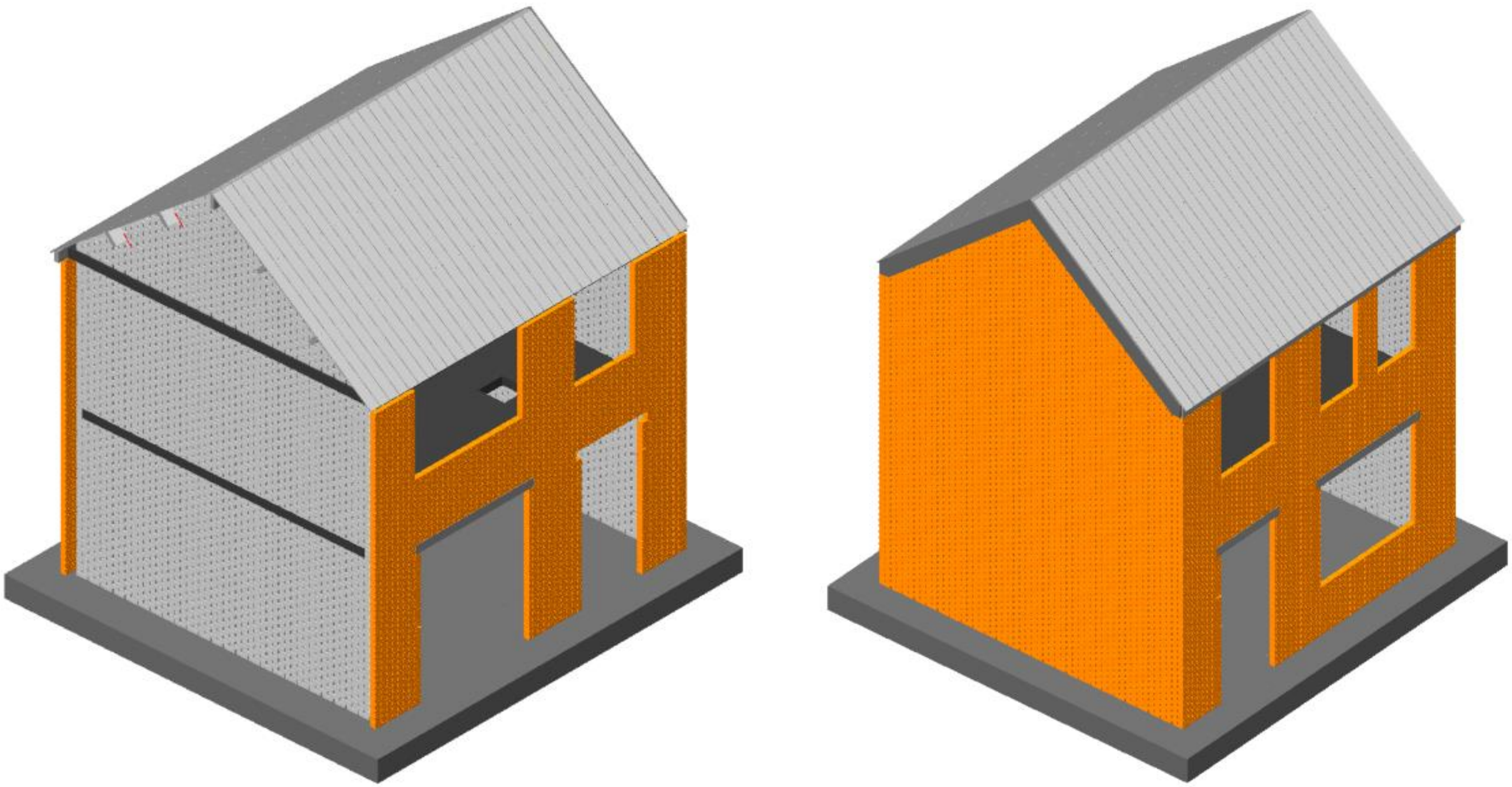

Screenshots of the EUC-BUILD1 numerical model (Mosayk, 2017b)

5. Numerical results for EUC-BUILD1

Numerical results:

- The following plots represent a comparison between the experimental (in **red**) PGA vs inter-storey drift (IDR) and PGA vs roof IDR against their numerical counterparts (in **grey**)

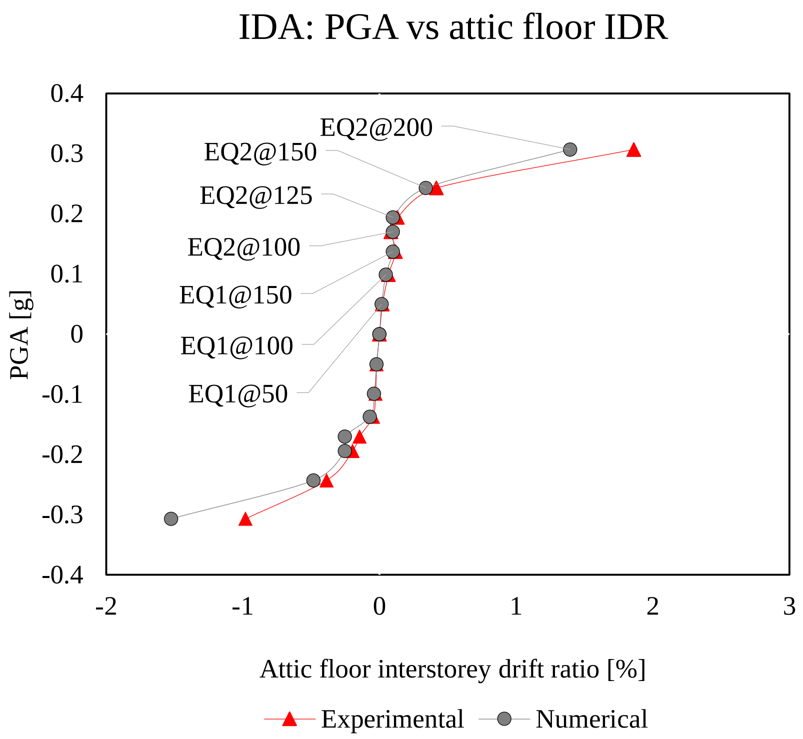

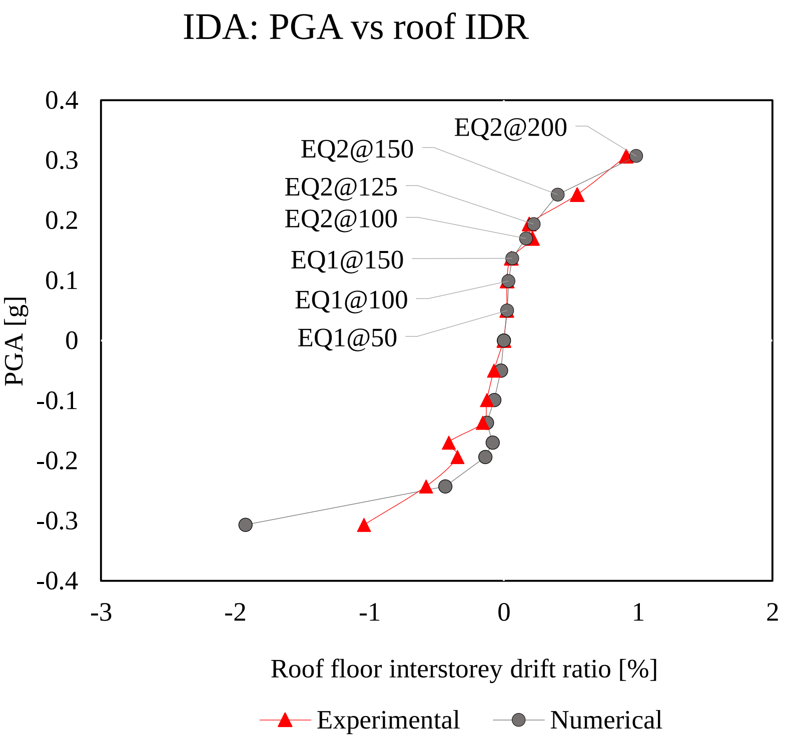

5. Numerical results for EUC-BUILD1

Numerical results:

- The following plot represents a comparison between the experimental (in **grey**) horizontal displacement at the attic floor [mm] versus base shear [kN] and their numerical counterparts (in **black**)

Attic displacement [mm] vs base shear [kN]

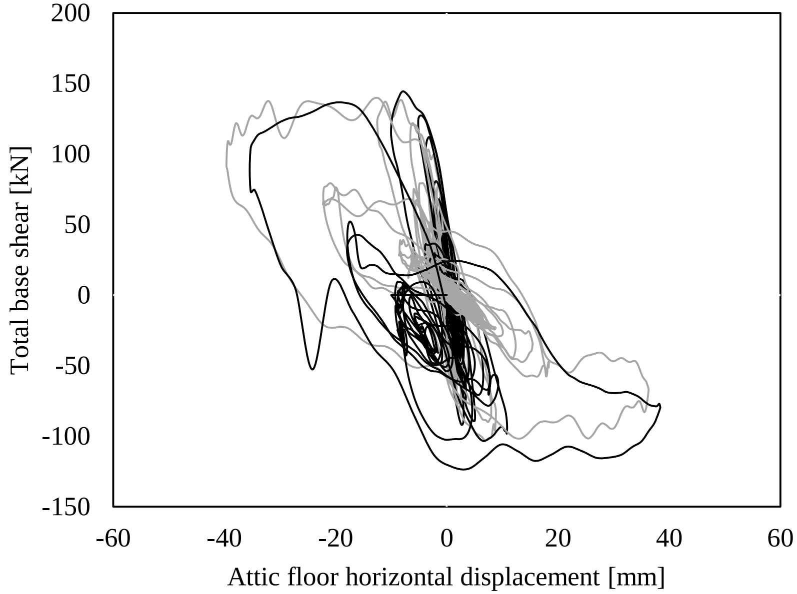

Deformed shape of AEM model at instant of peak deformation (magnified x5)

Attic displacement [mm] vs base shear [kN]

and deformed shape of AEM model at instant of peak deformation (magnified x5)

(Mosayk, 2017b)

5. Numerical results for EUC-BUILD1

Final considerations

- The AEM adequately captured the overall hysteretic behaviour of the specimen
- Numerical and experimental near-collapse condition occurred at the same loading phase
- The roof response was satisfactorily replicated, as reported in the associated IDA curve

Attic displacement [mm] vs base shear [kN]

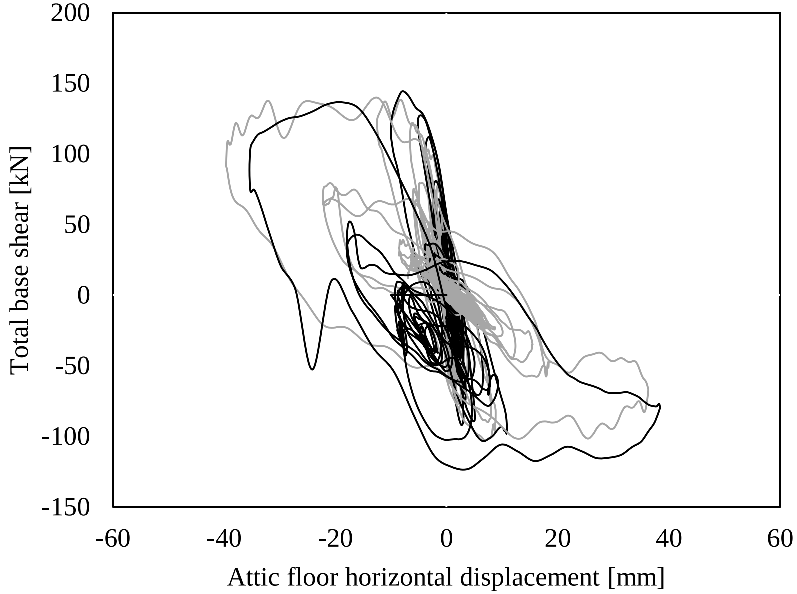

Deformed shape of AEM model at instant of peak deformation (magnified x5)

Attic displacement [mm] vs base shear [kN]

and deformed shape of AEM model at instant of peak deformation (magnified x5)

(Mosayk, 2017b)

Summary

1. Applied Element Method (AEM) overview
2. AEM for masonry structures
3. Modelling of the in-plane cyclic response of URM piers
4. Modelling of the out-of-plane dynamic response of URM piers
5. Numerical results for EUC-BUILD1
6. Numerical results for EUC-BUILD2
7. Numerical results for LNEC-BUILD1
8. Modelling of flexible diaphragms – LNEC-BUILD2
9. Index buildings

6. Numerical results for EUC-BUILD2

Brief description of test and specimen:

- The in-plan dimensions of the specimen were 5.33 m x 5.77 m, with a height of about 6.23 m
- The total mass was 32.6 t
- The loadbearing structural system is provided by 208-mm-thick, double-wythe unreinforced masonry walls, characterized by a Dutch cross bond pattern

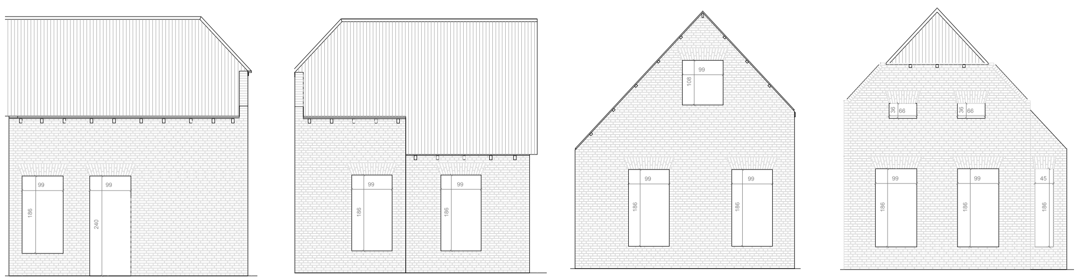

Elevation views of the specimen (Graziotti et al., 2016)

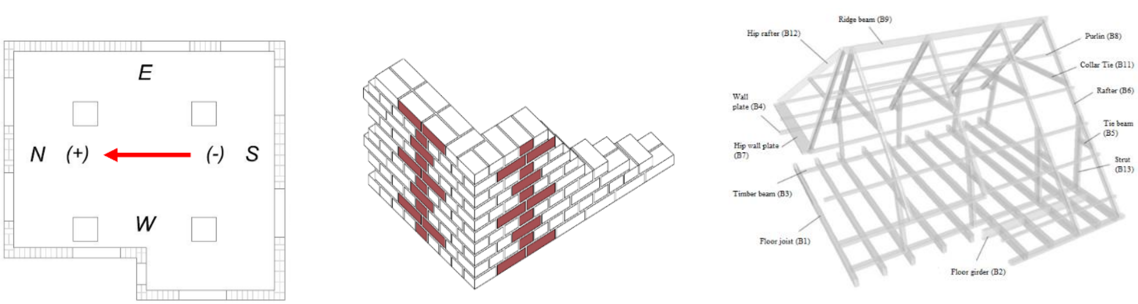

Plan view of the ground floor (left), Dutch cross bond representation and details of roof structure (right) (Graziotti et al., 2016)

6. Numerical results for EUC-BUILD2

Brief description of test and specimen:

- Two different records were imposed: EQ1 (from 25 to 100%) and EQ2 (from 50 to 400%)
- The tested building behaviour was mainly governed by the out-of-plane response of the gables, albeit diffuse damage was also observed with activation of both in-plane and out-of-plane failure mechanisms involving all of the façades of the building

EQ2@300

EQ2@400

Significant damage detected at EQ2@300 and EQ2@400 (Graziotti et al., 2016)

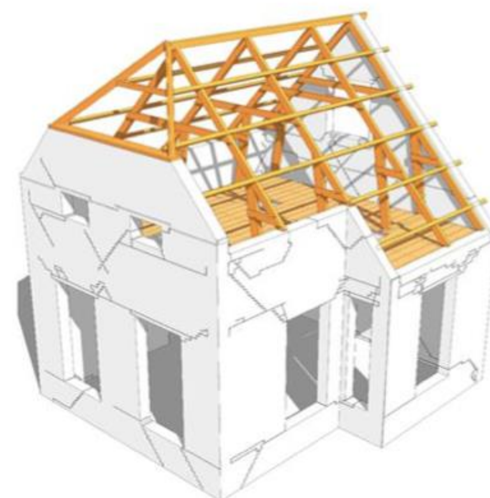

Damage pattern at end of testing (Graziotti et al., 2016)

6. Numerical results for EUC-BUILD2

Modelling assumptions:

Input	Modelling assumption
Boundary condition	Structure connected by mortar interfaces to a fixed slab
Roof diaphragm	Equivalent membrane elements
First-floor diaphragm/wall connection	Mortar interface
Timber beam/wall connection	Mortar interface
Connection between roof girders and wooden diaphragm	Nailed connection between membrane and beams modelled as equivalent spring interfaces characterised by an elastic-perfectly-plastic behaviour
Wall-to-wall connection	45-degrees connections between adjacent walls
Double-leaf brickwork	The influence of brick arrangement was not accounted (i.e. no perpendicular bricks to the bed joints were introduced)

6. Numerical results for EUC-BUILD2

Screenshots of the numerical model:

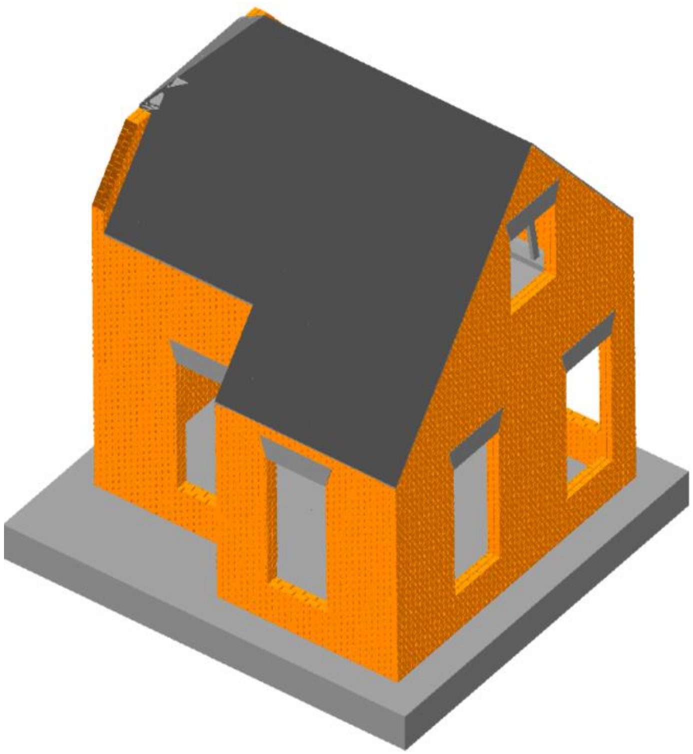

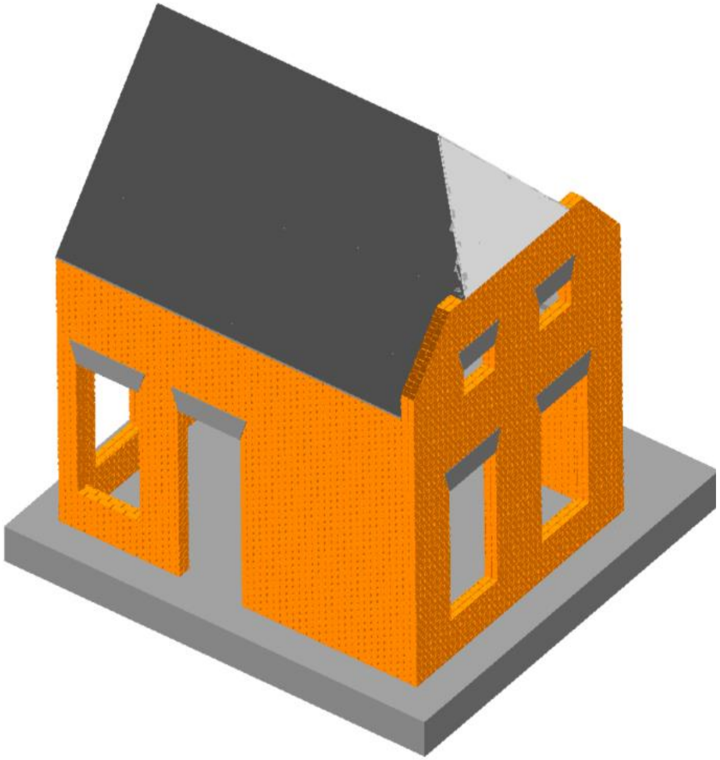

Screenshots of the EUC-BUILD2 numerical model (Mosayk, 2017b)

6. Numerical results for EUC-BUILD2

Numerical results:

- The following plots represent a comparison between the numerical (in **red**) PGA vs inter-storey drift (IDR) and PGA vs roof IDR against their experimental counterparts (in **grey**)

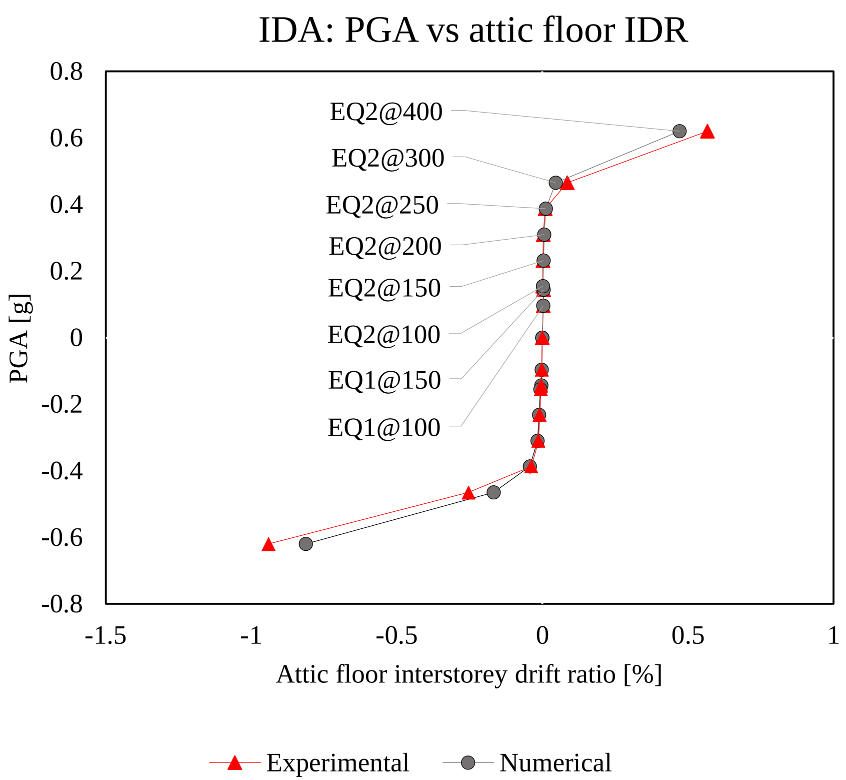

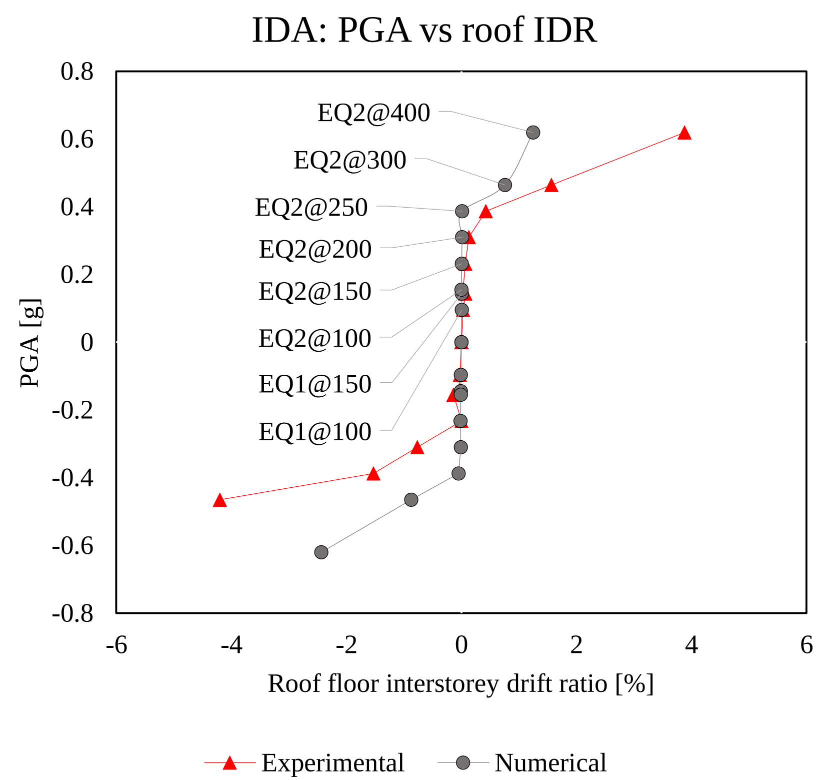

6. Numerical results for EUC-BUILD2

Numerical results:

- The following plot represents a comparison between the experimental (in **grey**) horizontal displacement at the attic floor[mm] versus base shear [kN] and their numerical counterparts (in **black**)

Attic displacement [mm] vs base shear [kN]

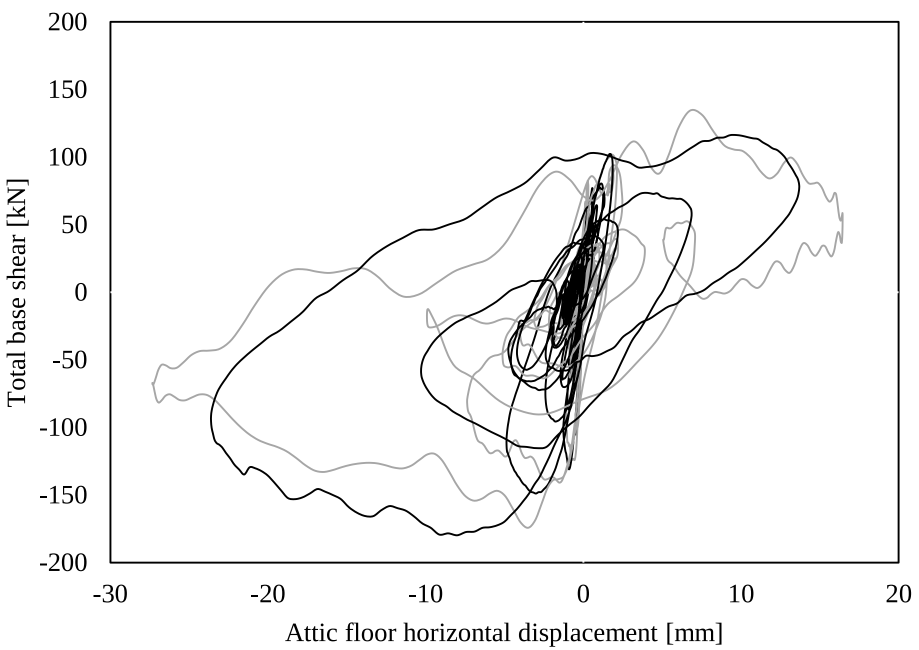

Deformed shape of AEM model at instant of peak deformation

Attic displacement [mm] vs base shear [kN]

and deformed shape of AEM model at instant of peak deformation (magnified x5)

(Mosayk, 2017b)

6. Numerical results for EUC-BUILD2

Final considerations

- The overall hysteretic response was predicted accurately by the model
- The damage and the crack patterns were adequately captured
- The simulation of this particular type of roof is still challenging

Attic displacement [mm] vs base shear [kN]

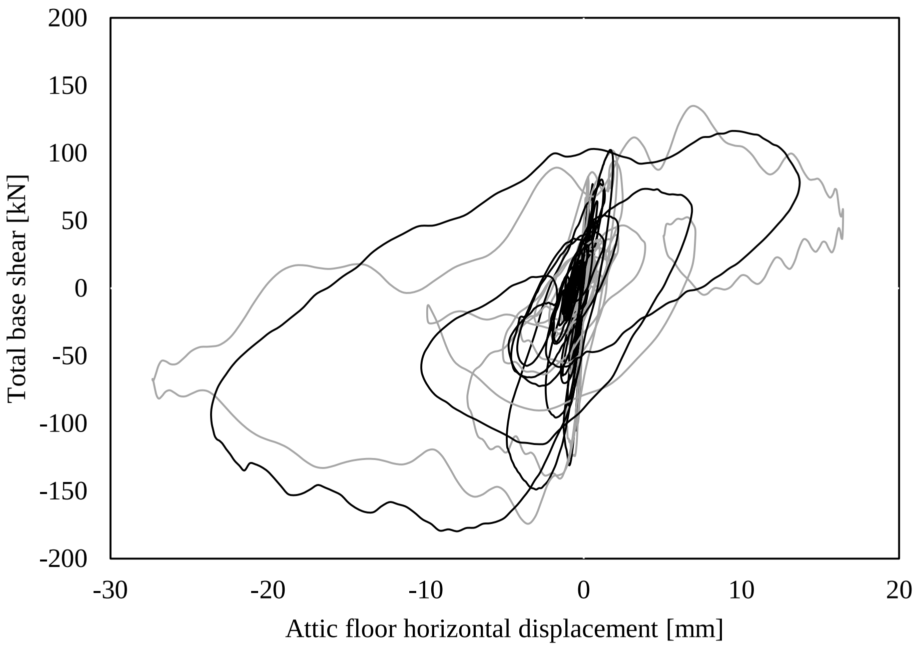

Deformed shape of AEM model at instant of peak deformation

Attic displacement [mm] vs base shear [kN]

and deformed shape of AEM model at instant of peak deformation

(Mosayk, 2017b)

Summary

1. Applied Element Method (AEM) overview
2. AEM for masonry structures
3. Modelling of the in-plane cyclic response of URM piers
4. Modelling of the out-of-plane dynamic response of URM piers
5. Numerical results for EUC-BUILD1
6. Numerical results for EUC-BUILD2
7. Numerical results for LNEC-BUILD1
8. Modelling of flexible diaphragms – LNEC-BUILD2
9. Index buildings

7. Numerical results for LNEC-BUILD1

Brief description of test and specimen:

- LNEC-BUILD1 basically consists in the upper portion of EUC-BUILD1, and it is 5.82 m long, 5.46 m wide and 4.93 m high with a total mass of 31 t
- The cavity-wall system consisted in an inner loadbearing leaf made of calcium silicate (CS) bricks (supporting the first floor reinforced concrete slab) whereas the external leaf was a clay brick (CL) veneer without any loadbearing function

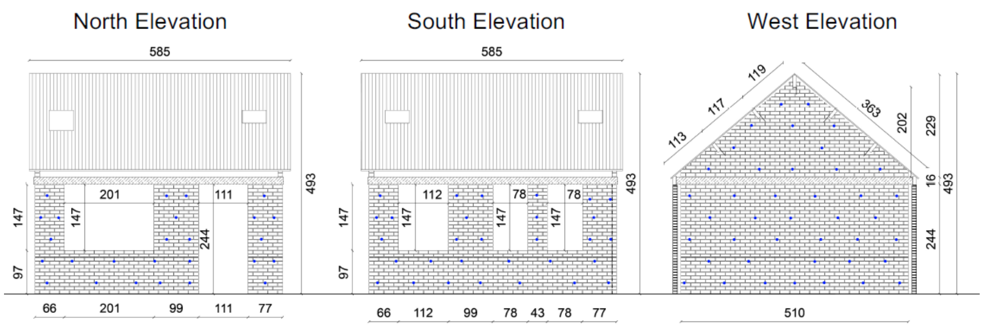

Elevation views of the specimen's CS inner leaf (Tomassetti et al. 2017a)

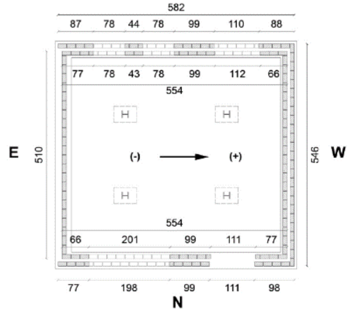

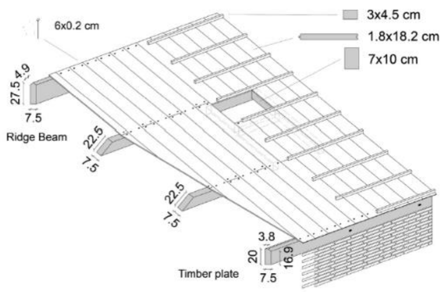

Plan view of the ground floor (left) and
details of roof structure (right) (Tomassetti et al. 2017a)

7. Numerical results for LNEC-BUILD1

Brief description of test and specimen:

- Two different records were imposed: EQ1 (from 25 to 100%) and EQ2 (from 50 to 300%)
- No relevant damage was detected until EQ1@150, when the front/back inner CS leafs started rocking
- During EQ2@300, an OOP mechanism of the South CS wall occurred, and the test was stopped. This phenomenon was associated to the loss of boundary conditions of the wall, due to the RC slab uplift caused by the increase in the rocking demand of the longitudinal piers

Significant damage detected at EQ2@300 (Tomassetti et al. 2017a)

7. Numerical results for LNEC-BUILD1

Modelling assumptions (prior to the test, blind prediction mode):

Input	Modelling assumption
Boundary condition	Structure connected by mortar interfaces to a fixed slab
Roof diaphragm	Nailed connection between planks and beams modelled as equivalent spring interfaces characterised by an elastic-perfectly-plastic behaviour
Wall ties	Elastic-perfectly-plastic beam elements
Attic floor slab and front/back inner leaves connection	Mortar interface (active after the static/gravity loading stage)
Timber beam and front/back outer leaves connection	Mortar interface (active after the static/gravity loading stage)
Attic floor slab and end/party walls connection	Mortar interface
Connection between roof girders and end/party walls	Mortar interface plus elastic-perfectly plastic L-steel anchors

7. Numerical results for LNEC-BUILD1

Screenshots of the numerical model:

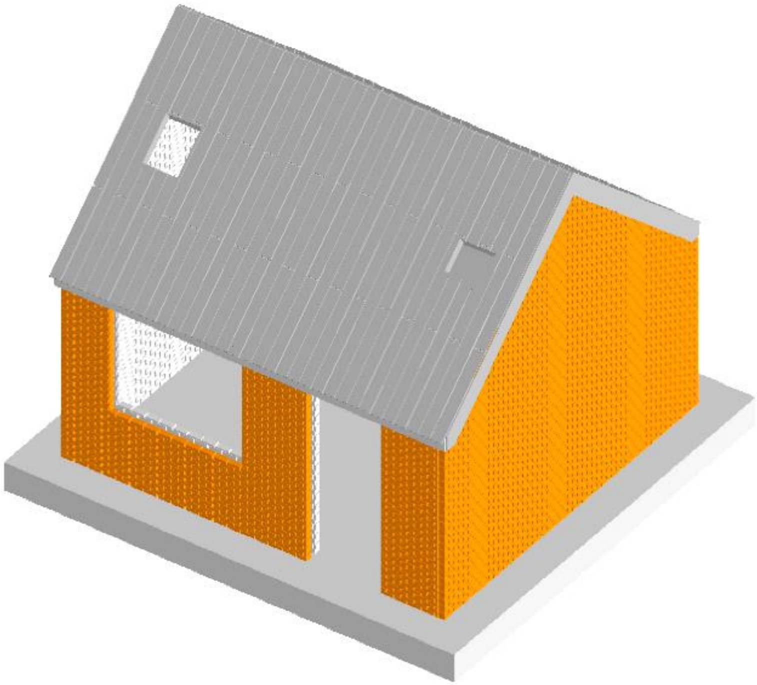

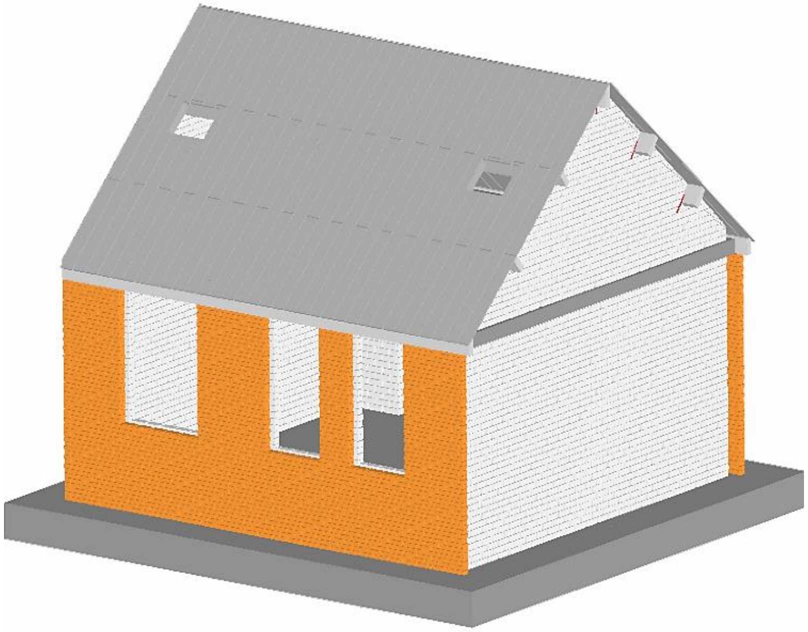

Screenshots of the LNEC-BUILD1 numerical model (Mosayk, 2017c)

7. Numerical results for LNEC-BUILD1

Numerical results prior to the test (blind prediction mode):

- The following plots represent a comparison between the experimental (in **red**) PGA vs inter-storey drift (IDR) and PGA vs roof IDR against their numerical counterparts (in **grey**)

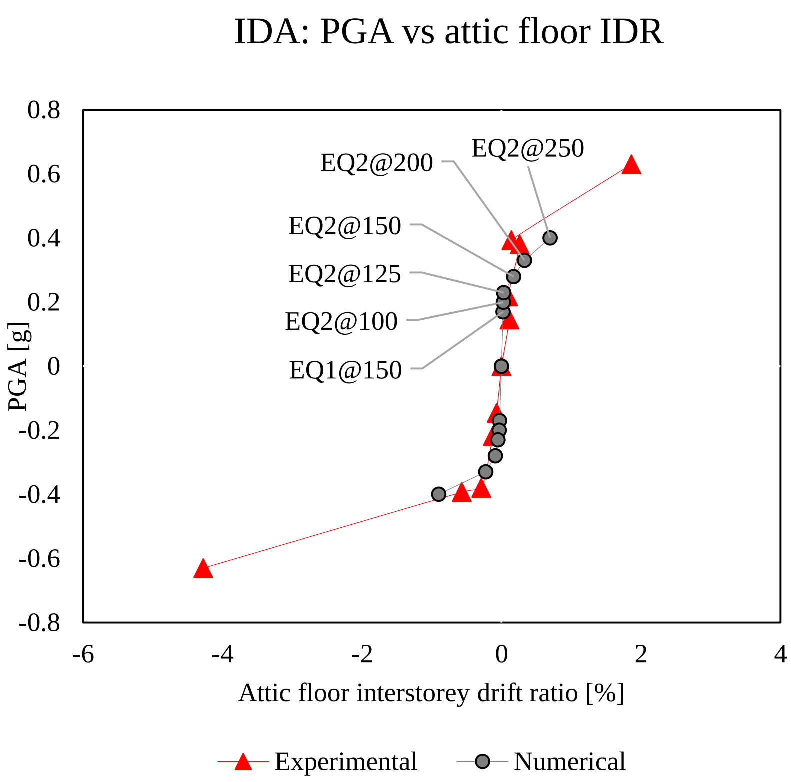

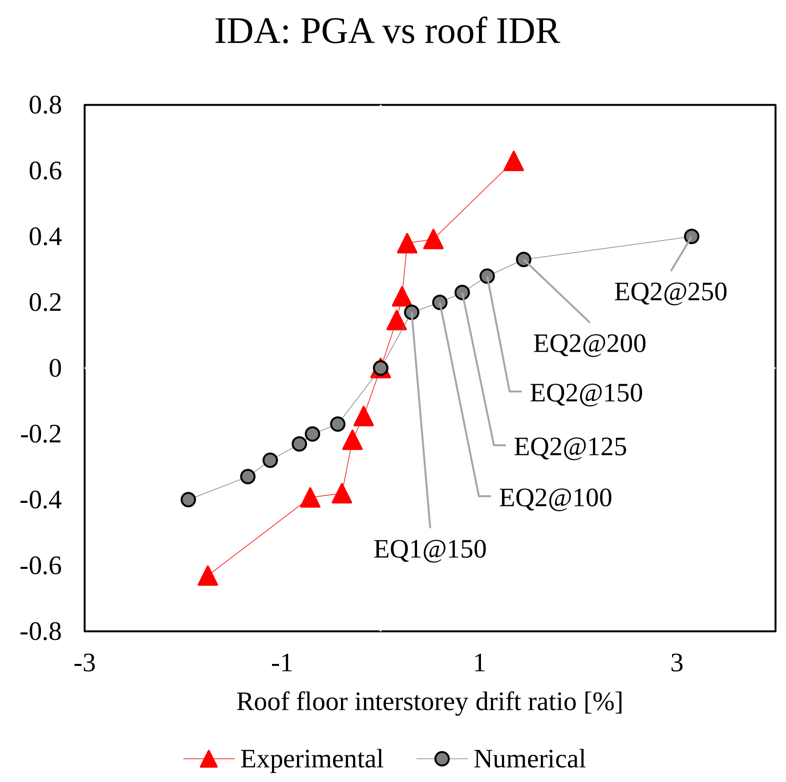

7. Numerical results for LNEC-BUILD1

Numerical results prior to the test (blind prediction mode):

- The following plot represents a comparison between the experimental (in **grey**) horizontal displacement at the ridge beam [mm] versus base shear [kN] and their numerical counterparts (in **black**)

Attic displacement [mm] vs base shear [kN]

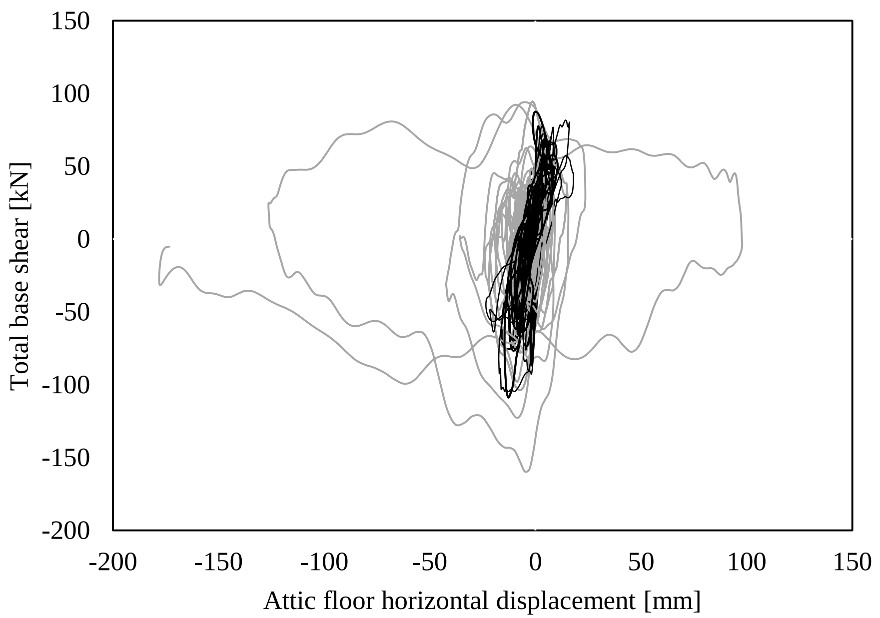

Deformed shape of AEM model at instant of peak deformation (magnified x5)

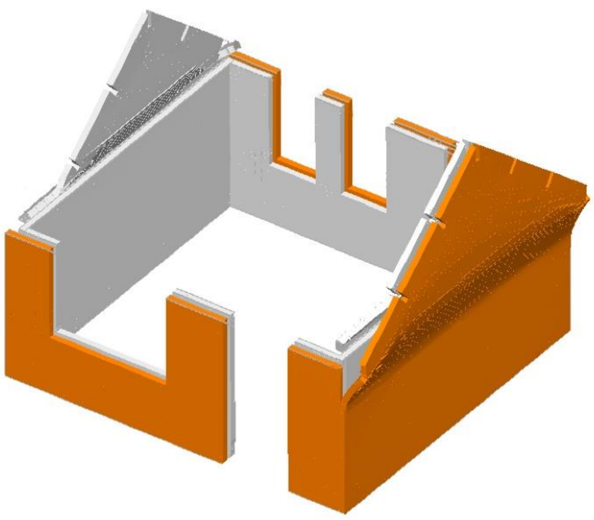

Attic displacement [mm] vs base shear [kN]

and deformed shape of AEM model at instant of peak deformation (magnified x5)

(Mosayk, 2017c)

7. Numerical results for LNEC-BUILD1

Modelling assumptions (after the test, refined model):

Input	Modelling assumption
Boundary condition	Structure connected by mortar interfaces to a fixed slab
Roof diaphragm	Nailed connection between planks and beams modelled as equivalent spring interfaces characterised by an elastic-perfectly-plastic behaviour
Wall ties	Elastic-perfectly-plastic beam elements
Attic floor slab-front/back inner leaves connection	*Cracked mortar interface* accounting for the damage occurred during transportation phases (active after the static/gravity loading stage)
Timber beam-front/back outer leaves connection	*Cracked mortar interface* accounting for the damage occurred during transportation phases (active after the static/gravity loading stage)
Attic floor slab and end/party walls connection	Mortar interface
Connection between roof girders and end/party walls	Mortar interface plus elastic-perfectly plastic L-steel anchors
Wall-to-wall connection	*45-degrees connections between adjacent walls*

7. Numerical results for LNEC-BUILD1

Numerical results after the test (refined model):

- The following plots represent a comparison between the experimental (in **red**) PGA vs inter-storey drift (IDR) and PGA vs roof IDR against their numerical counterparts (in **grey**)

IDA: PGA vs attic floor IDR

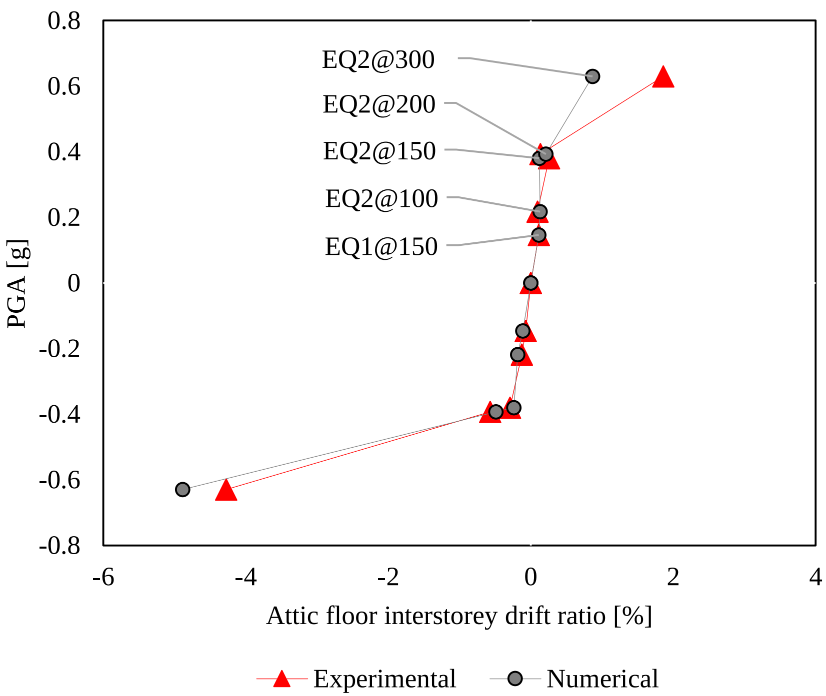

IDA: PGA vs roof IDR

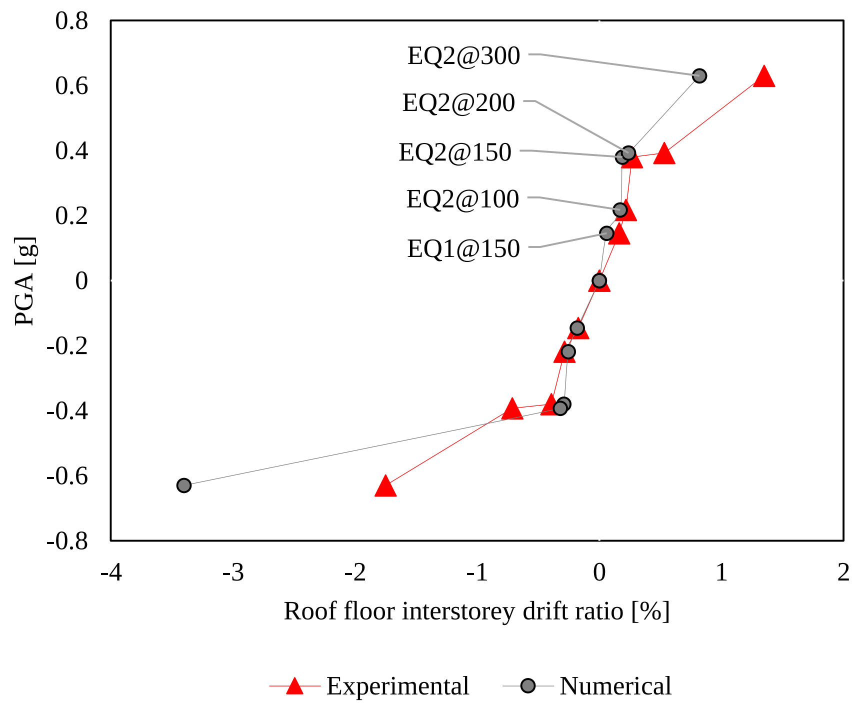

MOSAYK
Modelling and Structural Analysis Konsulting

7. Numerical results for LNEC-BUILD1

Numerical results:

- The following plot represents a comparison between the experimental (in **grey**) horizontal displacement at the ridge beam [mm] versus base shear [kN] and their numerical counterparts (in **black**)

Attic displacement [mm] vs base shear [kN]

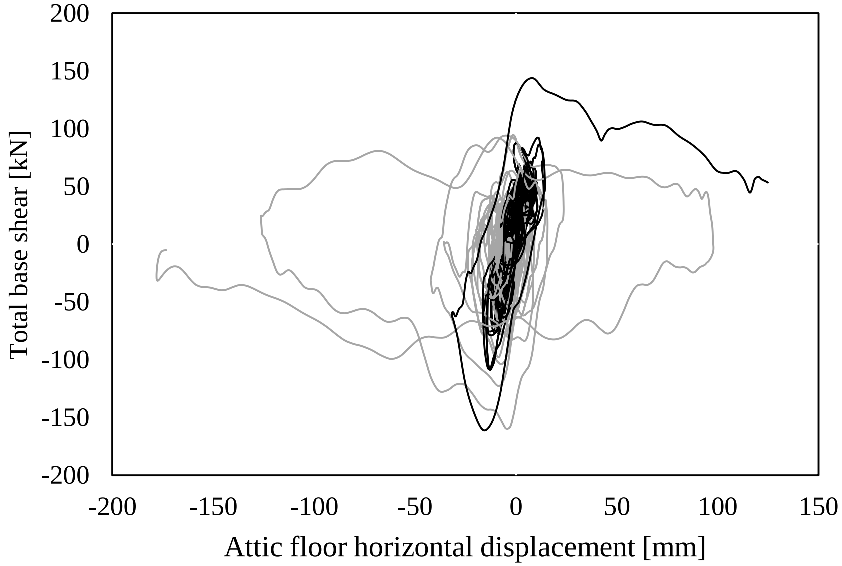

Partial collapse of the AEM model

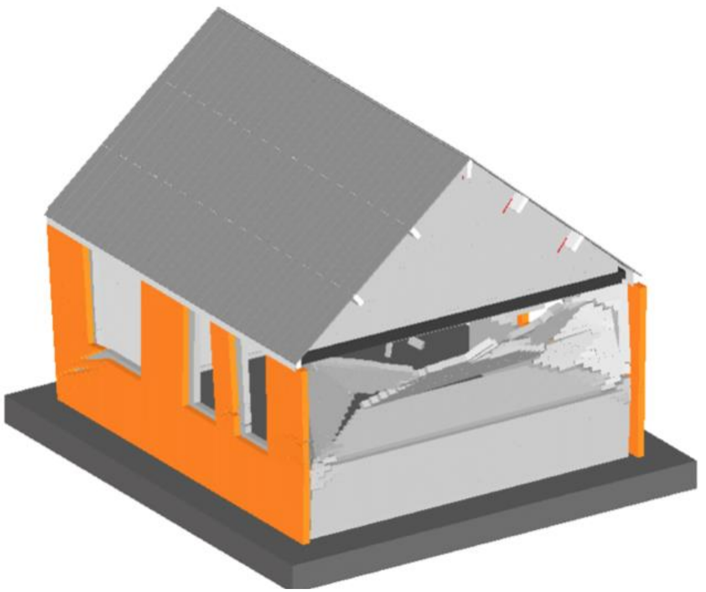

Attic displacement [mm] vs base shear [kN]

and deformed shape of AEM model at instant of peak deformation (magnified x5)

(Mosayk, 2017c)

7. Numerical results for LNEC-BUILD1

Numerical results:

- The numerical model successfully predicted the RC slab uplift and thus the loss of contact between RC slab and CS party wall (which resulted in the alteration of the initial boundary conditions of the wall). Since this phenomenon was not expected, the vertical displacement of the RC slab was not recorded by the laboratory instrumentation. However, the numerical prediction of 30 mm seems to be reasonable

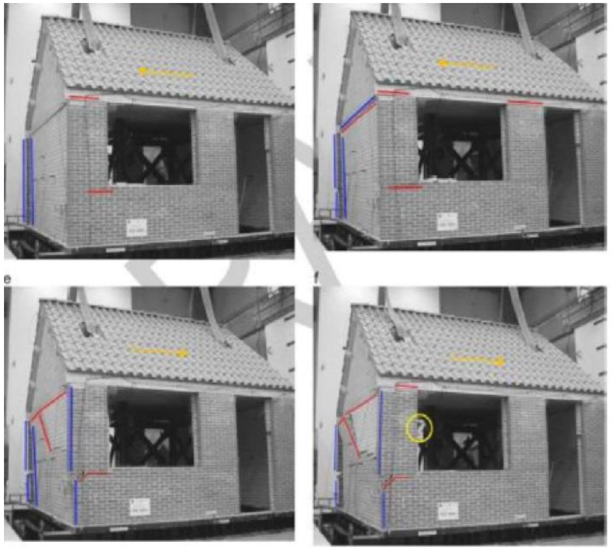

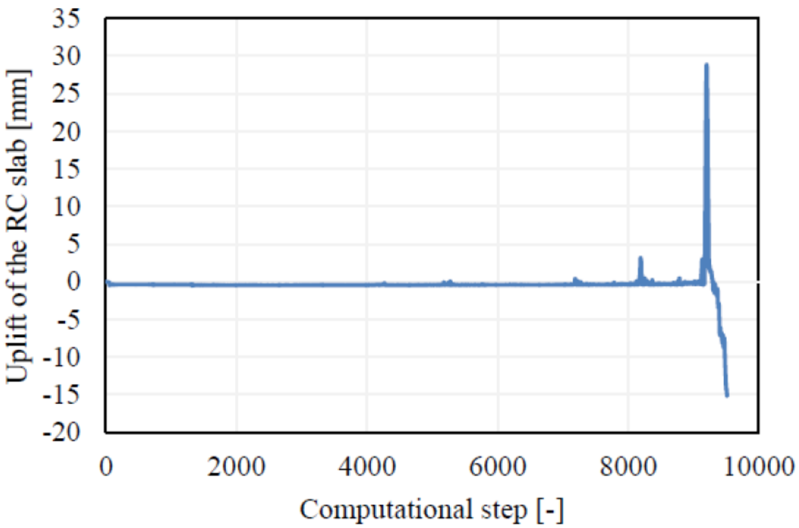

Experimental failure mechanisms and numerical RC slab uplift

7. Numerical results for LNEC-BUILD1

Final remarks:

- The blind prediction model shown an acceptable agreement with its experimental counterpart, although the partial OOP collapse was not captured
- The post-test refined model adequately represented the overall dynamic response of the specimen, although it overestimated the stiffness of the roof in the last cycle
- The predicted area of debris was comparable with the experimental one

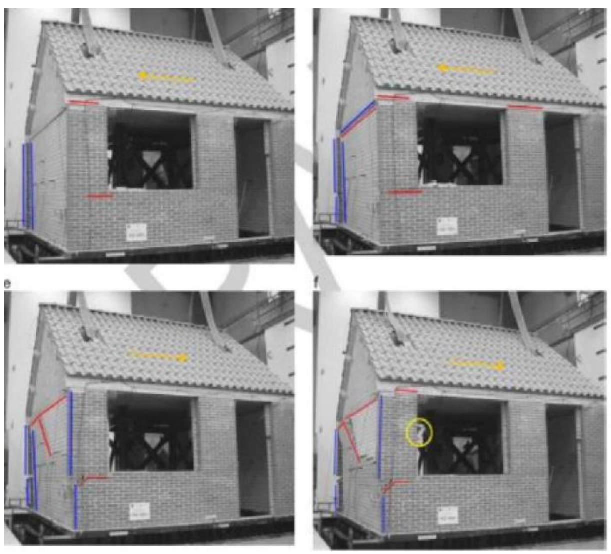

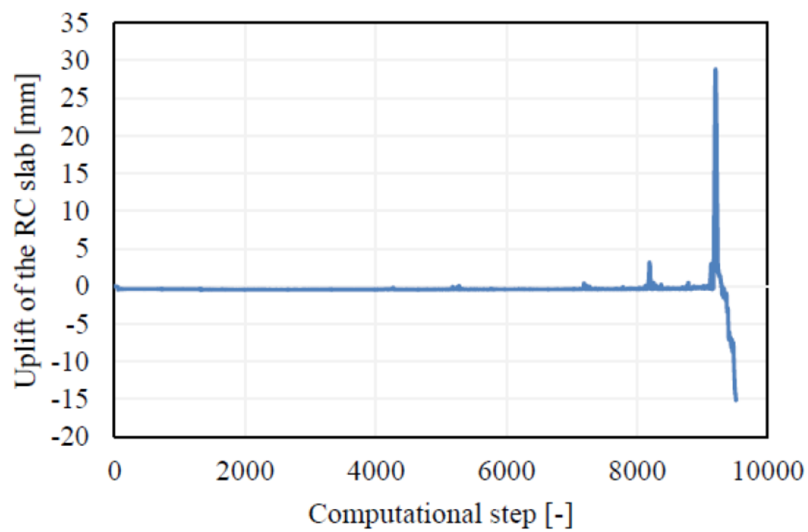

Experimental failure mechanisms and numerical RC slab uplift

Summary

1. Applied Element Method (AEM) overview
2. AEM for masonry structures
3. Modelling of the in-plane cyclic response of URM piers
4. Modelling of the out-of-plane dynamic response of URM piers
5. Numerical results for EUC-BUILD1
6. Numerical results for EUC-BUILD2
7. Numerical results for LNEC-BUILD1
8. Modelling of flexible diaphragms – LNEC-BUILD2
9. Index buildings

8. Numerical results for LNEC-BUILD2

Brief description of test and specimen:

- The full-scale test specimen LNEC-BUILD2 built in the LNEC laboratory in Lisbon is the roof substructure of the EUC-BUILD1 specimen tested in the Eucentre laboratory in 2015
- The seismic input introduced at the base of LNEC-BUILD2 specimen corresponded to the second floor accelerations that had been recorded during the EUC-BUILD1 test
- The aim of this test was to enhance further the knowledge of the seismic response of a flexible roof diaphragm + gable walls substructure up to collapse

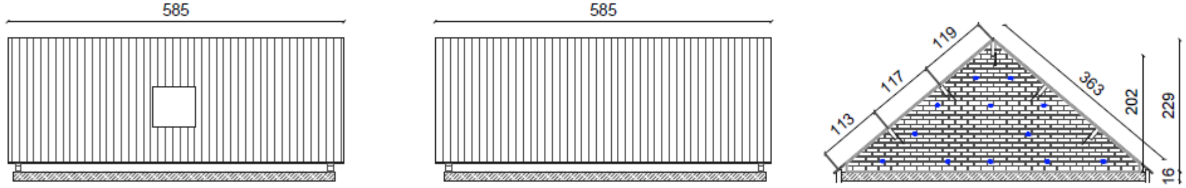

Elevation views of the LNEC-BUILD2 specimen (Tomassetti et al. 2017b)

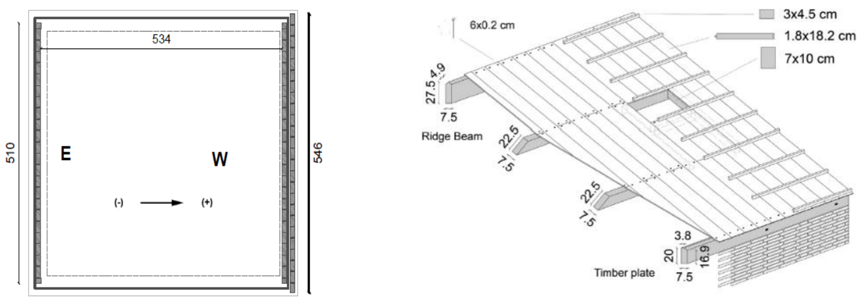

Plan view of the LNEC-BUILD2 specimen (left) and details of roof structure (right)
(Tomassetti et al. 2017b)

8. Numerical results for LNEC-BUILD2

Brief description of test and specimen:

- Two different records were imposed: EQ1 (from 50 to 150%) and EQ2 (from 50 to 600%)
- The first visible damage associated to shake-table motion was detected during test EQ1@100%
- The specimen collapsed in OOP fashion: the East gable (single leaf) wall had a full collapse towards the interior of the model.

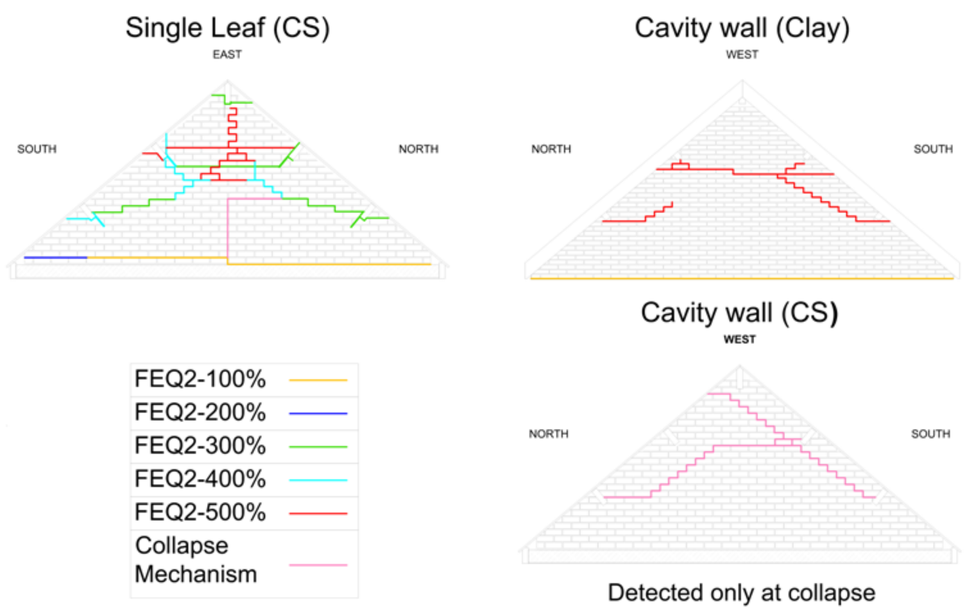

Evolution of the crack pattern in the gable walls along the test stages (Tomassetti et al. 2017b)

8. Numerical results for LNEC-BUILD2

Modelling assumptions:

Input	Modelling assumption
Boundary condition	Structure connected by mortar interfaces to a fixed slab
Beam/plank connection	Nailed connection between planks and beams modelled as equivalent spring interfaces characterised by an elastic behaviour
Plank elements	Bilinear material with an equivalent shear modulus accounting for flexural and shear deformations and an equivalent yield stress
Wall ties	Elastic-perfectly-plastic beam elements
RC slab/wall connection	Mortar interface
Connection between roof girders and end/party walls	Mortar interface plus elastic-perfectly plastic L-steel anchors

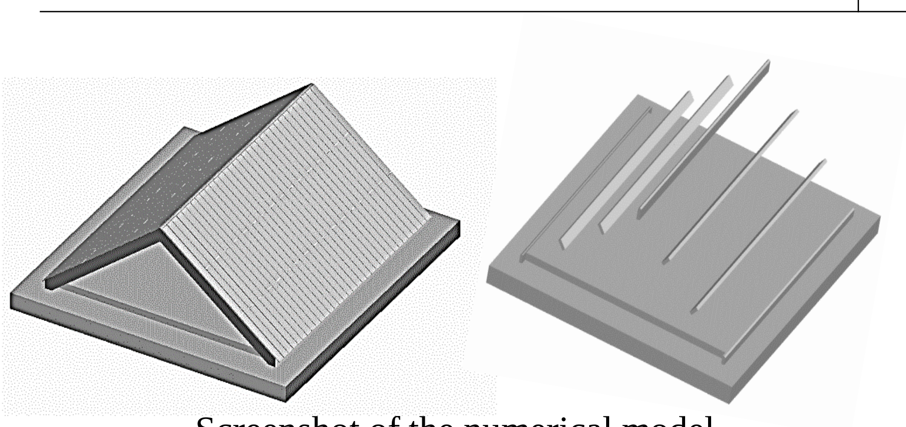

Screenshot of the numerical model

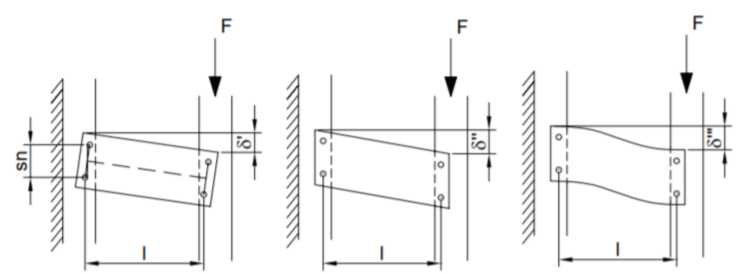

Rigid rotation of the board due to nails slip,
board shear deformation, board flexural deformation.

8. Numerical results for LNEC-BUILD2

Numerical results:

- The following plot represents a comparison between the experimental (in **grey**) horizontal displacement at the ridge beam [mm] versus base shear [kN] and their numerical counterparts (in **black**)

Ridge displacement [mm] vs base shear [kN]

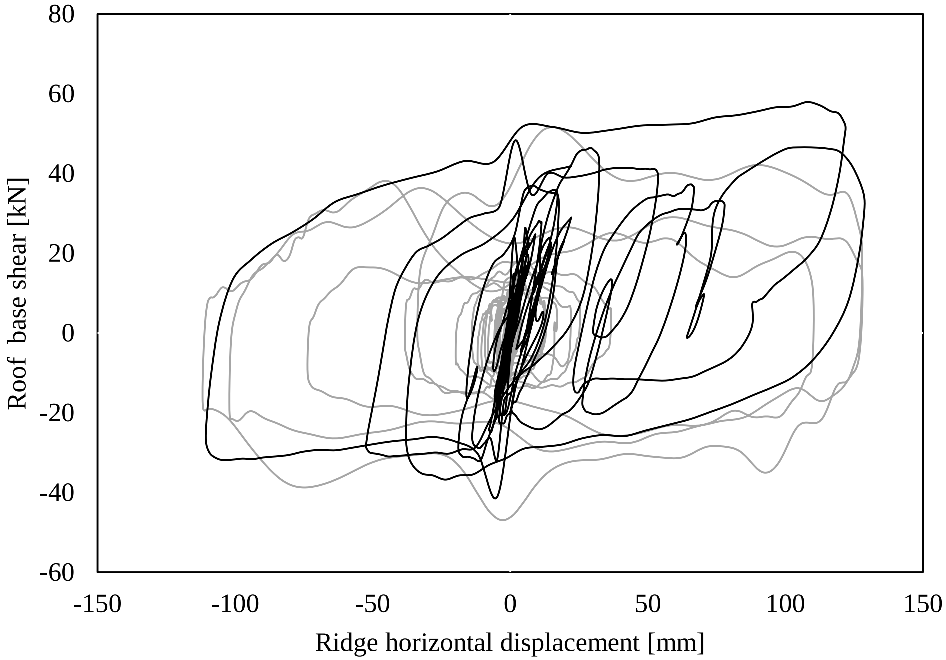

Global collapse of the AEM model

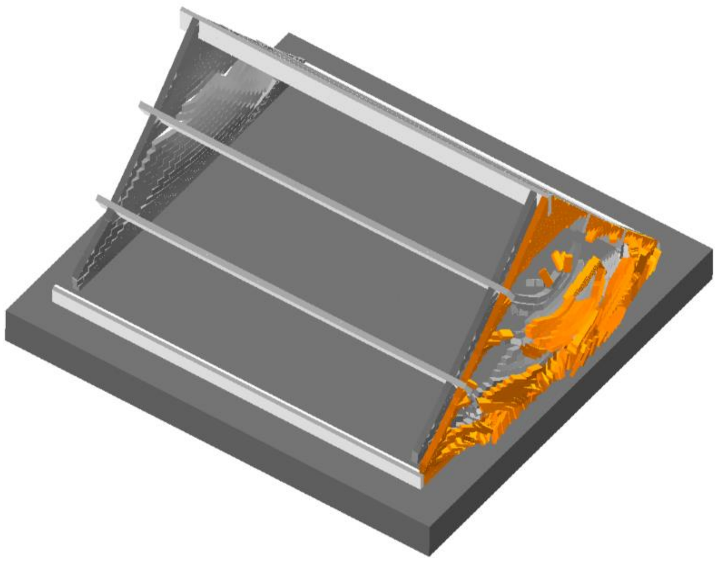

Ridge displacement [mm] vs base shear [kN]

and deformed shape of AEM model at instant of peak deformation (Mosayk, 2017d)

8. Numerical results for LNEC-BUILD2

Final considerations:

- The AEM predicted adequately the dynamic response of the structure
- The in-plane mechanism of the plank-joists assembly was successfully captured
- The OOP collapse mechanisms, unlike the test, started on the cavity wall side
- The debris area was slightly overestimated (+15% c.a.)

Ridge displacement [mm] vs base shear [kN]

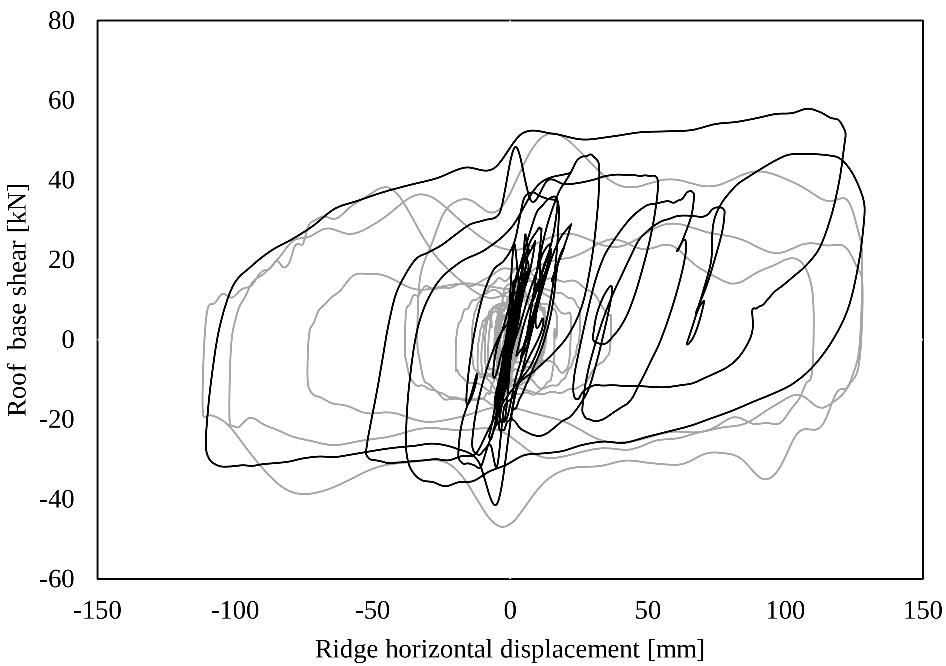

Global collapse of the AEM model

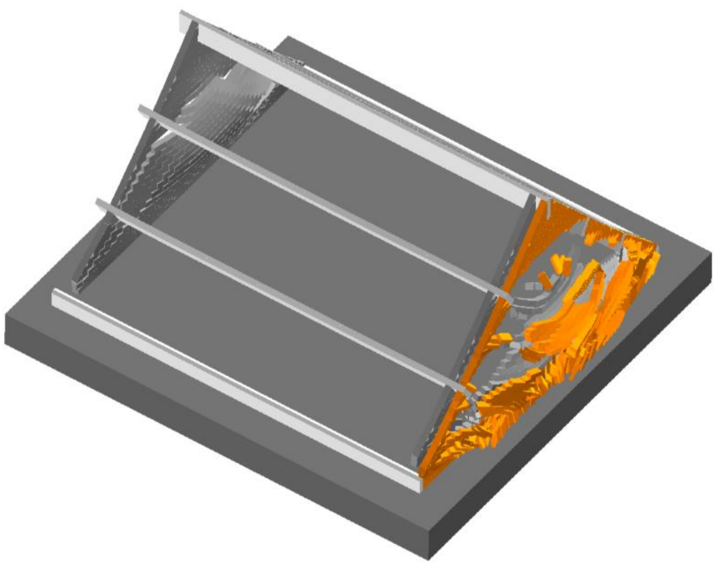

Ridge displacement [mm] vs base shear [kN]

and deformed shape of AEM model at instant of peak deformation (Mosayk, 2017d)

Summary

1. Applied Element Method (AEM) overview
2. AEM for masonry structures
3. Modelling of the in-plane cyclic response of URM piers
4. Modelling of the out-of-plane dynamic response of URM piers
5. Numerical results for EUC-BUILD1
6. Numerical results for EUC-BUILD2
7. Numerical results for LNEC-BUILD1
8. Modelling of flexible diaphragms – LNEC-BUILD2
9. Index buildings

8. Index buildings

Scope:

- The fragility and consequence models used in NAM's hazard and risk assessment are developed using single degree of freedom (SDOF) models
- The hysteretic response of these SDOF models is calibrated using the nonlinear dynamic analysis results of multi-degree-of-freedom (MDOF) models of index buildings from the Groningen region (Crowley and Pinho, 2017)
- Thus, a series of nonlinear dynamic analyses were perfomed using 11 different ground motions, which have been selected to cover a range of intensities, described in terms of AvgSa (Kohranghi et al., 2017), Arias Intensity, PGA and spectral acceleration at 0.1 seconds.

Building considered:

- In this framework, mainly the "**terraced house**" building typology has been scrutinized, except for Nieuwstraat (detached house typology)
- Thus, the following URM structures were considered:
  1. Zijlvest 25 (real building, Loppersum, NL - UBH- MUR/LN/MUR/LWAL/EW/FC)
  2. Julianalaan 52 (real building, Delfzijl, NL - UBH-MUR/LN/MUR /LWAL/EW/FC)
  3. EUC-BUILD-1 (test specimen)
  4. LNEC-BUILD1 (test specimen)
  5. Nieuwstraat (real building, Loppersum, NL- UBH-MUR/LN/MUR /LWAL/EWN/FW)

8. Index buildings

Ground motions:

- The metadata of the 11 ground motions that have been applied to all models presented herein is given in the Table below
- The horizontal component has been applied in the weak direction of each model, where this is identified *a priori* as that which is expected to have the lowest strength (i.e. base shear capacity). The other two components (horizontal and vertical) have also been applied to all models.

Ground motion	AvgSa (g)	Arias Intensity (m/s)	PGA (g)	Sa(0.1s)
N_00356L	0.07	0.07	0.09	0.11
E_00137_EW	0.09	0.26	0.19	0.44
N_00694T	0.14	0.46	0.23	0.38
N_00616T	0.22	0.49	0.24	0.49
N_00147T	0.27	0.51	0.25	0.67
N_00250L	0.34	1.53	0.88	0.87
E_17167_EW	0.40	1.20	0.53	0.72
N_00415L	0.46	1.74	0.70	1.02
N_00569T	0.46	2.25	0.52	0.68
N_00407L	0.57	3.54	0.82	1.26
N_00451T	0.74	3.85	1.25	1.49

8. Index buildings

Brief description of *Zijlvest*:

- Zijlvest 25 is terraced house which was built in 1976.
- The structure consists mainly of concrete and masonry, with timber roof joists.
- The building is a two-storey structure, with large openings at the ground floor
- A cavity wall system characterises this building typology, where the inner loadbearing walls are made of calcium silicate bricks. The outer veneer, instead, is made of clay bricks.
- CS and CL wall are connected by means of steel connectors (ties)

8. Index buildings

Numerical results for *Zijlvest* (one unit):

- Zijlvest was characterized by an asymmetrical distribution of the longitudinal walls at the ground floor. Thus due to the different in-plane strengths, the global response was mainly governed by torsional behaviour and flexural mechanisms
- Due to the large ground-floor openings, a soft-storey response was observed
- Considering the abovementioned 11 ground motions, the structure exhibited slightly damage at the end of the records only for 2 seismic inputs
- The near collapse condition or partial collapse was reached for 6 records
- Global collapse was reached for the last 3 inputs

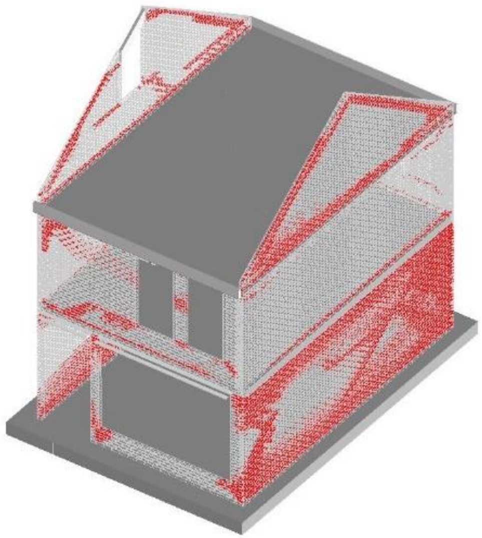

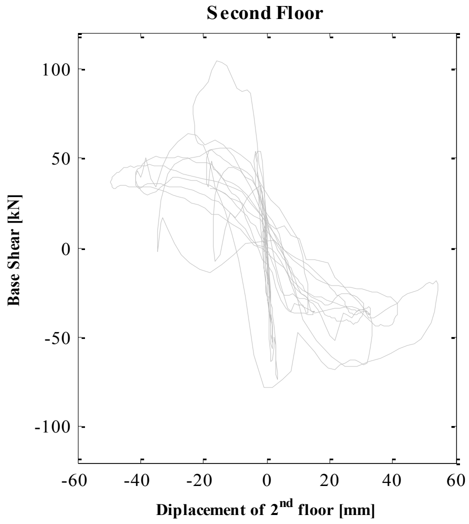

Soft-storey behaviour, inner CS walls damage and hysteretic response observed during the N-00250-L seismic input

8. Index buildings

Brief description of *Julianalaan*:

- Julianalaan is composed by two adjacent units, which are almost identical in plan. Each house is square in plan; approximately 6.5m x 6.5m.
- The houses comprise two habitable storeys plus an attic, accessible by a ladder. The building is a two-storey structure, with large openings at the ground floor
- A cavity wall system characterises this building typology, where the inner loadbearing walls are made of calcium silicate bricks. The outer veneer, instead, is made of clay bricks.
- CS and CL wall are connected by means of steel connectors (ties)

8. Index buildings

Numerical results for *Julianalaan* (one unit):

- The overall structural response was governed by the flexural response of the longitudinal walls
- The in-plane demand of the longitudinal piers induced OOP failure of the transversal ones
- Considering the abovementioned 11 ground motions, the structure exhibited slightly damage at the end of the records only for 2 seismic inputs
- The near collapse condition or partial collapse was reached for 6 records
- Global collapse was reached for the last 3 inputs

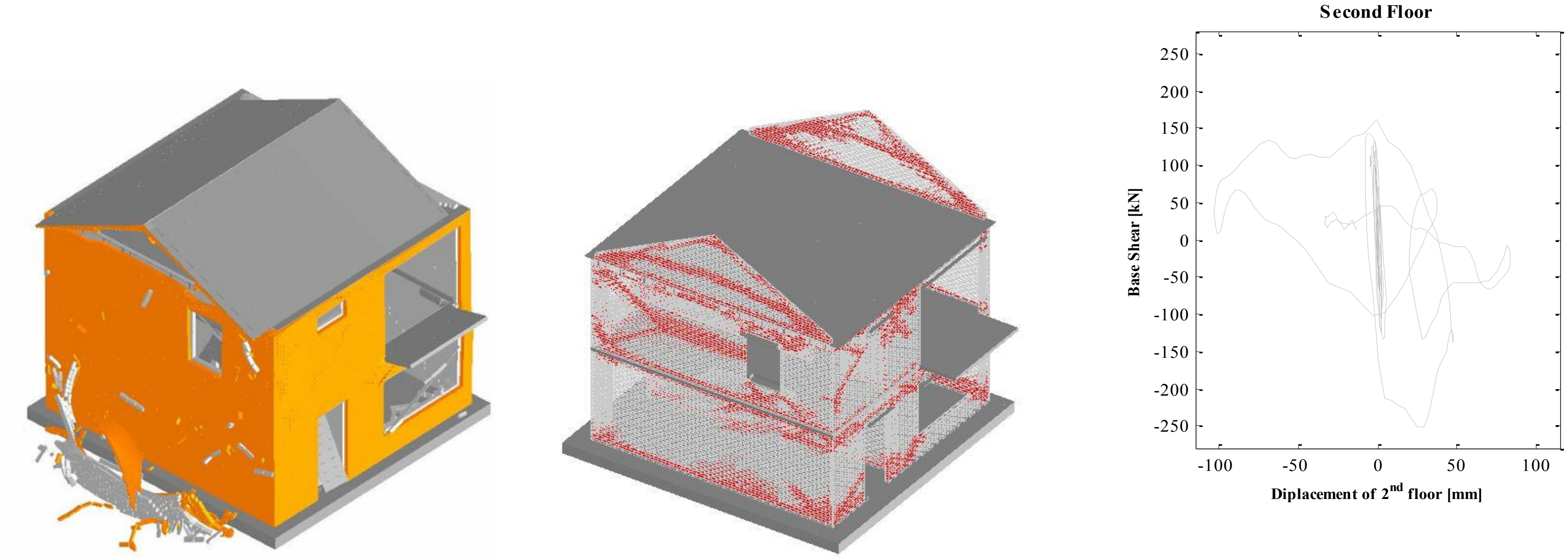

OOP partial collapse, inner CS walls damage and hysteretic response observed during the N-00407-L seismic input

8. Index buildings

Numerical results for *EUC-BUILD1* building specimen:

- The damage was mainly localised in the longitudinal walls and spandrels, which suffered several cracks due to diagonal shear
- The in-plane demand of the longitudinal piers induced OOP mechanisms of the transversal ones
- Considering the abovementioned 11 ground motions, the structure exhibited slightly damage at the end of the records for 5 seismic inputs
- The near collapse condition or partial collapse was reached for 3 records
- Global collapse was reached for the last 3 inputs

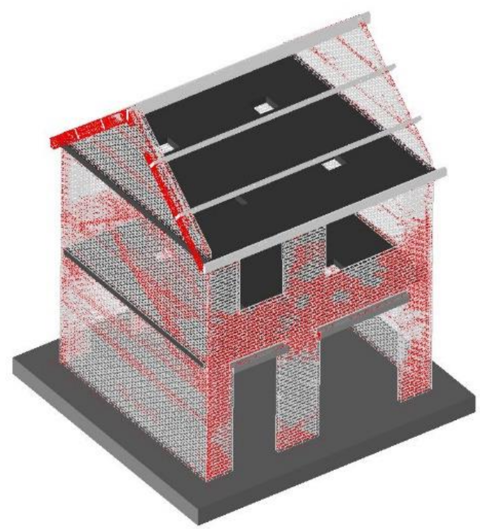

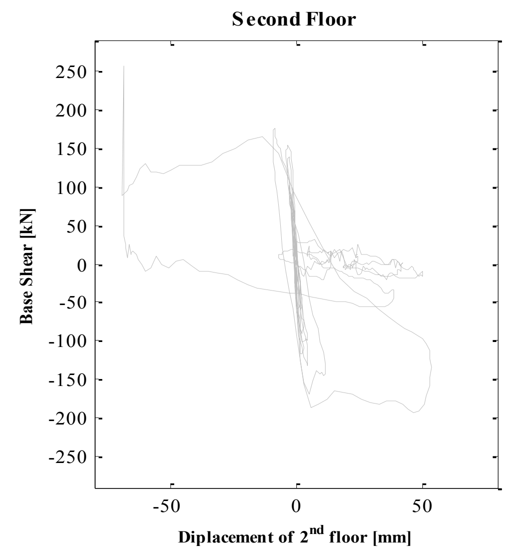

OOP collapse, inner CS walls damage and hysteretic response observed during the N-00250-L seismic input

MOSAYK Modelling and Structural Analysis Konsulting

8. Index buildings

Numerical results for *LNEC-BUILD1* building specimen:

- The observed damage was mainly due to the flexural mechanisms of the longitudinal piers
- In few cases, the in-plane demand of the longitudinal piers induced OOP failure mechanisms of the transversal ones
- Considering the abovementioned 11 ground motions, the structure exhibited slightly damage at the end of the records for 9 seismic inputs
- The near collapse condition or partial collapse was reached for 2 records
- No global collapses were observed

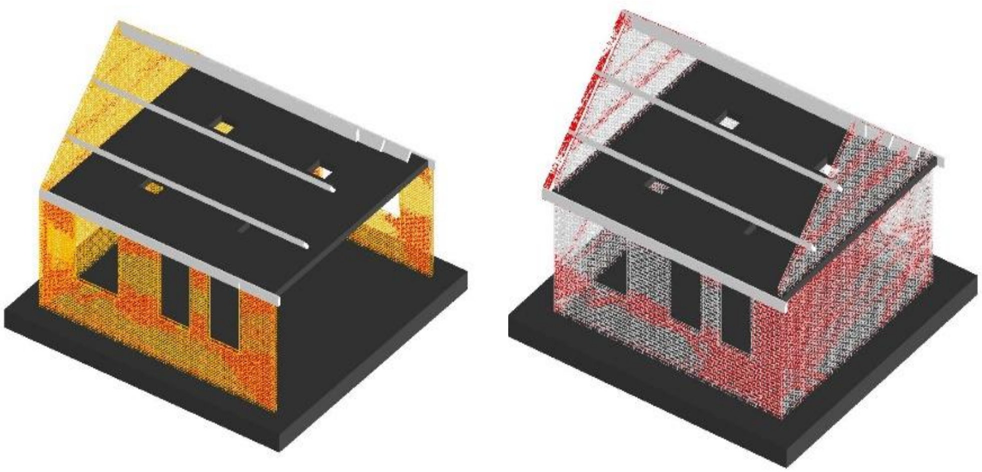

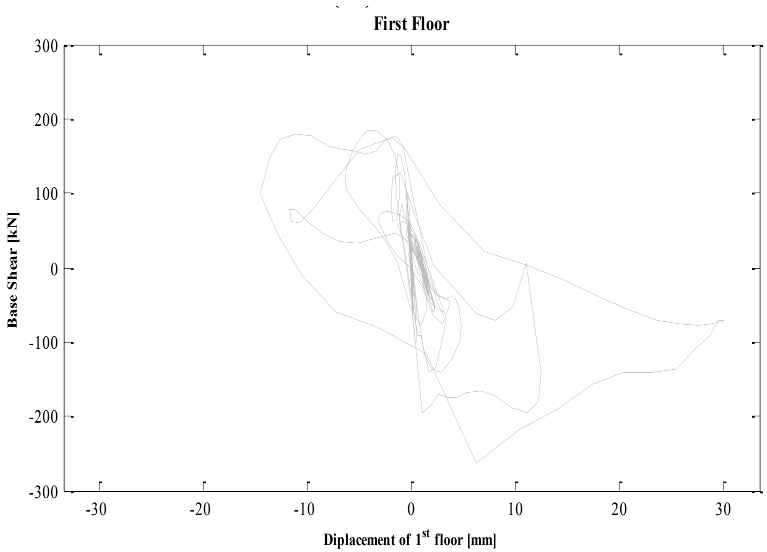

Damage of both inner an outer walls and hysteretic response observed during the N-00470-L seismic input

8. Index buildings

Brief description of *Nieuwstraat*:

- Nieuwstraat is an unreinforced masonry detached house with timber attic and roof diaphragms built around 1940.
- The overall height is 6.35 meters, the total mass around 100 tons
- The loadbearing function is provided by double wyhte clay brick masonry walls (200-mm thick)
- The façade openings distribution is irregular

8. Index buildings

Numerical results for *Nieuwstraat:*

- The observed failure modes involved both the OOP mechanisms of the gables and the shear damage of the longitudinal walls, but it is worth mentioning the first floor system was found to be very vulnerable. Indeed, most of the predicted collapses were caused by the partial unseating of the main floor beam.
- Considering the abovementioned 11 ground motions, the structure exhibited slightly damage at the end of the records only for the first record
- The near collapse condition or partial collapse was reached for 7 records
- Global collapse was reached for the last 3 inputs

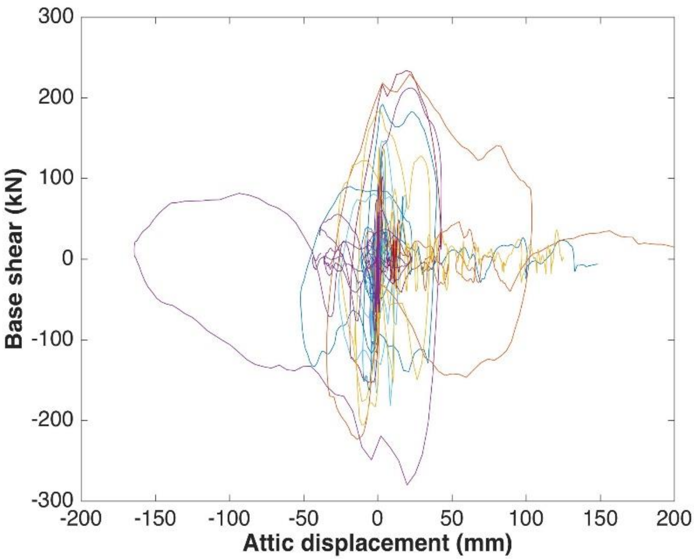

Screenshot of roof collapse mechanism observed during record N_00415L and hysteresis plots of the 11 recordings in the weak direction

Design of LNEC-BUILD3 full-scale specimen

- A new shake-table test on a URM building is proposed with the view to address some new questions that have arisen in the Dutch building fragility assessment, such as chimney seismic response and the first floor collapse due to the unseating of main floor beam observed in the Nieuwstraat model
- The specimen design was partially driven by the ELS model
- The prototype incorporates two additional distinctive features compared to previous investigated typologies (i.e. EUC_BUILD_1/LNEC_BUILD_1, and EUC_BUILD_2): an internal wall and two slender chimneys

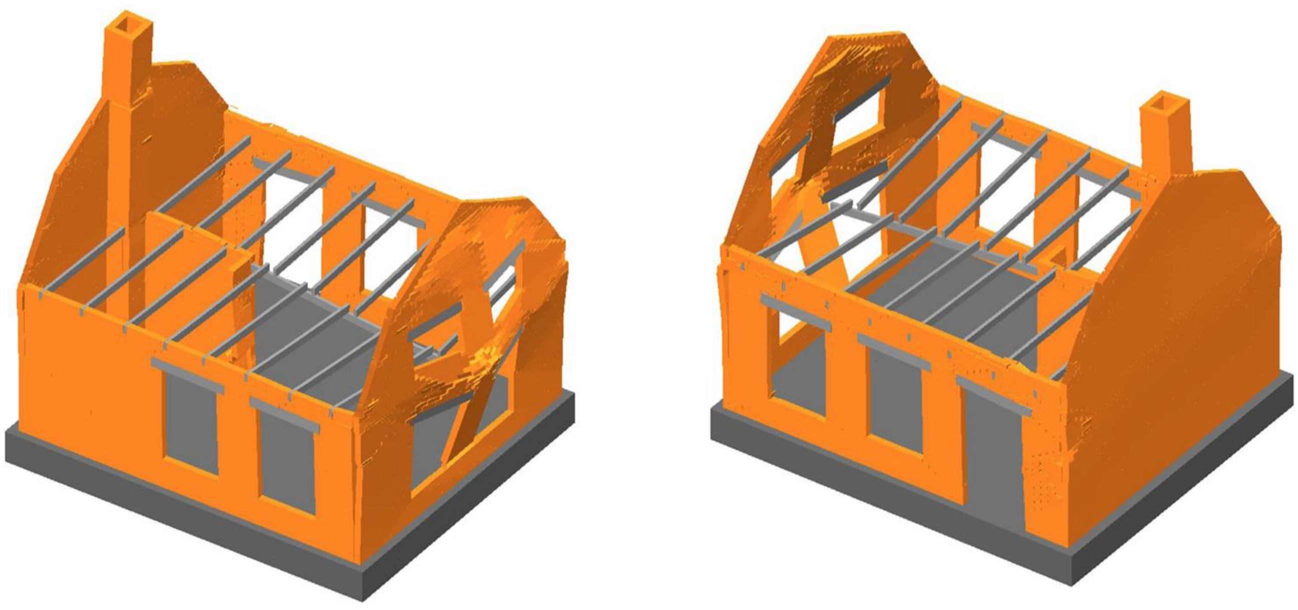

Screenshot of the OOP failure mode of the façade induced by the unseating of the main floor beam observed during EQ2@200% record

MOSAYK Modelling and Structural Analysis Konsulting

References (1/2)

1. Meguro K, Tagel-Din H. Applied element method for structural analysis: Theory and application for linear materials. JSCE-Structural Engineering/Earthquake Engineering, 2000; 17(1):21-35.
2. Cundall PA, Hart RD. Numerical modelling of discontinua. Engineering Computations 1992; 9(2):101-113. DOI: 10.1108/eb023851.
3. ASI (2017). Extreme Loading for Structures v5, Applied Science International LLC., Durham, USA.
4. Malomo D, Rui P, Penna A. Using the Applied Element Method for Modelling Calcium-Silicate Brick Masonry Subjected to In-Plane Cyclic Loading. Earthquake Engineering and Structural Dynamics, 2018 (in publishing).
5. Lourenco PB, Rots JG, Blaanwendraad J. Two approaches for the analysis of masonry structures: micro and macro-modeling. in Heron, Publication series of the Built Environment and Geosciences Department of the Delft University of Technology, The Netherlands, 1995; 40(4):314-343.
6. Graziotti F., Tomassetti U., Rossi A., Kallioras S., Mandirola M., Penna A., Magenes G. (2015). Experimental campaign on cavity-wall systems representative of the Groningen building stock, report n. EUC318/2015U, European Centre for Training and Research in Earthquake Engineering (EUCENTRE), Pavia, Italy. Available from URL: http://www.eucentre.it/nam-project.
7. Brooks JJ, Baker A. Modulus of elasticity of masonry. Masonry International, 1998; 12:58-63.
8. Matysek P, Janowski Z (1996). Analysis of factors affecting the modulus of elasticity of the walls, in Proceedings of the Conference of the Committee of Civil Engineering PZITB: Lublin, Poland. [in Polish]
9. Ciesielski R (1999), The dynamic module of elasticity of brick walls, in Proceedings of the Conference of the Committee of Civil Engineering PZITB: Wrocław-Krynica, Poland. [in Polish]
10. International Conference of Building Officials (1991), Uniform Building Code, Whittier, USA.

References (2/2)

11. Crowley H, Pinho R (2017). Report on the v5 Fragility and Consequence Models for the Groningen Field., available from http://www.nam.nl/feiten-en-cijfers/onderzoeksrapporten.html
12. Mosayk (2017a). Using the Applied Element Method to model the shake-table out-of-plane testing of full-scale URM wall specimens subjected to one-way bending. Report n. D9. Available from URL: http://www.nam.nl/feiten-en-cijfers/onderzoeksrapporten.html
13. Mosayk (2017b). Using the Applied Element Method to model the shake-table testing of two full-scale URM houses. Report n. D5. Available from http://www.nam.nl/feiten-en-cijfers/onderzoeksrapporten.html
14. Graziotti F, Tomassetti U, Rossi A, Marchesi B, Kallioras S, Mandirola M, Fragomeli A, Mellia E, Peloso S, Cuppari F, Guerrini G, Penna A, Magenes G (2016). Shaking table tests on a full-scale clay-brick masonry house representative of the Groningen building stock and related characterization tests. Report n. EUC128/2016U, European Centre for Training and Research in Earthquake Engineering (Eucentre), Pavia, IT. Available from URL: www.eucentre.it/nam-project
15. Tomasetti U, Correia AA, Graziotti F, Marques AI, Mandirola M, Candeias PX (2017a). Collapse shaking table test on a URM cavity wall building representative of a Dutch terraced house. European Centre for Training and Research in Earthquake Engineering (Eucentre), Pavia, IT. Available from URL: www.eucentre.it/nam-project
16. Mosayk (2017c). Using the Applied Element Method to model the collapse shake-table testing of a URM cavity wall structure. Report n. D6. Available from http://www.nam.nl/feiten-en-cijfers/onderzoeksrapporten.html
17. Tomassetti U., Kallioras S., Graziotti F., Correia A. (2017b) "Final report on the construction of the building prototype at the LNEC laboratory," European Centre for Training and Research in Earthquake Engineering (EUCENTRE), Pavia, Italy.
18. Mosayk (2017d). Using the Applied Element Method to model the collapse shake-table testing of a terraced house roof substructure. Report n. D7. Available from http://www.nam.nl/feiten-en-cijfers/onderzoeksrapporten.html

Assurance Meeting on Exposure, Fragility and Fatality Models for the Groningen Building Stock

Exposure, Fragility and Consequence models

Helen Crowley

Exposure model

Local Personal Risk

- Local Personal Risk (LPR)
  - the annual probability of fatality for a hypothetical person who is continuously present, without protection, in or near a building
- 'Near' a building is defined within 5 metres of the façade of the building
- In the risk engine, we calculate the average number of people/buildings in the field with a LPR above 10^{-4} and LPR above 10^{-5}
- We thus need a model of the location of people across the field and the building types they are situated within/near.

Exposure Database

Building ID
Coordinates
Building Year
Height
Footprint Area
Structural Layout
Structural System 1
Probability Structural System 1
Structural System 2
Probability Structural System 2
…
….
Number of people inside/near - day
Number of people outside/near - night

Exposure Model

Building ID

Coordinates

Building Typology 1

Probability Building Typology 1

Building Typology 2

Probability Building Typology 2

...

....

Number of people inside/near - day

Number of people outside/near - night

List of Building Typologies (for Fragility)

GEM Taxonomy Code	Short code	Short Description
CR+PC/LPB/CR+PC/LPB/EWN/FN/HBET:1,2	PC1L	Precast RC post and beam low-rise
CR+PC/LPB/CR+PC/LPB/EWN/FN/HBET:3,20	PC1M	Precast RC post and beam mid to high-rise
CR+PC/LWAL/CR+PC/LN/EWN/FC/HBET:1,2	PC2L	Precast RC wall-slab-wall low-rise no cladding
CR+PC/LWAL/CR+PC/LN/EW/FC/HBET:1,2	PC3L	Precast RC wall-slab-wall low-rise with cladding
CR+PC/LWAL/CR+PC/LN/EW/FC/HBET:3,20	PC3M	Precast RC wall-slab-wall mid to high-rise with cladding
CR+PC/LWAL/CR+PC/LWAL/EWN/FC/HBET:1,2	PC4L	Precast RC wall-wall low-rise no cladding
CR+PC/LWAL/CR+PC/LWAL/EWN/FC/HBET:3,20	PC4M	Precast RC wall-wall mid to high-rise no cladding
CR+PC/LWAL/CR+PC/LWAL/EW/FC/HBET:1,2	PC5L	Precast RC wall-wall low-rise with cladding
CR+CIP/LPB/CR+CIP/LPB/EWN/FN/HBET:1,2	RC1L	Cast-in-place RC post and beam low-rise
CR+CIP/LPB/CR+CIP/LPB/EWN/FN/HBET:3,20	RC1M	Cast-in-place RC post and beam mid to high-rise
CR+CIP/LFM/CR+CIP/LFM/EWN/FC/HBET:1,2	RC2L	Cast-in-place RC frame low-rise
CR+CIP/LFM/CR+CIP/LFM/EWN/FC/HBET:3,20	RC2M	Cast-in-place RC frame mid to high-rise
CR+CIP/LWAL/CR+CIP/LN/EW/FC/HBET:1,2	RC3L	Cast-in-place RC wall-slab-wall low-rise with cladding
CR+CIP/LWAL/CR+CIP/LN/EW/FC/HBET:3,20	RC3M	Cast-in-place RC wall-slab-wall mid to high-rise with cladding
CR+CIP/LWAL/CR+CIP/LWAL/EWN/FC/HBET:1,2	RC4L	Cast-in-place RC wall-wall low-rise no cladding
CR+CIP/LWAL/CR+CIP/LWAL/EWN/FC/HBET:3,20	RC4M	Cast-in-place RC wall-wall mid to high-rise no cladding
MUR/LH/MUR/LH/EWN/FW/HBET:1,2	URM1L	URM house and timber post and beam low-rise
MUR/LH/MUR/LH/EWN/FW/HBET:3,20	URM1M	URM house and timber post and beam mid to high-rise
MUR/LWAL/MUR/LN/EWN/FW/HBET:1,2	URM2L	URM wall-slab-wall with solid walls and timber floors low-rise
MUR/LW		
MUR/LW		
MUR/LW		
MUR/LW		
MUR/LW		
MUR/LW		
MUR/LW		
MUR/LW		
MUR/LW		
MUR/LW		
MUR/LW		
MUR/LW		
MUR/LW		
MUR/LW		
W/LPB/V		
W/LPB/V		
W/LWAL		
W/LWAL		
W/LWAL		
W/LWAL		
W/LWAL		
W/LWAL		
W/LWAL		
S/LPB/S/		
S/LPB/S/		
S/LFM/S/		
S/LFM/S/		
S/LFBR/V		
S/LFBR/V		
S/LFBR/S		
S/LFBR/S/LPB/EWN/FN/HBET:3,20	S3M	Steel portal frame with bracing in one direction mid to high-rise
S/LFBR/S/LFBR/EWN/FN/HBET:1,2	S4L	Steel braced frame with no floor low-rise
S/LFBR/S/LFBR/EWN/FN/HBET:3,20	S4M	Steel braced frame with no floor mid to high-rise
S/LFBR/S/LFBR/EWN/FC/HBET:1,2	S5L	Steel braced frame with concrete floor low-rise
S/LFBR/S/LFBR/EWN/FC/HBET:3,20	S5M	Steel braced frame with concrete floor mid to high-rise

- Added a height range attribute
- Mapped floors to either concrete or timber
- A small number of buildings had an unusual/unknown combination of attributes and so they were mapped to predominant building types.
- Separated terraced houses with concrete floors and cavity walls into two typologies as a function of openings at ground floor

Pre-cast RC

Cast-in-place RC

Unreinforced masonry

Timber

Steel

From Exposure Database to Model

- In a exposure database there were almost 60k buildings with the MUR/LWAL/MUR/LN/EW/FC structural system (i.e. terraced-like buildings with cavity walls and concrete floors).
- The maximum ground floor opening ratio (%) of these buildings was obtained from the terraced building database (TBDD):

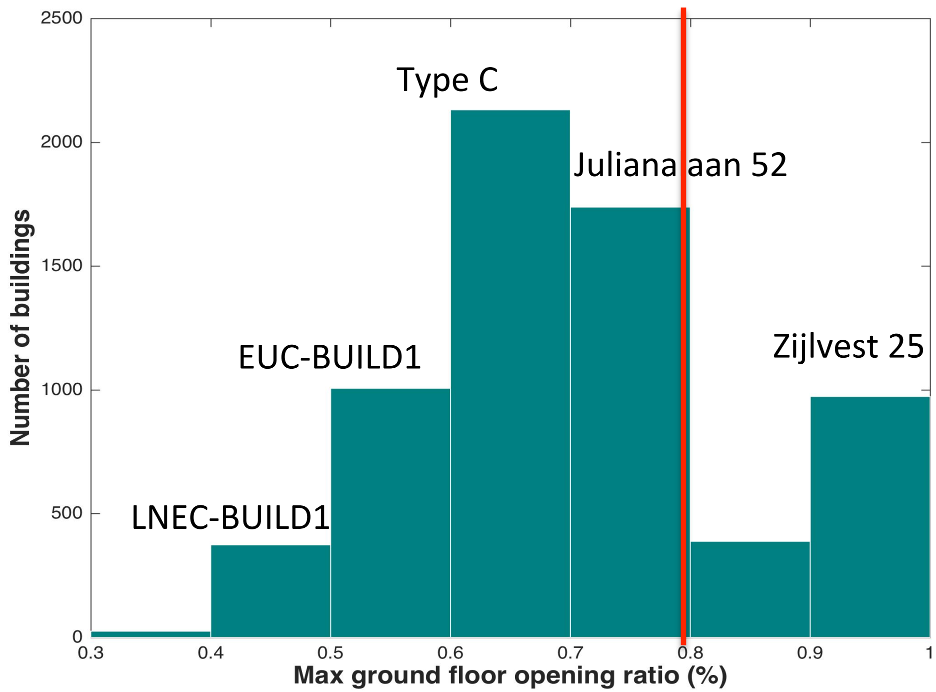

From Exposure Database to Model

- Hence MUR/LWAL/MUR/LN/EW/FC buildings with max. ground floor opening ratios ≥ 80% were separated into another structural system (identified using the 'change in vertical structure' attribute of the GEM Building Taxonomy).
- This data was available for 6635 inspected buildings, whereas an inference rule based on this data was applied to the buildings for which this information was not available.

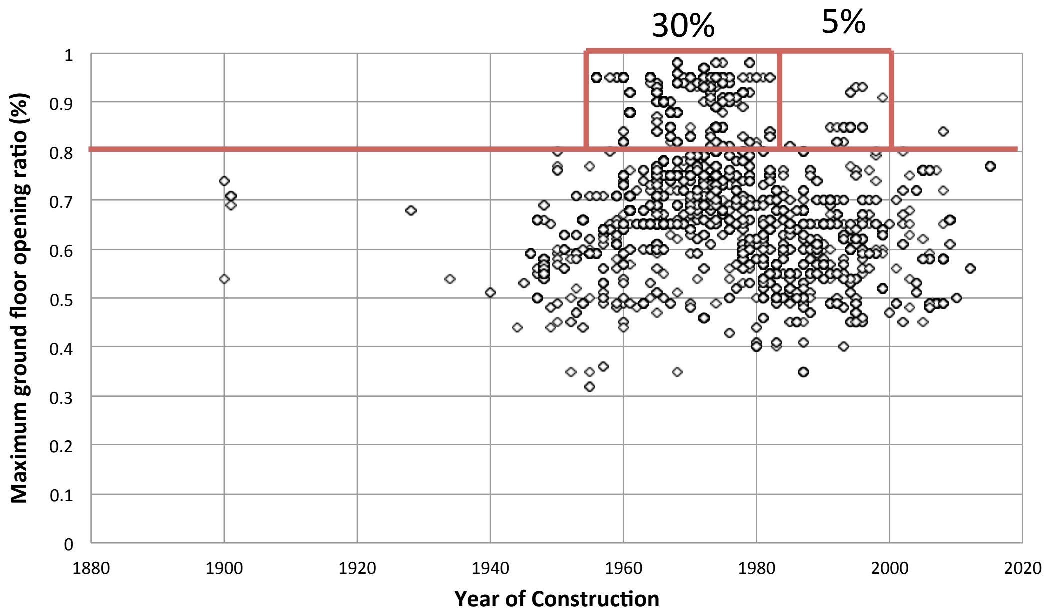

Distribution of Building Typologies

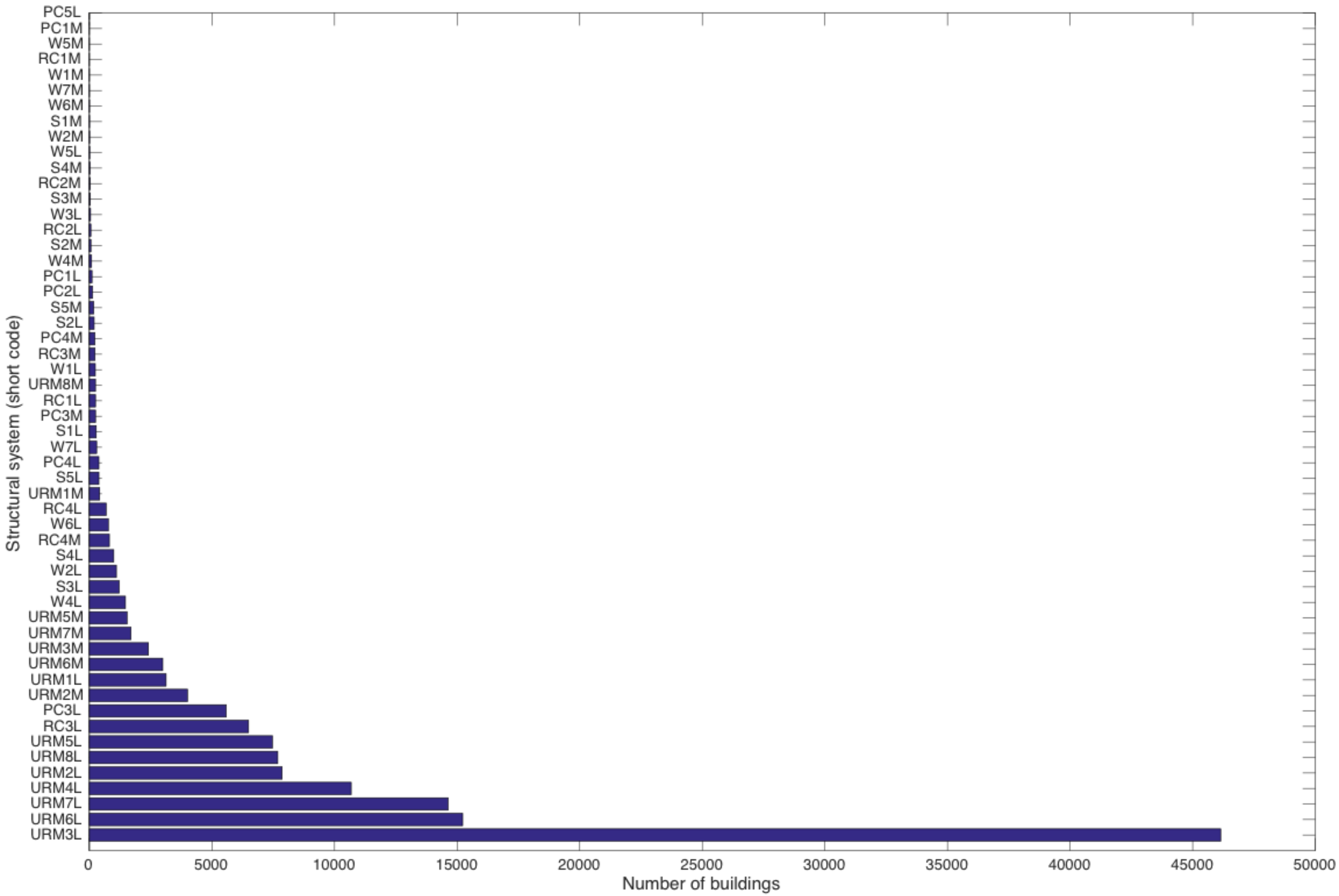

Index Buildings Representing Building Types

Index Building Name	GEM Taxonomy String
Precast RC post and beam*	CR+PC/LPB/CR+PC/LPB/EWN/FC/HBET:1,2
Precast RC wall-slab-wall*	CR+PC/LWAL/CR+PC/LN/EWN/FC/HBET:1,2
Cast-in-place RC post and beam*	CR+CIP/LPB/CR+CIP/LPB/EWN/FC/HBET:1,2
Cast-in-place RC wall-slab-wall*	CR+CIP/LWAL/CR+CIP/LN/EWN/FC/HBET:1,2
De Haver	MUR/LH/MUR/LH/EWN/FW/HBET:1,2
Solwerderstraat 55	MUR/LWAL/MUR/LN/EWN/FW/HBET:1,2
Julianalaan 52	MUR/LWAL/MUR/LN/EW/FC/HBET:1,2
Type C	MUR/LWAL/MUR/LN/EW/FC/HBET:1,2
Zijlvest 25	MUR/LWAL/MUR/LN/EW/FC/HBET:1,2/IRIR+IRVP:CHV
Koeriersterweg 20-21	MUR/LWAL/MUR/LN/EW/FC/HBET:3,20
Nieuwstraat 8	MUR/LWAL/MUR/LWAL/EWN/FW/HBET:1,2
Kwelder 1	MUR/LWAL/MUR/LWAL/EW/FC/HBET:1,2
Schuitenzandflat 2-56	MUR/LWAL/MUR/LWAL/EW/FC/HBET:3,20
Badweg 12	MUR/LWAL/MUR/LWAL/EW/FW/HBET:1,2
Kwelder 8	W/LWAL/W/LWAL/EW/FW/HBET:1,2
Steenweg 19	S/LFM/S/LFM/EWN/FC/HBET:1,2
Glulam portal frame*	S/LFBR/W/LPB/EWN/FN/HBET:1,2
Beneluxweg 15	S/LFBR/S/LPB/EWN/FN/HBET:1,2

* Generic model

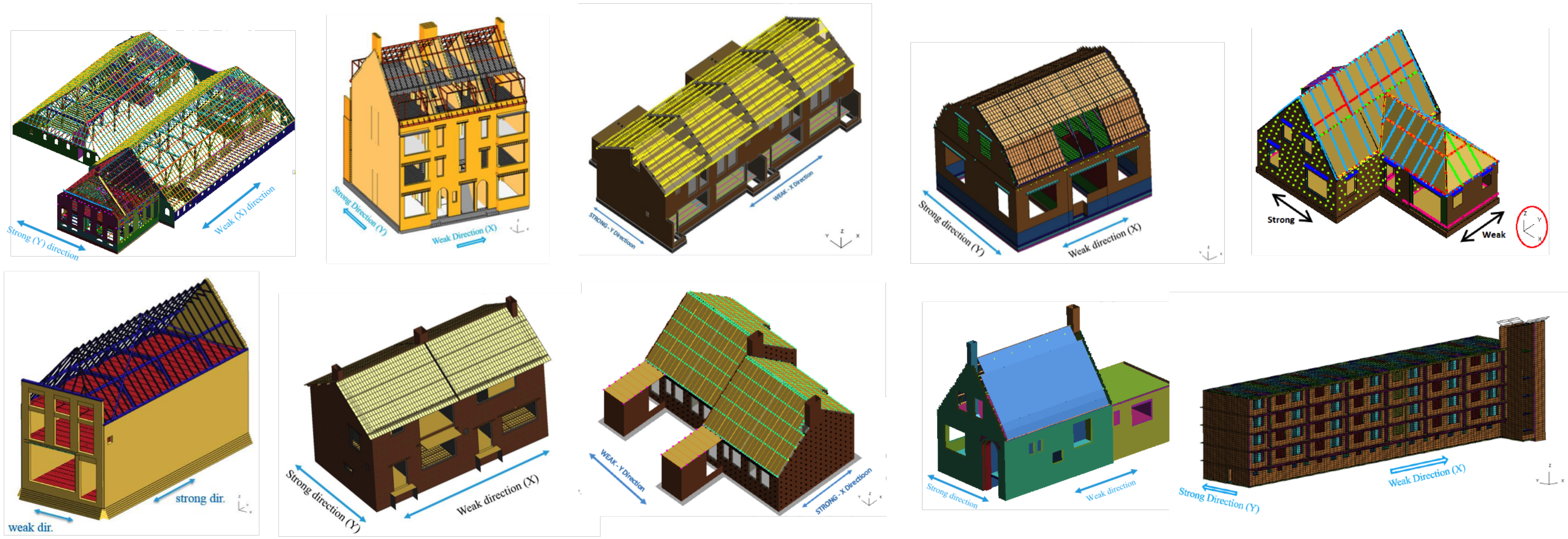

Index Buildings Representing Building Typologies

Index Building Name	GEM Taxonomy String
Precast RC post and beam*	CR+PC/LPB/CR+PC/LPB/EWN/FC/HBET:1,2
Precast RC wall-slab-wall*	CR+PC/LWAL/CR+PC/LN/EWN/FC/HBET:1,2
Cast-in-place RC post and beam*	CR+CIP/LPB/CR+CIP/LPB/EWN/FC/HBET:1,2
Cast-in-place RC wall-slab-wall*	CR+CIP/LWAL/CR+CIP/LN/EWN/FC/HBET:1,2
De Haver	MUR/LH/MUR/LH/EWN/FW/HBET:1,2
Solwerderstraat 55	MUR/LWAL/MUR/LN/EWN/FW/HBET:1,2
Julianalaan 52	MUR/LWAL/MUR/LN/EW/FC/HBET:1,2
Type C	MUR/LWAL/MUR/LN/EW/FC/HBET:1,2
Zijlvest 25	MUR/LWAL/MUR/LN/EW/FC/HBET:1,2/IRIR+IRVP:CHV
Koeriersterweg 20-21	MUR/LWAL/MUR/LN/EW/FC/HBET:3,20
Nieuwstraat 8	MUR/LWAL/MUR/LWAL/EWN/FW/HBET:1,2
Kwelder 1	MUR/LWAL/MUR/LWAL/EW/FC/HBET:1,2
Schuitenzandflat 2-56	MUR/LWAL/MUR/LWAL/EW/FC/HBET:3,20
Badweg 12	MUR/LWAL/MUR/LWAL/EW/FW/HBET:1,2
Kwelder 8	W/LWAL/W/LWAL/EW/FW/HBET:1,2
Steenweg 19	S/LFM/S/LFM/EWN/FC/HBET:1,2
Glulam portal frame*	S/LFBR/W/LPB/EWN/FN/HBET:1,2
Beneluxweg 15	S/LFBR/S/LPB/EWN/FN/HBET:1,2

* Generic model

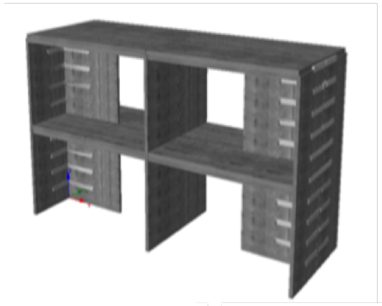

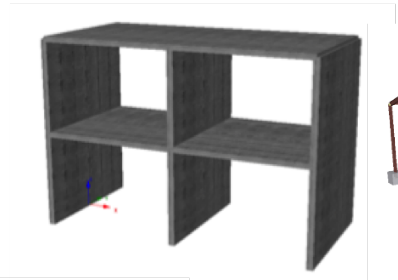

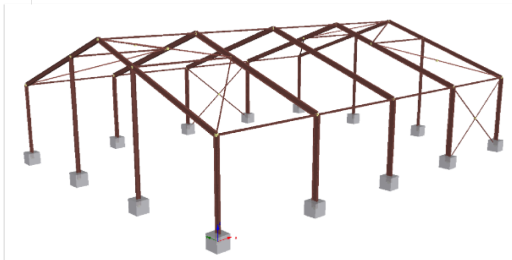

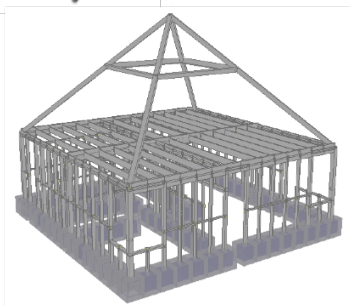

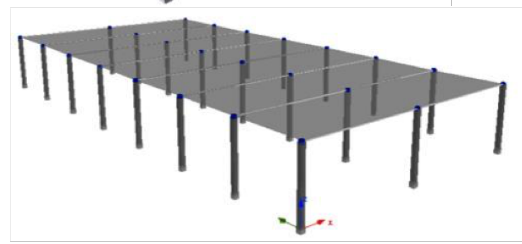

Distribution of Building Typologies

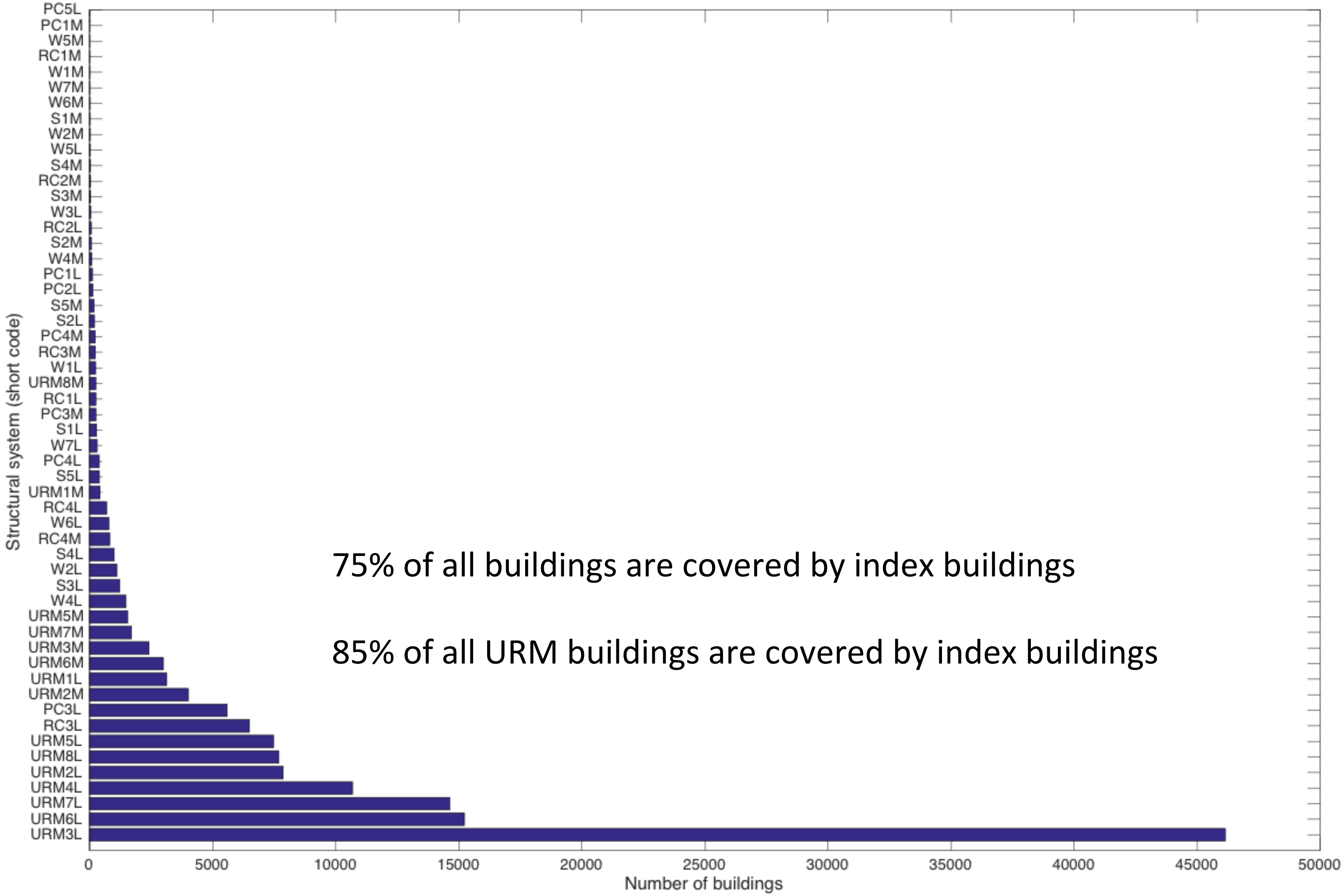

75% of all buildings are covered by index buildings

85% of all URM buildings are covered by index buildings

Coverage of Building Typologies

95% of all buildings with LPR > 10^{-5} are covered by index buildings:

Index Buildings:

- Zijlvest 25
- Badweg 12
- Koeriersterweg 20-21
- De Haver + House
- De Haver Barn
- EUC-BUILD 4/5 (with cladding)
- Nieuwstraat 8
- EUC-BUILD 4/5 (no cladding)
- De Haver + House

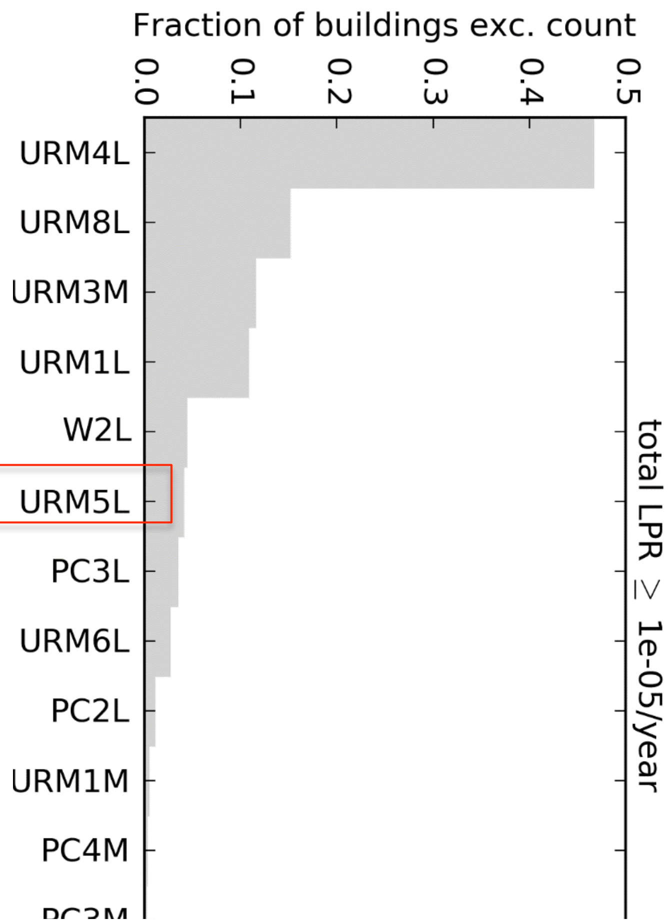

Representativeness of Building Typologies

v5 Exposure Database – distributions and mean properties

Structural System	Year of Construction	Structural Layout	Gutter Height (m)	Footprint Area (m^2)
CR+PC/LPB/CR+PC/LPB/EWN/FC/HBET:1,2	1980-1999	WBW	3.1-4	>300
CR+PC/LWAL/CR+PC/LN/EWN/FC/HBET:1,2	1980-1999	UBH	5.1-6	51-100
CR+CIP/LPB/CR+CIP/LPB/EWN/FC/HBET:1,2	1960-1979	WBW	3.1-4	>300
CR+CIP/LWAL/CR+CIP/LN/EWN/FC/HBET:1,2	1960-1979	UBH	5.1-6	51-100
MUR/LH/MUR/LH/EWN/FW/HBET:1,2	<1900	WBH	3.1-4	>300
MUR/LWAL/MUR/LN/EWN/FW/HBET:1,2	1920-1939	UBH	4.1-5	51-100
MUR/LWAL/MUR/LN/EW/FC/HBET:1,2	1960-1979	UBH	5.1-6	51-100
MUR/LWAL/MUR/LN/EW/FC/HBET:1,2	1960-1979	UBH	5.1-6	51-100
MUR/LWAL/MUR/LN/EW/FC/HBET:1,2/IRIR+IRVP:CHV	1960-1979	UBH	5.1-6	51-100
MUR/LWAL/MUR/LN/EW/FC/HBET:3,20	1960-1979	UBH	8.1-9	51-100
MUR/LWAL/MUR/LWAL/EWN/FW/HBET:1,2	1920-1939	UH	3.1-4	51-100
MUR/LWAL/MUR/LWAL/EW/FC/HBET:1,2	1980-1999	UH	4.1-5	101-150
MUR/LWAL/MUR/LWAL/EW/FC/HBET:3,20	1960-1979	BTN	>11	151-200
MUR/LWAL/MUR/LWAL/EW/FW/HBET:1,2	1920-1939	UH	3.1-4	101-150
W/LWAL/W/LWAL/EW/FW/HBET:1,2	1980-1999	UH	4.1-5	101-150
S/LFM/S/LFM/EWN/FC/HBET:1,2	1980-1999	UH	3.1-4	101-150
S/LFBR/W/LPB/EWN/FN/HBET:1,2	1980-1999	WBW	3.1-4	>300
S/LFBR/S/LPB/EWN/FN/HBET:1,2	1960-1979	WBW	3.1-4	>300

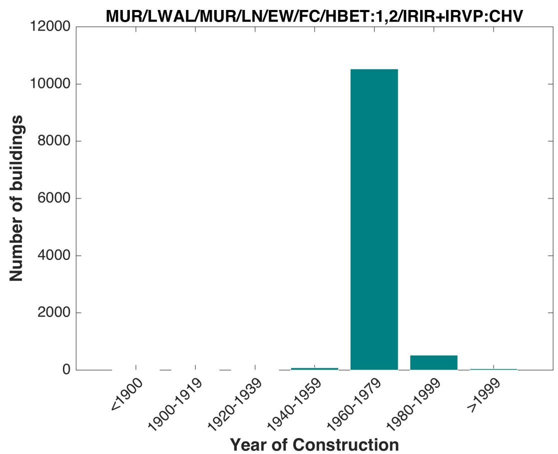

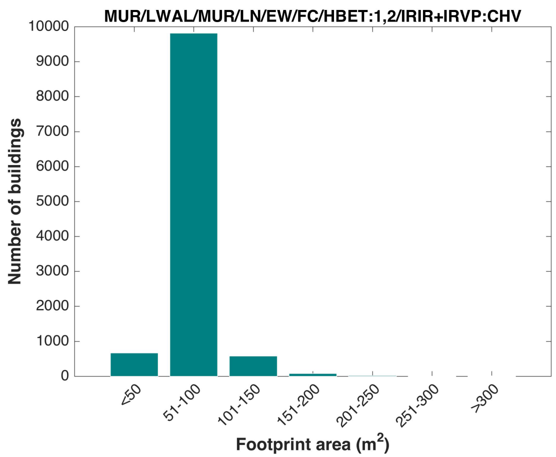

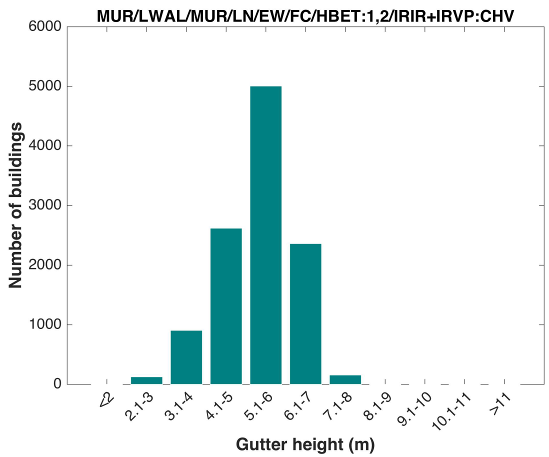

Representativeness of Building Typologies

Index Buildings

Index Building Name	Year of Construction	Structural Layout	Gutter Height (m)	Footprint area (m^2)
Precast RC post and beam	N/A	WBW	6.5	1880
Precast RC wall-slab-wall	N/A	UBH	5.52	44 per unit
Cast-in-place RC post and beam	N/A	WBW	6.5	1880
Cast-in-place RC wall-slab-wall	N/A	UBH	5.56	44 per unit
De Haver	1900's	WBH	2.9 (house) 3.7 (barn)	194 (house), 1530 (barn)
Solwerderstraat 55	<1945	UBA	6.1	113
Julianalaan 52	1950's	UBH	5.4	45 per unit
Type C	1970's	UBH	2.8	70 per unit
Zijlvest 25	1976	UBH	5.5	53 per unit
Koeriersterweg 20-21	TBD	UBH	8.59	50 per unit
Nieuwstraat 8	1940s	UH	3.0	70
Kwelder 1	TBD	UH	2.75	98
Schuitenzandflat 2-56	TBD	BTN	13.8	720
Badweg 12	1940's	UH	2.8	67
Kwelder 8	TBD	UH	2.75	76
Steenweg 19	2005	WBW	6.5	432
Glulam portal frame	N/A	WBW	4.0	460
Beneluxweg 15	2001	WBW	3.8	300

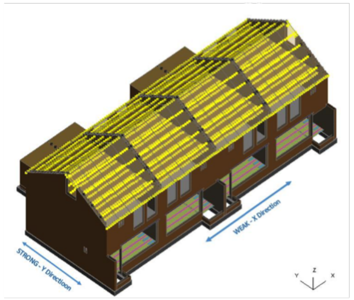

v5 Exposure Database – mean properties

Structural System	Year of Construction	Structural Layout	Gutter Height (m)	Footprint Area (m^2)
CR+PC/LPB/CR+PC/LPB/EWN/FC/HBET:1,2	1980-1999	WBW	3.1-4	>300
CR+PC/LWAL/CR+PC/LN/EWN/FC/HBET:1,2	1980-1999	UBH	5.1-6	51-100
CR+CIP/LPB/CR+CIP/LPB/EWN/FC/HBET:1,2	1960-1979	WBW	3.1-4	>300
CR+CIP/LWAL/CR+CIP/LN/EWN/FC/HBET:1,2	1960-1979	UBH	5.1-6	51-100
MUR/LH/MUR/LH/EWN/FW/HBET:1,2	<1900	WBH	3.1-4	>300
MUR/LWAL/MUR/LN/EWN/FW/HBET:1,2	1920-1939	UBH	4.1-5	51-100
MUR/LWAL/MUR/LN/EW/FC/HBET:1,2	1960-1979	UBH	5.1-6	51-100
MUR/LWAL/MUR/LN/EW/FC/HBET:1,2	1960-1979	UBH	5.1-6	51-100
MUR/LWAL/MUR/LN/EW/FC/HBET:1,2/IRIR+IRVP:CHV	1960-1979	UBH	5.1-6	51-100
MUR/LWAL/MUR/LN/EW/FC/HBET:3,20	1960-1979	UBH	8.1-9	51-100
MUR/LWAL/MUR/LWAL/EWN/FW/HBET:1,2	1920-1939	UH	3.1-4	51-100
MUR/LWAL/MUR/LWAL/EW/FC/HBET:1,2	1980-1999	UH	4.1-5	101-150
MUR/LWAL/MUR/LWAL/EW/FC/HBET:3,20	1960-1979	BTN	>11	151-200
MUR/LWAL/MUR/LWAL/EW/FW/HBET:1,2	1920-1939	UH	3.1-4	101-150
W/LWAL/W/LWAL/EW/FW/HBET:1,2	1980-1999	UH	4.1-5	101-150
S/LFM/S/LFM/EWN/FC/HBET:1,2	1980-1999	UH	3.1-4	101-150
S/LFBR/W/LPB/EWN/FN/HBET:1,2	1980-1999	WBW	3.1-4	>300
S/LFBR/S/LPB/EWN/FN/HBET:1,2	1960-1979	WBW	3.1-4	>300

Representativeness of Building Typologies

Index Buildings

Index Building Name	Year of Construction	Structural Layout	Gutter Height (m)	Footprint area (m^2)
Precast RC post and beam	N/A	WBW	6.5	1880
Precast RC wall-slab-wall	N/A	UBH	5.52	44 per unit
Cast-in-place RC post and beam	N/A	WBW	6.5	1880
Cast-in-place RC wall-slab-wall	N/A	UBH	5.56	44 per unit
De Haver	1900's	WBH	2.9 (house) 3.7 (barn)	194 (house), 1530 (barn)
Solwerderstraat 55	<1945	UBA	6.1	113
Julianalaan 52	1950's	UBH	5.4	45 per unit
Type C	1970's	UBH	2.8	70 per unit
Zijlvest 25	1976	UBH	5.5	53 per unit
Koeriersterweg 20-21	TBD	UBH	8.59	50 per unit
Nieuwstraat 8	1940s	UH	3.0	70
Kwelder 1	TBD	UH	2.75	98
Schuitenzandflat 2-56	TBD	BTN	13.8	720
Badweg 12	1940's	UH	2.8	67
Kwelder 8	TBD	UH	2.75	76
Steenweg 19	2005	WBW	6.5	432
Glulam portal frame	N/A	WBW	4.0	460
Beneluxweg 15	2001	WBW	3.8	300

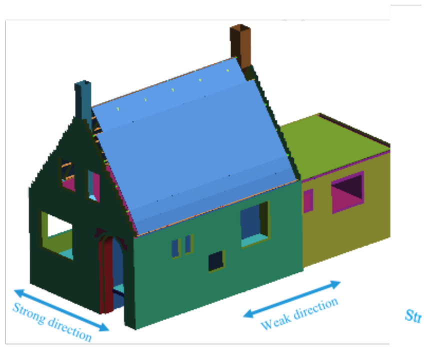

v5 Exposure Database – mean properties

Structural System	Year of Construction	Structural Layout	Gutter Height (m)	Footprint Area (m^2)
CR+PC/LPB/CR+PC/LPB/EWN/FC/HBET:1,2	1980-1999	WBW	3.1-4	>300
CR+PC/LWAL/CR+PC/LN/EWN/FC/HBET:1,2	1980-1999	UBH	5.1-6	51-100
CR+CIP/LPB/CR+CIP/LPB/EWN/FC/HBET:1,2	1960-1979	WBW	3.1-4	>300
CR+CIP/LWAL/CR+CIP/LN/EWN/FC/HBET:1,2	1960-1979	UBH	5.1-6	51-100
MUR/LH/MUR/LH/EWN/FW/HBET:1,2	<1900	WBH	3.1-4	>300
MUR/LWAL/MUR/LN/EWN/FW/HBET:1,2	1920-1939	UBH	4.1-5	51-100
MUR/LWAL/MUR/LN/EW/FC/HBET:1,2	1960-1979	UBH	5.1-6	51-100
MUR/LWAL/MUR/LN/EW/FC/HBET:1,2	1960-1979	UBH	5.1-6	51-100
MUR/LWAL/MUR/LN/EW/FC/HBET:1,2/IRIR+IRVP:CHV	1960-1979	UBH	5.1-6	51-100
MUR/LWAL/MUR/LN/EW/FC/HBET:3,20	1960-1979	UBH	8.1-9	51-100
MUR/LWAL/MUR/LWAL/EWN/FW/HBET:1,2	1920-1939	UH	3.1-4	51-100
MUR/LWAL/MUR/LWAL/EW/FC/HBET:1,2	1980-1999	UH	4.1-5	101-150
MUR/LWAL/MUR/LWAL/EW/FC/HBET:3,20	1960-1979	BTN	>11	151-200
MUR/LWAL/MUR/LWAL/EW/FW/HBET:1,2	1920-1939	UH	3.1-4	101-150
W/LWAL/W/LWAL/EW/FW/HBET:1,2	1980-1999	UH	4.1-5	101-150
S/LFM/S/LFM/EWN/FC/HBET:1,2	1980-1999	UH	3.1-4	101-150
S/LFBR/W/LPB/EWN/FN/HBET:1,2	1980-1999	WBW	3.1-4	>300
S/LFBR/S/LPB/EWN/FN/HBET:1,2	1960-1979	WBW	3.1-4	>300

Fragility model

Development of Fragility Functions

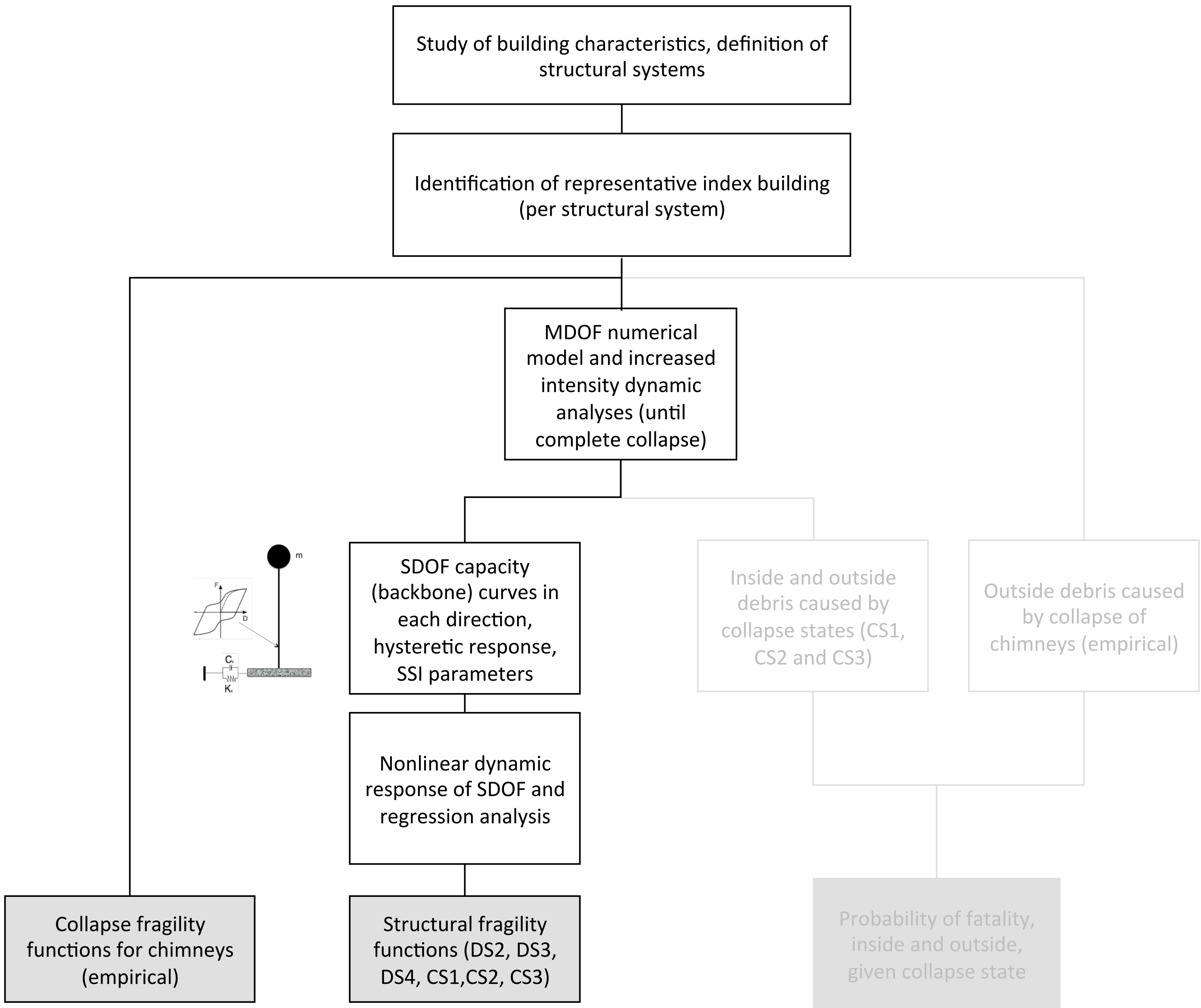

Nonlinear Dynamic Analysis

- A set of 11 tri-axial ground motions of increasing levels of intensity was applied to most index buildings (modelled using LS-DYNA, ELS and SeismoStruct). The strongest records led to collapse in all URM buildings.
- Hysteretic plots of base shear versus attic (i.e. highest level before roof) displacement were used to obtain peak base shear and corresponding displacement (with time lag) points:

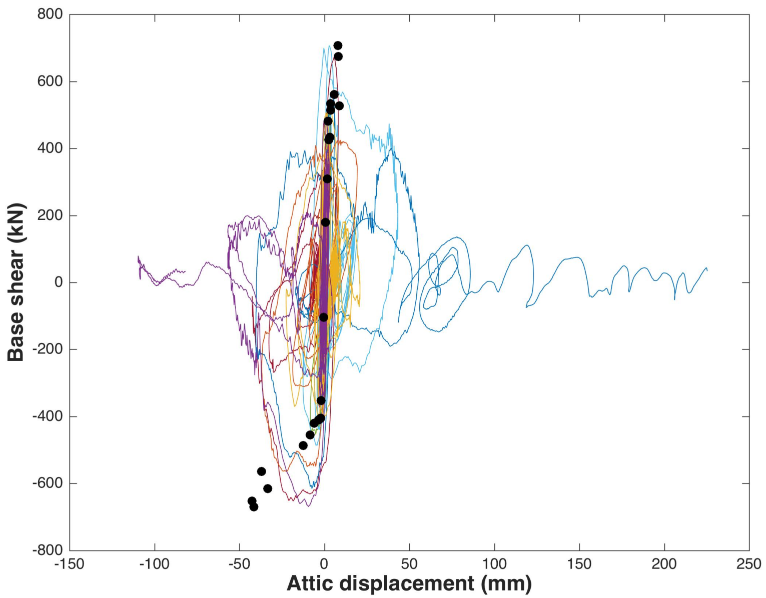

SDOF Models – Backbone Curves

- Peak base shear (V) and corresponding attic displacement (Δ_{max}) points transformed to SDOF system with base shear coefficient (BSC) and SDOF displacement (Sd) given by:

$$S_d = \frac{\Delta_{max}}{\Gamma_t} \qquad \Gamma_t = \frac{\sum m_i \phi_{it}}{\sum m_i \phi_{it}^2}$$

$$BSC = \frac{V}{m_{eff}} \qquad m_{eff} = \sum m_i \phi_{it} \Gamma_t$$

$$H_{eff} = \frac{\sum m_i \phi_{it} h_i}{\sum m_i \phi_{it}}$$

SDOF drift = S_d/H_{eff}

- Post-peak hysteretic response and collapse displacement used to complete the SDOF backbone curve.

SDOF Models – Backbone Curves

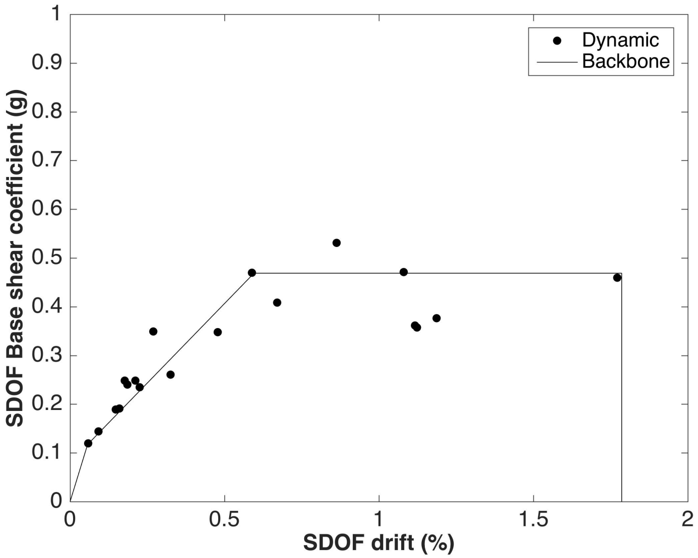

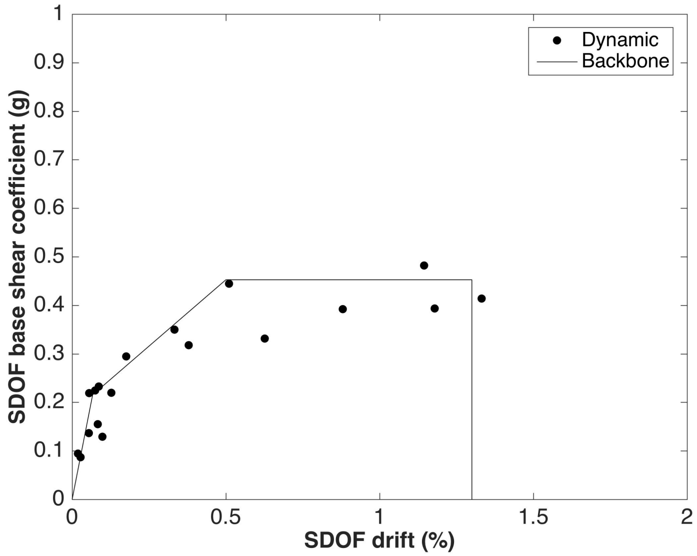

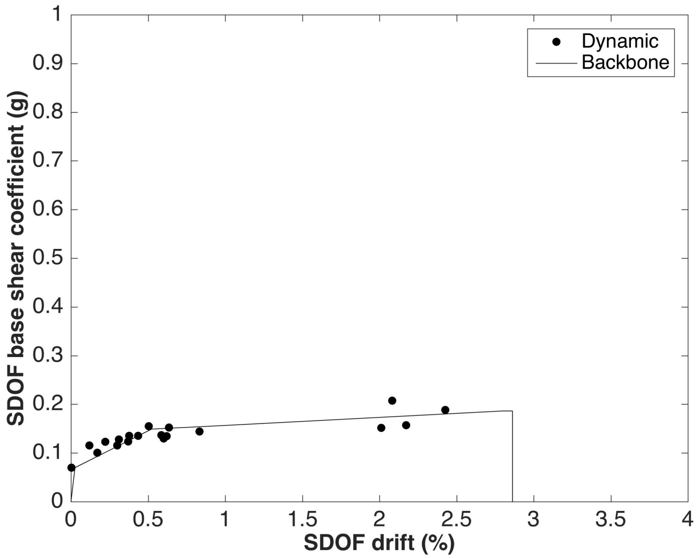

SDOF Models – Some Consistency Checks

- Backbone data has been obtained from EUC-BUILD1 and LNEC-BUILD1 (both same structural system) and transformed to equivalent SDOFs.

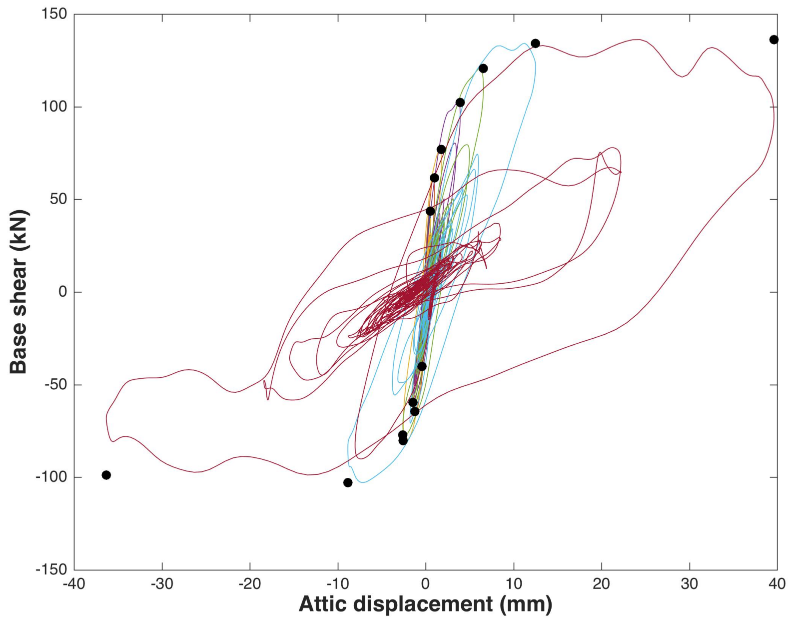

EUC-BUILD1

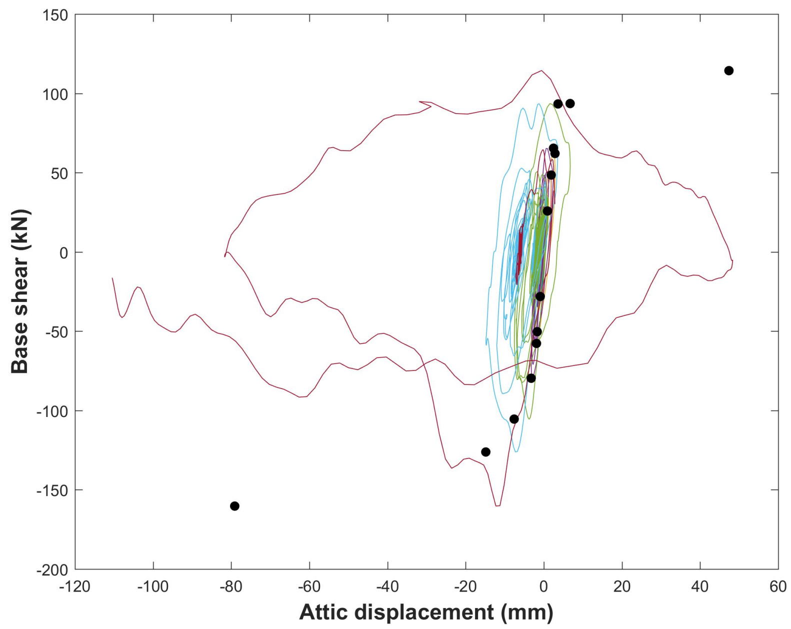

LNEC-BUILD1

SDOF Models – Some Consistency Checks

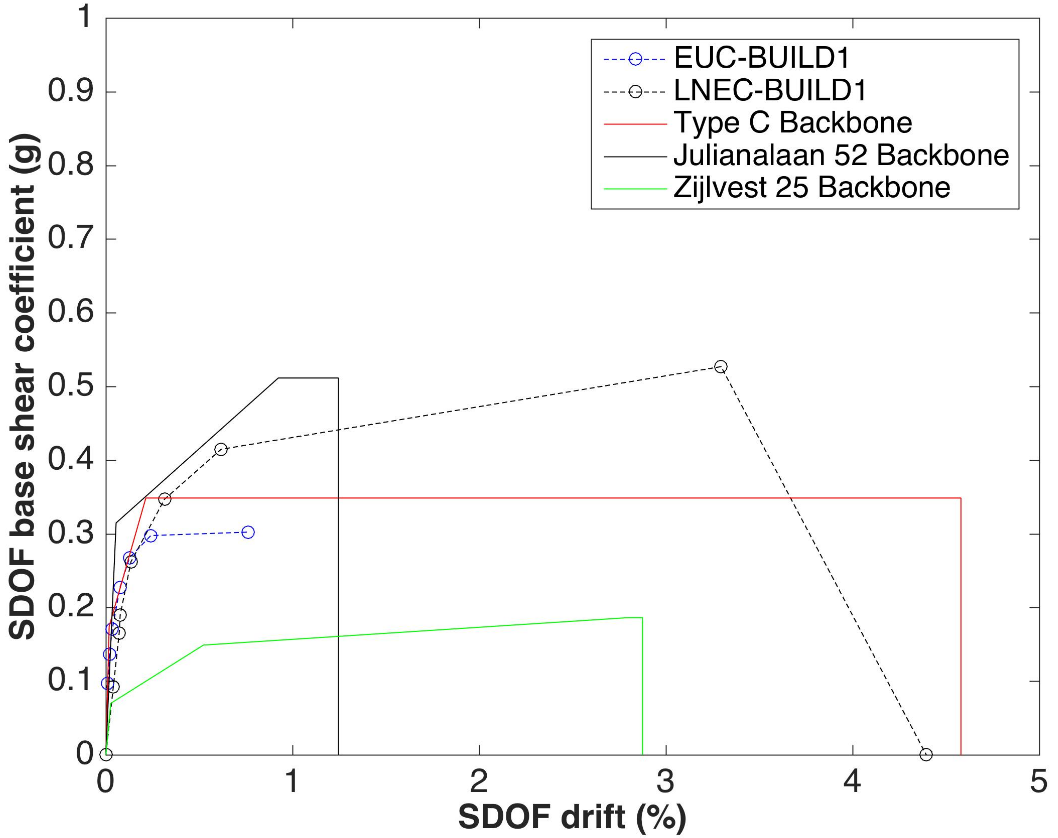

- Type C has one storey – similar base shear coefficient and collapse displacement to LNEC-BUILD1 (also one storey)
- Lower displacement capacity of Julianalaan 52 (two storeys) expected due to higher axial load on ground floor piers.

SDOF Models – Hysteretic Response

- OpenSees Hysteretic (which can model Takeda behaviour) and Multi-linear hysteresis models used. The degraded unloading stiffness (of Hysteretic) and damping values were modified for each system.

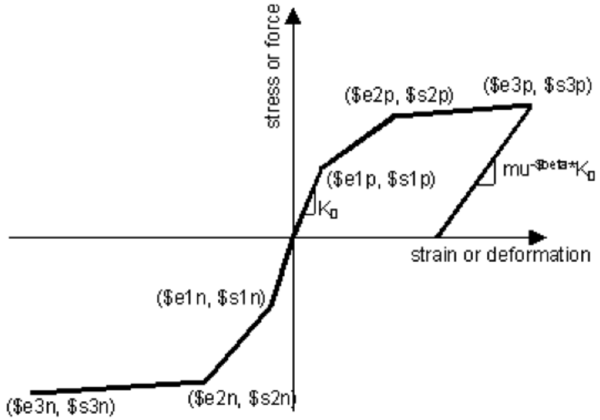

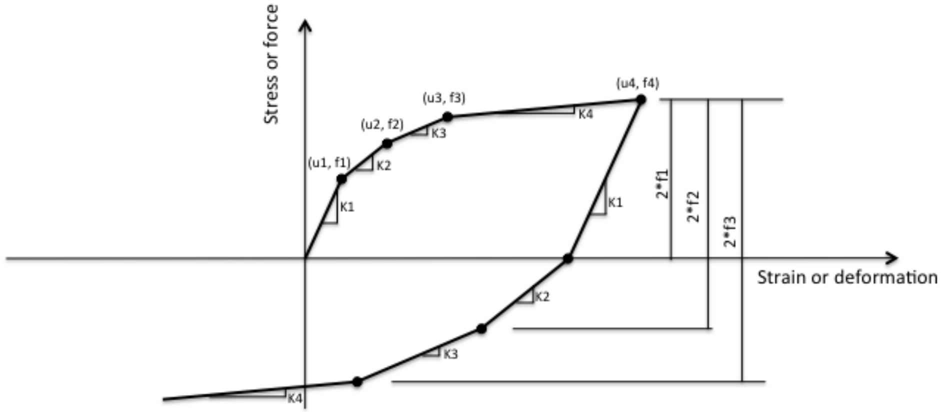

- A consistency check of the OpenSees SDOF maximum displacement response and transformed MDOF response was undertaken, mainly to ensure collapse predicted under same records and average ratio of displacements was ≈ 1.

SDOF Models – SSI Parameters

- Most probable foundation types have been identified for each URM structural system considering structural layout, age, soil stiffness (exposure database).
- Impedance functions developed by Mosayk (2015) have been used to assign the horizontal spring stiffness and damping at the base of the SDOF models, considering its fundamental period of vibration.

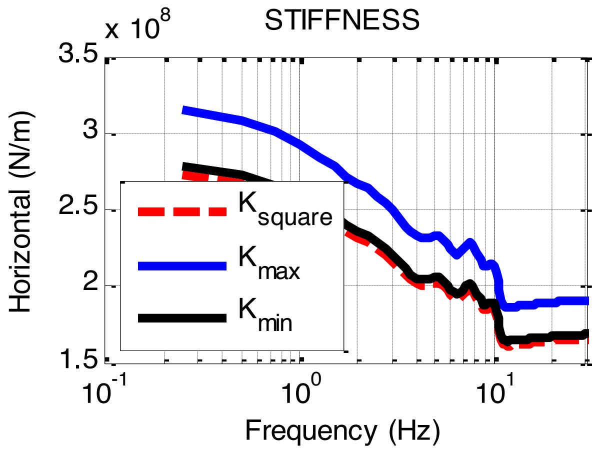

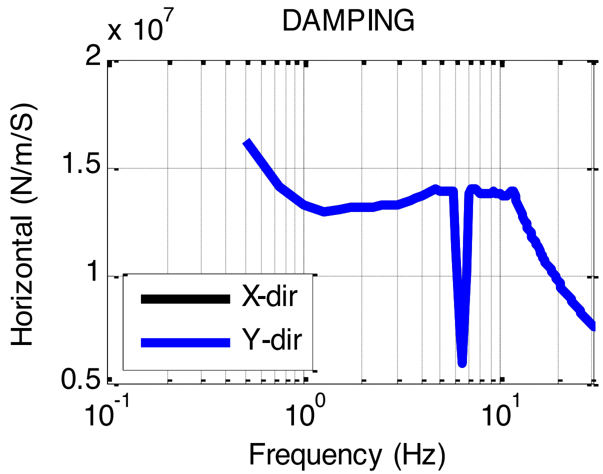

SDOF Models – Cloud Analysis

- Nonlinear dynamic analysis of the SDOF models has been undertaken considering hundreds of records.

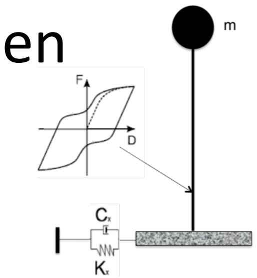

- Multivariate linear (censored) regression to obtain an equation that describes displacement response (Sd) given a vector of intensity measures.

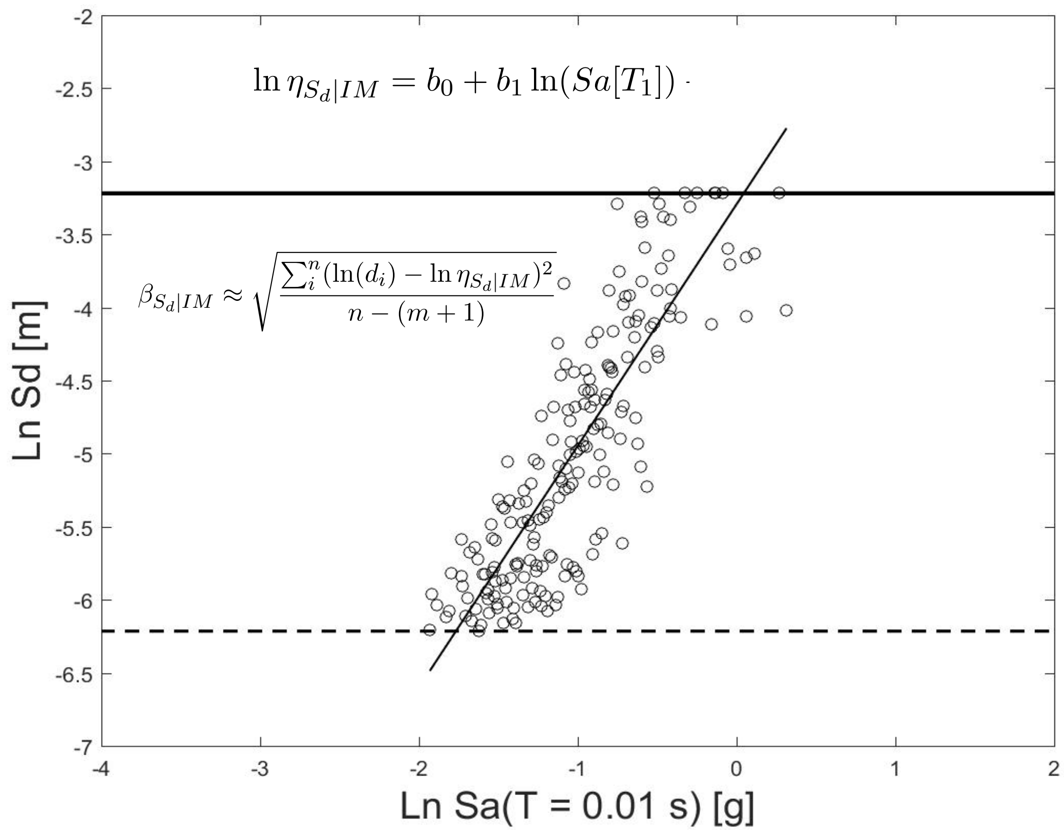

SDOF Model – Cloud Analysis

- Scalar intensity measure checked for sufficiency – i.e. linear regression of residuals against parameters of the events/ ground motions (M, R, $D_{5\text{-}75}$), p-value should be > 0.05 (coefficient of regression is not statistically significant)

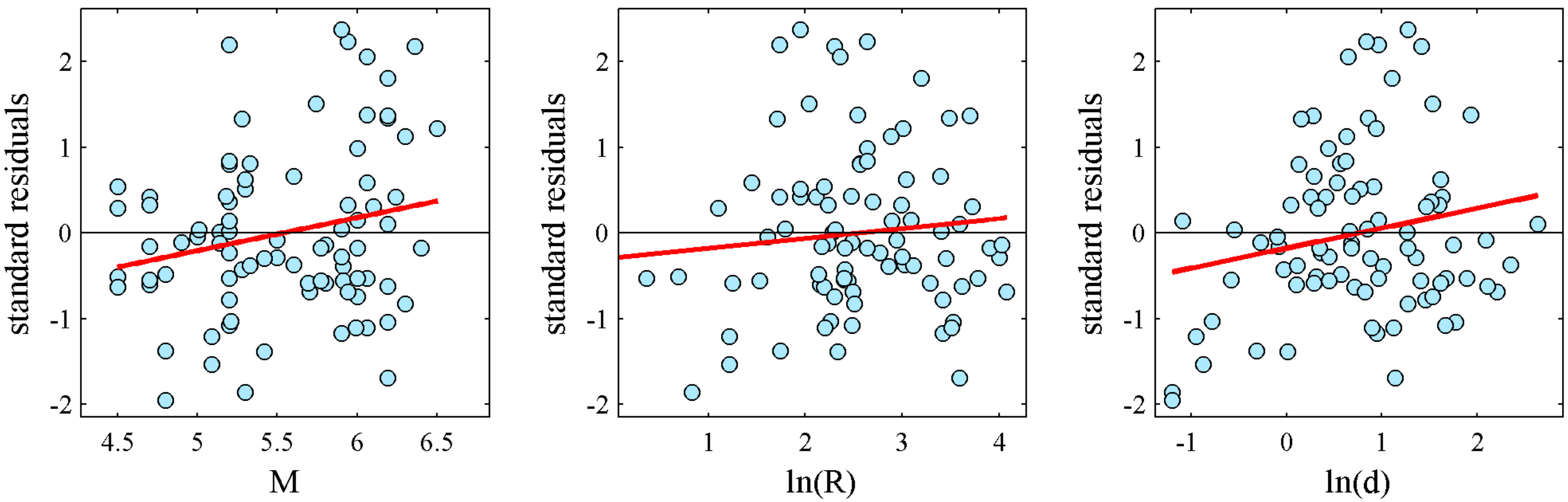

- If **insufficient**, consider various vector intensity measures:

$$\ln \eta_{S_d|IM} = b_0 + b_1 \ln(Sa[T_1]) + b_2 \ln(D_{S5-75}) + b_3 \ln(Sa[T_2])$$

SDOF Models – Building Variability

- Cloud plots have been developed using an index building that is considered to represent the median building of a given structural system.
- The variation in stiffness and strength of buildings within a given structural system is assumed to increase the dispersion of the regression.
- An assumed building to building (B-B) dispersion of 0.1 has been combined (through SRSS) with the record-to-record (R) variability obtained from the cloud regression.

SDOF Models – Building Variability

- To check this simple assumption, the cloud plots of two buildings of same structural system, but different values of stiffness and strength, were compared.
- Similar regression coefficients and values of dispersion (0.44 and 0.45). Increased dispersion of order of 0.1 seems reasonable.

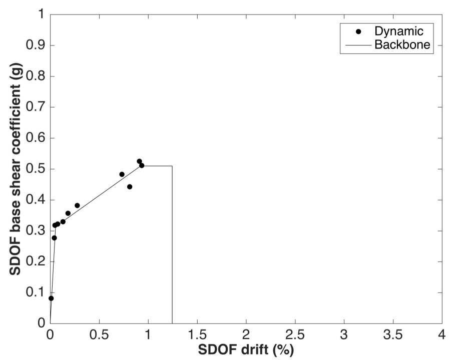

Julianalaan 52
(two storeys)

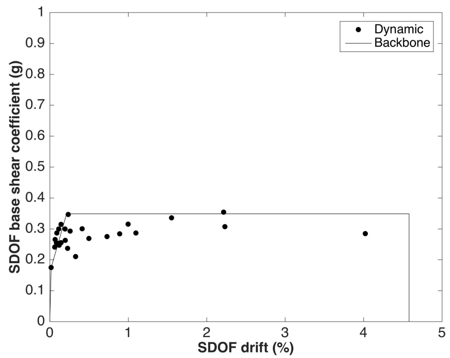

Type C
(one storey)

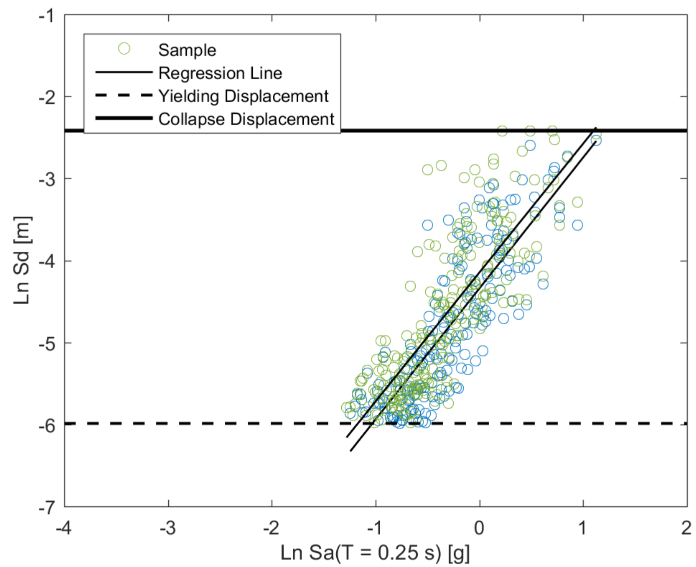

SDOF Models – Limit State Variability

- The main variability that influences the fragility functions is the damage/collapse state threshold variability (β_{DL}).

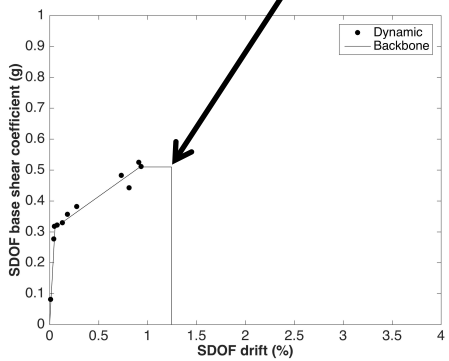

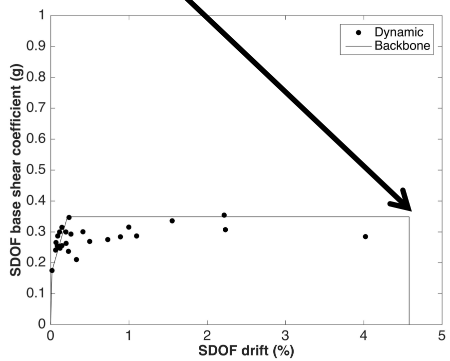

- A value of dispersion of 0.3 has been assumed based on values in the literature (e.g. Dymiotis, 2002; Borzi et al., 2008).
- The total response dispersion is thus:

$$\beta_s = \sqrt{\beta_R^2 + \beta_{BB}^2 + \beta_{DL}^2}$$

From cloud analysis (around 0.4)

0.1

0.3

SDOF Models – Model Uncertainty

- In addition to the aleatory variability in the displacement response, an epistemic (model) uncertainty has been included in the analyses.
- This model uncertainty accounts for inaccuracies in the structural models used to represent the response of a 'real' median building of a given structural system. It is modelled with a logic tree through a discrete three-point distribution (Miller and Rice, 1983).
- Based on recommendations in FEMA P-58, and considering that large scale testing and validation of software for URM buildings has been undertaken:

$$\beta_m = 0.27 \text{ for URM}$$

$$\beta_m = 0.47 \text{ for non-URM}$$

SDOF Models – Model Uncertainty

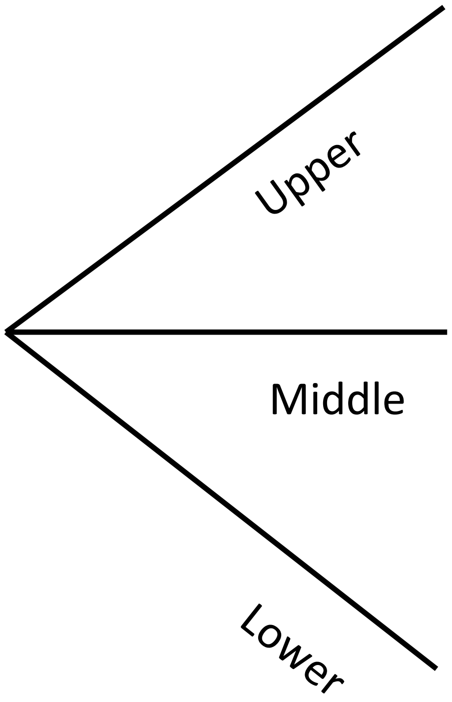

$$\ln \eta_{S_d|IM} = b_0 + b_1 \ln(Sa[T_1]) + b_2 \ln(D_{S5-75}) + b_3 \ln(Sa[T_2]) + 1.73\,\beta_m$$

w = 0.17

$$\ln \eta_{S_d|IM} = b_0 + b_1 \ln(Sa[T_1]) + b_2 \ln(D_{S5-75}) + b_3 \ln(Sa[T_2]) + 0\,\beta_m$$

w = 0.66

$$\ln \eta_{S_d|IM} = b_0 + b_1 \ln(Sa[T_1]) + b_2 \ln(D_{S5-75}) + b_3 \ln(Sa[T_2]) - 1.73\,\beta_m$$

w = 0.17

SDOF Models – Model Uncertainty

- In addition to the aleatory variability in the displacement response, an epistemic (model) uncertainty has been included in the analyses.
- This model uncertainty accounts for inaccuracies in the structural models used to represent the response of a 'real' median building of a given structural system. It is modelled with a logic tree through a discrete three-point distribution (Miller and Rice, 1983).
- Based on recommendations in FEMA P-58, and considering that large scale testing and validation of software for URM buildings has been undertaken:

$$\beta_m = 0.27 \text{ for URM}$$

$$\beta_m = 0.47 \text{ for non-URM}$$

- Partial correlation of model uncertainty between structural systems may exist, however it is currently conservatively modelled as fully correlated across all structural systems in the risk engine.

Fragility Functions

- Probability of exceeding the displacement limit (DL) to each structural damage (DS) or collapse (CS) state:

$$P_{eDL_{DSi}} = 1 - \Phi\left(\frac{\ln(DL_{DSi}) - \ln\eta_{S_d|IM}}{\beta_s}\right)$$

$$P_{eDL_{CSi}} = 1 - \Phi\left(\frac{\ln(DL_{CSi}) - \ln\eta_{S_d|IM}}{\beta_s}\right)$$

- Displacement limits for each damage and collapse state have been identified from a combination of analytical modelling, experimental tests and proposed values in literature.
- Assumptions:
  - Damage states are sequential.
  - Collapse states are sequential.

Damage Limit States

- Damage Limit States (illustrative)

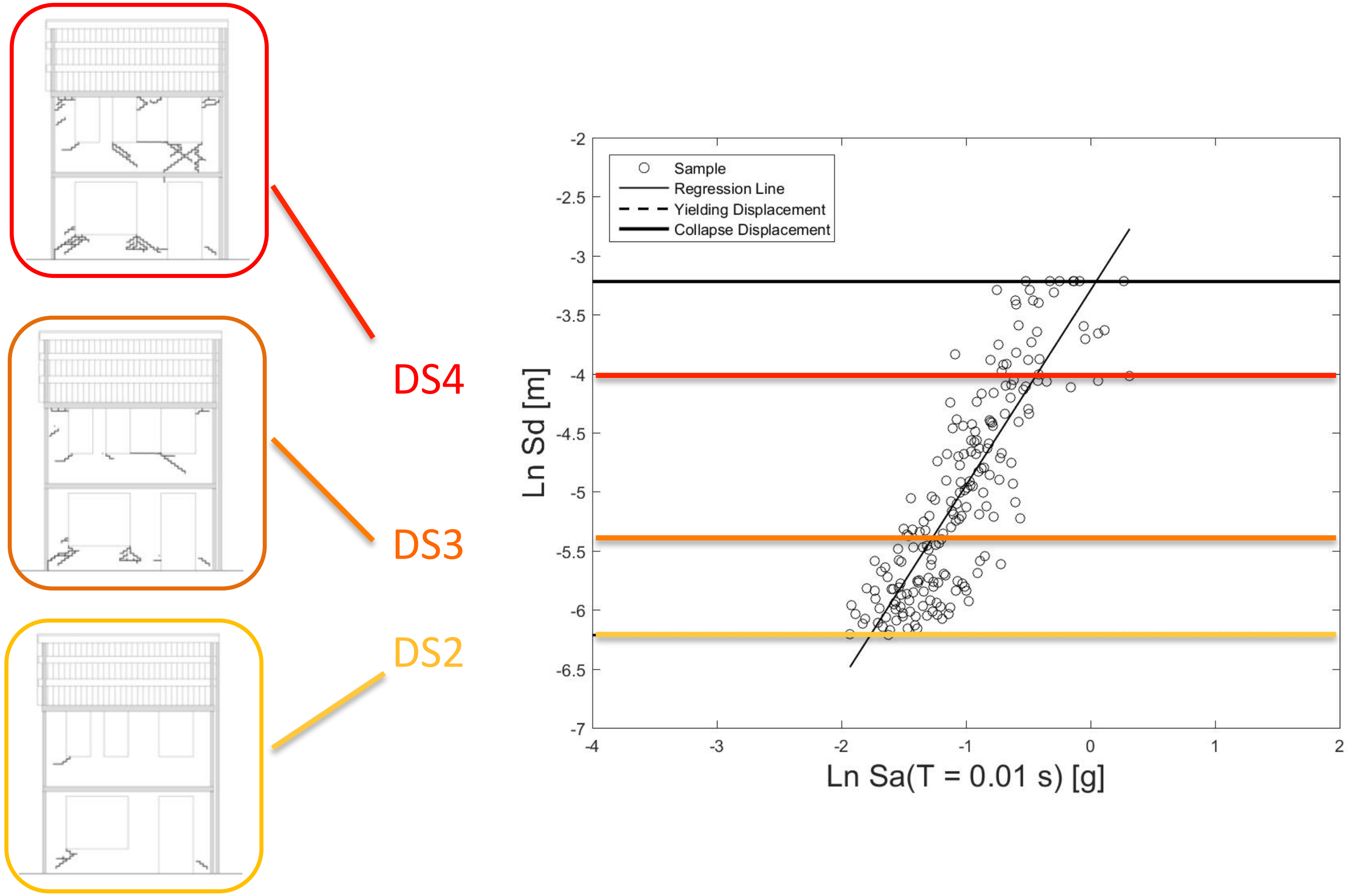

Damage Limit States

e.g. URM Buildings (from shake table tests)

- **DS2**: minor structural damage. It has been determined as the onset of cracking in primary resisting elements. The observed damage could be easily repaired.
- **DS3**: significant structural damage. This level of performance was associated with damage observed in all the piers contributing to the in-plane response of the building.
- **DS4**: severe damage leading to demolition associated to loss of stiffness and strength of the structural elements contributing to the lateral resistance.

Shake Table Test	$\theta_{SDOF,DL2}$ (%)	$\theta_{SDOF,DL3}$ (%)	$\theta_{SDOF,DL4}$ (%)
EUC-BUILD1	0.09	0.26	0.77
LNEC-BUILD1	0.13	0.30	0.59
EUC-BUILD2	0.01	0.25	0.94
Average	0.08	0.27	0.77

Damage Limit States

- Comparison with values from literature – wide range of values for DS2, more agreement for DS3 and DS4.

Source	$\theta_{SDOF,DL2}$ (%)	$\theta_{SDOF,DL3}$ (%)	$\theta_{SDOF,DL4}$ (%)
EUC-BUILD1	0.09	0.26	0.77
LNEC-BUILD1	0.13	0.30	0.59
EUC-BUILD2	0.01	0.25	0.94
Calvi (1999)	0.3	0.5	1.0
Lagomarsino & Cattari (2015)	0.15-0.3	0.25-0.5	0.55-0.7
Borzi et al. (2008)	0.13	0.35	0.72

- We have used the average values from the shake table tests, as they are based on materials from the region.

Damage Limit States

- Non-URM Structural Systems –cyclic tests on RC buildings and values from HAZUS (FEMA, 2004)

Cyclic Test	$\theta_{SDOF,DL2}$ (%)	$\theta_{SDOF,DL3}$ (%)	$\theta_{SDOF,DL4}$ (%)
EUC-BUILD3 (cast-in-place)	0.8	1.25	3.0
EUC-BUILD4 (pre-cast)	0.14	0.50	1.15

Structural System	$\theta_{SDOF,DL2}$ (%)	$\theta_{SDOF,DL3}$ (%)	$\theta_{SDOF,DL4}$ (%)
Cast-in-place wall-slab-wall mid-rise	0.54	0.84	2.0
Cast-in-place frame low-rise	0.4	0.64	1.6
Cast-in-place frame mid to high-rise	0.27	0.43	1.1
Cast-in-place post and beam low-rise	0.4	0.64	1.6
Cast-in-place post and beam mid to high-rise	0.27	0.43	1.1
Precast post and beam low-rise	0.4	0.64	1.6
Precast post and beam mid to high-rise	0.27	0.43	1.1

Structural System	$\theta_{SDOF,DL2}$ (%)	$\theta_{SDOF,DL3}$ (%)	$\theta_{SDOF,DL4}$ (%)
Wood, Light Frame	0.32	0.79	2.45
Steel, Light Braced Frame	0.4	0.64	1.6
Steel, Moment Frame low-rise	0.48	0.76	1.62
Steel, Moment Frame mid to high-rise	0.32	0.51	1.1
Steel, Braced Frame low-rise	0.4	0.64	1.6
Steel, Braced Frame mid to high-rise	0.27	0.43	1.1

Collapse Limit States

- Collapse Limit States (illustrative)

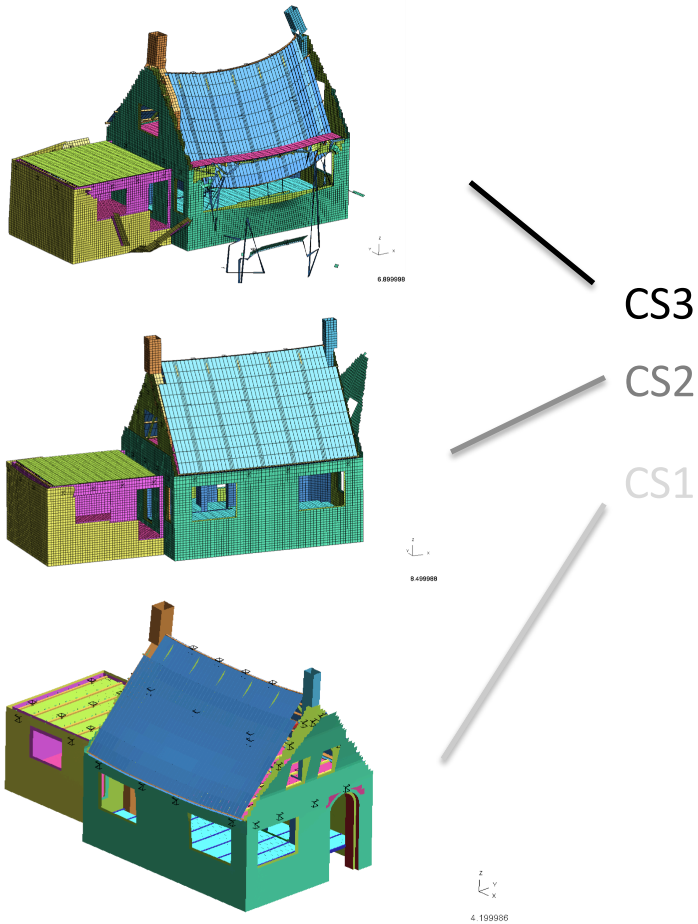

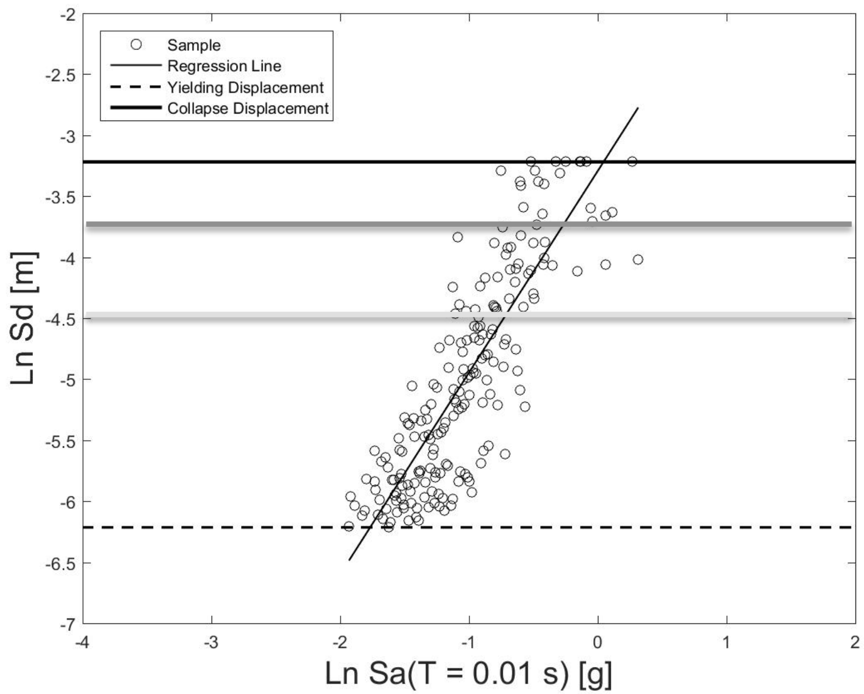

Collapse Limit States

- Collapse has been explicitly modelled with LS-DYNA and Extreme Loading for the URM buildings.
- For non-URM buildings the collapse state has been identified by the exceedance of displacements due to e.g. excessive rotation of joints, unseating.
- The SDOF displacement in the weak direction of the building at the occurrence of up to three collapse states has been identified.
- The collapse debris (inside and outside) has also been inferred from the analyses, for the fatality model.

Collapse Limit States

- MUR/LWAL/MUR/LWAL/EWN/FW/HBET:1,2

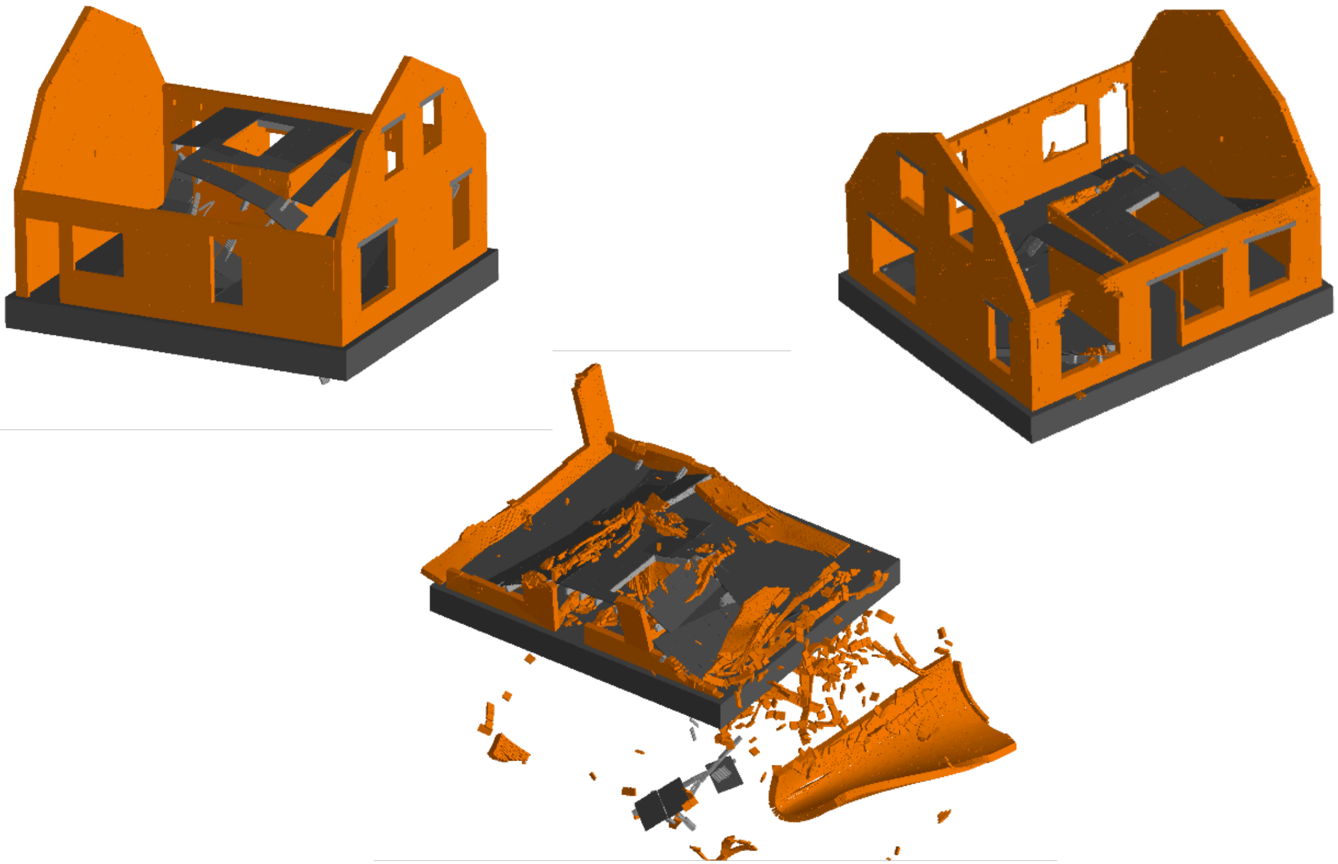

Collapse State Description	Attic displacement (mm)	θ_{SDOF}
Almost complete failure of floor	26.4	0.88
Almost complete failure of floor and wall collapse around windows	35.4	1.18
Global collapse	104	3.47

Collapse Limit States

- MUR/LWAL/MUR/LWAL/EW/FW/HBET:1,2

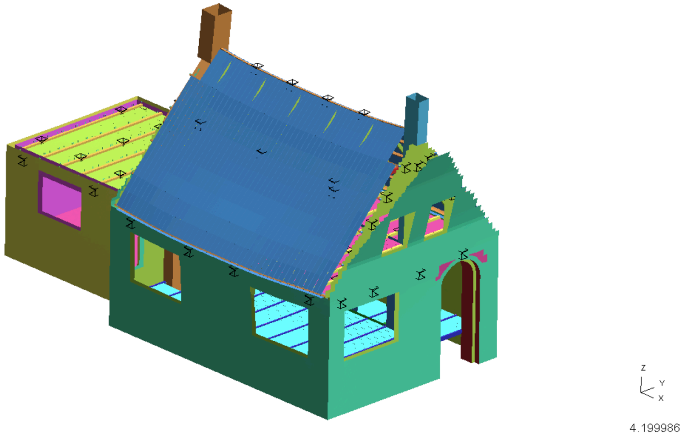

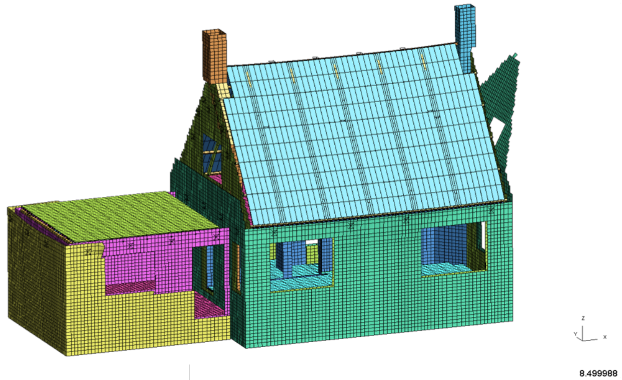

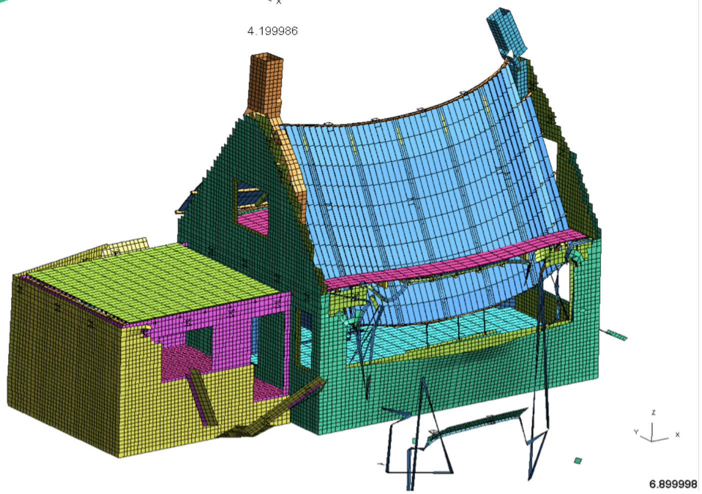

Collapse State Description	Attic displacement (mm)	θ_{SDOF}
OOP failure of external gable wall leaf	2.34	0.085
OOP failure of external gable wall leaf and part of longitudinal walls	9.52	0.34
Global collapse	17	0.59

Fragility Functions

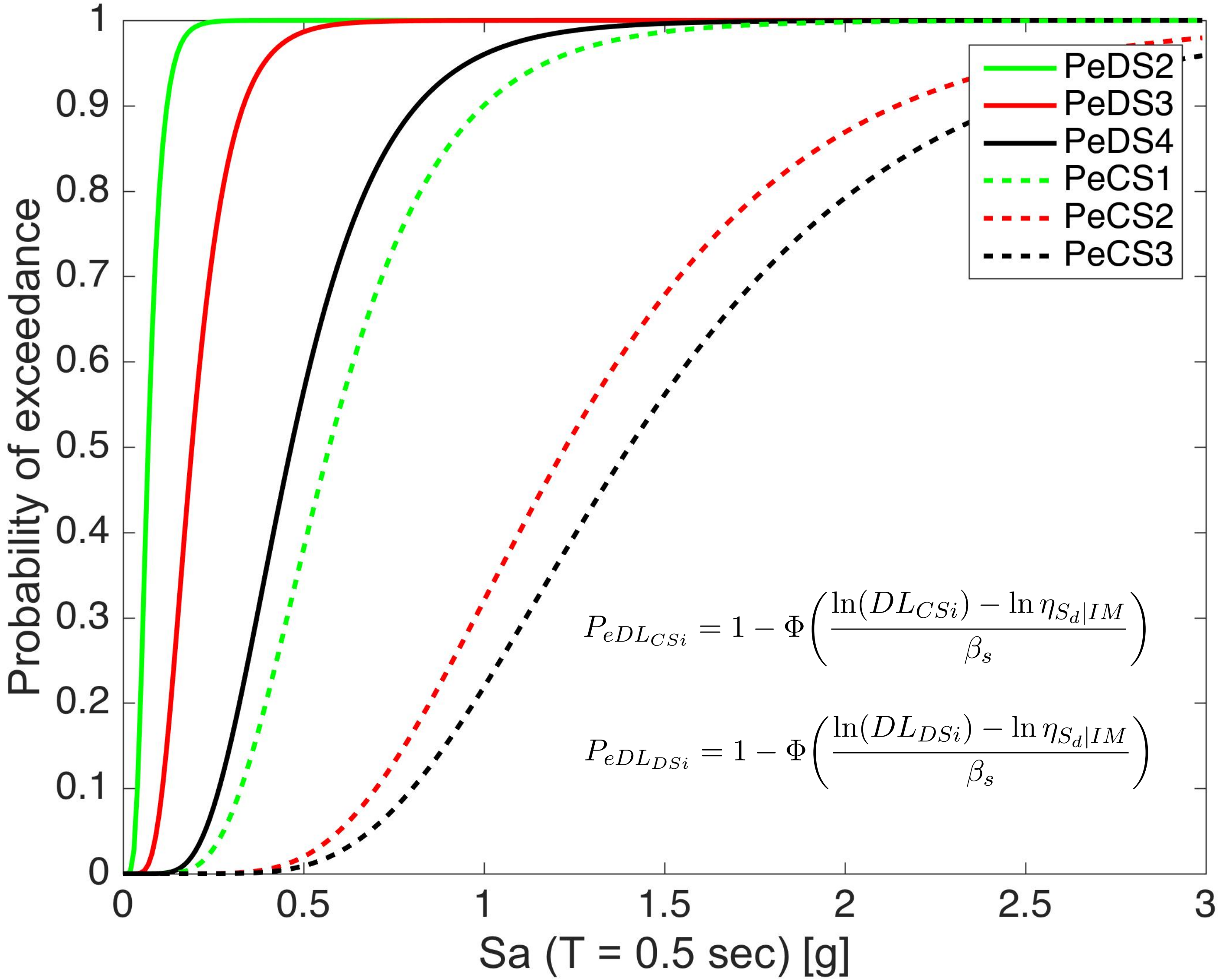

Fragility Functions

- Preliminary consistency checks on fragility functions based on average annual collapse (CS3) rate

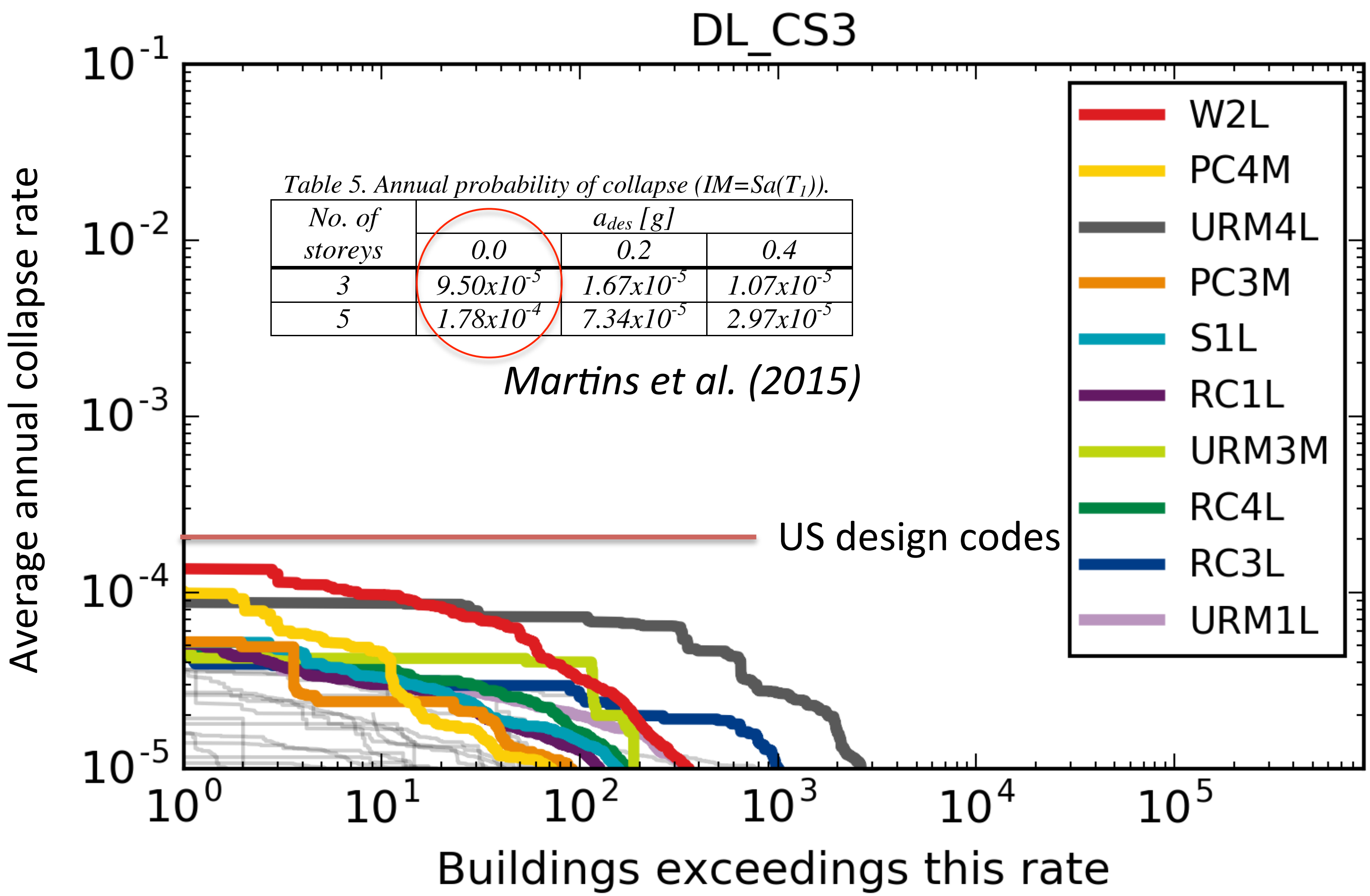

Disaggregation of LPR

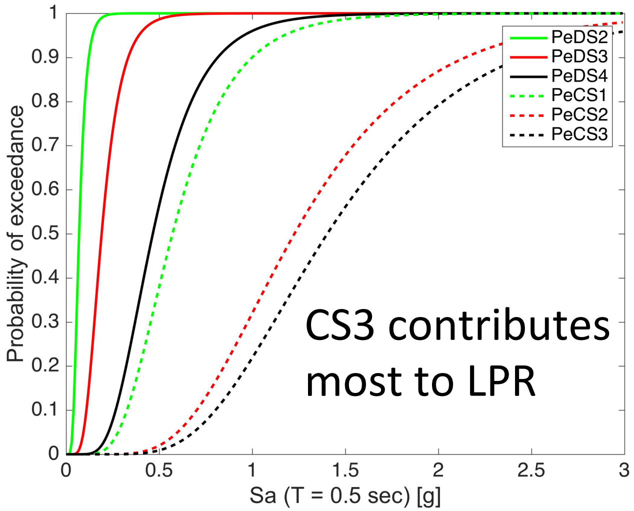

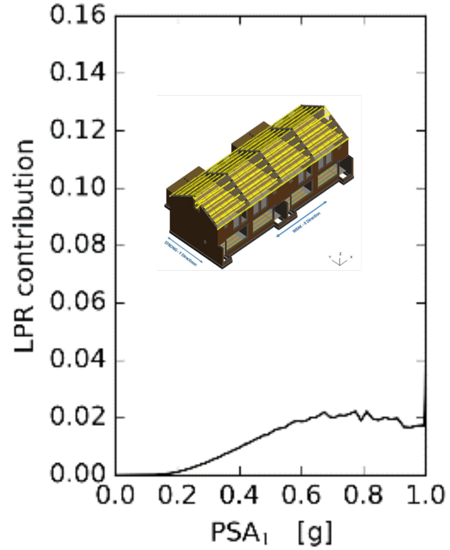

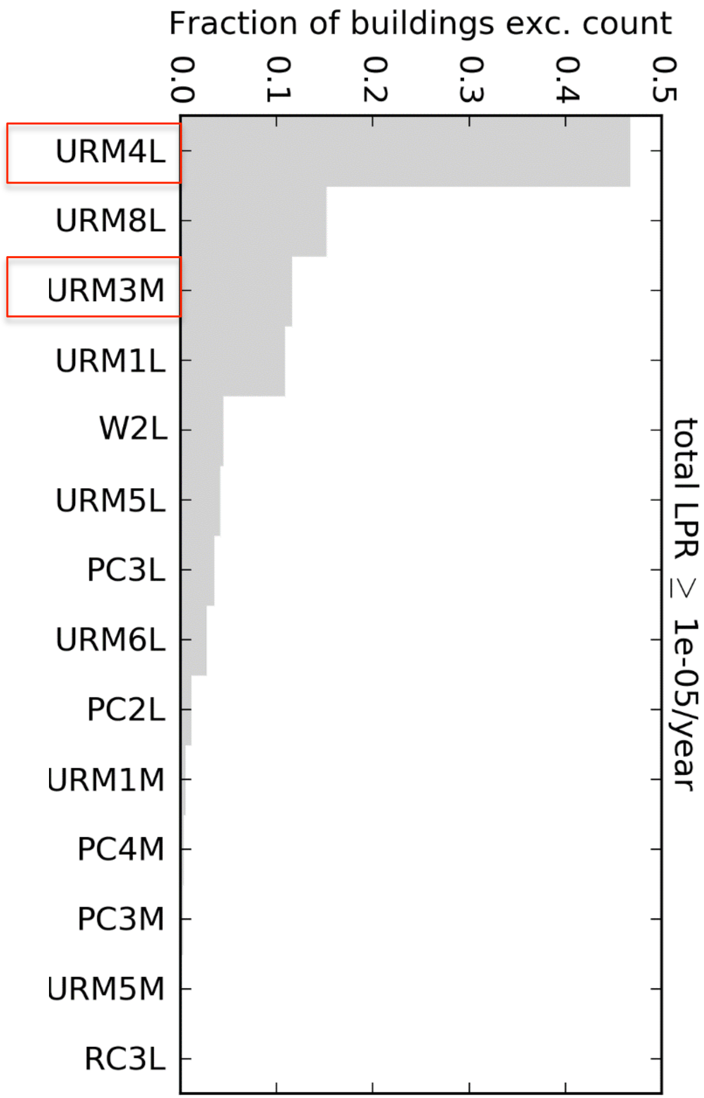

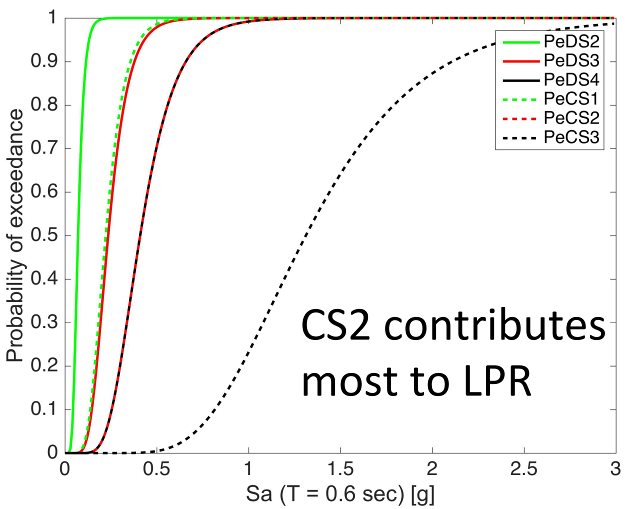

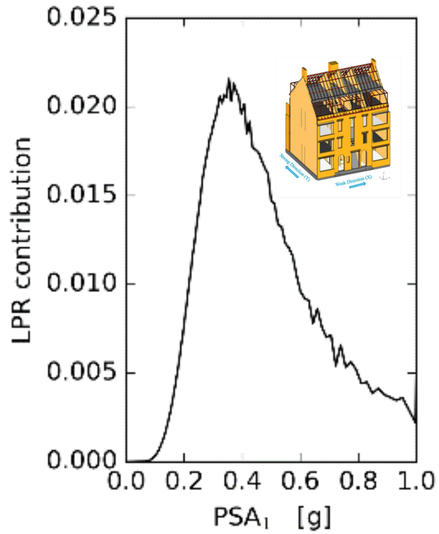

Chimney Collapse Fragility Functions

- Results of empirical study by Taig and Pickup (2016) have been employed.
- Lognormal distributions have been fit to the bands to produce lower, middle and upper branch fragility functions.

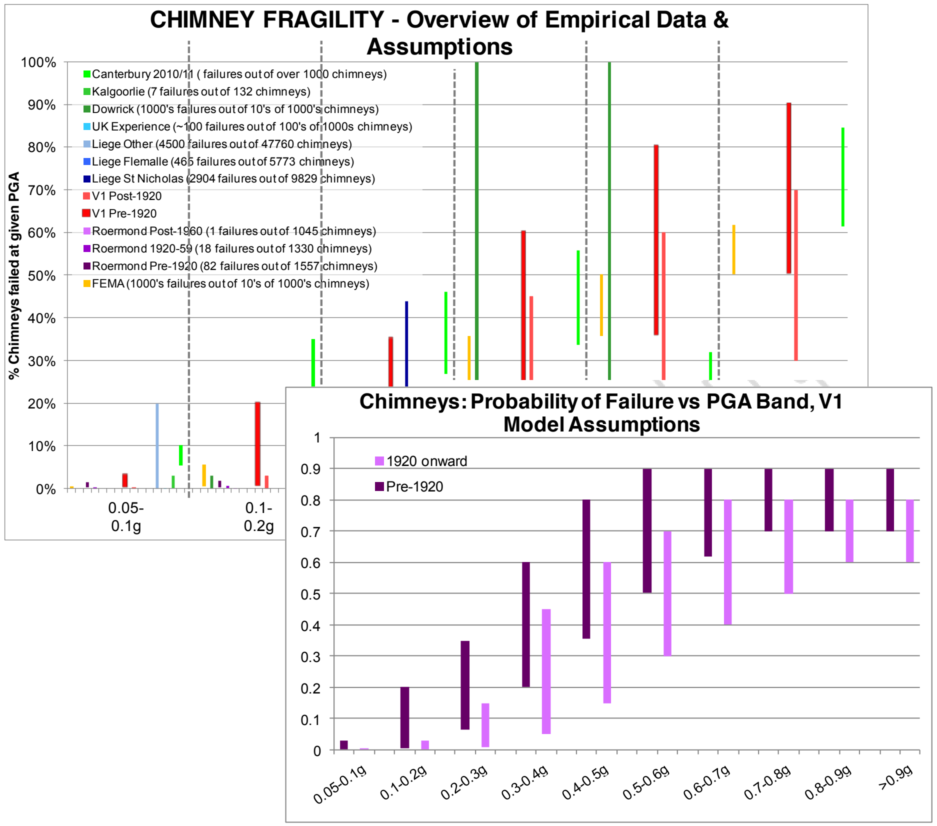

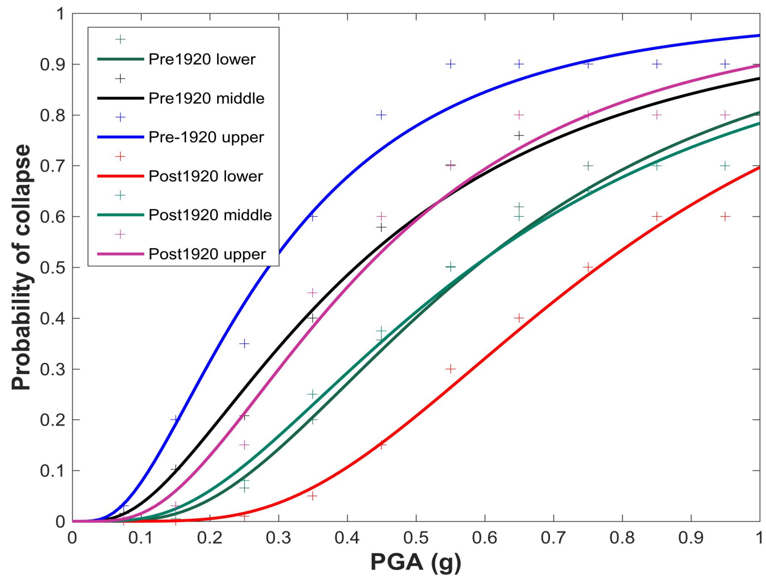

HRA model

Consequence model

Development of Consequence (Fatality) Functions

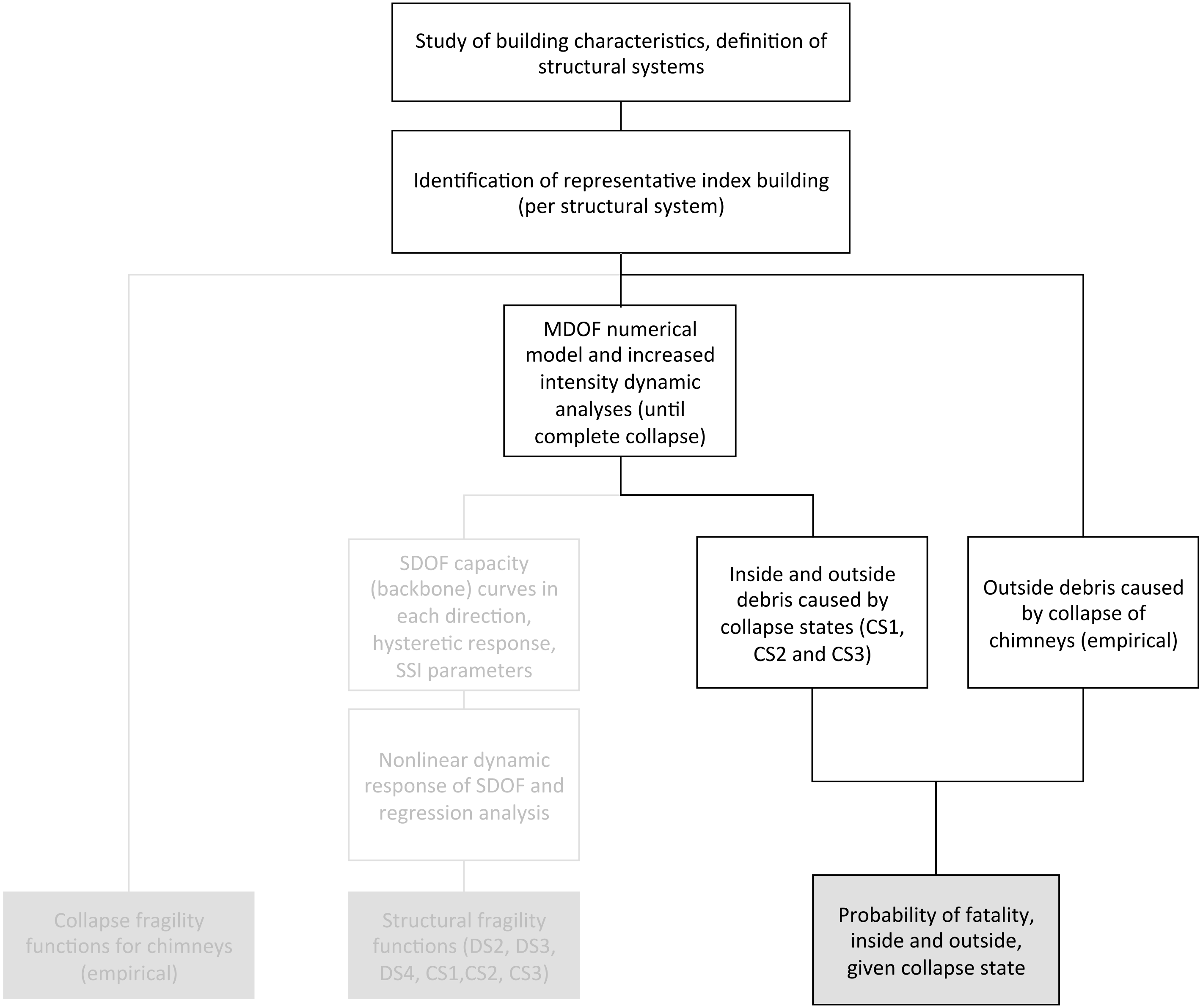

Fatality Risk

- Assumptions made when calculating fatality risk:
  - Structural collapse states are sequential.
  - Chimney collapse only contributes to the probability of dying outside the building.
  - Chimney collapse and structural collapse are assumed to be independent.
- Probability of dying, under given level of ground shaking:

$$P_{d_{inside}} = (P_{eDL_{CS1}} - P_{eDL_{CS2}}) \times P_{d_{inside|CS1}} + (P_{eDL_{CS2}} - P_{eDL_{CS3}}) \times P_{d_{inside|CS2}} + P_{eDL_{CS3}} \times P_{d_{inside|CS3}}$$

$$P_{d_{outside}} = (P_{eDL_{CS1}} - P_{eDL_{CS2}}) \times P_{d_{outside|CS1}} + (P_{eDL_{CS2}} - P_{eDL_{CS3}}) \times P_{d_{outside|CS2}} + P_{eDL_{CS3}} \times P_{d_{outside|CS3}} + (1 - P_{eDL_{CS1}}) \times P_{d_{outside|ChC}}$$

$$LPR = 0.99 \times ILPR + 0.01 \times OLPR$$

Fatality Model

- Probability of dying inside, given each collapse state, is based on the Coburn and Spence (2002) model:

$$N = M1 \times M2 \times M3 \times [M4 + M5 \times (1 - M4)]$$

- M1& M2 – used to evaluate number of people within the building at the time of the earthquake (not needed for local personal risk, included in exposure model for group risk)
- M3 – percentage of occupants that are trapped by collapse and are unable to escape. Replaced with the percentage of useable floor area impacted by collapsed debris.
- M4 – percentage of trapped occupants that are killed instantaneously, empirically estimated for timber, masonry, RC and steel buildings.
- M5 – percentage of surviving occupants that subsequently die, depending on search and rescue (SAR) efforts, empirically estimated for timber, masonry, and RC buildings.

$$P_{d_{inside|collapse}} = \frac{A_{debris_{inside}}}{A_{floor}}[M4 + M5 \times (1 - M4)]$$

Fatality Model

- Consistency check of the inside fatality model

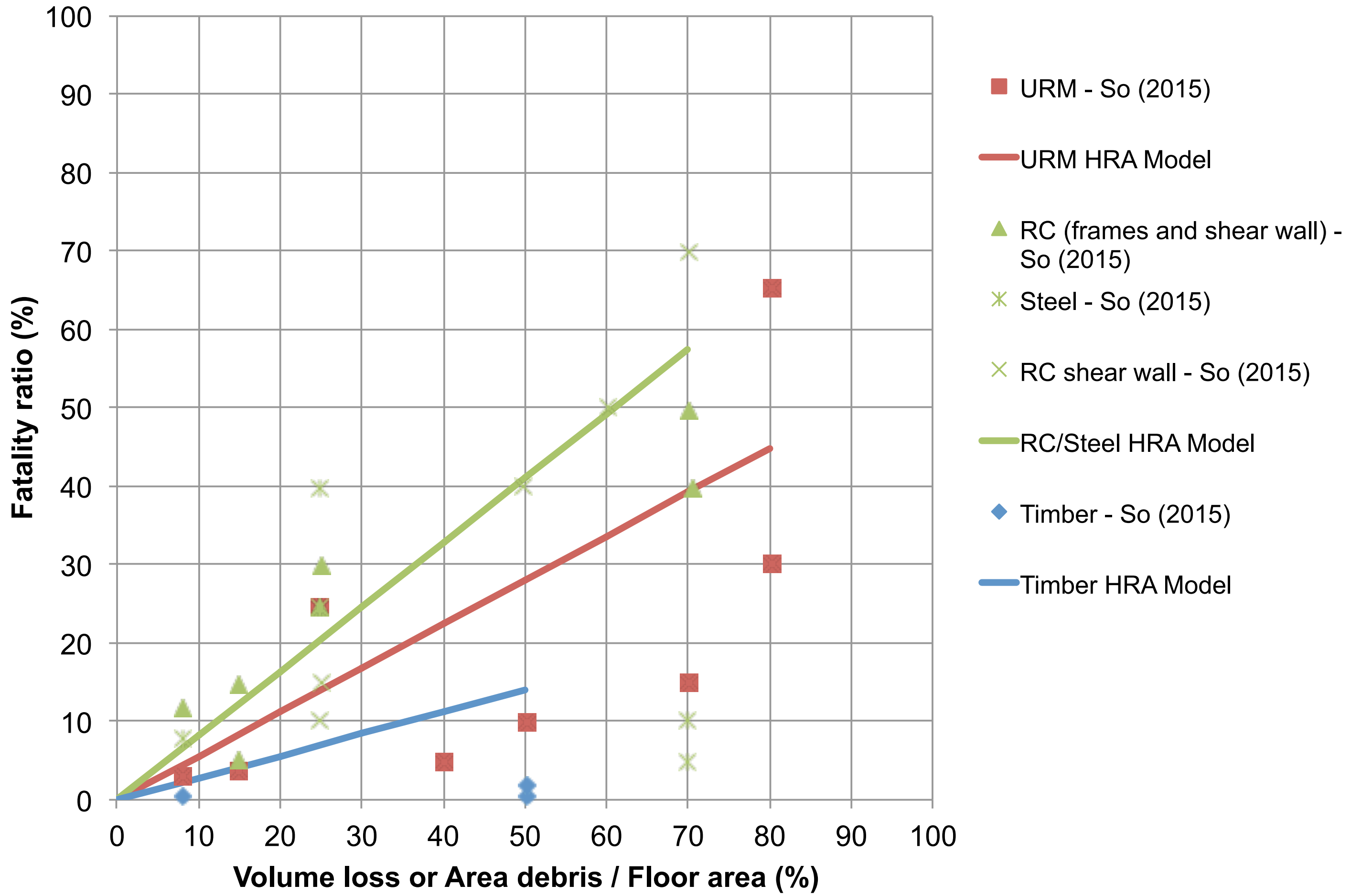

Fatality Model

- Probability of dying outside, given each collapse state, is taken equal to the ratio of area of outside debris to the total exposed area multiplied by 1, following the recommendations of Taig and Pickup (2016).

$$P_{d_{outside|collapse}} = \frac{A_{debris_{outside}}}{A_{exposed}}$$

Fatality Model

- Inside fatality ratios (middle branch) range from 0 % (for CS1 that occurs outside the building) to 42 % (for CS3 global collapse of URM buildings).
- Outside fatality ratios (middle branch) due to structural collapse can range from 0 % (for CS1 that occurs inside the building) to 75% (for CS3 global collapse of an aggregate building with small outside exposed area).
- A judgment-based logic tree considering upper and lower bound values of debris for each collapse state has been developed.

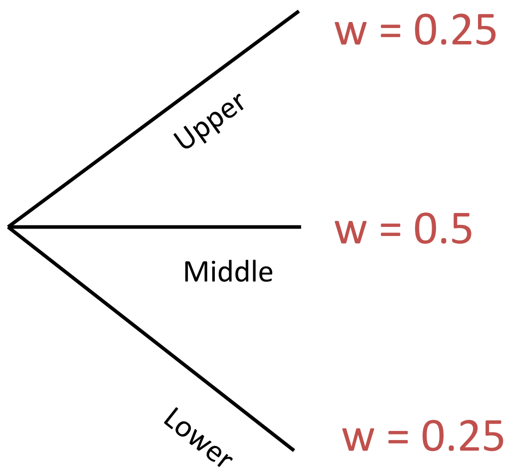

Publications

- Crowley H., Pinho R., Polidoro B., van Elk J. (2017) "Framework for Developing Fragility and Consequence Models for Local Personal Risk," *Earthquake Spectra*, Vol. 33, No. 4, pp. 1325–1345.
- Crowley H., Pinho R., Polidoro B., van Elk J. (2017) "Developing fragility and consequence models for buildings in the Groningen Field," *Netherlands Journal of Geosciences*, Vol. 96, No. 5, pp. s247-s257.
- Crowley, H., Polidoro, B., Pinho, R., van Elk, J., (2017) "Fragility and Consequence Models for Probabilistic Seismic Risk Assessment in the Groningen Gas Field," *16th European Conference on Earthquake Engineering* (16ECEE), Thessaloniki, Greece, June 18-21, 2018.

Probabilistic Seismic Risk Analysis Local Personal Risks associated with the 24 bcm/year Groningen gas production scenario

Stephen Bourne[1], Steve Oates[1], Assaf Mar-Or[1], Tomas Storck[2], Pourya Omidi[2], Julian Bommer[3], Rui Pinho[4], Helen Crowley[4]

[1] Projects & Technology, Shell Global Solutions International
[2] Alten Nederland, Rotterdam
[3] Imperial College, London
[4] EUCENTRE, Pavia

Assurance meeting for Exposure, Fragility and Fatality Models for the Groningen building stock
World Trade Center, Schiphol, 22st February, 2018

Probabilistic seismic risk model

- Five stochastic simulation models are sampled in the risk model:

Seismicity simulations	Ground motion simulations	Exposure database	Building damage simulations	Consequence simulations
Number, location, magnitude and rupture dimensions of earthquakes given gas production	Spectral accelerations and duration for a given surface site, earthquake location, magnitude and rupture dimensions	Location, type, & population of each building in and around the gas field	Probability and mode of building collapse given building type, *SA*, and *D*	Probability of injury given mode of building collapse and building type

Seismic Hazard

Damage Risk

Injury Risk

Monte Carlo procedure for simulating seismic risks

Simulate:

1. Event number

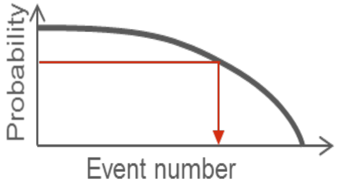

2. Event location

3. Event magnitude

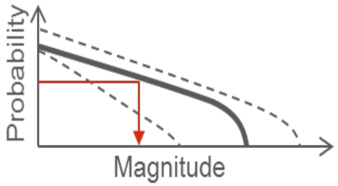

4. Aftershock number

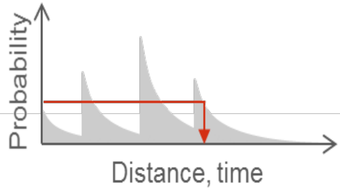

5. Ground motion

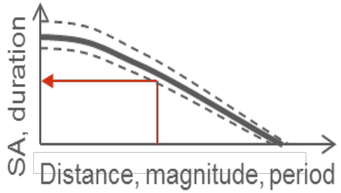

6. Surface amplification

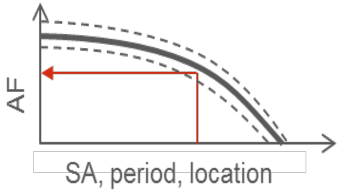

7. Building damage

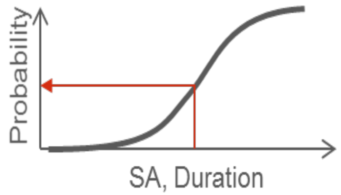

8. Injury severity

Monte Carlo procedure for simulating seismic risks - unpacked

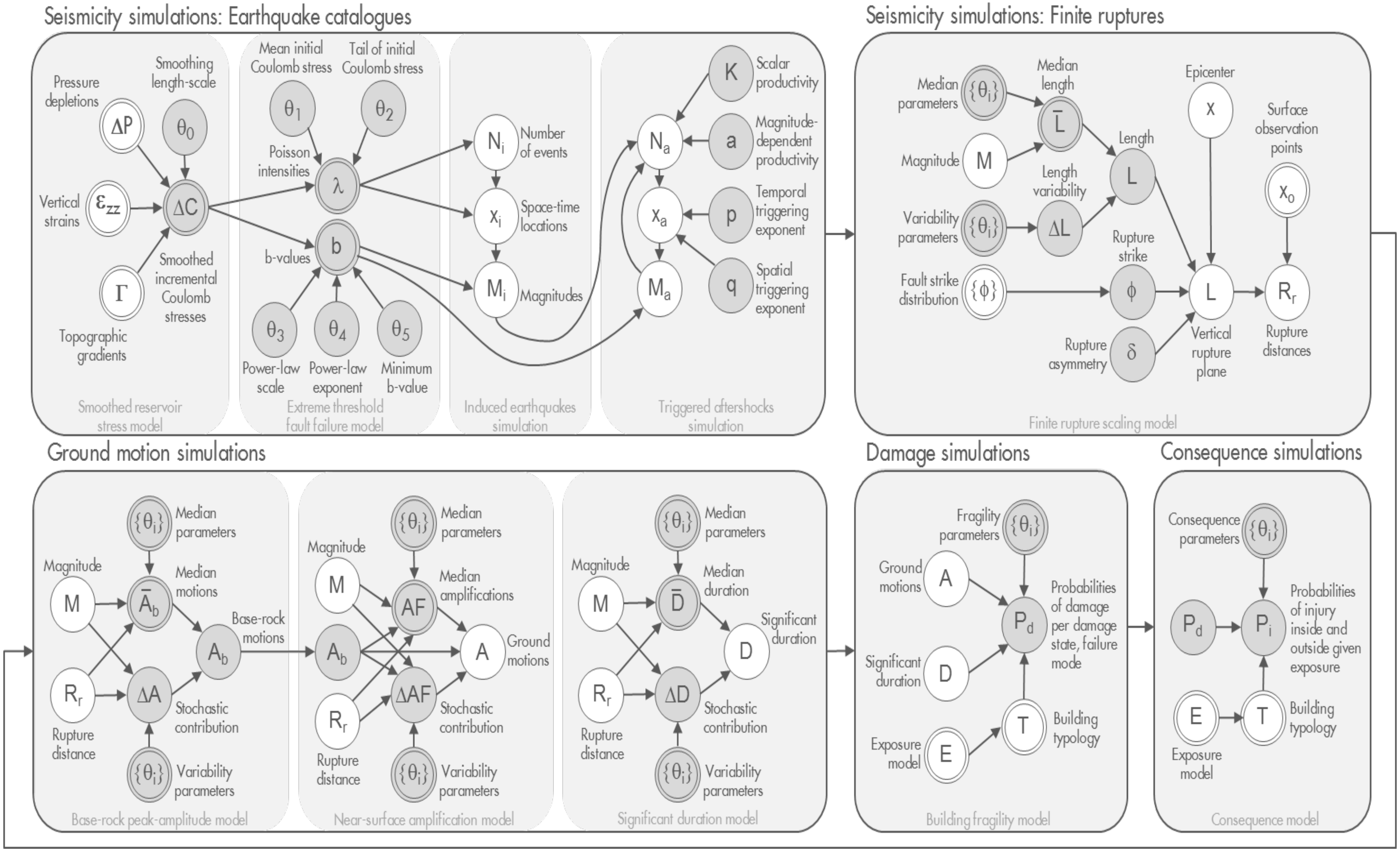

Analysis of the performance of potential control measures

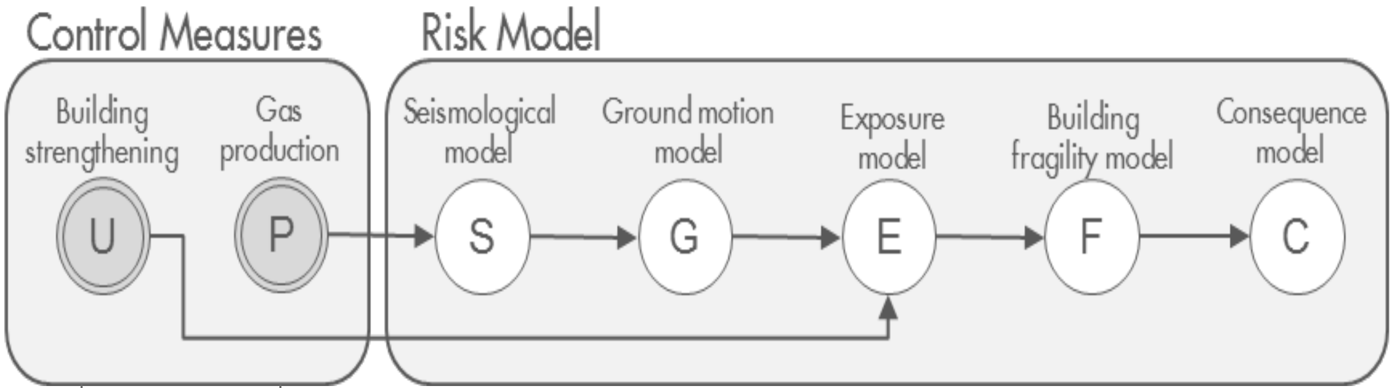

Individual buildings may be retrofitted through time

Gas production may be varied through time and re-distributed amongst each production cluster

Control options and epistemic uncertainties are incorporated in a combined decision tree and logic tree

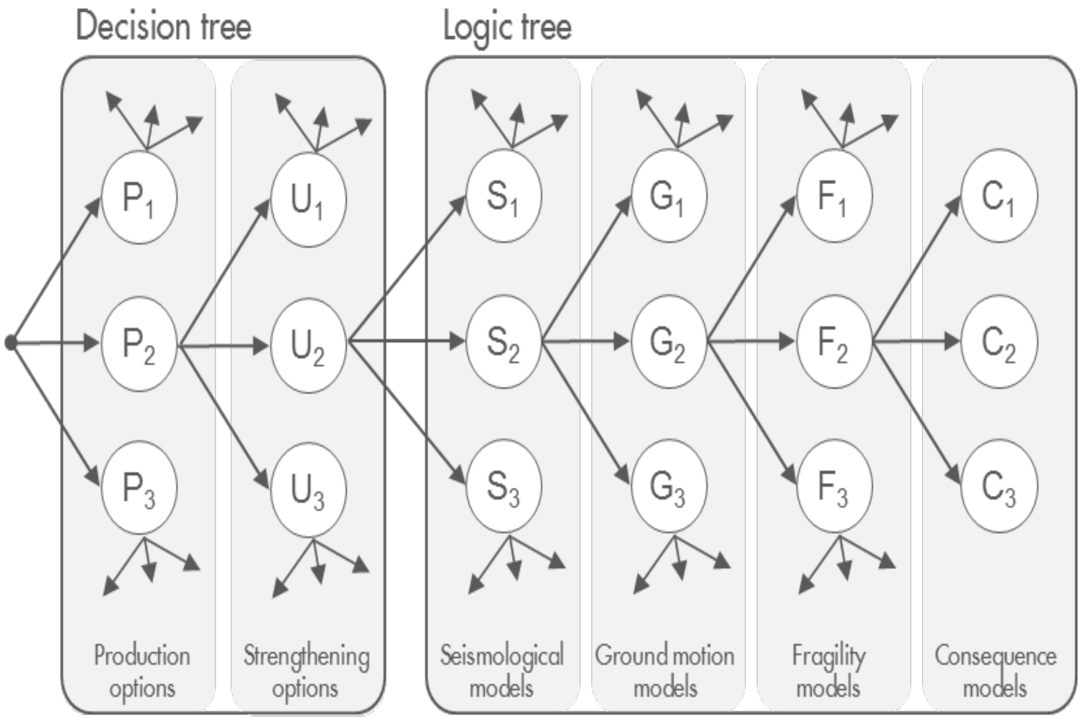

Logic tree description of epistemic uncertainties

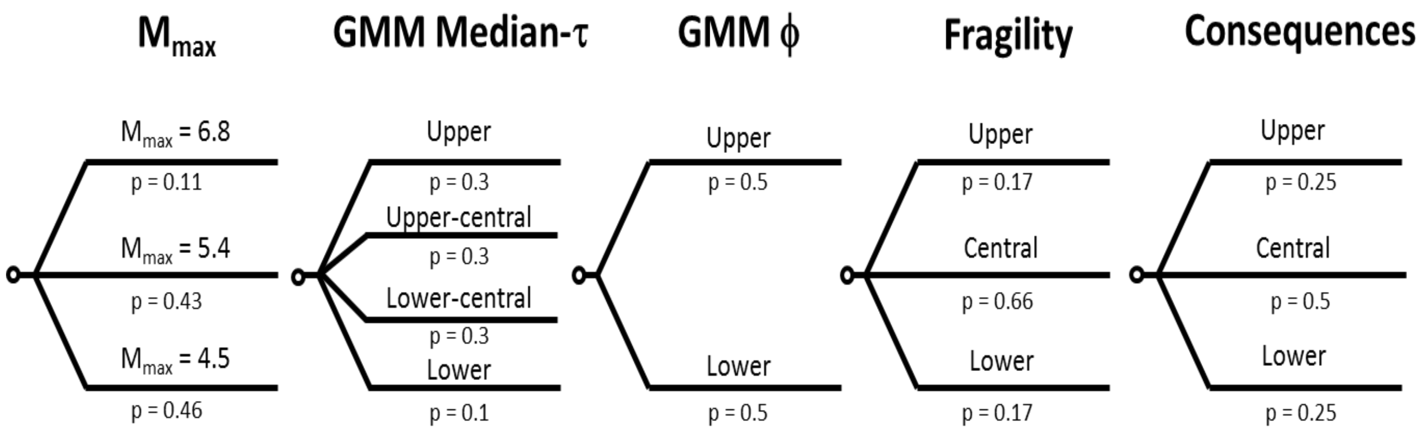

- 5 factors
- 3 x 4 x 2 x 3 x 3 levels
- 216 full-factorial combinations

Local personal risk exceedance curves – Relative to risk norms

- Assessment period: 1-1-2018 to 1-1-2023
- Production scenario: 24 bcm/year
- Strengthening scenario: Zero retrofitting

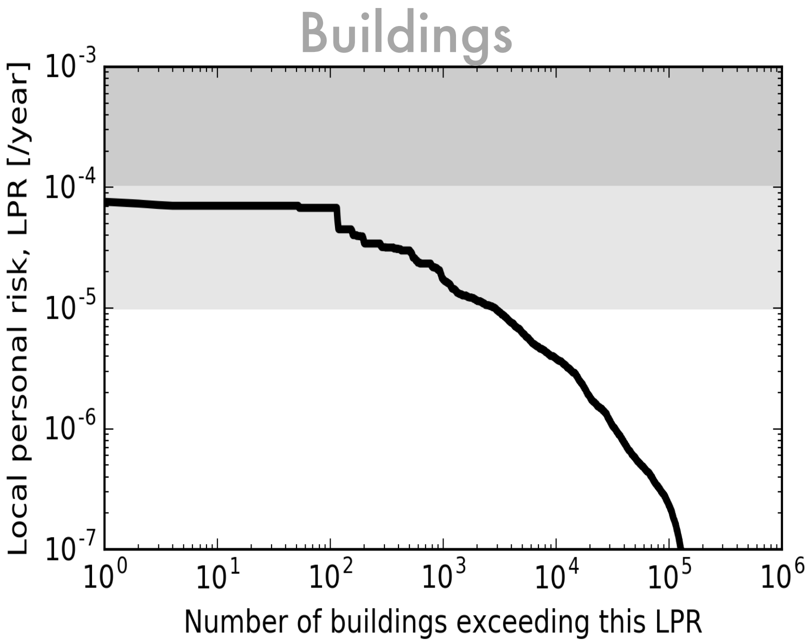

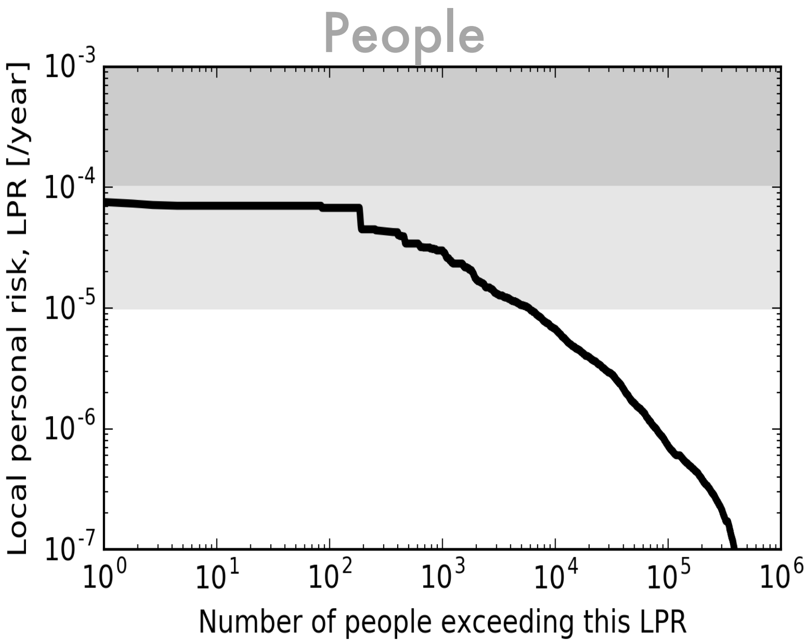

Local personal risk exceedance curves – Relative to 95% prediction interval

- Assessment period: 1-1-2018 to 1-1-2023
- Production scenario: 24 bcm/year
- Strengthening scenario: Zero retrofitting

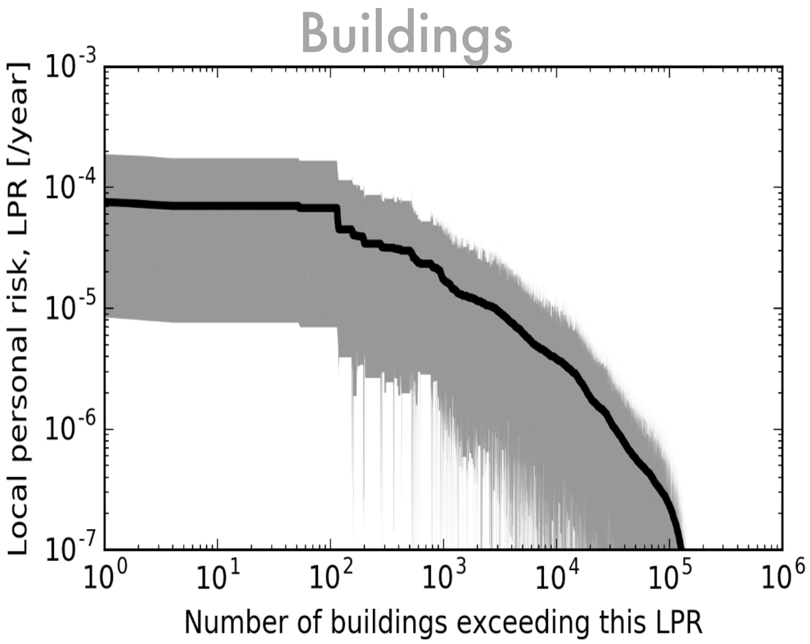

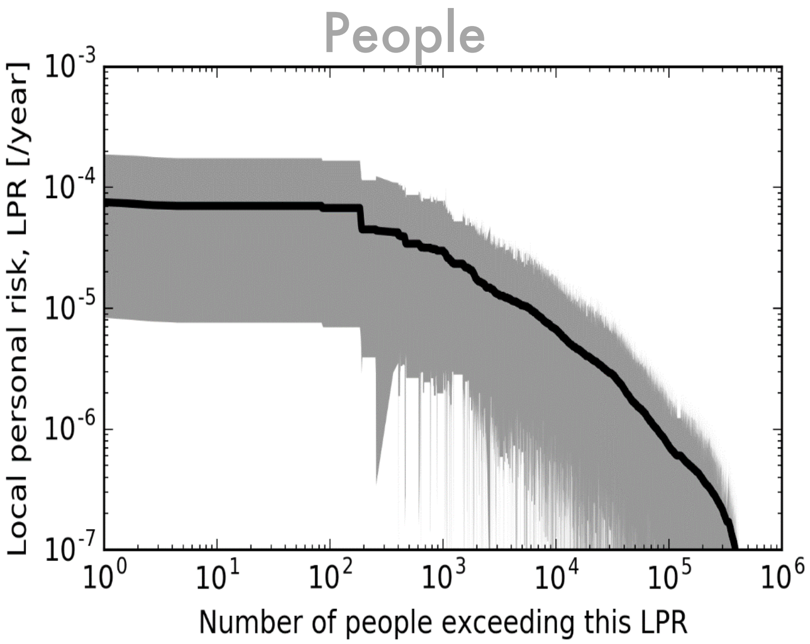

Local personal risk map

- Assessment period: 1-
- Production scenario: 2
- Strengthening scenari

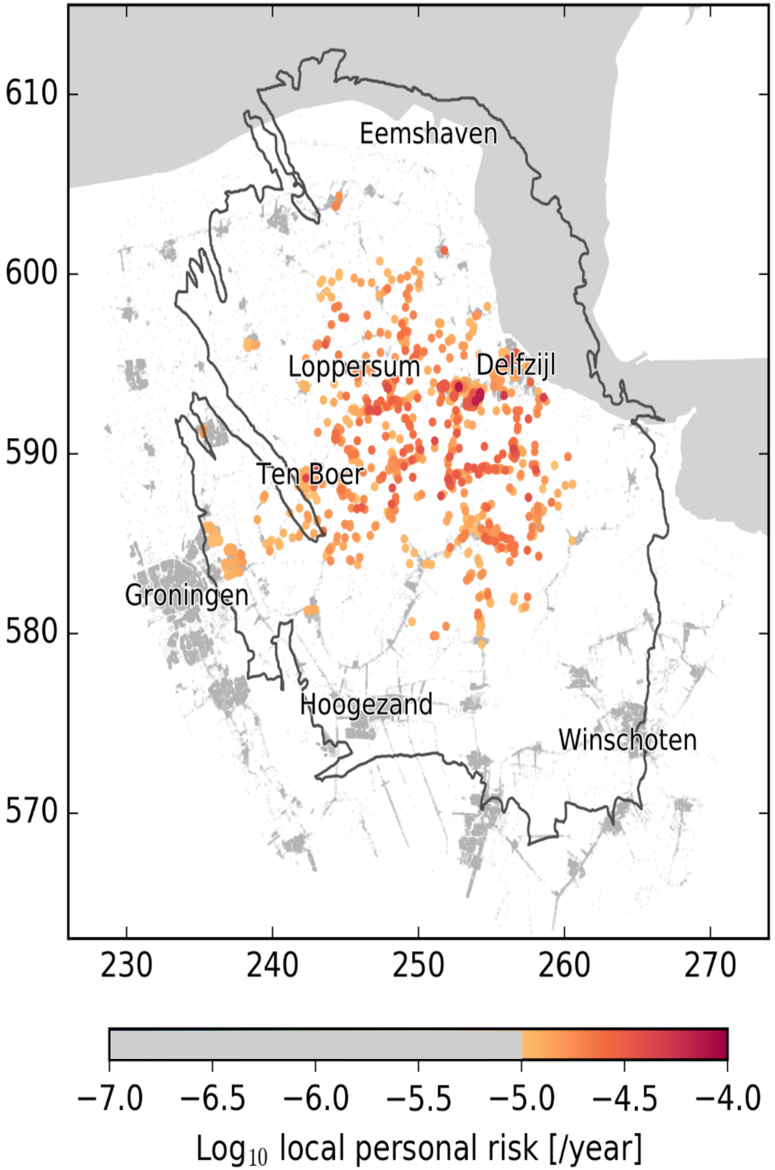

Which structural systems exceed the 10^{-5}/year risk norm?

- Assessment period: 1-1-2018 to 1-1-2023
- Production scenario: 24 bcm/year
- Strengthening scenario: Zero retrofitting

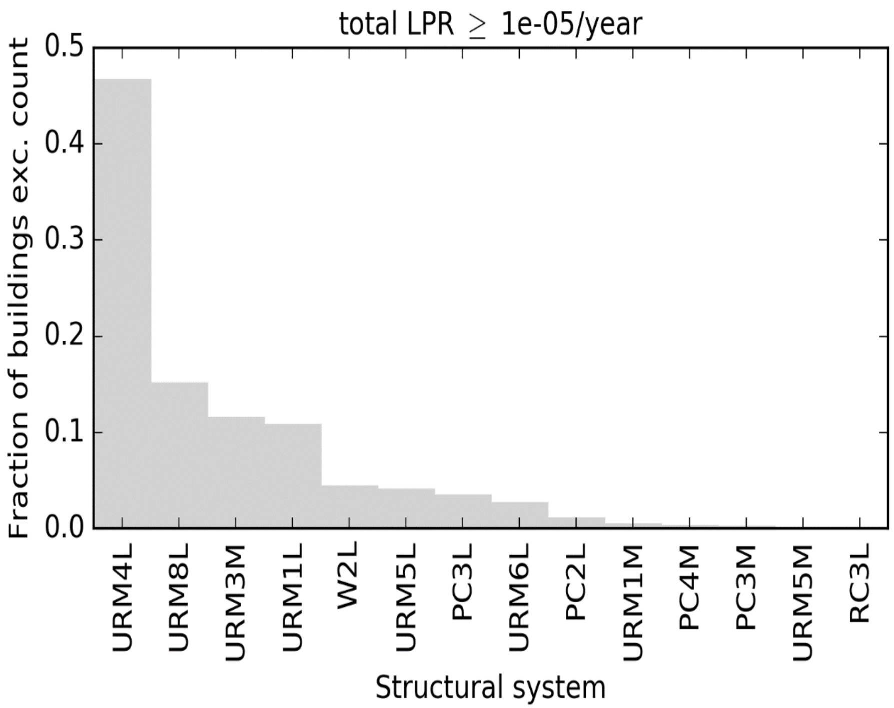

Sensitivity to epistemic uncertainty is dominated by M_{max}

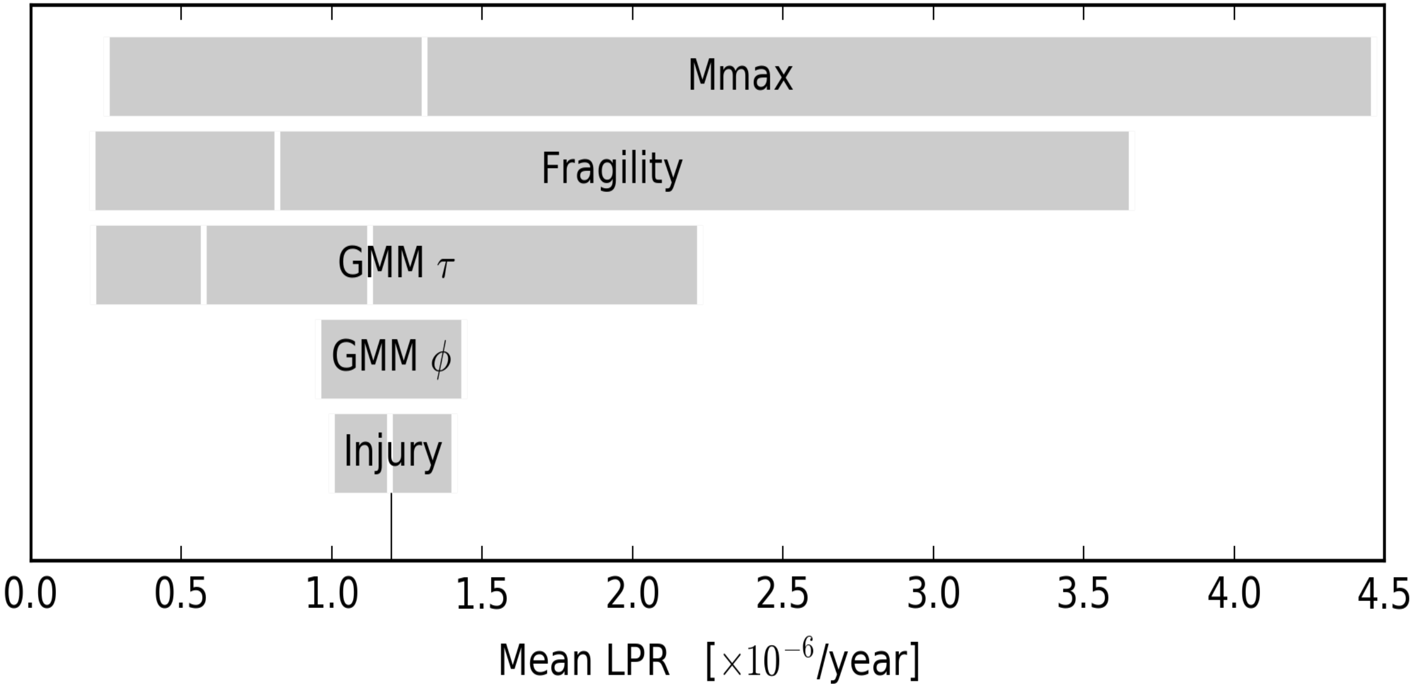

Sensitivity to epistemic uncertainty

- Assessment period: 1-1-2018 to 1-1-2023
- Production scenario: 24 bcm/year
- Strengthening scenario: Zero retrofitting

Logic-tree mean LPR is recomputed for every individual building given $M_{max} = 4.2$

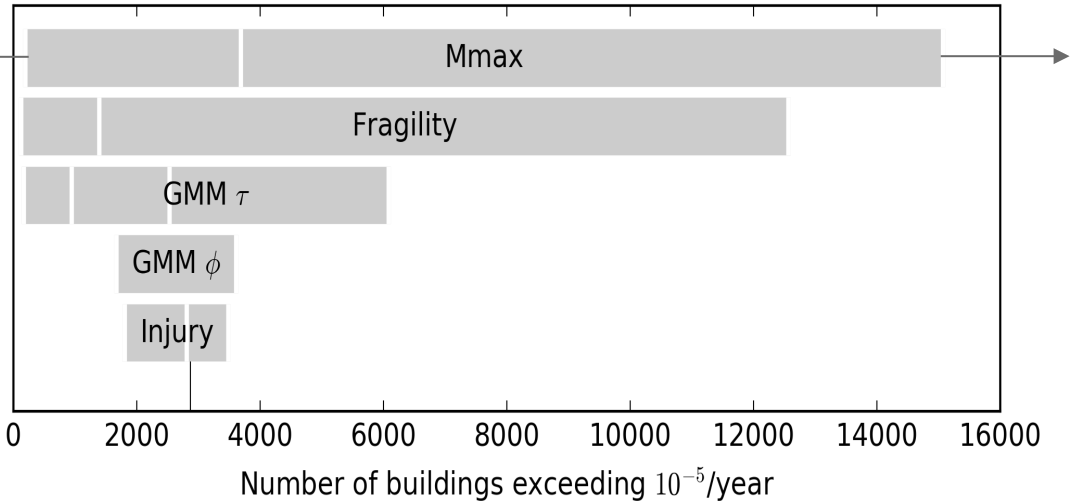

Logic-tree mean LPR is recomputed for every individual building given $M_{max} = 6.8$

Disaggregation of contributions to local personal risk – URM 4L

- Assessment period: 1-1-2018 to 1-1-2023
- Production scenario: 24 bcm/year
- Strengthening scenario: Zero retrofitting

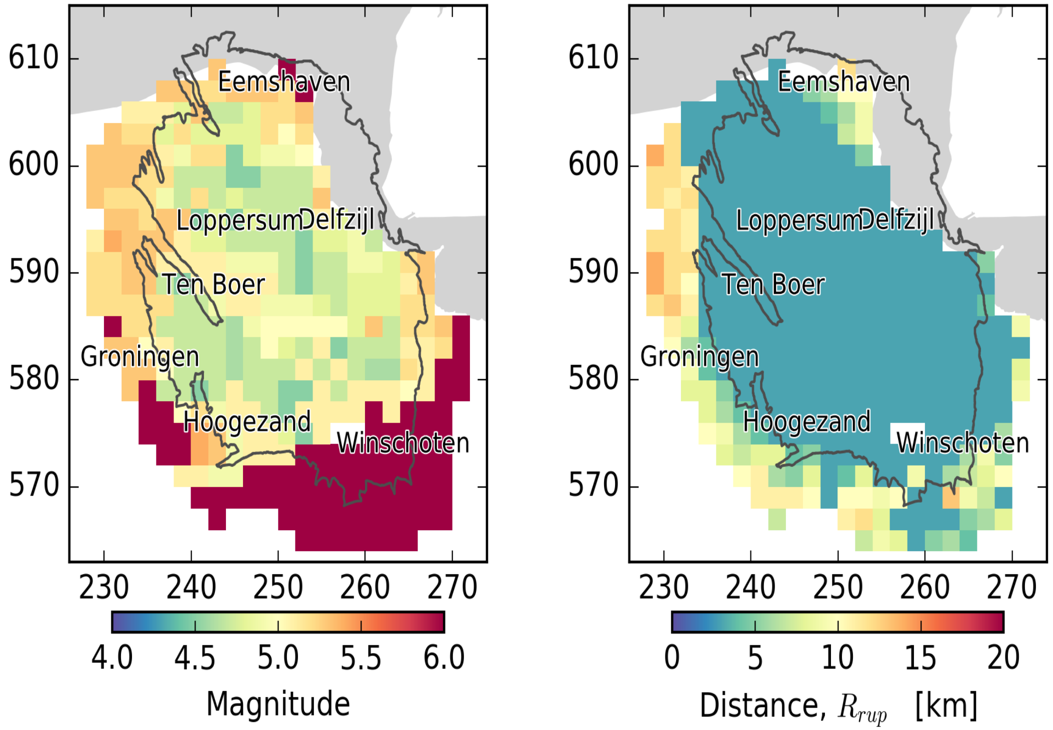

Maps of modal contributions to mean LPR

Disaggregation of contributions to local personal risk – URM 8L

- Assessment period: 1-1-2018 to 1-1-2023
- Production scenario: 24 bcm/year
- Strengthening scenario: Zero retrofitting

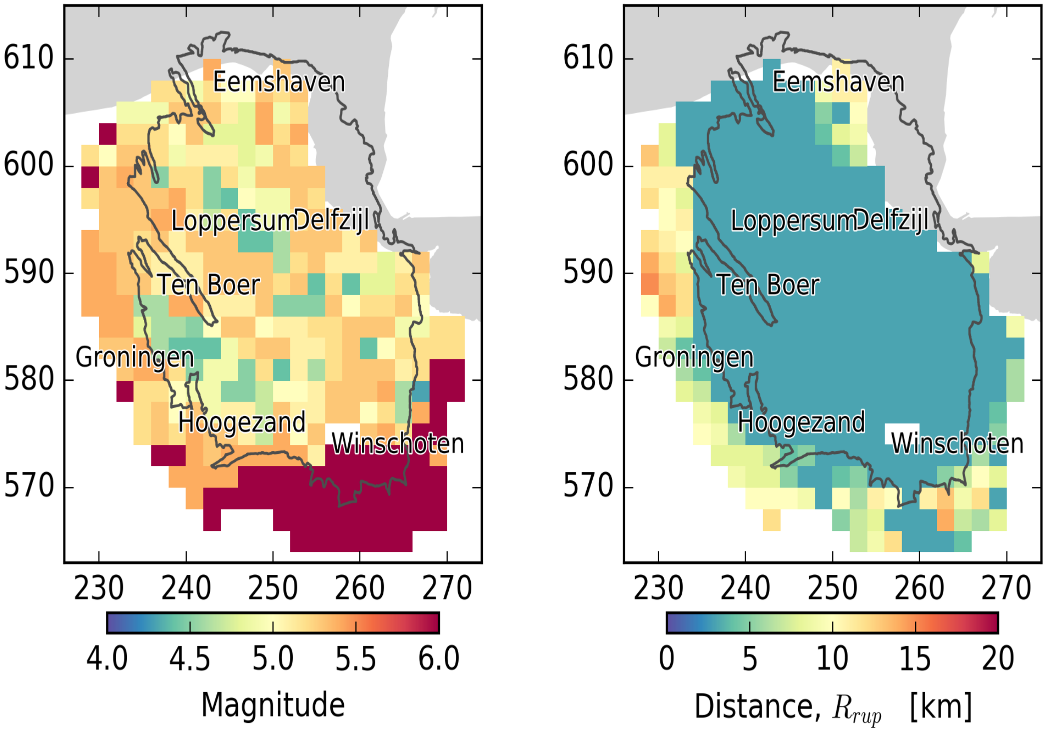

Maps of modal contributions to mean LPR

Disaggregation of contributions to local personal risk – URM 3M

- Assessment period: 1-1-2018 to 1-1-2023
- Production scenario: 24 bcm/year
- Strengthening scenario: Zero retrofitting

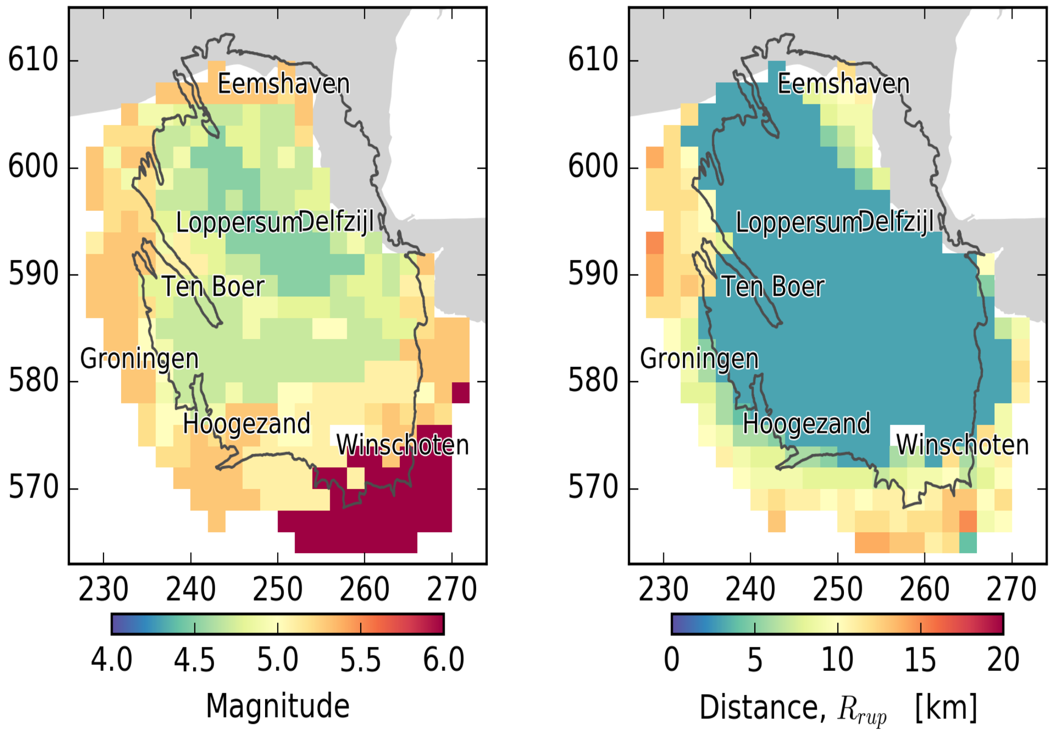

Maps of modal contributions to mean LPR

Prioritization for building strengthening inspections

- Assessment period: 1-1-2018 to 1-1-2023
- Production scenario: 24 bcm/year
- Strengthening scenario: Zero retrofitting

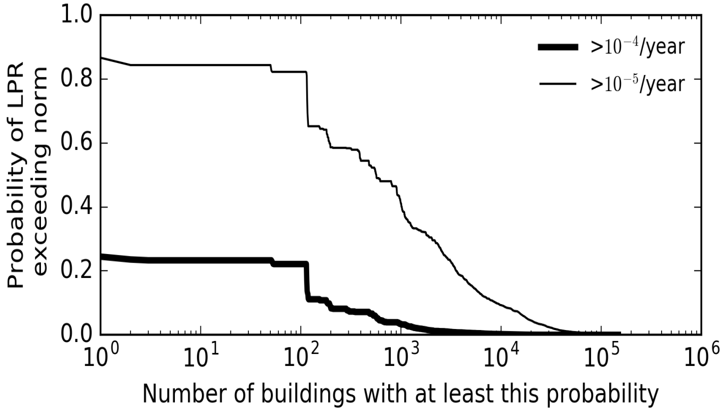

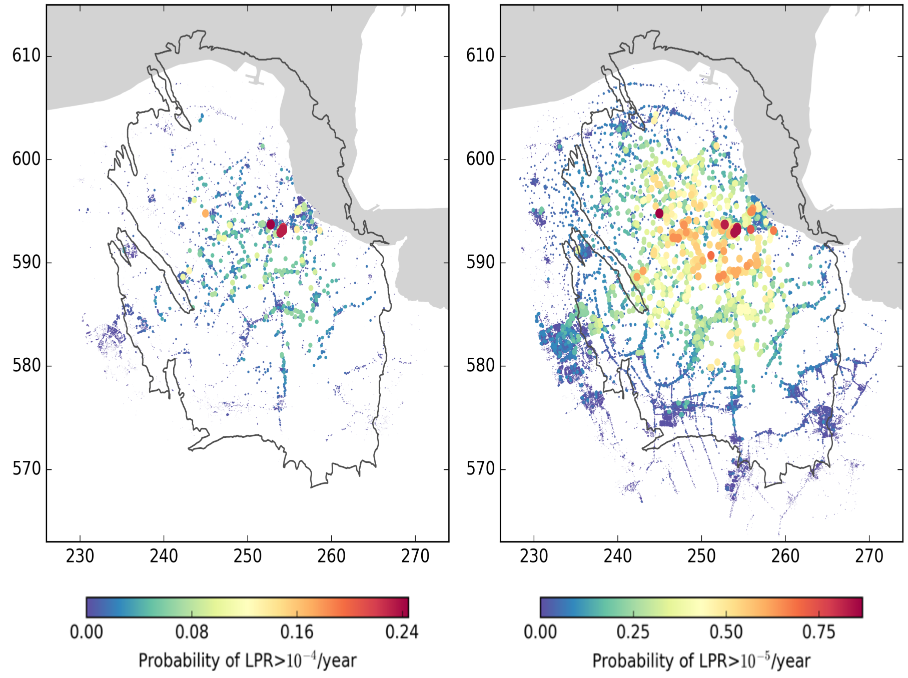

1. Buildings are ranked by probability of exceeding the given risk norm
2. Probability of exceedance computed as the probability-weighted fraction of logic tree branches and structural system combinations with an LPR exceeding the risk norm

Summary

- Seismic risk updated to include the V5 seismological, ground motion, exposure, fragility and consequence models
- Risk verification through replication by independent Python and C codes
- Optimization of MC PSHA code enables 250m resolution, full logic tree simulations overnight
- During the 5-year period from 2018 to 2022:
  - No occupied buildings with a mean local personal risk larger than 10^{-4}/year
  - About 3000 buildings with a mean local personal risk larger than 10^{-5}/year
- Assessment of alternative production and building strengthening options is ongoing